

NEWCASTLE UNIVERSITY

Design and Synthesis of Small-Molecule ERK5 Inhibitors for Anti-Cancer Therapy

Nick C Martin

September 2015

Declaration

The work carried out contributing to this thesis was conducted between October 2011 and September 2015 in the Medicinal Chemistry laboratories, Bedson Building, Northern Institute for Cancer Research at the Newcastle Cancer Centre, Newcastle University, Newcastle upon Tyne, NE1 7RU. The research was conducted in collaboration with the scientists at: Cancer Research Technology Discovery Laboratories, Jonas Webb Building, Babraham Research Campus, Cambridge, CB22 3AT; Laboratory of Signalling and Cell Fate, The Babraham Institute, Babraham Research Campus, Cambridge, CB22 3AT, UK; The Beatson Institute for Cancer Research, Garscube Estate, Switchback Road, Bearsden, Glasgow, G61 1BD.

All of the research presented in this thesis is original in content, and does not include any material or ideas previously published or presented by other authors except where due reference is given in the text.

No part of this thesis has been previously submitted for a degree, diploma or any qualification at any other university.

Acknowledgements

Foremost I would like to thank my supervisory team Dr Celine Cano, Dr Ian Hardcastle, Prof. Bernard Golding and Prof. Roger Griffin for their invaluable guidance, expertise and enthusiasm. The Medicinal chemistry group at the NICR has been a fantastic place to study and it's largely down to these individuals.

The chemistry team on the ERK5 project, past and present, have all been fantastic: Dr Stephanie Myers, Dr Lauren Molyneux, Dr Duncan Miller, Dr Tristan Reullion, Amy Heptinstall, Amy Roberts, Dr Ruth Bawn, Elina Boubouresi and Bebhinn Tully-Penon. I would also like to thank everybody I have shared the lab with: Dr Tim Blackburn, Dr Benoit Carbain, Dr Tommy Rennison, Dr Chris Matheson, Dr Sarah Cully, Dr David Turner, Dr Annalisa Bertoli, Dr Andy Q. Shouksmith, Dr Honrine Lebraud, Dr Suzannah Harnor, Dr Stephen Hobson, Dr Claire Wilson, Dr Elena costa, Daniela Cortese, Kevin Cuthbertson and of course Paul Shaw. Special mentions go to the Tuesday Club members Bian Zhang, James Pickles and Santosh Adhikari it has been a pleasure to go through my PhD along side you. I would also like to single out Lauren Molyneux and Stephanie Myers for being so incredibly helpful when I first started and throughout my PhD. The technical staff during my time at the NICR; Carlo Bawn, Karen Haggerty and Amy Heptistall also deserve thanks for the vital assistance they offered with NMR, HPLC and for maintaining a productive work enviroment.

Co-workers at the NICR have aslo made significant contributions to the work complied in this thesis, namely: Prof. Herbie Newell, Prof. Steve Wedge, Prof Jane Endicott, Prof Martin Noble, Dr Huw Thomas for all the *in vivo* experiments and Lan-Zhen Wang.

I would like to thank the staff at the Babaraham Instutute for making my placement there a very enjoyable one, chiefly Dr Pamela Lohead and Dr Simon Cook. Also collaborators Ai Ching Wong and Laurent Rigoreau at CRT, Dr Hing Leung at the Beatson Institute, Dr Susan Boyd for her assistance with molecular modelling and staff at Astex pharmaceuticals. I would also like to thank the medical research council for funding my PhD and the ERK5 project.

This thesis is the culmination of 8 years spent at university and I would like to thank all the people that have helped along the journey, especially my former supervisors; Prof.

Ray Jones of Loughborough University and Dr Paul Jenkins of the University of Leicester.

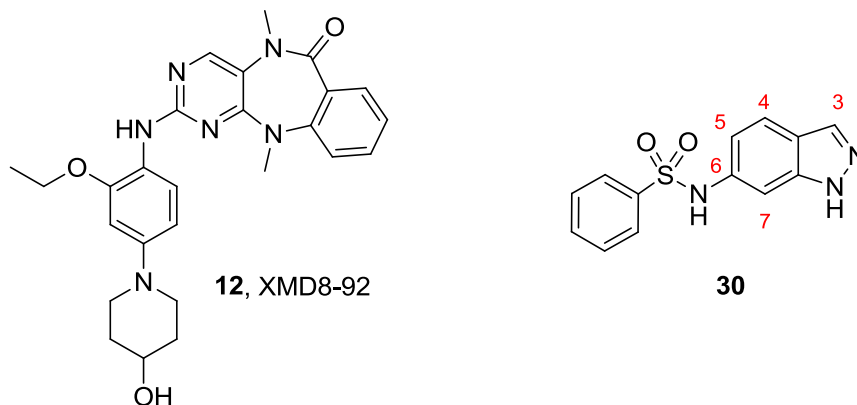
None of this would have been possible without the support of my family. My parents deserve the most thanks; their support has been unrelenting and goes far beyond the financial assistance I have received. I would also like to thank my brother Chris for the competition and his wife Harriet who has probably helped too. My girlfriend Cora has been of tremendous help throughout my time writing up, I don't think I would have ever finished without her support.

I would like to dedicate this thesis to my grandmother Joan Martin, who I have always used as motivation and Roger Griffin who was a fantastic role model and a privilege to work under.

Abstract

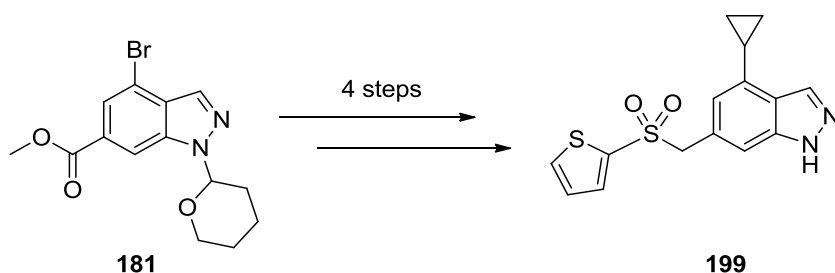
Extracellular signal-regulated kinase 5 (ERK5) is a member of the mitogen activated protein kinase (MAPK) family responsible for activating a number of transcription factors in the cell nucleus. Downstream effects of ERK5 activation have been linked to cell survival, proliferation and differentiation. Overexpression of ERK5 has been observed in a number of tumour cell lines and has been linked with poor prognosis in cancer patients. ERK5 gene knockout studies have proved it plays a role in angiogenesis. Inhibition of ERK5 with XMD8-92 (**12**) showed correlation with tumour growth. All ERK5 validation experiments to date have lacked a compound with good ERK5 potency, selectivity, cell permeability and metabolic stability. The aim of this project is to prove the role of ERK5 in cancer with a drug-like tool compound through *in vivo* validation experiments.

Small molecule ERK5 inhibitors have been discovered through a high-throughput screen revealing indazole-sulphonamide hit compounds with moderate potency, such as *N*-(1*H*-indazol-6-yl)benzenesulfonamide **30** (enzymatic ERK5 IC₅₀ = 4.7 ± 0.04 µM). Hit expansion *via* library synthesis identified a set of sulphonamide aromatic groups associated with good ERK5 inhibitory activity.



Structural optimisation around the sulphonamide linker elucidated a key binding interaction between Lys39 in the ERK5 active site and an S=O group. Removal of the hydrogen bond donor capacity of the sulphonamide yielded compounds with potency in the nM range. Alkylation or removal of heteroatoms in the indazole indicated that compounds form two hydrogen bonds with the hinge region of the kinase active site. Molecular modelling using GOLD predicted the 3- and 4-positions were suitable for substitution. Subsequent synthesis of key bromo intermediate **3** was conducted in a 68%

yield over five steps allowing for library synthesis of 4-alkyl indazoles, including current lead compound **199** (enzymatic ERK5 $IC_{50} = 12 \pm 7$ nM).



Compound **199** shows favourable drug-like properties (MW = 318, CLogP = 4.7, LE = 0.51, Caco-2 efflux ratio = 0.52) and good ERK5 potency in transfected HEK 293 cells (cellular ERK5 $IC_{50} = 24$ nM). However, the compound is rapidly metabolised in mouse liver microsomes (MLM $Cl_{int} = 378$ μ l/min/mg) and has a poor oral bioavailability in mice (24%). Compound **199** was also screened for activity against a panel of 456 kinases but unfortunately showed poor selectivity.

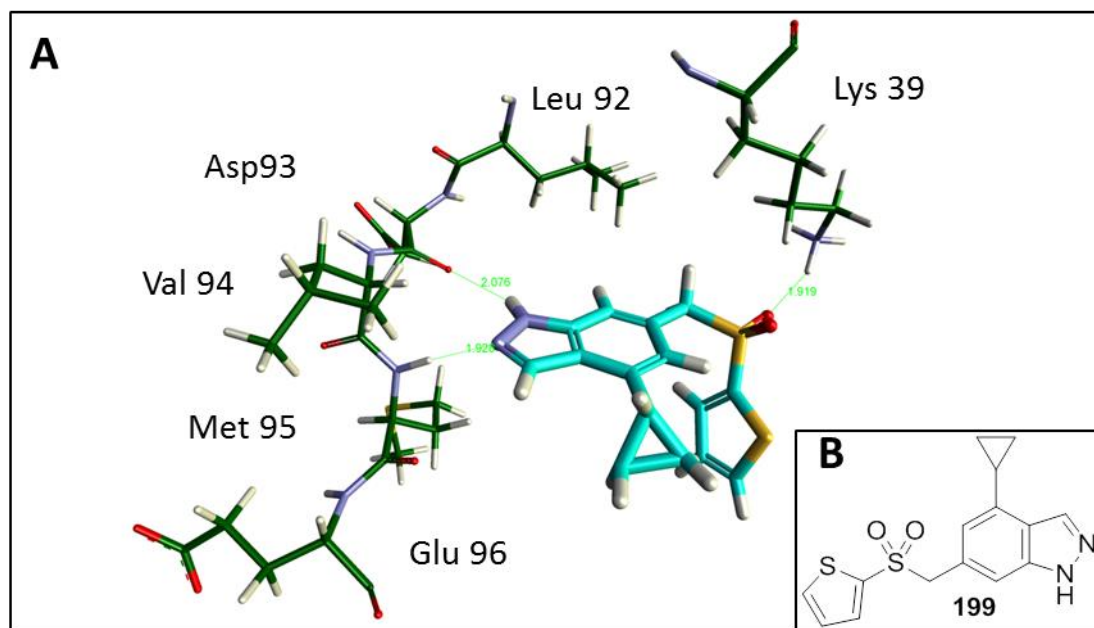


Figure 1. A) Key interactions made between compound **199** (cyan) in the ERK5 active site (green); (B) Structure of Compound **199**.

Metabolite identification conducted with **199** revealed oxidation of the indazole and cyclopropyl group as the major routes of metabolism by CYP enzymes. Unsubstituted 3-, 5-, and 7- positions around the indazole were systematically blocked from metabolism by chlorination, with data indicating the 3-position is most susceptible to oxidation. Improving the LogP of the series was explored by re-optimisation of the sulphonamide aryl group and substitution of the 3-position. It was found that 3-amino



CHAPTER 1: INTRODUCTION	1
1.1 Drug Discovery	1
1.1.1 The Inception of Drug Discovery	1
1.1.2 Modern Medicinal Chemistry	3
1.1.3 Hit Identification	4
1.1.4 Methods of Drug Administration	7
1.1.5 Metrics of Drug-Likeness	8
1.1.6 Ligand Efficiency Metrics	11
1.2 Anti-Cancer Drug Discovery	13
1.2.1 Introduction to Cancer	13
1.2.2 The Hallmarks of Cancer	13
1.2.3 Classical Chemotherapy	14
1.2.4 Targeted Therapies	16
1.3 Protein Kinases.....	18
1.3.1 Types of Kinase Inhibitors.....	22
1.3.2 Mitogen-Activated Protein Kinases (MAPKs)	22
1.4 Extracellular Signal-Regulated Kinase 5 (ERK5).....	26
1.4.1 The Biological Role of ERK5	26
1.4.2 The ERK5 Pathway	26
1.4.3 The Role of ERK5 in the Cell Cycle	28
1.4.4 The role of ERK5 in Cell Survival and Differentiation.....	29
1.4.5 The Role of ERK5 in Angiogenesis.....	30
1.4.6 Evidence of ERK5 in Carcinogenesis	30
1.4.7 MAP Kinase p38 α	32
1.4.8 ERK5 Inhibitors in the Literature	32
1.5 The Indazole Series of ERK5 inhibitors	37
1.5.1 Medicinal Chemistry Tools and Assays used on the ERK5 Project	37
1.5.2 ERK5 IMAP assay	38
1.5.3 p38 α LANCE assay	39
1.5.4 Molecular Modelling.....	39
1.5.5 Measuring Absorption, Distribution, Metabolism, Excretion and Toxicity (ADMET) <i>in vitro</i>	41
1.5.6 Indazoles and Sulphonamides in Medicinal Chemistry	42
1.5.7 Indazole Metabolism	46
1.5.8 Indazole Chemistry.....	46
1.5.8.1 Synthesis of Functionalised Indazoles	47
CHAPTER 2: THE INDAZOLE SERIES	50
2.1 Series Inception & Hit Validation.....	50
2.2 Proposed Libraries for the Indazole Series.....	53
2.3 Variation of the 6-Position Aryl-Sulphonamide	54
2.3.1 Synthetic Strategy Towards various 6-Position Aryl-Sulphonamide Indazoles.....	54
2.3.2 ERK5 structure activity relationships of indazole sulphonamides	58
2.3.2.1 Aromatic and aliphatic rings.....	58

2.3.2.2 Thiophene derivatives.....	59
2.3.2.3 Bicyclic rings	60
2.3.2.4 Substituted Phenyls	63
2.3.2.5 Di-substituted Phenyls	65
2.3.2.6 Cellular Potency of Selected Hit Compounds.....	67
2.4 Modifications Affecting the Indazole H-bonding Profile.....	69
2.4.1 Synthesis and SAR of <i>N</i> -(1-methyl-1 <i>H</i> -indazol-6-yl)benzenesulfonamide (75)	70
2.4.2 Synthesis and SAR of 6-Sulphonamide Indole Compounds.....	70
2.4.3 Molecular Modelling of Indazole Hinge Binding	72
2.5 Linker Modifications	73
2.5.1 Sulphonamide Alkylation.....	73
2.5.1.1 N-Methylation 6-sulphonamide indazoles.....	73
2.5.1.1.1 Alternate Aryl groups on N-Methyl Sulphonamide Indazoles	76
2.5.1.1.2 Selectivity of N-Methyl sulphonamide Indazoles	78
2.5.1.2 Sulphonamide N-Ethyl & N-Isopropyl Derivatives	80
2.5.2 Synthesis and SAR of 6-Amide Indazole Compounds	85
2.5.3 Synthesis and SAR of Cyclised Linker Indazoles.....	87
2.5.4 Synthesis and SAR of Reversed Indazole-6-Sulphonamide	91
2.5.5 Synthesis and SAR of 6-Sulphone indazoles	96
2.5.5.1 Synthetic targets	96
2.5.5.2 Synthesis of 6-Sulphone Indazoles.....	97
2.5.5.3 SAR of 6-Sulphone Indazoles.....	101
2.5.5.4 SAR of 6-Thioether Indazoles	104
2.5.5.5 Synthesis and SAR of 6-Sulphoxide Indazoles	104
2.6 Synthesis and SAR of 5-Substituted Indazoles.....	106
2.6.1 Synthesis of 5- Substituted Indazoles.....	107
2.6.2 Activity of 5-Substituted Indazoles.....	107
2.7 4,6- and 3,6- Disubstituted Indazoles	110
2.8 Substitution on the Indazole 4 & 6-Positions	112
2.8.1 Molecular Docking of 4,6-Substituted Indazoles	112
2.8.2 4 & 6-Substituted Indazole Sulphonamide/Sulphone Synthetic Targets.....	114
2.8.3 Revised Synthetic Scheme for 4 & 6-Substituted Indazole Sulphones	120
2.8.4 Structure Activity Relationships of 4 & 6 Substituted Indazoles.....	122
2.8.4.1 Large alkyl substituents in the Indazole 4-position	124
2.8.5 Cellular potency of 4 & 6-position substituted indazole	127
2.9 Full Profile of 4-Cyclopropyl-6-((thiophen-2-ylsulfonyl)methyl)-1<i>H</i>-indazole (199)	128
2.9.1 Physiochemical properties, in vitro pharmacology and in vitro DMPK profile of 199	128
2.9.2 Selectivity profile of 4-Cyclopropyl-6-((thiophen-2-ylsulfonyl)methyl)-1 <i>H</i> -indazole 199	130
2.9.2.1 CDK2-(4-Cyclopropyl-6-((thiophen-2-ylsulfonyl)methyl)-1 <i>H</i> -indazole) 199 crystal structure	134
2.9.3 Pharmacokinetic profile of 4-Cyclopropyl-6-((thiophen-2-ylsulfonyl)methyl)-1 <i>H</i> -indazole 199	135
2.9.4 Target validation using 4-Cyclopropyl-6-((thiophen-2-ylsulfonyl)methyl)-1 <i>H</i> -indazole 199.....	137
2.9.5 Synthesis and NMR Studies of 4-cyclopropyl-6-(difluoro(thiophen-2-ylsulfonyl)methyl)-1 <i>H</i> -indazole (211).....	137
2.9.5.1 Synthesis of 4-cyclopropyl-6-(difluoro(thiophen-2-ylsulfonyl)methyl)-1 <i>H</i> -indazole (211) .	137

2.9.5.2 F^{19} -NMR experiments with 211	141
2.9.6 Metabolite Identification Study of 199	142
2.9.6.1 Targets Arising from Metabolite Identification Study of 199	147
2.9.6.2 Synthesis of Chlorinated Derivatives of 199	148
2.9.6.3 Activity and Metabolism SARs of Chlorinated Derivatives of 199	151
2.10 3,6-Substituted Indazoles	152
2.10.1 Molecular Modelling of 3,6-Substituted Indazoles	152
2.10.2 Synthetic 3,6-Substituted Indazole Targets	155
2.10.3 Synthesis and evaluation of 3-Alkyl-6-Sulphonamide Indazoles	156
2.10.3.1 3-Alkyl-6-Sulphonamide Indazole Targets	156
2.10.3.2 Synthesis of 3-Alkyl-6-Sulphonamide Indazole Targets	156
2.10.3.3 SAR of 3-Alkyl-6-Sulphonamide Indazole Compounds	158
2.10.4 Synthesis and evaluation of 3-Carboxyl and Hydroxyl-6-Sulphonamide Indazoles	160
2.10.4.1 3-Carboxyl and Hydroxyl-6-Sulphonamide Indazole Targets	160
2.10.4.2 Synthesis of 3-Carboxyl /Hydroxyl-6-Sulphonamide Indazole Targets	160
2.10.4.3 SAR of 3-Carboxyl and Hydroxyl-6-Sulphonamide Indazole Compounds	162
2.10.5 Synthesis and Evaluation of 3-Amide-6-Sulphonamide Indazoles	164
2.10.5.1 3-Amide-6-Sulphonamide Indazole Targets	164
2.10.5.2 Synthesis of 3-Amide-6-Sulphonamide Indazole Compounds	164
2.10.5.3 SAR of 3-Amide-6-Sulphonamide Indazole Compounds	165
2.10.6 Synthesis and Evaluation 3-Amino-6-Sulphonamide Indazoles	165
2.10.6.1 3-Amino-6-Sulphonamide Indazole Targets	165
2.10.6.2 Synthesis of 3-Amino-6-Sulphonamide Indazole Targets	166
2.10.6.3 SAR of 3-Amino-6-Sulphonamide Indazole Compounds	171
2.10.15 SAR Summary of 3-Substituted-6-Sulphonamide Indazole Compounds	172
2.11 Metabolism SAR of the Indazole series	174
2.11.1 Re-optimisation of the Sulphonamide Aromatic	177
2.11.1.1 Decreasing the LogP by variation of the sulphonamide aryl group	177
2.11.1.2 Extension from the Sulphone Aromatic	180
2.11.1.2.1 Synthesis of Extended Phenyl and Triazole Sulphone Compounds	182
2.11.1.2.2 SAR of Extended Phenyl and Triazole Sulphone Compounds	182
2.11.2 4-Position Metabolism SAR	183
2.11.3 Metabolism SAR of 3,6-Substituted Indazoles	184
2.11.3.1 Synthesis and metabolism of N-(3-(difluoromethyl)-1H-indazol-6-yl)-N-methylthiophene-2-sulfonamide (322)	186
2.11.3.2 ERK5 activity and metabolism of N-(3-(difluoromethyl)-1H-indazol-6-yl)-N-methylthiophene-2-sulfonamide (322)	188
CHAPTER 3: THE PYRROLE SERIES	189
3.1 Initiation of the Pyrrole carboxamide series and early SARs	189
3.2 Pyrrole carboxamides 17 and 327	190
3.2.1 Resynthesis of Pyrrole Carboxamides 17 and 327	190
3.2.2 <i>In vitro</i> Pharmacokinetics of 17 and 327	191
3.2.3 <i>In vivo</i> Pharmacokinetics and Pharmacodynamics of 17	193
3.2.3.1 <i>Matrigel plug assay</i>	193
3.2.3.2 Human tumour xenograft models	194

3.3 Summary of Pyrroles Carboxamide SARs	195
3.3.1 Potential Combination of Indazole and Pyrrole Carboxamide Series.....	196
3.4 Investigating the Efflux of Lead Pyrrole Carboxamide Compounds	199
3.4.1 ABC Transporters.....	200
3.4.2 P-glycoproteins and Multidrug Resistance.....	201
3.4.3 Agents that Target P-gp.....	202
3.4.4 Designing drugs that do not interact with P-gps	202
3.4.5 Methods to Deduce Drug P-gp Interaction	203
3.4.6 Effects of Selected Pyrrole carboxamides on P-gp Expression.....	204
3.4.7 Summary of Pyrrole Carboxamide Efflux.....	208
 CHAPTER 4: CONCLUSIONS AND FUTURE WORK	 210
4.1 Summary of Further Indazole 4-position Exploration	210
4.1.1 Comparison of lead Sulphone Indazole Compounds with Sulphonamide Analogues	210
4.1.2 4-Substituted, 6-sulphonamide Indazoles – Heterocyclic Substituents	211
4.1.3 4-Substituted, 6-Sulphonamide Indazoles – Polar Substituents	211
4.2 Future work	213
4.2.1 Future Work at the Indazole 4-Position	213
4.2.2 Future Targets at the 3-Position.....	216
4.2.3 Substitution of 4,3 and 6 Positions.....	217
4.3 Conclusion	218
 CHAPTER 5: EXPERIMENTAL	 219
5.1 ERK5 and p38α Assay Protocols	219
5.1.1 ERK5 IMAP TM Assay Protocol.....	219
5.1.2 p38 α LANCE Assay	220
5.1.3 Hela cell-based densitometry assay protocol.....	221
5.1.4 Cellular Dual-Luciferase Reporter Assay	222
5.2 P-gp induction assessment.....	223
5.3 Molecular Docking Procedure	226
5.4 Analytical Techniques	226
5.5 General Procedures:	228
5.6 Synthetic Procedures	234
 ABBREVIATIONS.....	 378
 REFERENCES.....	 382

Chapter 1: Introduction

1.1 Drug Discovery

1.1.1 The Inception of Drug Discovery

The human race has been using medicines for centuries, however, the use of chemistry in the discovery of new drugs is much more recent. The field of chemistry reached a level of sophistication in the late 19th century which allowed its application in a pharmacological setting. Before agreement on Mendeleev's periodic table, Avogadro's atomic hypothesis, and the ability to determine the structure of organic molecules, the rational development of active drug compounds was not possible. Advances in the biological sciences such as the elucidation of the structure of DNA, protein synthesis and the amino acid structures facilitated the formation of a crossover discipline which could be described as medicinal chemistry.¹ When chemical dyes were studied by Paul Ehrlich in the 1870's an affinity between chemicals and living tissues was first described. His discoveries led to the development of Gram staining, used to categorise bacteria. He also proposed the chemical exploitation of differences in cells to a therapeutic end.

Arsphenamine (**1**) was the first synthetic drug and was prepared in Ehrlich's laboratory in 1907 for the treatment of Syphilis.² The arsenic based structure was associated with a host of side effects but was the treatment of choice until eventually superseded by Penicillin. Arsphenamine was the first example of lead optimisation, as Ehrlich's group synthesised, tested and modified structures to find the optimum anti-bacterial compound for a specific strain.

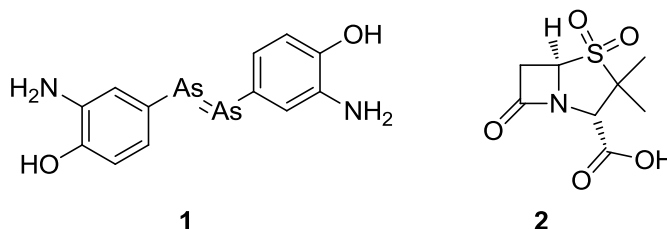


Figure 1. A possible structure of arsphenamine (**1**) and the structure of sulbactam (**2**).

A great number of medicinal products were isolated from natural sources, with opiates and penicillin among the most commercially successful. Penicillin was first isolated

from *Penicillium* mould, and subsequently, many other derivatives were also defined with varying properties. Chemical modification of natural products like Penicillin gave rise to the first semi-synthetic compounds such as sulbactam (**2**).³ The subtle differences in these compounds improved the understanding of their biological receptors and gave rise to some of the first structure-activity relationships (SAR).

An improved understanding of enzyme and receptor function, along with advances in X-ray crystallography, permitted the rational design and optimisation of drug molecules.⁴ The publication of the human genome project in 2003 supplied a great number of previously unknown possible drug targets to be investigated.⁵

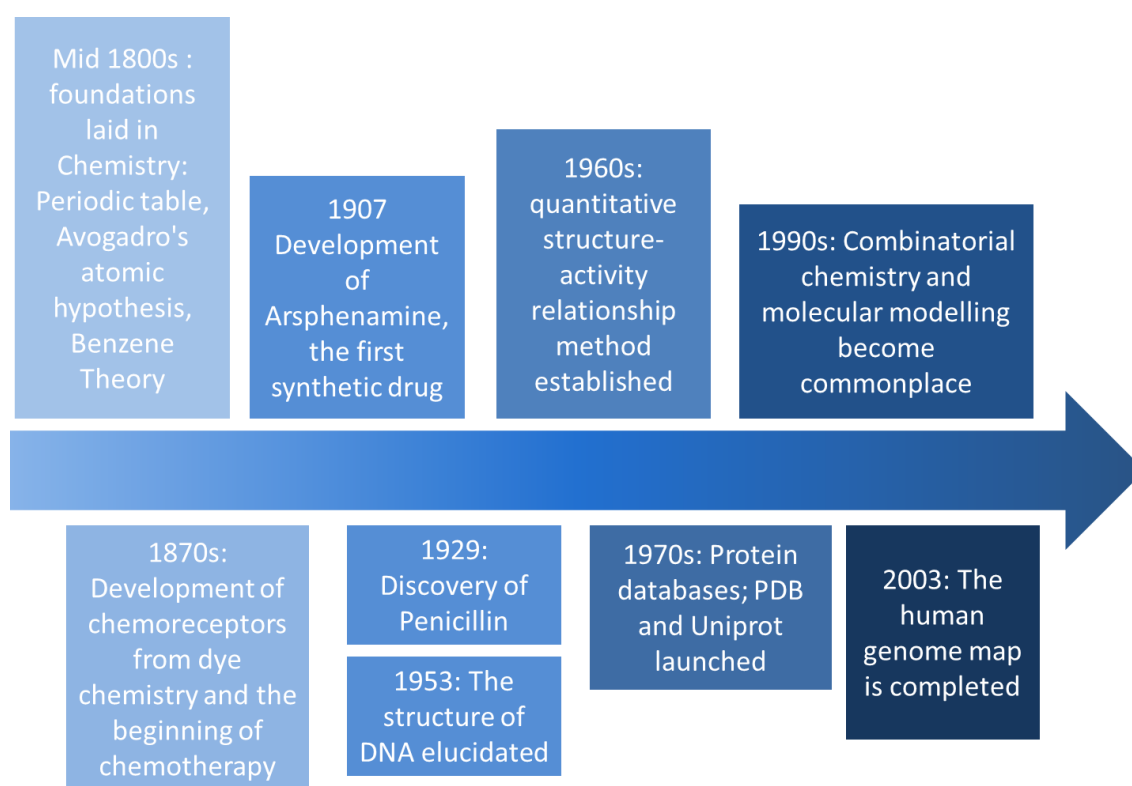


Figure 2. Timeline showing significant advances to aid, and leading to modern medicinal chemistry.

Advances in organic synthesis in the late 20th century gave rise to combinatorial chemistry that allows the synthesis of libraries of millions of compounds.⁴ The first clinical trials were conducted well before the inception of the Food and Drugs Administration (FDA), as early as 1747 with James Lind's documentation of his potential scurvy remedies.⁶ Over time the methods used have developed to include placebos, control groups, double blind controls, and randomised screening.

The FDA began in 1906 with the passing of the Pure Food and Drugs Act which regulated the quality of commercial medicines and foods in the USA.⁷ This body as well as European and regional equivalents have controlled the licencing of medicines to ensure the safety of the relevant populations and make the purveyors accountable for their products. Sanctions such as mandatory animal testing and the clinical trial tier system ensures that compounds are well vetted before general release. In modern practice a large amount of preclinical data must be obtained to prove compounds are of limited risk to the patients in phase 1 clinical trials.

The basic outline of clinical trials is shown in Table 1. Usually, clinical evaluation takes between 10 and 15 years. In comparison James Lind's trial lasted 6 days before the use of citrus fruit for the treatment of scurvy was declared curative, although this is only a dietary treatment.⁶

Table 1. Progression of clinical trials.

Phase	Size of study	Purpose	Typical Duration
Pre-clinical	-	<i>In vitro</i> and in animal assessment of biological effect and safety	3-4 years
Phase I	20-100 patients	Determine safe dosage regimen, pharmacokinetics and pharmacodynamics properties	8-10 years
Phase II	100's	Identify effect and any side effects	
Phase III	300-3000	Decide if new treatment is superior to those already in place	
Post Clinical trials	-	Continued monitoring of patients to conclude any long term side effects	1.5 years

1.1.2 Modern Medicinal Chemistry

The modern drug discovery cascade begins with a therapeutic need and target identification. Once the role of the target is determined and a therapeutic effect from its modulation has been demonstrated, an assay is required. If the target is a member of a well-studied protein family it is likely that an assay format can be

transferred/adapted, for example assays exist in some format for almost the entire kinome. However, consistent expression of protein and optimisation of the exact assay conditions can be time consuming. The primary assay is typically a high-throughput biochemical measure of a compound's affinity to the target as either an agonist or antagonist. For simplicity and speed, assays are often cell-free which gives the fewest variables, although this is not always possible and depends on the nature of the target.

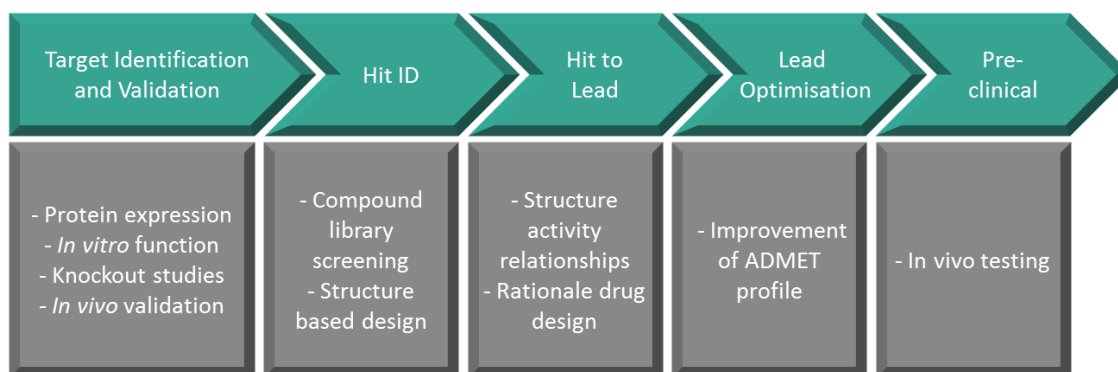


Figure 3. Progression of the modern drug discovery process.

1.1.3 Hit Identification

For well-established biological targets, active compounds or licenced drugs may have been disclosed. Literature data also exists on a wide range of natural products which regularly exhibit biological activities. Many drugs have come to market as unmodified natural products, such as epibatidine (**3**) and morphine (**4**) (Figure 4). Active compounds have been sourced from a wide diversity of life including plants, bacteria, fungi, marine life and animals. Natural products are often large macromolecules with a high degree of chirality. Synthesis of such molecules has become a sub-division of organic chemistry and has a reputation for pioneering novel synthetic methods.⁸ However, total syntheses are commonly low yielding and lengthy and not viable for scale up. Where possible natural products or precursors are isolated from an organism, for example paclitaxel (**9**) can be synthesised from a precursor isolated from European yew tree needles.⁹ It could be argued that a large portion of natural products are not suitable leads for a drug discovery campaigns due to their inherent complexity and large size. The lipase inhibitor orlistat (**5**) was derived from lipstatin (**6**), by a

medicinal chemistry campaign to optimise the SAR, and is one of many drugs discovered in this way (Figure 4).¹⁰

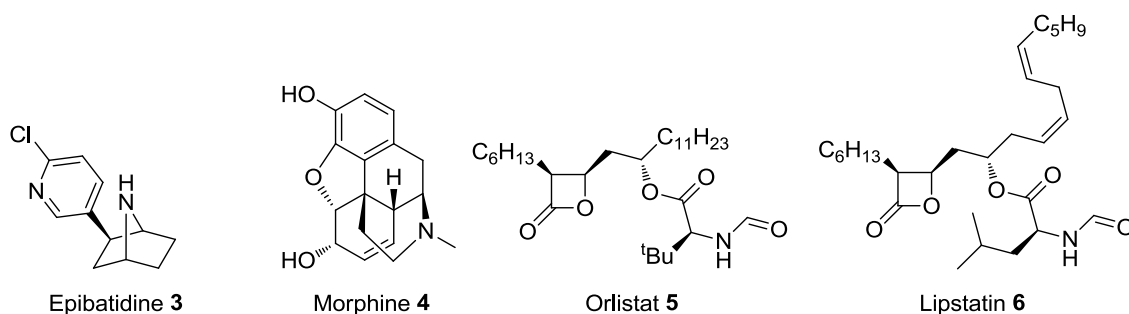
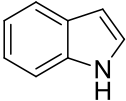
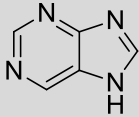
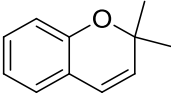
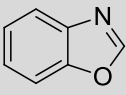
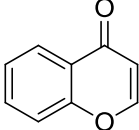


Figure 4. Structures of Epibatidine (**3**), Morphine (**4**), Orlistat (**6**) and Lipstatin (**7**).

Alternatively and increasingly popularly, hits are found in a library of synthetic scaffolds. Combinatorial chemistry along with microwave-assisted synthesis have simplified the production of drug-like compound libraries which can be screened for activity.¹¹ Library sizes range from a few thousand to millions of compounds. Organisations like the European Lead Factory allow the compounds in their possession (approximately 300,000) to be used by applicants, but most large pharmaceutical companies restrict access to their proprietary libraries.¹² Focussed libraries contain compounds that are most likely to have affinity to a particular class of target which saves time and resources. The pharmaceutical industry has driven a ‘fail fast, fail cheap’ philosophy to minimise losses on dead-end research which is inherent in the design of these large compound banks.

A well curated compound library should only contain compounds which make good lead compounds. High molecular weights (MW) and highly halogenated systems can lead to cul-de-sacs during development or are singletons in the first screen. Efforts have been made to remove toxicophores such as nitro groups, unstable ring systems and electrophilic species but maintain a representative library.¹³ Frequent hitting are structures which are routinely flagged up as potent against many targets and target types. Privileged structures appear in drug compounds, so starting a project from one can limit the novelty of the project and may present problems with intellectual property (Table 2).¹⁴ The heterocycles in Table 2 appear repeatedly in hit compounds due to their drug like structures, which is unsurprising given their abundance in nature.

Table 2. Selected privileged scaffolds and their appearance in biologically active compounds. Adapted from Welsh *et al.*¹⁴

Privileged scaffold	Drug examples	Natural product Examples
 Indole	Medmain Oxypertine Psilocybin	Okaramine Nostodione A Vinblastine
 Purine	Abacavir Pentoxifylline Cafaminol	Caffeine 1,3 Dimethylisoguanine 3,7 Dimethylisoguanine
 3,3-Dimethylbenzopyran	Nabilone Levchromaklim Centchroman	Metachromin T Phaseolin Acronycine
 Benzoxazole	Zoxazolamine Flumoxaprofen Benzoxaprofen	Pseudopteroxazole Antibiotic A 16886A Antibiotic A23187
 Chromone	Efloxate Favoxate Cromolyn	Tricin Homothamnione Cissampelflavone

It has been estimated that 10^{60} drug like structures are possible and that so far only an infinitesimal proportion of that space has been explored (estimated at 2.7×10^7 compounds).^{15, 16} With that in mind taking a privileged scaffold as an initial hit is unnecessary but, because of the way most high throughput screen (HTS) compound libraries are maintained, it is recurrent. A modern alternative to HTS of large compound libraries is fragment library screening. Fragment libraries are collections of low MW (<300 Da) structures. Complexity ranges from unsubstituted heterocycles to moderately functionalised heterocycles. By generating a hit from such a small compound there is greater freedom of development with regard to increasing LogP, MW and other such parameters defining drug likeness (Chapter 1.1.5). Hits from a fragment screen have lower affinity for the target than hits from a HTS but should have

a similar or improved ligand efficiency (LE). LE is a measure of a compound's affinity to the target in proportion to compound size (See Chapter 1.1.6 for full definition). Structure-based fragment discovery gives rise to hits with their interactions defined from the outset. In contrast, larger HTS hits may require preliminary SAR studies to identify their pharmacophore. It is possible for fragments to bind in one or more locations of the protein active site. In this case fragments can be linked or one grown to incorporate the interactions of others with isosteres. When crystallography is employed in the identification of fragments merging ligands is made simpler through visualisation data.

1.1.4 Methods of Drug Administration

The parameters defining drug likeness change depending on the method of administration. Topical treatments are applied directly to the target and need only to permeate the area whereas an oral drug is required to pass through the stomach and permeate the intestine to reach the blood before passing through the liver and eventually the cell membrane to reach the target (Table 3). Intravenous drugs only need to permeate the cell membrane but are less popular and are not commonly self-administered, therefore, most drug discovery projects aim to provide an orally available compound.

Table 3. Routes of drug administration.

Route of administration	Organs passed before reaching the blood	Advantages	Disadvantages
Oral	Stomach, Gut	Can be self-administered	Highest exposure to metabolic enzymes
Intravenous/ Subcutaneous	-	Rapid onset, lowest exposure to metabolic enzymes	Not favoured with patients
Topical	N/A	Non-invasive	Slow absorption, limited to skin disease
Inhaled	Lungs	Excellent for lung related illness	Dose received is highly variable
Suppository	Gut	Avoids stomach and hepatic portal vein (first pass metabolism)	Not favoured by patients

1.1.5 Metrics of Drug-Likeness

Lipinski *et al* was the first to define guidelines for the design of orally bioavailable drug compounds, known as Lipinski's rule of 5 (Table 4).¹⁷ The rules were deduced by analysing 2245 small molecule drug structures entering phase II clinical trials (not including peptides, polymers natural products or phosphates).¹⁷ It was found that a correlation exists between oral bioavailability and all the physiochemical properties give in Table 4.

Table 4. Lipinski's rule of five.

Parameter	Definition	Rule
MW	Mass of the compound	<500 Da
LogP	A measure of a compound's solubility in water by partition with octanol. $\text{LogP} = \text{Log}([\text{H}_2\text{O}]/[\text{octanol}])$	<5
HBA	Hydrogen bond acceptors	<10
HBD	Hydrogen bond donors	<5

A compound must be small enough to pass through the gut wall to reach systemic blood flow which generally requires a molecular weight below 500 Da. The compound must be soluble in H₂O/blood but also lipophilic enough to pass through the cell membrane which is of course made up of lipids. As ionised drugs cannot pass membranes the desirable range for LogP is between 0 and 5 but a better measure of this is LogD which takes into account the pK_a of the drug compound. HBA are better tolerated than HBD and both are relevant to the solvation of the compound in the body.

Since these guidelines were published in 1997 they have been widely adopted by the medicinal chemistry community but some flaws have been identified and refinements made. Expansions on Lipinski's metrics have been made to include; topological polar surface area (tPSA), number of aromatic rings, number of rotatable bonds and number of toxicophores to give a quantitative estimate of drug likeness (QED) (Table 5).¹⁸ Parameters were chosen based on known effects on drug-likeness, for instance the number of toxicophores, but also values easily measurable in a library of compounds where distinct trends exist.

Table 5. Factors that influence a compound's QED (quantitative drug-likeness) score plus Lipinski's Rules (Table 4)

Parameter	Desirable range
Topological polar surface area (tPSA) defined as Vander Waals radius of all HBDs and HBAs.	<140 Å
Number of aromatic rings	<3
Number of rotatable bonds	<10
Number of toxicophores	<2

There are many drugs which do not satisfy all of Lipinski's rules but are orally available, therefore a trigger for the definition of a new metric, QED, was to obtain a score function (0-1, where 1 is most drug-like) as apposed to a binary yes/no system. Compounds approved by the FDA are frequently at the upper limits of Lipinski's rules (median patented compound has a cLogP of 4.1 and MW of 450 Da) meaning that the majority of research is on compounds with poor drug QED scores (represented in Figure 5).¹⁹¹⁶ The pharmaceutical industry has a very poor attrition rate resulting in failure of 93-96% of candidate compounds in the clinic.²⁰ This may be attributed to the poor drug-likeness of compounds submitted.

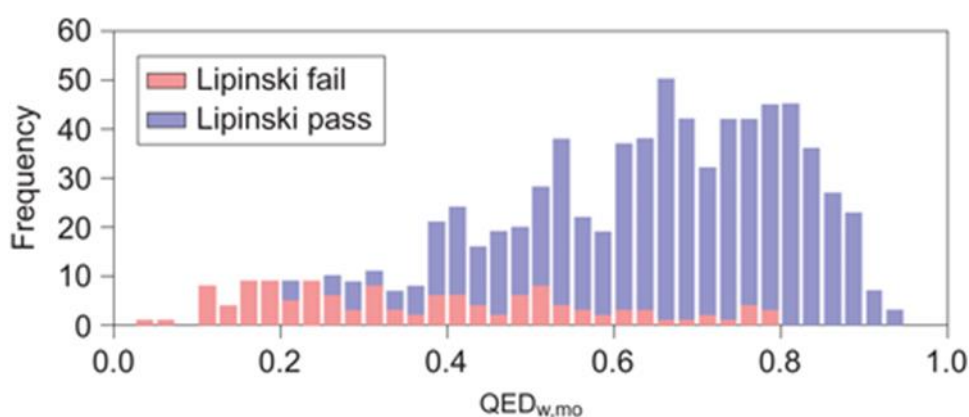


Figure 5. Graph showing distribution of QED scores and proportion of drugs that passed/failed Lipinski's rules of 771 FDA approved drugs.(taken from Hopkins *et al*)

1.1.6 Ligand Efficiency Metrics

The ligand efficiency (LE) is a method of quantifying each atoms contribution to potency given by; $LE = \Delta G/N$ where ΔG is Gibbs free energy and N is the number of heavy atoms i.e. not hydrogen. The equation can be transformed by substituting ΔG out to give:

$$LE = \frac{-1.37\text{Log}(IC_{50})}{N}$$

The formula above is representative of ligand binding energy per heavy atom and gives a high score for high efficiency (desirable values are over 0.3). This metric is particularly useful when identifying hit compounds and scrutinising functionalities. LE is commonly defined in simpler terms as $LE = pIC_{50}/N$ which is referred to as the ligand efficiency index (LEI).

Ligand efficiency can be modified to include other compound properties such as lipophilicity (lipophilic ligand efficiency, LLE or LipE). LLE is given by $LLE = pIC_{50} - CLogP$ with high scoring compounds having higher efficiency with regard to the lipophilicity and potency. LLE is useful when optimising the solubility of a compound as a drop in potency may actually be beneficial to a compound's overall profile if the LogP is affected enough.

Comparison of LE values can be done to determine differences between functionalities and also a group efficiency (GE) metric can be calculated by:

$$GE = \frac{[-1.37\text{Log}(IC_{50}^A)] - [-1.37\text{Log}(IC_{50}^B)]}{N^A - N^B}$$

GE can be used to compare different substituents and also predict potential benefits. When choosing functionalities to include the theoretical change in heavy atoms is known, as is the LE of original molecule. Therefore, the potency increase to maintain the LE can be calculated. For example an addition of 3 atoms (e.g. primary amide) on a molecule of 500 Da and an IC_{50} of 10 nM must improve potency 4.6 fold in order to maintain the LE.^{16, 21} Rough guidelines can be extracted from these type of calculations such as the addition of 1 heavy atom needs to improve potency ~2-fold to be worthwhile whilst the addition of a 6 membered ring needs to cause a potency

various groups, as shown in Figure 6.²¹

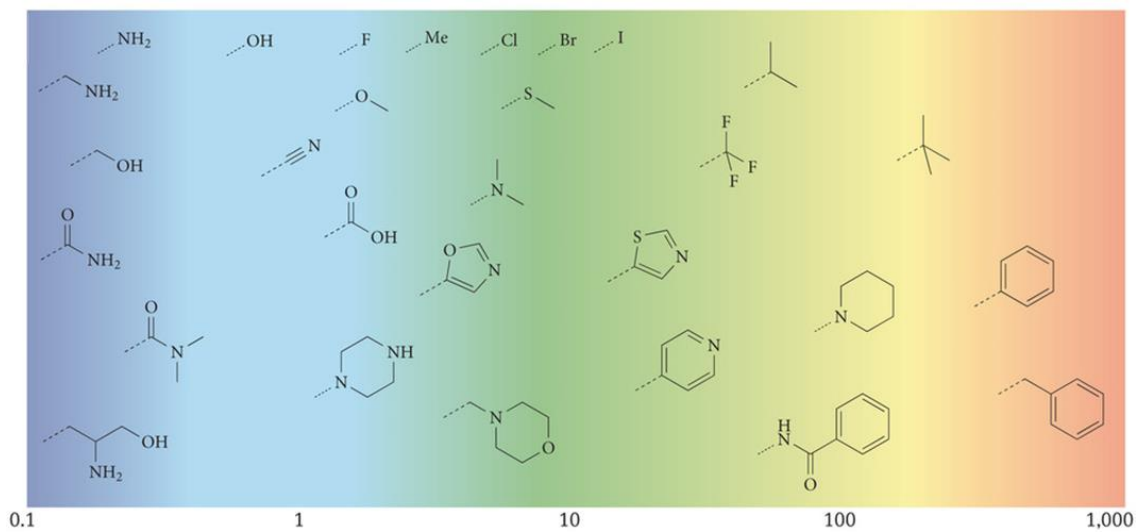


Figure 6. The fold increase in potency needed to maintain an LLE value of 0.3 of various substituents (taken from Hopkins *et al*²¹)

1.2 Anti-Cancer Drug Discovery

1.2.1 Introduction to Cancer

In 2012 Cancer Research UK estimated there were 8.2 million deaths as a direct result of cancer and 14.1 million new cases worldwide.²² A cancer cell can be defined as a cell that has escaped the intrinsic control mechanisms of the cell cycle. This change is brought about by a modification to the genetic makeup of the cell, caused by mutation. The total number of cells in the average human body is in the region of tens of trillions and therefore many mutation events occur as DNA is read and replicated in each cell. Due to the length of DNA, each cell is thought to produce over 10,000 replication errors each day.²³ The likelihood of mutation is further increased by overexposure to UV or radiation of any kind or the consumption of mutagens such as those found in cigarettes. Mutations ultimately affect the DNA code which leads to errors in the amino acid sequence of synthesised proteins. Commonly DNA mutations are identified by repair mechanisms in the cell, however, in some cases the cell cycle progresses resulting in a modified cell.

Some mutations, known as passenger mutations convey no benefit to the cell and can be described as biologically inert. These do not affect a cell's tendency to become cancerous.²⁴ If the mutation conveys a benefit over cells in the surrounding tissue it will prosper in a Darwinian 'survival of the fittest' manner. Mutations of this nature are called driver mutations as they are responsible for the cancerous properties of a malignant tumour when accumulated.²⁴ The development of cancer is thought to require a number of characteristic mutations in order to overcome certain processes which normally facilitate the prevention of tumour formation. Cancer cells are capable of invading tissues and therefore metastasising, resulting in multiple sites of tumour growth. Cancer fatality occurs when the function of vital organs is lost due to the overwhelming presence of cancer cells.

1.2.2 The Hallmarks of Cancer

The hallmarks of cancer (Figure 7) have been reported as a combination of properties which allow the cell to grow without regulation but with sufficient access to necessary resources.^{25, 26}

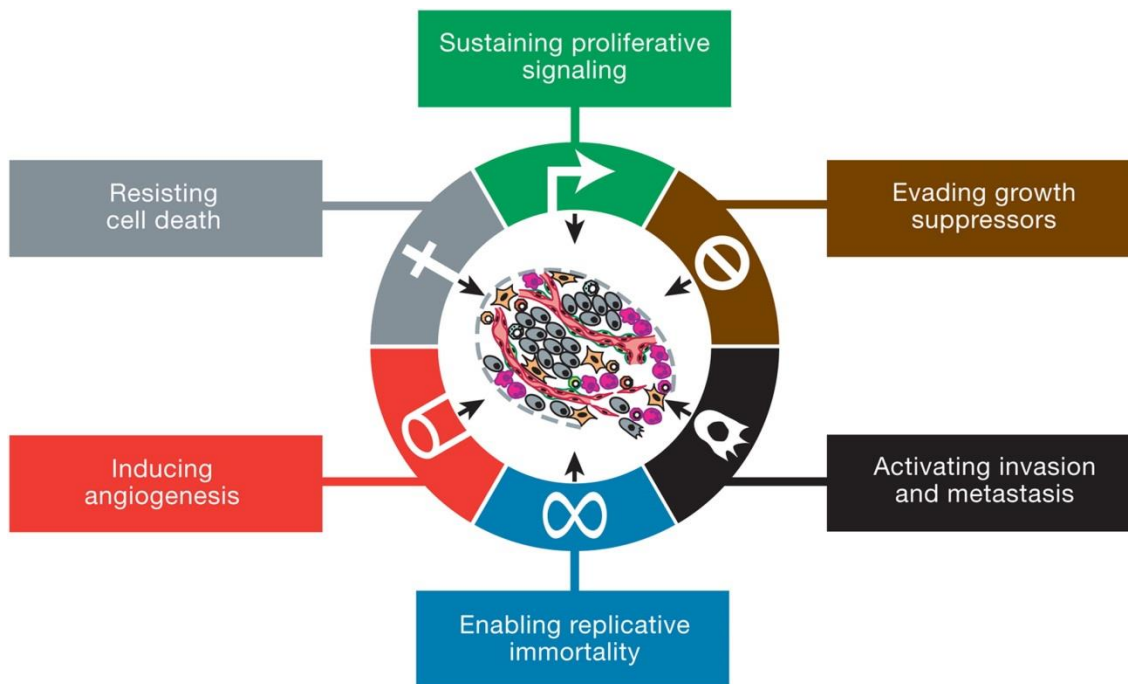


Figure 7. The Hallmarks of cancer (taken from Hanahan & Weinberg²⁵)

Almost all cancer driver mutations that occur in a cell can be attributed to one of the hallmarks of cancer. The order in which these mutations and properties occur is not consistent but typically all six are necessary for a malignant cancer. Driver mutations result in either the loss of function, by which the expression of tumour suppressors is suppressed or the expression of a natural cell cycle inhibitor is down regulated or a gain in function where a pathway becomes permanently active or expressed in greater concentrations. Angiogenesis allows a cancer tumour to propagate its own blood vessels ensuring an ample supply of resources necessary to sustain a constantly replicating group of cells. If this weren't the case a tumour would have a maximal size or rate of growth dependant on the tumour's location. Cancer cells are resistant to apoptosis which should be caused by recognition of the irregular genetic material, elevated levels of signalling and other physical stresses on the cell. Once pathways which control DNA replication are bypassed the cell is predisposed to garner more genetic variations causing rapid development into a cancer cell.

1.2.3 Classical Chemotherapy

The first chemical treatments for cancer were cytotoxic agents discovered as a result of research into the side-effects of chemical weapons used in warfare during the early 20th century. Chemical warfare was subsequently banned by the Geneva protocol in

1925 but mustard gasses were modified and repurposed as pharmaceuticals.²⁷ Whilst cancer is by no means a new disease, a deep understanding of the key principles was not present at this time and therefore treatments were highly toxic to the patient. Agents such as cyclophosphamide (**7**) are still used today and work by linking DNA bases together, typically the N-7 position of purine bases. DNA alkylation causes apoptosis or programmed cell death as the replication of genetic material is prevented. The nitrogen mustards gave birth to not only a class of anti-cancer drugs, DNA alkylating agents, but also the founding principles of chemotherapy.²⁸ Platinum based agents such as carboplatin (**8**) (Figure 7) also produce a therapeutic effect by forming DNA adducts and, like nitrogen mustards, are associated with toxic side effects.

Paclitaxel (**9**) prevents tubulin structures from disassembling causing the cell cycle to halt before reaching metaphase, leading to apoptosis. Some early chemotherapy relies on the higher rate of proliferation in cancer cells and therefore increased consumption of resources to produce a higher concentration of the drug compound in cancer cells. As a result most of these drugs cause cell death in normal body cells that are naturally dividing leading to hair loss, gastrointestinal disorder and weakening of the immune system.²⁷ It has been shown that normal cells are replaced quicker than cancer cells when put under the extreme stress of chemotherapy which may be due to the loss of some cellular process in the cancer cells. However, patients treated with cytotoxic agents suffer numerous side effects and extreme discomfort due to the narrow therapeutic index. Cisplatin, paclitaxel and vinblastine all cause nausea among more serious side effects such as loss of sight. It is questionable in some circumstances (when treatment is not curative) that the life extension they grant to a late stage cancer patient is not worth the pain and hardship that chemotherapy presents.²⁹

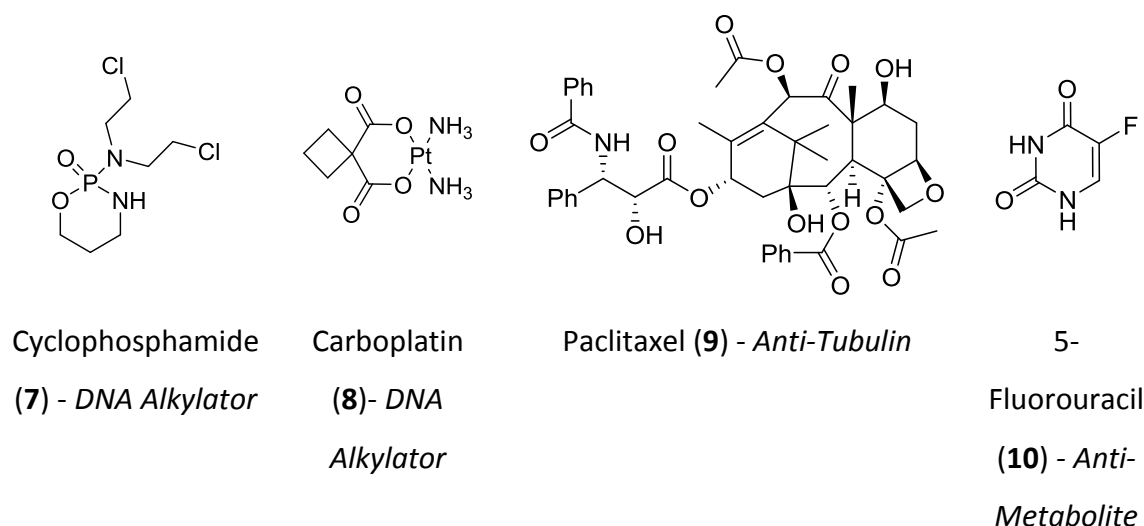


Figure 8. Structures and mode of action of cytotoxic chemotherapy agents.

Due to the way in which a cell becomes cancerous, a tumour may contain several cell lines that have achieved the hallmarks of cancer through different means and therefore possess different properties. Clonal evolution means that if one cancer cell line is sensitive to an administered agent another insensitive cancer cell line will prosper. This means that intrinsic or acquired resistance to therapy is very common as certain cell lines react differently to drugs. Genetic instability of the cancer genome causes many cell lines to be created from one cancer cell line making targeting a tumour even harder. Cytotoxic agents are generally administered as a cocktail of one or more active ingredients to limit the effects of toxicity. Resistance to drugs can develop in a number of ways such as increased expression of efflux pumps (Chapter 3.4).

1.2.4 Targeted Therapies

The hallmarks of cancer define the key differences between a normal and cancerous cell and each hallmark is brought about by a change in expression levels or activity of a relevant protein. Targeted therapies aim to regain control of one of the processes contributing to carcinogenesis or assisting tumour growth. A number of key driver proteins have been identified in particular cancer types that have been exploited with effective drug compounds (Figure 9). Tractable targets such as androgen or growth factor receptors have been exploited for the treatment of cancer as well as the inhibition of signalling pathways. The strategy behind this target selection is to create

better selectivity between cancerous and normal cells so a therapeutic effect is brought about without the side effects associated with cytotoxic agents.

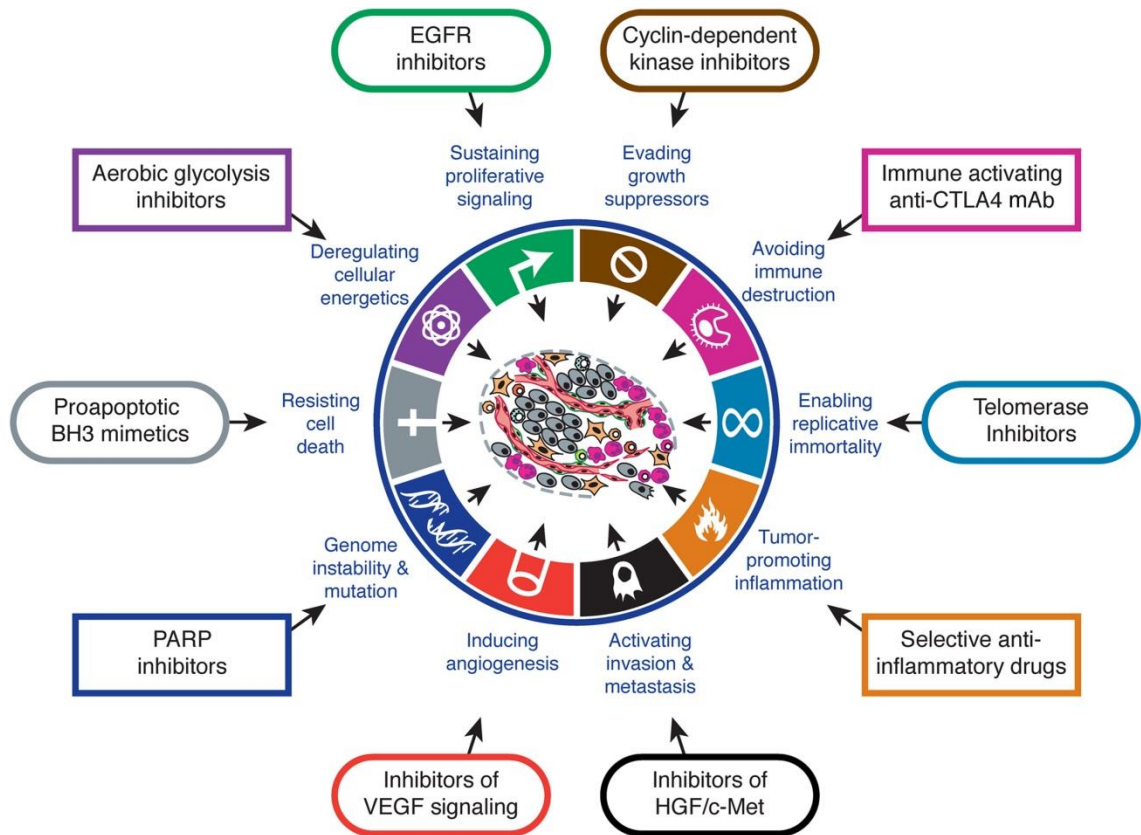
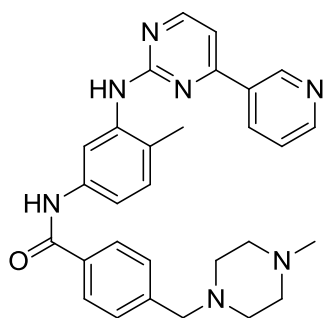


Figure 9. The Hall marks of cancer and associated therapeutic targets (taken from Hanahan & Weinberg²⁵)

One particular targeted therapy success story is the kinase inhibitor, imatinib (Gleevec®, **11**) which targets the Bcr-Abl kinase. This is a mutant kinase encoded by the Philadelphia chromosome, which is formed by a translocation event of chromosomes 9 and 22, and is expressed exclusively in chronic myeloid leukaemia cells. There are very few side effects associated with imatinib as the protein target is only present in cancer cells and the compound is sufficiently selectivity to not affect other kinase signalling pathways. Although the Bcr-Abl kinase is an isolated case of a mutant protein target, numerous other kinase targets have been identified as overexpressed or activated in cancerous cells.³⁰⁻³³



Imatinib (Gleevec) **11**

Figure 10. The structure of Imatinib (Gleevec) **11**.

1.3 Protein Kinases

The role of a kinase within a cell is to coordinate signalling through phosphorylation of proteins. The phosphorylation causes the activation or suppression of protein function by incurring a change in the conformation of the protein. The introduction of a phosphate group has a profound effect on the shape of a protein, although it is not a particularly large group the polarity is high and parts of the protein recoil due to unfavourable ionic interactions such as similarly charged dipoles or hydrophobic areas. Other functionalities embrace and accommodate the oxygens through hydrogen bonding and favourable dipole interactions. This change in shape presents a new active site for a specific substrate or de-activates a site so it no longer functions. In some cases the phosphorylation allows the protein to be recognised by another protein or be transported across an intercellular membrane.

For a phosphorylation to occur the kinase and substrate must be in the presence of adenosine triphosphate (ATP). This is the source of the phosphate group and is converted to adenosine diphosphate (ADP) during the process. ATP is abundant in the body not only for use in kinase action but also it is the body's principal source of cellular energy.

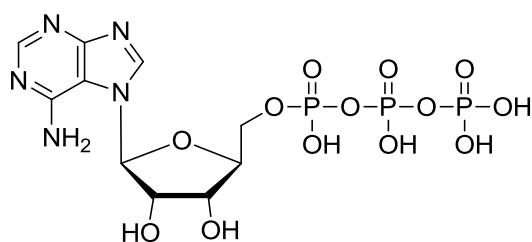


Figure 11. The structure of Adenosine Triphosphate (ATP)

The human genome encodes approximately 500 kinases. Within a single cell phosphorylation occurs thousands of times a second³⁴, and is the primary method for coordinating a cell's routine and is the mainstay of signal cascades and transduction. Kinases are located throughout the cell in the membrane, cytoplasm, and nucleus. There are three categories of protein kinases: Ser/Thr kinases that phosphorylate the side-chain hydroxyl group of serine or threonine; Tyr kinases that phosphorylate the phenolic hydroxyl group of tyrosine; and dual kinases which act at both. Even though all kinases have the same cofactor, i.e. ATP, there is enough variation between protein structures to give selectivity in a drug, as subtle residue changes in the active site are witnessed in all kinases. As expected, there are groups of kinases which display highly conserved active site sequence and structure and so designing selective drugs becomes more difficult. An attractive feature of kinase inhibition is the type of molecule that the active site demands. Compounds are typically entropically constrained meaning that there are limited permutations that can be performed on the structure. Most inhibitors are highly conjugated, have limited entropy and contain aromatic rings, carbonyl and amide groups. Heterocycles feature heavily, as expected when mimicking the binding of a purine base.³⁵ These moieties fit nicely within drug-like compound criteria and generally suit pharmacokinetic demands.

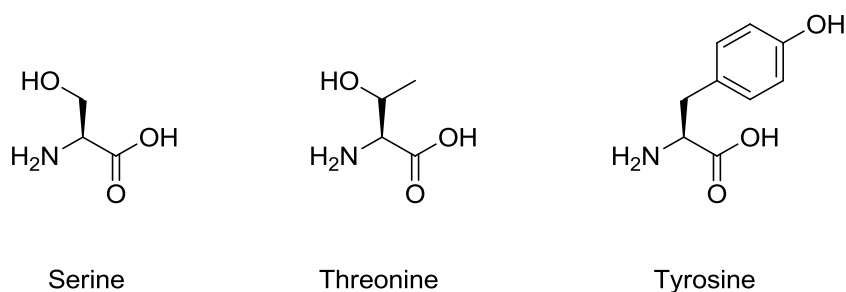


Figure 12. The structures of amino acid phosphorylation sites; serine, threonine and tyrosine.

Although the kinase active site varies between every kinase, the key features of the site and binding mode are conserved. The binding of ATP (Figure 13) shows the key areas to exploit in inhibitor design, most hydrogen bonding is found in the hinge region at the end of a bi-lobed cleft. A pocket accommodates the ribose with the phosphate chain projecting into solvent-exposed open space. Any area in this model not used by ATP holds potential to give a drug a competitive edge. These areas vary between proteins, however, a hydrophobic pocket behind a 'gatekeeper' residue is a staple of kinase structure. Around 82% of the gatekeepers are defined as small or medium residues and the most common is methionine, accounting for 40% of the currently mapped kinases.³⁶ The smaller the residue here the more accessible the pocket behind it becomes. As such from a drug design point of view, a small residue is favourable due to the potential for exploitation. Most active sites also contain a glutamic acid along the cleft which is not involved with ATP binding. This highly conserved feature can be utilised in the design of non-selective kinase inhibitors which are suggested to yield higher efficacy and safer drugs by synergistic effects and targeting multiple kinases.³⁷ However, selective kinase inhibitors remain the chief target to most research groups and as such drug interactions with highly conserved residues are avoided unless selectivity can be derived elsewhere. Previous crystal structures of kinase bound-ATP show that the association is not very strong, this is yet another attractive feature of protein kinases as a drug target. An inhibitor needs to form a stronger interaction than the substrate it is displacing to be competitive, if this original substrate complex has a weak binding energy the task is smaller to achieve greater energy.¹⁰

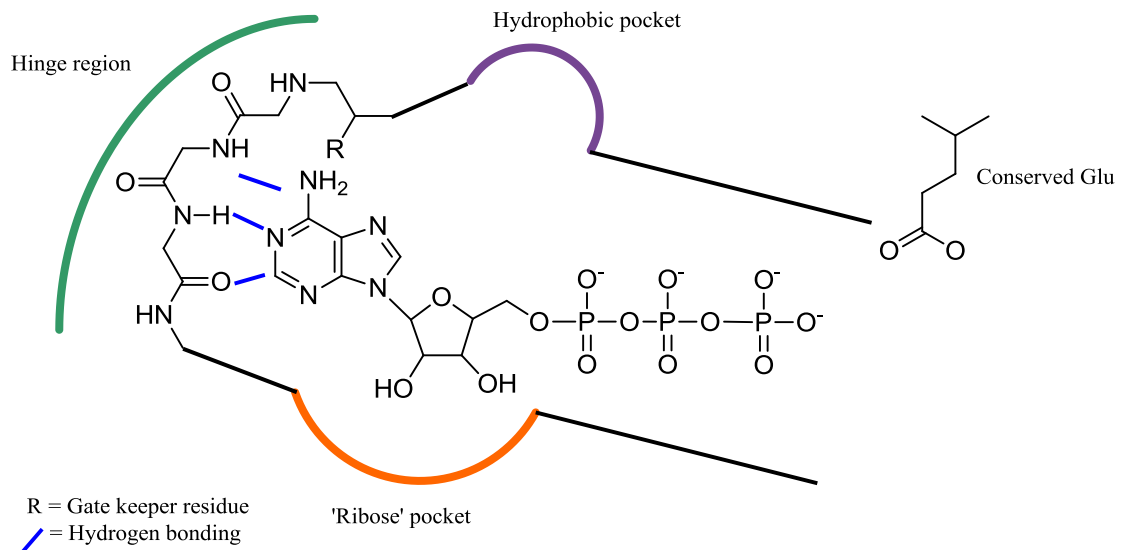


Figure 13. The Binding of ATP in a generic kinase active site.

A key aspect of the kinase activity is the activation loop which needs to adopt a particular conformation for the protein to accept its substrate. Although this is crucial in kinase activity it is the source of most variation as it is a moveable string of amino acids. The activation loop contains a conserved sequence of residues DFG (aspartate, phenylalanine, glycine) and activated kinases are referred to as 'DFG-in' or 'DFG-out' if inactive.

In the last 35 years there has been an explosion of research into the therapeutic application of these proteins due to the crucial roles many of them play in various pathways. It is quite common for kinases to be over-expressed, over activated or mutated in a cancer cell.

1.3.1 Types of Kinase Inhibitors

Kinase inhibitors can be classified by the key interactions they make with the kinase active site. Four classes exist, which are shown in Table 6.³⁸

Table 6. Kinase inhibitor classes.

Class of kinase inhibitor	Description
I	Mimics the interactions made by ATP at the hinge and adjacent pockets. Bind to the active or DFG-in kinase form
II	Compounds bind to the DFG-out or inactive kinase conformation and are therefore not ATP-competitive.
III	Compounds bind a site adjacent to the ATP binding location
IV	Allosteric kinase inhibitors

1.3.2 Mitogen-Activated Protein Kinases (MAPKs)

The Mitogen-activated protein kinase (MAPK) family is one of the largest described making up 8% of the kinome.³⁹ The MAPKs are a large family of proline-directed serine/threonine kinases that coordinate an important portion of cellular processes including cell differentiation, proliferation and apoptosis.^{40,41} MAPK pathways begin with an extracellular stimulus resulting in a kinase signalling cascade terminating at the activation of transcription factors or cytoplasmic substrates by the MAPK resulting in the expression or activation of a specific protein.

There are 14 MAPKs defined in mammalian cells which are characterised as typical and atypical.⁴² The typical MAPKs are further divided into four groups namely: Extracellular signal-regulated kinase 1/2 (ERK1/2), c-Jun amino N-terminal kinases or stress activated protein kinases 1/2/3 (JNK or SAPK1/2/3), p38 $\alpha/\beta/\gamma/\delta$ and ERK5. Atypical MAPKs are ERK3/4, ERK7 and Nemo-like kinase (NLK), however, much less is known about the function of these pathways.⁴²

MAPK signalling cascades are activated by mitogens, which are defined as chemical substances that trigger mitosis, and therefore largely consist of extracellular growth

factors, e.g. epidermal growth factor (EGF), platelet derived growth factor (PDGF) or nerve growth factor (NGF), cytokines and stress factors. Before the MAPKs are involved these extracellular signals bind to membrane bound receptor proteins such as tyrosine kinases or G-protein coupled receptors (GPCR) and downstream pathways are activated.⁴³

The conventional MAPKs are the focus of a three tiered pathway, beginning with the MAPK kinase kinase (MAPKKK) which activates the MAPK kinase (MAPKK) which subsequently activates the MAPK (Figure 14).⁴⁴ The MAPKK activates the MAPK by a dual phosphorylation event on a Thr-X-Tyr motif on the activation loop.⁴⁰ These two phosphorylation sites are separated by one residue which varies between each sub-group of MAPKs. In ERKs the separating residue is a glutamic acid, whereas it is a bulkier proline in JNK and a much smaller glycine in p38 isoforms. Once activated the MAPK goes on to phosphorylate either a protein upstream of a transcription factor or the factor itself which in turn causes the production of specific proteins related to a range of processes.

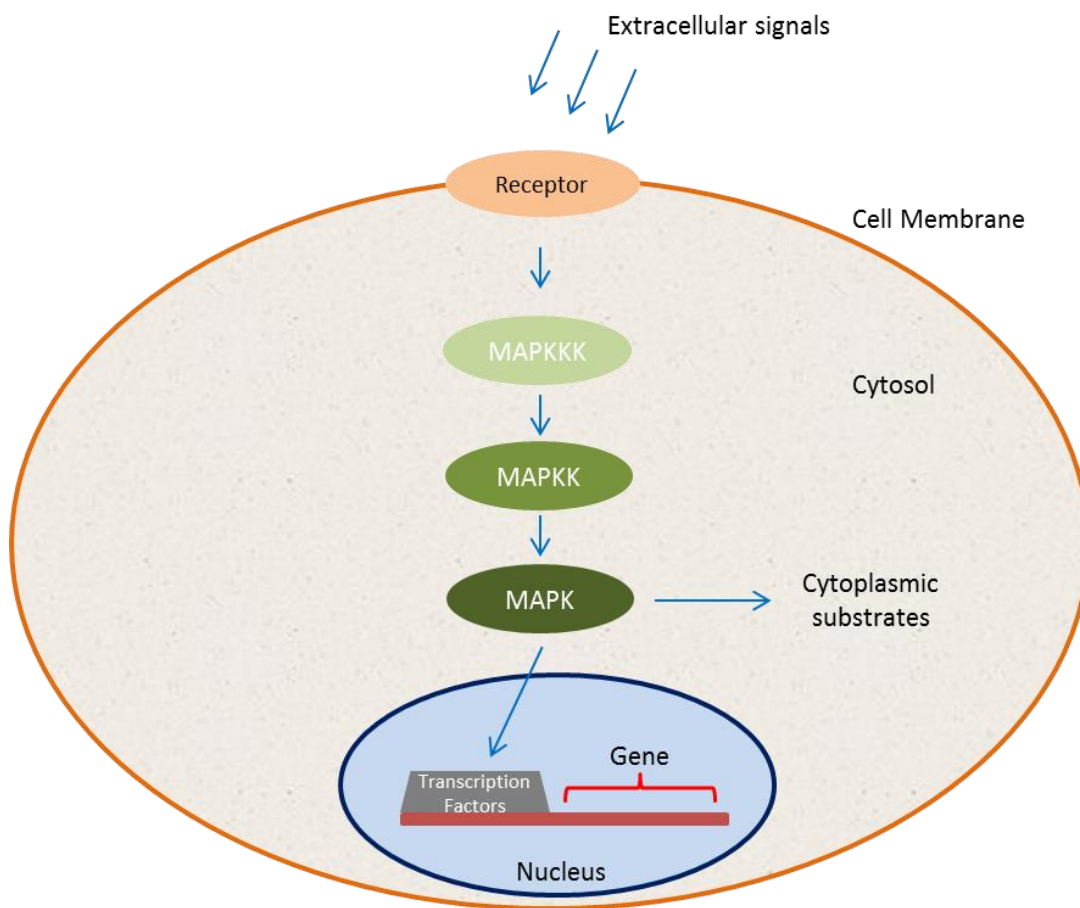


Figure 14. Typical MAPK signalling cascade.

Atypical kinase signalling is not consistently a three membered cascade and although all are activated by dual phosphorylation on the activation loop, the motif is not conserved, (only one atypical MAPK has the Thr-X-Tyr sequence (ERK7)). Unifying characteristics of all typical and atypical MAPKs include dual phosphorylation activation, high sequence homology in the kinase domain and downstream activation upon serine/threonine residues followed by proline (i.e. proline-directed).

MAPK pathways are predominantly found as part of a scaffold-bound complex containing all three members of the conventional three tier system and a specific scaffold protein⁴⁵. Cross pathway signalling is limited by the formation of these complexes despite the similar activation motifs and sequence homology between equivalent proteins. All MAPKs bind the upstream MAPKK by an ionic interaction between negatively charged residues on the MAPK and positive on the MAPKK but each of these protein-protein interactions is unique to the particular pathway.⁴⁶

Table 7. Details of Typical and Atypical MAPK signal cascades.

MAPK	MAPKKK	MAPKK	Activation loop motif	Gatekeeper residue
Typical/ conventional MAPKs				
ERK1/2	Raf-1/A/B, c-Mos	MEK1, MEK2	Thr-Glu-Tyr	Gln
p38 $\alpha/\beta/\gamma/\delta$	MEKK1-4, DLK, MLK2, Tpl-2, ASK1, TAK1, TAO1/2	MEK3, MEK6	Thr-Gly-Tyr	α = Thr
JNK1/2/3	MEKK1-4, DLK, MLK2, Tpl-2, ASK1, TAK1, TAO1/2	MEK4, MEK7	Thr-Pro-Tyr	-
ERK5	MEKK2/3, Tpl-2	MEK5	Thr-Glu-Tyr	Leu
Atypical/ non-conventional MAPKs				
ERK3	Unconfirmed		Ser-Glu-Gly	-
ERK4			Ser-Glu-Gly	-
ERK7/8			Thr-Glu-Tyr	-
NLK			Thr-Gln-Glu	-

The numerous members of the MAPK family are of particular interest in oncology because of the links to cell cycle progression and cell differentiation as well as other downstream effects related to the hallmarks of cancer.

1.4 Extracellular Signal-Regulated Kinase 5 (ERK5)

1.4.1 The Biological Role of ERK5

ERK5 was first described in 1995 as around twice the size of most MAPKs (816 amino acids) and is ubiquitously expressed in human cells.^{47, 48} ERK5 is encoded by the MAPK7 gene and has 10 consensus phosphorylation sites in its 400 residue excess (which shows no homology to any other MAPK).^{49, 40} It is implicated in a number of important cell functions such as proliferation, survival, and cell cycle progression among other processes that relate to the hallmarks of cancer.

1.4.2 The ERK5 Pathway

The ERK5 pathway consists of ERK5, which is activated by MEK5, which is in turn activated by MEKK2/3. It has been noted that MEKK2, which is activated by growth factors including the nerve growth factor (NGF) and oxidative stress, has higher affinity for MEK5 than MEKK3.⁵⁰ The role of Ras in the ERK5 signal cascade is not fully understood, but it is thought to be involved under epidermal growth factor (EGF) and NGF-stimulated signalling.⁵¹ Leukaemia inhibitory factor (LIF) is a cytokine which causes activation of the pathway by activation of surface bound tyrosine kinase GP130, which in turn activates Grb2-associated binder (GAB1) and protein tyrosine phosphatase (SHP2). Whether the GAB1-SHP2 complex activates MEKK2/3 is disputed but this trigger has only been witnessed in cardiomyocytes and causes elongation of the cell.⁵² Other routes have been described for the activation of the ERK5 signalling cascade and are shown schematically in Figure 15.⁵³

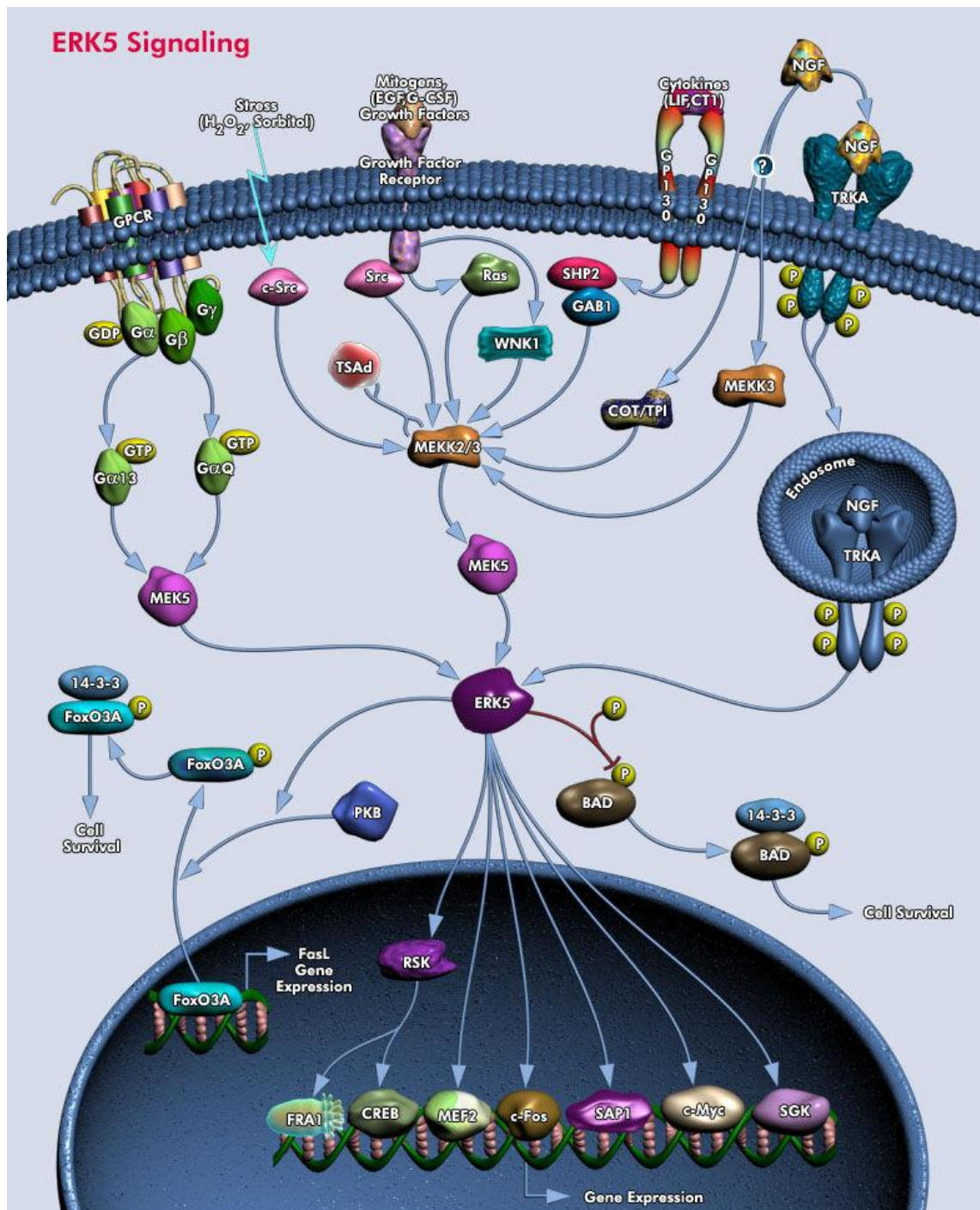


Figure 15. ERK5 signalling cascade (© 2009 QIAGEN, all rights reserved).⁵³

Like many other MAPK pathways the ERK5 pathway is supported by scaffold proteins when propagating signals.⁵⁴ The relevant kinases are joined together on a framework, which ensures that phosphorylation of the next kinase in the pathway is made quick and specific due to the proximity of the target. The activation of MEK5 by MEKK2 is aided by the Lck-associated adaptor (Lad) which increases the rate of association and therefore phosphorylation.⁵⁵ MEK5 is activated by dual phosphorylation on Ser 311

and Thr 315 by either MEKK2/3 and goes on to doubly phosphorylate ERK5 as discussed previously.^{56, 57} At present MEK5 is thought to be the only activator of ERK5 but can exist in two isoforms; MEK5 α and MEK5 β .⁵⁸ MEKK2/3 binds to MEK5 on the N-terminal lobe which is also the ERK5 binding site and therefore disassociation of the MAPKKK is required before ERK5 can be activated.⁵⁹

ERK5 can be differentiated from other typical MAPK family members ERK1/2 by its extended C-terminus despite, possessing the same Thr-Glu-Tyr activation motif. ERK5 has a nuclear localisation domain which allows transport from the cytosol into the cell nucleus and an additional transactivation domain (TAD), both of which are absent in all other typical MAPKs.⁴² The TAD regulates autophosphorylation which may be required for nuclear localisation and activation of ERK5 itself.⁶⁰ Once activated ERK5 is able to partially unfold allowing it to pass into the nucleus and activate several transcription factors such as c-Fos, c-Myc, Myocyte enhancer factor 2 (MEF2) and c-Jun affecting cell cycle progression, proliferation, differentiation and cell survival.⁶¹ ERK5 is deactivated by resuming its folded conformation which causes transportation back to the cytosol.⁶²

1.4.3 The Role of ERK5 in the Cell Cycle

Cell proliferation is induced by several transcription factors, importantly ERK5 has been shown to be essential in epidermal growth factor (EGF) activated cell division. Using an inactive mutant of ERK5, proliferation caused by EGF ceases, indicating ERK5's crucial involvement.⁶³

Transcription factors MEF2 and c-Jun are both implicated in cell proliferation and are substrates of ERK5. MEF2 also activates c-Jun, which drives the expression of cyclin D1.⁶⁴ Cyclin D1 is a cofactor of cyclin dependant kinase 4 and 6 (CDK4/6)(Figure 16). These CDKs are vital to the cell cycle check point between the first gap phase (G₁) and the synthesis phase (S) by inactivation of the retinoblastoma protein (Rb) which is a tumour and cell cycle suppressor.⁶⁵ As expression of the CDKs is constant throughout the cycle, the level of specific cyclins is the controlling factor. Expression of c-Jun is inversely proportional to expression of the tumour suppressor p53 by binding to the p53 promoter causing deregulated cell proliferation.⁶⁶ In cancer cells with up regulated ERK5 the production of cyclin D1 is increased and levels of natural CDK inhibitor p21

are reduced. Due to decreased p53 expression the cell can more readily enter the synthesis phase of the cell cycle.

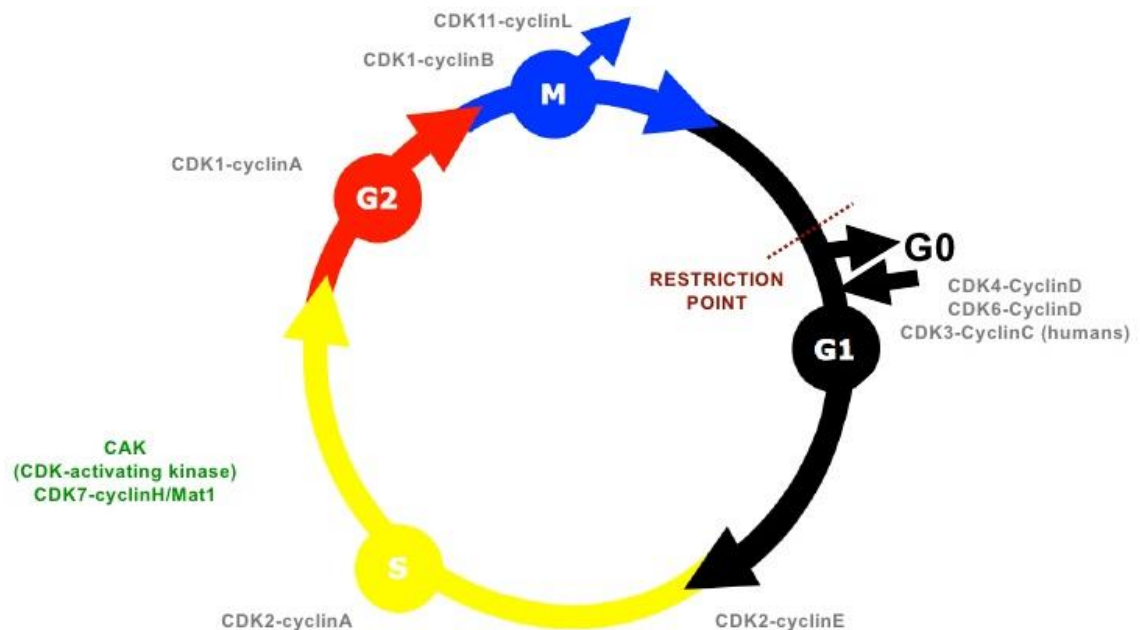


Figure 16. The Cell cycle showing the functions of Cyclin dependant kinase proteins (CDKs) and the various stages of cell division. (Taken from D. Morgan *Controlling the cell cycle* slides⁶⁷).

ERK5 has been shown to deactivate, by phosphorylation, the tumour suppressor capacity of promyelocytic leukaemia protein (PML).⁶⁸ PML, when active, upregulates the expression of p21, and therefore ERK5 activity contributes to cell proliferation by p21 suppression in two ways; activation of c-jun and deactivation of PML.⁶⁹

1.4.4 The role of ERK5 in Cell Survival and Differentiation

MEF2 is found in almost all cell types and is one of the oldest transcription factors in encoded in the human genome. MEF2 is known to assist in cell differentiation during embryogenesis and beyond during the formation of skeletal muscle, the heart, the brain/neurons, and bones.⁷⁰ These effects are achieved by ERK5 activation and also members of the p38 MAPK family.⁷¹ ERK5 knockout mice do not live longer than 10 days due to inhibited brain growth attributed to limited cell differentiation, however, this is not caused when ERK5 is only eliminated in neurons.^{72, 73}

The transcription factor forkhead box O3A (FoxO3A) and Bcl-2-associated death promoter (BAD) both lead to apoptosis when active in the nucleus and mitochondria respectively (Figure 15).⁵⁴ Phosphorylation of BAD and FoxO3A, which is caused by ERK5 directly (BAD) or by ERK5 activated serum- and glucocorticoid-inducible kinase (SGK)(FoxO3A) traps them in the cytoplasm thus inhibiting apoptosis.^{74, 75}

1.4.5 The Role of ERK5 in Angiogenesis

Ablation of ERK5 activity via a conditional mutation could be triggered in adult mice but caused death due to internal bleeding within 1 month.⁷⁶ It was concluded from this data that ERK5 plays an essential role in the maintenance of healthy blood vessels. However, the concept has not been proven in other tissues and studies require a specific inhibitor of the ERK5 pathway to eliminate the involvement of ERK1/2 in vascular endothelial growth factor (VEGF) induced angiogenesis.⁴⁷

1.4.6 Evidence of ERK5 in Carcinogenesis

The downstream effects of ERK5 discussed so far all have the potential to augment cancer development if unregulated. Remarkably, ERK5 is implicated in four of the six original hallmarks of cancer (i.e. resisting cell death, sustaining proliferative signalling, evading growth suppressors, and inducing angiogenesis). There is some evidence for ERK5 effecting invasion or cell migration by increasing levels of matrix metalloproteinase 1/2/9 (MMP1/2/9).⁷⁷ MMPs normally break down extracellular material to facilitate organ growth but are often found in high levels in aggressive cancer cells.⁷⁸ This means that ERK5 is of relevance to five out of six hallmarks. The ERK5 signalling pathway is also related to known oncogenes Ras and c-Myc and ERK5 has been shown to be overexpressed or constitutively active in a number of cancer cell lines.⁴⁹

The Myc family of transcription factors are one of the most commonly deregulated or mutated groups in cancers and trigger the expression of various proteins related to cell proliferation.^{79, 80} ERK5 is not the only activating pathway of c-Myc but when ERK5 is overexpressed in cancers, c-Myc is also found to be over active inducing a proliferative effect. Anaplastic lymphoma tyrosine kinase receptor (ALK) -induced activation of ERK5

causes the transcription of *c-MycN*, which has a strong correlation to proliferation in neuroblastoma cell proliferation.⁸¹

ERK5 over-expression has been witnessed in a number of common cancers such as triple negative breast cancer (TNBC) which comprises 15% of breast cancers, and prostate cancers which killed over 10,000 people in the UK in 2012.^{82, 83} MEK5/ERK5 has been shown to be overexpressed highly in 37% of malignant prostate cancers, showing correlation to tissue invasion.⁸⁴ Further to this high levels of ERK5 in the nucleus relate to poor patient prognosis and aggressive disease.⁸⁵ Similarly to this, ERK5 expression in TNBC is linked to an aggressive phenotype and evidence for its role in cell proliferation has been shown through gene knockout and pharmacological inhibition.⁸³ ERK5 is to be found constitutively active in Hodgkin lymphoma cells lines and shown to be responsible for cell proliferation and inhibited apoptosis.⁸⁶ High expression of ERK5 in oral squamous cell carcinoma is linked to tissue invasion.⁸⁷ ERK5 has also been shown to be pivotal in the cancerous capacity of leukaemia T cells, human mesothelioma cells and various other cell lines.⁸⁸⁻⁹⁰ In inflammation-driven cancer occurring in epidermal cells, ERK5 has been found to activate substrates that mediate inflammation, making it a potential target for these cancer types.⁹¹

ERK5 requires full validation as an anti-cancer target, despite the wide range of cell lines in which it is found in high levels and been shown to play a key role in growth or another cancer hallmark.^{61, 69} s.

1.4.7 MAP Kinase p38 α

p38 α shares a large amount of active site homology with ERK5: 48% sequence identity in the kinase domain and 56% in the ATP binding site, even though its closest family member is again ERK2, sharing 51% and 78% sequence identity respectively to ERK5. A key variation here comes from the gatekeeper residue in each active site. In ERK2 it is a large glutamine residue, whereas in ERK5 and p38 α , it is smaller (leucine and threonine, respectively). p38 α also known as SAPK2 is one of four isoforms of the p38 MAPK and is a stress activated protein kinase (SAPK). The stresses these kinases respond to include oxidative, ultraviolet light, osmolarity, cytokines and various others. The p38 pathway begins with the MAPKKK's ASK, TAK1, MEKK1-4, MLK3 and possibly others. These phosphorylate and activate MKK3/6, which activate the MAPKs p38 α / β / γ / δ . Like the ERK5 pathway this is the conventional route and the p38 isoforms go on to activate transcription factors and other kinase pathways. The main responses derived from the p38 pathway are inflammatory and immune responses, due to the nature of their activation. There is also evidence for p38 inhibiting the cell cycle by suppressing the release of cyclins and producing CDK inhibiting proteins.⁴² p38 activity may also play a role in initiation of apoptosis.

From evidence gathered to date it appears that p38 α only plays a suppressive role in the cell cycle, so inhibition of this site in cancer cells would likely induce a negative effect. p38 isoforms may be appropriate targets for the production of anti-inflammatory drugs, but for the purpose of this project, p38 α activity is not desirable.

^{92, 93} In order to minimise off-target effects, compounds made in this project are counter screened against p38 α .

1.4.8 ERK5 Inhibitors in the Literature

In 2010 Deng et al reported the discovery of benzo[e]pyrimido-[5,4-*b*][1,4]diazepin-6(11*H*)-ones as ERK5 inhibitors with good drug-like properties.^{94,95} Selected 2-amino-pyrido[2,3-*d*]pyrimidines were screened for potency against a wide range of kinases, showing moderate potency against ERK5. This series was developed into the more potent benzo[e]pyrimido-[5,4-*b*][1,4]diazepin-6(11*H*)-one (Figure 17).

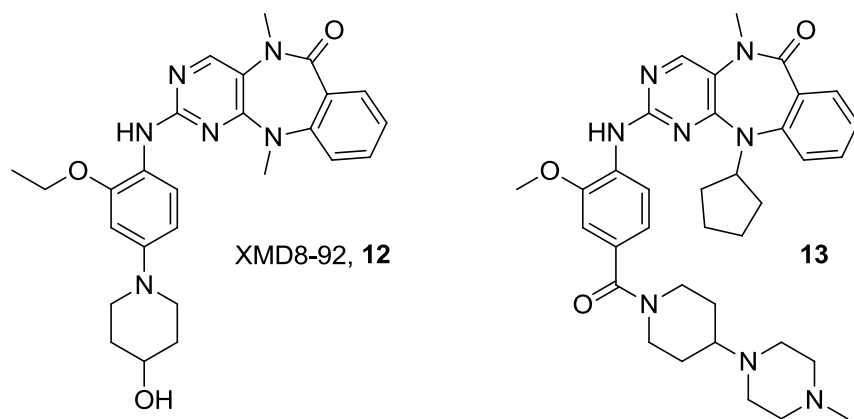


Figure 17. Structure of benzo[*e*]pyrimido-[5,4-*b*][1,4]diazepin-6(11*H*)-ones (XMD8-92, **12**) and closely related ERK5 inhibitor **13**.

SAR studies identified the hinge binding region of XMD-8-92 (Figure 18A) showing that the core structure is making two hydrogen bonds with the hinge region of the active site, while the rest of the molecule binds to the mainly hydrophilic periphery. This analysis was confirmed with the publication of a co-crystal structure of ERK5 with a closely related inhibitor **13** (Figure 18B/C).⁹⁶

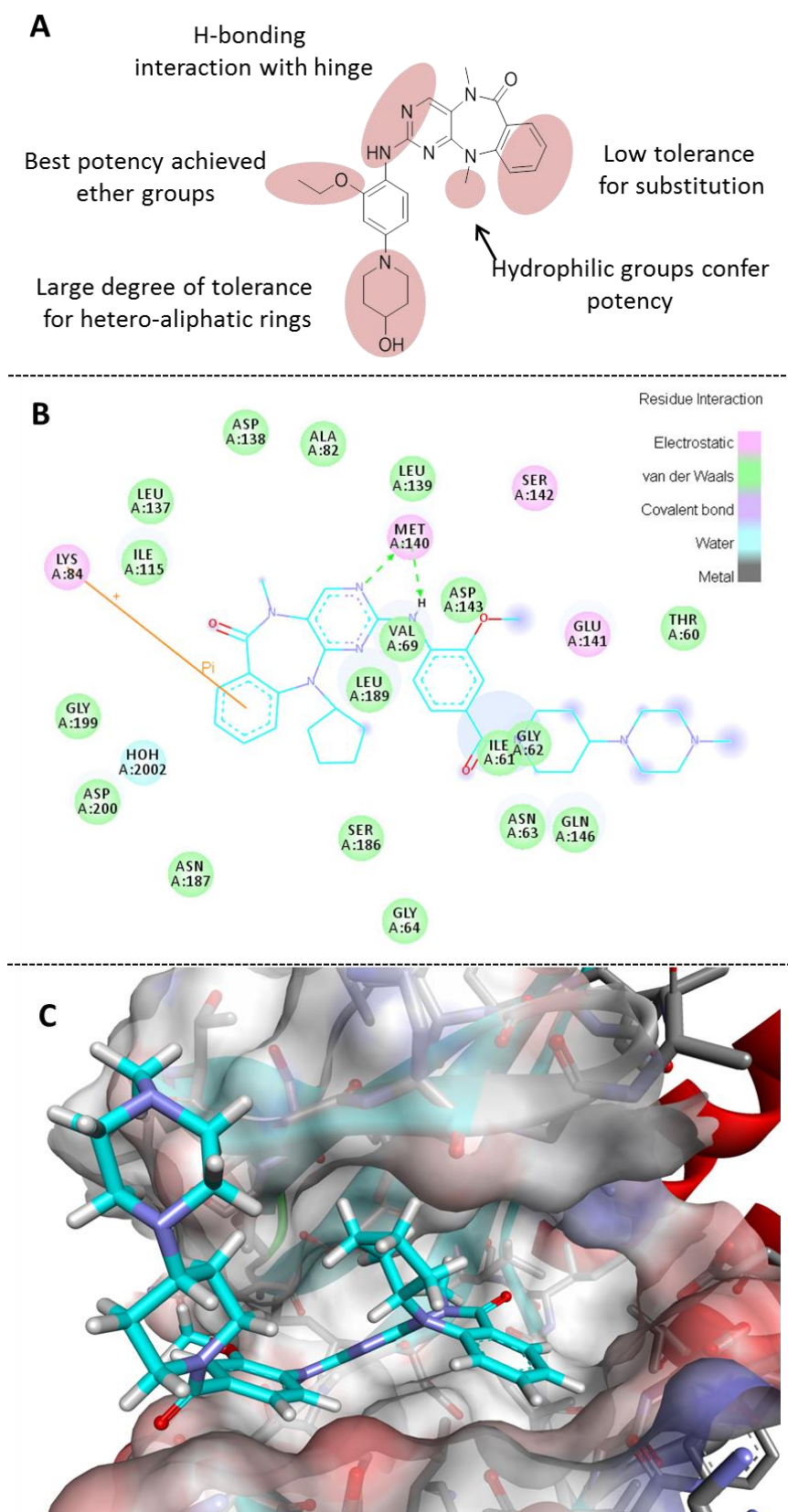


Figure 18. A) SARs developed by Deng *et al* on the benzo[e]pyrimido-[5,4-b][1,4]diazepin-6(11H)-one core shown on the structure of XMD8-92;^{94, 95} B) 2D representation of the binding of compound **13** (Cyan) and the ERK5 active site; C) 3D representation of the binding of compound **13** (Cyan) and the ERK5 active site (PDB code: 4B99).⁹⁶

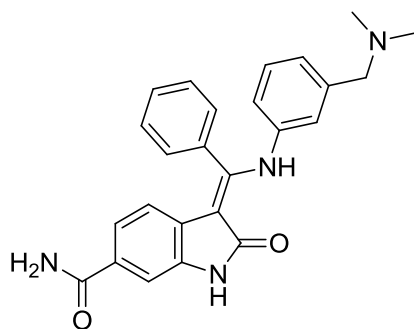
XMD8-92 (**12**, Figure 16) is the most widely used compound in *in vitro* and *in vivo* studies of ERK5 inhibition. Mice presenting tumour cells were treated with XMD8-92 at a dose of 50 mg/Kg twice a day for 1-4 weeks interperitoneally. The results showed that ERK5 was inhibited successfully and tumour growth significantly reduced. In this study of 24 animals there was limited evidence of side-effects or toxicity.⁶⁹ XMD8-92 has an IC₅₀ of 240 nM in an enzymatic assay achieving 76% inhibition of ERK5 at 0.5µM.⁹⁴ *In vivo* data collected in rats shows XMD8-92 (**12**) to have good bioavailability (69%) and a good PK profile overall (Table 8).⁹⁴

Table 8. *In vivo* Pharmacokinetic data collected in Rat for XMD8-92 (**12**).⁹⁷

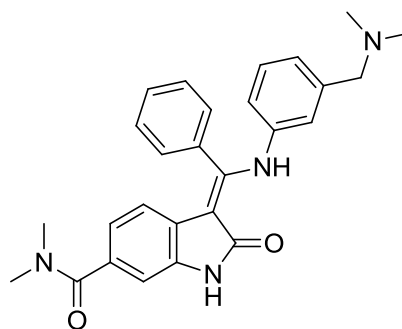
Parameter	XMD8-92 (12)
ERK5 IC ₅₀ (nM)	240
t _{1/2} (min)	204
Clearance (ml/min/kg)	37
V _d (L/kg)	3.4
Bioavailability (%)	68.6

Indole-based compounds BIX02188 (**14**) and BIX02189 (**15**) are potent MEK5/ERK5 dual inhibitors (Figure 19). Cellular IC₅₀s were obtained in HeLa and HEK293 cells.

Compound **15** is the more potent in a cellfree assay with a range of 260-530 nM versus 820-1150 nM for compound **14**. Despite being non-selective on the ERK5 pathway, good selectivity is seen over other MAPK families including MEK1/2, ERK1 and JNK2. Good selectivity has also been demonstrated in HeLa cells by Western blotting that showed reduced levels of phosphorylated ERK5 substrate MEF2 but no effect on MAPKs.⁹⁸



BIX02188, **14**
 MEK5 IC₅₀ = 4.3 nM
 ERK5 IC₅₀ = 810 nM



BIX02189, **15**
 MEK5 IC₅₀ = 1.5 nM
 ERK5 IC₅₀ = 59 nM

Figure 169. Structures of MEK5 inhibitors BIX02188 (**14**) and BIX02189 (**15**).

TG02 (**16**) is a non-selective ERK5 inhibitor that has been used in identifying ERK5 as a target in triple negative breast cancer.⁸³ TG02 (**16**) shows good potency against ERK5 (IC₅₀ = 43 nM) but also CDKs 1, 2, 3, 5 and 9 (IC₅₀ = 3-9 nM) and a wide range of other kinases at sub 100 nM levels. The compound has shown evidence of limiting leukaemia growth but due to the lack of kinase selectivity this cannot be attributed to the inhibition of any defined signalling pathway.⁹⁹

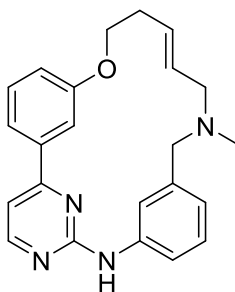


Figure 20. Structure of TG02 (**16**).

1.5 The Indazole Series of ERK5 inhibitors

Work in Newcastle began with the identification of the pyrrole carboxamide scaffold from a high-throughput screen at Cancer Research Technology Discovery Labs (CRT-DL) (Figure 21). After development of this series to good potency, challenges regarding the pharmacokinetic profile have delayed progression in the lead optimisation phase and so the need for a back-up series was established (see Chapter 3). In 2009, a kinase-focussed library of compounds were screened for activity against ERK5 by CRT-DL and identified a number of potential scaffolds. The indazole series (Figure 21) was selected for further development because of its low molecular weight, moderate potency, and chemical accessibility.

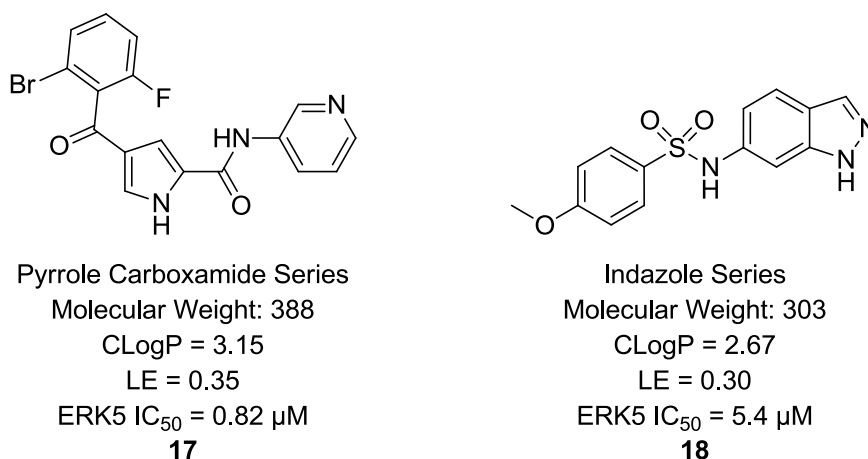


Figure 21. Representative structures of the Pyrrole (**17**) and Indazole (**18**) Series.

1.5.1 Medicinal Chemistry Tools and Assays used on the ERK5 Project

Final compounds synthesised on the project were first subjected to the primary ERK5 enzymatic assay and the p38 α assay to determine selectivity. Potency of the compound in the primary assay determined if the compound would then be tested in the cellular assay. If the compound met the criteria for potency and selectivity mouse microsomal clearance data was obtained along with plasma protein binding and solubility. Following this, compounds were further profiled by permeability (measured in a Caco-2 assay) and wider kinase selectivity panel. Compounds meeting the criteria for progression were then profiled for mouse pharmacokinetics and then *in vivo* xenograft tumour regression experiments (Figure 22).



Figure 22. ERK5 drug discovery cascade.

1.5.2 ERK5 IMAP assay

ERK5 IC₅₀ values were obtained through a cell free IMAP (immobilised metal affinity polarisation) assay that is conducted by staff at CRT.¹⁰⁰ ERK5 is expressed and incubated with a potential inhibitor before the introduction of a specific peptide with a fluorescent tag. The peptide is phosphorylated by ERK5 which enables binding to the IMAP agent and a measurable fluorescence directly proportional to the amount of

phosphorylated peptide present and therefore the inhibition of ERK5 (Figure 23). The ATP concentration of this assay is 350 μ M.

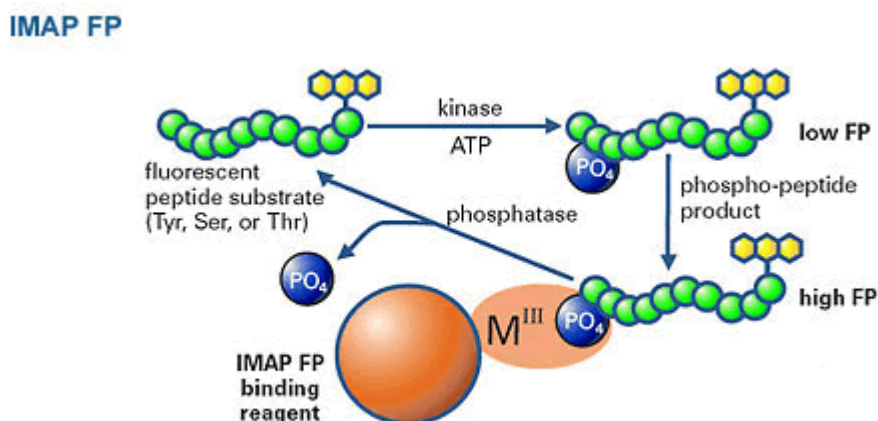


Figure 23. Schematic representation of the IMAP assay.¹⁰⁰

1.5.3 p38 α LANCE assay

All compounds submitted for biological testing are screened against both ERK5 and the close homologue p38 α in a Lance assay. The kinase is incubated in solution with ATP (350 μ M), the chosen inhibitor and a specific peptide substrate labelled with a Ulight tag. This substrate, without the presence of any inhibitor is phosphorylated, the location of which is recognised by a Europium tagged antibody. The Europium is excited by light at a wavelength of 320 nm. This irradiation excites all the Europium in the system regardless of its binding to the peptide, however the fluorescence given off by the Ulight tag varies depending on its proximity to the Europium. Fluorescence at 665 nm denotes the phosphorylated peptide and 630 nm the non-phosphorylated. The inhibitory effect on ERK5 can be quantified by the ratio of these two outputs and therefore a percent inhibition or IC₅₀ calculated.

1.5.4 Molecular Modelling

Protein crystallography was first developed by Dorothy Hodgkin and John Bernal at Cambridge in 1932. Since then it has become common place in drug discovery, with particular focus on co-crystal structures of proteins and small molecules. Once this type of crystal structure becomes available informed simulations can be run *in silico* to predict SAR using docking programmes such as GOLD. Tools like this make it possible for potent, selective structures to be reached more quickly, without the need for

synthesis of excessively large compound libraries. Docking programmes consider a number of parameters which are condensed into a scoring function and visualisation. Ideally the binding conformation of a compound is similar to its most energetically favourable conformation and any deviation from this is taken into account by the programme as well as clashes or repulsion with functionalities on the protein (See Table 33 Chapter 2.8.1 for full scoring breakdown). The ERK5 crystal structure has been published with a bound inhibitor and has been used on the project for molecular modelling using GOLD software.⁹⁶

1.5.5 Measuring Absorption, Distribution, Metabolism, Excretion and Toxicity (ADMET) *in vitro*

ADMET data was collected on the project to define lead compounds and quantify the quality of leads. Table 9 shows the data types collected and the rationale for each assay.

Table 9. *in vitro* assays to determine ADMET properties.

Assay	Rationale
Caco-2	The Caco-2 assay measures compound permeation through a colon carcinoma cell monolayer. The cells include transporter proteins and measurements are made in both directions; A2B and B2A where A denotes the extracellular matrix and B the intracellular matrix. An efflux ratio is generated by dividing B2A divided by A2B and is ideally 2 or lower, however, it is important that A2B is high no matter the ratio.
Plasma protein binding (PPB)	Denotes what fraction of compound is bound to plasma proteins in the blood. Ideally a compound is less than 99.9% bound.
Mouse liver microsome	Metabolism by Cyp enzymes found in the liver of mice. A human assay is also available but was rarely used in the project. The results of this assay indicate the metabolism/clearance of a compound. Ideal values are less than 50 $\mu\text{L}/\text{ml}/\text{mg}$
hERG	Human ether-a-go-go related gene product is an ion channel that when inhibited causes severe cardiac arrhythmias. Ideally the compound has very little effect on this target.
CYP inhibition	Accumulation of drug compounds can be caused by Cyp inhibition leading to unpredictable side effects. Drug-drug interactions are avoided if common Cyp enzymes are not inhibited.

1.5.6 Indazoles and Sulphonamides in Medicinal Chemistry

The indazole is an attractive scaffold for drug design, in particular as a protein kinase inhibitor. This two ring heterocycle meets some of the key criteria described earlier that are typical of kinase inhibitors. In particular, it has groups capable of hydrogen bonding and has a rigid structure with scope for conjugation into its ring systems from suitable substitutions. The ring system is able to establish π -stacking and hydrophobic interactions with appropriate amino acids, completing the structure's set of attributes. It is, therefore, not surprising that this pharmacophore appears in numerous drug structures, is a regular feature in HTS libraries, and appears in a large number of patents. Two FDA approved drugs, axitinib (**19**) and granisetron (**20**), contain an indazole group (Figure 24).

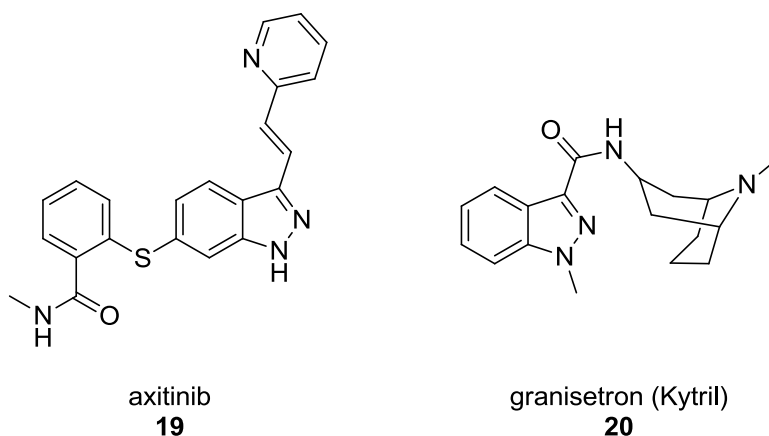


Figure 24. Structures of indazole based drugs axitinib (**19**) and granisetron (**20**).

Axitinib (**19**) is an angiogenic inhibitor specifically targeting the tyrosine kinase vascular endothelial growth factor receptors 1, 2 and 3.¹⁰¹ It has been approved for use in advanced renal cell carcinoma as of January 2012. Granisetron (**20**) is a much older compound first used in the UK in 1991 for the treatment of nausea as a serotonin receptor antagonist. There are an abundance of papers that feature an indazole moiety in kinase inhibitor compound. Kinases such as JNK3¹⁰², Lck¹⁰³, EphB4¹⁰⁴, KDR¹⁰⁵, Aurora kinases¹⁰⁶, B-Raf¹⁰⁷, ROCK-II¹⁰⁸, Chk1¹⁰⁹, Rho¹¹⁰, Tpl2¹¹¹, B/Akt¹¹², CDKs¹¹³, c-ABL¹¹⁴, CDC7¹¹⁵, PI3K/mTOR¹¹⁶, I kappa kinase¹¹⁷ and PKC-zeta¹¹⁸ are reportedly inhibited by derivatised indazole. The co-crystal structure of indazole **21** has been described for inhibition of cell cycle checkpoint kinase Chk1 with an IC₅₀ of 42 nM.¹⁰⁹ Compound **21** is a 6-substituted indazole but has a benzimidazole group attached in the 3-position

(Figure 25). The most transferable aspect of this crystal structure is the dual binding of the indazole, with both nitrogens forming hydrogen bonds with the backbone of the hinge region amino acids. The geometry of the phenyl group in the 6-position is not very similar to our series as there is no form of linker between the aromatic groups however, it can be seen that this rather large di-substituted phenyl group is well accommodated. Perhaps an interesting feature is the presence of a hydrogen bond donor two bonds away from the 3-position, which is able to form another interaction with the hinge region.

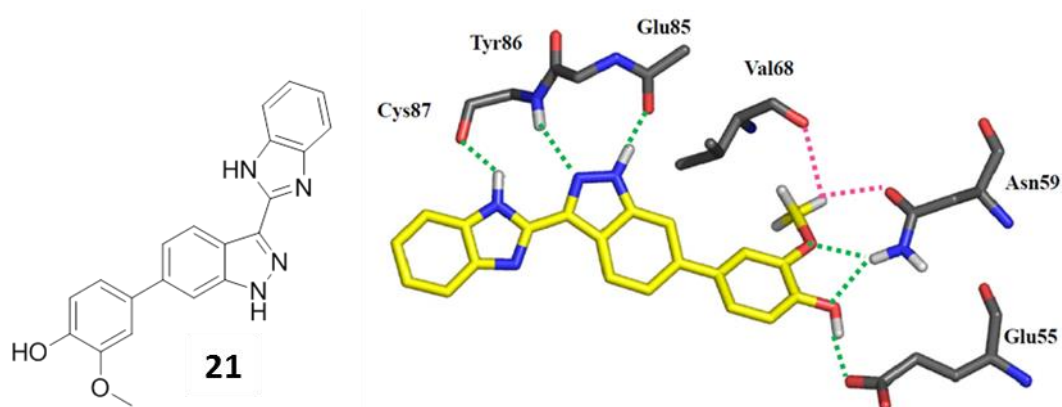


Figure 25. Binding mode of indazole-containing compound **14** in the Chk1 active site (PDB: 1IA8).

Another MAPK under investigation is the c-Jun N-terminal kinase-3 (JNK3) with inhibitors proposed to have a neurological effect.¹⁰² These compounds also possess p38 α activity, the MAPK which shows the greatest active site homology to ERK5. Inhibitors in development are 3,6 substituted indazoles with a homologous NH at the 6-position equivalent to the sulphonamide NH in the indazole hits generated for ERK5 series. The crystal structure of the lead compound (**22**) shows how it sits in the binding site and exploits areas not used by ADP (Figure 26). Both indazole nitrogens are involved in hydrogen bonding with the kinase hinge.

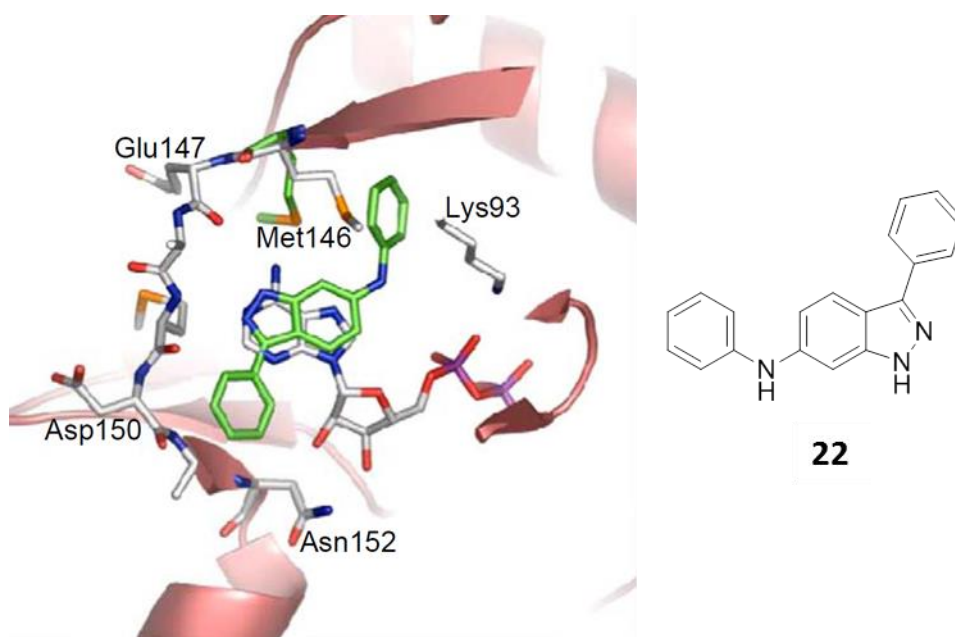


Figure 26. X-ray crystal structure of compound **22** (green) bound in JNK3, overlaid on ADP binding (white)(PDB: 2B1P).

Sulphonamides are especially abundant in drug design featuring in 9% of all candidate drugs.¹¹⁹ They present a centre with excellent hydrogen bonding potential and therefore solubility. They are often incorporated into drugs to improve solubility and also as an isostere to amides. Unless sterically hindered sulphonamides are readily metabolised to a number of products undergoing acylation, hydroxylation and glucoronidation.¹²⁰

The design of an indazole sulphonamide (**23**) has been described in the literature for action as a nucleosidase inhibitor (Figure 27). The lead described is a mono-substituted indazole with the sulphonamide unit in the five position with developments being made in the three and seven positions. In the X-ray structure the indazole nitrogens are seen making two hydrogen-bond interactions with the backbone of leucine 152. The sulphonamide also forms two bonds through the sulfonyl oxygens, and the attached aromatic forms π - π interactions with surrounding phenylalanine residues.¹²¹ Whilst the structure investigated here (**23**) is very similar to the hits proposed for ERK5 inhibition the biological targets are fundamentally different.

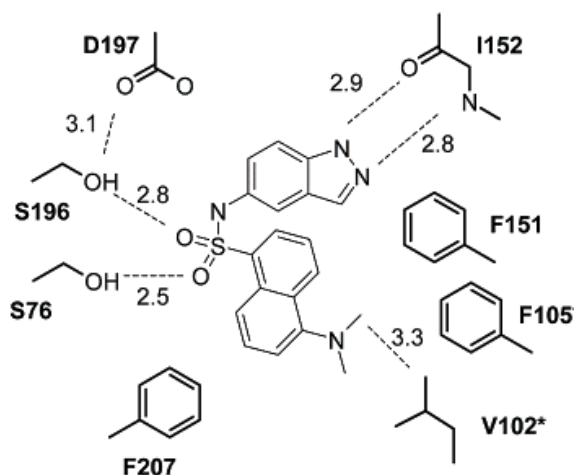


Figure 27. Schematic representation compound **23** bound in SAH/MTA nucleosidase created using homology modelling (not available on the PDB).

Functionalised indazoles have been investigated previously for the inhibition of CDK2 as it makes a strong interaction with the hinge region of the kinase domain.¹²²

An indazole based inhibitor (**24**, Figure 28) of ERK1/2 has also been described in the literature.¹²³ The compound shows strong cellular potency and shows good selectivity for the MAPKs ERK1 and ERK2 over related kinases and has been shown to cause reduced tumour growth in xenograft studies. It is typical of kinase inhibitors to possess 2-4 ring systems but **24** exceeds this with 5 aromatic and 2 aliphatic cyclic systems.

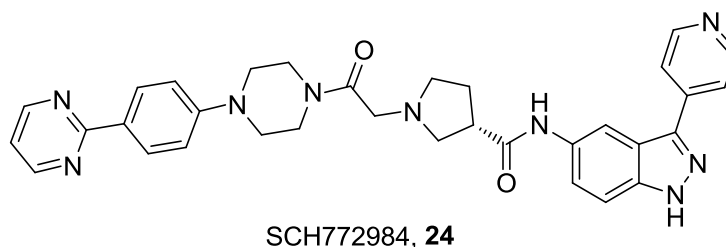


Figure 28. Structure of ERK1/2 inhibitor **24**.

1.5.7 Indazole Metabolism

Many drug examples including an indazole moiety have been described which is testament to the stability of the system towards metabolism and the low inherent toxicity despite being a masked aniline. Indazoles are less susceptible to oxidative cleavage than other two heteroatom heterocycles such as thiazoles, oxazoles and imidazoles, although there is some precedent.¹²⁴ The 3-position of the indazole can be oxidised by CYP enzymes and then exists in equilibrium as either tautomer **25** or **26** (Figure 29). The indazole one position can also undergo glucuronidation (**27**) or conjugation with ribose (**28**, Figure 29).

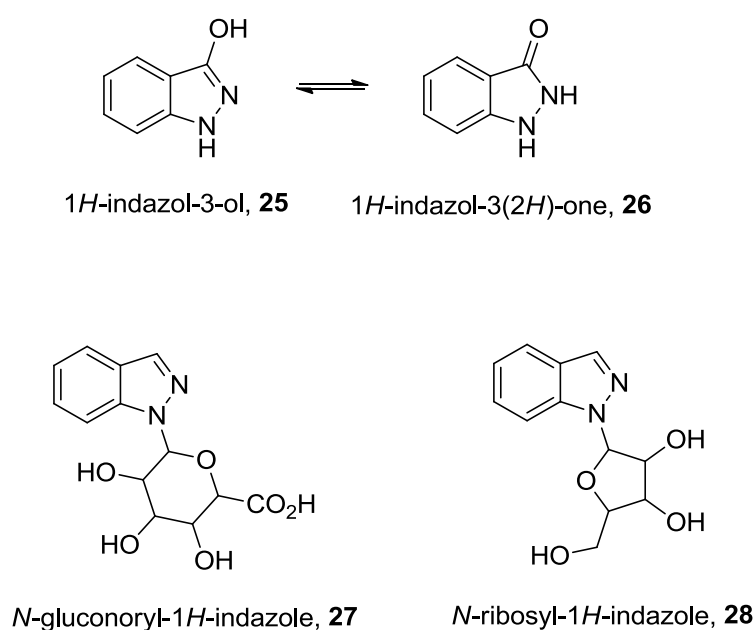


Figure 29. Metabolites of indazoles

Dealkylation of the indazole 1-position is witnessed in drug molecules benzydamine and granisetron (**20**).¹²⁴

1.5.8 Indazole Chemistry

Indazole has a predicted LogP of 1.32 which is an acceptable solubility for any drug compound (logP is a factor of lipophilicity with a value below 5 being desirable for a drug compound).¹⁰ It has pK_a values of 13.86 and 1.25 for the protonated and non-protonated nitrogen units respectively making it mildly acidic.¹²⁵ Unsubstituted pyrazoles have a pK_a of 19.9 and are therefore subtly more basic, essentially however the chemistry of both the indazole and pyrazole 1, 2, and 3 positions is analogous.

There are three possible tautomeric forms of Indazole possible (Figure 30) but the *1H* and *2H* forms are more commonly found than the *3H*. The most stable form is the *1H* tautomer by $2.3 \text{ kcal mol}^{-1}$ in either ground or excited state and is typically the only visible form by NMR in solvent.¹²⁶

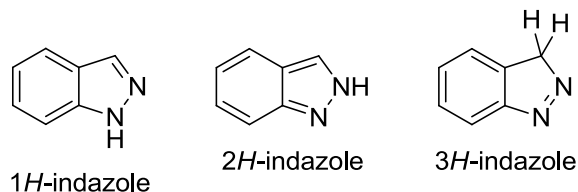


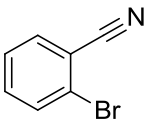
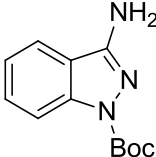
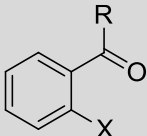
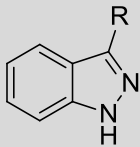
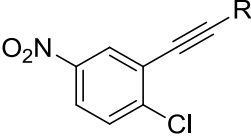
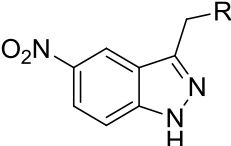
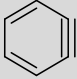
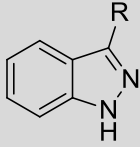
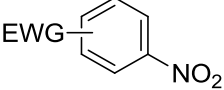
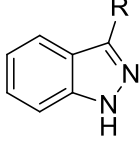
Figure 30. Tautomers of Indazole.

1.5.8.1 Synthesis of Functionalised Indazoles

Indazoles can be synthesised in a number of different ways. Table 10 summarises some of the described methods.

Table 10. Common methods of indazole synthesis.

	Functionalised benzene	Reagents	Product	Reference
1		AcOH, NaNO ₂ , H ₂ O		127
2		NHNH ₂ , NaOBu ^t [Pd(cinnamyl)Cl ₂]		128
3		Na ₂ WO ₄ , H ₂ O ₂		129
4		CsF, TMSCH ₂ N ₂		130
5		NHNH ₂		131
6		NHNH ₂		132

7		CuBr, Boc-NHNH ₂ , K ₂ CO ₃		133
8	 X = F, Cl, OMs	NHNH ₂		126
9		NaNO ₂ , HCl, H ₂ O		134
10		RCHN ₂		135
11		i) RCHNNHTs, Cs ₂ CO ₃ ii) NaH		136

In most of the examples in Table 10 the introduction of the azo group is the key step in the synthesis that is most commonly done using hydrazine or a derivative but can also be done by diazotisation of an aniline. Once the hydrazine moiety is introduced, either through S_NAr or another method, it attacks an electrophilic centre such as carbonyl or nitrile to close the ring and form the aromaticity of the pyrazole portion of the molecule. In reactions 6-11 in Table 10, the indazole is formed with functionalization in the 3-position and also with the indazole NH protected by a Boc group in reaction 7. The 3-position of the molecule is accessible after ring closing by selective halogenation using a hydroxide base which can then be exploited for further functionalization.¹³⁷ The 3-position is most readily exploited using palladium or copper coupling reactions upon halogenated aromatics.¹³⁸⁻¹⁴¹

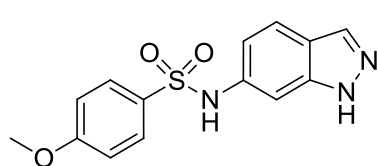
The most acidic position on indazole is the protonated nitrogen which can be abstracted with a strong base and is also sufficiently acidic to undergo a Mitsunobu reaction.¹⁴² Protection of this position can be done using a tetrahydropyran (THP), *tert*-

butyloxycarbonyl (Boc) or trimethylsilylethoxymethyl (SEM) groups amongst others.^{143,}
^{144, 133} The 5-position is the favoured site for electrophilic aromatic substitution on an unprotected indazole due to the conjugated *para*-azo group. There is no literature precedent for substitution at the 4, 6 or 7 position on a protected or unprotected indazole. Functionalities can more easily be introduced by a ring closing reaction on a functionalised phenyl ring such as the examples shown in Table 10.

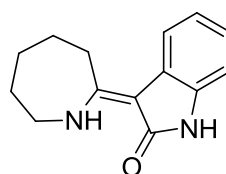
Chapter 2: The Indazole Series

2.1 Series Inception & Hit Validation

In 2009 a kinase-focussed library of compounds were screened for activity against ERK5 by Cancer Research Technology Discovery Labs (CRT-DL) revealing a number of potential scaffolds for development. Eight distinct chemotypes were identified of which two were considered for further structure activity relationship studies (Figure 31). The oxindole and indazole functionalities occur in numerous drug molecules and many patents already exist for both compound classes and therefore may create difficulties when filing a patent of our own with a unique molecule and application. Both molecules (**18** & **29**) have a low molecular weight and good predicted lipophilicity. The geometry of oxindole **29** suggests an intramolecular hydrogen bond may form, which not only may reduce the measured solubility of the compound but also means the molecule is very flat. As both compounds are equipotent, ligand efficiency (LE) informs that the oxindole scaffold is superior with regards to the contribution each atom has to potency. However, this parameter considers very few factors and the profile of the indazole compound is arguably better. The indazole series has three conserved rotatable bonds, which is preferable as flexibility generally improves solubility, selectivity and reduces the likelihood of CYP inhibition. For these reasons and the feasibility of a synthetic campaign, the indazole series was chosen for further exploration.



Indazole series
Molecular Weight: 303.34
CLogP = 2.67
LE = 0.30
ERK5 IC₅₀ = 5.4 μ M
18



Oxindole series
Molecular Weight: 228.29
CLogP = 2.65
LE = 0.42
ERK5 IC₅₀ = 5.8 μ M
29

Figure 31. ERK5 hits from a kinase-focussed library

To determine the selectivity of the selected series a counter screen of 40 kinases representing all major families was performed by Millipore using compound **18**. No

significant inhibition of p38 α or any other kinase was observed (Table 11). The indazole scaffold is well known in the literature as a kinase inhibitor (Chapter 1.5.6) due to the adjacent hydrogen bond donor and acceptor motif which can bind favourably to the kinase hinge. It is therefore encouraging to find the selectivity results so favourable for such a discreetly functionalised core.

Table 11. Millipore counter screen results for **18**. Values represent the percent inhibition of the Kinases in the presence of 10 μ M of the compound.

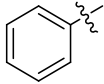
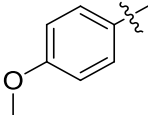
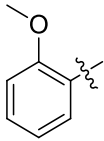
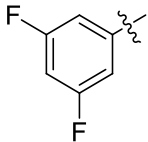
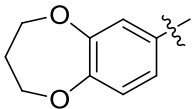
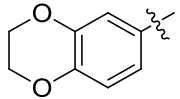
Percentage		Percentage	
Kinase	inhibition at 10 μ M	Kinase	inhibition at 10 μ M
Abl	-37	MAPKAP-K2	-1
Aurora-A	-1	MEK1	-6
CDK2/cyclinA	11	Met	3
CDK7/cyclinH/MAT1	3	MSK1	-9
c-RAF	2	MST1	-16
cSRC	1	mTOR	-9
DAPK1	0	NEK2	-17
EGFR	-2	NLK	3
GSK3 α	29	p70S6K	-1
HIPK1	-6	PAK4	-3
IKK α	-8	PDK1	-3
IR	-11	PKA	-2
IRAK4	1	PKB β	2
JAK3	-8	PKC α	0
JNK1 α 1	-5	Plk3	3
KDR	-8	ROCK-I	-7
LIMK1	-3	ROCK-II	-6
MAPK1	6	Rsk1	-6
MAPK2	-4	Rsk2	6
SGK	3	SAPK2a	-3

With the exception of the pyrrole carboxamide series (Chapter 3) hit validation previously undertaken on this project has not been fruitful, as potency seen in the HTS

was not replicated when compounds were re-synthesised. Confidence in a chemical series is gained if a number of examples appear in a HTS with similar potency. To prove a chemotype's potency active molecules were re-synthesised and re-tested as HTS samples can become contaminated or degrade in prolonged storage.

Six indazole compounds were present in the HTS library which showed comparable potency to **18**, all of which were re-synthesised in house *via* a facile, one step synthesis (Scheme 1)(synthesis conducted by Elina Boubouresi, except **31**). These compounds were fully characterised and resubmitted to CRT for testing at a high purity (>95%). The results (Table 12) show good correlation between potency of HTS and re-synthesised samples encouraging further exploration of this series.

Table 12. SAR for ERK5 inhibition: Comparison of HTS samples and resynthesized samples.

Compound	R ¹	ERK5 ^a IC ₅₀ (μM)	
		HTS Results	Resynthesised in house
30		4.8	4.7 ± 0.04
18		5.4	7.4 ± 0.4
31		9.3	24 ± 5.5
32		34	26 ± 0.4
33^b		87	-
34^c		-	20 ± 1.4

^a ERK5 IC₅₀ values generated by IMAP cell free assay (350 μ M ATP); ^b This compound was not resynthesized, instead a close analogue was submitted instead; ^c Close analogue of **33**.

2.2 Proposed Libraries for the Indazole Series

There are 6 positions around the indazole pharmacophore which are amenable to investigated (Figure 32). The most logical starting point, as some variants already exist in the original hits, is the 6-position aryl sulphonamide. A large library of analogues are accessible by the coupling of various sulphonyl chlorides with 6-aminoindazole to form the sulphonamide linker (Chapter 2.3).

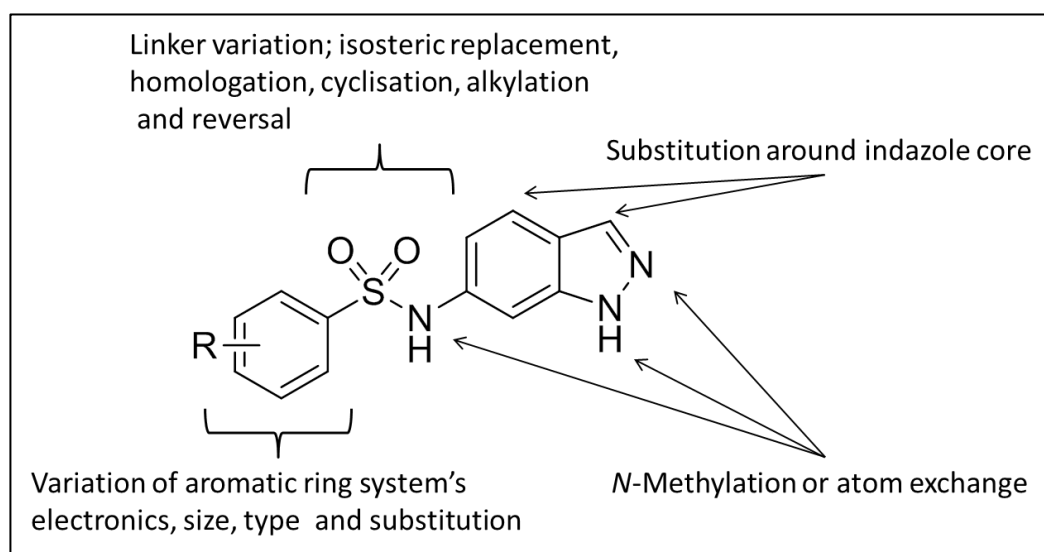


Figure 32. Proposed structure activity relationship studies around the indazole core.

A primary objective was to determine the nature of any hinge binding motif present on the hits. It is likely that the indazole core forms a pair of hydrogen bonds with the backbone of the amino acid chain in the kinase active site. One way to define this is by the sequential removal of the H-bonding character within the molecule i.e. methylation of the indazole NH and swapping the indazole for an indole will also reveal the role of the second indazole nitrogen (Chapter 2.4.2).

The role of the sulphonamide linker can be better understood by isosteric replacement and removal of the hydrogen bonding capability it carries. Replacement of the group with an amide reduces the flexibility of the whole molecule and also diminishes the capacity to accept H-bonds. Reversal of the linker will maintain the flexibility but significantly disturb any interactions the sulphonamide makes. Replacement of the

nitrogen with an sp^3 carbon again changes the hydrogen bonding profile. The synthesis of the sulphone also facilitates the synthesis of thioether and sulfoxide compounds which establish the role of the S=O groups in ERK5 activity.

The indazole molecule, at this stage, is substituted only in the 6 position leaving the 1, 3, 4, 5 and 7 positions free for further elaboration. Molecular modelling data was used when prioritising positions and selecting functionalities for inclusion.

2.3 Variation of the 6-Position Aryl-Sulphonamide

2.3.1 Synthetic Strategy Towards various 6-Position Aryl-Sulphonamide Indazoles

The initial HTS hits provided an excellent starting point to commence SAR development. However, in the absence of an ERK5 co-crystal structure a hit-expansion library was designed for synthesis based on commercially available building blocks. The 'hit explosion' technique consists of the synthesis of a large number of diverse compounds related to a hit compound. In this case the aryl-sulphonamide was varied. Target molecule selection was based on the feasibility of synthesis, the cost of building block and length of synthetic scheme. Variation of the aryl-sulphonamide is seen to be tolerated in the SAR of the validated hits (Table 12). To ascertain the significance of these groups, synthetic targets were selected to represent electron rich and poor aromatic systems including a range of substitution patterns, fused ring systems and heterocycles (Figure 33). All 41 building blocks chosen, with one exception, are aromatic systems and were sourced from major chemical suppliers without excessive expense. The overall aim of this target set was to identify a refined set of compounds with an ERK5 IC_{50} below 10 μ M to progress into the hit to lead process. The secondary aim was to draw conclusions about this area of the molecule and begin to develop a robust SAR.

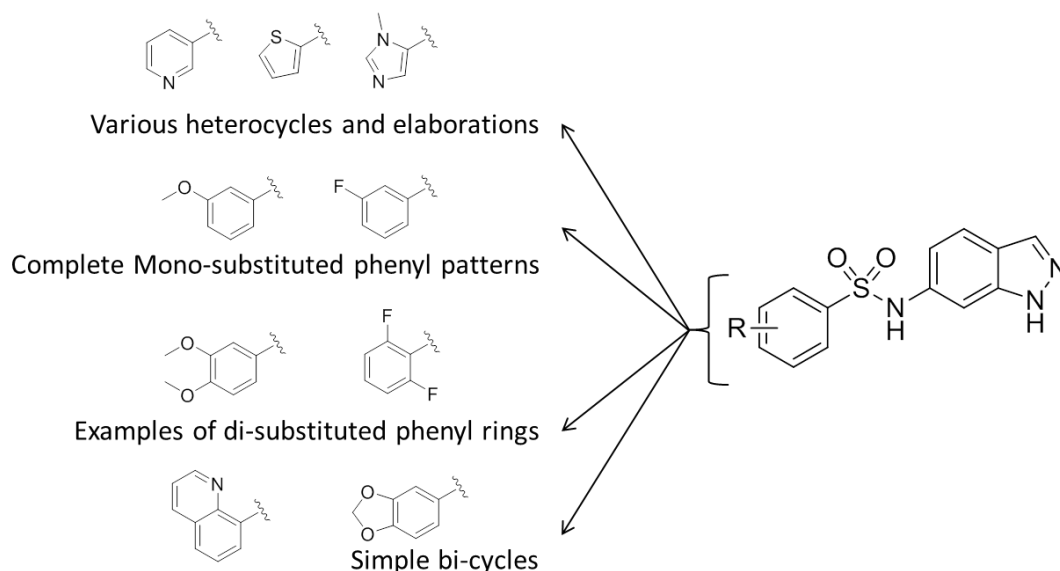
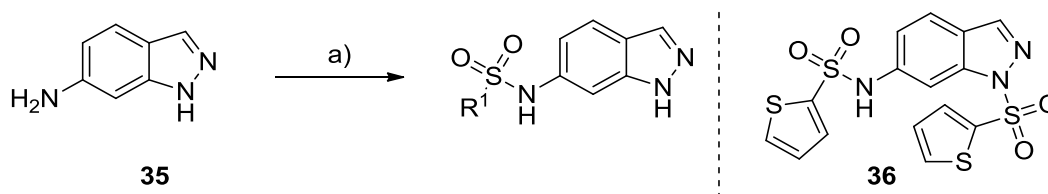


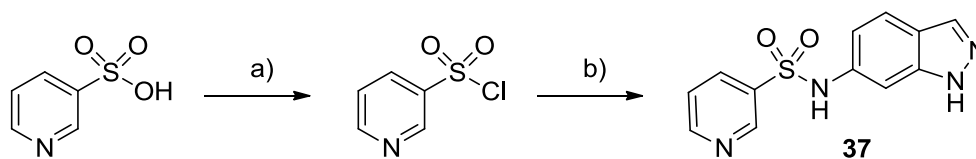
Figure 33. Target compound libraries with selected examples.

Final compounds were synthesised in one step using 6-amino indazole and various sulphonyl chloride building blocks in pyridine. Other methods exist for the synthesis of sulphonamides, however, this simple procedure was chosen due to its suitability for parallel synthesis. A stock solution of 6-aminoindazole in pyridine was used for numerous reactions, reducing reaction set up time and allowing for simultaneous synthesis. A limited amount of di-substitution was witnessed as both the indazole NH and the free amine are sufficiently nucleophilic to attack the electrophilic centre. Formation of the by-product ((**36**), Scheme 1) formed in the synthesis of thiophene target **38** could be controlled by reducing the temperature to 0 °C in the first instance and also by using a 1:1 solvent mix of THF and pyridine to lower the basicity of the system. All the targets were synthesised using this refined procedure which routinely gave the desired molecules in high yields. The employment of a Biotage v10 instrument for the rapid removal of high boiling solvents meant that the use of pyridine did not impede the work up time. The reaction mixture was concentrated to a residue which was then suspended in a saturated sodium hydrogen carbonate solution and extracted with EtOAc before purification by flash chromatography.



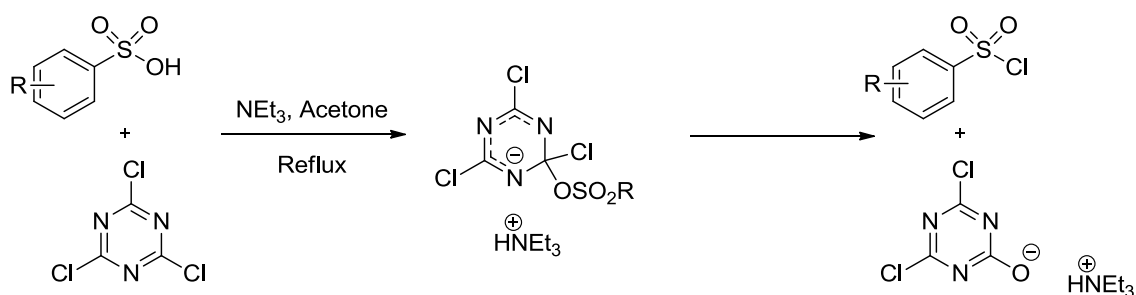
Scheme 1. Reagents and conditions; a) R^1-SO_2Cl , Pyr:THF (1:1), 3-6 h, 0 °C-RT 9-70%.

In a select number of cases a desired sulphonyl chloride was not available and therefore a longer synthesis was required. Literature precedent exists for the synthesis of sulphonyl chlorides from thiols in a one pot procedure or from sulphonic acids.¹⁴⁵⁻¹⁴⁶ Conversion of pyridine-3-sulphonic acid into the corresponding sulphonyl chloride was attempted using PCl_5 giving the product in a very low yield, 16% final product **37**, and so was deemed an unsuitable procedure for library synthesis. It was found that isolation of the sulphonyl chloride further reduced the yield due to exposure to aqueous solution in the work up and hydrolysis of the product. For this reason the crude material was used directly in the sulphonamide formation reaction.



Scheme 2. Formation of pyridine-3-sulphonylchloride. Reagents and conditions; a) PCl_5 , $POCl_3$, 120 °C, overnight; b) Pyr:THF (1:1), 3-6 h, 0 °C-RT 16% (over two steps).

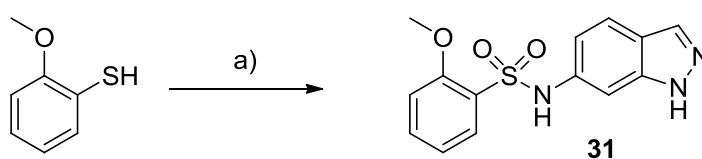
The conversion of sulphonic acids to sulphonyl chlorides using cyanuric trichloride has been reported.¹⁴⁷ The reaction proceeds in the presence of a base and a low boiling solvent at reflux as shown in Scheme 3.¹⁴⁷ Conversion of pyridine-3-sulphonic acid was conducted showing some product formation. However, the stability of the sulphonyl chloride formed was brought in to question when the product was not isolated after a low temperature work up.



Scheme 3. Formation of sulphonyl chlorides using cyanuric trichloride.

Sulphonyl fluorides are reportedly more stable than sulphonyl chlorides due to the electronegativity of fluorine and therefore an analogous reaction was conducted using cyanuric trifluoride. In this instance no product formation was witnessed and therefore a method was sought for the conversion of alternate starting materials.

A one pot conversion of thiols to sulphonyl chlorides has been described using hydrogen peroxide and thionyl chloride in high yields and a short timeframe.¹⁴⁵ This procedure also describes the direct conversion of thiols to sulphonamides *via* the sulphonyl chloride intermediate, making the scheme particularly attractive (Scheme 4).



Scheme 4. Formation of sulphonyl chlorides and *in situ* amine coupling. Reagents and conditions; a) i) H_2O_2 , SOCl_2 , MeCN, RT. ii) 6-Aminoindazole, pyridine, RT (7% over 2 steps)

Addition of hydrogen peroxide to the thiol and thionyl chloride was exothermic and therefore the poor conversion witnessed was attributed to the escape of volatile materials or overheating. The desired final product (**31**) was isolated only after an addition of 6-amino indazole to the crude sulphonyl chloride product (Scheme 4) to give the sulphonamide in a 7% yield overall.

Due to difficulties experienced in formation of sulphonyl chlorides the selection of starting materials was limited to sulphonyl chlorides, with the exception of compounds **37** and **31** detailed above.

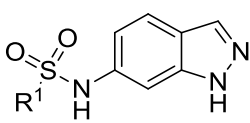
2.3.2 ERK5 structure activity relationships of indazole sulphonamides

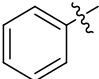
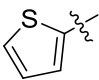
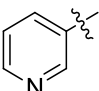
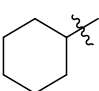
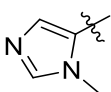
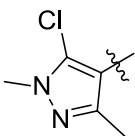
Final compounds of purity over 95% by HPLC were tested for inhibitory activity against ERK5 and p38 α in the cell free, enzymatic IMAP and LANCE assays, respectively. This library of compounds was completed before any further design decisions were made. Compounds have been defined into groups for ease of comparison. Compounds showing potency below 10 μ M (IC_{50}) were selected as templates for further modifications. Synthesis of compounds in this section (2.3.2) not appearing in the experimental section of this thesis was conducted, under supervision, by MChem project student Amy Roberts.

2.3.2.1 Aromatic and aliphatic rings

The results in Table 13 show the different ring systems which differed from the substituted phenyl derivatives present in the original hits. The cyclohexane group (**39**) gives a very poor IC_{50} value because, even though the compound has a predicted $LogP$ of 2.47, the compound was not soluble in the assay. Addition of a nitrogen atom to the ring (Pyridine, **37**) reduces the potency significantly (> 10-fold) when compared to the phenyl (**30**). It may be that in this position the nitrogen lone pair is forming a negative interaction in the active site. It is therefore not possible, at this stage, to conclude that the 2 and 4 pyridines will also show a drop in activity. Pyrazole (**41**) and imidazole (**40**) compounds show no or very poor ERK5 activity, although the other 5-membered ring, thiophene (**38**), is 2-fold more potent than phenyl **30**. Further thiophene derivatives are discussed in the following section (Chapter 2.3.2.2).

Table 13. Enzymatic activity data of compounds **30**, **37-41** against ERK5 and p38 α .



Compound	R ¹	IC ₅₀ (μM)	
		ERK5 ^a	p38 α ^b
30		4.7 ± 0.04	>120
38		2.2 ± 1.1	>120
37		59 ± 1.3	>120
39^c		>120	>120
40		>120	>120
41		64 ± 9.1	>120

^a ERK5 IC₅₀ values generated by IMAP cell free assay (350 μM ATP); ^b p38 α IC₅₀ values generated by Lance assay (350 μM ATP). ^c Insoluble in IMAP and Lance assay.

2.3.2.2 Thiophene derivatives

Compound **38** (Table 13) shows marginally improved potency compared with the parent phenyl compound highlighting the fact that there is potential for an electron rich system or even a possible dipole interaction. However, various thiophene substitution patterns, also included in this library, do not confer any additional potency (Table 14).

Table 14. Enzymatic activity data of compounds **38**, **42-47** against ERK5 and p38 α .

Compound	R ¹	IC ₅₀ (μM)	
		ERK5 ^a	p38 α ^b
38		2.2 ± 1.1	>120
42		22 ± 3.5	>120
43		41 ^d	>120
44		79 ^d	>120
45^c		>120	>120
46^c		>120	>120
47^c		>120	>120

^a ERK5 IC₅₀ values generated by IMAP cell free assay (350 μM ATP); ^b p38 α IC₅₀ values generated by Lance assay (350 μM ATP). ^c Insoluble in IMAP and Lance assay. ^d n=1 therefore no calculable error.

Compounds **45-47** possess poor solubility and therefore an accurate assay result could not be obtained. This data suggests that only an unsubstituted thiophene is tolerated. However, the dataset is not conclusive as a diverse range of sulphonyl chloride building blocks was not available.

2.3.2.3 Bicyclic rings

A small number of bicyclic compounds were included in the library, shown in Table 15, producing some encouraging results. In the case of compound **48** and **52** the potency was maintained showing a large amount of tolerance in both 2,3- and 3,4- substituted

bicyclic systems. Comparisons between compounds **52** and **53** suggest that the oxindole derivative may form a hydrogen bond interaction either through the carbonyl group or the free NH whilst the oxazolone analogue (**53**) shows that there is no favourable interaction to be gained by including the additional oxygen. This may be due to a negative interaction by the oxygen or the effect it has on the hydrogen bonding strength of the adjacent hetero atoms. It is also possible that because of the hydrogen bond donor-acceptor array, the oxindole can replicate the assumed hinge binding interaction of the indazole thus giving two binding modes for this compound. The discrepancy between compounds **52** and **53** could be explained by hydrogen bonding strength. These theories are tested by a reversed sulphonamide series of compounds (Chapter 2.5.4).

Table 15. Enzymatic activity data of compounds **30**, **34**, **48-54** against ERK5 and p38 α .

Compound	R ¹	IC ₅₀ (μM)	
		ERK5 ^a	p38 α ^b
30		4.7 ± 0.04	>120
48		3.5 ± 1.7	>120
49		79 ^d	>120
34		20 ± 1.4	>120
50		16 ± 0.8	>120
51		11 ± 1.8	>120
52		1.5 ± 0.4	>120
53		9.5 ± 2.4	>120
54^c		>120	>120

^a ERK5 IC₅₀ values generated by IMAP cell free assay (350 μM ATP); ^b p38 α IC₅₀ values generated by Lance assay (350 μM ATP). ^c Insoluble in IMAP and Lance assay. ^d n = 1

Quinoline compound **48** shows good potency, which is interesting considering the result of pyridine **37** shown earlier. Pyridine and quinoline are both electron deficient aromatics, however, the difference in potency here is over 15-fold in favour of the larger group. The potency may be derived from a superior conformation or lipophilic

interaction. Unfortunately compound **48** is the only example of a 2,3-bicyclic system in the library so an SAR cannot be defined.

Cyclic-ether compounds **33-34** and **50-51** show a reduction in potency as their complexity increases (these gains are not significant enough to extrapolate a sensible SAR). These results do indicate, along with compounds **52** and **53**, that there is room for 3,4-fused bicycles in the ERK5 active site.

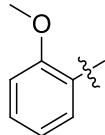
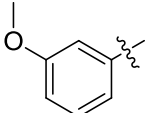
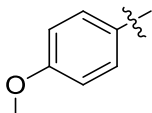
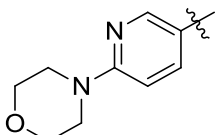
2.3.2.4 Substituted Phenyls

A set of compounds was chosen to explore the substitution pattern around the ring including electron withdrawing and donating substituents. Table 16 shows the results indicating that no apparent trend exists, but significant differences are seen between matched pairs. *para*-substituted compounds **61** and **63** (CN and CF₃) exhibit potency at least a factor of two better than the corresponding *meta*-substituted analogues (**60** and **62**). This relationship suggests that the *para*-position could be a source of potency although this is not supported by the whole data set.

para-Fluoro compound **57** has poor potency (IC₅₀ 33 ± 4.7 µM) and whilst both *meta* and *ortho* substituted analogues (**56** and **55**) have only moderate potency both results are superior. In the case of the electron rich, methoxy compounds, *meta* (**66**) and *para* (**18**) substitution gives reasonable potency (the only examples in the data set below 10 µM (IC₅₀)). There is no improvement over the unsubstituted phenyl (**30**) in this set of compounds, which suggest, contrary to the bicycle library, that space around the sulphonamide aryl is limited.

Table 16. Enzymatic activity data of compounds **18**, **30-31**, **55-67** against ERK5 and p38 α .

Compound	R ¹	IC ₅₀ (μM)	
		ERK5 ^a	p38 α ^b
30		4.7 ± 0.04	>120
55		23 ± 0.8	98 ± 2.7
56		22 ± 1.5	82 ± 0.03
57		33 ± 4.7	>120
58		12 ± 0.3	>120
59		14 ± 1.3	>120
60		47 ± 4.7	>120
61		17 ± 1.0	>120
62		>120	>120
63		69 ± 16	>120
64		70 ± 4.0	>120
65		73 ± 11	>120

31		24 ± 5.5	>120
66		7.0 ± 0.4	>120
18		7.4 ± 0.4	>120
67		71 ± 12	>120

^a ERK5 IC₅₀ values generated by IMAP cell free assay (350 μM ATP); ^b p38α IC₅₀ values generated by Lance assay (350 μM ATP).

2.3.2.5 Di-substituted Phenyls

The di-substituted compound set shows a little difference between the various substitution patterns. The 2,6-difluoro compound (**70**) shows good potency, which is presumably due to the twist this substitution pattern imposes on the ring. The conformation invoked in compound **70** should also be seen with the mono-substituted derivative **55** but an almost 3-fold potency difference exists which indicates there may be other contributing factors. It is important to note, in both cases where the 3,5 and 2,4 substitution patterns are repeated with both fluorine and another halogen (Cl and Br respectively) that the fluorinated derivative has higher activity. Bromine and chlorine atoms are much larger than fluorine and therefore the space around the aromatic group could be restricted.

Table 17. Enzymatic activity data of compounds **30**, **68-74** against ERK5 and p38 α .

Compound	R ¹	IC ₅₀ (μM)	
		ERK5 ^a	p38 α ^b
30		4.7 ± 0.04	>120
68		37 ± 3.4	>120
69		72 ± 0.4	>120
70		7.7 ± 0.3	44 ± 8.6
71		80 ± 4.7	>120
72		26 ± 0.4	>120
73		>120	>120
74		>120	>120

^a ERK5 IC₅₀ values generated by IMAP cell free assay (350 μM ATP); ^b p38 α IC₅₀ values generated by Lance assay (350 μM ATP).

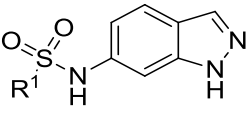
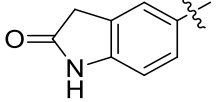
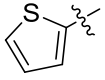
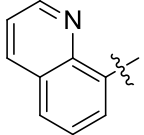
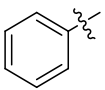
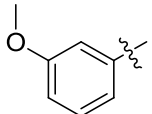
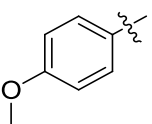
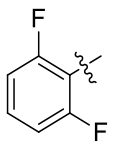
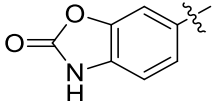
Compound **70** is the first example synthesised of interest that also shows activity against p38 α . Other fluorine containing compounds **55** and **56** also show measurable activity against p38 α suggesting that an electron deficient ring system confers potency or a beneficial interaction with a fluorine might exist.

2.3.2.6 Cellular Potency of Selected Hit Compounds

The small library synthesis revealed eight compounds with IC₅₀ values lower than 10 µM which were deemed suitable for future optimisation (Table 18). There is no clear unifying property that these compounds share meaning that the SAR remains largely unknown. The purpose of this screen was achieved as compounds suitable for further exploration have been identified without any prior knowledge of SARs. Future derivatives feature the potent aryl sulphonamide groups when possible, to generate broad and reliable SARs.

Cellular potency gathered on select compounds in this set show that in most cases the enzymatic potency is representative of cellular activity. Oxindole compound **52** shows a discrepancy between the two assay types, however, this was not a major concern at this stage of the project.

Table 18. Enzymatic and cellular ERK5 activity data of compounds showing ERK5 IC₅₀ below 10 μM.

			
Compound	R ¹	ERK5 IC ₅₀ (μM) ^a	Cellular Reporter assay IC ₅₀ (μM)
52		1.5 ± 0.4	13.5 ± 4.1
38		2.2 ± 1.1	-
48		3.5 ± 1.7	3.58 ± 0.3
30		4.7 ± 0.04	5.4 ± 0.8
66		7.0 ± 0.4	-
18		7.4 ± 0.4	6 ^b
70		7.7 ± 0.3	-
53		9.5 ± 2.4	-

^a ERK5 IC₅₀ values generated by IMAP cell free assay (350 μM ATP); ^b n=1 therefore no error available.

2.4 Modifications Affecting the Indazole H-bonding Profile

To establish the role of the indazole binding to the ERK5 active site a strategy was devised to systematically remove the H-bond capacity of the structure. Two distinct targets were devised to answer these questions. Methylation of the Indazole NH removes its capacity to donate a Hydrogen bond but is only a small change which should not perturb other interactions greatly (Figure 34). Exchange of the indazole for an indole eliminates the H-bond acceptor capacity at the 2-position without introducing any significant changes to the shape or size of the molecule (Figure 34). Both changes were investigated in the context of the best sulphonamide substituents identified previously. Synthesis of these compounds was conducted, under supervision by MChem project students Amy Roberts (**75**) and Amy Heptinstall (**76-80**)

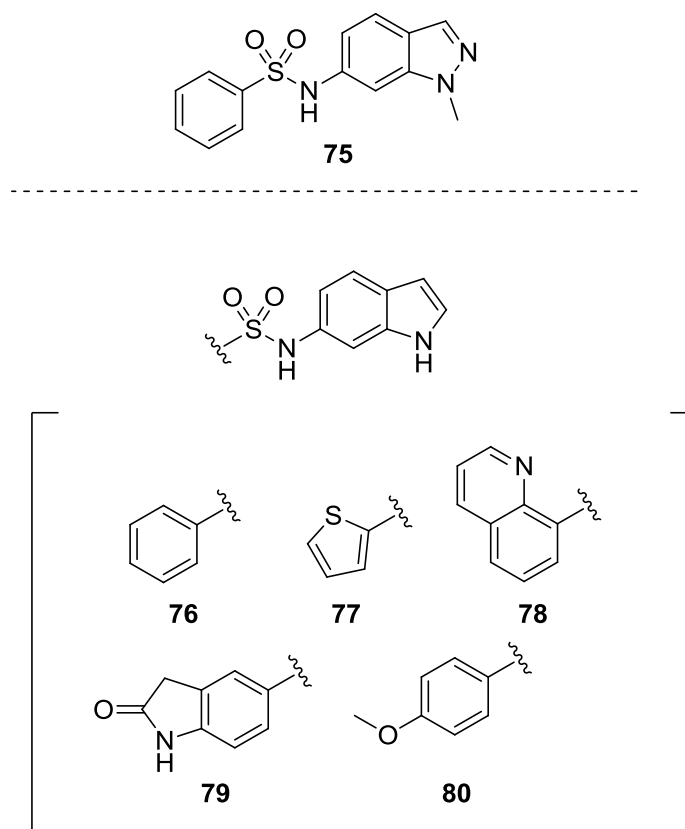
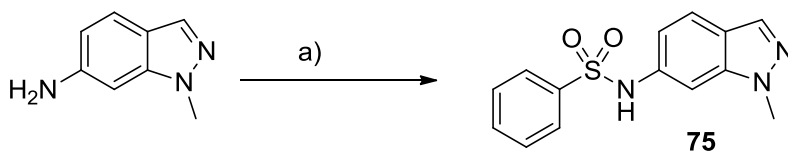


Figure 34. Indazole H-bonding modification targets.

2.4.1 Synthesis and SAR of *N*-(1-methyl-1*H*-indazol-6-yl)benzenesulfonamide (**75**)

The synthesis of **75** was completed in one step from the commercially available 1-methyl-1*H*-indazol-6-amine and benzenesulphonyl chloride in the same way as the previous library was synthesised (Scheme 5, Synthesis conducted by Amy Roberts).



Scheme 5. Reagents and conditions; a) RSO₂Cl, Pyr, 3-6 h, 0 °C-RT.

The activity data (Table 19) shows that potency is completely lost when a 1-methyl group is introduced on the indazole and therefore gives strong reason to believe the indazole NH plays a crucial role in binding.

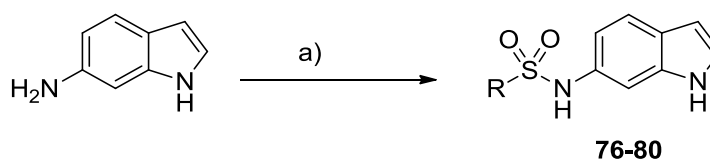
Table 19. Enzymatic activity data of compounds **30** and **75** against ERK5 and p38α.

Compound	Structure	IC ₅₀ (μM)	
		ERK5 ^a	p38α ^b
30		4.7 ± 0.04	>120
75		>120	>120

^a ERK5 IC₅₀ values generated by IMAP cell free assay (350 μM ATP); ^b p38α IC₅₀ values generated by Lance assay (350 μM ATP).

2.4.2 Synthesis and SAR of 6-Sulphonamide Indole Compounds

Synthesis was carried out in an analogous manner to previous sulphonamide libraries (Scheme 6) which again gave good yields despite the instability of 6-aminoindole which is known to decompose at room temperature. (Synthesis was carried out by Amy Heptinstall)



Scheme 6. Reagents and conditions; a) RSO_2Cl , Pyr, 3-6 h, 0 °C-RT.

The ERK5 activity results show complete abolition of activity thus proving the hydrogen bond acceptor role of the indazole in binding. This conclusion can be made with confidence due to the range of sulphonamide-aryl groups included in the data set and the range of properties represented.

Table 20. Enzymatic activity data of compounds **30**, **76-80** against ERK5 and p38 α .

Compound	Structure	IC ₅₀ (μM)	
		ERK5 ^a	p38 α ^b
30		4.7 ± 0.04	>120
76		>120	>120
80		>120	>120
78		>120	>120
79		>120	>120
77		>120	>120

^a ERK5 IC₅₀ values generated by IMAP cell free assay (350 μM ATP); ^b p38 α IC₅₀ values generated by Lance assay (350 μM ATP).

2.4.3 Molecular Modelling of Indazole Hinge Binding

Molecular modelling software (GOLD) has been used to propose an ERK5 binding interaction with compound **30** (Figure 35). The indazole is suggested to sit an appropriate distance from the hinge region to hydrogen bond i.e. 1.5-2.5 Å. Simulations have speculated that interactions exist between the indazole NH and Asp95 backbone carbonyl and the second indazole nitrogen with the NH of Met93.

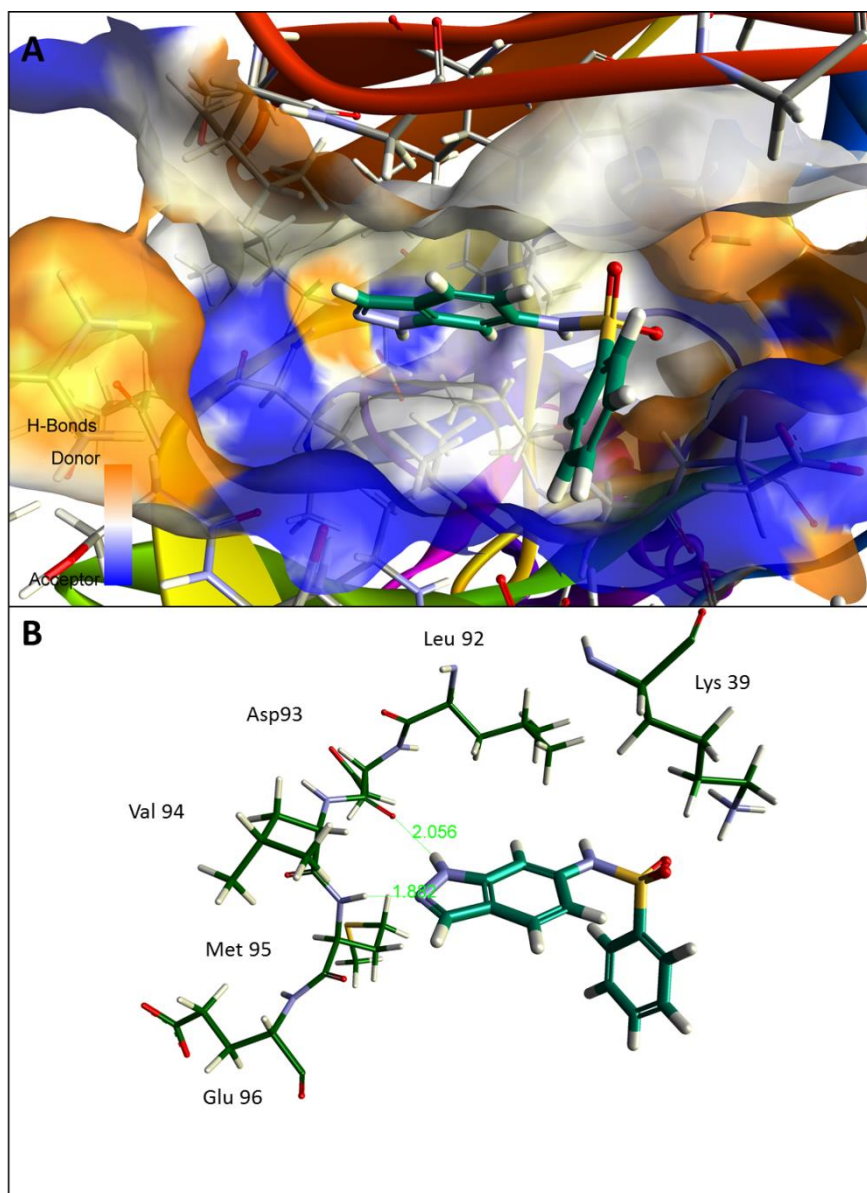


Figure 35. Molecular modelling of compound **30** (teal) in the crystallised ERK5 kinase domain (PDB: 4IC8) with active site surface shown in blue (H-bond acceptor) to orange (H-bond donor) and the ERK5 protein (rainbow). A) Proposed shape of compound **30** in the ERK5 active site. B) Key interactions with the ERK5 hinge region and compound **30** (teal) showing h-bond distances in angstroms (Å).

2.5 Linker Modifications

The role of these target compound sets was to improve potency by defining the role of the sulphonamide linker. Systematic removal or attenuation of hydrogen bonding capabilities and modification of the linker conformation was conducted.

2.5.1 Sulphonamide Alkylation

2.5.1.1 *N*-Methylation 6-sulphonamide indazoles

Sulphonamides have a pK_a value of around 6-7, depending on adjacent groups, and can therefore be deprotonated at physiological pH. The B-Raf inhibitor Vemurafenib (**81**, Figure 36) is an example of a drug compound which is deprotonated to facilitate binding. In this case the sulphonamide is adjacent to an electron deficient difluorophenylketone which contributes to the low pK_a (7.17). Without conducting a pH study on our compounds, we can only estimate the ionisation state and therefore it is unknown if the sulphonamide retains or loses its capacity as a hydrogen bond donator.

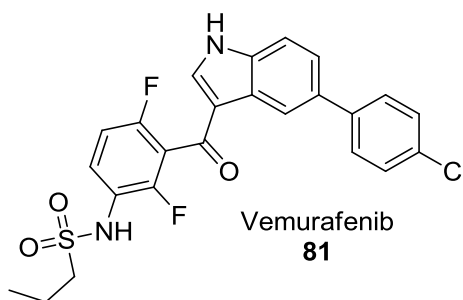
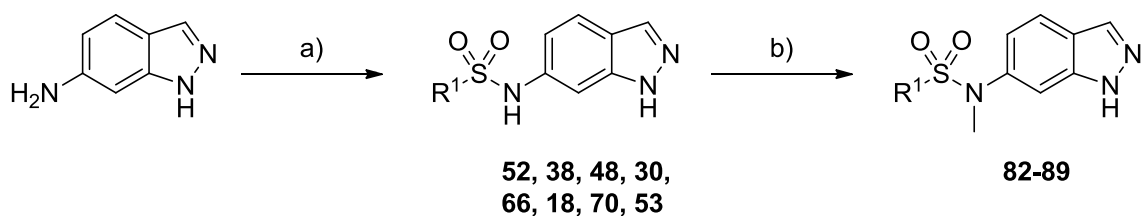


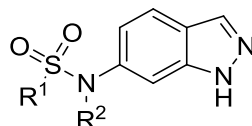
Figure 36. Structure of B-Raf inhibitor Vemurafenib.

To ascertain the role of this moiety in the molecule, a methyl group was introduced to the sulphonamide nitrogen atom removing the possibility of deprotonation and the ability to interact favourably with δ^- groups. To make the methylated sulphonamide, compounds in Table 18 were treated with methyl iodide and K_2CO_3 in DMF (Scheme 7). Good selectivity was found between the sulphonamide and indazole NH, due to the difference in pK_a (\sim 6-8 and 13.2 respectively).



Scheme 7. Reagents and conditions; a) $\text{R}^1\text{SO}_2\text{Cl}$, Pyr, 3-6 h, 0°C -RT. b) MeI, K_2CO_3 , DMF, 8h 0°C -RT.

The products formed were significantly more active against ERK5 than the unmethylated counterparts with an average 4-fold improvement and no p38 α activity. Overall the results show that no beneficial interaction is made by the H-bond donor unit in question whether protonated or not.

Table 21. Enzymatic activity data of compounds **82-89** against ERK5 and p38 α .

Compound	R ¹	R ²	IC ₅₀ (μM)	
			ERK5 ^a	p38 α ^b
30		H	4.7 ± 0.04	>120
82		Me	1.1 ± 0.6	>120
52		H	1.5 ± 0.4	>120
83		Me	0.33 ± 0.17	>120
38		H	2.2 ± 1.1	>120
84		Me	0.45 ± 0.09	>120
48		H	3.5 ± 1.7	>120
85		Me	1.5 ± 0.4	>120
66		H	7.0 ± 0.4	>120
86		Me	3.2 ± 0.4	>120
18		H	7.4 ± 0.4	>120
87		Me	0.35 ± 0.04	>120
70		H	7.7 ± 0.3	44 ± 8.6
88		Me	2.6 ± 0.4	>120
53		H	9.5 ± 2.4	>120
89		Me	1.7 ± 0.97	>120

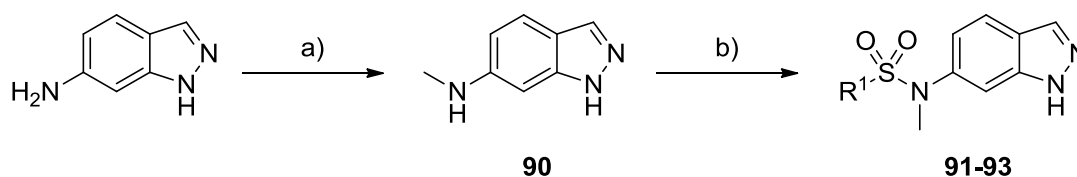
^a ERK5 IC₅₀ values generated by IMAP cell free assay (350 μM ATP); ^b p38 α IC₅₀ values generated by Lance assay (350 μM ATP).

Three compounds show an IC₅₀ value below 1 μM (**83**, **84** & **87**) but again there is not a unifying characteristic between these compounds. A distinction can be made between the two methoxy compounds **86** and **87** as the *para*-positioning gives ten-fold better activity than the *meta*.

2.5.1.1.1 Alternate Aryl groups on *N*-Methyl Sulphonamide Indazoles

Three further *N*-methyl sulphonamide compounds were synthesised with variation of the aryl R¹ group. The use of benzylsulphonyl chloride produced a compound with an extended linker by introduction of a benzyl carbon atom. A cyclopropyl group was installed as an aliphatic group that was predicted to be soluble in the assay conditions. A furan ring was also included in the data set as a close analogue to thiophene **84** which has shown good potency.

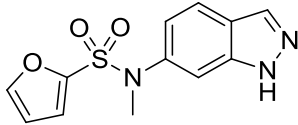
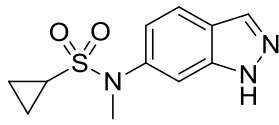
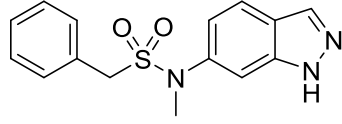
For ease of synthesis *N*-methyl-1*H*-indazol-6-amine (**90**) was synthesised to truncate the scheme to one step from a common intermediate (Scheme 8). Mono-methylation of 6-amino indazole was achieved by forming an imine using paraformaldehyde in the presence of a base and subsequent reduction using sodium borohydride in a one pot procedure. Yields of the sulphonamide formation were generally improved via this route due to the increased nucleophilicity of the reactive centre by the alkyl group.



Scheme 8. Reagents and conditions; a) i) paraformaldehyde, NaOMe, MeOH, 5h RT. ii) NaBH₄, 80 °C, 2 h, (38%) b) R¹SO₂Cl, Pyr, 3-6 h, 0 °C-RT (39-79%).

As predicted the furan derivative (**91**) had moderate potency however the close analogue (**84** thiophene) is significantly more potent.

Table 22. Enzymatic activity data of compounds **91-93** against ERK5 and p38 α .

Compound	Structure	IC ₅₀ (μ M)	
		ERK5 ^a	p38 α ^b
91		3.7 \pm 0.5	>120
92		19.7 ^c	>120
93		>120	>120

^a ERK5 IC₅₀ values generated by IMAP cell free assay (350 μ M ATP); ^b p38 α IC₅₀ values generated by Lance assay (350 μ M ATP). ^c no duplicate result available therefore no calculable error.

The cyclopropyl derivative (**92**) is not aromatic and therefore possesses protons directed out of plane with the 3-membered ring (Figure 37). This means that even though it doesn't project as far as the thiophene it occupies different space immediately next to the sulphonamide centre, which may affect the orientation or create a clash with the protein surface. It is possible that the aromatic groups included here are making a π - π or π -dipole interaction. However no correlation has yet been seen between electronics of the ring and activity.

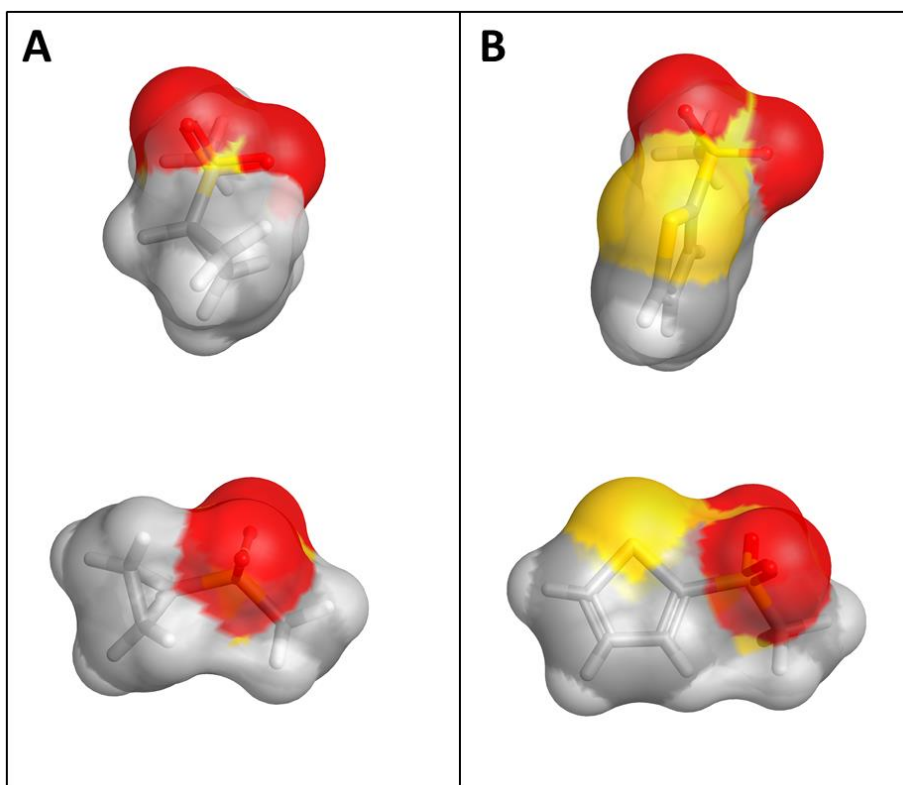


Figure 37. Simulations created using Torchlight (Cresset) to show the shape of both cyclopropane methylsulphone (A) and 2-thiophene methylsulphone (B).

Homologation of the linker (**93**) resulted in a complete loss of potency in spite of the good potency of considerably larger groups such as bicycles **48** and **52**. It is likely that the vector required to orientate the phenyl ring in the most favourable position in the active site is not achieved by the inclusion of the extra benzylic carbon.

2.5.1.1.2 Selectivity of *N*-Methyl sulphonamide Indazoles

For all compounds tested for ERK5 activity to date, p38 α activity has also been collected. p38 α is a member of the MAP kinase family and a close homologue of ERK5, particularly in the kinase domain. No significant activity has been seen for p38 α but the wider kinome shares a large amount of structural features in the active site and so inhibition of other kinases may occur. To determine the selectivity profile of the indazole sulphonamide scaffold, phenyl compound **82** was submitted for a wide kinase screen. 131 Kinases were screened with results given as a percent inhibition at 1 μ M concentration of compound **82**. The overall profile was good and only moderate inhibition of ERK8 (48%) and CDK2/A (52%) was seen (these values are directly comparable to potency against ERK5 (IC_{50} of 1.1 μ M i.e. ~50% at 1 μ M).

An assay had previously been established in house for CDK2, so a number of close analogues to **82** were tested including the corresponding un-methylated sulphonamides.

Table 23. Enzymatic activity data of compounds against ERK5, p38 α and CDK2/A.

Compound	R ¹	R ²	IC ₅₀ (μM)		
			ERK5 ^a	p38 α ^b	CDK2/A
30		H	4.7 ± 0.04	>120	19.2
82		Me	1.1 ± 0.6	>120	2.1
52		H	1.5 ± 0.4	>120	12.9
83		Me	0.33 ± 0.17	>120	5.8
38		H	2.2 ± 1.1	>120	18.4
84		Me	0.45 ± 0.09	>120	1.3
48		H	3.5 ± 1.7	>120	2.1
85		Me	1.5 ± 0.4	>120	0.19
18		H	7.4 ± 0.4	>120	69.7
87		Me	0.35 ± 0.04	>120	6.7
70		H	7.7 ± 0.3	44 ± 8.6	46.9
88		Me	2.6 ± 0.4	>120	0.48

^a ERK5 IC₅₀ values generated by IMAP cell free assay (350 μM ATP); ^b p38 α IC₅₀ values generated by Lance assay (350 μM ATP).

Unlike p38 α , compounds showed significant activity against CDK2/A. In some cases such as **85**, **48** and **88** greater affinity is seen for CDK2/A than ERK5. As is the case with ERK5 activity, methylation of the sulphonamide improves potency of compounds against CDK2/A with an average 10-fold increase. These results show the quinolone moiety could be associated with CDK2/A activity making it a less interesting group for the design of ERK5 inhibitors.

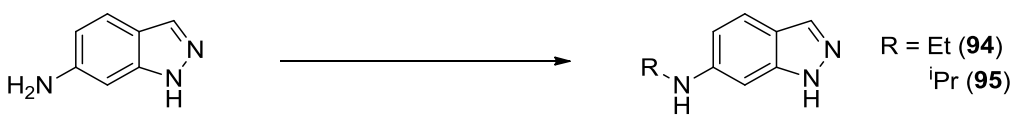
From this point in the project CDK2 activity has been closely monitored whilst further structural modifications were made. At this stage of the project it was deemed unnecessary to commit to designing out CDK2 activity as a thorough SAR for ERK5 activity had not yet been built.

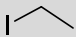
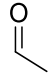
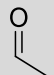
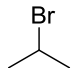
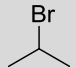
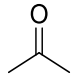
2.5.1.2 Sulphonamide *N*-Ethyl & *N*-Isopropyl Derivatives

It has been shown that methylation of the sulphonamide nitrogen increases ERK5 inhibition. To investigate this gain further, progressively larger alkyl groups (ethyl and isopropyl) were introduced to the sulphonamide. The potency gain achieved by *N*-methyl sulphonamides may have been due to the removal of an unfavourable interaction or the creation of a beneficial interaction. If the increase in alkyl substituent size improves potency it is likely that a new interaction has been identified. However if potency decreases it shows that masking the H-bond potential of the sulphonamide was the sole reason for improved potency.

A strategy was devised to synthesise compounds first by a mono alkylation upon 6-aminoindazole followed by a sulphonyl chloride coupling. Alkylation of the indazole NH₂ prior to the formation of the sulphonamide presented a more efficient reaction sequence. Mono-alkylation has been achieved previously through reductive amination which worked to a satisfactory degree to give *N*-methyl-1*H*-indazol-6-amine (**90**, Scheme 8). The reductive animation using acetaldehyde and AcOH (Reaction 2, Table 24) gave poor conversion (12%) . However, when TFE (2,2,2-trifluoroethanol) was used in place of solvent and acting as the acid a significant improvement is made to conversion¹⁴⁸. This is presumably due to the acidity of TFE which is sufficient to catalyse the reaction without the addition of strong acid such as AcOH, HCl or H₂SO₄. The reductive amination conducted to give *N*-isopropyl-1*H*-indazol-6-amine (**95**) progressed with the use of H₂SO₄ in a comparable yield owing to the increased stability of the carbonyl reagent.

Table 24. Conditions and yields of N-alkylation reactions.



Reaction	Reagent	Conditions	Yield / %	Comments / reference
1		CsOH.H ₂ O, DMF, 4Å MS	10	Major product was 6-diethylaminoindazole
2		i) DCM, AcOH ii) NaBH ₄	12	-
3		i) TFE ii) NaBH ₄	38	¹⁴⁸
4		CsOH.H ₂ O, DMF, 4Å MS	38	Major product was 1-isopropylaminoindazole
5		KI, MeCN, 170°C μ-wave, 10 mins	20	-
6		i) H ₂ SO ₄ ii) NaBH ₄	39	-

Yields of S_N2 alkylations varied from poor to modest due to a number of factors (Table 24, reactions 1, 4 and 5). There is competition between formation of primary and secondary amines at the 1- and 6- positions as well as the possibility for dialkylation of the 6-amino group. Reactions 1 and 4 rely on the ‘caesium effect’, which is reported to give monoalkylated amines. Cesium coordinates strongly to the lone pair on the amine nitrogen and because of the large size of the atom multiple alkylation reactions are blocked (Figure 38)¹⁴⁹. Reactions of ethyl iodide (1) or 2-bromo propane (4) gave low yields of the desired product accompanied by a diethyl product and the 1-propyl product respectively. The literature describes the use of bromoalkanes for this transformation and therefore the use of the more reactive iodoethane may be the cause of over-alkylation. The 1-NH-position is less nucleophilic than the free amine and therefore would be expected to react second to the aniline portion. However, coordination of the caesium may take precedent over the alkylation causing a paradoxical result.

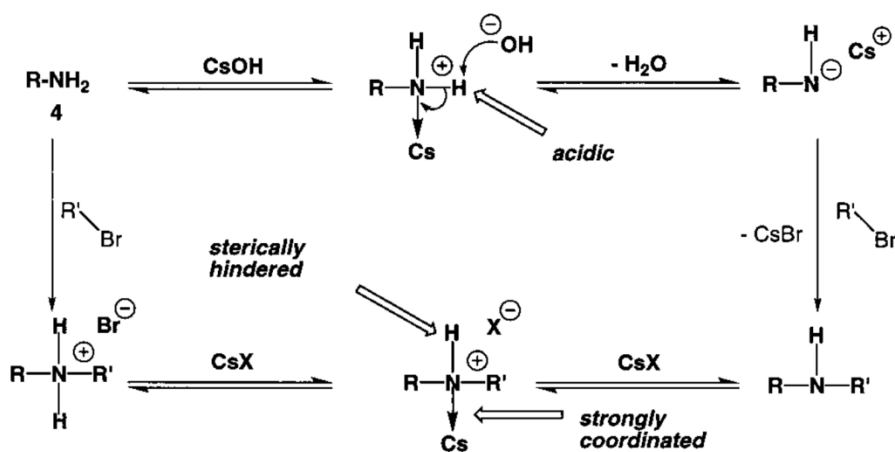
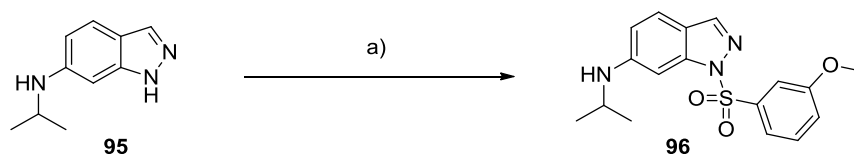


Figure 38. The proposed 'Caesium effect' resulting in mono *N*-alkylation¹⁴⁹.

Stoichiometric control was used in the microwave assisted reaction 5 (Table 24) which gave the desired product in a 20% yield. The potassium iodide in the reaction is expected to convert the bromopropane to the iodopropane *in situ* which is the more reactive species and should therefore decrease reaction time¹⁵⁰. The limitation of this reaction was the inefficient use of the amine species (3:1 equivalence with the bromo alkane) and therefore a more elegant procedure was sought.

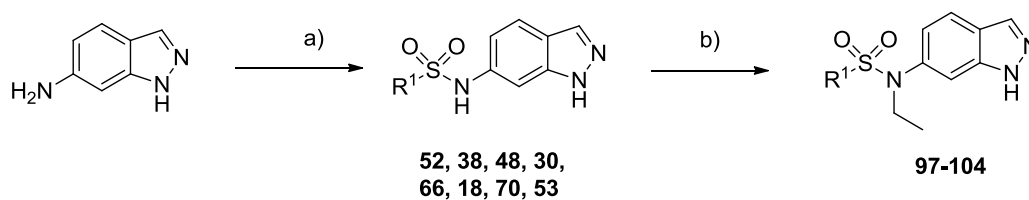
Material isolated from alkylation test reactions was used to test the sulphonyl chloride coupling, now with a larger degree of steric hindrance. The reaction requires the attack of the nucleophilic nitrogen upon the aromatic sulphonyl chloride in close proximity and therefore reactivity is limited by large alkyl groups attached to the nucleophile. In the case of the isopropyl compound **95** this resulted in sulphonamide formation at the indazole NH to give **96** (Scheme 9), and as a result none of the isopropyl desired targets were synthesised.



Scheme 9. Reagents and conditions; i) Pyridine, THF, RSO₂Cl, RT, 3h.

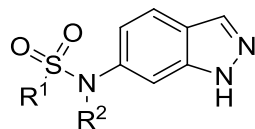
Limited success of the sulphonyl chloride coupling reaction and poor conversion to monoalkylated species meant that the target compounds were synthesised by other means (Scheme 10). In an analogous manner to the *N*-methylsulphonamide compound

synthesis intermediates were subjected to ethylation conditions using ethyl iodide, Cs_2CO_3 in DMF which gave the desired products in satisfactory yields.



Scheme 10. *Reagents and conditions;* a) Pyridine, THF, RSO_2Cl , RT, 3h, (40-70%). b) EtI , K_2CO_3 , DMF, 0°C -RT, 4h, (30-60%).

The activity results conclusively show that the *N*-ethyl group is not well tolerated in comparison to the *N*-methyl and consequently *N*-isopropyl analogues were not pursued further. Potency has fallen on average 20-fold between the methyl and ethyl analogues despite compounds **98**, **99** and **102** achieving potency below 10 μM .

Table 25. Enzymatic activity data of compounds **97-104** against ERK5 and p38 α .

Compound	R ¹	R ²	IC ₅₀ (μM)	
			ERK5 ^a	p38 α ^b
97		Et	17 ± 7	>120
82		Me	1.1 ± 0.6	>120
98		Et	7.5 ± 2.2	>120
83		Me	0.33 ± 0.17	>120
99		Et	8.7 ± 2.5	>120
84		Me	0.45 ± 0.09	>120
100		Et	18 ± 1	>120
85		Me	1.5 ± 0.4	>120
101		Et	57 ± 3	>120
86		Me	3.2 ± 0.4	>120
102		Et	7.0 ± 2.9	>120
87		Me	0.35 ± 0.04	>120
103		Et	40 ± 9	44 ± 8.6
88		Me	2.6 ± 0.4	>120
104		Et	67 ± 24	>120
89		Me	1.7 ± 0.97	>120

^a ERK5 IC₅₀ values generated by IMAP cell free assay (350 μM ATP); ^b p38 α IC₅₀ values generated by Lance assay (350 μM ATP).

This data suggests that this region of the active site cannot accommodate a group as big as an ethyl and that the previous gain in potency between SO₂NH and SO₂NMe derivatives was because of the removal of the ionisable centre or hydrogen bonding potential.

2.5.2 Synthesis and SAR of 6-Amide Indazole Compounds

One isostere of a sulphonamide is an amide, both groups have hydrogen bonding donor and acceptor moieties at equivalent proximities. The major difference of the sulphonamide is the presence of a second oxygen atom and the hybridisation of the sulphur atom. To identify if the shape of this linker is important in binding a number of amide targets were proposed (Figure 39). Compounds appearing in this section were synthesised by MChem student Amy Roberts.

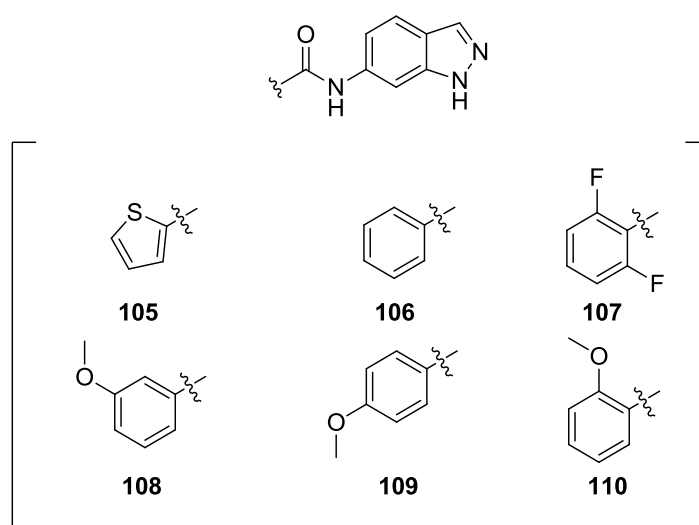
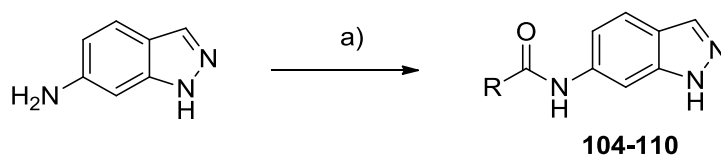


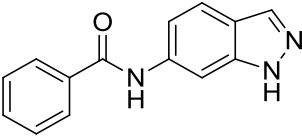
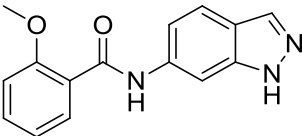
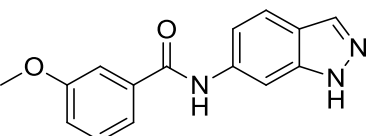
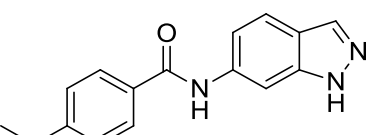
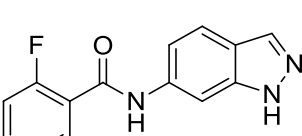
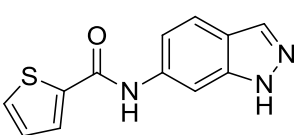
Figure 39. Amide Linker Targets.

1,1'-Carbonyldiimidazole (CDI) was used with various carboxylic acids in an amide coupling reaction which proceeded favourably with 6-aminoindazole (Scheme 11). Sulphonamide aryl systems exhibiting moderate potency were selected for synthesis when starting materials were commercially available as carboxylic acids (Figure 39).



Scheme 11. Reagents and conditions; i) CDI, R-COOH, THF.

Table 26. Enzymatic activity data of compounds **105-110** against ERK5 and p38 α .

Compound	Structure	IC ₅₀ (μ M)	
		ERK5 ^a	p38 α ^b
106		>120	>120
110		>120	>120
108		>120	>120
109		>120	>120
107		>120	>120
105		>120	>120

^a ERK5 IC₅₀ values generated by IMAP cell free assay (350 μ M ATP); ^b p38 α IC₅₀ values generated by Lance assay (350 μ M ATP).

The results (Table 26) show that all compounds made were inactive in the enzymatic assay. Although both linkers are capable of making similar interactions, the shape of each moiety is very different. The sulphur centre is tetrahedral whereas the carbonyl sp² centre of an amide is planar. The amide is a conjugated system with partial double bond character. Further conjugation exists with the adjacent indazole and aryl ring systems. Typically, only strong steric effects can force an aromatic ring out of plane with an amide, as the conformation is more favourable when electron density is spread over a larger area, which is only possible in plane.

It is proposed that the planarity of the amide linker compounds **104-110** is a potential reason for the sharp drop in potency and therefore the bend in the molecule (Figure

40) facilitated by the sulphonamide is in part responsible for the potency observed. Modelling data has suggested that the linker portion of the molecule is in close proximity to a Lys39 which is capable of forming an interaction with a hydrogen bond acceptor. It is possible that this interaction is present in the sulphonamide compounds but not in the amides due to the shape of the linker. It is therefore possible that planarity is tolerated and potency is lost only due to the loss of the H-bond interaction.

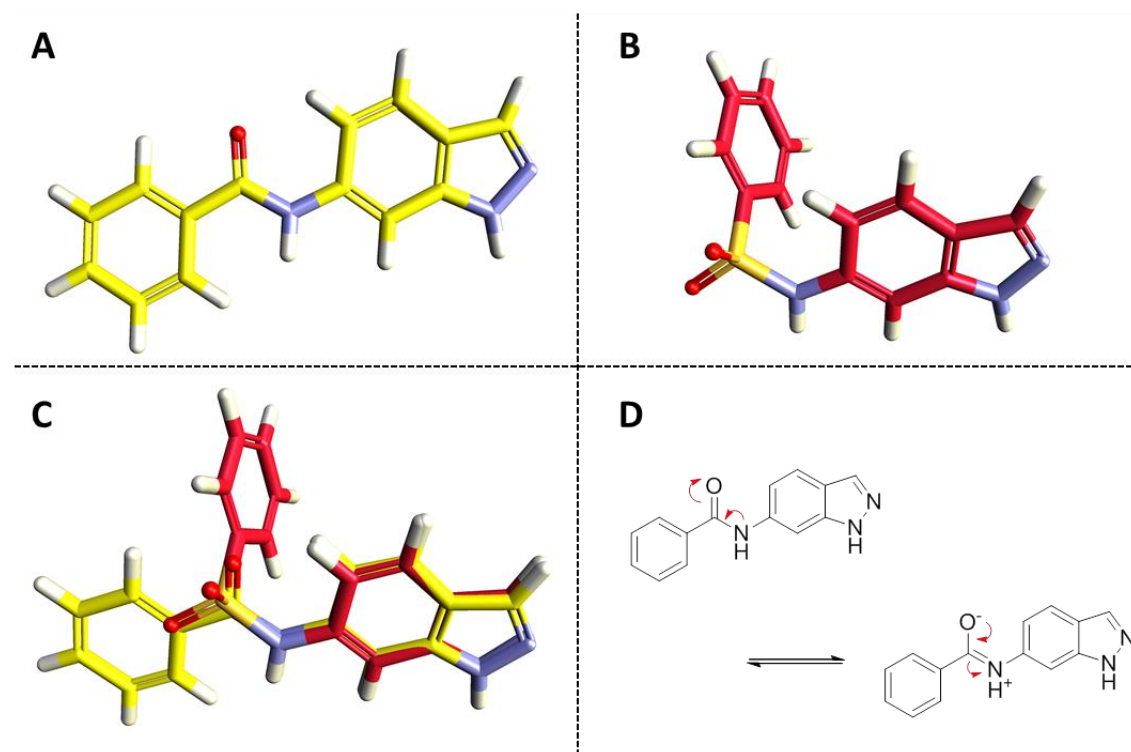


Figure 40. Energetically favourable conformation of: amide (**106**) (A); sulphonamide (**30**) (B); amide(**106**, yellow) and sulphonamide(**30**, red) (C); amide (**106**) resonance (D)

2.5.3 Synthesis and SAR of Cyclised Linker Indazoles

To investigate if the amide linker series of compounds lost potency due to lost hydrogen bonding interactions or the planarity of the molecule a synthetic target was proposed which preserves the planarity of the amide and a tetrahedral linker centre. In light of molecular modelling data (Figure 41) it appears that a pocket may exist that can accommodate an aryl group that is in plane with the indazole. By exchanging the aromatic and linker portion of the molecule, for a benzothiophenedioxide the compound will have a tetrahedral sulphonyl centre and an energetically favourable planar conformation.

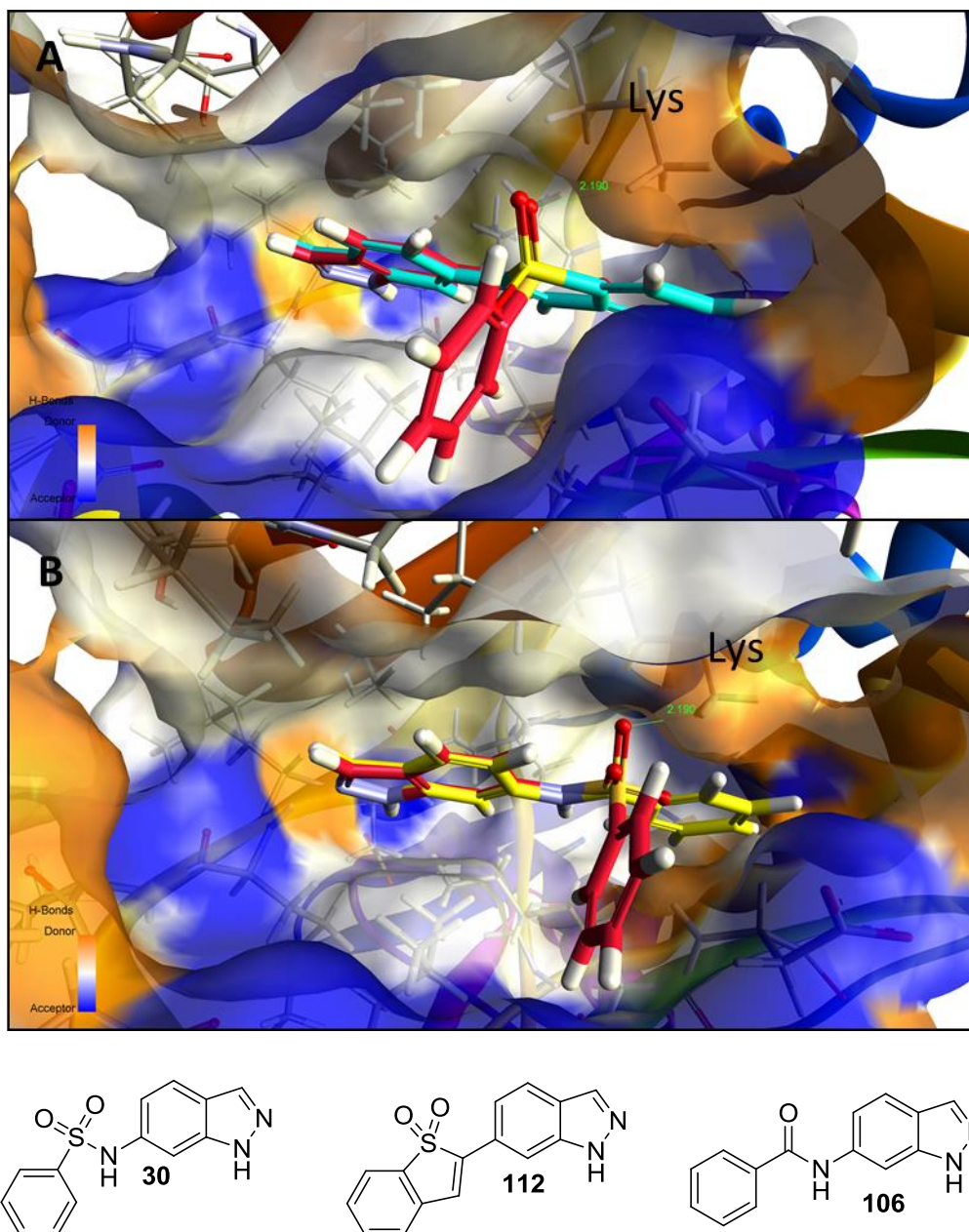
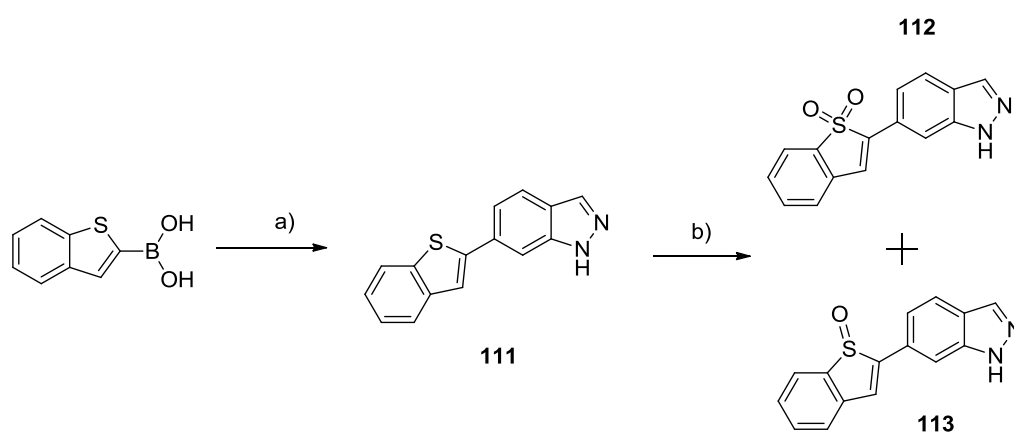


Figure 41. Molecular modelling of compounds **112** (cyan), **30** (red) and **106** (yellow) in the ERK5 active site (PDB: 4IC8) showing the linearity of **112** and **106** in comparison to the 'bent' (more potent) conformation of **30**.

The entropy of a compound can be decreased by making it more conjugated, planar or by reducing the number of rotatable bonds. Kinase inhibitors are generally entropically constrained and highly conjugated¹⁵¹. Cyclisation of the linker in the indazole series reduces the number of rotatable bonds from three to one (not including any rotatable bonds on various aryl-sulphonamide groups). This design change also creates a completely aromatic system with the potential to be entirely planar. By installing a benzothiophene in the 6-position of the indazole and oxidising to the di-oxide a subtle

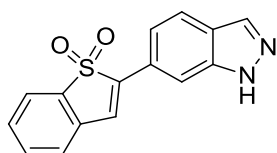
change is made to the compound's physiochemical properties and the placement of functionalities, whilst the conformation is changed significantly.

The compound **111** was synthesised via a Suzuki coupling using 6-bromoindazole and 2-boronic acid benzothiophene to give the product in a good yield, without having to protect the indazole nitrogen (Scheme 12). Compound **111** was oxidised using *m*-CPBA to give the desired sulphone **112** and sulfoxide **113**. The aromaticity of the thiophene ring detracts from the nucleophilicity of the sulphur as one lone pair is delocalised within the ring system. In this case the strong oxidising agent *m*-CPBA was used, which readily oxidises thiophenes to thiophene dioxide.



Scheme 12. Reagents and conditions; a) 6-bromoindazole, Pd(PPh₃)₄, Na₂CO₃, Dioxane, H₂O, μ -wave 110°C, 30mins, (77%). b) DCM, *m*-CPBA, 0°C-RT.

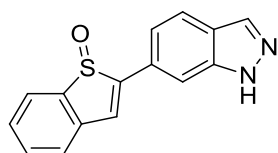
Compounds **112** and **113** were screened for activity against ERK5 and p38 α with all results showing less than 50% inhibition at a concentration of 120 μ M (Figure 42). Although the conformation of compound **112** matches **30** with regard to hydrogen bonding capacity they do not have comparable potency and therefore we can confirm that this class of ERK5 inhibitors require the bend in conformation shown by molecular modelling (Figure 43).



112

ERK5^a; IC₅₀ >120 μM

p38α^b; IC₅₀ > 120 μM



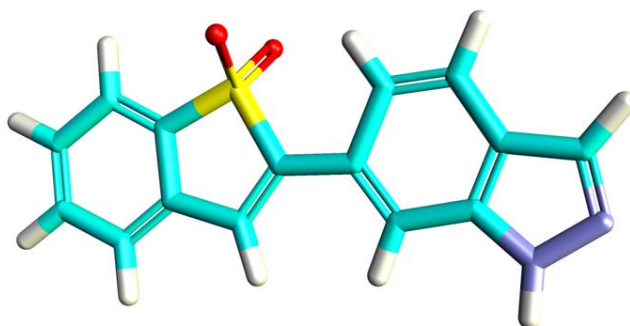
113

ERK5^a; IC₅₀ > 120 μM

p38α^b; IC₅₀ > 120 μM

Figure 42. Activity data for the cyclised linker compounds **112** and **113**. ^a ERK5 IC₅₀ values generated by IMAP cell free assay (350 μM ATP); ^b p38α IC₅₀ values generated by Lance assay (350 μM ATP).

A



B

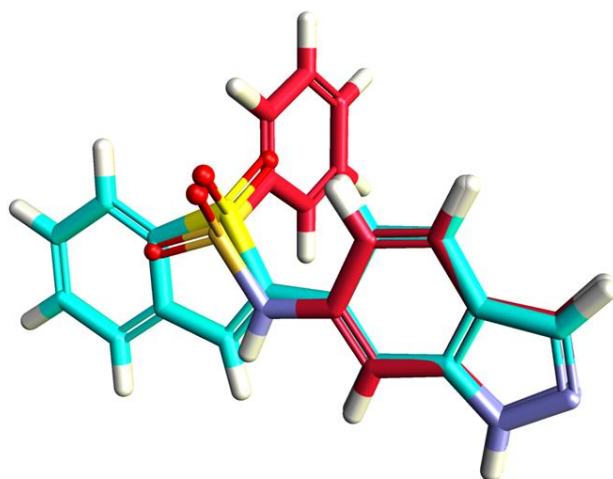


Figure 43. Energy minimised structure of **112** showing the structure to be completely planar (A); overlay of compound **112** (blue) and the more potent compound **30** (red) (B).

2.5.4 Synthesis and SAR of Reversed Indazole-6-Sulphonamide

Having established that linear molecules, such as amides and benzothiophene compounds (Chapter 2.5.2 & 2.5.3), are not potent against ERK5, linker moieties which retain a bent conformation were investigated. A bend can be achieved with a number of groups such as a carbon chain, sulphone, ether as well as a sulphonamide. The physiochemical properties of the molecule are maintained when the sulphonamide is reversed but potentially interacting groups are moved. The reversal of the linker may add additional potency if the binding groups in the linker now find themselves at a preferable proximity or angle to complementing groups in the active site. The positioning of the sulphonamide NH in original hit compounds is known to be unfavourable as methylation improved potency (Table 21, Chapter 2.5.1.1). A small group of compounds were selected based on available materials and previously identified potent aryl groups (Figure 44). Because of the bend in these compounds any interactions made by the indazole and aromatic groups should be retained.

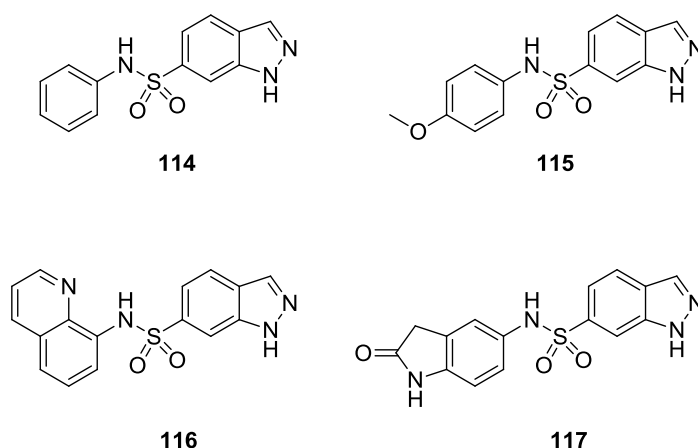


Figure 44. Synthetic targets for reversed sulphonamide series of compounds.

The synthesis of reversed sulphonamides **114-117** required the synthesis of indazole-6-sulphonyl chloride **118**. The sulphonyl chloride can be synthesised from 6-aminoindazole *via* diazotisation followed by variations on the Sandmeyer reaction using either a thiol species or by forming the sulphuryl dichloride/sulphonyl chloride cuprate *in situ* (Figure 45). The latter was chosen as the introduction of the thiol would require oxidation to the sulphonic acid and subsequent conversion into the sulphonyl chloride, which had proved troublesome earlier in the project (Chapter 2.3.1).

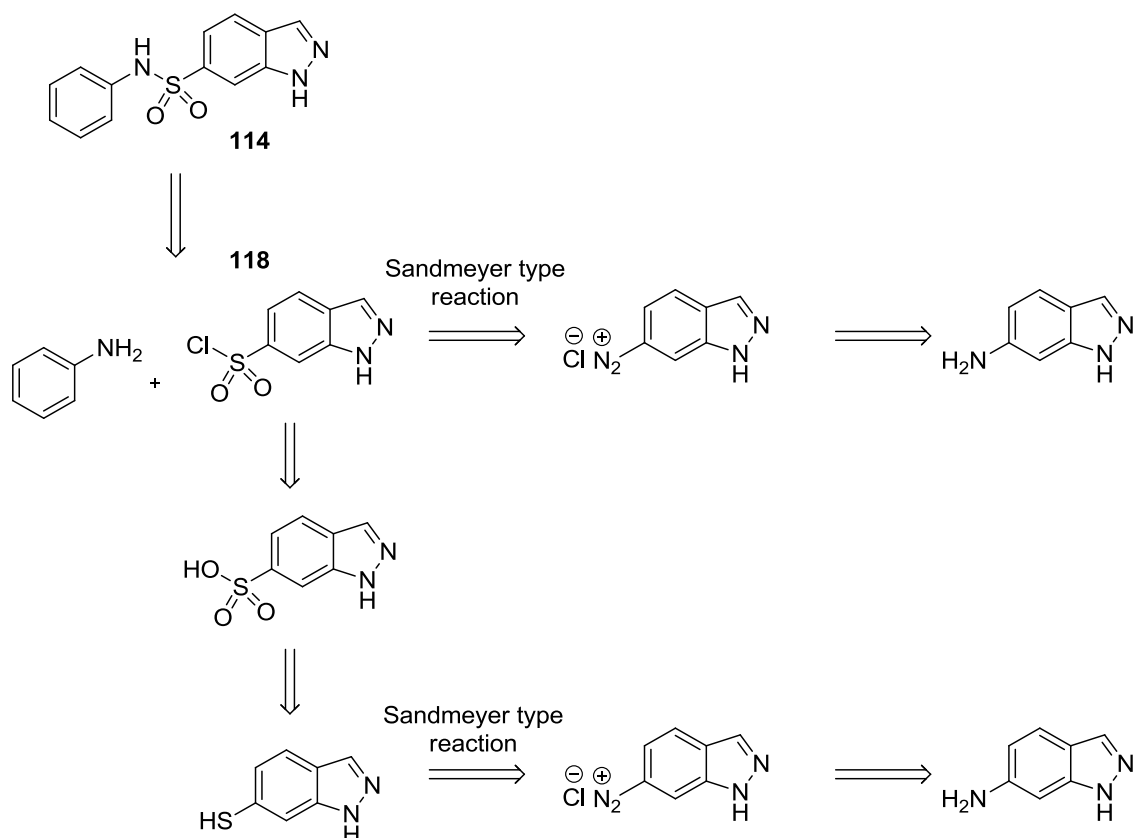
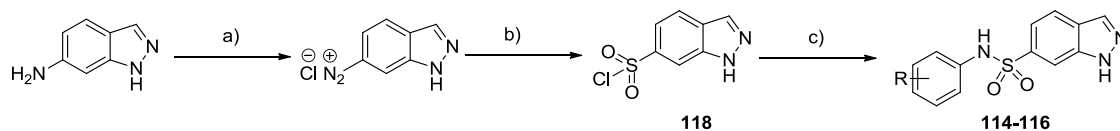


Figure 45. Retrosynthetic approach to reversed sulphonamide compounds.

Using a literature method, the conversion of 6-aminoindazole was undertaken *via* diazonium formation followed by chlorosulfonylation and sulphonamide formation (Scheme 13)¹⁵²⁻¹⁵⁵. This series of reactions was conducted without isolation of intermediates due to their reactivity. Diazonium formation was conducted in concentrated HCl with the minimum amount of water used to dissolve the sodium nitrite. The presence of the diazonium ion was confirmed by disappearance of the starting material peaks on both TLC and LCMS and with potassium iodide-starch paper (liberation of iodine on contact with an oxidising agent causes a dark blue colour when it chelates to starch, this is triggered by the presence of diazonium species). Diazonium salts pose an explosion risk at temperatures in excess of 10°C as diatomic nitrogen is released triggering a dramatic increase in volume. These temperamental materials were not allowed to crystallise and were kept chilled unless in the reaction mixture of the following step. Isolation of the diazonium is possible as a tetrafluoroborate salt which can be stable at room temperature.

Once all the starting material had been converted into the diazonium-chloride salt, the solution was added to a pre-saturated solution of sulphur dioxide in acetic acid with

copper(II) chloride and SO₂ gas was continuously driven through the reaction mixture. Sulphonyl chlorides are unstable in aqueous conditions, forming the sulphonic acid if not properly temperature or pH controlled. For this reason the sulphonyl chlorides were freshly synthesised for each aniline coupling.



Scheme 13. Reagents and conditions; a) HCl, NaNO₂, H₂O, 0°C, 1h; b) SO₂, CuCl₂, AcOH, RT, 1h; c) Pyridine, RNH₂, THF, RT, 3h (5-11% over three steps)

Formation of 6-chloroindazole (**119**) was observed as an undesired product. This material was formed in roughly a 10% yield using CuCl₂. This reaction goes via a Sandmeyer reaction mechanism which is typically used for the conversion of anilines to halogenated aromatics.¹⁵⁶ Optimisation of the reaction was undertaken by varying the copper species. The use of Copper(I) chloride, copper(II) chloride and copper(II) chloride dehydrate, however, resulted in no significant difference and copper(II) chloride became the reagent of choice only due to slightly improved conversion to the product irrespective of side products.

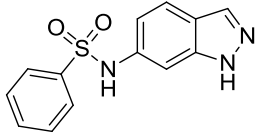
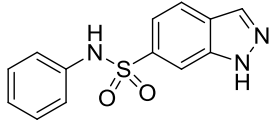
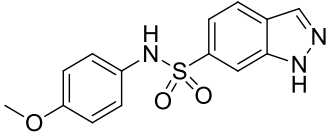
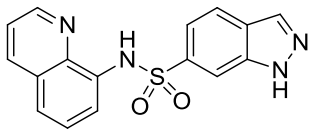


Scheme 14. Sandmeyer side reaction.

Sulphonyl chloride (**118**) formation is estimated to have been achieved in yields under 50% based on crude material isolated. An attempt to purify this material was made by chromatography on silica, however, it was found that significant amounts of material were lost and purification was not optimised.

Crude materials were used directly in the sulphonamide formation (Scheme 13) and products were formed with the overall yields shown in Table 27.

Table 27. Yield and activity data for the reversed linker compounds synthesised.

Compound	Structure	Overall yield (%)	IC ₅₀ (μM)	
			ERK5 ^a	p38α ^b
30		-	4.7 ± 0.04	120
114		6	32 ± 3	>120
115		11	>120	>120
116		5	>120	>120

^a ERK5 IC₅₀ values generated by IMAP cell free assay (350 μM ATP); ^b p38α IC₅₀ values generated by Lance assay (350 μM ATP).

The ERK5 IC₅₀ results illustrate that the reversed linker provides no benefit and that the superior isomer is in fact the more straight forward to synthesise. Measureable potency was seen for compound **114**, however, this is almost 7-fold less active than the isomer **30**, which has an IC₅₀ of 4.7 μM against ERK5 and therefore reflects the loss of one strong interaction. Modelling predictions show that these compounds are not able to form the important interaction with Lys39, even though the general shape of the molecule is very similar (Figure 46). The sulphonyl group of compound **114** (Figure 46, gold) is too far away from the Lys residue, even with flexibility of this residue simulated. If this set of reversed linker compounds had given high potency the next stages of SAR development would have proceeded through N-methylation and CH₂ replacement as well as the reversed amide isosteric replacement. However, this work becomes redundant based on these results.

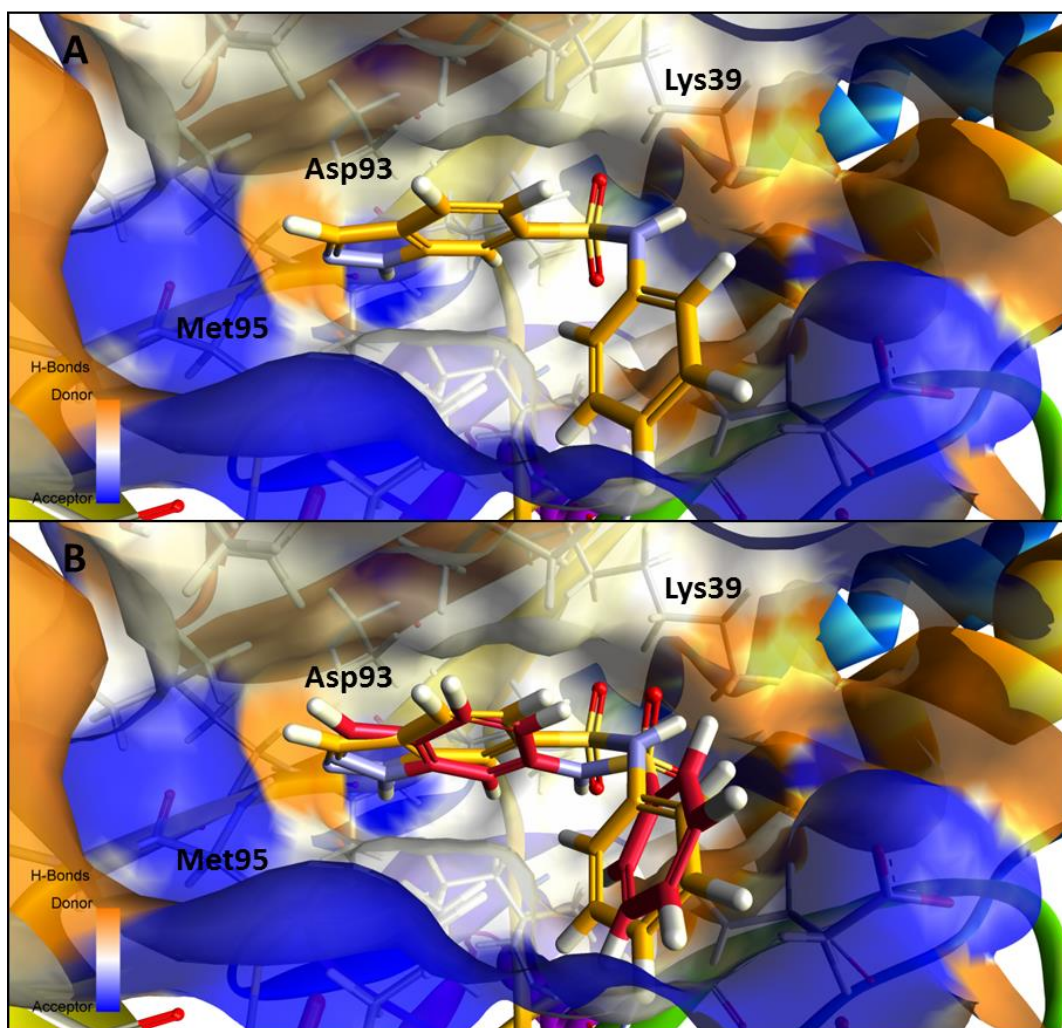


Figure 46. Molecular modelling of compounds in the ERK5 active site; A, Compound **114** (gold); B, Compound **114** (gold) and compound **30** (red) (PDB: 4IC8).

Synthesis of the reversed sulphonamide oxindole compound (**117**) was not completed due to low yielding steps and prioritisation of other series. Based on the results obtained (**114-116**, Table 27) good potency from compound **117** would have meant that the oxindole was able to make the key hinge interaction in place of the indazole which is also likely to be tolerated in the aryl pocket. However, modelling data has shown that this is unlikely (Figure 47).

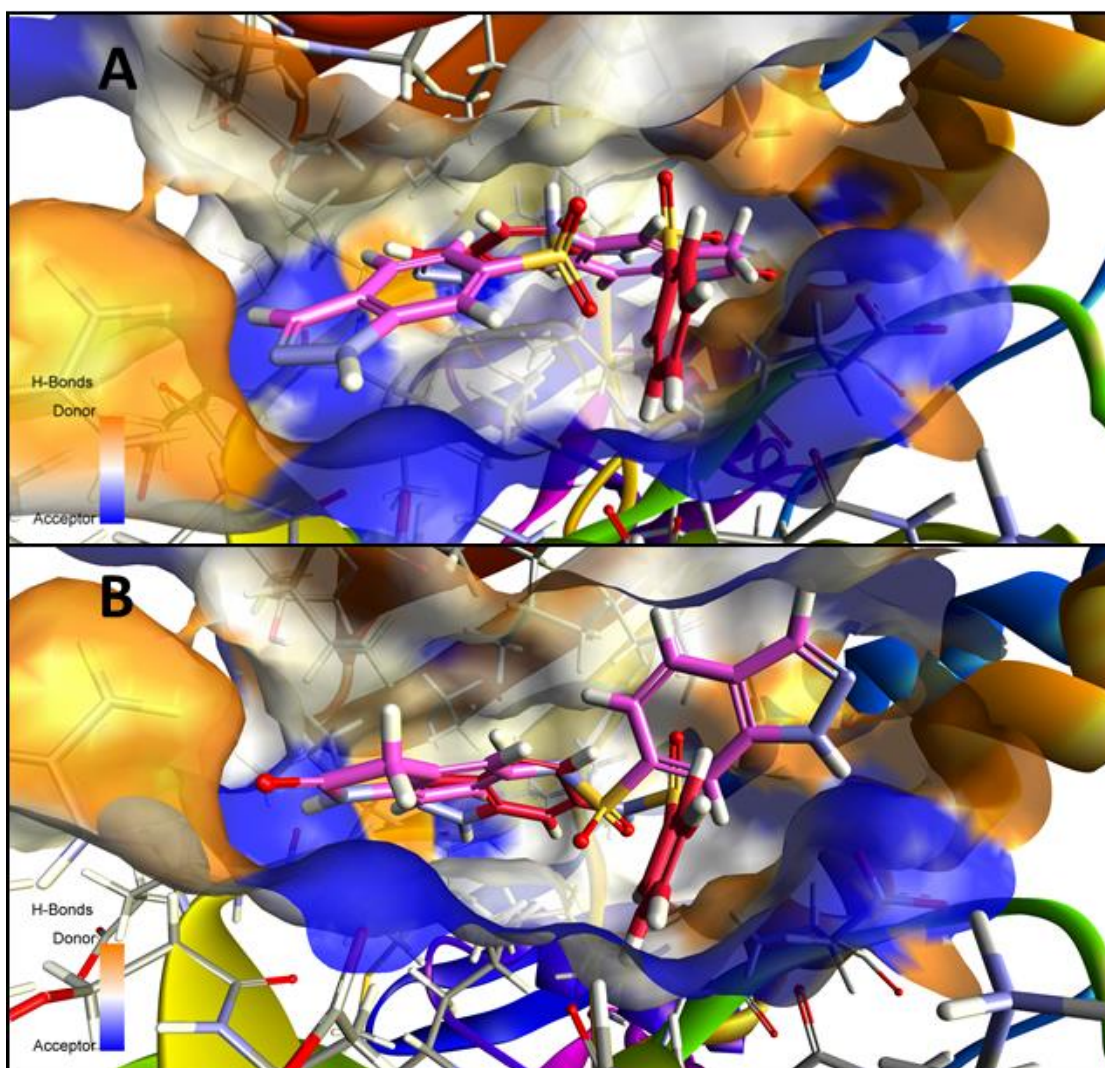


Figure 47. Modelling images of compound **117** (pink) in two suggested poses showing very abstract conformations from the assumed potent conformation of **30** (red); A and B.

Two *in silico* binding solutions of compound **117** are shown in Figure 47, neither of which show similar binding to compound **30** (the solutions shown (Figure 47, pink) are representative of the whole dataset). If the two compounds showed similar hinge binding then it is possible that compound **52** would have two binding modes. However, This theoretical result suggests that the oxindole compound **52** has good potency because of binding in the aryl pocket and not a dual binding mode.

2.5.5 Synthesis and SAR of 6-Sulphone indazoles

2.5.5.1 Synthetic targets

Investigation into the sulphonamide linker has shown that the NH is redundant in compound binding and that N-Me sulphonamides conveyed better potency than the

un-methylated analogue (Chapter 2.5.1.1). Permutations of the linker such as reversal, isosteric replacement, cyclisation and alkylation did not yield an improvement to potency over the *N*-methylated sulphonamide. It is clear that an exploitable, lipophilic pocket or hydrogen bond acceptor is not present at this location in the active site. Exchange of the sulphonamide nitrogen for a carbon in the linker remained to be explored. This linker maintains the bent conformation in the molecule proven necessary from the planar molecules synthesised (Chapter 2.5.2 and 2.5.3) and the positioning of the sulphonyl groups to make the interaction with Lys39. Previously identified, potent aryl groups were selected for incorporation into the molecule when starting materials were available (Figure 48).

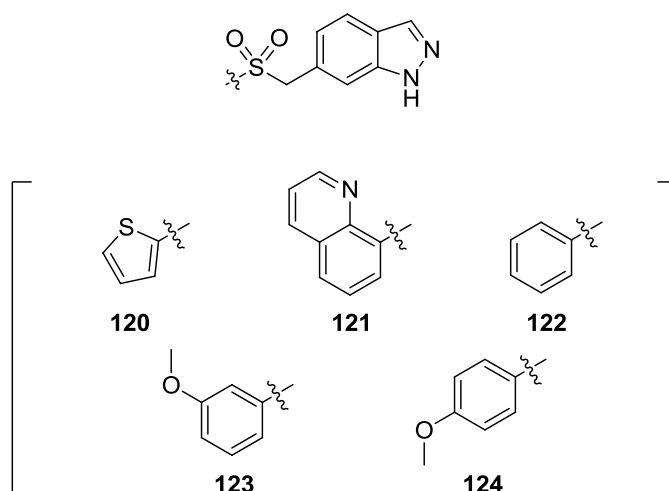


Figure 48. Synthetic targets incorporating sulphone linker.

2.5.5.2 Synthesis of 6-Sulphone Indazoles

Target sulphone compounds (Figure 48) were synthesised using a four step synthesis (Scheme 15). 1*H*-Indazole-6-carbaldehyde was reduced to the alcohol (**125**) using sodium borohydride in a high yield and short reaction time. Two different bromination procedures were trialled using PBr_3 or SOBr_2 as the bromine sources with the latter found to be preferable. The bromination of hydroxyl groups to alkyl bromides has been described in the literature using catalytic DMF and also without DMF for the conversion of phenol groups. However, omission of DMF from this reaction significantly reduced product formation over the 4 hour reaction time.^{157,158} The increased reaction rate in the presence of DMF was therefore attributed to the formation of a Vilsmeier type reagent (Figure 49). This is contrary to the proposed

mechanism of Nagle *et al* which describe a nucleophilic attack on the thionyl group to release the bromo anion.¹⁵⁷

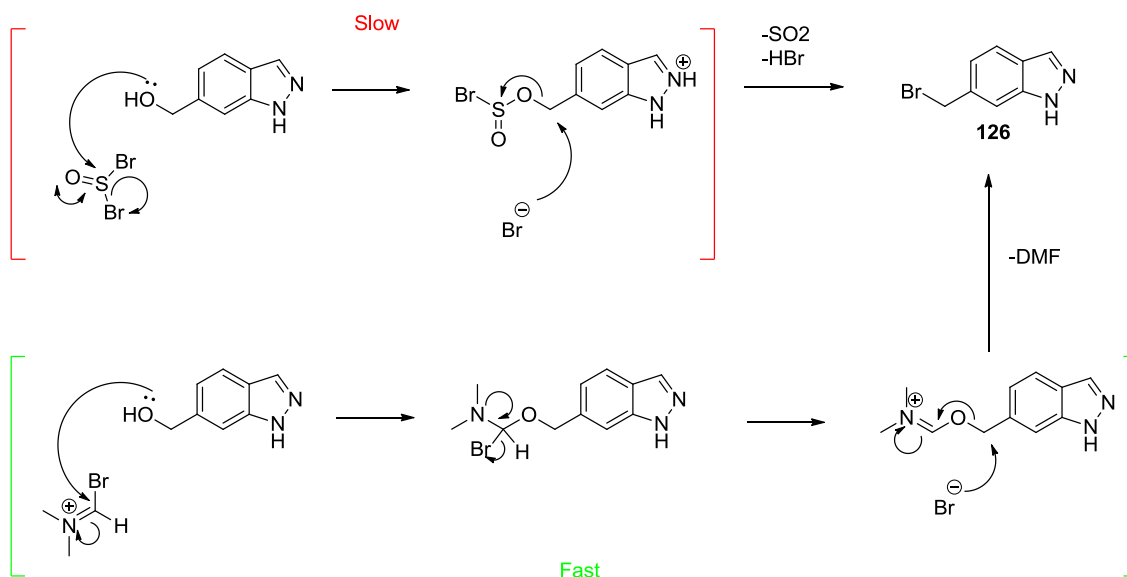
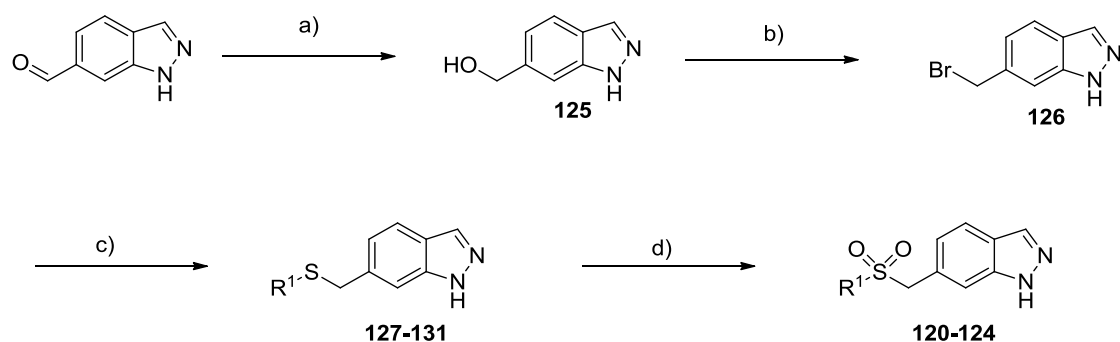


Figure 49. The proposed mechanism for bromination using SOBr_2 with (green) and without (red) DMF on the hydroxy indazole.

A one step indium/zinc mediated coupling reaction was identified for the formation of the sulphone using the benzylic bromide species and sulphonyl chlorides. However the procedure was found to be unrepeatable after testing multiple conditions.^{159, 160} The bromo-indazole was also treated with magnesium to perform a Grignard reaction, as a literature precedent for reaction on sulphonyl chlorides exists, but unfortunately none of the desired product was formed.¹⁶¹ The conversion of sulphonyl chlorides to sodium sulfinates was also conducted to then combine with bromo-indazole material.


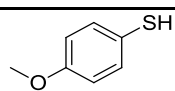
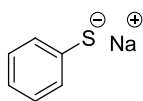
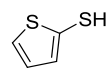
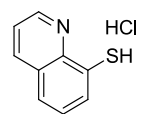
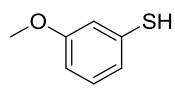
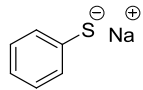
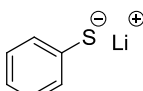
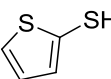
However, a model reaction of this was not successful and therefore an alternate scheme to form the sulphone *via* a thioether was chosen (Scheme 15).¹⁶² This new scheme beneficially, facilitated the synthesis of a number of secondary targets (Chapter 2.5.5.4 & 2.5.5.5).



Scheme 15. *Reagents and conditions;* a) NaBH_4 , EtOH, RT, 3h, 86%. b) SOBr_2 , DMF, DCM, 0°C -RT, 4h, 92%. c) $\text{R}^1\text{-SH}$, NaOH, TBAB, H_2O , Toluene, RT, 18h, 36%. d) KHSO_5 , MeOH, H_2O , RT, 18h, 19-72%.

The $\text{S}_{\text{N}}2$, thioether formation conditions shown in Scheme 15 are biphasic utilising the phase transfer catalyst tetrabutylammonium bromide (TBAB). Although the desired products were formed, solubility was an issue in this reaction when thiol species were varied. Further optimisation has taken place when this thioether formation was revisited during synthesis of later targets yielding the desired products in a faster reaction time and in repeatable yields. Optimisation of this reaction is shown in Table 28 illustrating where compounds relate to this set of targets.

Table 2. Optimisation of S_N2 reaction with various aromatic thiols.

				
	R ⁴	Substrate (R ¹)	Conditions	Yield (Conversion by LCMS)
1	H		NaOH, EtOH	42%
2	H		EtOH	48%
3	H		CsCO ₃ , THF	35%
4	H		Toluene, H ₂ O, TBAB, NaOH (2.2 eq)	36%
5	H		NaOH, H ₂ O	20%
6 ^a	Br		Toluene, H ₂ O, TBAB,	(5%)
7 ^a	Br		DMF	28%
8	Br	 1M in THF	THF	66%
9	Br		CsCO ₃ , DMF	92%
10	Br		K ₂ CO ₃ , DMF	78%
11	Br		Pyridine	92%

All reactions were conducted at room temperature.^a Sodium thiophenolate had degraded and was therefore responsible for the low yield.

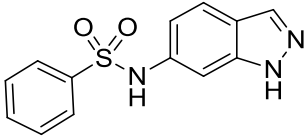
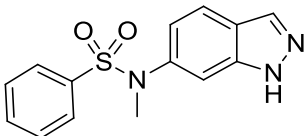
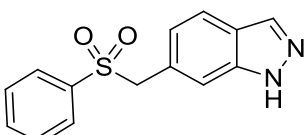
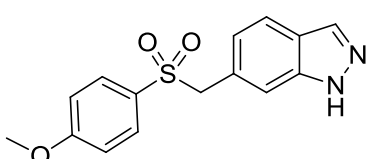
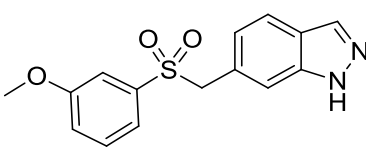
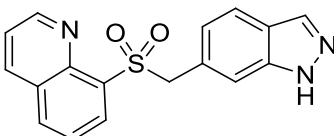
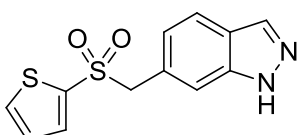
The yield increase is explained by the solvation of all reagents in one reaction solvent and therefore the more efficient mixing of materials. Yields were low in water and ethanol presumably due to a side reaction in which a hydroxyl group is added or the ethyl ether is formed, both of which form an unreactive by-product. In the last three reactions (9-11) an aprotic base and solvent were used which reduced the risk of side reactions completely. A small assessment of base solubility in DMF and acetonitrile was done with the former proving superior and therefore used.

For the final oxidation step of the thioether to the sulphone, two sets of conditions were considered using potassium permanganate or potassium peroxymonosulfate (Oxone®)¹⁶³. The use of Oxone® prevailed due to the handling requirements and the reaction progress which facilitated, in some cases, the isolation of the sulphone and sulfoxide species which were desired as a secondary targets.

2.5.5.3 SAR of 6-Sulphone Indazoles

The sulphone compounds in Table 29 all have good potency between 2.2 – 0.59 μM which is directly comparable to the corresponding *N*-Me sulphonamides which have a similar range (3.2-0.45 μM). all these compounds can be regarded as equipotent and therefore prove that the unique properties of the nitrogen, such as the H-bond acceptor capacity or the influence it has on the electronics of the rest of the compound, play no role in binding to the ERK5 active site. The ERK5 IC₅₀ values show, explicitly, that the sulphonamide nitrogen is not required for potency.

Table 29. Activity data of sulphone compounds **120-124** compared to sulphonamides **30** and **82**.

Compound	Structure	IC ₅₀ (μM)	
		ERK5 ^a	p38α ^b
30		4.7 ± 0.04	>120
82		1.1 ± 0.6	>120
122		0.91 ± 0.15	>120
124		0.71 ± 0.25	>120
123		2.2 ± 0.2	>120
121		0.59 ± 0.07	>120
120		1.1 ± 0.2	>120

^a ERK5 IC₅₀ values generated by IMAP cell free assay (350 μM ATP); ^b p38α IC₅₀ values generated by Lance assay (350 μM ATP).

These compounds are assumed to mimic the conformation of the sulphonamide derivatives giving similar bond angles and therefore occupying the same space in the active site. A molecular modelling overlay of compounds **30** and **122** in the binding pocket illustrates the similarity in conformation (Figure 50).

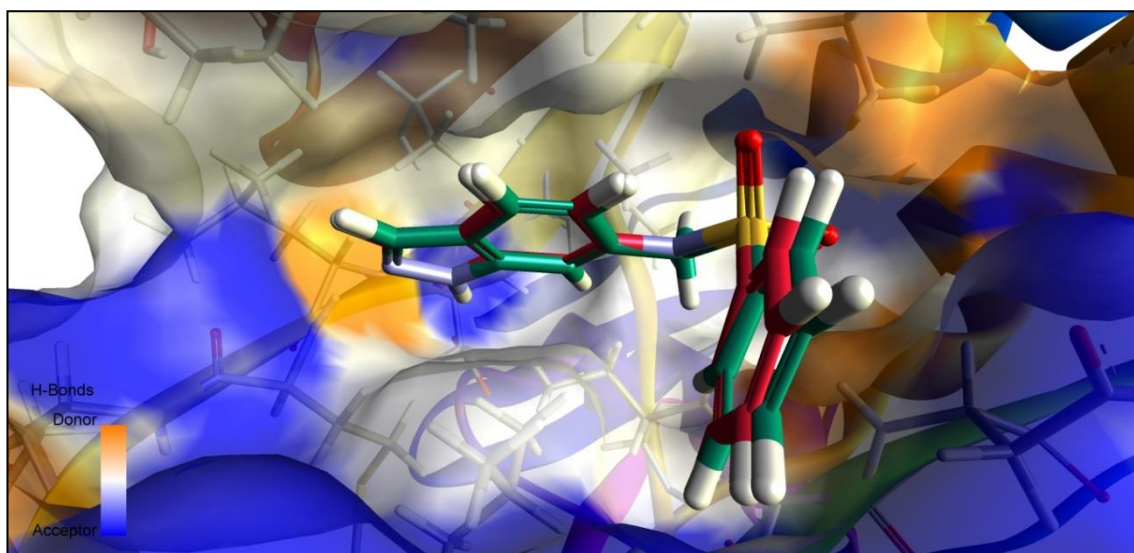
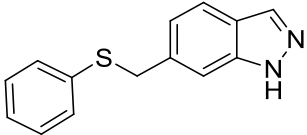
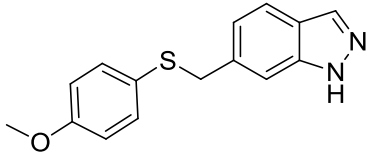
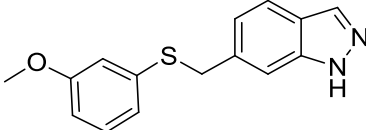
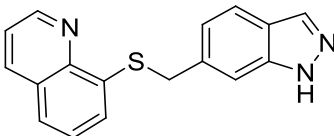
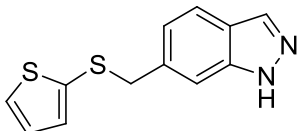


Figure 50. Overlay of compound **30** (red) and **122** (teal) in the ERK5 active site showing almost identical binding conformations. (PDB: 4IC8).

2.5.5.4 SAR of 6-Thioether Indazoles

Thioethers (**127-131**) from Scheme 15 were also tested for potency showing complete inactivity except for one example, **130** (Table 30). These results suggest that a key interaction must exist between Lys39 and at least one sulphonyl group.

Table 30. Activity data of thioether compounds **127-131**.

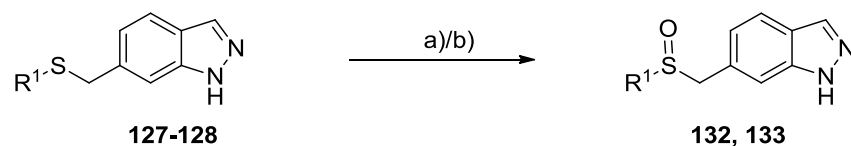
Compound	Structure	IC ₅₀ (μM)	
		ERK5 ^a	p38α ^b
127		>120	>120
128		>120	>120
129		>120	>120
130		17 ± 1	>120
131		>120	>120

^a ERK5 IC₅₀ values generated by IMAP cell free assay (350 μM ATP); ^b p38α IC₅₀ values generated by Lance assay (350 μM ATP).

2.5.5.5 Synthesis and SAR of 6-Sulphoxide Indazoles

Synthesis of sulphoxide linker compounds was possible by slight modification of the sulphone synthesis (Scheme 16). Sulphoxide compound **132** and sulphone compound **122** were isolated from the same reaction by terminating the Oxone® oxidation before complete conversion. It was found that conversion of thioethers to sulphoxides was quicker than the subsequent oxidation to the sulphone and therefore compounds **132** and **122** were isolated without any unreacted starting material present in the reaction mixture. Compound **133** was synthesised from thioether **128** using sodium periodate

which oxidises only to the sulfoxide due to the reduced nucleophilicity of the sulphur and reactivity of the oxidising agent.¹⁹



Scheme 16. Reagents and conditions; a) KHSO₅, MeOH, H₂O, RT, 18h, 45% (**132**). b) NaIO₄, MeOH, 0°C-RT, 18 h, 80% (**133**).

Table 31. Activity data of sulfoxide compounds **132** and **133**.

Compound	Structure	IC ₅₀ (μM)	
		ERK5 ^a	p38α ^b
132		15 ± 3	>120
133		14 ± 2	>120

^a ERK5 IC₅₀ values generated by IMAP cell free assay (350 μM ATP); ^b p38α IC₅₀ values generated by Lance assay (350 μM ATP).

The hybridisation of the sulphur atom in the linker gives a tetrahedral shape which as the sulfoxide forms a stereocentre. Sulfoxides do not readily invert and therefore give stable a racemic mixture at room temperature. All results gathered are for unresolved mixtures in ca. 1:1 ratio. Activity data shows that at least one isomer is capable of making a hydrogen bond through the sulfoxide group to Lys39 whilst the other has reduced activity. Molecular modelling suggests that only one interaction is made through a salt bridge to Lys39 (Figure 51). The area that would be occupied by the second oxygen is an open area with very little activity to be gained. It is possible that one enantiomer would have better potency than the equivalent sulphone compound.. However, the additional oxygen in the sulphone may align the compounds in a more favourable conformation and also affects the electronics on the adjacent aromatic. Neither of these postulations has been further investigated by resolving the racemic mixture and repeating the assay.

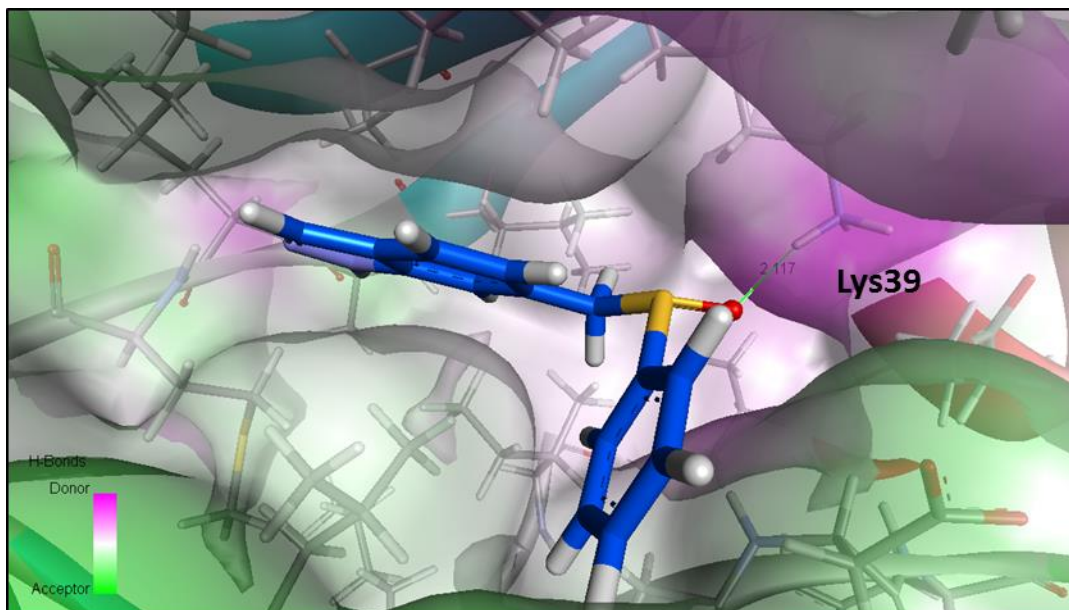


Figure 51. Proposed binding of the sulfoxide compound (**132**) showing an interaction with Lys39 (PDB: 4IC8).

The sulphone linker compounds show that the oxidation of the sulphone is critical and as a result this scaffold has been used to develop further SARs elsewhere on the molecule.

2.6 Synthesis and SAR of 5-Substituted Indazoles

The 5-position of an indazole is the most reactive to electrophilic aromatic substitution due to the conjugation with the heteroatom lone pairs. This means that synthesis of compounds substituted at this position is well described. The targets here proposed are isomers of the potent compounds **82-89** with *N*-methylated sulphonamide linker. Both 5 and 6-substituted indazoles project into similar space in the active site and the new targets have the potential to make the crucial interaction with Lys39. This set of target compounds can be viewed in two ways (Figure 52). If the linker interaction is conserved in compound binding the flipped indazole may find a new interaction with the hinge region of the active site which contains numerous, exposed H-bonding sites. Without a crystal structure it can only be speculated which binding mode, if either (Figure 52), is adopted even with the aid of molecular modelling.

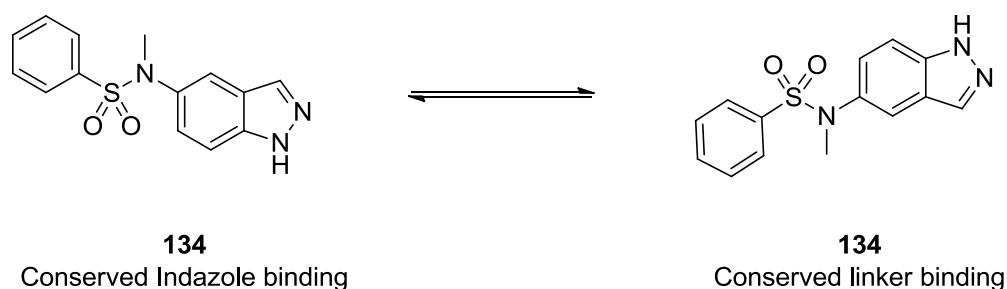
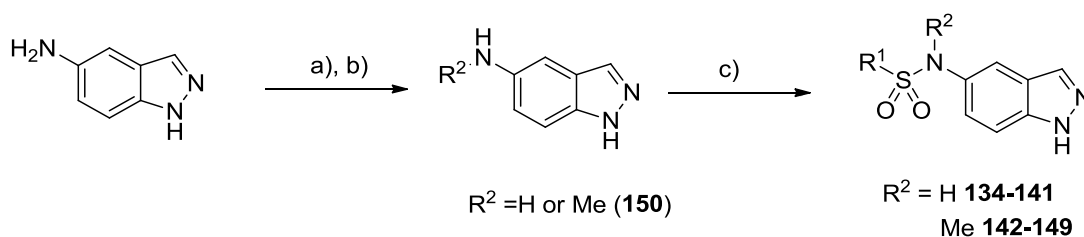


Figure 52. Proposed binding modes of 5-substituted indazole **134**.

2.6.1 Synthesis of 5- Substituted Indazoles

Synthesis of compounds (**134-149**) was performed in an analogous procedure to the 6-position sulphonamides (Scheme 17). By allowing longer for the amination and subsequent reduction, *N*-methyl-1*H*-indazol-5-amine (**150**) was obtained in a higher yield (62%) compared to *N*-methyl-1*H*-indazol-6-amine (**90**, 38%) made when synthesising the 6-position analogues.

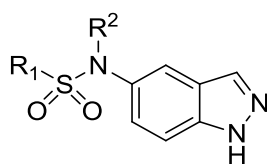


Scheme 17. Reagents and conditions; a) paraformaldehyde, NaOMe, MeOH, RT, 18h, b) NaBH_4 , 60°C , 5h (62% over two steps), c) Pyridine, THF, $\text{R}^1\text{-SO}_2\text{Cl}$, RT, 3h (50-80%).

2.6.2 Activity of 5-Substituted Indazoles

Methylated and unsubstituted sulphonamide compounds were submitted to the ERK5 assay to ascertain the role of the sulphonamide NH in this modified series. Table 32 shows activity data for both linker types with variation at R^1 .

Table 32. Enzymatic activity data of sulphonamides **134-141** and *N*-methyl sulphonamides **142-149** against ERK5 and p38 α .



Compound	R ¹	R ²	IC ₅₀ (μM)	
			ERK5 ^a	p38 α ^b
134		H	30 ± 6	>120
142		Me	4.7 ± 0.46	>120
135		H	4.1 ± 0.3	>120
143		Me	3.1 ± 1.5	>120
136		H	6.4 ± 0.1	>120
144		Me	4.1 ± 0.1	>120
137		H	82 ± 14	>120
145		Me	23 ± 1	>120
138		H	46 ± 6	>120
146		Me	31 ± 4	>120
139		H	51 ± 4	>120
147		Me	10 ± 1	>120
140		H	75 ± 7	44 ± 8.6
148		Me	24 ± 3	>120
141		H	27 ± 4	>120
149		Me	8.6 ± 1.0	>120

^a ERK5 IC₅₀ values generated by IMAP cell free assay (350 μM ATP); ^b p38 α IC₅₀ values generated by Lance assay (350 μM ATP).

Potency of the *N*-methylated derivatives **142-149** is comparable to the 6-position analogues but overall the series has suffered a 10-fold loss in potency and no single analogue is more potent in the 5-position series than the 6-position. As seen with *N*-methylated 6-sulphonamides the introduction of the small alkyl group improves

potency for all 5-sulphonamide matched pairs. This trend suggests that the sulphonamide interaction is retained and the indazole hinge binding is modified. If the same hinge interaction between the indazole and protein were retained, the alkylation of the sulphonamide should have little effect on potency as the group projects towards solvent when simulated.

Molecular modelling in this instance does not entirely agree with the binding mode suggested as the R¹ aromatic does not occupy the same space in **82** as it does in compound **142** (Figure 53). An interaction may exist with Lys39 and the linker as flexibility of this residue was included in the docking study but is not visualised in Figure 53. Regardless of the mode, this set of compounds has not changed the lead compound as both potency and the binding score from GOLD are inferior to the matched pairs of the 6-position sulphonamide compounds.

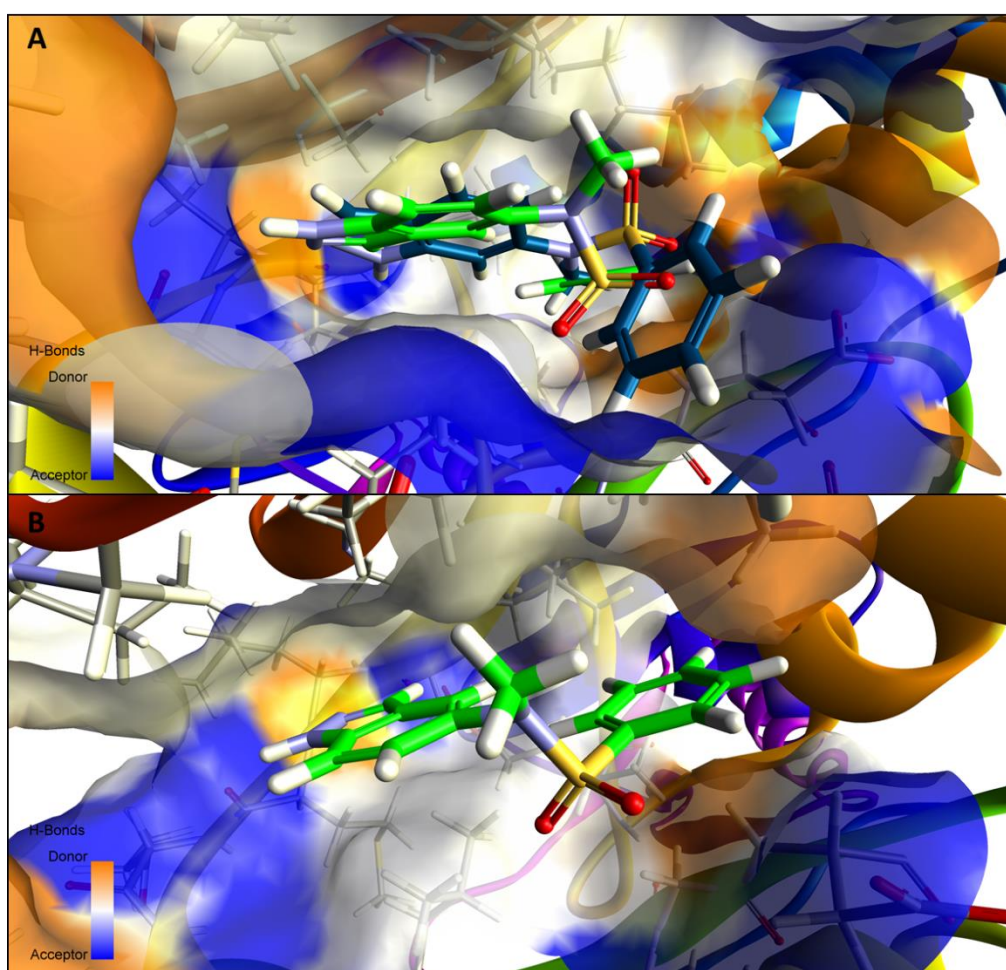


Figure 53. A) Molecular modelling of compounds **142** (green) and **82** (blue) in the ERK5 active site showing the hinge binding of **142** is not consistent and with the established binding mode. B) conformation of compound **142** (green) alone in the ERK5 active site. (PDB: 4IC8).

2.7 4,6- and 3,6- Disubstituted Indazoles

The SAR of the indazole and linker interactions are now well established (Figure 54), revealing the hinge binding between the indazole and ERK5, and the interaction between sulphonyl functionalities and Lys39 in the active site. A number of potency providing, sulphonamide aryl groups have been identified but no unifying properties exist regarding electronics or size. Further potency may be gained by substitution of other positions around the indazole. Substitution of the indazole 1-position (compound **75**) showed complete loss of potency as the hinge interaction was disturbed. Investigation of the 5-position showed that there may be room in this area, although it is likely that when both the 5- and 6-positions are substituted the sulphonyl linker interaction will be reduced in strength, due to steric effects of the adjacent substitution. The 7-position, according to molecular modelling, directs towards confined space in the active site and is not expected to yield potency through substitution. Both the 3- and 4-positions point into open space with part of the ERK5 active site in close proximity and therefore it was predicted that potency could be gained by substitution at either position.

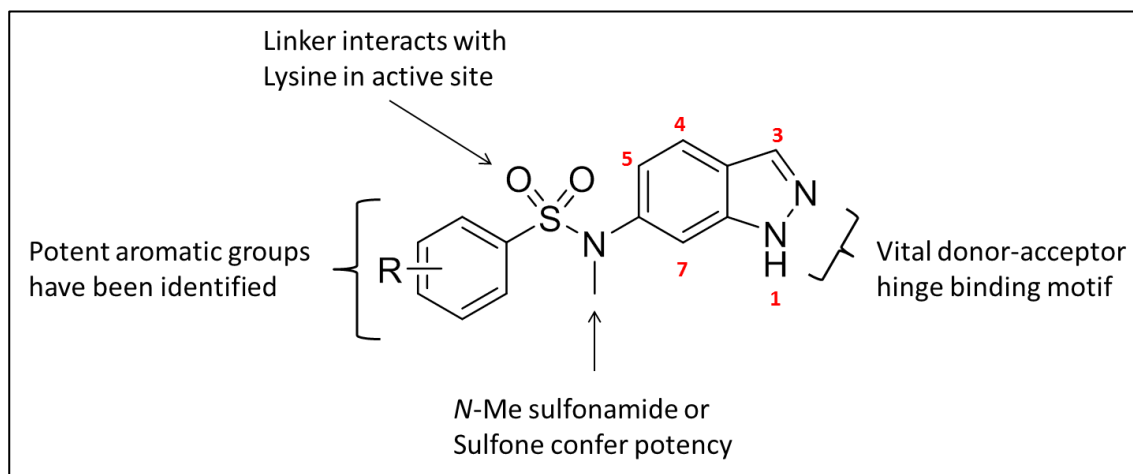


Figure 54. SARs developed in previous chapters.

Existing indazole based kinase inhibitors are frequently di-substituted and commonly the 3-position is occupied, such as in axitinib (**19**, Figure 24). The proposed binding mode of lead indazole compounds is typical of kinase inhibitors. A strong hinge binding interaction is present in almost all marketed kinase inhibitors. This area of the enzyme active site is rich in functionalities capable of hydrogen bonding, usually through the

amino acid backbone. Molecular modelling of lead compounds suggests that the 3-position of the indazole directs along the hinge region in good proximity to install polar substituents and form an additional hydrogen bond (Figure 55). Incorporation of a hydrogen bond donor-acceptor-donor motif is likely to be potent in a large number of kinases thus reducing the selectivity of the series. This is largely because the motif is replicated in the binding of ATP.

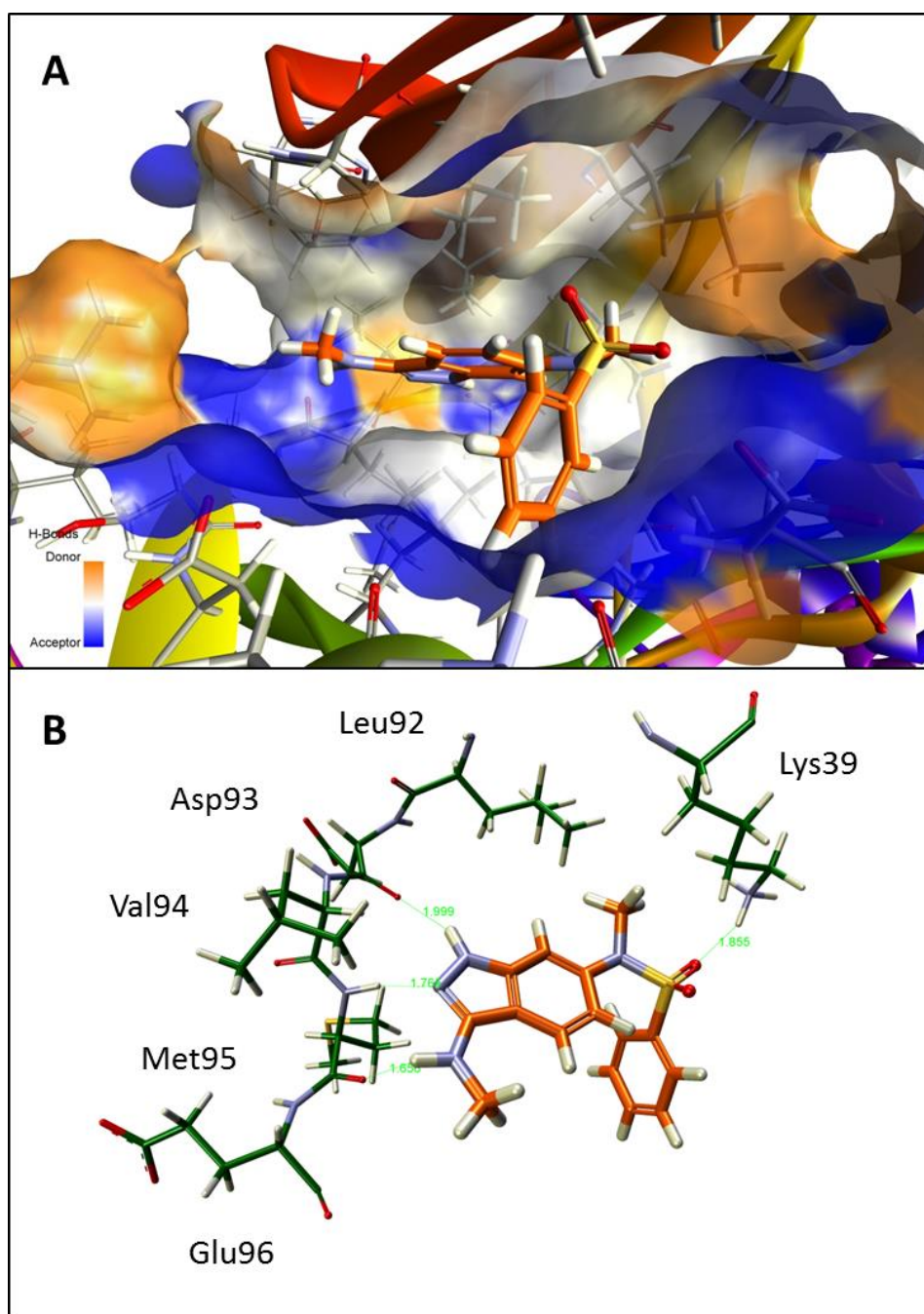


Figure 55. Molecular modelling image of *N*-methyl-*N*-(3-(methylamino)-1*H*-indazol-6-yl)benzenesulfonamide **232** (orange) in the ERK5 active site (A) and in selected binding residues (B).

The 4-position, according to molecular modelling, projects towards the ceiling of the active site in the direction of solvent (Figure 55). The space around this position suggests that alkyl or hydrophobic groups should be well accommodated but further out towards solvent, polar functionalities may be beneficial. The ceiling of the site is the glycine rich loop which is known to be highly flexible and therefore predicting anything but a broad interaction here is not possible. A valine residue sits over the indazole 4-position surrounded by other similar alkyl amino acid residues, therefore, the first set of groups to probe this position were a set of progressively larger alkyl groups.

2.8 Substitution on the Indazole 4 & 6-Positions

2.8.1 Molecular Docking of 4,6-Substituted Indazoles

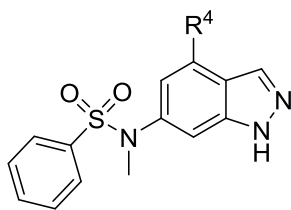
Using the described crystal structure of ERK5, potential synthetic targets were docked into the active site using 'GOLD' docking software.¹⁶⁴ The docking study was run to a high efficiency with *ca.* 12 poses simulated for each compound. The active site was treated as rigid for the study with the exception of Lys39 which was permitted free rotation. Data generated by the programme indicates which compounds make the strongest interactions with ERK5, but results are not as accurate as measured activity in the biochemical assay. The GOLD fitness score is an amalgamation of all scoring functions provided by the program to give a high score designed to reflect compound binding enthalpy (scoring breakdown shown in Table 33). All compounds chosen are synthetically plausible and include the *N*-methyl sulphonamide.

Table 33. GOLD Molecular docking scoring functions.

Score function	Explanation
Fitness	Total fitness value of docked ligand (combination of all other scores)
PLP	All other piecewise linear potential (PLP) terms plus chemscore clash and internal energy term
PLP-Part H-Bond	Protein to ligand H-bond score - A hydrogen bond is deemed to be present if the distance between the acceptor and the donor heavy atoms are within the range $2.85 \text{ \AA} \pm 0.45$, the acceptor angle is within $145^\circ \pm 65$ and the donor angle is within $115^\circ \pm 40$.
PLP-Part Buried	Buried interaction types i.e. H-bond donor/acceptor of either protein or ligand buried in a non-polar region of the corresponding structure.
PLP-Part Non-Polar	Non-polar interactions e.g. lipophilic
PLP-Part Repulsive	Repulsion between protein and ligand
PLP-Ligand clash	Penalty of protein and ligand clash
PLP-Ligand torsion	Penalty for unfavourable internal ligand torsion angles
Chemscore H-Bond	Alternate Protein-ligand H-bond score
Chemscore CH-O Score	Weak aromatic (CH) to O H-bonding - an interaction is deemed to be present if the distance between the acceptor and the aromatic carbon is within the range $3.35 \text{ \AA} \pm 0.65$, the acceptor angle is within $145^\circ \pm 65$, the donor angle is within $115^\circ \pm 40$ and the CH...O bond is not more than 30° out of the aromatic plane
Chemscore Protein Energy	Penalty for protein clashes when flexible side chains are used
Chemscore Internal Correction	Ligand internal energy offset

Adapted from the GOLD User Guide

Table 34. Molecular docking data gathered for compounds **151-158** in the ERK5 active site using GOLD.



Compound	R ⁴	GOLD Fitness highscore
151	Et	64.4
152	ⁱ Pr	67.2
153	^{Cyc} Pr	70.4
154	Ph	68.0
155	Benzyl	79.0
156	NMe ₂	65.0
157	Piperidine	65.7
158	CONHMe	63.7

The program has a bias towards larger compounds, making comparisons between compounds **151** and **155** less meaningful than those of similar molecular weight such as **152**, **153** and **156**. When comparing tertiary amine **156** with propyl groups **152** and **153**, it is clear that the lipophilic groups are better tolerated, and furthermore the polar amide **158** has the worst score in the set. It is most likely, from looking at this data and the empty crystal structure, that alkyl or lipophilic groups would be best tolerated in this area. Compound **155** probes furthest into the space and has the highest score value leaving us to assume a large lipophilic space is available for exploitation.

2.8.2 4 & 6-Substituted Indazole Sulphonamide/Sulphone Synthetic Targets

The initial set of targets probed the space at the 4-position with progressively larger alkyl substituents i.e. methyl, ethyl, cyclopropyl. As equivalent potency is seen for sulphone and *N*-methyl sulphonamide matched pairs, the decision of which to include was made based on synthetic feasibility. For this series of compounds the number of aryl sulphonamide systems examined was reduced from eight to four as the 2-

thiophene, 4-methoxyphenyl, phenyl and 8-quinoline groups had consistently given superior potency.

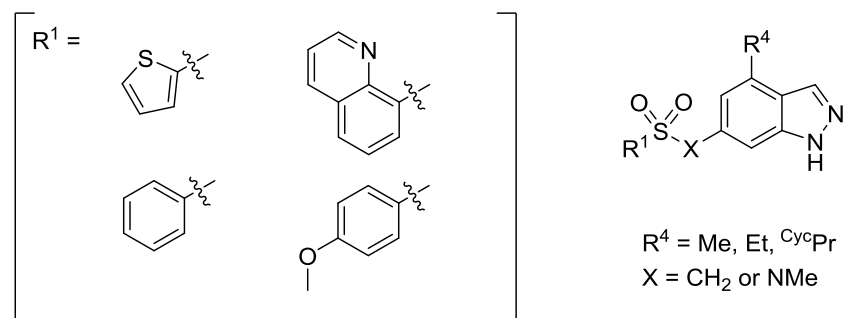


Figure 56. Synthetic targets exploring the 4-position

Suitable starting materials could not be sourced that possessed the required functionalization without employment of an indazole ring-closing procedure. Retrosynthetic analysis to a derivatised 2-amino toluene revealed a commercially available starting material (Figure 57).

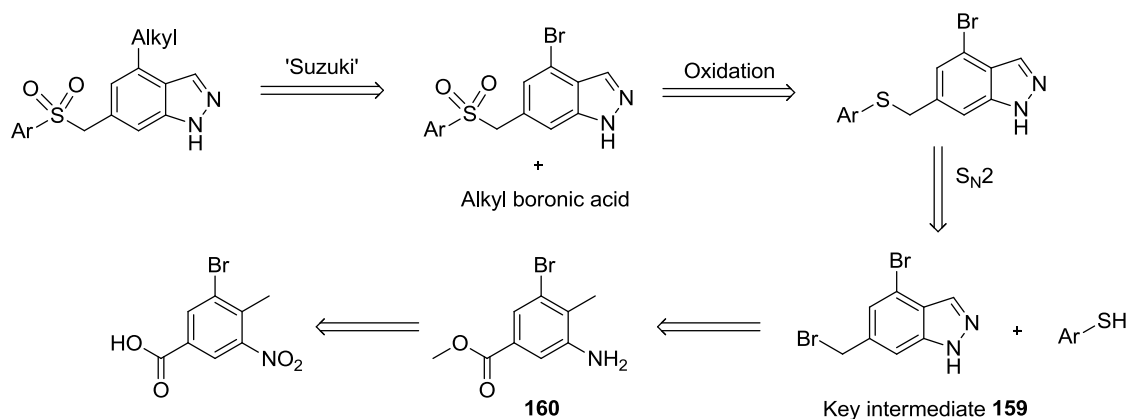
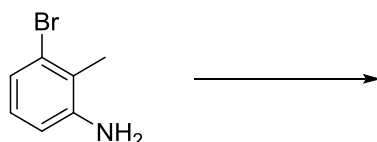


Figure 57. Retrosynthetic analysis of desired compound set.

The indazole ring-closure method progresses *via* diazonium formation upon the aniline and subsequent attack by the adjacent methyl group. Model reactions were set up using 3-bromo-2-methylaniline with two sets of conditions to test the critical ring-closure step of the synthesis before commencement of the lengthy scheme (Table 35).¹²⁷

Table 35. Model reaction conditions for indazole ring closure.

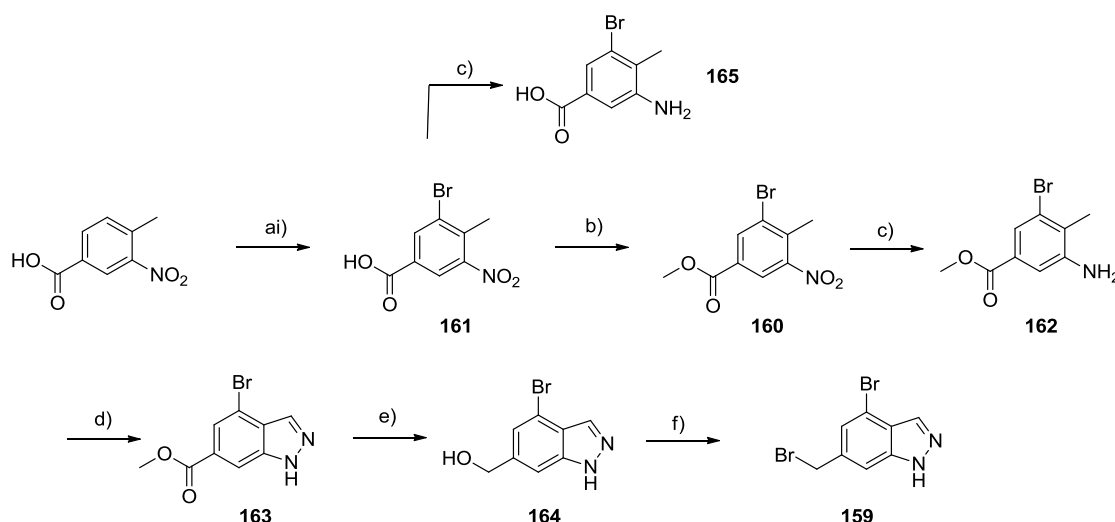
	Product	Conditions	Yield	Comments	Ref
1		i) HBF ₄ (aq), NaNO ₂ , H ₂ O, 0 °C –RT, 2 h ii) KOAc, 18-crown-6, DCM, RT, 2 h	29%	Starting material was poorly soluble in H ₂ O.	127
2		Acetic anhydride, KOAc, Toluene, Isoamyl nitrite; 60 °C, 72 h	67%		internal

Reaction 1 (Table 35) presented solubility issues despite the literature conditions described being employed on the same substrate.¹²⁷ The procedure also required the isolation of a stable diazonium salt, however, this can be hazardous and introduces an unnecessary opportunity to lose material. At this stage reaction 2 was preferred due to an improved yield and minimised handling. Isoamyl nitrite used in place of sodium nitrite allows the diazonium formation without the use of water to solubilise inorganic materials and therefore reagents are more readily dissolved in reaction 2. The product is in a protected form which may prove beneficial to the overall synthesis.

Retrosynthetic analysis of the desired compounds (Figure 57) led to key, dibrominated indazole **159** from which steps previously developed in the synthesis of sulphone compounds (Scheme 15, Chapter 2.5.5) could be used alongside a Suzuki reaction. It was also determined that because of the need for an aniline-like species to undergo ring-closing that installing the sulphone linker would simplify the scheme. A halogen at the 4-position also means that intermediates generated in this synthesis can be used to perform Ullman, carbonylation or lithium-halogen exchange reactions to synthesise alternate compound libraries.

A scheme was proposed to reach the key dibromoindazole (**159**) intermediate in six steps using typical methods and the previously modelled ring closure. The success of the ring closing reaction meant that functionalised benzene rings could be investigated

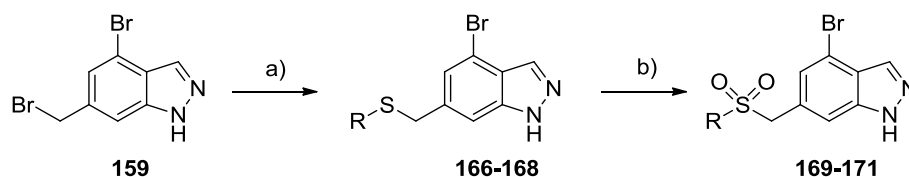
as potential starting materials leading to identification of 4-methyl-3-nitrobenzoic acid and a high yielding literature procedure for a regioselective bromination using dibromoisocyanuric acid (DBI) (Scheme 18)¹⁶⁵. The nitro group was reduced to an amine to form unnatural amino acid **165** which was highly water soluble and found to be unrecoverable from aqueous media. This situation was remedied by the esterification of the acid prior to nitro reduction (**160**). Esterification was conducted in a high yield, as was the following zinc/acetic acid reduction of the nitro group giving **162**. Ring closure was attempted using the model reaction conditions. However, slow progress of the acetylation step meant that alternate conditions were used. Intermediate amine **162** was dissolved in acetic acid and a solution of NaNO₂ in H₂O was added which gave the 4,6-functionalised indazole **163** in a 94% yield. The presence of a minimal amount of water to solubilise NaNO₂ did not affect the solubility of the aniline starting material.



Scheme 18. Reagents and conditions; a) DBI, H₂SO₄, 60 °C, 3h, 98%. b) MeOH, H₂SO₄, 60 °C, 18h, 92%. c) Zn, AcOH, MeOH, 50 °C, 1h, 98% (yield for compound **162**). d) AcOH, NaNO₂, H₂O, RT, 15 mins, 94%. e) LiAlH₄, THF, 0 °C-RT, 4h, 82%. f) SOBr₂, DMF, DCM, 0 °C-RT, 4h, 58%.

Conversion of the ester to benzylic bromine **159** was achieved via LiAlH₄ reduction of **163** to the alcohol **164** and the use of SOBr₂ to put in place the bromine as discussed in Chapter 2.5.5.¹⁶⁶ Despite the key intermediate presenting two bromine derived, active centres, selectivity is gained through the hybridization of each. The sp³ centre is sensitive to an S_N2 reaction whereas the S_NAr, which can occur at the 4-position under the same conditions is, much slower (Scheme 19). The conditions previously optimised for S_N2 reactions in DMF with Cs₂CO₃ gave the desired thioethers **166-168** in good

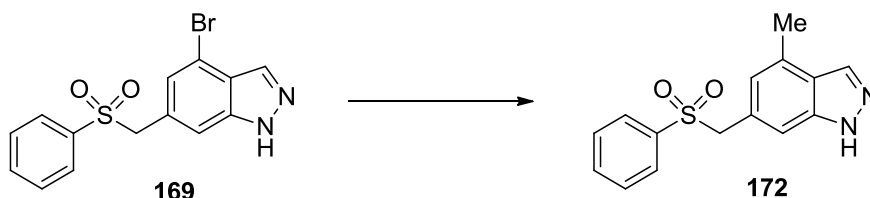
yields. Oxidations proceeded well giving substrates for Suzuki reaction optimisation and relevant intermediate compounds **169-171** to send for testing.



Scheme 19. Reagents and conditions; a) R^1-SH , $CsCO_3$, DMF, RT, 6h, 73-91%. b) $KHSO_5$, MeOH, H_2O , RT, 18h, 65-95%.

Suzuki conditions previously optimised for the cyclised linker compounds (Chapter 2.5.3) were employed but the mild palladium tetrakis catalyst and trimethylboroxine did not yield any product formation (Table 36). The reaction was repeated using an alternate boron species, methylboronic acid, but no improvement was witnessed. Previously developed conditions using $(Pd[(P^tBu)_2C_5H_4]_2Fe)Cl_2$ and Cs_2CO_3 were applied, however, the highly activated catalyst did not aid product formation only resulting in the dehalogenation of a small amount of starting material. Cs_2CO_3 is often used in place of sodium or potassium carbonates as it is more soluble in organic solvent due to the reduced charge density of the metal ion.¹⁶⁷

Table 36. Optimisation of Suzuki reaction on 4-methyl-6-((phenylsulfonyl)methyl)-1H-indazole (**169**).

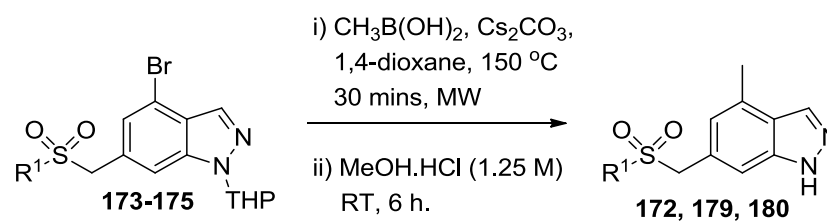
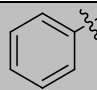
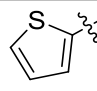
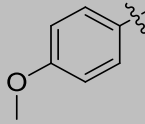


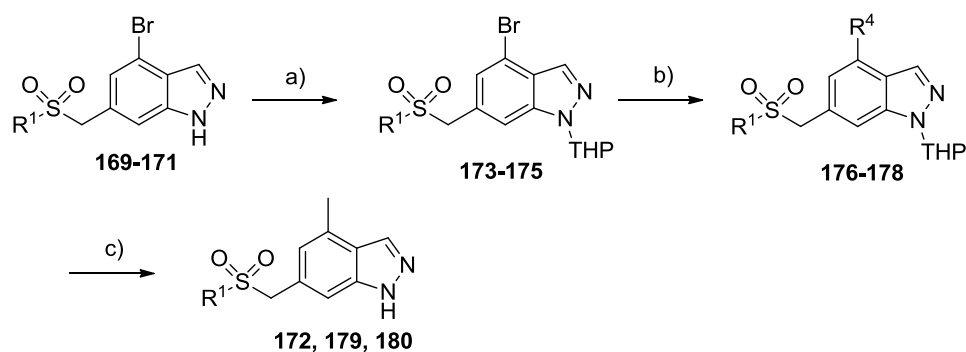
	Boron species	Palladium	Base	Solvent system	Heating	Conversion
1	Trimethylboroxine (1 eq)	$Pd(PPh_3)_4$ (10 mol%)	Na_2CO_3 (2 eq)	1,4-Dioxane and H_2O	150 °C, 30 min, MW	No reaction
2	Methylboronic acid (3 eq)	$Pd[(P^tBu)_2C_5H_4]_2Fe$ Cl_2 (10 mol%)	Cs_2CO_3 (1.5 eq)	1,4-Dioxane	150 °C, 30 min, MW	13 % de-halogenated (compound 122)

^aConversion estimated by LCMS.

As reaction 2 (Table 36) showed evidence of palladium oxidative addition/ bond insertion these conditions were used on a protected version of compound **169**. The indazole NH was protected with tetrahydropyran (THP). A facile procedure using dihydropyran (DHP), *p*-toluenesulfonic acid (*p*-TSA) in DCM giving good conversion (Scheme 19).¹⁴⁴ The Suzuki reaction on **173** using conditions described in Table 37 gave the desired methyl product in a high yield. However, a significant amount of de-halogenated material was generated and, therefore, a milder catalyst (Pd(dppf)Cl₂) was used in later reactions. A persistent, close running, impurity was identified after the Suzuki reaction as de-halogenated material which was carried forward through the THP deprotection using HCl in MeOH. Standard, amine and reversed phase silica were all used but did not remove the impurity; only semi-preparative HPLC afforded the pure products, impacting on the overall yield and throughput of the scheme.

Table 37. Yields of various Suzuki reactions on bromo compounds **173-175**.

			
	R ¹	Palladium Species	Yield over steps i) & ii)
172		Pd[(P(^t Bu) ₂ C ₅ H ₄) ₂ Fe]Cl ₂ (10 mol%)	41%
179		Pd[(P(Ph) ₂ C ₅ H ₄) ₂ Fe]Cl ₂ .DCM (10 mol%)	54%
180		Pd[(P(Ph) ₂ C ₅ H ₄) ₂ Fe]Cl ₂ .DCM (10 mol%)	52%



Scheme 19. Reagents and conditions; a) DHP, *p*-TSA, DCM, RT, 6h 58-80%. b) Pd[(P(Ph)₂C₅H₄)₂Fe]Cl₂.DCM, CH₃B(OH)₂, Cs₂CO₃, 1,4-dioxane, 150 °C, MW, 0.5 h. c) MeOH.HCl (1.25 M), 18 h followed by HPLC, 30-54% (over two steps).

2.8.3 Revised Synthetic Scheme for 4 & 6-Substituted Indazole Sulphones

The remaining synthetic targets were synthesised in a revised order which avoided the use of semi-preparative HPLC purification (Scheme 20). By installing the alkyl R⁴ group earlier in the scheme, products were separable by reversed phase MPLC (medium pressure liquid chromatography) but the total number of intermediate compounds was increased. It was seen previously that compound **159** (dibromo) was able to dimerise (Figure 58). By protecting the indazole earlier in the scheme, to perform the Suzuki reaction, it was hoped that the homo-dimer formation would cease. In the SOBr₂ bromination, the THP is partially removed during the reaction by HBr generated *in situ*. Because of this, the reaction was pushed to complete deprotection by the addition of HCl and therefore unprotected bromo compounds **186-187** were produced. This did not greatly impact the synthesis as dimer formation was found to be concentration-dependant and therefore easily avoided.

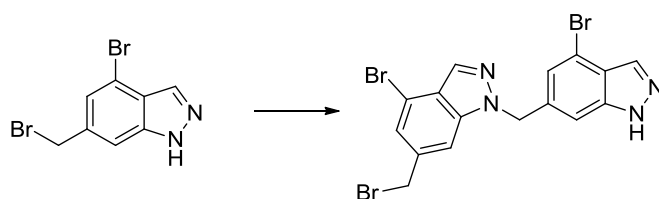
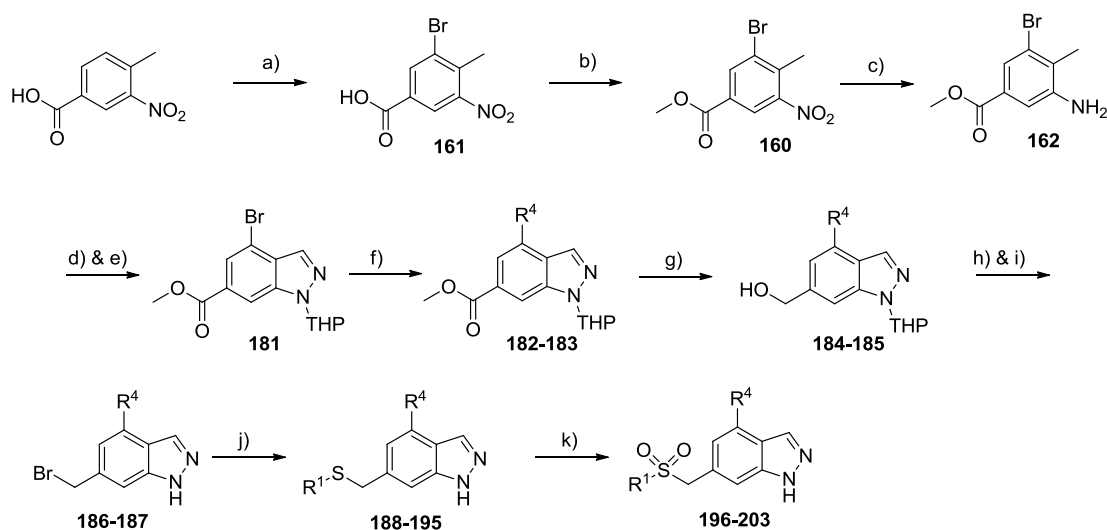


Figure 58. Spontaneous dimer formation of bromine compound **159** in solution.

The yield of the Suzuki reaction was improved significantly (from ~50% to 71-87%) when performed on the 6-ester, THP protected indazole (**181**). Final products were obtainable from the revised scheme without further optimisation of previously used reaction procedures (Scheme 20). The overall yield of this scheme was comparable

with the initial scheme but could be performed more rapidly due to simplified purifications.



Scheme 20. Reagents and conditions; a) DBI, H_2SO_4 , 60 °C, 3h, 98%. b) MeOH, H_2SO_4 , 60 °C, 18h, 92%. c) Zn, AcOH, MeOH, 50 °C, 1h, 98%. d) AcOH, $NaNO_2$, H_2O , RT, 15 mins, 94%. e) DHP, *p*-TSA, DCM, RT, 6h 82%. f) $Pd[(P(Ph)_2C_5H_4)_2Fe]Cl_2 \cdot DCM$, R^4 -B(OH) $_2$, Cs_2CO_3 , 1,4-dioxane, 150 °C, MW, 0.5 h. 71-87%. g) $LiAlH_4$, THF, 0 °C-RT, 4h, 86-93%. h) $SOBr_2$, DMF, DCM, 0 °C-RT, 4h. i) MeOH.HCl (1.25 M), 18 h, 64-91% (over two steps). j) R^1 -SH, $CsCO_3$, DMF, RT, 6h, 61-97%. k) $KHSO_5$, MeOH, H_2O , RT, 18h, 34-99%.

2.8.4 Structure Activity Relationships of 4 & 6 Substituted Indazoles

Pure final compounds and 4-bromo intermediates were screened for activity against ERK5 and p38 α . Results are shown in Table 38.

Table 38. Enzymatic activity data of 4 & 6 substituted indazoles against ERK5 and p38 α .

Compound	R ¹	R ⁴	IC ₅₀ (μM)	
			ERK5 ^a	p38 α ^b
122		H	0.91 ± 0.15	>120
169		Br	0.87 ± 0.47	>120
172		Me	0.18 ± 0.04	>120
196		Et	0.04 ± 0.01	>120
197		CycPr	0.03 ± 0.01	>120
120		H	1.1 ± 0.2	>120
170		Br	0.52 ± 0.31	>120
179		Me	0.14 ± 0.04	>120
198		Et	0.08 ± 0.01	>120
199		CycPr	0.01 ± 0.01	>120
124		H	0.71 ± 0.25	>120
171		Br	1.7 ± 1.0	>120
180		Me	0.22 ± 0.03	>120
200		Et	0.09 ± 0.01	>120
201		CycPr	0.08 ± 0.01	>120
121		H	0.59 ± 0.07	>120
-		Br	-	-
-		Me	-	-
202		Et	0.05 ± 0.01	-
203		CycPr	0.03 ± 0.01	-

^a ERK5 IC₅₀ values generated by IMAP cell free assay (350 μM ATP); ^b p38 α IC₅₀ values generated by Lance assay (350 μM ATP).

It is clear from the results that substitution at the 4-position is well tolerated and can have a dramatic improvement on potency. With the exception of 4-bromo derivatives

(**169-170**) potency has increased with the size of R⁴ substituents from methyl to cyclopropyl. This trend can be seen in Figure 59, R⁴ groups increase in size impacting overall lipophilicity (represented by cLogp) as potency improves (represented by pIC₅₀ (pIC₅₀ = -Log(IC₅₀))). This relationship applies to all three complete compound sets with a fixed 6-position substituent (disregarding data for the brominated compounds). It is expected that the trend (Figure 59) will adopt a bell shape as the size of the groups increases eventually revealing an optimal size and lipophilicity before larger groups are less potent. More potency values are needed to prove this hypothesis such as cyclobutyl, cyclopentyl and cyclohexyl substituents (Chapter 2.4.1).

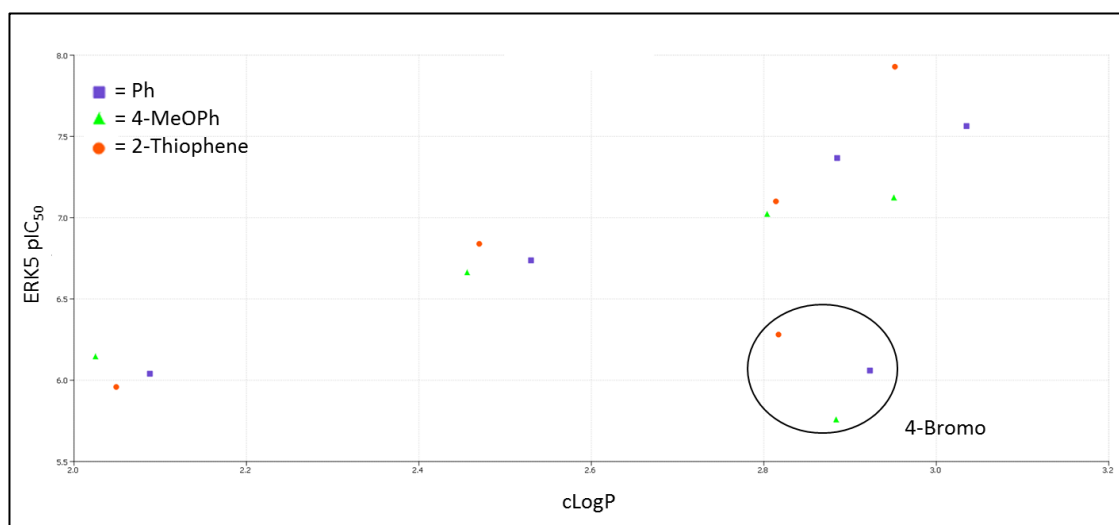


Figure 59. Graph of ERK5 potency vs CLogP showing a near linear relationship.

Comparing the 4-H and 4-cyclopropyl in each compound set the average improvement in potency is 42-fold. This is most likely due to the lipophilic space being occupied with the small alkyl group pointing along the ceiling of the active site producing a beneficial interaction. It is also possible that the introduction of this group changes the most energetically favourable conformation of the compound so that it better aligns with the ERK5 binding conformation (Figure 60).

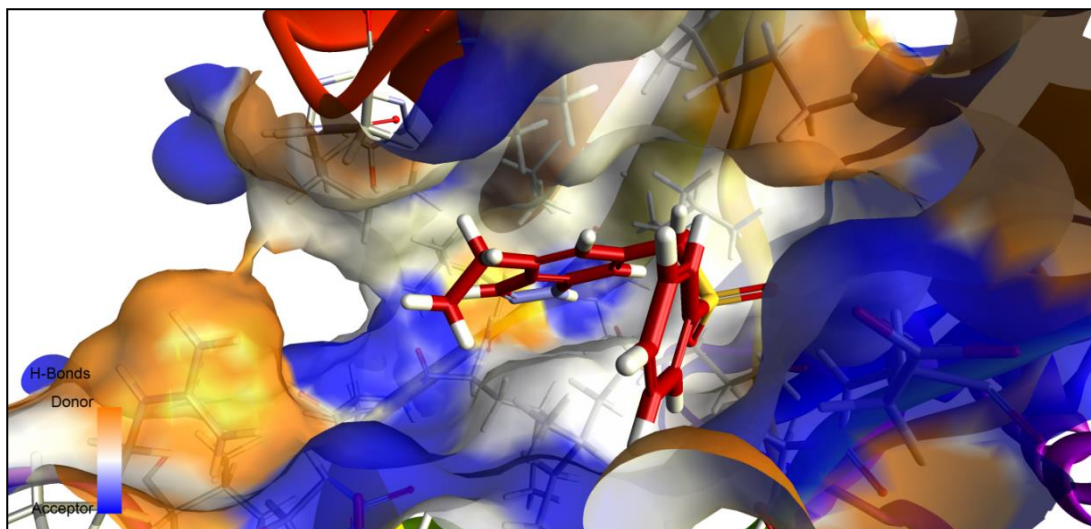


Figure 60. Compound **196** (red) docked into the ERK5 active site showing the vector of the 4-position pointing along the ceiling of the active site, towards solvent. (PDB: 4IC8).

2.4.1 Large alkyl substituents in the Indazole 4-position

After the success of introducing alkyl groups in the 4-position and the gain in potency observed, the limits of this space were further investigated with progressively larger alkyl groups. Three aliphatic rings were chosen for incorporation increasing methodically in size (Figure 61).

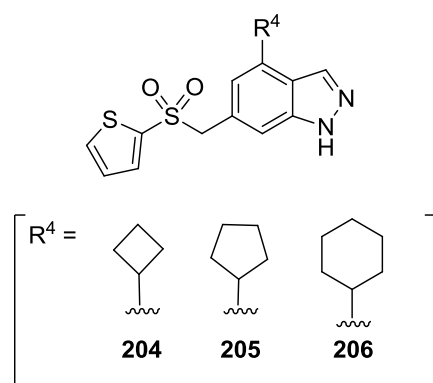
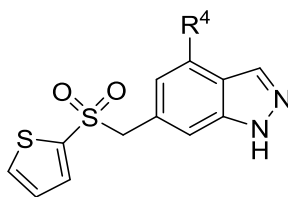


Figure 61. Synthetic targets exploring the 4-position

These targets were synthesised using the same procedures developed in Scheme 20, however, large amounts of material were lost during the second bromination step due to formation of dimers (Figure 58). Sufficient material was not available to facilitate a thorough purification and therefore activity data was collected on material of purity below 95% by HPLC. Cyclopentyl compound **205** could not be synthesised. It is important to note that neither NMR nor HPLC showed a major impurity in either compound **204** or **206**.

Table 39. Enzymatic activity data of compounds **204-205** against ERK5 and p38 α .

Compound	Purity by HPLC (acid/basic)	R ⁴	IC ₅₀ (μ M)	
			ERK5 ^a	p38 α ^b
120	>95%/>95%	H	1.1 \pm 0.2	>120
179	>95%/>95%	Me	0.14 \pm 0.04	>120
198	>95%/>95%	Et	0.08 \pm 0.01	>120
199	>95%/>95%	^{Cyc} Pr	0.01 \pm 0.47	>120
204	87%/85%	Cyclobutyl	0.33 \pm 0.01	-
205	-	Cyclopentyl	-	-
206	82%/82%	Cyclohexyl	1.6 \pm 0.1	-

^a ERK5 IC₅₀ values generated by IMAP cell free assay (350 μ M ATP); ^b p38 α IC₅₀ values generated by Lance assay (350 μ M ATP).

This data is less accurate than activity values shown previously, however, the results gathered show a drop in potency and presumably the potency limit for alkyl substituents in the 4-position. According to Figure 62 the optimally sized alkyl substituent at the 4-position is, the most potent, cyclopropyl (**199**). The graph displays the clear drop in potency as units increase in size beyond the C₃H₅ unit. These probes only elucidate the lipophilic space available at this position and therefore future targets were devised to introduce polarity in space beyond the reach of a cyclopropyl group.

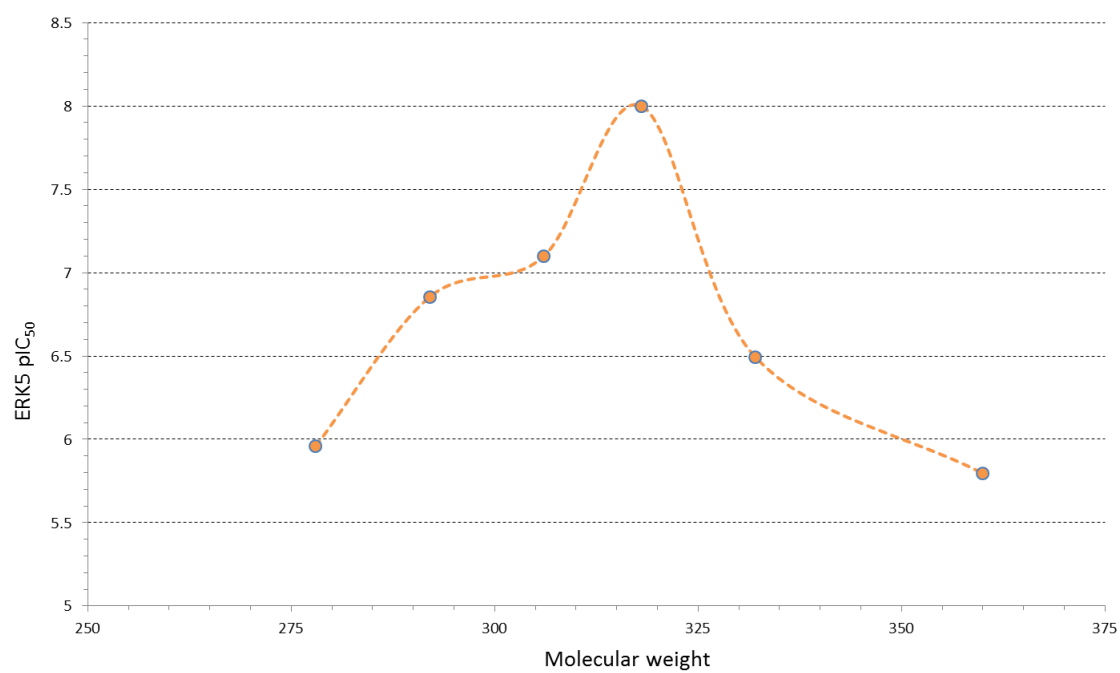


Figure 62. Graph of ERK5 pIC₅₀ vs molecular weight for 2-thiophene compounds **120, 179, 198, 199, 204, 206** (Table 39).

2.8.5 Cellular potency of 4 & 6-position substituted indazole

The most potent compounds from this series were tested for ERK5 activity in two cell lines, in different assays; a reporter assay in HEK293 cells and a Western blotting assay in HeLa cells.

Table 40. Enzymatic and cellular ERK5 potency for 4,6-substituted indazole compounds.

Compound	R ¹	R ⁴	ERK5	Cellular IC ₅₀ (μM)	
			Enzymatic IC ₅₀ (μM)	HeLa ^a	HEK293 ^b
172		Me	0.18 ± 0.04	-	1.07
196		Et	0.04 ± 0.01	1.3 ± 0.8	0.16
197		CycPr	0.03 ± 0.01	0.08 ± 0.01	0.03
179		Me	0.14 ± 0.04	-	0.20
198		Et	0.08 ± 0.01	0.02 ^c	0.08
199		CycPr	0.01 ± 0.01	0.04 ± 0.04	0.024
180		Me	0.22 ± 0.03	-	0.75
200		Et	0.09 ± 0.01	0.66 ± 0.06	0.15
201		CycPr	0.08 ± 0.01	0.27 ± 0.04	-

^a Western blot assay; ^b MEF2D, luciferase reporter assay; ^c n=1 therefore no errors.

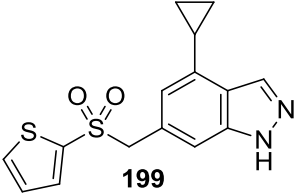
Both cellular assays show good correlation to enzymatic data and encouraging cellular potency is seen for all tested ligands. 4-Cyclopropyl compounds **197** and **199** show 50% inhibition at sub 100 nM concentrations. However, the thiophene compound **199** performs best in all assay types and was therefore nominated as the lead compound in the series and selected for further investigation.

2.9 Full Profile of 4-Cyclopropyl-6-((thiophen-2-ylsulfonyl)methyl)-1*H*-indazole (**199**)

2.9.1 Physiochemical properties, in vitro pharmacology and in vitro DMPK profile of **199**

The physiochemical properties of **199** are favourable as it satisfies all of Lipinski's rules whilst having 4 rotatable bonds and 3 aromatic rings, which is within the typical range described by licenced kinase inhibitors.¹⁶⁸ The molecular weight is low (318 Da) meaning that the ligand efficiency of this molecule is exceptionally high (0.51), reflecting the fact that all parts of the molecule contribute to activity. There is good selectivity between ERK5 and p38 α , however, a wider kinase screen has been carried out on this molecule and is discussed in Chapter 2.9.2.

Table 41. Medicinal chemistry profile of 4-cyclopropyl-6-((thiophen-2-ylsulfonyl)methyl)-1*H*-indazole (**199**). Good results are highlighted in green, undesirable in amber and poor in red. Solubility and metabolism data supplied by Cyprotex.

Criteria	Desired value for lead	 199	
ERK5 IC ₅₀ (cell free)	< 0.1 μM	0.012 ± 0.007 (n=6)	
ERK5 cellular potency (Hela)	<1 μM	0.04 ± 0.04 (n=2)	
ERK5 cellular potency (HEK293)	<1 μM	0.24 (n=1)	
Selectivity	>10-fold	p38α IC ₅₀ >120 μM + kinase screen (Chapter 2.9.2)	
ERK5 Ligand Efficiency	>0.3	0.51	
xLogP	<5	4.8	
TPSA	75-100	63	
MW	<500	318	
Plasma Protein binding	<99%	92	
Caco-2 A2B/B2A Efflux Ratio	>1 x10 ⁻⁶ cm/s <2	39/20 0.52	
Solubility (Lower/Upper)	>50 μM	100/100	
Mouse microsomal clearance	<48 μl/min/mg	378	
hERG inhibition	IC ₅₀ >25 μM	27% at 25 μM	
CYP1A inhibition	IC ₅₀ >10 μM	25	
CYP2C19 inhibition	IC ₅₀ >10 μM	11	
CYP2C9 inhibition	IC ₅₀ >10 μM	25	
CYP2D6 inhibition	IC ₅₀ >10 μM	15	
CYP3A inhibition	IC ₅₀ >10 μM	6	

No concern is raised by values for plasma protein binding, solubility or efflux ratio, all of which are within the desired range. Inhibition of hERG and selected CYP metabolic enzymes was found to be adequate therefore there is not a strong reason to expect toxicity from the compound in mice.

Metabolism data collected in mouse liver microsomes shows that **199** is cleared very quickly; this is discussed in much greater depth in Chapter 2.9.6.

2.9.2 Selectivity profile of 4-Cyclopropyl-6-((thiophen-2-ylsulfonyl)methyl)-1*H*-indazole **199**

4-Cyclopropyl-6-((thiophen-2-ylsulfonyl)methyl)-1*H*-indazole **199** was screened for activity against 139 kinases, this data shows some degree of off target kinase inhibition. Results are gathered as percentage remaining activity at 1 μ M drug concentration. Table 42 shows all kinases with remaining activity lower the 50% and therefore a theoretical IC₅₀ below 1 μ M.

Table 42. Selectivity data gathered for 4-Cyclopropyl-6-((thiophen-2-ylsulfonyl)methyl)-1*H*-indazole **199**. Only inhibited kinases are shown.

Kinase	Remaining activity at 1 μ M /%	Notes
IRAK1	1	
CDK9-Cyclin T1	2	CDK family
ERK8/7	3	MAPK family
CDK2-Cyclin A	7	CDK family
PRK2	8	
CLK2	9	
TrkA	13	
DYRK1A	16	
DYRK2	16	
CAMKKb	17	
AMPK (hum)	19	
IRAK4	23	
HIPK2	27	
BRSK2	27	
STK33	31	
BRSK1	31	
JAK2	33	
DYRK3	34	
MAP4K3	39	MAPK family
TAO1	40	
ERK5	42	MAPK family – Target
ULK1	43	
ULK2	43	
TSSK1	48	
Aurora A	49	
ERK1	52	MAPK family
ERK2	58	MAPK family

Despite **199** showing poor activity against ERK5 in this selectivity panel, we are confident that our assay gives a more dependable result due to the repeatability and high ATP concentration.

Collectively this data shows 23 kinase targets where **199** shows a theoretical IC₅₀ below 1 μ M. A number of MAPK family targets (ERK1/2) are susceptible to inhibition by this

compound, which was not entirely unexpected given the shared sequence homology with ERK5. As this data showed a wide spread of inhibition, it was decided that a wider profile of kinases needed to be screened, therefore **199** was submitted to DiscoverX for a kinomescan™ which measures activity against 456 kinase targets.

Activity is given as %ctrl given by $(\text{test signal} - +\text{ve ctrl signal}) / (-\text{ve ctrl signal} - +\text{ve ctrl signal}) \times 100$. Low values indicate strongly inhibited proteins. In this assay ERK5 is identified as a strongly inhibited target (0.05 %ctrl) and MEK5, the upstream ERK5 activating kinase, shows limited inhibition (82% ctrl). It may be desirable to inhibit both enzymes as it is currently believed the sole role of MEK5 is the activation of ERK5 making it an equally valuable target.

Overall the results of this assay showed that **199** possess relatively ambiguous binding properties. 29 Targets have a % ctrl value of 1 or less, representing a number of important kinase families. Data has been mapped onto the kinome (Figure 63) showing a number of cases of subfamily associated activity. Notably, the subfamilies are a mixture of serine/threonine, tyrosine and dual specificity kinases.

Kinome Activity Map

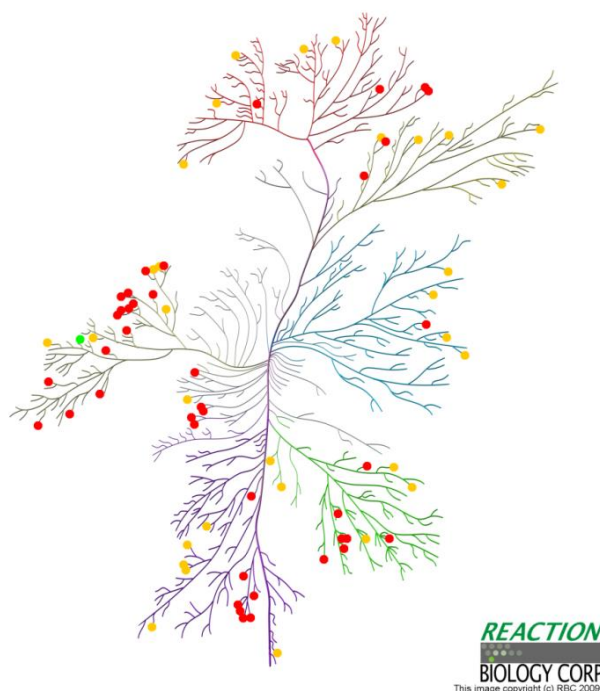


Figure 63. Kinase Activity map for **199** on the known kinome. Red spots show <2 %ctrl, orange <10 %ctrl, green = ERK5.¹⁶⁹

The selectivity of this compound is undesirable as some key kinase families are inhibited as well as ERK5 by **199** (Table 43). Ideally a lead compound should show at least ten-fold better potency for the target over closely related targets and one hundred fold for a drug candidate. In this case there are a range of kinase targets for which compound **199** is more active than ERK5 and therefore any effect of this compound *in vivo* cannot be directly attributed to ERK5 inhibition.

Table 43. Selectivity data gathered for 4-Cyclopropyl-6-((thiophen-2-ylsulfonyl)methyl)-1*H*-indazole **199**. Only inhibited kinases are shown.

Kinase subfamily	Inhibitory range (%Ctrl)	Inhibited Members/ Subfamily Members	Name
CAMK	3.3-5.6	4/9	Calcium/calmodulin-dependent protein kinase
CAMKK	1.2-1.7	2/2	Calcium/calmodulin-dependent protein kinase kinase
ULK	4.2-4.6	2/4	Unc-51-Like Kinases
CLK	1.4-3.5	4/4	Dual specificity kinase acting on both serine/threonine and tyrosine-containing substrates
HIPK	0.25-2	3/4	Homeodomain-interacting protein kinase
DYRK	0.25-16	3/5	Dual specificity Tyrosine Regulated Kinase
CDK	0-5.4	4/11	Cyclin-dependent kinases
ROCK	0.3-3.2	2/2	Rho-associated protein kinase
IRAK	0-0.7	2/4	Interleukin-1 receptor-associated kinase
JAK	0-0.6	2/4	Janus kinase

2.9.2.1 CDK2-(4-Cyclopropyl-6-((thiophen-2-ylsulfonyl)methyl)-1H-indazole) **199** crystal structure

CDK2 inhibition by an indazole compound has been noted previously (Chapter 2.5.1.1.2) and again with 4-cyclopropyl-6-((thiophen-2-ylsulfonyl)methyl)-1H-indazole **199**. As CDK2 activity has been maintained it was further investigated by the crystallisation of **199** in the CDK2 active site (Figure 64) with the aim of designing out the unwanted activity.

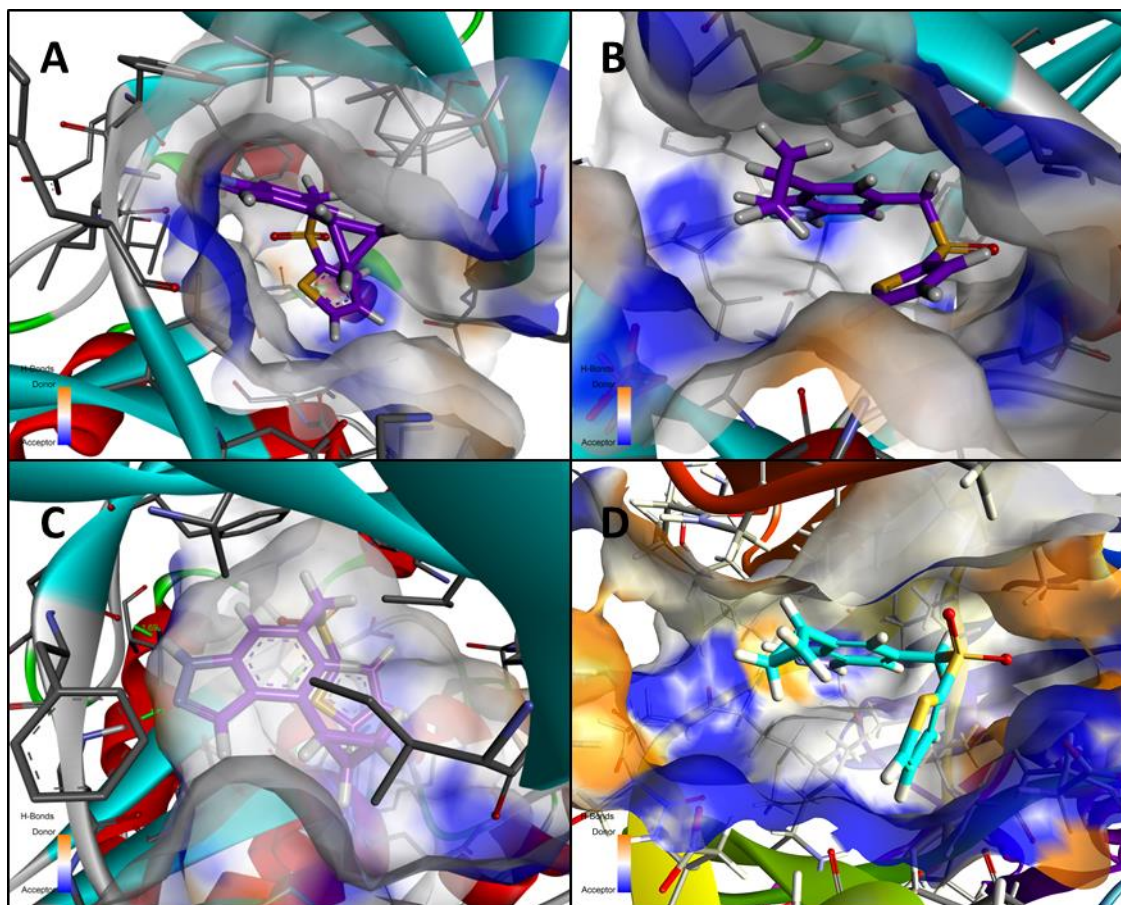


Figure 64. A-C, Crystal structure of **199** (purple) in the CDK2 active site visualised from three angles to show orientation of the sulphonamide aromatic and conserved hinge binding; D, molecular modeling of **199** in the ERK5 active site.

The CDK2 binding mode is very similar to the suggested binding of **199** in the ERK5 active site. Subtle differences include the orientation of the thiophene ring which in the CDK2 structure is proposed to form a π - π stacking interaction with the indazole and so the rings lie in parallel planes. The geometry of the sulphonyl groups is fixed by this intramolecular interaction but they do not make an interaction in the site as seen with the ERK5 modelling. The 8-quinoline compound **85** (CDK2 IC₅₀ = 0.19 μ M) showed

high CDK2 activity, presumably due to the increased overlap of the quinoline and indazole π -clouds therefore fixing the structure in the binding conformation. In the ERK5 structure the sulphonamide aryl plane is almost perpendicular to the indazole and therefore the aromatic group possesses a very different vector array. By adding groups to the sulphonamide aryl to disrupt the π - π stacking seen in the CDK structure selectivity may be improved.

2.9.3 Pharmacokinetic profile of 4-Cyclopropyl-6-((thiophen-2-ylsulfonyl)methyl)-1*H*-indazole **199**

Pharmacokinetic data for **199** was collected in mice after dosing at 10 mg/Kg (Table 44). Three dosing methods were used; intravenous (IV), intraperitoneal (IP) and oral (PO). IV and IP produce very similar data however IP was conducted in this case as administration is preferable. The total volume tolerated through IP is higher than IV allowing for an easier formulation. For IP dosing the drug compound was taken in 10% *N*-methyl-2-pyrrolidone (NMP), 30% polyethylene glycol (PEG) and 60% encapsin; a solution which could not be used for IV. From a practical point of view IP administration is much easier to conduct than IV due to the size of veins in a mouse. All *in vivo* pharmacokinetic studies were performed by Dr Huw Thomas in the NICR, Newcastle-upon-Tyne.

Table 44. Pharmacokinetic data for **199**.

Parameter	Intravenous Dose (IV)	Oral Dose (PO)	Intraperitoneal Dose (IP)
Dose (mg/kg)	10	10	10
AUC ($\mu\text{g/ml}\cdot\text{min}$)	74	17	79
C_{max} ($\mu\text{g/ml}$)	5.4	0.25	3.2
t_{max} (min)	5	30	5
$t_{1/2}$ (min)	49	81	55
Clearance (ml/min/kg)	136	-	126
V_{dss} (L/kg)	2.2	-	3.8
Bioavailability (%)	-	24	-

AUC = Area under curve; V_{dss} = volume of distribution at steady state.

The compound is cleared at approximately the same rate as the mouse liver blood flow (90 -110 ml/min/kg) which was to be expected given the high value for mouse microsomal clearance (378 μ l/min/mg, Table 41).¹⁷⁰ The compound had unremarkable plasma-protein binding figure of 92% which means that the blood clearance of the unbound fraction ($CL_u = CL/f_u$) is extremely high \sim 1600 ml/min/kg. The volume of distribution values are typical of a neutral compound and reflect the absorption of the compound. The bioavailability (24%) is therefore low due to the rapid clearance as we know from Caco-2 assay data (Table 41) that the compound has good cell permeability.

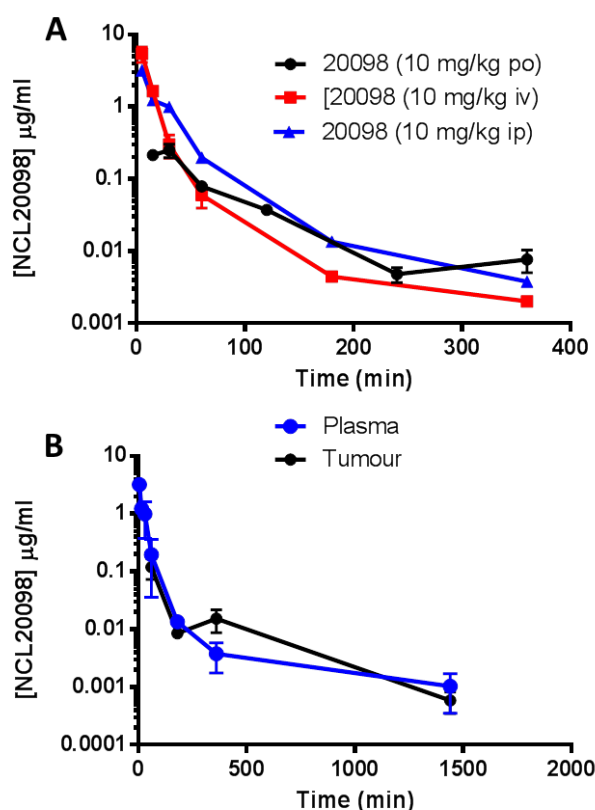


Figure 65. A) Plasma drug concentrations following administration of 10 mg/kg **199** by three different routes (PO, IV, IP); B) plasma and tumour drug levels following IP administration of 10 mg/kg **199**.

Graphical data (Figure 65A) shows that drug plasma concentrations fall evenly in all dosing methods. A pharmacokinetic experiment was also conducted using mice with a tumour xenograft to ascertain the drug concentration in the tumour (Figure 65B). This analysis showed the plasma and tumour concentrations are equivalent over the measured time period. This data shows that cellular uptake of the compound is good

and with a better clearance profile this compound would be an appropriate tool for an *in vivo* ERK5 target validation experiment.

2.9.4 Target validation using 4-Cyclopropyl-6-((thiophen-2-ylsulfonyl)methyl)-1H-indazole **199**

199 Has been used in a number of biological experiments in a bid to validate ERK5 as a target and this compound series as useful inhibitors. Results have been generated regarding the effect of ERK5 in angiogenesis by a matrigel plug assay and cell invasion by scratch assays. However, given the selectivity of compound **199** the positive results generated cannot solely be attributed to the effect of ERK5 inhibition.

2.9.5 Synthesis and NMR Studies of 4-cyclopropyl-6-(difluoro(thiophen-2-ylsulfonyl)methyl)-1H-indazole (211**)**

*2.9.5.1 Synthesis of 4-cyclopropyl-6-(difluoro(thiophen-2-ylsulfonyl)methyl)-1H-indazole (**211**)*

In a bid to determine the metabolites of **199** a fluorinated derivative of this compound was synthesised. Orally dosing mice with a fluorinated compound and running an F¹⁹-NMR experiment with the collected animal material is often used to determine several properties such as where a compound accumulates, where it is metabolised and the biological half-life.¹⁷¹⁻¹⁷³ Determining the structure of metabolites in this manner is difficult as gaining a spectrum with which the structure can be determined (i.e. C¹³/H¹-NMR) requires a large amount of sample. Alternatively, once a fluorine NMR is obtained using animal urine the shift of the metabolite peaks are recorded and oxidation reactions upon the parent compound can be performed in an effort to match shifts and thus predict metabolites.

In the case of establishing the metabolism of **199** the F¹⁹-NMR spectra collected was proposed to be used to identify the number of major metabolites and the quantity in which each is formed. At this time the nature of **199** metabolism was unknown and therefore the desired synthetic target for this experiment would reveal all metabolites regardless of which area of the parent compound was affected. Potential targets

(Figure 66) were proposed based on synthetic feasibility and availability of starting materials utilising adapted versions of Scheme 19.

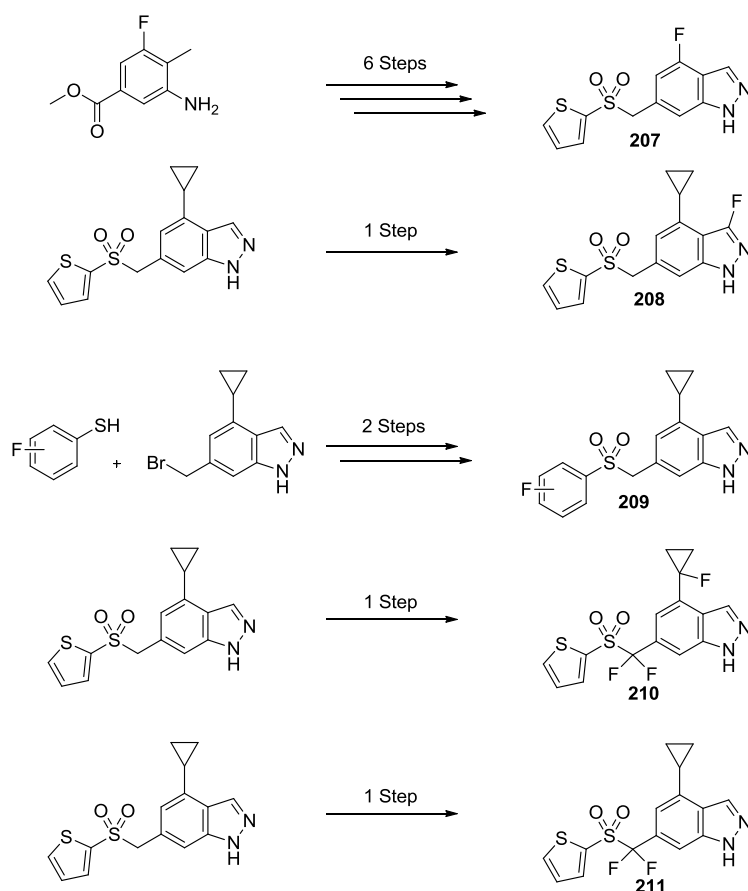
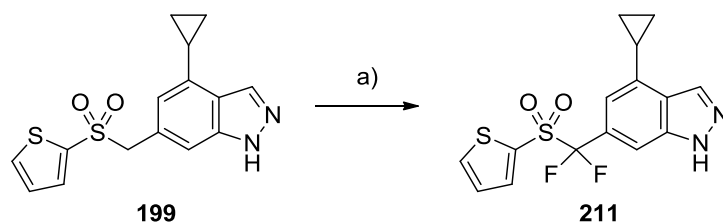


Figure 66. Proposed fluorinated targets **207-211** and the proposed forward synthesis from a commercially available starting material or intermediate of Scheme 19.

4-Fluoro (**207**) and fluorophenyl (**209**) targets were disregarded because of their significant structural difference to **199**. Both the thiophene and cyclopropyl units could be sites of metabolism and therefore exclusion of these groups would not give a true picture of metabolism in the F^{19} -NMR. Fluorinated compound **210** was not synthesised as the addition of three fluorines in two different environments will not only affect the complexity of the spectra but also the properties of the molecule, more so than desired. A silver mediated, radical procedure was found which allows fluorination of benzyl positions, two of which are present on **199** and therefore it was assumed selectivity would not be obtained.¹⁷⁴ This target may be more attractive if synthesised in the sulphonamide series as a pose to the sulphone as only one benzylic centre is present.

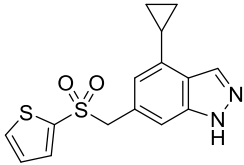
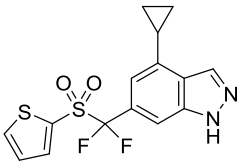
Due to the central location of the fluorinated centre, compound **211** (fluorinated sulphone) was chosen for synthesis. It was postulated that metabolism of the indazole or thiophene would both perturb the chemical shift of the fluorine signal of compound **211**, which would most likely not be the case with compound **208**.

The synthesis of **211** was adapted from a literature procedure describing the fluorination of benzyl sulphonic acids and phosphonates using NaHMDS and either diethylaminosulfur trifluoride (DAST) or *N*-fluorobenzenesulfonimide (NFSI).¹⁷² Both reactions are driven by the breaking of a weak heteroatom (N or S) to fluorine bond and formation of a strong C-F bond. In this case the carbon centre is activated by deprotonation by a strong base. Both NaHMDS and *n*-butyl lithium were tested for the deprotonation with better results derived from the latter, stronger base. NFSI was used as the fluorinating agent which gave satisfactory results and was not further investigated (Scheme 21). The pure product was obtained and tested for enzymatic and cellular activity as well as mouse microsomal clearance and solubility (Table 45).



Scheme 21. Synthesis of **211**; Reagents and conditions; a) *n*-Buli, NFSI, THF, -78 °C-RT, 18 h, 49%.

Table 45. Potency, Clearance and Lipophilicity data regarding **199** and **211**.

Structure		
Compound	199	211
ERK5 Enzymatic IC ₅₀ (μM)	0.012 ± 0.007	0.019 ± 0.003
ERK5 Cellular IC ₅₀ (μM)	0.04 ± 0.04 ^a	0.003 ± 0.04 ^b
Mouse Microsomal Clearance (μl/min/mg)	378	604
cLogp	4.83	5.45
Caco-2 A2B/B2A	39/20	11.8/10.7
Efflux Ratio	0.52	1.11

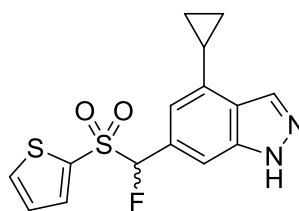
^a HeLa western blot assay; ^b MEF2D reporter assay

Both **211** and the parent compound **199** possess excellent enzymatic and cellular potency against ERK5. As potency is maintained it suggests there is room for a small group at the sulphone position which may improve potency. However, it is crucial to recall the *N*-ethyl sulphonamides synthesised in Chapter 2.5.1.2 which showed a reduction.

The fluorination of the sulphone resulted in an increase in microsomal metabolism indicating that the benzyl position is not a centre of metabolism, as fluorination of this centre removes any possibility of oxidation. It is most likely that this increase in the rate of metabolism is caused by the increase in lipophilicity and therefore better recognition by CYP enzymes. The increased lipophilicity also means that compound **211** has inferior solubility to the parent (**199**) but remains sufficiently soluble for both activity assays to be completed and an *in vivo* formulation to be prepared.

Isolation of a racemic mixture of mono-fluorinated **199** derivatives (*rac*-**212**) was possible upon scale up of the synthesis expected to yield **211** (Scheme 21). This mixture was tested for ERK5 activity in the enzymatic assay measuring a similar potency of 0.015 ± 0.006 μM to **199** and **211** (Figure 67). The activity of this compound (*rac*-**212**) reflects the same SAR generated for **211**, tentatively indicating there is some

space for substitution at the sulphone. This compound was not used in any subsequent analysis due to the limited amount isolated. The mixture has not been chirally resolved.



212

Enzymatic ERK5 IC₅₀ = 0.015 ± 0.006 μM

Figure 67. Structure of monofluorinated compound **212**.

2.9.5.2 F^{19} -NMR experiments with **211**

A formulation of **211** was made up and mice were dosed via IP at 100 mg/Kg and kept in a metabolic cage for 24 hrs. Urine of both test and control mice was collected during this time and stored at -20 °C. This work was conducted by Dr Huw Thomas in the NICR, Newcastle-upon-Tyne.

After calibration of the NMR to the fluorine signal of the positive control both urine samples were run giving the spectra shown in Figure 68. The NMR data shows that **211** is almost entirely metabolised inside the 24 hour time period to one major metabolite. A remnant of un-metabolised sample is visible in the dosed animal urine but indicating rapid clearance. Only one new peak appears in the dosed animal urine which is unlikely to refer to two or more metabolites with the same chemical shift.

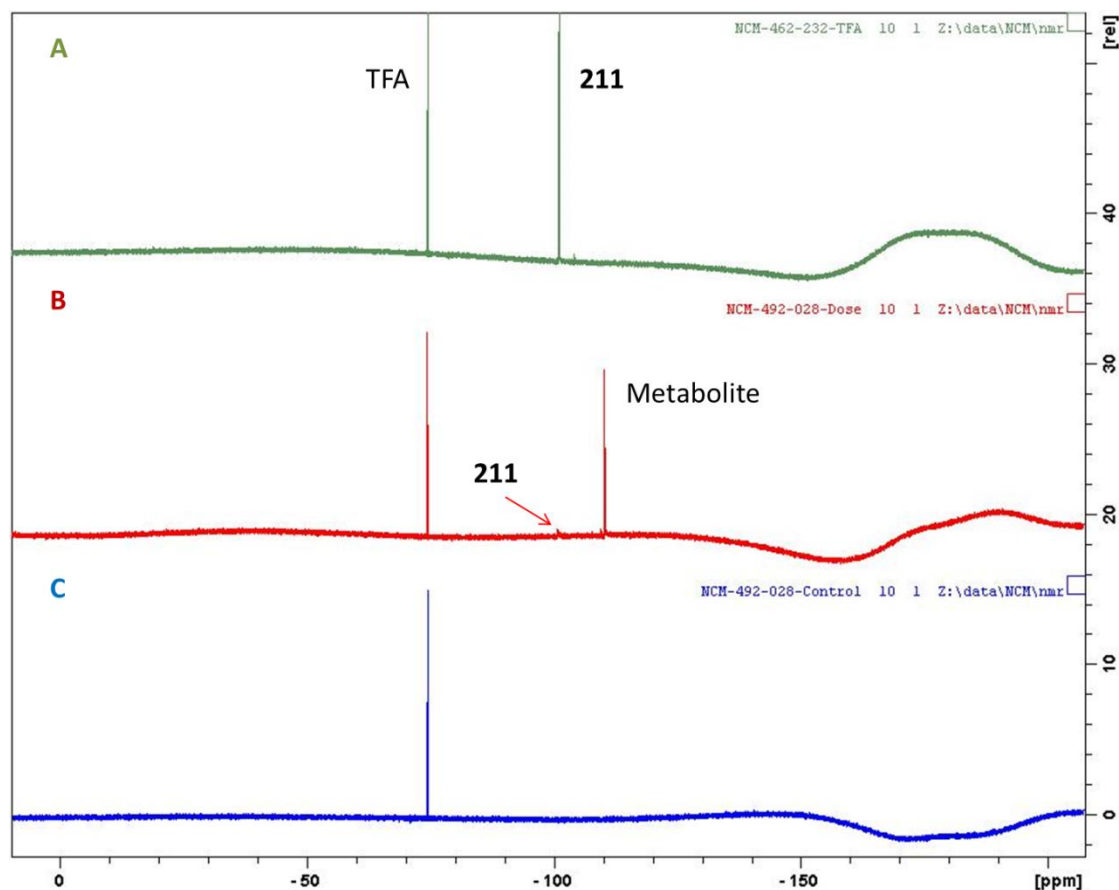


Figure 68. F^{19} -NMR Spectra A) positive control (200 μ L DMSO- d_6 , 200 μ L H $_2$ O, 44 μ L TFA H $_2$ O; green); B) dosed mouse urine (200 μ L DMSO- d_6 , 200 μ L dosed animal urine, 44 μ L TFA H $_2$ O; red); C) negative control (200 μ L DMSO- d_6 , 200 μ L negative control urine, 44 μ L TFA H $_2$ O; blue).

This data suggests only one metabolite exists which would simplify optimising the metabolic profile of the series, however, an out-sourced metabolite identification study showed that this data was not representative of **199** metabolism (Chapter 2.9.6). It is known from microsomal data that **211** is less metabolically stable than **199** and it is therefore expected that that sensitivity to different routes differs between the two molecules.

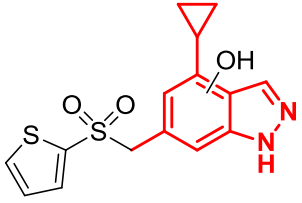
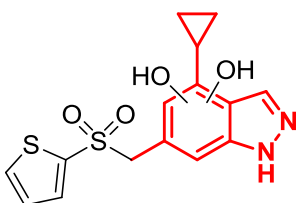
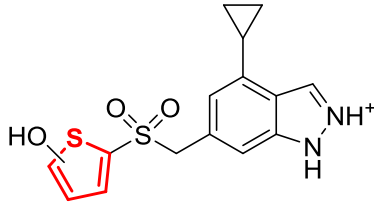
Although the findings here have not improved knowledge of **199** pharmacokinetics, the discovery of an equipotent compound with rapid, but simple metabolism may prove important later in the development of indazole ERK5 inhibitors.

2.9.6 Metabolite Identification Study of **199**

A metabolite identification experiment was outsourced to Cyprotex for **199** revealing five major metabolites. The study was conducted by incubating the compound (**199**) with mouse liver microsomes for 15 minutes and analysis of the resulting solution by

LCMS. Mouse liver microsomes contain a mixture of CYP and other membrane bound metabolising enzymes found in hepatocytes. The findings of the study are summarised in Table 46. This study reconfirms the initial microsomal clearance data which showed the rapid clearance of the compound. This is made clear by the fact that almost 80% of the sample is metabolised in the 15 minute time frame.

Table 46. Metabolite ID study of 199.

Type/location	Peak Area at 15 mins (%)	m/z Found	Retention Time (min)
Parent compound 199	32.4	319.0570	8.14
Indazole Oxidation	12.5	335.0519	6.00
	11.4	335.0518	6.62
	17.5	335.0511	6.92
Indazole di-oxidation			
	19.4	351.0473	5.40
Thiophene oxidation			
	6.9	335.0513	7.54

The study identified single oxidation of the indazole as the major metabolite. The experiment is not able to distinguish between the five different possible sites of oxidation on the cyclopropyl indazole. Metabolites are identified by mass

spectrometry fragmentation patterns. Compound **199** typically fragments across the sulphone bond which means the location of metabolites can only be determined to be on either the indazole or thiophene halves of the molecule. A second oxidation occurs on the indazole in 20% of the sample and interestingly only one metabolite is shown. As three singly oxidised metabolites are present it would be expected that three doubly oxidised metabolites would also exist. The fact that only one exists may mean that oxidation at certain positions on the indazole prevents further (second) oxidation. It is also possible that the doubly oxidised metabolite is oxidised at one or more different positions to the singly metabolised peaks. There are six positions which could potentially be oxidised on the indazole portion of the molecule highlighted in Table 46, not including *N*-oxidation (Figure 69).

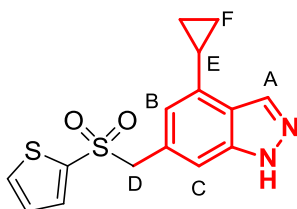


Figure 69. Potential oxidation sites on the indazole core.

Position D has been discounted as an oxidation site due to synthesis of di-fluoro sulphone compound **211** which did not improve the metabolic profile (Chapter 2.9.5). Rapid oxidation of benzylic positions such as E (Figure 69) is well documented and is likely to have been oxidised in this case.

Oxidation on the thiophene occurs in 7% of the sample which is the smallest portion of metabolites. This data only shows the effects of phase 1 metabolism caused by CYP enzymes but this is not necessarily the limit of compound modifications. Once oxidised thiophenes are susceptible to nucleophilic attack producing toxicophores depending on the nature of the nucleophile. If thiophene-glutathione conjugates form, renal excretion is increased. However, if protein or CYP enzymes act as the nucleophile toxicity generally increases. The real danger posed by the thiophene ring is the nature of the metabolites. Production of epoxides, thiols, thials and aldehydes by ring opening or other pathways and the formation of Michael acceptors *via* S-oxidation means numerous highly reactive species are released (Figure 70).

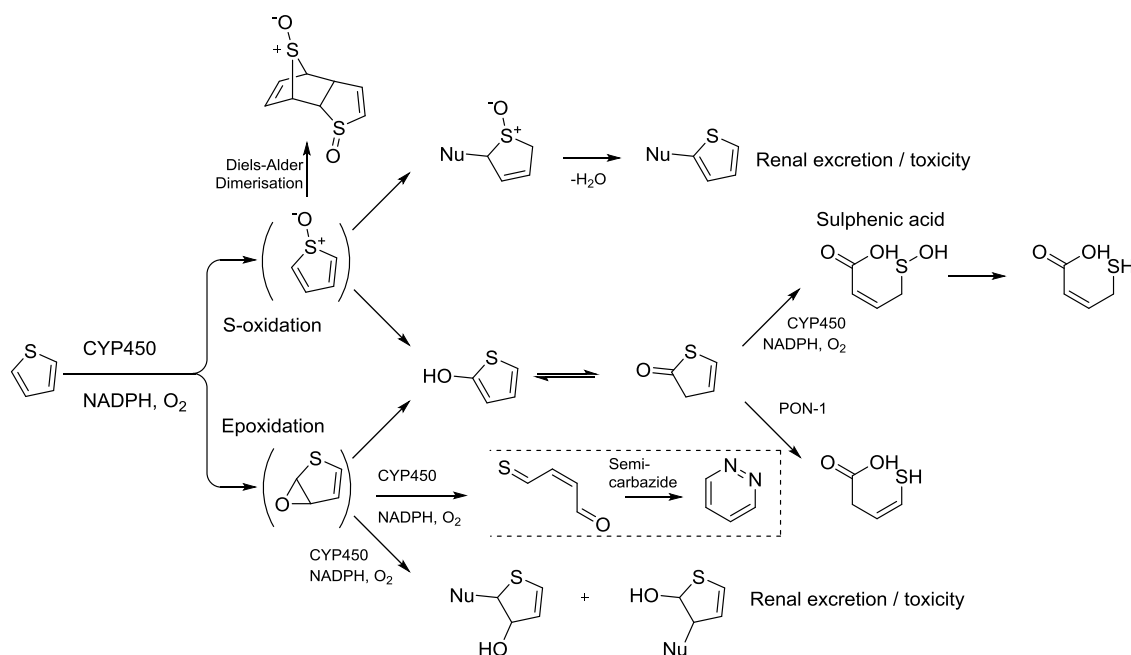
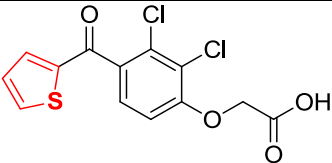
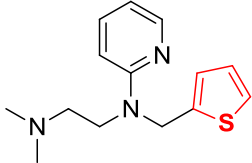
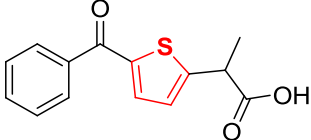
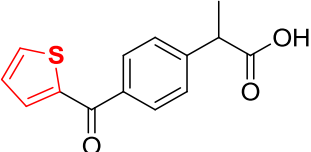
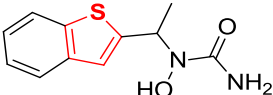


Figure 70. Biotransformations of the thiophene ring, adapted from Dolenc *Et al.*^{124, 175}

The most common reason for a drug to be withdrawn from the market is idiosyncratic toxicity derived from formation of reactive metabolites.¹⁷⁶ Numerous drugs on the market contain the thiophene moiety testifying to its suitability to drug-like structure. In some examples the thiophene is the major source of metabolic changes to the molecule and is associated with various toxicities (Table 47). Oxidation of the sulphur is common across these drug structures with some evidence for epoxidation also. Toxicity is commonly associated with the liver and also the kidneys as these are the major sites of metabolism. CYP inhibition by Tienilic acid (**213**) metabolites is critical due to the prevalence of CYP2C9 which is speculated to metabolise 15% of all drugs.^{177, 178} The chance of drug-drug interactions is significantly increased when a fundamental enzyme such as CYP2C9 is inactivated increasing the chance of adverse effects.¹⁷⁹

Table 47. Drugs containing a thiophene ring, the metabolic pathway and any associated toxicity. Adapted from Dolenc *et al.*¹⁷⁵

# - Name	Drug Structure	Reactive Thiophene Metabolite	Toxicity of Daily Dose
Drugs containing metabolically labile thiophene:			
213-Tienilic acid		S-oxide, epoxide	CYP2C9 inactivator
214-Methapyrilene		S-oxide	Liver toxicity in rats, Periportal necrosis
215-Tiaprofenic acid		Not reported	Acute cystitis
216-Suprofen		S-oxide, epoxide	Renal toxicity in humans
217-Zileuton		S-oxide	Hepatotoxic

In every case of the drug examples included in Table 47 the thiophene is substituted in the 2-position and the 4-position is unoccupied. As seen in Figure 70 all five positions around the thiophene ring can be oxidised unless substituted meaning that only a completely masked thiophene, including S-oxidation, would attenuate the metabolism beyond doubt. Examples of both electron-rich and -deficient thiophenes are included in Table 47 with no clear distinction between the metabolism of either.

Figure 71 shows thiophene containing drugs in which the thiophene is not the major route of metabolism. Structurally these compounds are unrelated and the properties cannot be correlated to aid design decisions regarding progression of **199** though it is encouraging that two cases of mono-substituted thiophenes exist without metabolic liability.

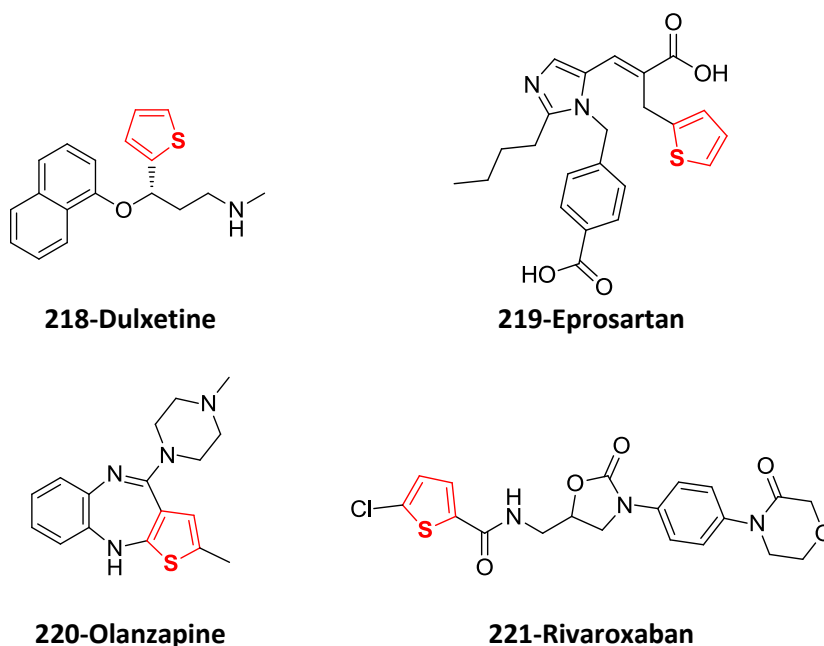
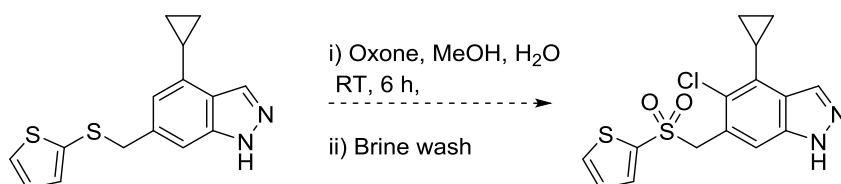


Figure 71. Drugs containing a thiophene ring which are not metabolised via biotransformations of thiophene. Adapted from Dolenc *et al*¹⁷⁵.

Metabolism of the thiophene accounts for 10% of metabolites identified in the study and is known to produce reactive and therefore toxic metabolites. For this reason replacement heterocycle systems were investigated to improve the metabolic liability of the moiety and the overall LogP of the compound (see Chapter 2.11.1).

2.9.6.1 Targets Arising from Metabolite Identification Study of **199**

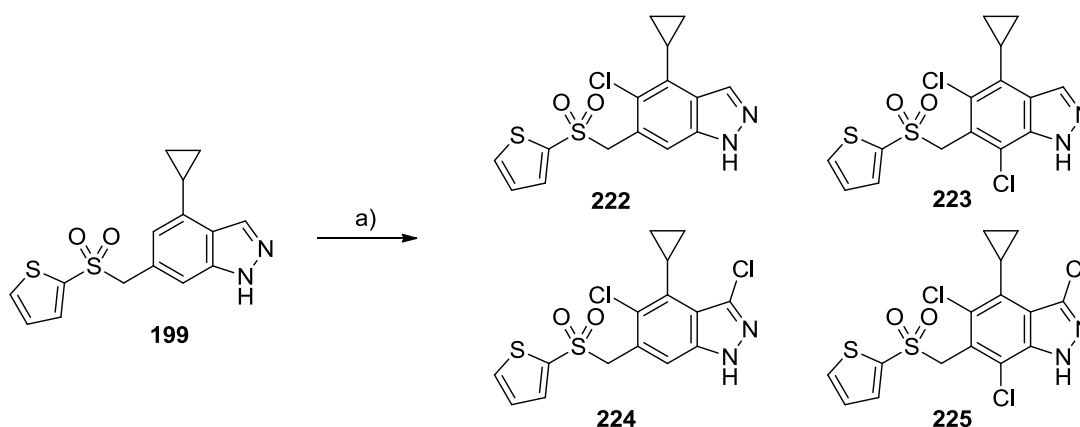
The results of the metabolite ID study show that oxidation of the indazole and cyclopropyl are the major causes of fast excretion in mice. No indication is given in the study as to which positions on the structure are the most labile and at least three different positions are affected in almost equal measure. A 5-chloro indazole (**222**) derivative of **199** was proposed for synthesis to better understand the reactivity of the 5-position. Introducing a halogen to the aromatic ring blocks any metabolism at that position thus if microsomal stability fluctuates a relationship can be established. A procedure to give compound **222** was found serendipitously when investigating thiophene replacement groups (Chapter 2.11.1). During thioether oxidation to sulphone, it was noted that a small amount of chlorination took place selectively at the 5-position (Scheme 22). This transformation occurred due to the presence of both Oxone® and NaCl in the work up of the oxidation reaction.



Scheme 22. Hypothetical reaction of thioether **191** in Oxone® and brine to produce chlorinated derivative **222**.

2.9.6.2 Synthesis of Chlorinated Derivatives of **199**

The reaction was repeated on the sulphone compound **199** with an excess of brine in order to establish the limits of chlorination. Two equivalence of Oxone® in H₂O, one equivalence of **199** in MeOH and brine were used to make a 1:1 ratio of aqueous and organic solvent. The solution was stirred overnight at room temperature and showed full conversion of the starting material to four products by LCMS after this time (Scheme 23).



Scheme 23. Formation of chlorinated derivatives of **199**; Reagents and conditions; a) Oxone, Brine, H₂O, MeOH, RT, 18 h, Quantative (**222** 36%, **223** 24%, **224** 21%, **225** 21%).

All four products (**222-225**) were separable by standard phase MPLC and produced in a quantative yield regarding starting material. The major product was the mono-chlorinated compound **222** (36%) and the remaining doubly and triply chlorinated compounds were isolated in near equal measure. Substitution patterns were easily identifiable by H¹-NMR after using 2D spectra to full assign **199** with high confidence. Proton peaks corresponding to chlorinated positions can be seen to disappear in Figure 72 as the degree of chlorination increases.

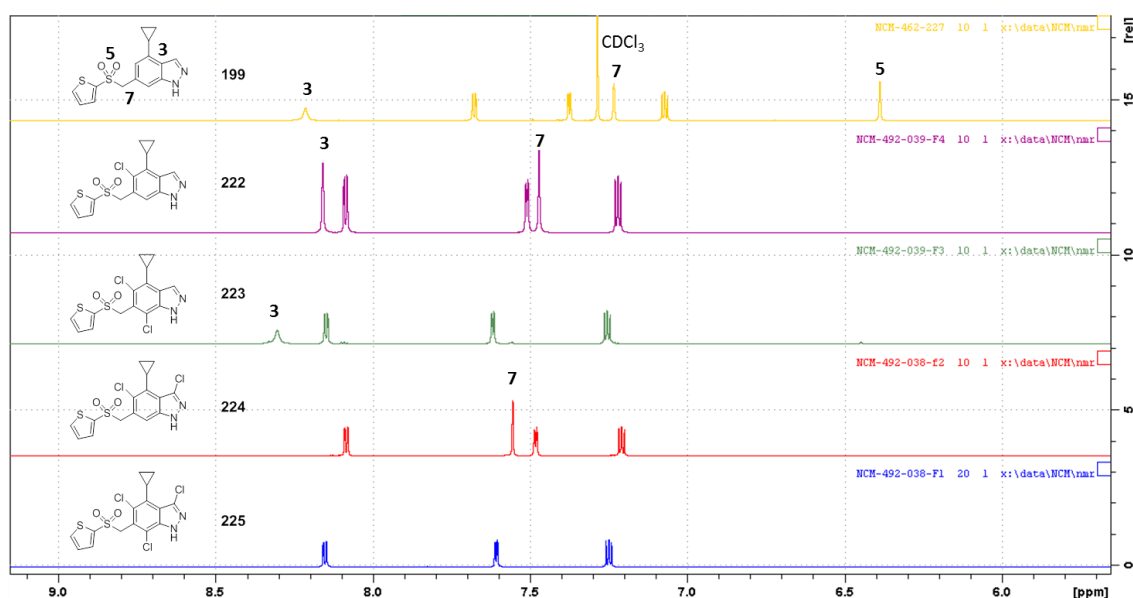


Figure 72. ^1H -NMR spectra of **199** and **222-225** aromatic regions. **199** sample in CDCl_3 , **222-225** all in $\text{DMSO}-d_6$.

The chlorination is an electrophilic aromatic substitution ($\text{S}_{\text{E}}\text{Ar}$) caused by the formation of hypochlorous acid from the radical decomposition of peroxymonosulfate (active salt in Oxone®)(Figure 73).¹⁸⁰ Hypochlorous acid is a highly reactive source of Cl^+ and so the indazole positions conjugated to the NH are readily chlorinated, which are the unoccupied 3-, 5- and 7-positions. The electron withdrawing effects of halogenation of indazole are not so great that the nucleophilicity is completely diminished and therefore multiple chlorinations occur on one substrate leading to the di- and tri-halogenated compounds **222-225**.

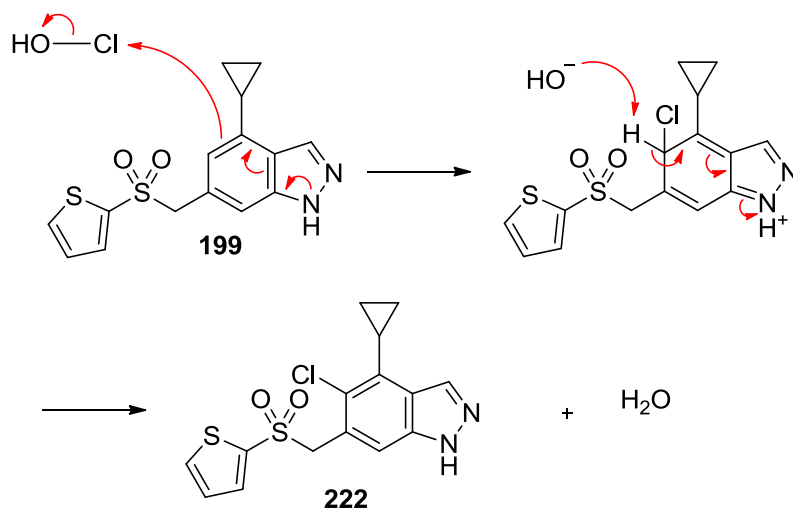
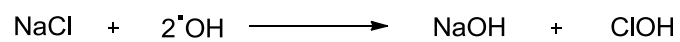
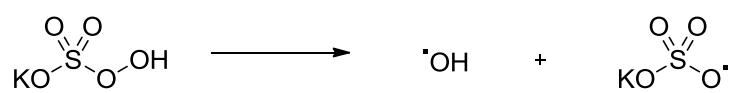
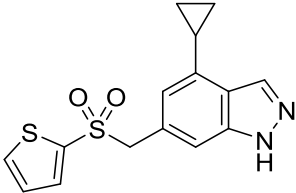
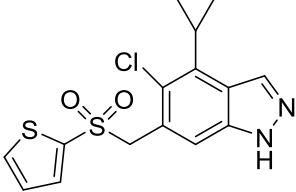
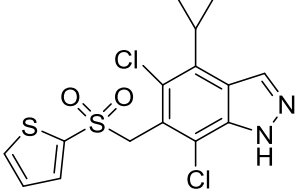
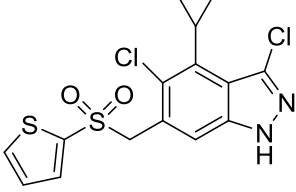
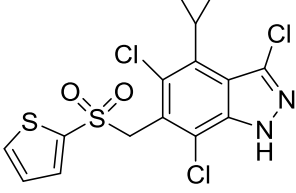


Figure 73. Mechanism of Oxone[®] mediated chlorination of **199**.

2.9.6.3 Activity and Metabolism SARs of Chlorinated Derivatives of **199**

Indazoles **222-225** were tested for ERK5 activity and mouse liver microsome stability. As expected potency was diminished particularly in compounds **224** and **225** which both present 3-chloro groups (Table 48).

Table 48. ERK5 activity, microsomal stability and lipophilicity of compounds **222-225**.

	Structure	ERK5 enzymatic IC ₅₀ (μM) ^a	Mouse liver microsomal stability (μl/min/mg)	CLogP
199		0.012 ± 0.007	378	4.83
222		0.28 ± 0.14	604	5.45
223		0.18 ± 0.05	696	6.07
224		4.6 ± 1.9	390	6.47
225		3.4 ± 0.3	148	7.09

^a ERK5 IC₅₀ values generated by IMAP cell free assay (350 μM ATP).

Metabolism data shows that all compounds are rapidly cleared, however, this was not unexpected due to increase made to LogP and the fact that some susceptible parts of the molecule remain exposed. Comparison of **199** and **222** indicates that the 5-position

is not a major site of oxidation due to the large increase in clearance. A similar difference in clearance is seen between **223** and **224** indicating that the occupation of the 3-position has a larger effect on metabolism than substitution of the 7-position. This conclusion is further confirmed by the clearance result of **225** which is significantly superior to **224** and therefore oxidation at the 3-position of **199** is more prevalent than the 5- or 7-positions.

This data suggests that substitution at the indazole 3-position may yield an improvement to metabolism. A large number of compounds have been synthesised exploring the 3-position (Chapter 2.10) and the metabolic trends of these compounds are discussed in Chapter 2.11.

2.10 3,6-Substituted Indazoles

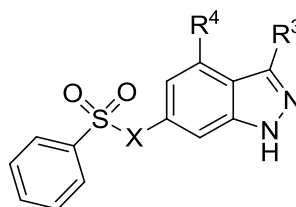
Substitution of the indazole 3-position presents a potentially fruitful vector along the hinge region of the ERK5 active site. As discussed previously, many drug molecules include 3-substituted indazoles. The indazole structure is capable of making two close proximity hydrogen bonds and therefore is commonly seen to interact with the amino acid backbone in the kinase hinge region. Frequently an extra interaction can be gained by introducing a further hydrogen bonding group at the 3-position.

2.10.1 Molecular Modelling of 3,6-Substituted Indazoles

Using the published crystal structure of ERK5, potential synthetic targets were docked into the active site using docking software 'GOLD'.¹⁶⁴ The compounds were chosen to assess which linker system may be preferred (sulphone or *N*-methyl sulphonamide) and what type of group would be best tolerated in the 3-position. In total 33 speculative compounds were proposed, 6 of which have direct relevance to the 3-position (Table 49). Compound **226** is included for reference as a compound that was synthesised and tested for activity. Therefore the docking score can be related to a real ERK5 activity value. The docking study was run to a high efficiency with *ca.* 12 solutions predicted for each compound. The active site was treated as rigid for the study with the exception of Lys39 which was permitted free rotation. Whilst results generated in this way are not as accurate as measured activity they serve as a guide to prioritise synthesis. The GOLD fitness score is an amalgamation of all scoring functions provided

by the program giving a high score that should in theory be comparable to binding enthalpy (see Chapter 2.8.1 for details). All compounds chosen are synthetically plausible and represent 3 classes of targets, namely; alkyl (**227/228**) amide (**229/230**) and amine (**231/232**).

Table 49. Molecular docking data gathered for compounds **226-232** in the ERK5 active site using GOLD.



Compound	X	R ³	R ⁴	GOLD Fitness score (ERK5 IC ₅₀)
226	NMe	H	Et	64.4 (43 nM)
227	CH ₂	Me	H	59.6
228	NMe			55.1
229	CH ₂	CONHMe	H	61.3
230	NMe			56.3
231	CH ₂	NHMe	H	67.9
232	NMe			59.3

There is a clear trend in this data set suggesting that the sulphone linker is superior to the *N*-methyl sulphonamide. This conclusion is entirely due to the ligand torsion and ligand clash scores given by the programme which predict that the *N*-methyl group on compounds **226**, **228**, **230** and **232** prevents compounds adopting the binding conformation without a steric penalty. The results also show that the introduction of small amine groups at the 3-position is the most promising compound set of three due to an improved hydrogen bonding profile. All scores are in a range suitable for synthesis and the visualisations show reason to believe that larger groups will also be tolerated (Figure 74).

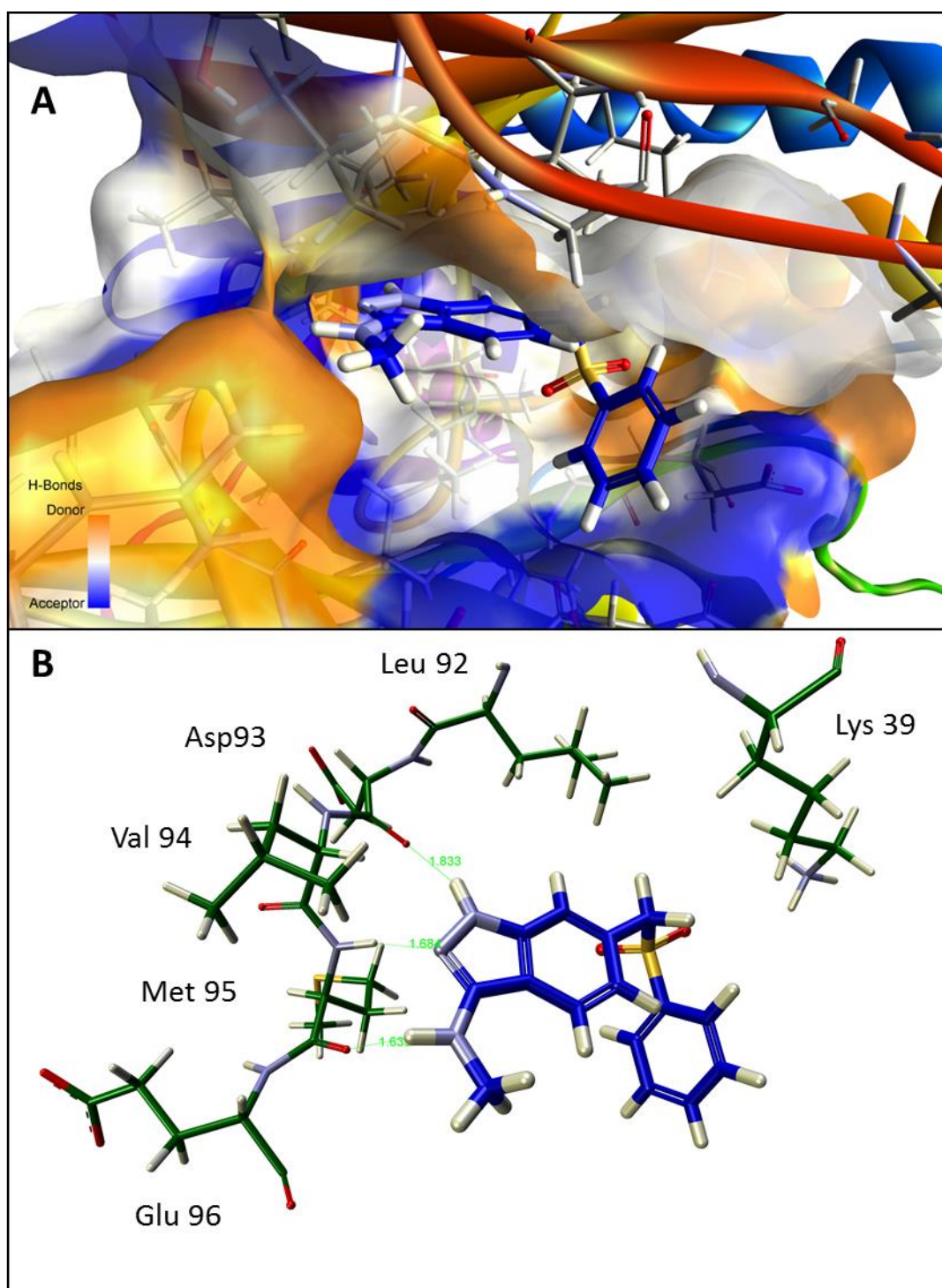


Figure 74. Best scoring docking pose of compound **231** (blue) in the ERK5 active site. A) ERK5 protein surface shown, B) Key interacting residues of ERK5 (green) with Compound **231** (blue). (PDB: 4IC8)

2.10.2 Synthetic 3,6-Substituted Indazole Targets

Three compound sets were designed for investigating interactions at the 3-position; alkyl, amine and amide. It is hypothesised that all three can be made from one common halogenated intermediate using various synthetic procedures (Figure 75).

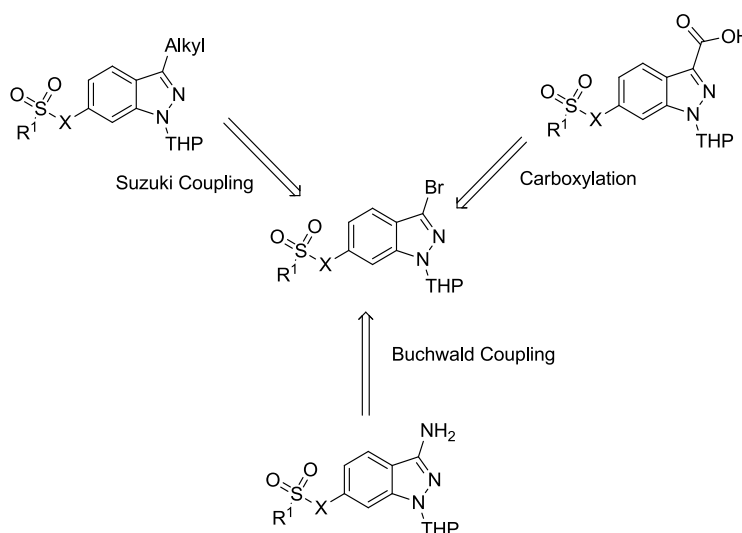
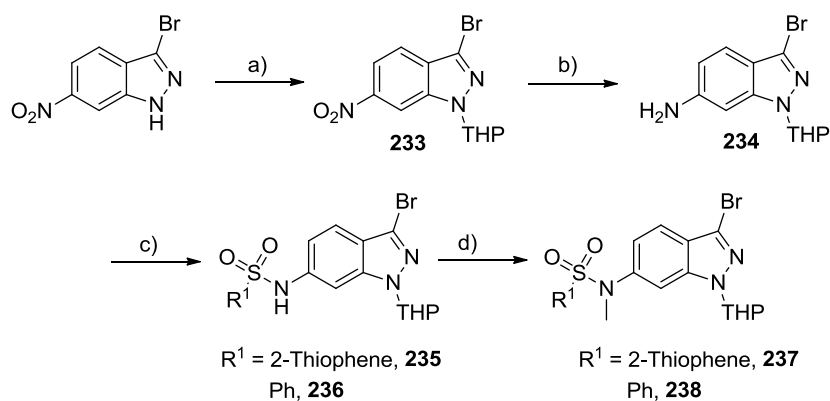


Figure 75. Retrosynthetic analysis of 3-substituted indazoles, X = CH₂ or NMe, R¹ = Ph, 2-thiophene or 4-MeOPh, Alkyl = Me, Et, ^{Cyc}Pr, Ph.

Synthesis of both linker types was investigated and it was decided that this series of compounds would be made with the N-Me sulphonamide linker due to the availability of 3-bromo-6-nitro-1*H*-indazole starting material. The guidance of molecular modelling data means that sulphone compounds are expected to be superior to the alkylated sulphonamide, however, a parallel SAR is expected for 3-position substituents for both linkers.

The key intermediates **237/238** were synthesised in 4 steps commencing with a THP protection (Scheme 24). The nitro reduction was conducted using Pd/C and H₂ in a Thales H-cube flow reactor which gave complete conversion to **234** without the need for optimisation or purification. The sulphonamide formation was conducted using previously optimised conditions in pyridine and was methylated using methyl iodide in DMF with Cs₂CO₃. For these compound sets only phenyl and 2-thiophene R¹ groups were included with the major focus on 2-thiophene derivatives.



Scheme 24. Synthesis of key intermediates **237/238**. *Reagents and conditions:* a) DHP, p-TSA, DCM, RT, 6 h, 86%; b) Pd/C, H₂, EtOAc, 40 °C, 6 h, 99%; c) R¹-SO₂Cl, Pyr, RT, 16 h, 90%; d) MeI, K₂CO₃, DMF, RT, 4 h, 90-98%.

2.10.3 Synthesis and evaluation of 3-Alkyl-6-Sulphonamide Indazoles

2.10.3.1 3-Alkyl-6-Sulphonamide Indazole Targets

Synthetic targets are shown in Figure 76 all of which are accessible via Suzuki reaction on the key intermediate **237/238**. Small probing groups have been chosen up to a large phenyl group which is predicted to be too large for the space. This data set revealed the volume of space open to the 3-position vector and some encouraging potency results.

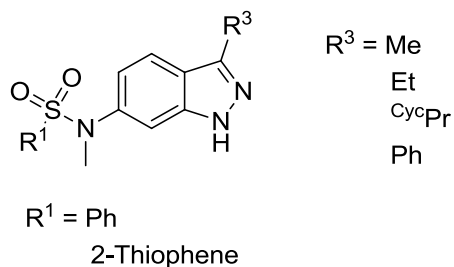
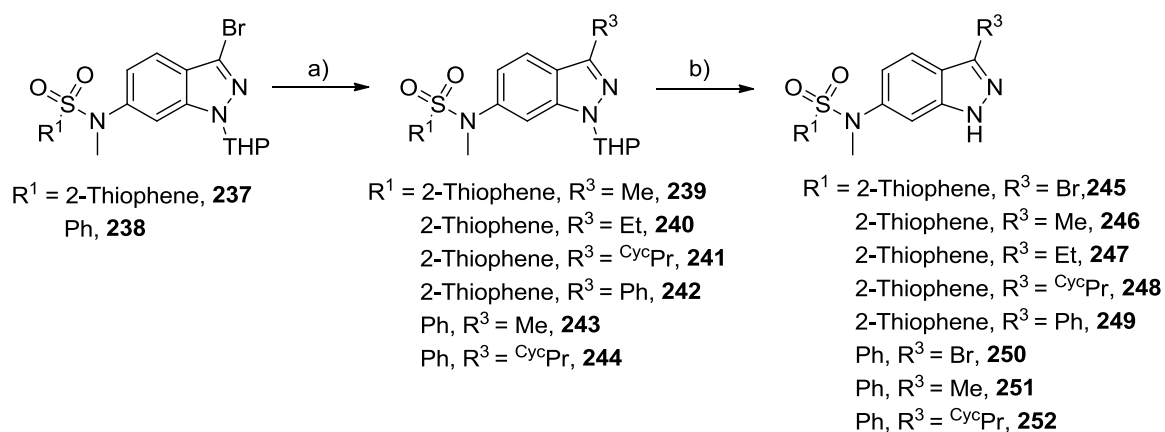


Figure 76. Synthetic targets for 3-alkyl indazole sulphonamides.

2.10.3.2 Synthesis of 3-Alkyl-6-Sulphonamide Indazole Targets

Using the Suzuki conditions employed to install alkyl groups at the indazole 4-position (Chapter 2.8.3) followed by THP deprotection (Scheme 25) all targets were synthesised in high yields (Table 50).

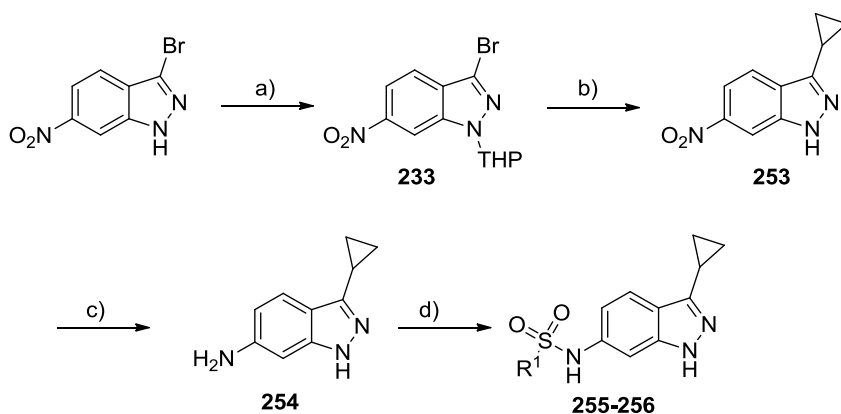


Scheme 25. Reagents and conditions: a) Pd(dppf)Cl_2 , $R^3\text{-B(OH)}_2$, Cs_2CO_3 , 1,4-dioxane, MW, 150°C , 0.5 h, 67-99%; b) MeOH.HCl , RT, 6 h, 31-92%.

Table 51. Yields of Suzuki reactions to form compounds **239-244**.

Compound	R^1	R^3	Boron Species	Yield
239		Me	Trimethyl boroxine	85%
240		Et	EtB(OH)_2	67%
241		Cyc Pr	Cyc PrB(OH)_2	96%
242		Ph	PhB(OH)_2	99%
243		Me	Trimethyl boroxine	99%
244		Cyc Pr	Cyc PrB(OH)_2	80%

Two non-methylated sulphonamide targets were synthesised to maintain confidence in the linker SAR developed in Chapter 2.5.1 which concluded the *N*-methyl sulphonamide was superior. Targets were synthesised using the same procedures as Schemes 24 and 25 but the order was changed to avoid the presence of protonated nitrogen in the Suzuki reaction (Scheme 26). Unexpectedly, during the Suzuki reaction significant deprotection was witnessed resulting in the isolation of compound **253** as the major product in an approximately 3:2 ratio with the protected derivative. This synthesis yielded both final compounds, however, yields were reduced in the final step due to formation of 6-disulphonamide and 1,6-sulphonamides (Figure 77) in small quantities. Had the THP deprotection been conducted last as initially planned this formation would have been limited.



Scheme 26. Reagents and conditions: a) DHP, p-TSA, DCM, RT, 6 h, 86%; b) Pd(dppf)Cl₂, ^{cyc}Pr-B(OH)₂, Cs₂CO₃, 1,4-dioxane, MW, 150 °C, 0.5 h, 58%; c) Pd/C, H₂, EtOAc, 40 °C, 6 h, 93%; d) R₁-SOCl, Pyr, RT, 16 h, 17-46%.

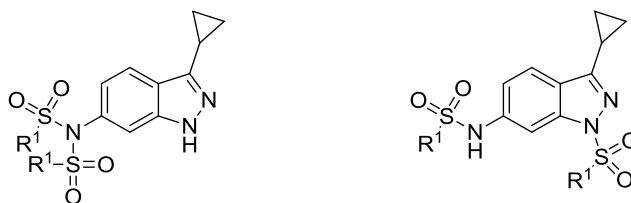
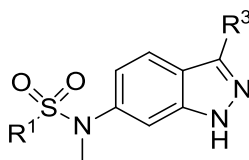


Figure 77. By-products of sulphonamide formation reaction

2.10.3.3 SAR of 3-Alkyl-6-Sulphonamide Indazole Compounds

Compounds were tested for activity against ERK5 and p38α showing a mixed range of potency. As was seen with the 4-substituted series, the bromine is not tolerated in either matched pair (Table 52). An increase in potency is seen when small alkyl groups are introduced, most profoundly in the complete 2-thiophene data set. Ethyl compound **247** shows excellent activity, however, potency dropped when a slightly larger cyclopropyl group (**248**) was introduced. This data set suggests there is room for a small group at the three position with alkyl properties. Compound **249** with a phenyl group also has good potency at 100 nM suggesting aromatic groups may also be tolerated.

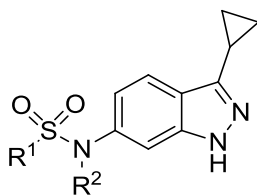
Table 52. Enzymatic activity data of compounds **245-250** against ERK5 and p38 α .

Compound	R ¹	R ³	IC ₅₀ (μM)	
			ERK5 ^a	p38 α ^b
82		H	1.1 ± 0.6	>120
250		Br	2.4 ± 0.1	>120
251		Me	0.48 ± 0.05	>120
252		CycPr	0.32 ± 0.18	>120
84		H	0.45 ± 0.09	>120
245		Br	3.6 ± 0.6	>120
246		Me	0.16 ± 0.05	>120
247		Et	0.05 ± 0.05	>120
248		CycPr	0.29 ± 0.05	>120
249		Ph	0.10 ± 0.01	>120

^a ERK5 IC₅₀ values generated by IMAP cell free assay (350 μM ATP); ^b p38 α IC₅₀ values generated by Lance assay (350 μM ATP).

Cellular data collected in the HeLa cell Western blot assay shows 3-ethyl compound **247** to have an IC₅₀ of 0.17 μM and 3-phenyl **249** an IC₅₀ of 0.09 μM. Correlation between the enzymatic and cellular data is good in this case and both compounds have reasonable potency in cells.

Overall, potency has increased over unsubstituted 3-position compounds (**82** and **84**) and therefore this substitution could be combined with substitution at the 4-position which may further increase potency. The sulphonamide linker targets **255-256** showed a consistent SAR as potency was found to be inferior to the methylated match pairs **30** and **38** (Table 53).

Table 53. Enzymatic activity data of compounds **253-254** against ERK5 and p38 α .

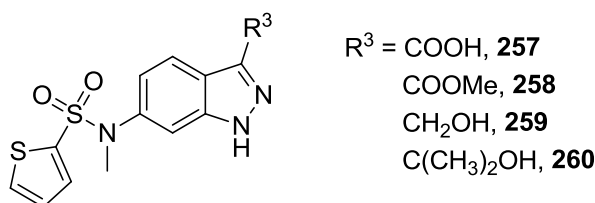
Compound	R ¹	R ²	IC ₅₀ (μM)	
			ERK5 ^a	p38 α ^b
255		H	1.3 ± 0.1	>120
252		Me	0.32 ± 0.18	>120
256		H	1.2 ± 0.6	>120
248		Me	0.29 ± 0.05	>120

^a ERK5 IC₅₀ values generated by IMAP cell free assay (350 μM ATP); ^b p38 α IC₅₀ values generated by Lance assay (350 μM ATP).

2.10.4 Synthesis and evaluation of 3-Carboxyl and Hydroxyl-6-Sulphonamide Indazoles

2.10.4.1 3-Carboxyl and Hydroxyl-6-Sulphonamide Indazole Targets

Targets in this set are polar in nature and therefore will benefit from a good LogP and solubility profile. This small set of compounds will help establish the hydrogen bonding capability in the extended hinge region of the kinase active site. Typically acidic groups are not desirable in a drug molecule as ionised drugs cannot pass through the cell membrane thus limiting the bioavailability. The functionality is also a known substrate for glucuronidation. Carboxylic acid target **257** is a useful intermediate for the synthesis of the remaining targets and therefore was also tested for activity.

**Figure 78.** Synthetic targets exploring the 3-position with carbonyl and hydroxyl groups.

2.10.4.2 Synthesis of 3-Carboxyl /Hydroxyl-6-Sulphonamide Indazole Targets

There are numerous examples of carbonylation reactions in the literature describing conditions amenable to a halogenated substrate.¹⁸¹⁻¹⁸⁴ To avoid the use of gaseous

carbon monoxide, a procedure was selected which included the *in situ* formation of the reagent from Ac_2O . Bromo indazole **237** was dissolved in THF with a palladium catalyst and phosphor ligand, xantphos, and lithium formate. Addition of Ac_2O causes the release of gas and is added through a septum to the sealed flask. The reaction proceeds through bond insertion by the palladium complex in the C-Br bond of the indazole and addition of the formate, the Ac_2O triggers the formation of carbon monoxide which then follows a typical palladium-mediated carbonylation mechanism (Figure 79).¹⁸⁵ This modified carbonylation procedure facilitated the conversion of the 3-bromo-indazole intermediate **237**, to the carboxylic acid **261** in a 95% yield (Scheme 27).

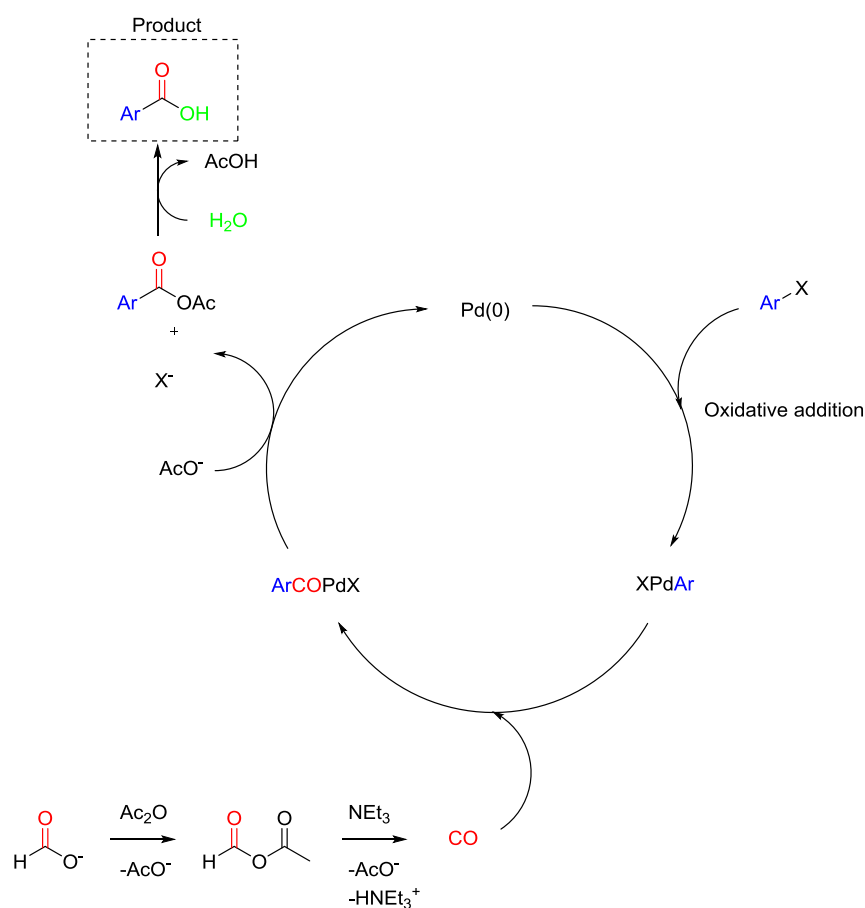
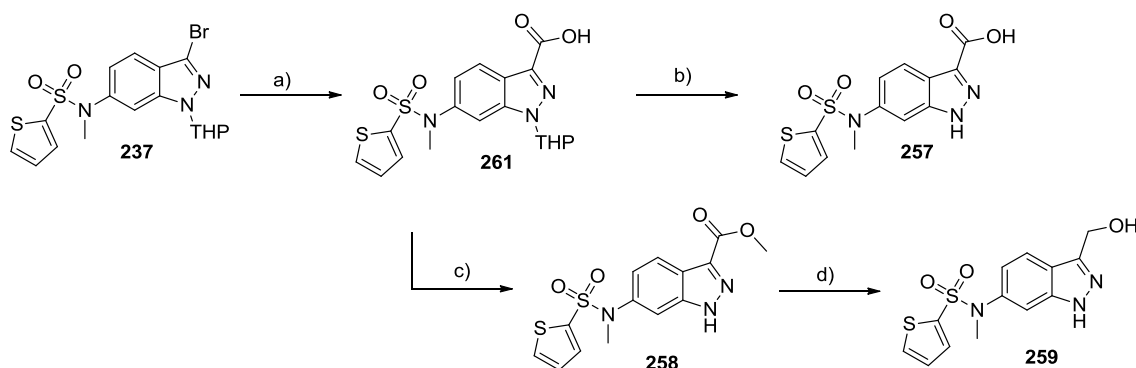


Figure 79. Mechanism of palladium mediated carbonylation using *in situ* generated CO from Ac_2O and lithium formate; adapted from Cacchi *et al.*¹⁸⁵

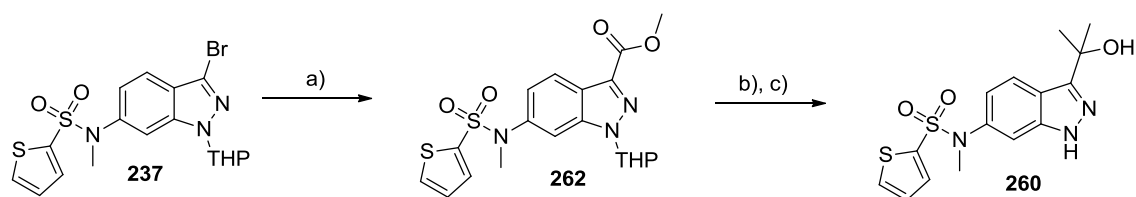
Deprotection of the indazole using a low concentration of HCl gave the desired acid target. By using a strong acid, H_2SO_4 , at a high concentration in MeOH a simultaneous esterification/deprotection reaction was performed giving the desired methyl ester

compound **258** (Scheme 27). The ester product (**258**) was reduced using LiAlH_4 to yield the hydroxyl target **259**.



Scheme 27. Synthesis of final compounds **257**, **258**, **259**. Reagents and conditions: a) $\text{Pd}(\text{OAc})_2$, Xantphos, Et_3N , $\text{HCO}_2\text{Li}\cdot\text{H}_2\text{O}$, Ac_2O DMF, 90°C , 2 h, 95%; b) $\text{MeOH}\cdot\text{HCl}$, RT, 6 h, 69%; c) MeOH , H_2SO_4 , RT, 18h 47%. iv) LiAlH_4 , THF, 4 h 90%;

To synthesise dimethyl-carbinol **260**, a modified version of the palladium-mediated carbonylation was conducted using methylformate in place of lithium formate to give methyl 6-(*N*-methylthiophene-2-sulfonamido)-1-(tetrahydro-2*H*-pyran-2-yl)-1*H*-indazole-3-carboxylate **262** (Scheme 28). The ester was formed in a satisfactory yield (53%) and importantly retained the THP protecting group. Compound **262** was exposed to a small excess of methyl magnesium bromide to give the tertiary alcohol in an excellent yield. Deprotection of this product was not trivial and it was found that a strong acid and a long reaction time was required to remove the THP group due to the now electron rich 3-position.



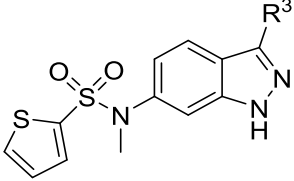
Scheme 28. Synthesis of final compounds **260**. Reagents and conditions: a) $\text{Pd}(\text{OAc})_2$, Xantphos, Et_3N , HCO_2Me , Ac_2O DMF, 90°C , 2 h, 53%; b) MeMgBr , THF, 0°C - RT, 2 h, 87%; c) H_2SO_4 , THF, RT, 72 h, 39%.

2.10.4.3 SAR of 3-Carboxyl and Hydroxyl-6-Sulphonamide Indazole Compounds

Compounds show a range of potencies from poor to moderate. The carboxylic acid (**257**) has poor ERK5 affinity whilst the methyl ester (**258**) analogue shows ten-fold superiority at $1.7\ \mu\text{M}$. The ester **258** is equipotent with the unsubstituted 3-*H* compound **84** indicating no benefit is associated with the addition of the hydrogen

bond acceptor functionality. Neither the carbinol (**260**) nor hydroxyl (**259**) make an improvement to potency, however, the result of the ester **258** and acid **257** compounds suggests that ether versions of these compounds may confer extra potency.

Table 54. Enzymatic activity data of compounds **257-260** against ERK5 and p38 α .

			
Compound	R ³	IC ₅₀ (μM)	
		ERK5 ^a	p38 α ^b
84	H	0.45 ± 0.09	>120
257	COOH	16 ± 0.2	>120
258	COOMe	1.7 ± 0.1	>120
259	CH ₂ OH	3.7 ± 0.2	>120
260	C(CH ₃) ₂ OH	2.8 ± 0.5	>120

^a ERK5 IC₅₀ values generated by IMAP cell free assay (350 μM ATP); ^b p38 α IC₅₀ values generated by Lance assay (350 μM ATP).

A potential problem with the synthesis of the suggested ether targets is their potential for elimination. The indazole is an electron rich aromatic and elimination of groups has been seen at the 4-position when a potential leaving group such as an amine is present in acidic reaction conditions. This elimination is also possible at the 3-position by a similar mechanism (Figure 80). Aqueous acidic conditions are likely to yield compound **259**.

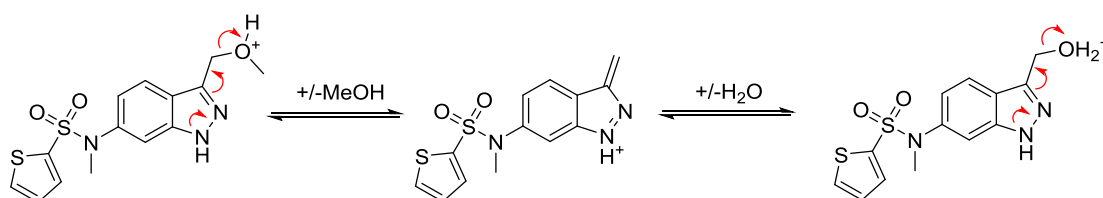


Figure 80. Elimination mechanism of conjugated 3,6-substituted Indazole sulphonamides

2.10.5 Synthesis and Evaluation of 3-Amide-6-Sulphonamide Indazoles

2.10.5.1 3-Amide-6-Sulphonamide Indazole Targets

A set of simple amides were designed to investigate the hydrogen bonding potential at the amide. Progressive alkylation of a primary amide will show if a hydrogen bond donor is beneficial at the 3-position, three bonds away from the indazole hinge binding motif. This target set represents similar chemical space to the acid and ester compounds **257** and **258** but amides are more 'drug like' as rapid metabolism is a lesser concern. Flexibility of these targets is expected to be limited due to the conjugation between the amide and aromatic indazole.

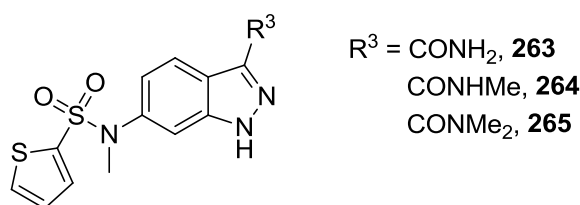
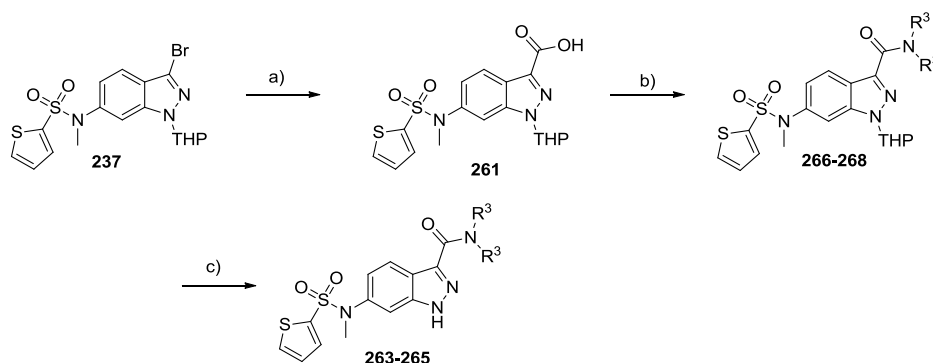


Figure 81. Synthetic targets in the 3-position; amide data set.

2.10.5.2 Synthesis of 3-Amide-6-Sulphonamide Indazole Compounds

From the previously synthesised 3-carboxylic acid **261** a number of amide coupling reactions followed by an elongated deprotection reaction gave the products in a facile manner (Scheme 29). Carbonyldiimidazole (CDI) was used as the acid activating reagent in the amide coupling, giving satisfactory yields of **263-265** without rigorous optimisation.

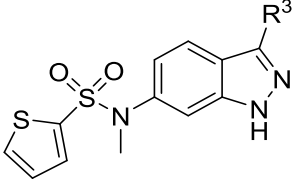


Scheme 29. Synthesis of final compounds **263-265** Reagents and conditions: a) $\text{Pd}(\text{OAc})_2$, Xantphos, Et_3N , $\text{HCO}_2\text{Li}\cdot\text{H}_2\text{O}$, Ac_2O DMF, 90°C , 2 h, 90%; b) CDI, NHR^3_2 , THF, 70°C , 18 h, 27-99%; c) $\text{MeOH}\cdot\text{HCl}$, RT, 72 h, 34-47%.

2.10.5.3 SAR of 3-Amide-6-Sulphonamide Indazole Compounds

ERK5 assay results of the amide data set show a drop in potency over the unsubstituted indazole matched pair **84**. Methylated amides **264** and **265** have superior ERK5 activity to the primary amide **263** indicating that no benefit is gained by the hydrogen bond donor. These values can be compared with those for the methyl ester compound **258** which has an IC₅₀ value of 1.7 ± 0.1 µM and is therefore equipotent to the alkylated amides.

Table 55. Enzymatic activity data of compounds **263-265** against ERK5 and p38α.

			
Compound	R ³	IC ₅₀ (µM)	
		ERK5 ^a	p38α ^b
84	H	0.45 ± 0.09	>120
263	CONH ₂	>30	>120
264	CONHMe	3.5 ± 0.1	>120
265	CONMe ₂	3.8 ± 0.7	>120

^a ERK5 IC₅₀ values generated by IMAP cell free assay (350 µM ATP); ^b p38α IC₅₀ values generated by Lance assay (350 µM ATP).

Similarly to the targets arising from carboxyl and hydroxyl compound sets, the removal of the carbonyl group to leave the alkylated amines appears to be most promising. Again it is expected that these targets may be unstable due to the potential for elimination.

2.10.6 Synthesis and Evaluation 3-Amino-6-Sulphonamide Indazoles

2.10.6.1 3-Amino-6-Sulphonamide Indazole Targets

Simple synthetic targets were chosen in this data set to represent all possible hydrogen bonding profiles immediately adjacent to the core, at the 3-position (Figure 82). Introduction of these groups is predicted to decrease the hydrogen bond strength of the indazole H-bond donor and increase the effect of the H-bond acceptor through the conjugation of the amine lone electron pair. The SAR of this effect is very difficult

to conclude as two parameters are changed simultaneously. It is known that both heteroatoms in the indazole core form hydrogen bonds and it is therefore predicted that the change in electronics will have little effect on the overall hinge binding.

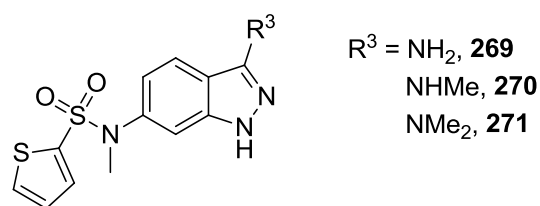
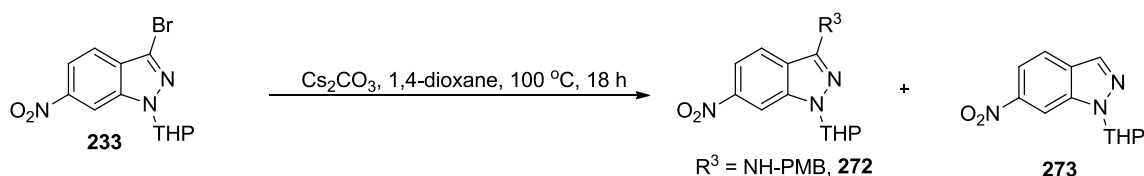


Figure 82. Synthetic targets in the 3-position; amine data set.

2.10.6.2 Synthesis of 3-Amino-6-Sulphonamide Indazole Targets

The synthesis of the amine compounds was conceived incorporating a Buchwald-Hartwig reaction upon bromo intermediate **237**. Investigation of this reaction was conducted on the 6-nitro,3-bromo, THP protected, indazole **233** to optimise conditions before application to the sulphonamide intermediate **237** (Table 56).

Table 56. Optimisation of Buchwald-Hartwig reaction on 3-bromo-6-nitro-1-(tetrahydro-2H-pyran-2-yl)-1H-indazole, **233**.



Reaction	Catalyst	Amine/ R^3	Conversion
1	$\text{Pd}(\text{OAc})_2$, Xantphos	Me_2NH	No reaction
2	$\text{Pd}(\text{OAc})_2$, Xantphos	MeNH_2	Major product is 273
3	$\text{Pd}(\text{OAc})_2$, Xantphos	PMB-NH_2	53% 272
4	$\text{Pd}(\text{dppf})\text{Cl}_2 \cdot \text{DCM}$	PMB-NH_2	No reaction
5	$\text{Pd}_2(\text{dba})_3$, Johnphos	PMB-NH_2	61% 272 , 15% 273
6	$\text{Pd}(\text{OAc})_2$, Johnphos	PMB-NH_2	No reaction
7	$\text{Pd}(\text{PPh}_3)_4$	PMB-NH_2	43% 273
8	$\text{Pd}_2(\text{dba})_3$, Brettphos	PMB-NH_2	91% 272

PMB = *Para*-methoxybenzyl

Palladium acetate and Xantphos ligand were used according to a procedure developed in house. Reactions (1 and 2) with simple methylated amines failed to give the desired product at the 3-position. The loss of the bromine in the reaction was common

resulting in an unusable product, **273**. Microwave irradiation was employed as an alternative to conventional heating but it was found that vials were susceptible to rupture and yields were not improved. Significant improvements were made to the yield once the *para*-methoxybenzylamine(PMB-NH₂) was used. Further improvements were made by changing the catalyst to Pd₂(dba)₃ and the phosphine ligand to Brettphos (Table 56, Reaction 8). Buchwald reactions require a phosphorous ligand on palladium, this usually comes as a palladium (0) catalyst and a specific phosphine ligand such as those listed in the Table; Xantphos, JohnPhos and BrettPhos (Figure 83). Reactions 4 and 7 in Table 56 do not include separate Pd catalyst and phosphine ligand and, interestingly, no product formation was seen in either example, although there was evidence for initial oxidative addition by the formation of the de-halogenated product **273**.

Selection of the phosphine catalyst is crucial as subtleties in the structure effect different stages of the Buchwald-Hartwig catalytic cycle (Figure 83 & 84). Only two of the dialkylbiaryl phosphine ligand class were used before a suitable yield was achieved so a relationship between the substitution pattern of the ligand and the progress of the reaction could not be established for this particular transformation on an indazole.

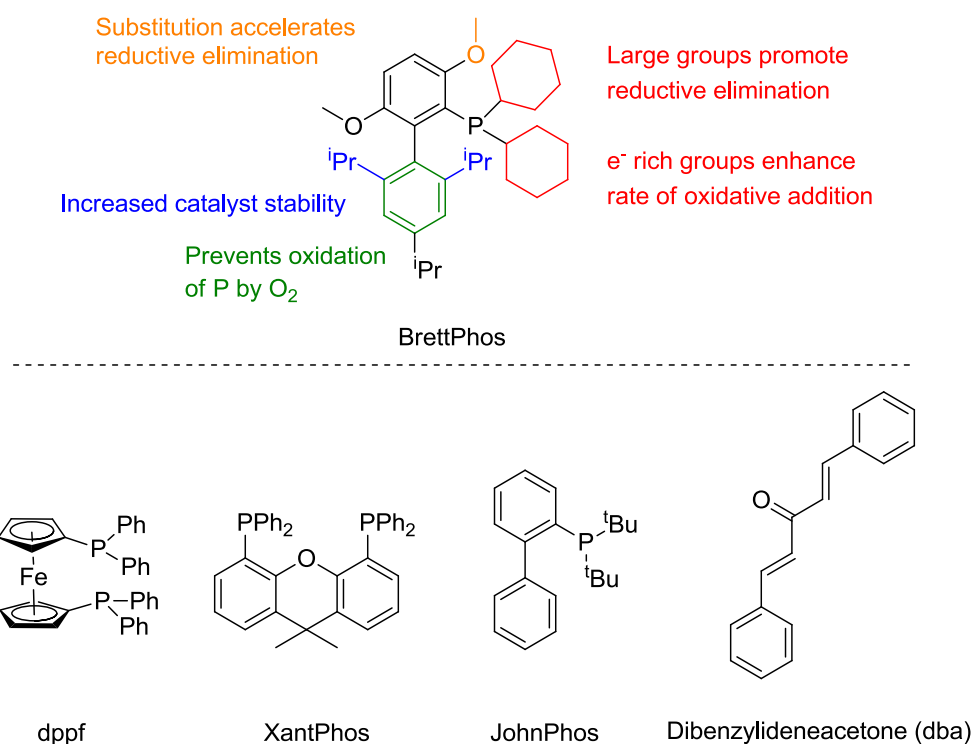


Figure 83. Structural features of dialkylbiaryl phosphine ligands adapted from Buchwald *et al*¹⁸⁶ and the structures of ligands used in optimisation.

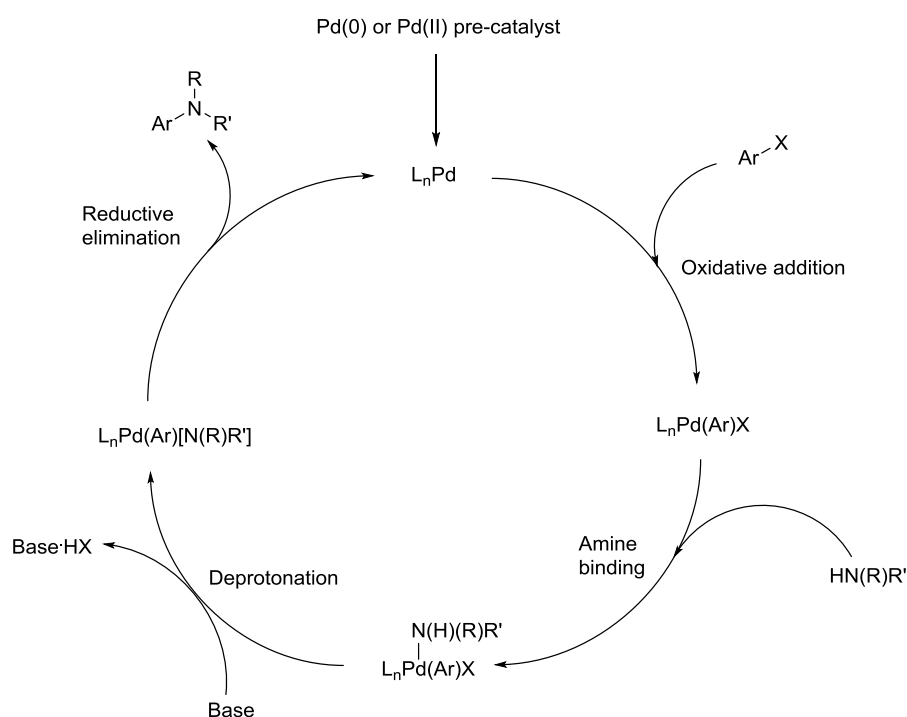
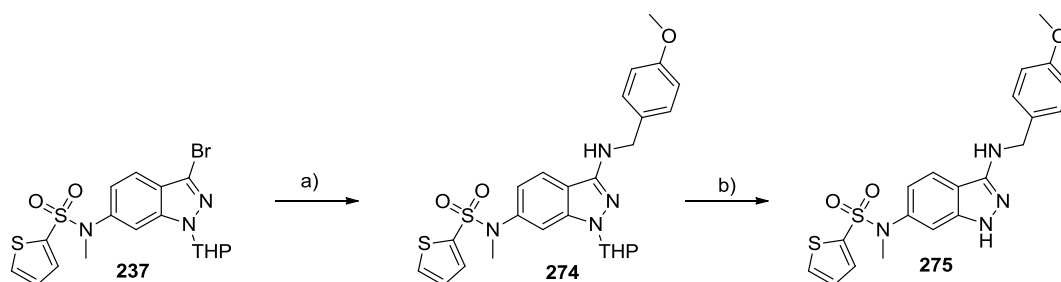


Figure 84. Generalised Buchwald-Hartwig catalytic cycle adapted from Buchwald *et al*¹⁸⁶.

After the success of the Buchwald reaction (8, Table 56) on a test substrate the same conditions were applied to the more elaborate intermediate **237** (Scheme 30). This

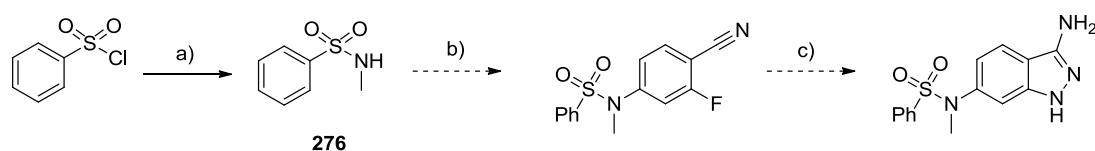
gave the PMB protected amine **274** in a reduced yield of 51% which was deemed satisfactory. The THP deprotection was modified to give compound **275** as a final target retaining the large 3-position group.



Scheme 30. Synthesis of final compound **275**. Reagents and conditions: a) $\text{Pd}_2(\text{dba})_3$, Brettphos, Cs_2CO_3 , 1,4-dioxane, 100°C , 18 h, 51%; b) AcOH , MeOH , 70°C , 2 h, 43%.

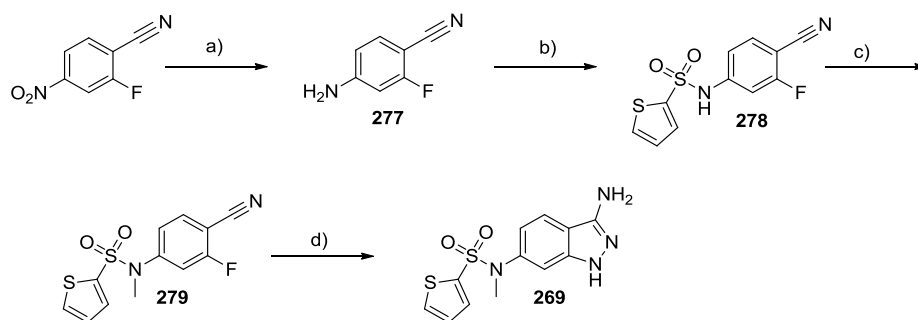
Compound **275** was subjected to hydrogenation in an attempt to selectively remove the PMB group however this resulted in over cleavage giving the 3-H indazole sulphonamide **84**. The use of MeOH.HCl , commonly used for THP deprotection, also gave this product. Methylation of intermediate **274** was found to be incredibly slow and poor yielding. Exchanging the PMB for the more labile dimethoxy benzyl (DMB) did not solve the deprotection issue. It became apparent that this strategy would not yield the desired compounds in a repeatable manner, which was desired for the broadening of this target library at a later date. Therefore an alternate scheme was devised.

A scheme was proposed using literature procedures which would give 3-amino targets in three steps without the use of a protection strategy (Scheme 31).¹⁸⁷⁻¹⁸⁹ The scheme was embarked upon using benzenesulfonyl chloride to maintain conditions as close to those given by Deng *et al* in the second step which was identified as key.¹⁸⁷ Formation of the methyl sulphonamide **276** was conducted in a high yield, however, the following copper mediated coupling was found to be unrepeatable.¹⁸⁹ This is presumably because of the presence of the cyano or fluorine group which are not represented in the test step of compounds for this reaction. This scheme was abandoned and a more simplistic but longer route was adopted.



Scheme 31. Reagents and conditions: a) MeNH₂, DCM, 60 °C, 2 h, 94%¹⁸⁹; b) 4-bromo-2-fluorobenzonitrile, CuI, *N,N*-dimethylglycine, K₃PO₄, DMF, reflux, 48 h¹⁸⁷; c) N₂H₄·H₂O, THF, reflux, 48 h¹⁸⁸.

A route to the products via an analogous ring closing strategy was completed using more conventional methods to form the methylated sulphonamide (Scheme 32).

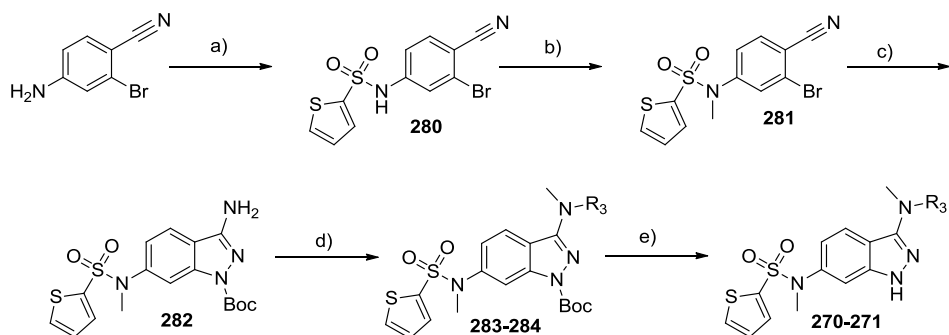


Scheme 32. Synthesis of final compound **269**. Reagents and conditions: a) Zn, AcOH, MeOH, 50 °C, 4 h, RT, 61%; b) 2-thiophene sulphonyl chloride, Pyr, RT, 3 h, 54%; c) MeI, K₂CO₃, DMF, RT, 4 h, 99%; d) NHNH₂, THF, RT, 18 h, 59%;

Reduction of nitro starting material followed by sulphonamide formation and alkylation gave intermediate **279** in good yields. When *N*-(4-cyano-3-fluorophenyl)-*N*-methylthiophene-2-sulfonamide **279** was treated with hydrazine the ring closing reaction is facilitated by an S_NAr on the fluoroaromatic and nucleophilic attack by the hydrazine on the nitrile group to form the imidamide. Final product **269** was obtained from this scheme, however, alkylation of the primary amine could not be completed selectively without the protection of the indazole NH. Incidentally, the protection of this material (**269**) would not progress selectively using standard conditions for THP protection. Attempts were made to install a pre-protected indazole functionality in the hydrazine ring closing step by use of *t*-butylcarbazate in a copper mediated reaction. This reaction would not proceed, presumably due to the strong F-C bond preventing bond insertion by the copper reagent. To solve this problem bromo intermediate **281** was proposed which complies better with literature conditions for this transformation and was easily synthesised. The procedures in Scheme 33 were used upon a brominated starting material to give Boc protected indazole **282**.

A strong base (NaH) was required to facilitate the methylation of the secondary amine which was attributed to the effect of the carbamate formed on the indazole drawing

electron density away from the nucleophilic group. The scheme allows the synthesis of a wide range of amines or amine derived compounds to be made by further reactions on intermediate **282**.

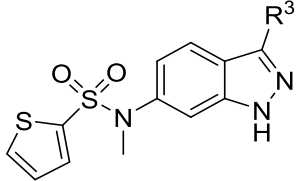


Scheme 33. Synthesis of final compounds **270-271**. Reagents and conditions: a) 2-thiophene-SO₂Cl, Pyr, RT, 3 h, 60%; b) MeI, K₂CO₃, DMF, RT, 4 h, 99%; c) CuBr, Boc-NHNH₂, K₂CO₃, DMSO, 80 °C, 18 h, 43%; d) NaH, MeI, DMF, 0 °C-RT, 6h 23-37% (eq varied to acquire products **283** and **284** selectively); e) TFA, DCM, RT, 2 h, 57-66%.

2.10.6.3 SAR of 3-Amino-6-Sulphonamide Indazole Compounds

The primary amine (**269**) shows moderate potency (Table 57) which is comparable to the unsubstituted derivative (**84**, ERK5 IC₅₀ = 0.45 ± 0.09 μM), however, the dimethyl (**271**) and mono-methyl (**270**) show significantly worse activity. These results suggest neither the presence of a hydrogen bond acceptor or donor is beneficial adjacent to the pyrazole functionality as potency is either lost or unchanged. Intermediate **275**, which was also sent for testing, showing that space at this position is not limited. However it is possible that this compound, due to its significant differences in size and properties, adopts a different binding mode. The most likely conformation of **275** is with the ring folded back to accommodate the lipophilic space at the 4-position.

Table 57. Enzymatic activity data of compounds **269-271** & **275** against ERK5 and p38 α .

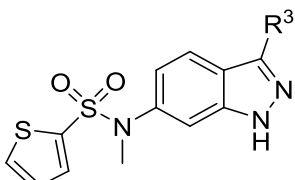

			
Compound	R ³	IC ₅₀ (μM)	
		ERK5 ^a	p38 α ^b
84	H	0.45 ± 0.09	>120
269	NH ₂	0.79 ± 0.08	>30
270	NHMe	>30	>30
271	NMe ₂	7.2 ± 0.2	>30
275	NH-PMB	0.73 ± 0.3	>30

^a ERK5 IC₅₀ values generated by IMAP cell free assay (350 μM ATP); ^b p38 α IC₅₀ values generated by Lance assay (350 μM ATP).

2.10.15 SAR Summary of 3-Substituted-6-Sulphonamide Indazole Compounds

A set of 17 compounds possessing the 2-thiophene R¹ group and variation at the 3-position is compared in Table 58. The data clearly shows, by colour coding, that lipophilic groups at the 3-position confer the best potency and largely the polar groups included showed poor ERK5 affinity.

Table 58. Enzymatic activity data of 3-Substituted-6-Sulphonamide Indazole compounds against ERK5 and p38 α .

				
Compound	R ³	IC ₅₀ (μM)		
		ERK5 ^a	p38α ^b	
84	H	0.45 ± 0.09	>120	
269	NH ₂	0.79 ± 0.08	>30	
270	NHMe	>30	>30	
271	NMe ₂	7.2 ± 0.2	>30	
275	NH-PMB	0.73 ± 0.3	>30	
257	COOH	16 ± 0.2	>120	
258	COOMe	1.7 ± 0.1	>120	
259	CH ₂ OH	3.7 ± 0.2	>120	
260	C(CH ₃) ₂ OH	2.8 ± 0.5	>120	
263	CONH ₂	>30	>120	
264	CONHMe	3.5 ± 0.1	>120	
265	CONMe ₂	3.8 ± 0.7	>120	
245	Br	3.6 ± 0.6	>120	
246	Me	0.16 ± 0.05	>120	
247	Et	0.05 ± 0.05	>120	
248	^{Cyc} Pr	0.29 ± 0.05	>120	
249	Ph	0.10 ± 0.01	>120	

^a ERK5 IC₅₀ values generated by IMAP cell free assay (350 μM ATP); ^b p38 α IC₅₀ values generated by Lance assay (350 μM ATP). Colour code base on ERK5 IC₅₀: green < 1 μM; orange > 1, < 10 μM; red > 10 μM.

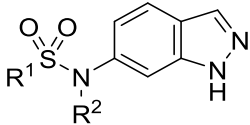
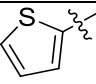
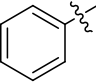
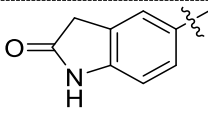
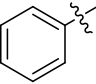
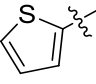
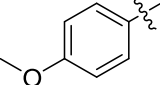
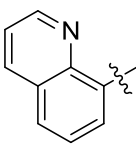
Substitution of the 3-position has produced significant benefits to ERK5 activity with two compounds reaching sub 100 nM IC₅₀ (**247** and **249**). All compounds in Table 58 contain the sulphonamide linker and it is possible that further potency could be gained by synthesising matched pairs of **247** and **249** with a sulphone linker.

2.11 Metabolism SAR of the Indazole series

Metabolism data has been collected thus far in the form of microsomal clearance which determines the magnitude of metabolism caused by cytochrome p450 (CYP) enzymes. This is a good measure of how susceptible a compound is to phase 1 metabolism reactions.

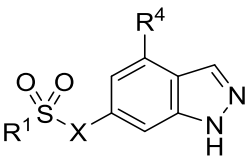
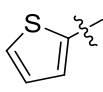
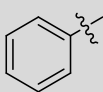
Metabolism data has been collected on selected compounds where matched pairs exist or where significant changes to physiochemical properties have been made. Initially the simple compounds synthesised with a sulphonamide linker displaying moderate μM potency showed good clearance data, below the criteria of $<48 \mu\text{l/min/mg}$ (Table 59). Once the *N*-methylated linker was identified as beneficial for potency a faster rate of metabolism is observed (Table 59). This may be because of a demethylation process or better recognition by CYP enzymes due to the increase in LogP. Metabolism is clearly affected by the R^1 ring system in this data set but no correlation exists between LogP and microsomal stability.

Table 59. Mouse microsomal clearance data of sulphonamide linker compounds.

				
Compound	R ¹	R ²	Mouse Microsomal Clearance (μl/min/mg)	XLogP
38		H	21	3.60
30		H	41	3.16
83		Me	24	2.44
82		Me	47	3.34
84		Me	81	3.78
87		Me	102	3.30
85		Me	174	3.48

Further metabolism data was collected on the sulphone linker and 4-substituted compounds along with 4-substituted sulphonamide compounds **285 - 288** which were synthesised by Dr Stephanie Myers. This data shows a clear trend in substitution at the 4-position causing a significant increase in the rate of metabolism (Table 60).

Table 60. Metabolism data of various linkers and substitution in the 2-thiophene and phenyl data sets.

						
Compound	R ¹	R ⁴	X	Mouse Microsomal	ERK5	XLogP
				Clearance ($\mu\text{l/min/mg}$)	Enzymatic IC ₅₀ (μM)	
38		H	NH	21	2.2 \pm 1.1	3.60
84		H	NMe	81	0.45 \pm 0.09	3.78
120		H	CH ₂	86	1.1 \pm 0.2	4.05
285		CycPr	NH	126	0.09 \pm 0.03	4.38
286		CycPr	NMe	432	0.43 \pm 0.05	4.56
199		CycPr	CH ₂	378	0.01 \pm 0.01	4.83
30		H	NH	41	4.7 \pm 0.04	3.16
82		H	NMe	47	1.1 \pm 0.6	3.34
122		H	CH ₂	83	0.91 \pm 0.15	3.61
287		CycPr	NH	94	0.20 \pm 0.06	3.95
288		CycPr	NMe	200	0.99 \pm 0.08	4.12
197		CycPr	CH ₂	319	0.03 \pm 0.01	4.40

A convincing trend exists between clearance and XLogP (Figure 85) showing that increases in lipophilicity, giving better potency in some cases, results in a higher rate of metabolism in almost all cases. This finding means that a strategy could be put in place to improve this parameter and therefore the metabolic profile of the series.

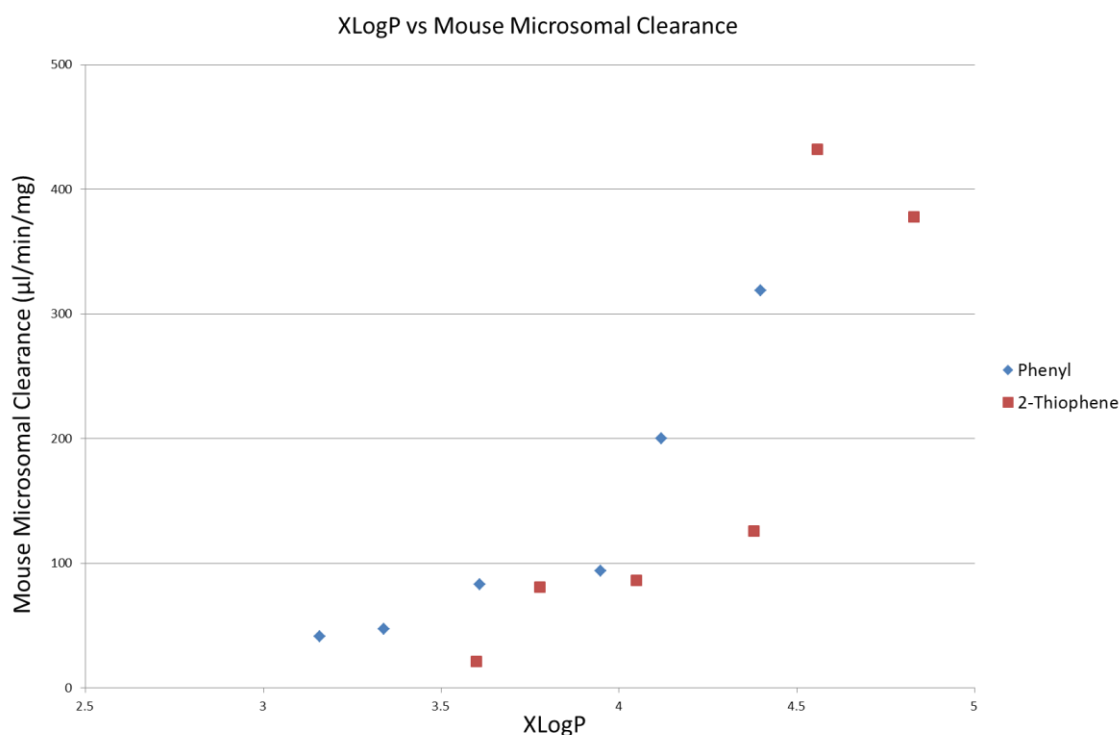
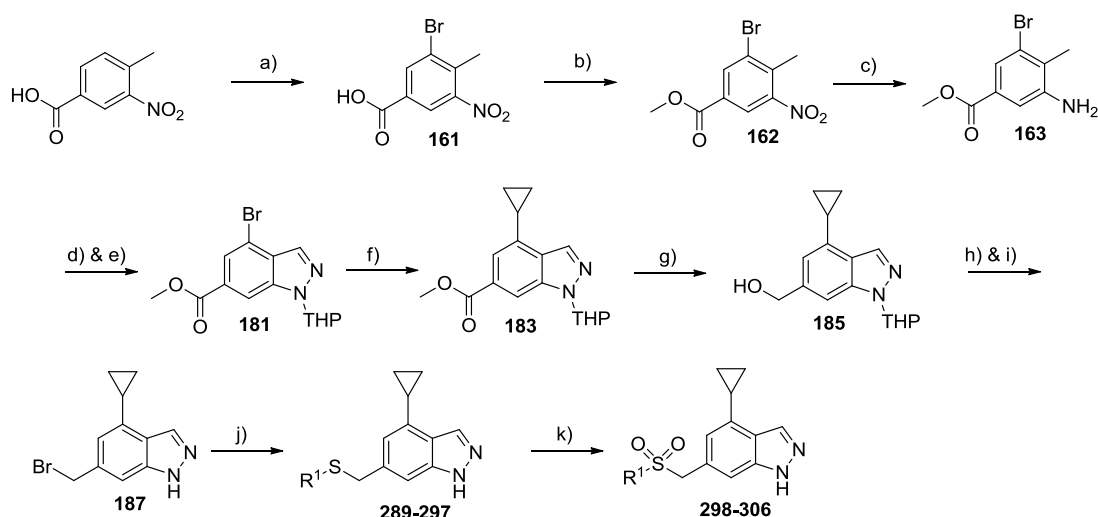


Figure 85. Graph showing the relationship between microsomal clearance in mice and XLogP.

2.11.1 Re-optimisation of the Sulphonamide Aromatic

2.11.1.1 Decreasing the LogP by variation of the sulphonamide aryl group

The most straightforward position to vary is the sulphonamide aromatic system whilst maintaining the potent cyclopropyl group at the 4-position. Chapter 2.3 describes the synthesis of a library of sulphonamide aromatics which exhausted viable commercially available sulphonyl chlorides. The sulphone linker has since been identified as equipotent to the *N*-methyl sulphonamides and therefore a novel reagent pool was available in the form of aromatic thiols. The groups chosen lower the overall lipophilicity of the molecule over matched pairs **199** and compound **197** (phenyl) which are two of the most potent, but metabolically labile compounds. Small heterocycles are not typically metabolically unstable, due to polarity and strong aromatic systems and therefore if this portion of the molecule is causing the high rate of metabolism, these modifications would alleviate it. Thiol starting materials were sourced and synthesis completed according to Scheme 34.

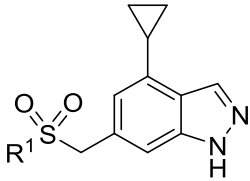


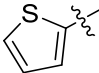
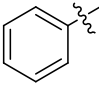
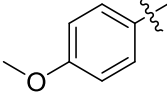
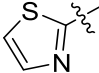
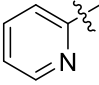
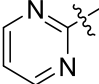
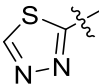
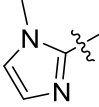
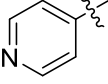
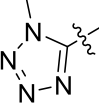
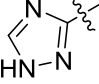
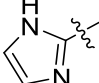
Scheme 34. Reagents and conditions; a) DBI, H_2SO_4 , 60°C , 3h, 98%. b) MeOH, H_2SO_4 , 60°C , 18h, 92%. c) Zn, AcOH, MeOH, 50°C , 1h, 98%. d) AcOH, NaNO_2 , H_2O , RT, 15 mins, 94%. e) DHP, *p*-TSA, DCM, RT, 6h 82%. f) $\text{Pd}[(\text{P}(\text{Ph})_2\text{C}_5\text{H}_4)_2\text{Fe}]\text{Cl}_2$.DCM, $^{\text{Cyc}}\text{Pr-B}(\text{OH})_2$, Cs_2CO_3 , 1,4-dioxane, 150°C , MW, 0.5 h. 71%. g) LiAlH_4 , THF, 0°C -RT, 4h, 93%. h) SOBr_2 , DMF, DCM, 0°C -RT, 4h. i) MeOH.HCl (1.25 M), 18 h, 91% (over two steps). j) $\text{R}^1\text{-SH}$, CsCO_3 , DMF, RT, 6h, 83-99%. k) KHSO_5 , MeOH, H_2O , RT, 18h, 56-80%.

Compound synthesis was completed using the same scheme used in the synthesis of **199** and was completed in high yields. Some complications occurred in the final oxidation step as residual oxone was present during a brine wash of the organic layer during work up. This caused an unwanted chlorination of indazole and the synthesis had to be repeated for those compounds (**302**, **298** & **305**) with the omission of brine from the work up. This unwanted chlorination was later used to investigate the metabolism of **199** (See Chapter 2.9.6.2).

Isolated products were tested for ERK5 activity and metabolism data was also collected on selected compounds based on potency or unique properties (Table 61).

Table 61. Activity data for re-optimisation of the sulphonamide aromatic group.



Compound	R ¹	ERK5 Enzymatic IC ₅₀ (μM)	Mouse Microsomal Clearance (μl/min/mg)	XLogP
199		0.01 ± 0.47	378	4.83
197		0.03 ± 0.01	319	4.40
201		0.08 ± 0.01	342	4.36
298		0.06 ± 0.02	-	4.33
299		0.08 ± 0.01	200	3.49
300		0.10 ± 0.09	160	2.99
301		0.36 ± 0.15	335	4.01
302		0.46 ± 0.14	-	3.99
303		0.60 ± 0.16	-	3.09
304		0.88 ± 0.48	398	2.21
305		2.2 ± 0.1	-	4.29
306		2.6 ± 1.4	190	3.53

No significant improvements were made to potency. However, compounds **298** and **299** possess <100 nM potency which means the thiazole and pyridine groups will be considered as thiophene replacements due to the improved LogP of the compounds.

Similarly, metabolism data has not revealed a useable improvement as values are higher than that required to retain a good drug concentration in an *in vivo* model (typically < 50 $\mu\text{l}/\text{min}/\text{mg}$). There is no visible correlation between predicted LogP and clearance data indicating that this position of the molecule is not a metabolic hot spot and that CYP enzyme recognition is not greatly affected by these modifications.

2.11.1.2 Extension from the Sulphone Aromatic

To further investigate the space around the sulphone aromatic position a set of elongated groups were selected for synthesis. It was proposed that potential for maintaining or improving potency would be possible by extending from two vectors on triazole **305** and phenyl **197** to probe new space with a polar moiety. Despite the poor activity of **305** this ring was chosen for further development because it gives chemical accessibility to a desirable vector towards the edge of the active site (Figure 81). Targets were based on synthetic feasibility with potential to expand the library to include ethers and amines should promising results be obtained (Figure 82).

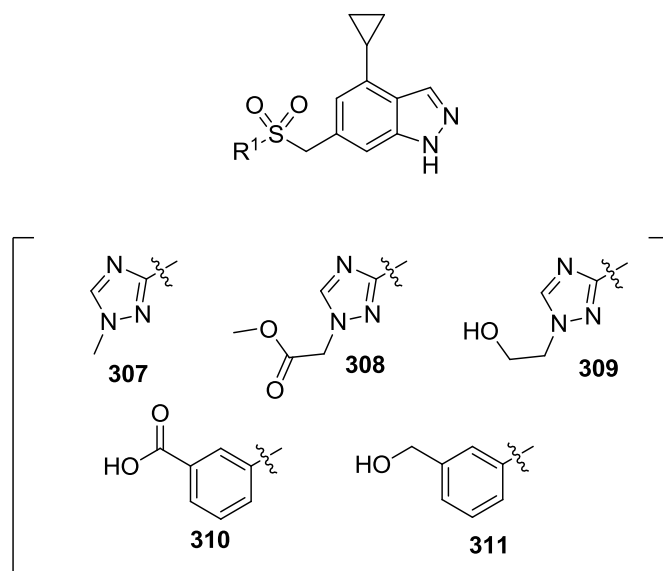


Figure 81. Synthetic targets extension from the sulphonamide aromatic.

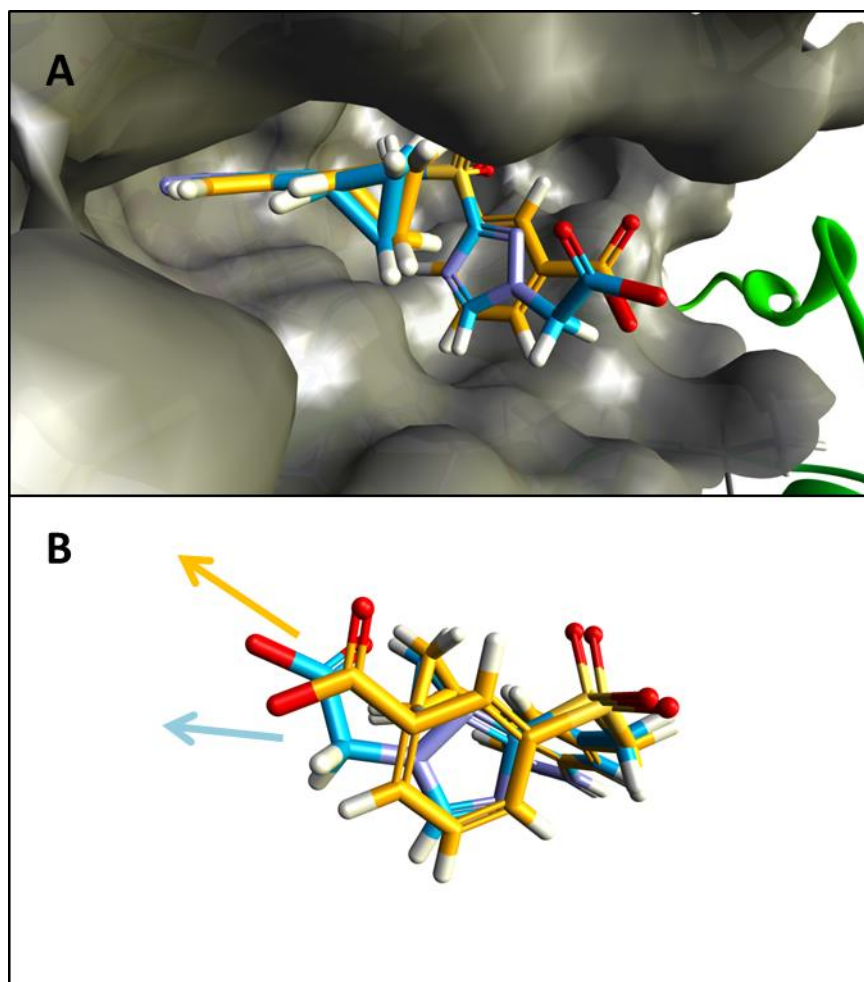
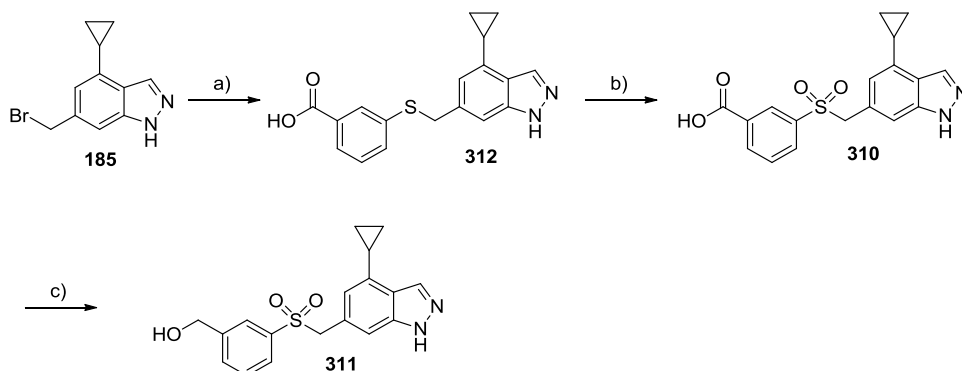


Figure 82. A) Overlay of compounds **308** (blue) and **310** (orange) in the ERK5 active site (grey) showing the opposed vectors each provides; B) with ERK5 removed and colour coded arrows to denote each vector.

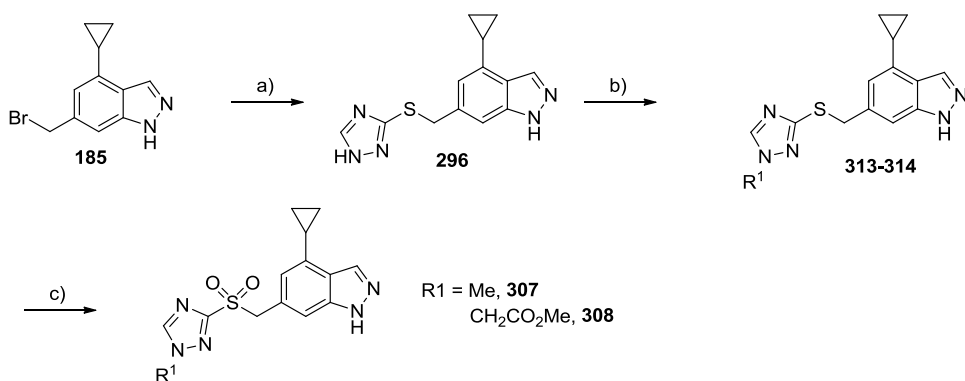
2.11.1.2.1 Synthesis of Extended Phenyl and Triazole Sulphone Compounds

Phenyl derivatives **310** and **311** were synthesised by varying the thiol species in the S_N2 reaction of Scheme 35. The unprotected indazole compound **312** was then oxidised and the carboxylic acid reduced using borane to give both desired products.



Scheme 35. Reagents and conditions; a) 3-mercaptobenzoic acid, CsCO_3 , DMF, RT, 6h, 92%; b) KHSO_5 , MeOH, H_2O , RT, 18h, 30%; c) Borane.THF, THF, 0°C , 4 h, 33%.

Triazole targets **307-309** proved more difficult to synthesise as an alkylation reaction was conducted on the unprotected indazole which inherently lead to selectivity issues. Final compounds were synthesised according to Scheme 36, however, insufficient material remained to complete the reduction of the ester to the hydroxyl target **309**.



Scheme 36. Reagents and conditions; a) 3-mercaptobenzoic acid, CsCO_3 , DMF, RT, 6h, 92%; b) Cs_2CO_3 , MeI or methylbromoacetate, DMF, RT, 8h, 9-18%; c) KHSO_5 , MeOH, H_2O , RT, 18h, 30-63%

2.11.1.2.2 SAR of Extended Phenyl and Triazole Sulphone Compounds

Compounds were tested in the enzymatic assay for activity against ERK5 however no major improvements were made to activity. The *N*-methylated triazole **307** is over 2-fold more active than the non-methylated derivative **305** (Table 62) but potency is not improved over the current lead compound **199**.

Table 62. Activity data for Sulphonamide Aromatic Extension Compounds.

Compound	R ¹	ERK5 Enzymatic IC ₅₀ (μM)	XLogP
197		0.03 ± 0.01	4.40
310		1.5 ± 0.8	3.60
311		0.29 ± 0.05	3.77
305		2.2 ± 0.1	4.29
307		0.77 ± 0.05	3.67
308		6.8 ^b	3.40

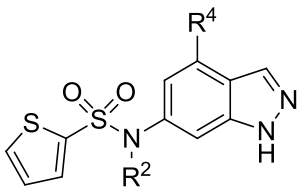
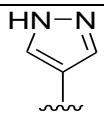
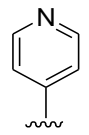
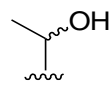
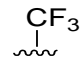
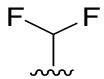
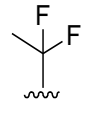
^b n=1.

2.11.2 4-Position Metabolism SAR

A number of compounds synthesised by Dr Stephanie Myers were submitted for mouse liver microsome, metabolic stability assessment with the sulphonamide linkers and variation in the 4-position (Table 63). Pyrazole and pyridine heterocycles did not show an advantageous improvement to clearance when compared to current lead **199** (378 μl/min/mg). Similarly the ethyl hydroxyl compound **317b** is cleared at the same rate as ethyl compound **321b**. Di-fluoro compound **320b** is cleared at a slower rate than **321b** and therefore highlights the alkyl group as a metabolic site. This finding is backed up by the clearance of trifluoromethyl compound **318b** but contradicted by **319b**. It is highly likely that the 4-position alkyl groups are centres for metabolism but based on this data it is not confirmed.

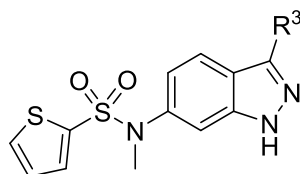
Comparison of *N*-methyl and non-methylated sulphonamides show the latter to be much more stable to CYP enzymes. This suggests that *N*-demethylation is a metabolic pathway for these compounds.

Table 63. Metabolism of selected 4,6-substituted indazole sulphonamides.

<div style="text-align: center;">  </div>		
	R^4	MLM Cl_{int} (μ l/min/mg)
		$R^2 = H$ $R^2 = Me$
315a/b		- 327
316a/b		- 238
317a/b		- 412
318a/b		46 161
319a/b		65 409
320a/b		- 225
321a/b	Et	- 436

2.11.3 Metabolism SAR of 3,6-Substituted Indazoles

Clearance of compounds substituted in the 4-position is poor, however, the effects of substitution at the 3-position on metabolism are not known. Microsomal clearance data was collected on a number of compounds with various interesting 3-position substituents. Table 64 shows the activity and clearance data of selected compounds.

Table 64. ERK5 activity and metabolism data of selected 3,6-substitued indazole sulphonamides

Compound	R ³	ERK5 Enzymatic IC ₅₀ (μM)	Mouse	XLogP
			Microsomal Clearance (μl/min/mg)	
84	H	0.45 ± 0.09	81	3.78
247	Et	0.05 ± 0.05	1010	4.39
248	CycPr	0.29 ± 0.05	287	4.47
269	NH ₂	0.79 ± 0.08	8.3	3.43

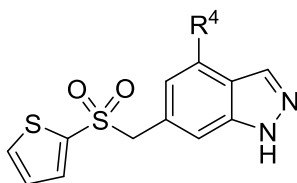
Amine compound **269** has an excellent clearance value and is the most metabolically stable compound made and measured in the series so far. **269** is 10-fold more stable than the unsubstituted compound **84** and is well within the acceptable range of microsomal clearance values desired (<48 μl/min/mg). The drop in clearance may be attributed to the net reduction in LogP. However, this does not seem significant and previously has not correlated with clearance (Chapter 2.11.1.1). The stability of **269** may be due to the placement of the solubilising group which affects the CYP enzyme's ability to act upon the 3-position or other positions on the indazole. Typically, increasing the nucleophilicity of a ring system results in an increase in metabolism due to the increase in reactivity. With this in mind it is therefore most likely that the compound's affinity for the CYP enzyme is lost due to the placement of this amine group. Unfortunately, compound **269** does not possess good potency, but the concept of increasing polarity at the 3-position of the molecule is incorporated into future targets to retain the good clearance profile and improve potency.

It is proposed that during CYP oxidation a proton is first abstracted from the substrate before the introduction of the hydroxyl group and therefore the rate is dependent on the strength of the bond being broken and the nucleophilicity of the resulting structure.¹⁹⁰ Ethyl compound **247** has the worst microsomal stability of all compounds tested and is cleared over 3-fold quicker than the cyclopropyl compound **248**. This

relationship between ethyl and cyclopropyl groups is expected due to the comparative bond strength of C-H bonds in each group. Cyclopropyl C-H bonds have an energy of 109.0 kcal mol⁻¹ compared to ethane at 101.2 kcal mol⁻¹. This translates to the metabolic stability witnessed.¹⁹¹

Both ethyl and cyclopropyl groups have also been incorporated in the 4-position of the indazole in a separate data set and a similar relationship is seen (Table 65). Although the difference in clearance is less pronounced, ethyl compound **198** is metabolised at a higher rate (513 µl/min/mg) than the cyclopropyl analogue **199** (378 µl/min/mg). This conserved relationship indicates that in both the 3- and 4-substituted indazoles the alkyl appendage is a metabolic centre.

Table 65. ERK5 activity and metabolism data of selected 4,6-substituted indazole sulphones



Compound	R ⁴	ERK5 Enzymatic IC ₅₀ (µM)	Mouse	XLogP
			Microsomal Clearance (µl/min/mg)	
198	Et	0.08 ± 0.01	513	4.75
199	CycPr	0.01 ± 0.01	378	4.83

2.11.3.1 Synthesis and metabolism of *N*-(3-(difluoromethyl)-1*H*-indazol-6-yl)-*N*-methylthiophene-2-sulfonamide (**322**)

Although the metabolism of 3-substituted compounds was improved drastically by the introduction of an amino group there was no associated benefit to potency. Introduction of alkyl groups did improve potency but the metabolic profile of these compounds was disappointing. In order to remove the liability of the introduced metabolic centres synthesis of the fluorinated derivatives was attempted. Compound

322, the 3-CHF₂ compound (Figure 83) was the only example synthesized due to the relative ease by which it could be made from intermediates already in hand.

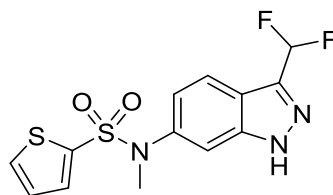
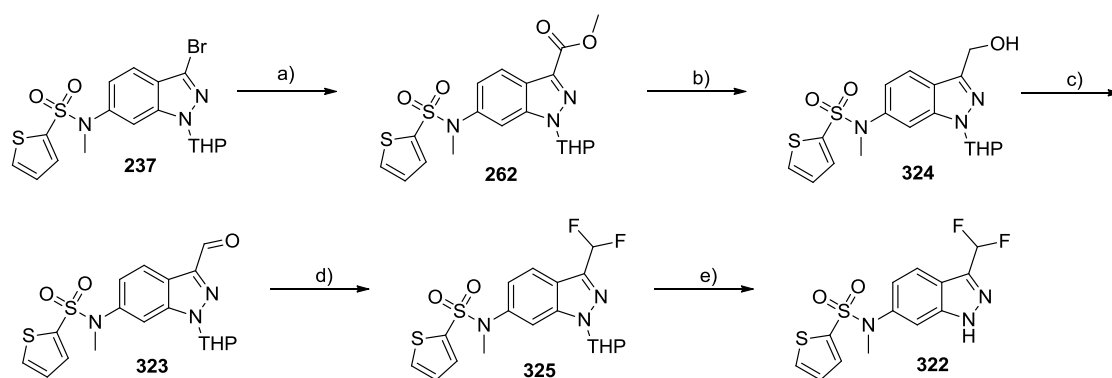


Figure 83. Difluoro compound **322**.

The synthesis of compound **322** was achieved by the successful fluorination of 3-C(O)H compound **323** (Scheme 37). Repetition of the palladium mediated carbonylation of key intermediate **237** was conducted and the methyl ester product **262** was reduced to the hydroxyl **324** using DIBAL-H in a 90% yield. Compound **324** was then oxidised using Dess-Martin Periodinane to the corresponding aldehyde **323** in a high yield (96%) with no observed oxidation of the thiophene moiety. The resulting aldehyde **323** was taken in DCM with diethylaminosulfur trifluoride (DAST) and stirred overnight for 18 hours at room temperature. The starting material was recovered in its entirety from this reaction but upon repetition an alternate fluorine source was used in the form of Deoxo-Fluor[®]. The solvent was also switched to toluene which gave the di-fluoro methyl compound **325** in an acceptable yield. The THP protecting group was removed in the next step to give the desired final product **322** (Scheme 37).

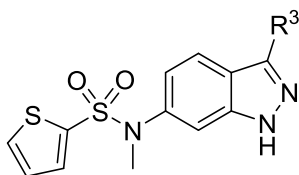


Scheme 37. Synthesis of difluoro-methyl compound **322**. Reagents and conditions: a) Pd(OAc)₂, Xantphos, Et₃N, HCO₂Me, Ac₂O DMF, 90 °C, 2 h, 53%; b) DIBAL-H, THF, -78 °C, 2 h, 90%; c) DMP (0.3M), DCM, RT, 3 h, 96%; d) Deoxo-Fluor[®], 18 h, 60 °C, 37%; e) MeOH.HCl, RT, 6 h, 95%.

2.11.3.2 ERK5 activity and metabolism of *N*-(3-(difluoromethyl)-1*H*-indazol-6-yl)-*N*-methylthiophene-2-sulfonamide (**322**)

The di-fluoromethyl compound **322** was subjected to the ERK5 enzymatic assay as well as the mouse liver microsome screen (Table 66). The collected data shows that the di-fluoro compound **322** has lost potency when compared to the methyl analogue **246** (7-fold decrease). When comparing the metabolism value of the highly cleared ethyl compound **247** with the difluoro **322** a significant improvement is made, however, the compound is outside the desired value for this assay type. Further fluorinated analogues at the 3-position have not been synthesised due to the tenuous benefit this result indicates and instead future focus is around 3-amino compounds which showed excellent metabolism properties.

Table 66. ERK5 activity and metabolism data of fluorinated 3,6-substituted indazole sulphonamide **322** and corresponding matched pairs.



Compound	R ³	ERK5 Enzymatic IC ₅₀ (μM)	Mouse	XLogP
			Microsomal Clearance (μl/min/mg)	
84	H	0.45 ± 0.09	81	3.78
247	Et	0.05 ± 0.05	1010	4.39
322	CHF ₂	1.1 ± 0.2	157	4.32
246	Me	0.15 ± 0.03	-	3.97

Chapter 3: The Pyrrole Series

3.1 Initiation of the Pyrrole carboxamide series and early SARs

A HTS campaign of 48,500 and 9,000 compounds from diverse and kinase focussed compound libraries revealed three ERK5 inhibitory chemotypes, one of which was a pyrrole carboxamide. Hits such as **326** (Figure 89) were validated by resynthesis and retesting and consistently displayed potency below 10 μM (IC_{50}) in the ERK5 enzymatic assay. This series of compounds was developed by colleagues; Dr Sandrine Vidot, Dr Ruth Bawn, Dr Stephanie Myers and Dr Lauren Molyneux to reveal SARs and lead compound **17** (Figure 89).

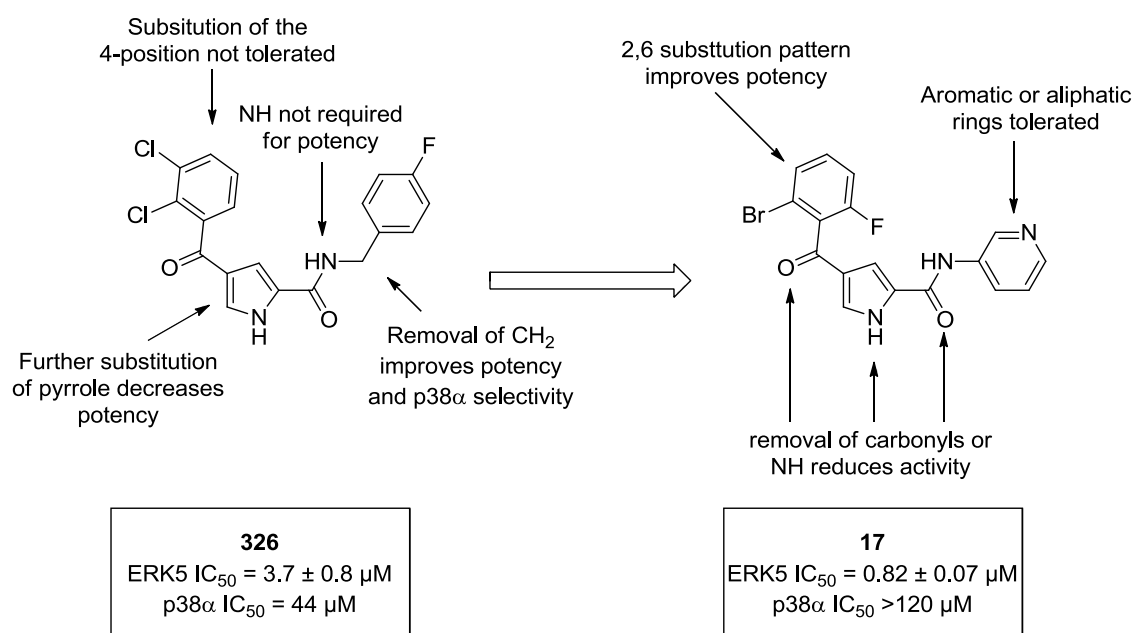


Figure 89. Structures of **326** and **17** and relevant SARs of the pyrrole carboxamide series.

Molecular modelling has shown that the compounds interact with the ERK5 active site through the ketone to Lys39, pyrrole NH to Asp93 and amide carbonyl to Met95. The presence of the 2,6 disubstitution pattern on the phenyl group of **17** induces a twist on the geometry so the ketone and aromatic group are out of plane allowing both to be accommodated in the ERK5 active site (Figure 90).

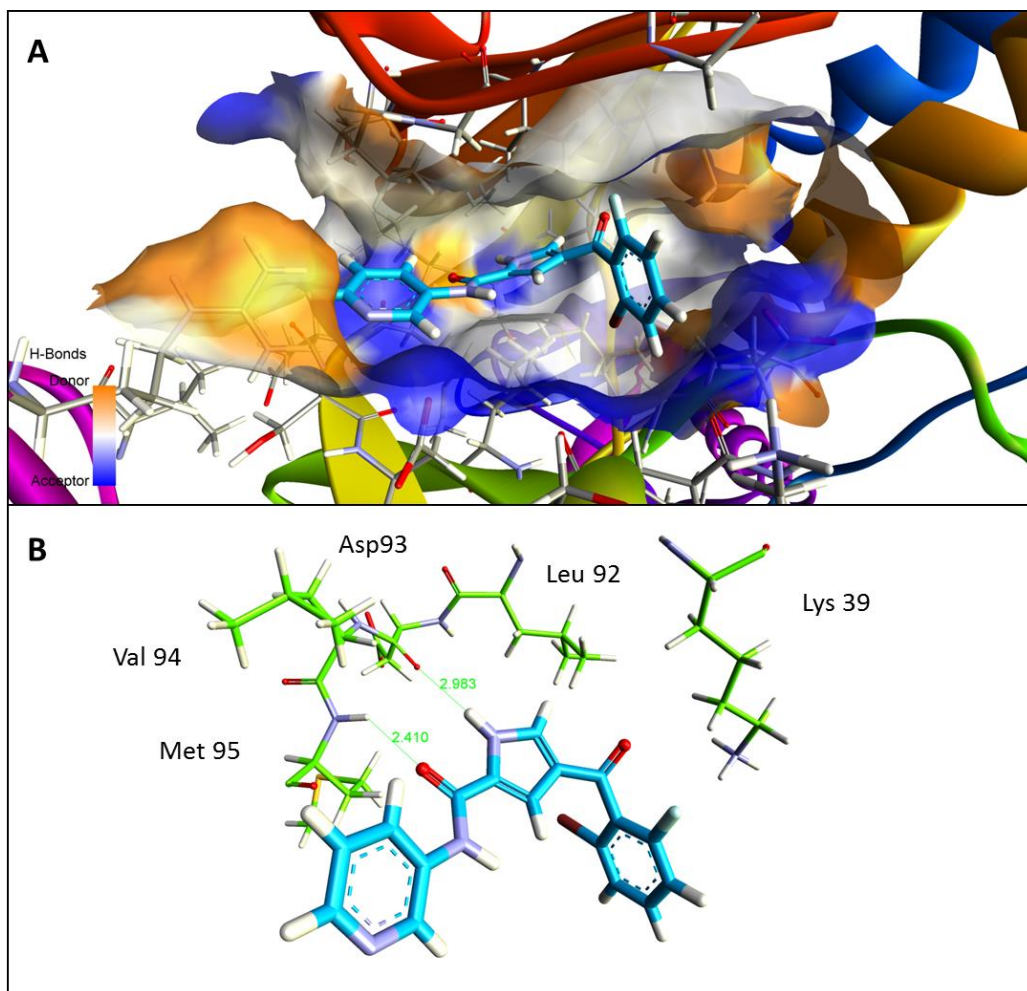
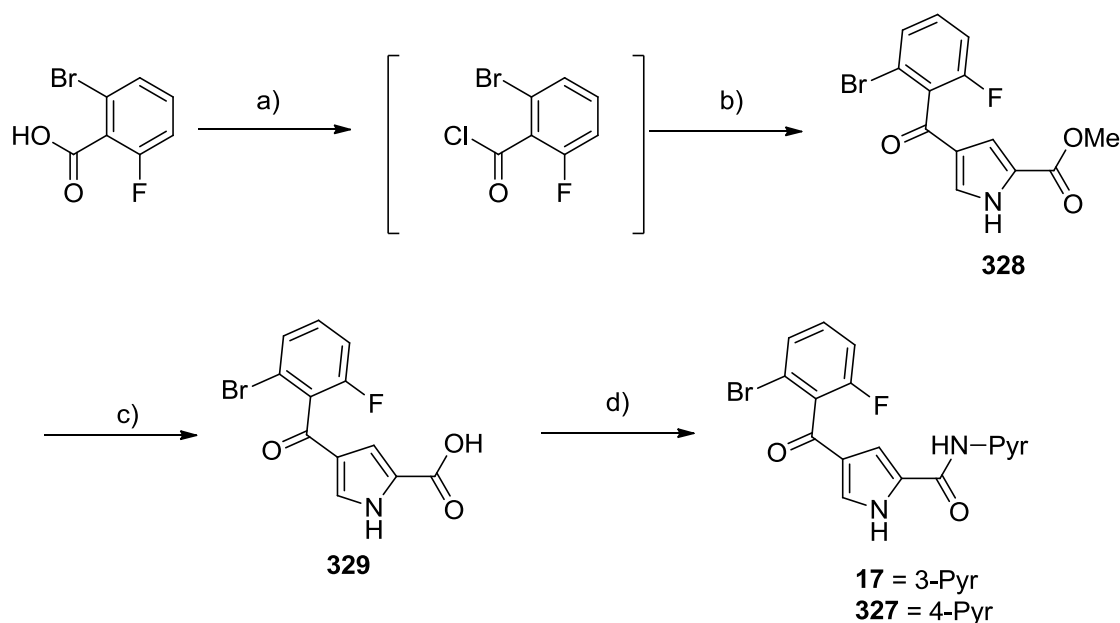


Figure 90. Proposed binding of **17** (blue) in the ERK5 active site. A) showing the ERK5 protein and surface of active site. B) select ERK5 hinge residues (green) and interactions with **17** (blue).

3.2 Pyrrole carboxamides **17** and **327**

3.2.1 Resynthesis of Pyrrole Carboxamides **17** and **327**

Compound **17** and close analogue **327** were desired for use in pharmacokinetic and pharmacodynamics studies and therefore a scale up synthesis was conducted. The synthesis of these compounds was achieved in four steps beginning with the activation of 2-bromo-6-fluorobenzoic acid for a Friedel-Crafts acylation which proceeded in an 85% yield over the two steps (Scheme 38). The resulting pyrrole ester (**328**) was hydrolysed to the carboxylic acid **329** and then subjected to an amide coupling reaction using PCl_3 and the desired amino-pyridine. The route has been optimised via the synthesis of numerous related compounds and the final compounds were obtained in high yields.

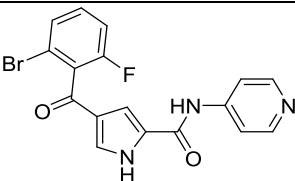
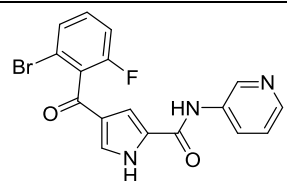


Scheme 38. *Reagents and conditions*; a) SOCl_2 , DMF (cat.), THF, RT, 3h, (not isolated); b) AlCl_3 , methyl 1H-pyrrole-2-carboxylate, DCM, RT, 18h, 85% (over 2 steps); c) LiOH , H_2O , THF, 65°C , 16 h, 99%; d) 3/4-aminopyridine, PCl_3 , MeCN, 150°C MW, 5 mins, 69-74%.

3.2.2 *In vitro* Pharmacokinetics of **17** and **327**

Both compounds displayed good properties and potency at that point of the project (Table 67). At the time **17** was the most promising compound synthesised and was therefore subjected to further selectivity and metabolism screening. The data collected shows the compound was of some promise but is hindered by CYP inhibition results. It is an extremely undesirable characteristic in a drug to exhibit CYP enzyme inhibition as it leads to drug-drug interactions and toxicity. As maybe expected compound **327** has very similar properties to **17** and is only inferior in solubility which was the primary reason this molecule (**327**) was not pursued into further *in vitro* and *in vivo* assays.

Table 67. Medicinal chemistry profile of **17** and **327**. For **17** only: good results are highlighted in green, undesirable in amber and poor in red. Solubility and metabolism data supplied by Cyprotex.

Criteria	Desired value for lead	 327	 17	
ERK5 IC ₅₀ (cell free)	< 0.1 µM	0.67 ± 0.15	0.82 ± 0.07	
ERK5 cellular potency (Hela)	<1 µM	-	1.9 (n=1)	
ERK5 cellular potency (HEK293)	<1 µM	4.0 ± 2.8	3.8 ± 2.2	
Selectivity	>10-fold	p38α IC ₅₀ >120 µM	p38α IC ₅₀ >120 µM	
ERK5 Ligand Efficiency	>0.3	0.35	0.35	
xLogP	<5	3.15	3.15	
TPSA	75-100	75	75	
MW	<500	388	388	
Plasma Protein binding	<99%	99.9	99.9	
Caco-2 A2B/B2A Efflux Ratio	>1 x10 ⁻⁶ cm/s <2	-	34/28 0.82	
Solubility (Lower/Upper)	>50 µM	30/100	100/100	
Mouse microsomal clearance	<48 µl/min/mg	36.9	25.7	
hERG inhibition	IC ₅₀ >25 µM	-	38% at 25 µM	
CYP1A inhibition	IC ₅₀ >10 µM	-	6.0	
CYP2C19 inhibition	IC ₅₀ >10 µM	-	8.5	
CYP2C9 inhibition	IC ₅₀ >10 µM	-	13.8	
CYP2D6 inhibition	IC ₅₀ >10 µM	-	9.2	
CYP3A inhibition	IC ₅₀ >10 µM	-	8.4	

3.2.3 *In vivo* Pharmacokinetics and Pharmacodynamics of 17

17 Was dosed at 10 mg/kg in mice and pharmacokinetic data collected (Table 68) this shows the compound behaves favourably in animals as it has a respectable biological half-life and clearance resulting in a good bioavailability value of 68%. Animal studies were all conducted by Dr Huw Thomas.

Table 68. Pharmacokinetic data for **17**

Parameter	Intravenous Dose (IV)	Oral Dose (PO)	Intraperitoneal Dose (IP)
Dose (mg/kg)	10	10	10
AUC ($\mu\text{g/ml}\cdot\text{min}$)	372	254	398
C_{max} ($\mu\text{g/ml}$)	25	6	12
t_{max} (min)	5	15	15
$t_{1/2}$ (min)	38	65	43
Clearance (ml/min/kg)	27	-	25
V_{dss} (L/kg)	1.2	-	-
Bioavailability (%)	-	68	-

AUC = Area under curve; V_{dss} = volume of distribution at steady state.

3.2.3.1 Matrigel plug assay

17 Was used in a Matrigel plug assay to deduce the effect of ERK5 inhibition on angiogenesis.¹⁹² Matrigel plugs doped with fibroblast growth factor (bFGF) were implanted subcutaneously in mice and animals were dosed over 7 days. After this time mice were euthanized, plugs were removed and assessed for blood content by colorimetric analysis of haemoglobin levels (Figure 91).

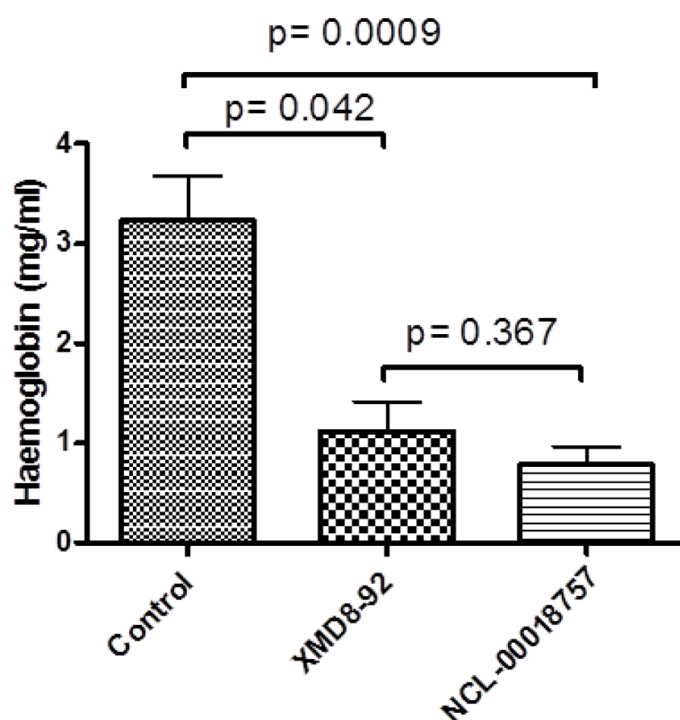


Figure 91. Haemoglobin levels in matrigel plugs retrieved from mice after 7 days dosing twice daily with either vehicle (control), 50 mg/kg XMD8-92 **12** (IP) and **17** 50 mg/kg (PO).

Data gathered from matrigel plugs reveals a notable antiangiogenic effect of ERK5 inhibition by **17** which is comparable to the positive control, XMD8-92 (**12**).

3.2.3.2 Human tumour xenograft models

17 Was assessed for tumour growth inhibition with XMD8-92 (**12**) as a positive control. Mice were inoculated with human ovarian carcinoma cells (A2780) and after 7 days without any drug, tumours were established subcutaneously at an average volume of 72 mm³. Mice were dosed with vehicle control, XMD8-92 or **17** over 11 days and the tumour volumes measured (RTV). The data (Figure 92) shows **17** to produce the same growth inhibitory effect as XMD8-92, although at twice the dose. During the study no animal weight loss was associated with administration of **17** indicating a good tolerance for the high dose of compound and therefore good toxicity profile.

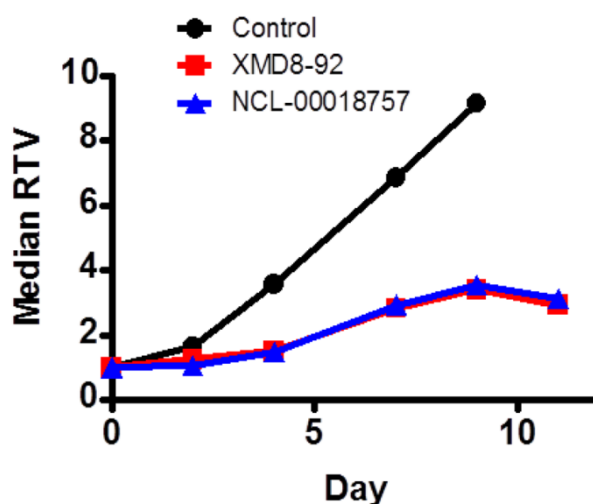


Figure 92. Xenograft tumour volume vs time for subcutaneous A2780 xenografts in mice dosed with vehicle (control), XMD8-92 (**12**) 50 mg/kg and **17** 100 mg/kg.

3.3 Summary of Pyrroles Carboxamide SARs

Further development of this series of compounds by Dr Lauren Molyneux, Dr Duncan Miller and Dr Tristan Reuillon improved the potency of the lead compound extensively. Figure 93 shows the structure of **331** which has been used in further pharmacokinetic and pharmacodynamics experiments.

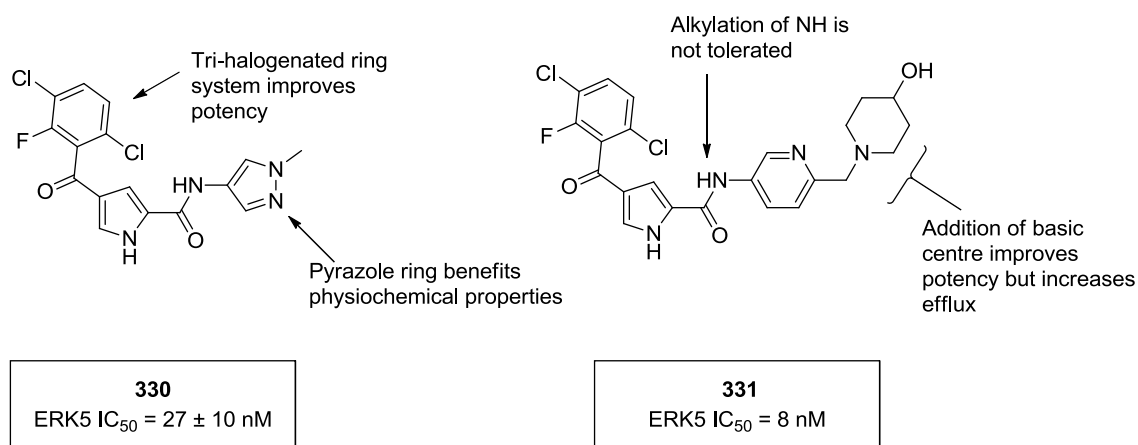


Figure 93. SARs of the pyrrole carboxamide series around compounds **330** and **331**.

The series now exhibits excellent potency and physiochemical properties, however, progression to a clinical candidate has been impeded by the poor efflux of lead compounds. During development the CYP inhibition witnessed for **17** was designed out. Efforts to remove the poor efflux properties have not been successful and included

biological experiments to identify SAR between pyrrole carboxamides and P-gp expression (Chapter 3.4). The Indazole series development was run simultaneously to the pyrrole series and both ran into different problems at a similar time point. It is possible that combination of the two series may aid both the efflux and metabolism problems that each series faces.

3.3.1 Potential Combination of Indazole and Pyrrole Carboxamide Series

Developments on the pyrrole carboxamide series have shown potency can be derived from the portion of the active site beyond the hinge, towards solvent. Molecular modelling of both indazole and pyrrole series shows that the 3-position of the indazole directs towards the space in which potency is gained in the pyrrole series (Figure 94). Inclusion of an aromatic ring and basic centre beyond it at the indazole 3-position would simulate the potent groups discovered on the pyrrole series. It has been shown that substitution at the 3-position can boost potency and 3-amino compound **269** has excellent metabolic stability. For these reasons it is plausible that a suitable *in vivo* tool compound may be identified through further exploitation of the 3-position. Interestingly compound **275**, which was originally a synthetic intermediate serves as a suitable mimic for **17** and is equipotent (ERK5 IC₅₀ = 0.73 ± 0.3 µM) (Figure 95).

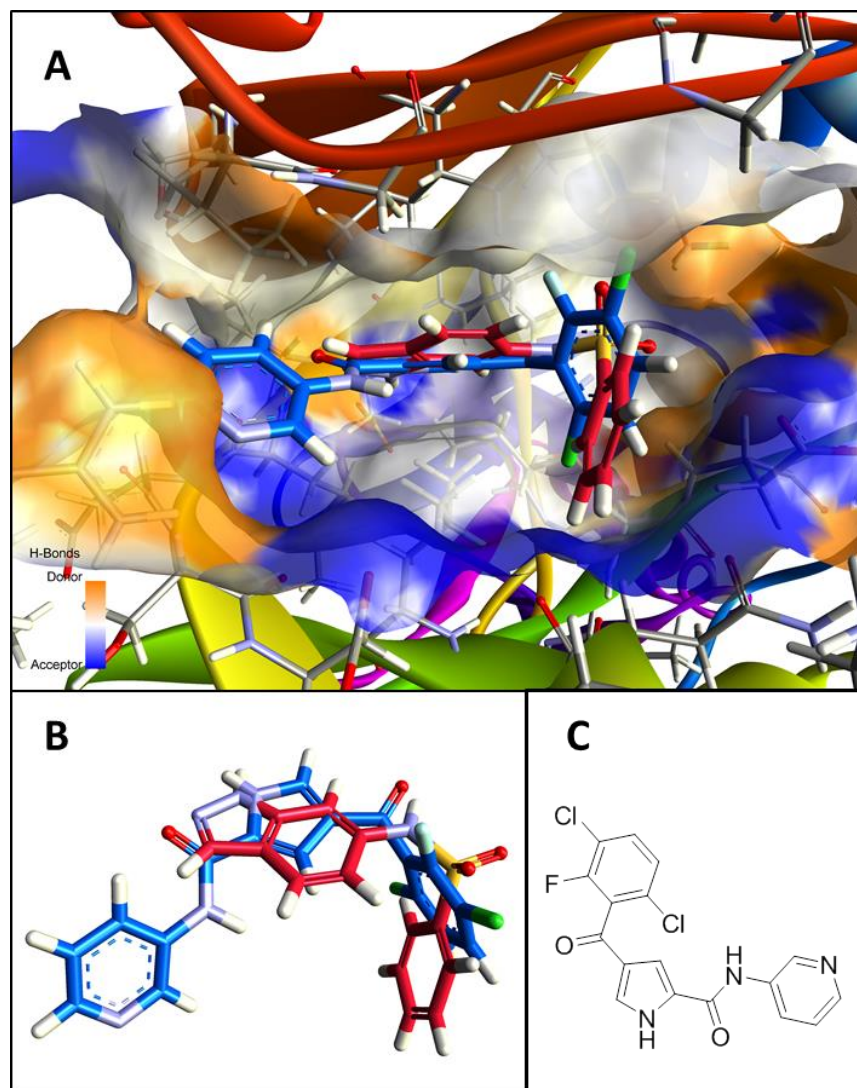


Figure 94. A) Overlay of indazole **30** (red) and pyrrole carboxamide **332** (blue) docked in the ERK5 active site; B) Overlay of indazole **30** (red) and pyrrole carboxamide **332** (blue); C) Chemical structure of pyrrole carboxamide compound **332**.

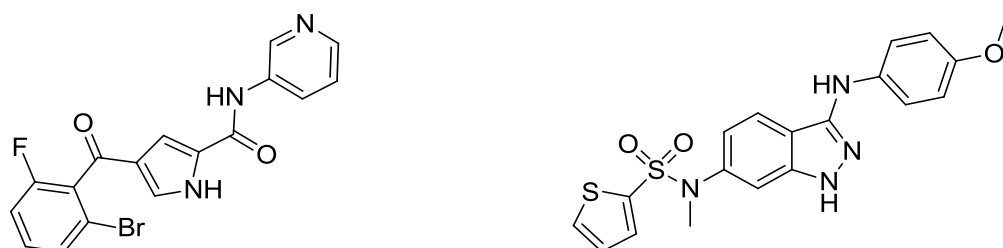


Figure 95. Equivalent compounds in the pyrrole carboxamide (**17**) and indazole sulphonamide (**275**) series.

Combination of the two series may improve potency but it has been shown that the potent basic chain incorporated into pyrrole compounds is associated with poor efflux. It is therefore reasonable to believe that this property would also be introduced when the same functionality is incorporated in the indazole 3-position (Figure 96A). Although

it is possible that the indazole compound **334** may not suffer the same efflux effects due to the subtle differences in the structure and the positioning of polar groups. A synthetic campaign to reach this compound would systematically build the molecule as was originally done in the Pyrrole series. Synthesis of the Boc-protected 3-amino indazole **282** has been shown previously and would allow for a series of S_NAr reactions to be conducted to install the various required groups (Figure 96B). Alternately in the same manner that compound **275** was synthesised, an optimised Buchwald-Hartwig reaction would enable the introduction of the desired amine groups.

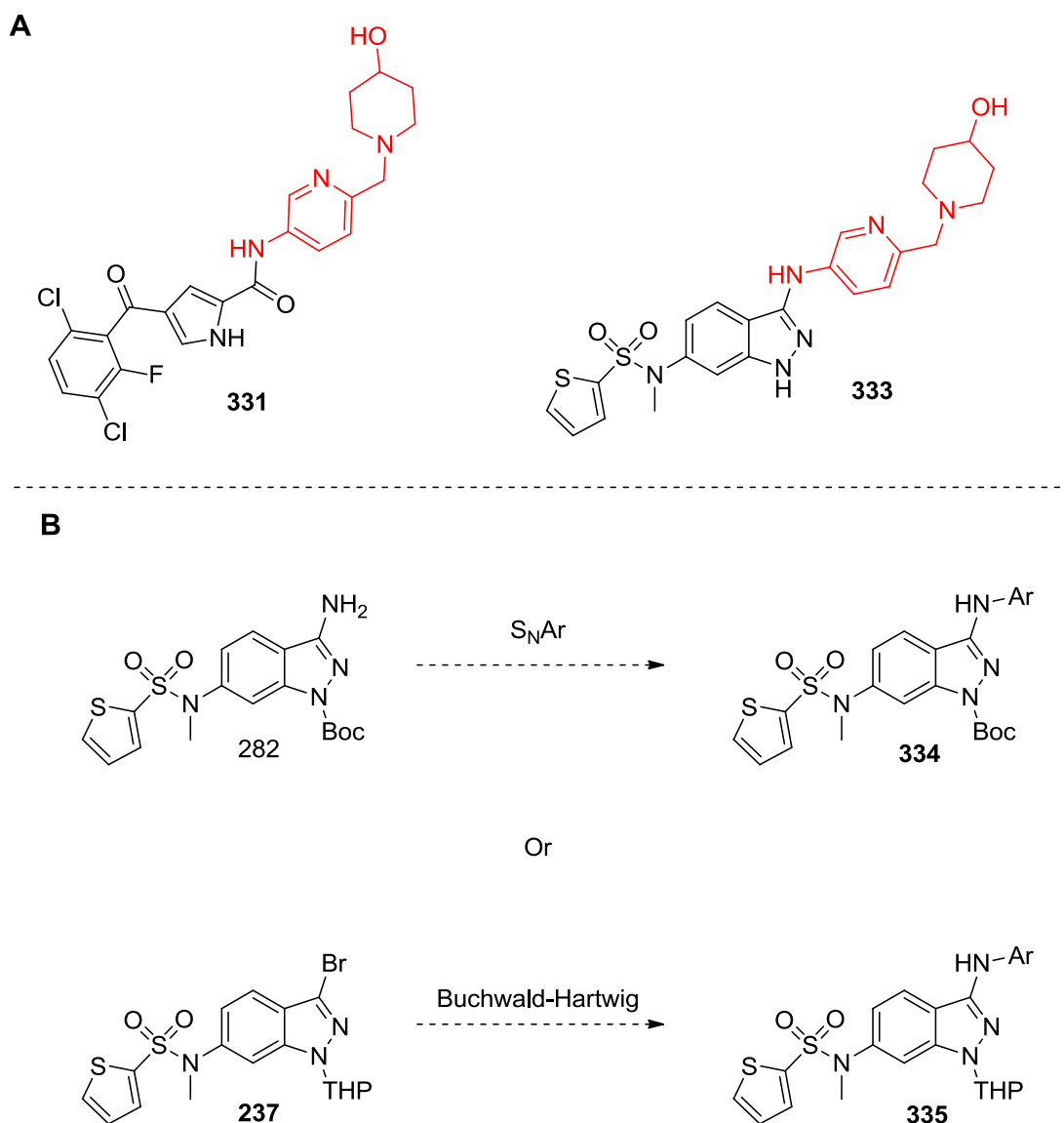


Figure 96. A) potential targets combining the indazole and pyrrole carboximide series **333** and **334**; B) Potential synthetic routes to compound **334**.

Inclusion of potent indazole moieties would lead to alkylation of the pyrrole carboxamide core at the 3-position (Figure 97). This modification has been

investigated and the compounds lost potency, presumably because of the congested space and the orientation of the adjacent systems.

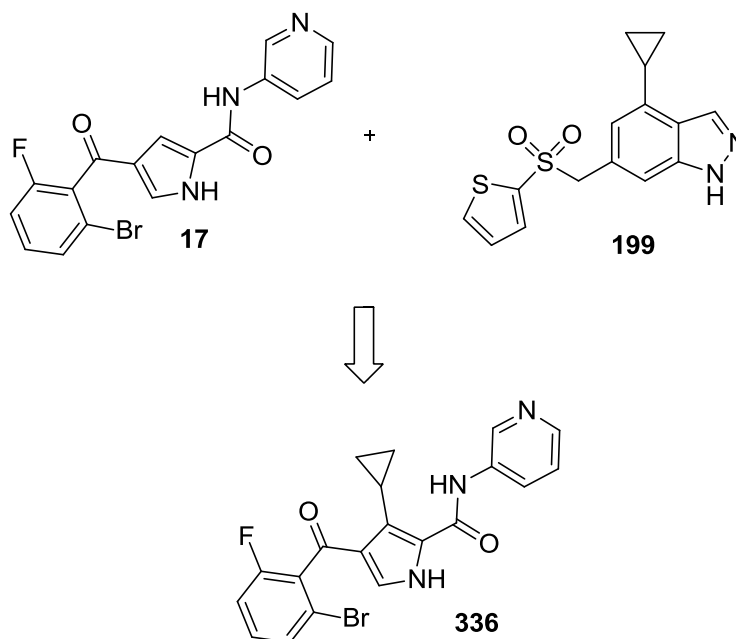


Figure 97. Pyrrole carboxamide target **336** incorporating potent indazole series moieties.

Combination of the two series has not been thoroughly investigated to date as it requires a crystal structure of both chemotypes in the ERK5 active site before any accurately informed design decisions can be made. A more coalescent pathway to develop the indazole series would be to combine the SARs developed at the 3- and 4-positions of the molecule (Chapter 4).

3.4 Investigating the Efflux of Lead Pyrrole Carboxamide Compounds

Experiments were conducted to determine if a cellular presence of selected pyrrole carboxamide compounds causes an increase in the expression of transporter protein P-gp. Resistance to drugs can be caused by efficient efflux of a drug molecule from the cell, preventing it from reaching its target. This resistance can be caused by a high affinity between the efflux protein and the drug which is generally associated with up-regulated expression. Ten pyrrole carboxamide compounds were chosen displaying high potency but poor cell permeability properties, in particularly poor efflux.

3.4.1 ABC Transporters

Membrane transporter proteins are an abundant family of proteins in living organisms. They span biological membranes and facilitate the passage of vital materials, such as ions, small molecules and macromolecules across the membrane. The movement of substances is mediated either by passive diffusion (high to a low concentration) or by active transport (from low to high concentration) which normally requires energy in the form of ATP.

ATP binding cassette (ABC) transporters are primary active transporters; they utilize ATP to transport substrates across extra-and intra-cellular membranes. Their role within the human body serves to remove foreign or unrecognised material from the cell. This process aids the body by eliminating toxic entities from cells and eventually from the body.

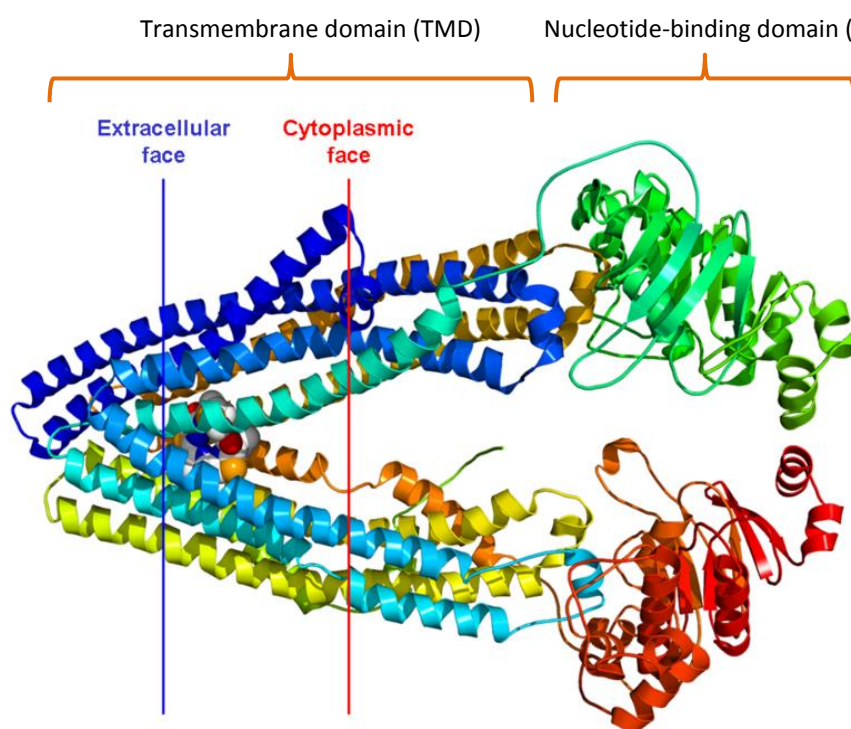


Figure 98. Generic structure of ABC transporters.

These proteins are made up of a transmembrane domain (TMD) and a nucleotide binding domain (NBD)^{193,194}. The TMD, largely made up of α -helices, has a high affinity site on the cell interior which binds to the substrate, and a low affinity site on the exterior which permits dissociation of the material after transfer to the extracellular

face. When ATP binds to the NBD, the conformation of the transporter changes such that any substrate bound to the interior of the TMD passes to the low affinity site on the other side of the membrane and is released. The release of ADP from the NBD resets the transporter to its ground state, ready to bind another substrate. The system consumes two ATP molecules per cycle and therefore has poor energy economy, though this does imply a high importance in the cellular hierarchy.

3.4.2 P-glycoproteins and Multidrug Resistance

P-glycoprotein (P-gp) also known as multidrug resistance 1 (MDR1) and ABCB1 is a 170 kDa protein present in endothelial and epithelial cells of the liver, lungs kidneys, testes and brain, among others. P-gp is the most studied member of the ABC transporter family accounting for over 400 related publications in 2012 alone. This is largely due to P-gp's implication in multidrug resistance (MDR). Many drug compounds are substrates of P-gp and are expelled from cells. This lowers the drug's overall bioavailability, as it reduces the total time an effective drug concentration is present in the cell. Such a drug will have a poor pharmacokinetic profile as a result.

Expression of P-gp is not necessarily intrinsic to the cell and expression can be induced by exposure to a compound or a mutation. The conventional chemotherapeutic agents, taxanes, epipodophyllotoxins and vinca alkaloids, are all known substrates for P-gp. Chemotherapy regimens involving these (and other compounds) become much less effective following P-gp overexpression¹⁹⁵. This phenomenon is a contributing factor to a patient developing MDR and also identifies P-gp as a therapeutic target. Thus, combinatorial therapy of a P-gp inhibitor such as verapamil, **337**, and a chemotherapeutic agent can potentially negate the drugs efflux and restore the intracellular concentration of the desired agent.

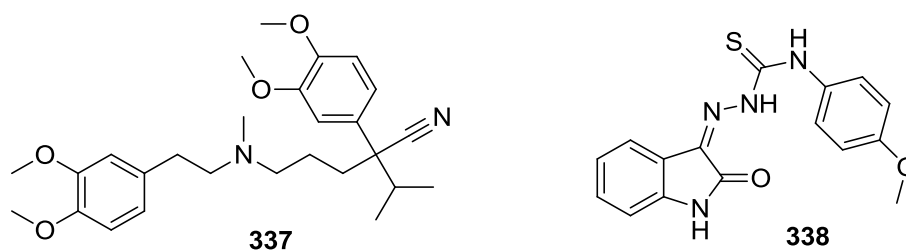


Figure 99. Chemical structures of Verapamil, **337** and NSC73306, **338**.

3.4.3 Agents that Target P-gp

A P-gp inhibitor, like any drug compound, must meet certain safety criteria and so far toxicity has limited development of a clinical compound specifically designed for P-gp inhibition.¹⁹⁵ A study in 2006 identified a novel compound, NSC73306 (**338**) (Figure 99), which increased the cytotoxicity of various tumour cell lines to cytotoxic agents in correlation to P-gp over-expression.¹⁹⁴ However, the mode of action appears to bypass an interaction between the intended transporter and **338**, presenting another, so far unidentified, target to combat MDR.

Verapamil is an FDA approved calcium channel inhibitor used as a treatment for various conditions of the cardiovascular system. It has also become widely used as a tool compound in cell biology for the inhibition of P-gp ($IC_{50} = 0.5 \mu M$).¹⁹⁶ The compound has been shown to reduce the passage of materials by P-gp whilst remaining relatively non-toxic to the cell, the primary reason for its widespread use. Verapamil itself has a moderate bioavailability and a biological half-life of less than 12 hours because of metabolism in the liver. The side effects attributed to P-gp inhibition are currently unknown however verapamil is known to cause headaches, nausea and dizziness.

3.4.4 Designing drugs that do not interact with P-gps

The substrate binding domain of P-gp does not contain a conserved binding motif: this fact means that designing compounds to avoid efflux is very difficult. Ambudkar *et al* demonstrated a limited number of SARs by making small structural modifications to known P-gp substrates.¹⁹⁷ This exposed planar lipophilic groups and lipophilic, tertiary amines as common moieties causing drug efflux. However, these groups are present

on many drug compounds that do not suffer from accelerated cell elimination, highlighting the difficulty in defining the parameters of P-gp-substrate binding.

It has also been reported that moderating hydrogen bond strength can have a profound impact on P-gp recognition; this is typically done by the introduction of a fluorine atom to withdraw electron density.¹⁹⁸ The strategy is to identify and disrupt a key hydrogen bond between the transporter and the molecule by reducing its strength. Maintaining high potency for the therapeutic target whilst altering the electronics of key functionality to prevent efflux presents a difficult challenge.

Another strategy to combat P-gp elimination is to improve the pharmacokinetic properties and potency of the compound so that elimination by P-gp no longer has a significant effect on the therapeutic concentration obtained in the body. This is perhaps the most difficult method to employ as many parameters need to be addressed at once.

3.4.5 Methods to Deduce Drug P-gp Interaction

To satisfy the specification of a clinical candidate compound, cell permeability must provide an in cell concentration sufficient for a therapeutic effect at a tolerable dose. A widely used indicator of cell permeability is the Caco-2 assay; this provides data on both influx and efflux of material. Caco-2 is a colon carcinoma cell line which has tight junctions and expresses a comprehensive variety of transporter proteins including P-gp. The compound in question is added in solution on top of the Caco-2 membrane and the concentration of compound is measured on the other side to give a value of permeability. Because of the tight junctions between the cells it is deemed that any amount of compound measured on the other side must have passed through the cell. Results are routinely quoted as an efflux ratio which takes the values of B to A (the reverse of the assay) over A to B giving a value proportional to excretion. When this assay is run on a compound in the presence of a P-gp inhibitor any increase in the efflux ratio eludes to an interaction with P-gp.

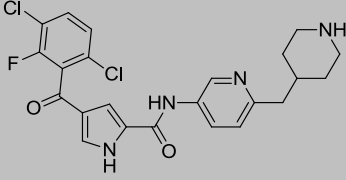
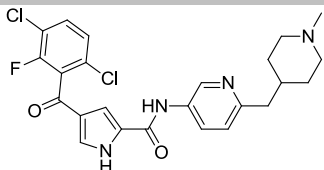
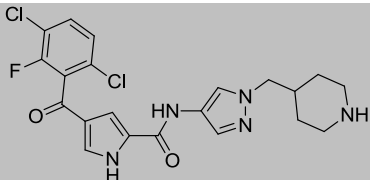
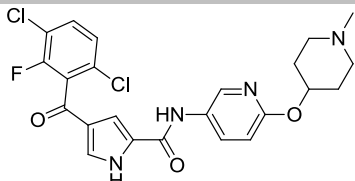
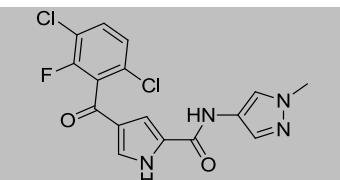
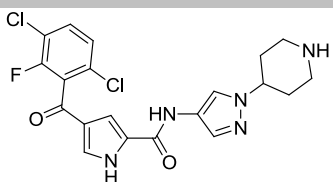
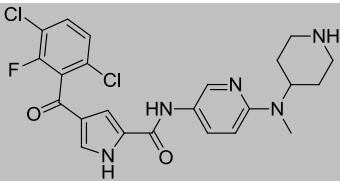
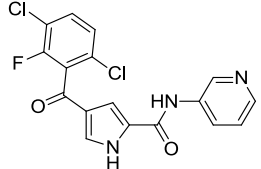
To determine the activity of an ATP consuming transporter, an ATPase assay can be conducted. This quantifies activity by measuring the phosphate level produced as a result of ATP hydrolysis, typically by colorimetry. A vesicular transport assay

determines the amount of drug remaining in a system after a given time by using inverted vesicles possessing ABC transporters. Any drug that is a transporter substrate is taken up into the vesicles which can be filtered off and the concentration of the remaining media analysed.

3.4.6 Effects of Selected Pyrrole carboxamides on P-gp Expression

A number of potent compounds from the pyrrole core series were selected for *in vitro* pharmacokinetic screening consisting of: solubility assessment, mouse microsomal clearance and Caco-2 assessment (Table 69). The results showed only one compound is not completely soluble (**344** (10/65)) with generally good microsomal clearance. As we already know, the efflux ratios across a Caco-2 membrane gave cause for concern for pyrrole carboxamides. The potency of these compounds in the enzymatic ERK5 IMAP assay is good (65-4.8 nM). However, since the inclusion of the tri-halogenated aromatic ring and extension of the scaffold with multiple heterocycles off the pyrrole amide, a decrease in cell permeability has been witnessed. These groups have increased ERK5 inhibition but it is now crucial to understand, firstly if the reason for the poor Caco-2 profile is due to a transporter protein and secondly which, if any group is the source of this activity. Typically a Caco-2 efflux ratio less than 2 is desired as it indicates that material is not ejected from the cell at a great rate. However, all but two compounds (**330** and **345**) gave poor results indicating that a transporter protein may be identifying and transferring the molecules out of the cell.

Table 69. Pharmacokinetic and potency data for selected pyrrole compounds (Caco-2 ratio = amount eliminated/amount absorbed)

Structure	Caco-2 Ratio	Mouse		IMAP ERK5 IC ₅₀ (nM)
		Microsomal Clearance (µl/min/mg)	xLog P	
339 	5.42	4.3	4.0	4.8
340 	28.3	34	4.5	5.9
341 	4.52	0.3	3.6	7.3
342 	8.22	50	4.0	13.4
330 	0.94	28	3.6	18.4
343 	18.4	8.2	3.3	18.7
344 	38.3	20	3.5	23.3
345 	0.66	46.8	3.8	65.6

Another reason to suspect that compounds are being ejected from the cell is the cellular assay data. Although the curves generated have a steep gradient, as expected for a potent compound, the maximal inhibition remains very high (Figure 100). A potential cause for the early plateau could be an induction of P-gp expression and therefore excretion due to the presence of the compound at higher concentrations. To ascertain whether selected compounds in the pyrrole series are substrates for P-gp a number of protocols were devised.

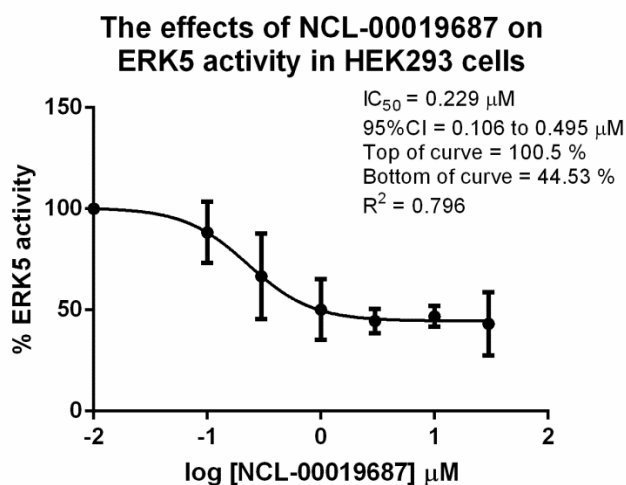


Figure 100. Cellular inhibition curve for compound **345**.

The ERK5 cellular assay was conducted in HEK293 cells with and without a known P-gp inhibitor (verapamil, **337**). There is no variation in the curves with both showing poor maximum inhibition (Figure 101). This suggests that P-gp is not responsible for the reduced activity. To control for verapamil (**337**) activity, paclitaxel resistant MCF7 cells were used. This breast cancer cell line has elevated P-gp levels in response to chronic exposure to paclitaxel; this underlines resistance to paclitaxel in this cell line. Treatment of paclitaxel resistant MCF7 cells with paclitaxel in the presence or absence of verapamil for 24h shows that inhibition of P-gp with verapamil reduces cell proliferation due to inhibition of P-gp, thus demonstrating that the verapamil used in this study is active (Figure 102).

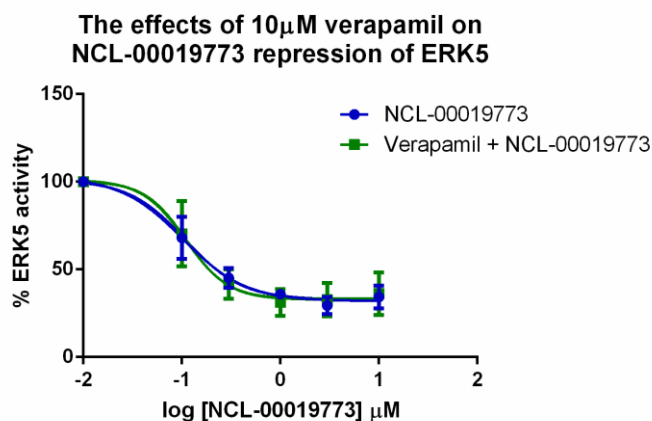


Figure 101. Activity curve of compound **341** with (green) and without (blue) verapamil, **337**.

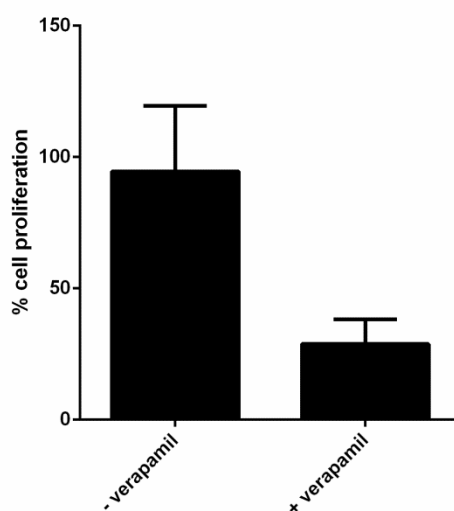


Figure 102. Verapamil, **337** sensitises paclitaxel Resistant MCF7 cells to paclitaxel treatment.

P-gp expression can be induced by the presence of a drug; therefore we monitored the level of P-gp in cells in the presence of a number of selected ERK5 inhibitors. Using HEK293 cells, as they are used in the cellular IC₅₀ determination assay, a dose of 10 μ M inhibitor was added and incubated overnight. This concentration, in all cases is enough to cause significant inhibition of ERK5 and assumed to be high enough to induce P-gp expression, if the event occurs. This is also a dose tolerated by the cells so toxicity should not lead to a false result. After incubation the cells are lysed, the lysate separated by SDS-PAGE and then visualised by Western blotting. ERK1 expression is used to verify the amount of protein loaded on the gel and an MDR1 polyclonal antibody is used to show the amount of P-gp expressed. MCF7 cells showing resistance

to paclitaxel (MCF7Tax^R) are known to up-regulate P-gp expression when grown in the presence of Taxol and were therefore used as a positive control with HEK293 cultured in the absence of a drug fulfilling the negative control (Figure 103). These results show that P-gp was detected in all lanes and that there was no substantial induction of P-gp expression following incubation with any of the compounds tested.

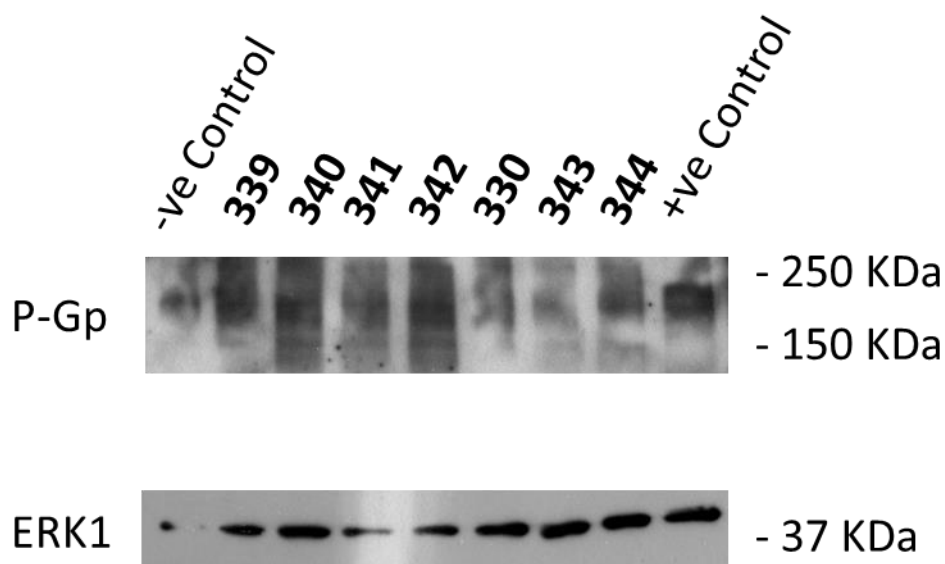


Figure 103. Transferred and visualised 10% SDS poly acrylamide gel (SDS-PAGE), showing (left to right); -ve control (HEK293 cell lysate in the absence of drug), compounds 3-9 (HEK293 cells cultured with corresponding compound), +ve control (MCF7TaxR cells grown in 6 nM paclitaxel to over express P-gp). ERK1 bands show variation in sample loading.

These results show that HEK293 cells, which are used for the ERK5 in-cell luciferase assay, express P-gp. However, P-gp expression was not altered with any of the selected inhibitors. No correlation is witnessed between poor Caco-2 efflux and P-gp expression. However, one limitation of this experiment is that only induction of P-gp expression is monitored and it may be that select compounds in this series are substrates for P-gp without increasing expression.

3.4.7 Summary of Pyrrole Carboxamide Efflux

With regard to both experiments run it is deemed that the pyrrole pharmacophore does not suffer from low maximum inhibition due to the action of P-gp. There is no change whatsoever to the cellular inhibition isotherm when P-gp is eliminated through inhibition which suggests it is not the reason for the poor profile. This suggests that compounds are not eliminated from the cell by P-gp. Western blotting of P-gp

expression showed that the HEK293 cell line does express P-gp, however, a significant variation in expression was not seen between positive/negative controls and the compounds under investigation. Induction of P-gp does not correlate to the efflux ratio witnessed in the Caco-2 assay but elimination from the cell by P-gp needn't, in all cases, induce P-gp expression. Susceptibility to P-gp transport alone could be investigated by running a Caco-2 membrane assay in the presence of a P-gp inhibitor. A decrease in the efflux ratio in this case would indicate that P-gp was responsible for the poor pharmacokinetics. It is also possible that another member of the ABC transporter family acts on the pharmacophore but an experiment to investigate this theory is not being pursued.

The data generated suggests P-gp does not interact with compounds in the pyrrole series and therefore the findings cannot aid the design of further compounds. To eliminate P-gp from the investigation into the poor Caco-2 permeability, the Caco-2 assay should be repeated with a P-gp inhibitor present.

Chapter 4: Conclusions and Future work

4.1 Summary of Further Indazole 4-position Exploration

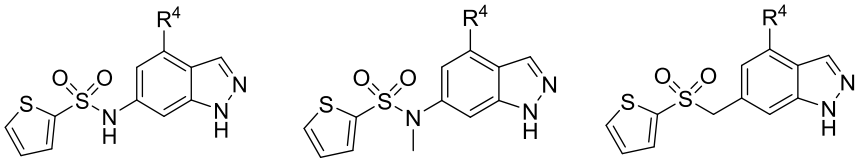
A large library of 4-substituted indazole compounds have been synthesised with the sulphonamide linker as a pose to the sulphone compounds discussed in Chapter 2.8. Compound sets were devised to investigate the difference between the sulphone and sulphonamide linkers by introducing small heterocycles and polar systems.

4.1.1 Comparison of lead Sulphone Indazole Compounds with Sulphonamide

Analogues

The first sulphone compounds synthesised were equipotent to *N*-methyl sulphonamide matched pairs when unsubstituted in the 4-position (Chapter 2.5.5). The sole reason for selecting the sulphone series for progression was the simplicity of synthesis of 4-position analogues. Subsequently sulphonamide matched pairs have been synthesised by Dr Stephanie Myers. Sulphonamide analogues of sulphones **179**, **198** and **199** all show inferior potency in both *N*-methyl and unmethylated sulphonamide (Table 70). Interestingly the previously established activity hierarchy of *N*-methyl sulphonamide lending higher potency than the un-substituted is contradicted by compound **348a** and **348b** in which the relationship is reversed. Lead compound **199** is between 10 and 40-fold more potent than the sulphonamide matched pairs indicating that the sulphone linker is superior on the elaborated indazole scaffold.

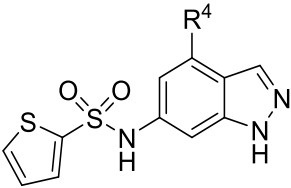
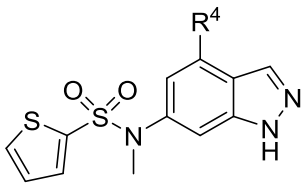
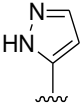
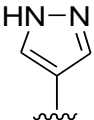
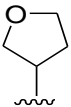

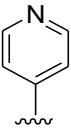
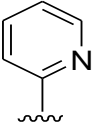
Table 70. Activity results of Indazole sulphonamide compounds.

				
	R ⁴	Enzymatic ERK5 IC ₅₀ (μM)		
346a/b, 179	Me	1.1 ± 0.02	0.27 ± 0.10	0.14 ± 0.04
347a/b, 198	Et	1.1 ± 0.2	0.10 ± 0.01	0.08 ± 0.01
348a/b, 199	^{Cyc} Pr	0.11 ± 0.01	0.43 ± 0.05	0.01 ± 0.01
349a/b	Ph	6.2 ± 4.5	2.3 ± 0.7	-

4.1.2 4-Substituted, 6-sulphonamide Indazoles – Heterocyclic Substituents

Heterocyclic rings were installed in the indazole 4-position to improve the solubility profile of the series, a limitation of lead compound **199**. Although good potency was obtained and properties improved, ligand efficiency is not improved and therefore inclusion of these groups holds no net benefit.

Table 71. Activity results of compounds **350a/b** – **355a/b**

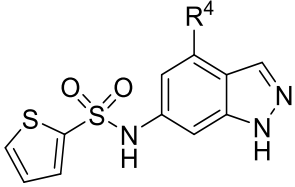
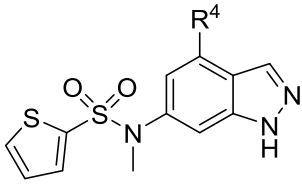


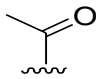
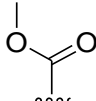
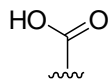
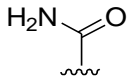
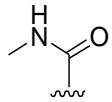
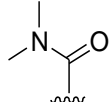
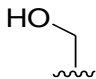
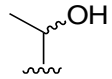
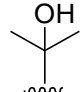
			
	R ⁴	ERK5 IC ₅₀ (μM)	
350a/b		1.87 ± 1.2	0.21 ± 0.10
351a/b		1.46 ± 0.28	0.11 ± 0.01
352a/b		0.72 ± 0.07	0.13 ± 0.01
353a/b		1.32 ± 0.18	0.18 ± 0.03
354a/b		0.45 ± 0.06	0.13 ± 0.05
355a/b		1.75 ± 0.5	1.05 ± 0.06

4.1.3 4-Substituted, 6-Sulphonamide Indazoles – Polar Substituents

Numerous carbonyl possessing groups were introduced to the indazole to improve solubility however potency significantly suffered. With the exception of ester compound **359b** all results are over 1 μM. Alkyne **356b** is 4-fold more potent than the cyano **357b** indicating that a lone pair of electrons cannot make a favourable

interaction in the enzyme at this location. Compounds **366a/b** are the only compounds tested so far which have a benzylic sp^3 centre but no benzylic hydrogen. The poor potency of compound **366b** suggests that space at this position is confined.

Table 72. Summary of ERK5 SARs for indazoles **356a/b-366a/b**.

		
	R^4	ERK5 IC_{50} (μM)
356a/b		2.5 ± 0.2 1.3 ± 0.0
357a/b		5.9 ± 0.6 4.4 ± 0.2
358a/b		2.5 ± 0.7 1.1 ± 0.02
359a/b		1.6 ± 0.4 0.43 ± 0.1
360a/b		>120 20.3 ± 0.5
361a/b		8.1 ± 1.0 1.9 ± 0.02
362a/b		9.2 ± 0.05 1.8 ± 0.1
363a/b		10.5 ± 4.9 4.3 ± 0.1
364a/b		2.8 ± 0.3 0.52 ± 0.08
365a/b		- 0.12 ± 0.02
366a/b		1.8 ± 0.5 3.3 ± 0.5

4.2 Future work

4.2.1 Future Work at the Indazole 4-Position

To understand the SAR of the benzylic 4-position of the indazole, groups have been categorised by hybridisation of this carbon, and in the case of sp^3 centres by degree of substitution. It has been observed that tertiary sp^3 benzylic centres have poor potency when compared to primary and secondary centres. Sp^2 and aromatic groups are tolerated with regard to potency and it is possible that the reason for the loss in potency is the polarity of these groups not the hybridisation. The 4-position vector is out towards the solvent and into the roof of the active site at the glycine rich loop. Figure 103 shows the binding of lead compound **199** and a hypothetical 4-^tbutyl indazole **367** illustrating a subtle change in the angle of the indazole core, which will affect the hinge binding. Hydrogen bonds are strongest when the lone pair and proton align at 180° . By affecting the angle of the hinge binding motif through substitution of the 4-position the strength of the hydrogen bonds is likely to be affected and may well be the reason for the sharp drop in potency.

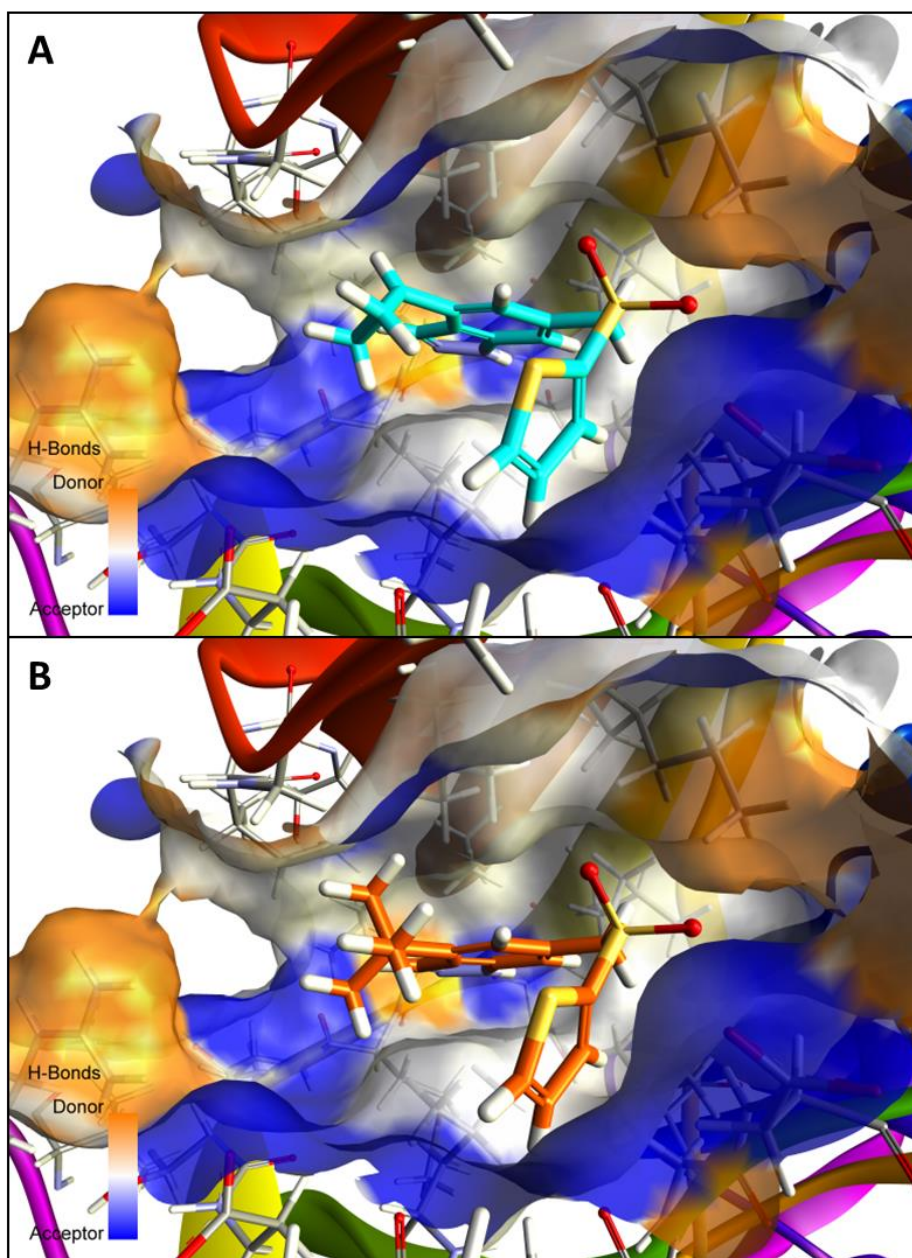


Figure 103. Molecular modelling of compound **199** (A, cyan) and hypothetical ^tbutyl compound **367** (B, Orange) in the ERK5 active site.

Considering modelling images in Figure 103 and all activity data generated from the sulphonamide series it is proposed that a ‘good substituent’ at the 4-position must satisfy two requirements:

1. The benzylic carbon of the 4-position groups must either be an sp^3 with at least one proton attached or an sp^2 centre.

Although most of the substituents with an sp^2 centre at this position have shown poor activity (Table 72) these groups are all highly polar. It is known that a small lipophilic group gives excellent potency at this position and therefore compounds **358a/b** -

365a/b in Table 72 have poor ERK5 affinity because of polarity not the planarity of the group.

2. 4-position substituents must make a contribution to LogP within the first 3-4 bond lengths.

Figure 104 shows the limits of potency obtained by only alkyl substituents revealing the cyclopropyl to be the frontier of this positive SAR. This means that introducing solubility beyond this point should improve potency further. Heterocyclic compounds shown in Table 71 agree with the above statement. Comparison of pyrazole compounds **350b** and **351b** shows that positioning the heteroatoms 3 bond lengths from the indazole lends more potency than the nearest heteroatom being situated 2 bond lengths away. This translates to a 2-fold difference in potency. Pyridine compounds **354b** and **355b** show the same relationship as the 4-pyridyl group is almost 10-fold more potent than the 2-pyridyl.

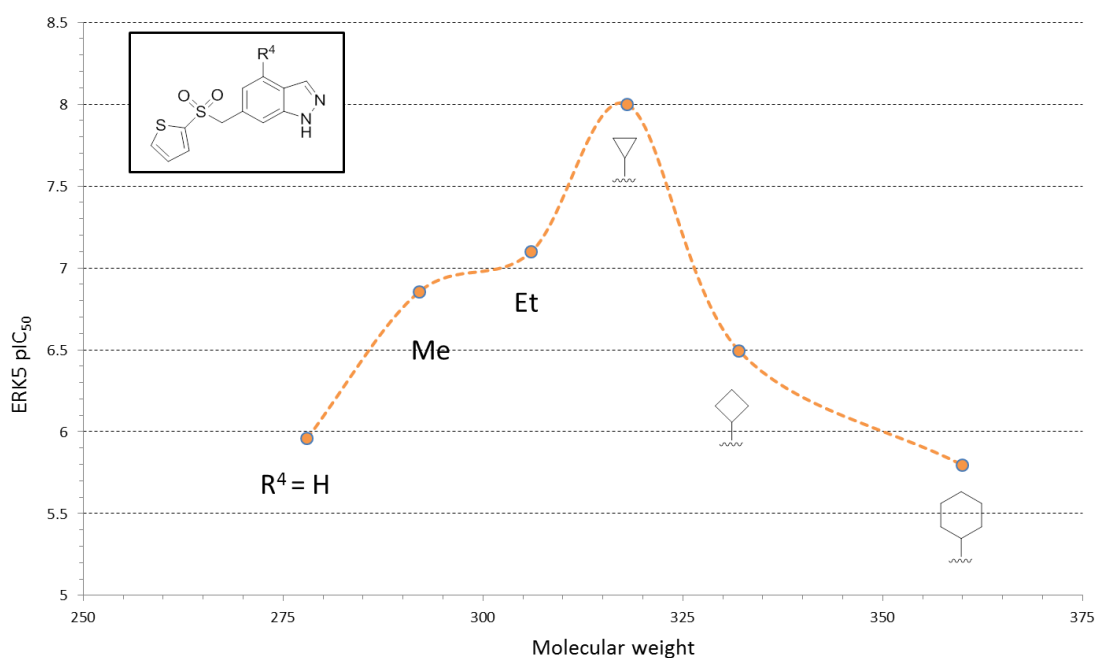


Figure 104. Graph of ERK5 pIC₅₀ vs Molecular weight for 2-thiophene sulphone compounds with alkyl 4-substituents.

3-Tetrahydrofuran compound **352b** (Table 71) shows good potency but it is proposed that the heteroatom is still too close to the indazole to make the most of the lipophilic relationship. Proposed targets are shown in Figure 105 and aim to establish the optimum proximity of a heteroatom to the core.

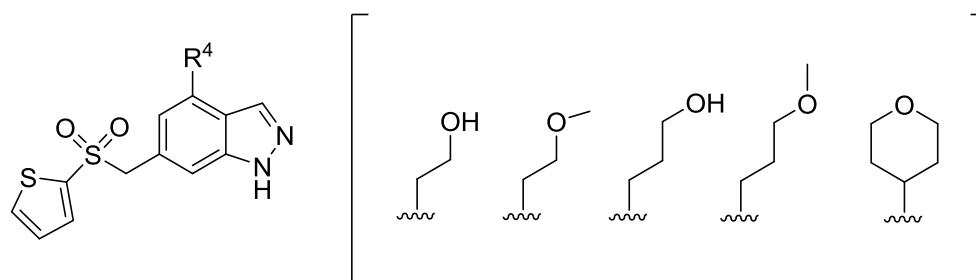
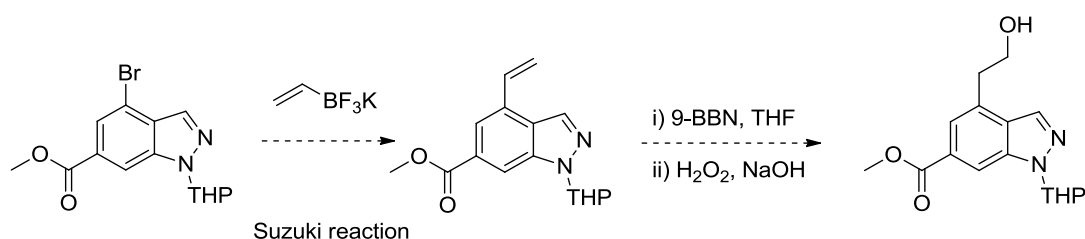


Figure 105. Proposed future targets to explore the properties of the 4-position.

Synthesis of these compounds is possible by introducing a vinyl group to the 4-position by the same Suzuki reaction used to obtain the 4-alkyl targets (scheme 38) and hydroxylation of this material via hydroboration and oxidation.



Scheme 38. Key steps involved in the synthesis of 4-position future targets.

4.2.2 Future Targets at the 3-Position

A number of targets have arisen from the 3-substituted indazole sulphonamide data set. Lipophilic compounds **247-249** show good potency but also reach the limit of the lipophilic interaction and therefore new targets need to incorporate polarity (Figure 106). A new data set systematically moving hydrogen bond acceptor/donor motifs away from the indazole core should reveal a new interaction and therefore improvement in potency and potentially properties of the compound.

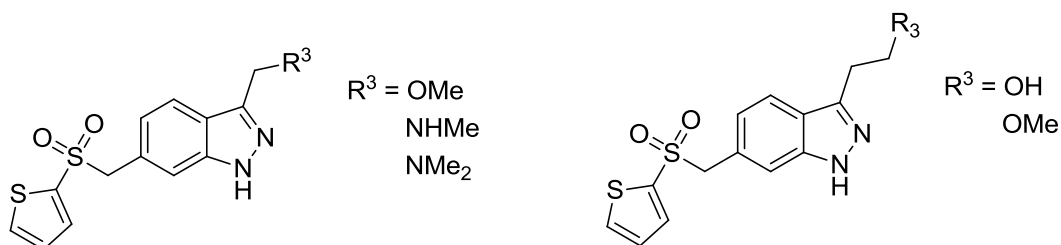


Figure 106. Future synthetic targets at the indazole 3-position.

Synthesis of these targets with a sulphone linker as a pose to the sulphonamide should also improve potency.

4.2.3 Substitution of 4,3 and 6 Positions

Substitution at the 4-position with alkyl groups has given the best potency and current lead compound **199**. Exploration of the 3-position also revealed potential for more potency and possibly the attenuation of the metabolic problem the series faces (Figure 107). Combination of these groups has yet to be attempted.

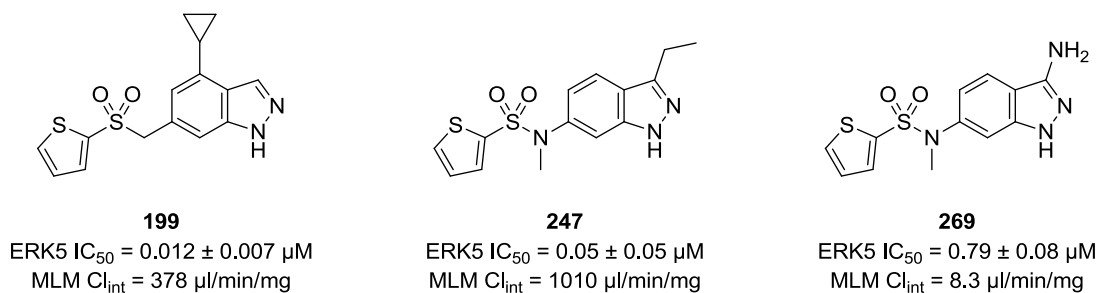


Figure 107. Significant results of compounds **199**, **247** and **269**

To date, substitution of the 3, 4 and 6-position of the indazole has not been undertaken due the lengthy synthesis. Targets shown in Figure 108 show both cyclised and separate 3,4-substituents. It is expected that due to the proximity of the 3 and 4-position independent substituents will affect the orientation of potent functionalities and therefore optimisation may be required. Targets **368** and **370** do not appear particularly drug-like and will almost undoubtedly show very high clearance, however ERK5 potency is predicted to be very good. The incorporation of a hetero atom to targets **369** and **371** may balance potency and metabolism or at least give a starting point for further investigation.

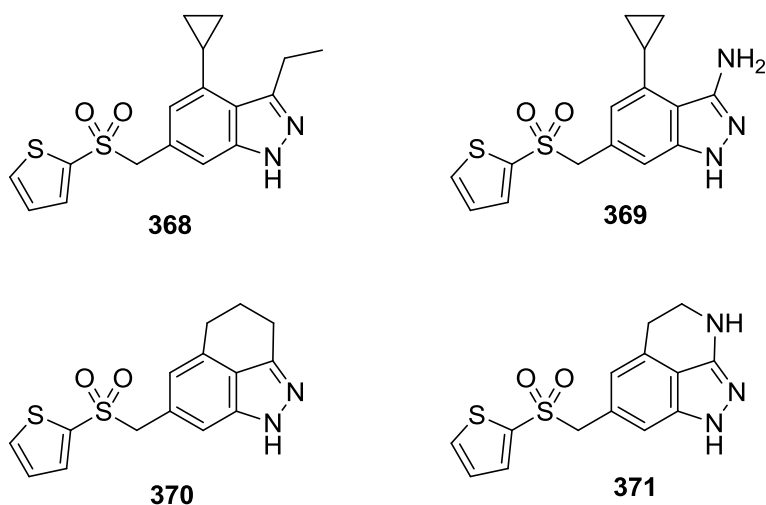


Figure 108. Potential targets combining potent groups in both the 3 and 4 position.

4.3 Conclusion

Investigations conducted on the Indazole series have moved from hit validation through hit to lead and into lead optimisation with the synthesis of over 130 final compounds. An array of SARs have been developed revealing the likely binding mode of indazole compounds in the ERK5 active site. Activity for ERK5 has been increased 1000-fold between the original hits and lead compound **199**. Compound **199** has good solubility and potency but suffers from rapid metabolism by CYP enzymes and undesirable selectivity among other kinases. *In vivo* pharmacokinetic studies with **199** revealed a bioavailability of 24% which requires improvement before the role of ERK5 inhibition in cancer can be proven in an animal model. Synthesis of 4-substituted indazoles has been heavily optimised to give a high yielding scheme over nine steps

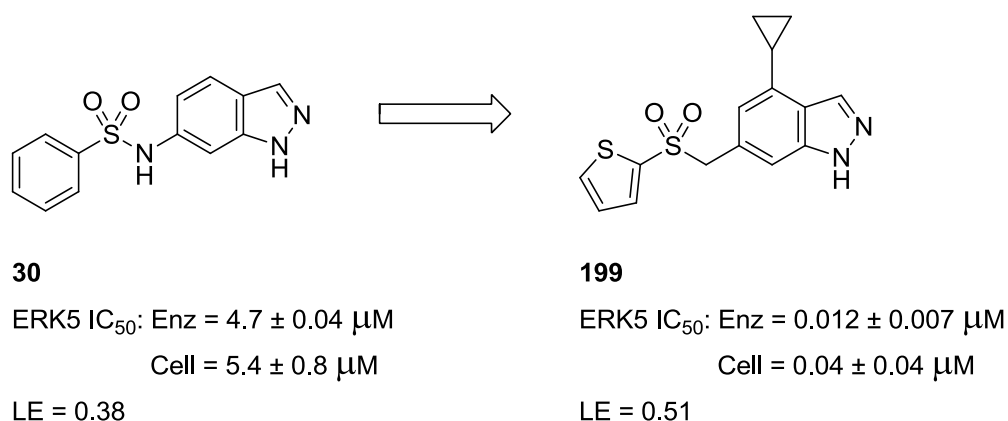


Figure 109. Progression of the indazole series activity.

Efforts to improve the metabolic profile of the series has led to 3-aminoindazole compound **269** which exhibits excellent metabolic stability and will be used to inform further compound design to retain both metabolic stability and potency.

Chapter 5: Experimental

5.1 ERK5 and p38 α Assay Protocols

The ERK5 biological assays were performed by Ms Ai Ching Wong at Cancer Research Technology Discovery Research Laboratories, London, by Dr Pamela Lochhead at the Babraham Institute, Cambridge, by Ms Lan-Zhen Wang and Dr Noel Edwards at the Paul O’Gorman Building, Newcastle Cancer Centre, Newcastle upon Tyne.

5.1.1 ERK5 IMAPTM Assay Protocol

Preparation of assay buffer (1x)

The assay buffer was prepared using 0.01% Tween[®]-20 5x stock, supplied as part of IMAPTM FP Progressive Binding System Kit (Molecular Devices R7436) and diluted to 1x using milliQ H₂O. 1 μ L of a 1 M DTT stock was added for every 1 mL of 1x assay buffer to give a final concentration of 1 mM DTT.

Preparation of ERK5 working solution

The final dilution was dependent on activity of the enzyme batches. The initial batch (08/08/08) was used at a 1 in 1 in 350 final dilution in assay buffer. A 1:175 dilution of ERK5 stock was performed in 1x assay buffer. For 1 plate, 13 μ L of ERK5 stock was added to 2262 μ L of 1x assay buffer. ERK5 was expressed and purified at CRT by Leon Pang and Sue Young. Aliquots were stored at -80 °C. Batch PO080808 was used at a stock concentration of 73.4 ng/ μ L.

Preparation of ATP/substrate working solution

For one plate, ATP disodium salt (90 μ L, 20 mM) (Sigma A7699) and FAM-EGFR-derived peptide (15 μ L, 100 μ M) (LVEPLTPSGEAPNQ(K-5FAM)-COOH) (Molecular Devices RP7129; reconstituted in milliQ H₂O to a stock concentration of 100 μ M; stored at -20 °C) was added to 2295 μ L of 1x assay buffer.

Preparation of IMAPTM binding solution

For one plate, 20.5 μ L of IMAPTM binding reagent stock, 1476 μ L of 1x binding buffer A (60%), and 984 μ L of binding buffer B (40%) (IMAPTM FP Progressive screening express kit (Molecular Devices R8127) was added to 9819.5 μ L of milliQ H₂O.

Assay procedure

1 μL of inhibitor (in 60:40 H_2O /DMSO) or control/blanks (60:40 H_2O /DMSO) were dry-spotted into the relevant wells of a 384-well assay plate using the MATRIX PlateMate® Plus. 5 μL of ERK5 working solution was added to test and control wells, and 5 μL of 1x assay buffer added to blanks; 4 μL of ATP/substrate working solution was added to all wells using a Matrix multichannel pipette. The plate was sealed using DMSO resistant clear seal and incubated for 2 h at 37 °C. 1 μL of the kinase reaction mixture from the first plate was dry spotted into a second 384-well assay plate using the MATRIX PlateMate® Plus. 9 μL of assay buffer was added, followed by 30 μL of IMAP™ binding solution using a multichannel pipette. The plate was incubated at RT in darkness for 2 h. The assay plate was then read on an Analyst HT plate reader (Molecular Devices) using the settings described below:

Measurement mode = Fluorescence polarisation; Method ID = ERK5; Integration time = 100 ms; Excitation filter = Fluorescein 485-20; Emission filter = 530-25; Dichroic mirror = 505 nm; Plate definition file = Corning 384 black fb; Z-height = 5.715 mm (middle); G-factor = 1; Attenuator = out; Detector counting = Smartread+; Sensitivity = 2.

5.1.2 p38 α LANCE Assay

Preparation of assay buffer (1x)

1x assay buffer was prepared consisting of the following reagents; 250 mM tris(hydroxymethyl)aminomethane (Tris) pH 7.5, 25 mM MgCl_2 , 2.5 mM ethylene glycol tetraacetic acid (EGTA), 10 mM DTT and 0.05% Triton X100 in milliQ H_2O (NB: 1x buffer final assay concentrations were 5x lower than stated above).

Preparation of p38 α /SAPK2 working solution

The p38 α /SAPK2 working solution was prepared using active N-terminal GST-tagged recombinant full length protein (Millipore 14-251) supplied as a 10 $\mu\text{g}/4 \mu\text{L}$ stock. This was diluted to a 10 $\mu\text{g}/40 \mu\text{L}$ (1 μM) concentration by addition of 156 μL of Tris/HCl (pH 7.5, 50 mM), NaCl (150 mM), EGTA (0.1 mM), Brij-35 surfactant (0.03%), glycerol (50%) and 0.1% 2-mercaptoethanol (0.1%). The final dilution was dependent on activity of the enzyme batches. The p38 α concentration used in the assay was 1 nM. A 2x working stock solution (2 nM, 500 fold dilution of 1 μM stock) in 1x assay buffer was prepared. For one plate, 9.4 μL of p38 α (1 μM) was added to 1870.6 μL of milliQ H_2O .

Preparation of ATP/substrate working solution

For one plate, ATP disodium salt (17.5 μ L, 200 mM stock), (Sigma A7699) and Ulight-MBP Peptide (50 μ L, 5 μ M stock) (Perkin Elmer TRF0109), which were added to 400 μ L of 5x assay buffer and 1532.5 μ L of milliQ H₂O.

Preparation of EDTA/antibody detection reagent

For one plate, 84 μ L of ethylenediaminetetraacetic acid (EDTA) (0.5 M) (Sigma E4378-100G) and 27 μ L of Europium-anti-phospho-MBP antibody (0.625 μ M) (Perkin Elmer) was added to 420 μ L of LANCE detection buffer (1x) and 3669 of milliQ H₂O.

Assay procedure

1 μ L of compound (in 80:20 H₂O/DMSO) or control/blank (80:20 H₂O/DMSO) was dry-spotted into the relevant wells of a 384-well assay plate using the MATRIX PlateMate Plus. 5 μ L of p38 α working solution was added to test and control wells, and 5 μ L of assay buffer added to blanks; 4 μ L of ATP/substrate working solution was added to all wells using a Thermo Multidrop Combi or Matrix multichannel pipette. The plate was sealed using DMSO resistant clear seal and incubated for 1 h at 37 °C. 10 μ L of the EDTA/antibody working solution was added to all wells using a Thermo Multidrop Combi or Matrix multichannel pipette. The plate was incubated at RT in darkness for 2 h. The assay plate was then read on a PheraStar microplate reader using the settings described below:

Pherastar: Measurement mode = TRF; Method ID = LANCE HTRF ERK5; Optic Module: 337, 665, 620 nm. Focal Height = 6.0, Positioning delay, 0.1 sec, Number of flashes per well = 100, Integration start = 60 μ s, Integration time = 200 μ s, Simultaneous dual emission, Ratio multiplier = 1000.

5.1.3 HeLa cell-based densitometry assay protocol

HeLa cells were serum starved overnight followed by treatment with ERK5 inhibitors for 1 h. Cells were then stimulated with 100 ng/ml EGF for 10 min. The cells were harvested and lysed at 4 °C for 5–10 min in Laemmli buffer containing Halt protease and phosphate inhibitors (Pierce). The lysates were boiled for 10 min at 100 °C. Twenty microliters samples were run on 6% Tris–glycine gels and transferred to nitrocellulose. Western blotting was done with ERK5 antibody (Cell signalling #3372S). The IC₅₀ was calculated from densitometry of top bands.

5.1.4 Cellular Dual-Luciferase Reporter Assay

Cell Trypsinisation

Cell stocks of HEK293 and MCF7 were removed from incubation and the media was removed. Cells were washed with PBS (15 mL) and trypsinised using 0.05% Trypsin EDTA solution (1 mL). Cells were then counted under a microscope and the media solution was diluted with DMEM accordingly to give 80 mL of 0.2×10^6 cells/mL solution which was transferred to 8 x 96 well plates (84 µL/well) which were incubated overnight.

Lipofection

A lipofection solution made up of Lipofectamine™ 2000 transfection reagent (Invitrogen 11668019) was combined with a solution of DNA master mix A (61.5 µL) in 1500 µL Opti-MEM® growth media (reduced serum medium, Invitrogen 31985070) and left for twenty minutes before 16 µL was added to each of the wells (except for controls) previously prepared. The control experiment was set up in the same way but with DNA master mix B in 250 µL of Opti-MEM® growth media, plates were then incubated for 4 hours.

DNA master mix A: MEF2D-Gal4 (15 µL, 0.25mg/mL stock), Gal4-Luc (15 µL, 1.25 mg/mL stock), Renilla Luciferase (15 µL, 0.1 mg/mL stock), EGFP-MEK5D construct (1.5 µL, 0.5 mg/mL stock), HA-ERK5 wt (wild type)(15 µL, 0.5 mg/mL stock).

DNA master mix B: MEF2D-Gal4 (2.5 µL, 0.25 mg/mL stock), Gal4-Luc (2.5 µL, 1.25 mg/mL stock), Renilla Luciferase (2.5 µL, 0.1 mg/mL stock), EGFP construct, containing no MEK5D (0.25 µL, 0.5 mg/mL stock), and HA-ERK5 wt (2.5 µL, 0.5 mg/mL stock)

Addition of drugs

Compounds were prepared as a 10 mM solution in DMSO, from which serial dilutions were conducted to give concentrations of 10 mM, 1 mM, 0.1 mM, 3 mM, 0.3 mM and 0.03 mM. 3 µL of each of these solutions was added to 0.5 mL of DMEM and 100 µL of each of these solutions was added to corresponding wells in a 96-well plate containing 100 µL of transfected cell media to give final drug concentrations of; 30 µM, 3 µM, 0.3 µM, 10 µM, 1 µM and 0.1 µM. Controls of C3 and 5D were made up using only DMSO instead of drug plus DMSO. A further control using BIX02189 in equal drug concentrations was also prepared.

Cell Lysis

The media was removed from the assay plates by aspiration and 20 μ L of passive lysis buffer (PLB) was dispensed into each well, the plates were then shaken for 10 min.

Quantification of cellular ERK5 Inhibition

A Dual-Luciferase[®] Reporter Assay System (Promega[®] E1960) kit was prepared according to the manufacturer's guidelines by combining Luciferase assay buffer and Luciferase assay substrate separately to a combination of Stop and Glo[®] assay buffer and Stop and Glo[®]. 50 μ L of the Luciferase system was added to each well of a 96 well plate using a multichannel pipette and luminescence was quantified by an EG&G Berthold Microumat Plus luminometer. A further addition of Stop and Glo[®] system (50 μ L) was added and the analysis repeated. The technical replicates generated were transformed in Excel and data was then transformed using GraphPad Prism to a curve and absolute IC₅₀.

5.2 P-gp induction assessment

Cell preparation and compound addition

Cell stocks of HEK293 and MCF7 were removed from incubation and the media was removed. Cells were washed with PBS (15 mL) and trypsinised using Trypsin/EDTA solution (1 mL). MCF7Tax^R cells were suspended in DMEM-Tax^R media and counted on glass slip under a microscope showing 1.37×10^6 cells/mL. A cell count of 1.5×10^5 is required per plate therefore 1.1 mL of cell solution was combined with 8.9 mL of DMEM-Tax^R on a 10 cm circular cell plate and incubated overnight.

HEK293 cells were suspended in DMEM (19 mL) after trypsinisation and counted, showing 1.06×10^6 cells/mL therefore 16 mL of cell solution was combined with 64 mL of DMEM to give a 1.5×10^5 cells/mL which was used to make 9x10 mL circular cell plates which were incubated overnight. After this time drug was added to the cells to a final concentration of 10 μ M, the cells were then returned to the incubator for a further 18 hours.

Cell lysate preparation

The media was then removed and the cells washed with PBS solution (5 mL). Cells were lysed using TG lysis buffer (250 μ L) and this solution was transferred to a 1.25 mL eppendorf tube and centrifuged at 13000 rpm, 4°C for 10 minutes to remove cell debris, and the supernatant collected. A Bradford assay was performed to ensure equal protein loading whilst the supernatant (150 μ L) was combined with loading buffer (50 μ L) and heated to 95°C for 5

minutes. Equal amount of protein was loaded for each sample according to the Bradford assay results. *Dual colour protein ladder* (10µL) was loaded in the final well.

Bradford Assay

The supernatant (5 µL) was added to Bradford assay solution (995 µL) and this mixture (200 µL) was added to a 96 well plate in duplicate. The absorbance was measured at 595 nm and protein loading volumes calibrated to the lowest absorbing sample to give 45 µg in each well.

SDS-Polyacrylamide gel electrophoresis

A 6% stacking gel and either 8 or 10% resolving gels were made up and poured according to the quantities shown (Table 72). Gels were run at 25 mA for 2-4 hours, until the dye present in the loading buffer elutes off the gel.

Table 72. Material quantities (in order of addition) for making up gels of specified strength.

Resolving Gel	8%	10%
Deionised H ₂ O / mL	27.6	24
1.5 M Tris pH 8.8 (ml)	15	15
30% Acrylamide/Bis (ml)	16.2	19.8
20% SDS (ml)	0.6	0.6
APS (ml)	0.6	0.6
TEMED (µl)	60	60

Stacking Gel	6%
Deionised H ₂ O / mL	10.6
0.5 M Tris pH 6.8 (ml)	5
30% Acrylamide/Bis (ml)	4
20% SDS (ml)	0.2
APS (ml)	0.2
TEMED (µl)	25

Protein Transfer

A Polyvinylidene fluoride (PVDF) membranes activated in methanol and washed in transfer buffer was layed on the gel and electroblotted in a Biorad mini-transblot tank for ca. 80 minutes at 300 mA.

Immunodetection

Membranes were washed in TBST solution and blocked for 1 hour at room temperature in 5% (W/V) milk-TBST solution. The Primary polyclonal antibodies; P-gp (P-gp, Santa Cruz biotechnology, inc. MDR (H-241): sc-8313) and ERK1 (BD transduction labs 610031) were added (6 µL in 6 mL 5% (W/V) milk-TBST solution) to the membrane and incubated overnight

at 4°C. Following this membranes were washed in TBST solution and the secondary antibodies (mouse for visualising ERK1, Rabbit for visualising P-gp (2 µL in 6 mL 5% (W/V) milk-TBST solution) were added. The membranes were left for one hour then washed in TBST and subjected to immunodetection solution (ECL, peroxide and luminol enhancer) according to the manufacturer's instructions. Film exposures were made for various durations in complete darkness and digital files made by scanning marked films.

Cell lines:

HEK293

HEK293 cells are an epithelial-like human embryonic kidney cell line transformed with adenovirus 5 DNA and were a kind gift from Dr Nicholas Ktistakis, The Babraham Institute.

HEK293 growth media: DMEM-HEK293 (Dulbecco's Modified Eagle Medium): 100 µg ml⁻¹ penicillin, 100 µg ml⁻¹ streptomycin, 1 mM L-glutamine, 10% (v/v) foetal bovine serum.

MCF7Tax^R

MCF7Tax^R cells are an epithelial-like breast adenocarcinoma cell line established from a 69 year old female Caucasian patient with acquired resistance to 6 nM paclitaxel (Taxol)⁷. Cells were kindly provided by Dr Helen Coley, University of Surrey.

MCF7Tax^R (*Taxol resistant*) growth media: DMEM-Tax^R (Dulbecco's Modified Eagle Medium): 100 U ml⁻¹ penicillin, 100 µg ml⁻¹ streptomycin, 1mM L-glutamine, 10% (v/v) foetal bovine serum, 6 nM paclitaxel.

Cell Maintenance

All cells were incubated at 37°C in a humidified incubator with 95% (v/v) air and 5% (v/v) carbon dioxide. Cells were generally passaged every three days when the density reaches *ca.* 80% confluency. Media is removed by aspiration and cells rinsed with PBS (4 mL) then detached by Trypsin/EDTA (2 mL). Cells were counted and resuspended in the appropriate media at a concentration of 0.2x10⁶ cells/mL.

Solutions:

Bradford assay solution: 795 µl distilled water, 200 µl Bradford reagent

Phosphate buffer solution (PBS (10x)): NaCl (4% w/v), KCl (0.1% w/v), Na₂HPO₄·7H₂O (0.6% w/v), KH₂PO₄ (0.1% w/v), NaN₃ (0.01% w/v) in distilled H₂O.

Trypsin/EDTA: (0.5% Trypsin-EDTA (1x), Gibco®)

Loading Buffer: Tris-Cl (50 mM), sodium dodecyl sulphate (SDS, 2% w/v), bromophenol blue (0.1% w/v), glycerol (10% v/v), dithiothreitol (100 mM) in distilled H₂O.

TG lysis buffer: 20 mM Tris-Cl, pH 7.5, 137 mM NaCl, 1 mM EGTA, 1% (v/v) Triton X-100, 10% (v/v) glycerol, 1.5 mM MgCl₂, 1 mM Na₃VO₄, 1 mM PMSF, 10 µg ml⁻¹ leupeptin, 10 µg ml⁻¹ aprotinin, 50 mM NaF.

Transfer buffer: 192 mM glycine, 25 mM Tris base, 20% (v/v) methanol.

Running buffer: 192 mM glycine, 25 mM Tris base, 0.1% (w/v) SDS.

TBS-T: 50 mM Tris-HCl, pH 7.6, 150 mM NaCl, 0.1% (v/v) Tween 20, Tris-Buffered Saline Tween-20

Passive lysis buffer: PLB (Dual-Luciferase Reporter Assay System (5x), Promega®) in H₂O, (1:5)

5.3 Molecular Docking Procedure

Molecular docking was conducted using GOLD software. Selected structures were drawn in ChemDraw, saved in .SDF format and docked in the active site of ERK5 (PDB: 4IC7). A 12 Å radius sphere centred on Met93 (C2) was defined as the docking space and free rotation was permitted on Lys39 (all other residues were treated as rigid). Water was eliminated from the structure. The Chemscore docking protocol was run at the highest level of efficiency.

5.4 Analytical Techniques

All commercial reagents were purchased from Sigma-Aldrich Chemical Company, Alfa Aesar, Apollo Scientific, Tokyo Chemical Industry UK Ltd or Fluorchem. Unless otherwise stated, chemicals were used as supplied without further purification. Anhydrous solvents were obtained from AcroSeal™ or Aldrich SureSeal™ bottles and were stored under nitrogen. Petrol refers to the fraction with a boiling point between 40 and 60 °C.

NMR samples were run on a Bruker Avance III (500 MHz) NMR spectrometer in deuterated solvent. Chemical shifts are reported in parts per million (ppm) and coupling constants in Hertz (Hz). Spin multiplicity is denoted in the following format: s = singlet, d = doublet, t = triplet, q = quartet, quint = quintet, m = multiplet and br = broad. Notations can also be found combined to denote the following dt = doublet of triplets, dd = doublet of doublets etc. Homonuclear and

heteronuclear two dimensional NMR experiments were used where appropriate to facilitate assignment of chemical shifts.

Low resolution mass spectrometry data were collected from a Waters Acquity UPLC system, through a Aquity UPLC® BEH C18 1.7µm, 2.1 x 50mm column with PDA and ELSD with both positive and negative electrospray ionisation. High resolution mass spectra were obtained from EPSRC UK National Mass Spectrometry Facility (NMSF), University of Wales, Singleton Park, Swansea, SAZ 8PP.

Liquid chromatography purification was performed by medium pressure liquid chromatography (MPLC) using Davisil silica gel (40 -63µm) on a Biotage SP4 system using pre-packed Aligent Si 50, Si 35 or Graceresolve Si 40 columns. Thin layer chromatography (TLC) was performed on aluminium backed Merck TLC silica gel 60 F254 plates and visualised under short wave ultraviolet light (254nm).

All samples submitted for biological assay were greater than 95% purity by integration. Analytical HPLC values were acquired from a Waters XTerra RP18, 5 M (4.6 x 150 mm) column at 1 ml/min. Both acidic and basic values were taken using 0.1% aqueous formic acid and 0.1% aqueous ammonia in acetonitrile respectively on a gradient of 5-100% over 15 minutes.

All FTIR (fourier transform infrared) spectra were run on a Bio-Rad FTS 3000MX diamond ATR as a neat sample or an Agilent Cary 630 FTIR as a neat sample.

Melting points were obtained on a Stuart Scientific SMP3.

Ultraviolet spectra were gathered on a Hitachi UV-U2800A spectrophotometer in ethanol.

Microwave reactions were carried out in a Biotage initiator with Sixty robot.

5.5 General Procedures:

Except where water was included in the reaction mixture, all reactions were carried out under strict anhydrous conditions with oven-dried glassware and cooled under nitrogen. Temperatures quoted refer to heating block temperatures.

General procedure A: The preparation of Sulphonamides:

Sulphonyl chloride (1.1 eq) was dissolved in pyridine and added dropwise to amino indazole (1 eq) in pyridine (1.5 mL per 100 mg) at 0 °C. The reaction mixture was stirred for 4 h under N₂ and allowed to warm to RT. After this time the solution was reduced under vacuum and resuspended in saturated NaHCO₃ solution and extracted with EtOAc. Combined organic fractions were washed with brine, dried over Na₂SO₄ and purified by MPLC (0-80% EtOAc in petroleum ether) giving the pure product.

General procedure B: Sulphonamide Alkylation:

In oven dried glassware, a sulphonamide (1 eq) was dissolved in DMF (1 mL per 0.18 mmol) and potassium carbonate (1 eq) was added and the mixture stirred at 0 °C under N₂ for 15 mins. After this time ethyl/methyliodide (1.5 eq) was added and the reaction was allowed to warm to RT. This was left to stir overnight before being reduced to a residue *in vacuo* and suspended in water before extraction with EtOAc. Organic fractions were combined and washed with brine. The pure product was obtained by MPLC (10 - 60% EtOAc in petroleum ether).

General procedure C: Indazole-THP protection

The indazole derivative (1 eq) was dissolved in DCM (3 mL/mmol) and DHP (3 eq) added followed by *p*-TSA (0.1 eq). The solution was stirred at RT for ca. 6 h then saturated aqueous sodium hydrogen carbonate solution (2 mL/mmol) was added and the solution extracted with DCM (3 x 1.5 mL/mmol). Organic fractions were combined and dried using a phase separator. The solution was reduced *in vacuo* and the pure product obtained by MPLC (0-80% EtOAc in petroleum ether).

General procedure D: Indazole-THP Deprotection

THP protected indazole (1 eq) is dissolved in an excess of methanolic HCl (1.25 M) solution and stirred at room temperature for *ca.* 3 h before evaporation of the volatiles and redissolving in EtOAc. The organic solution was washed with saturated NaHCO₃ solution (aq) and dried over Na₂SO₄. The pure product was obtained by MPLC (0-80% EtOAc in petroleum ether).

General procedure E: Aromatic Nitro reduction

A nitro-indazole compound (1 eq) was dissolved in EtOAc to a maximum concentration of 0.05 M and cycled through a Thales 'H-Cube' instrument with a 10% Pd/C catalyst cartridge on full H₂ mode at 40°C with a flow rate of 1 mL/min until complete conversion was witnessed by TLC/LCMS. The volatiles were removed and the clean product isolated without purification.

General procedure F: Suzuki reaction

A bromo-indazole compound (1 eq), a boronic acid species (3 eq), Cs₂CO₃ (1.5 eq) and Pd(dppf)Cl₂.DCM (0.1 eq) were deposited in a dry microwave vial under N₂ and dissolved in 1,4-dioxane (12 mL/ mmol). The solution was degassed with N₂ for *ca.* 10 minutes before being subjected to microwave irradiation for 30 minutes, to a temperature of 150 °C. The solution was allowed to cool, filtered through Celite® and the reduced to a residue under vacuum. The pure product was obtained by reversed phase MPLC (0-80% MeCN (0.1% HCOOH) in H₂O (0.1% HCOOH)).

General procedure G: LiAlH₄ Ester Reduction

Methylester-indazole (1 eq) was dissolved in anhydrous THF (10 mL/mmol) under N₂ at 0 °C and LiAlH₄ (1 M in THF, 2 eq) added dropwise. The reaction was stirred for 3 h before addition of EtOAc (5 mL/mmol) and a further stirring period of 15 minutes. Water was added dropwise until effervescence ceased. The reaction mix was then filtered through Celite® and washed with MeOH. The solution was reduced to a residue by rotary evaporator and resuspended in DCM, partitioned with water, washed with brine and dried by phase separator before purification by MPLC (0-80% EtOAc in petroleum ether).

General procedure H: Bromination and Simultaneous Indazole-THP Deprotection

A Methanol-indazole derivative (1 eq) was dissolved in anhydrous DCM (20 mL/mmol) under N₂ at 0 °C and DMF (0.1 eq) was added. SOBr₂ (2 eq) was added dropwise and the reaction allowed to reach room temperature over 6 h with stirring. After this time the reaction mix was concentrated in vacuo and resuspended in methanolic HCl (1.25 M, 10 eq). This mixture was stirred for 3 h before volatiles were removed *in vacuo* and the residue redissolved in EtOAc. The organic solution was washed with saturated NaHCO₃ solution (aq) and dried over Na₂SO₄. The pure product was obtained by MPLC (0-80% EtOAc in petroleum ether).

General procedure I: Thiol-Alkyl Bromide S_N2

A Thiol species (1.5 eq) was dissolved in anhydrous DMF (10 mL/mmol) under N₂ and Cs₂CO₃ (1.1 eq) added. This mixture was stirred for 5 minutes before the addition of the bromomethyl-indazole species (1 eq). The reaction was stirred at room temperature for 6 h then reduced to a residue on by high vacuum and heat (Biotage V10 instrument), resuspended in DCM and partitioned with H₂O. The aqueous layer was extracted with DCM (3 x 10 mL) and combined organic fractions were washed with brine and dried via phase separator. The product was obtained by MPLC (0-80% EtOAc in petroleum ether).

General procedure J: Secondary Sulphonamide Formation

Methylamine (2 M in THF, 2.1 eq) was added to a solution of a sulphonylchloride (1 eq) in DCM (3 mL/mmol) and heated at reflux for 2 h whilst stirring. After this time water (2 mL/mmol) was added and the organic fraction separated, washed with brine (2 mL/mmol) and dried using a phase separator. The product was obtained by MPLC (0-80% EtOAc in petroleum ether).

General procedure K: Oxone® Thioether Oxidation

Indazole-thioether was dissolved in MeOH (20 mL/mmol) and a solution of Oxone® (6 eq) in H₂O (20 mL/mmol) was added in one portion. The reaction mix was stirred for 18 h then volatiles were removed by rotary evaporator. The remaining solution was diluted with H₂O and extracted with DCM (3 x 10 mL) and the combined organic

fractions dried via phase separator. The product was obtained by MPLC (0-80% EtOAc in petroleum ether).

General procedure L: Suzuki and THP Deprotection

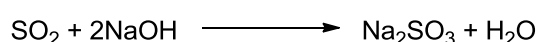
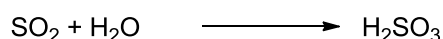
Bromo-indazole compound (1 eq), a boronic acid species (3 eq), Cs_2CO_3 (1.5 eq) and $\text{Pd(dppf)Cl}_2\cdot\text{DCM}$ (0.1 eq) were deposited in a dry microwave vial under nitrogen and subsequently dissolved in dioxane (12 mL/ mmol). The solution was degassed with N_2 for *ca.* 10 minutes before being subjected to microwave irradiation for 30 minutes, to a temperature of 150°C . The solution was allowed to cool, filtered through Celite® and the filtrate reduced to a residue under vacuum. This resulting material was dissolved in an excess of methanolic HCl (1.25 M) solution and stirred at room temperature for *ca.* 3 h before volatiles were removed *in vacuo* and the residue redissolved in EtOAc. The organic solution was washed with a saturated NaHCO_3 solution (aq) and dried over Na_2SO_4 . The product was obtained by semi-preparative HPLC (MeCN:H₂O (0.1% CHOOH)).

General procedure M: Sequential Diazotisation, Sulphonylchloride and sulphonamide formation

6-Aminoindazole (100 mg, 0.75 mmol) was dissolved in concentrated hydrochloric acid (0.25 mL, 3.00 mmol) and water (1 mL) and stirred at 0°C . A solution of sodium nitrite (62 mg, 9.0 mmol) in water (0.5 mL) was added drop wise over 10 minutes. After 30 minutes this reaction mixture was added drop wise to a solution of copper (II) chloride (300 mg, 2.25 mmol) in concentrated acetic acid (12 mL) under SO_2 over 5 minutes. Sulphur dioxide was vigorously bubbled through this mixture for 40 minutes at RT before being diluted with DCM (40 mL) and cooled in ice. Cold water (20 mL) was added and the organic layer was isolated, dried and reduced *in vacuo*, this gave the intermediate sulphonyl chloride which was used directly without purification. The residue was taken in pyridine (2 mL) and the relevant aromatic amine (0.75 mmol) in pyridine (1 mL) was added slowly under N_2 . This was stirred at RT for 18h before being reduced to a residue under vacuum and suspended in saturated sodium bicarbonate solution. This was extracted with EtOAc (3 x 10 mL) and combined organic extracts

were washed with brine (10 mL) then dried over Na₂SO₄. Desired products were isolated by MPLC (0-80% EtOAc in petroleum ether).

SO₂ is a toxic gas and therefore release to the environment is prohibited; this was managed by allowing excess gas from the reaction to pass through water and a separate sodium hydroxide solution to convert SO₂ to safer substances namely sulfurous acid and sodium sulphite which can be neutralised and disposed of in a typical manor for aqueous solutions (Scheme 39).



Scheme 39. Quenching methods for the sanitation of SO₂ gas.

General procedure N: Palladium Mediated Carboxylation

A bromo-indazole compound (1 eq), Pd(OAc)₂ (0.1 eq), XantPhos (4,5-Bis(diphenylphosphino)-9,9-dimethylxanthene, 0.2 eq) and lithium/methyl formate (4 eq) were deposited in a dry microwave vial under N₂ and dissolved in DMF (12 mL/mmol). After addition of Et₃N (4 eq) the solution was degassed with N₂ for *ca.* 10 minutes and Ac₂O (4 eq) added then reaction vessel was sealed. The solution was heated to 90 °C for 18 hours then allowed to cool, filtered through Celite® and reduced to a residue under vacuum. The pure product was obtained by MPLC (0-80% EtOAc in petrol).

General procedure O: CDI Mediated Amide Coupling

A solution of carbonyldiimidazole (2.0 eq.) and the relevant carboxylic acid (1.0 eq.) in THF (5 mL/mmol) was heated to 70 °C for 3 h. The appropriate amine (2.5 eq.) was added and the mixture heated at 50 °C for 3 h then RT for 16 h. The solution was diluted with H₂O (10 mL), extracted with EtOAc (2 x 10 mL), washed with brine (10 mL) and dried over Na₂SO₄. The desired product was purified by MPLC (0-80% EtOAc in petrol).

General procedure P: Amine Alkylation:

In oven dried glassware an amino indazole (1 eq) was taken in DMF (1 mL per 0.18 mmol) with NaH (1 eq/ 2 eq) and stirred at 0 °C under N₂ for 30 mins. After this time methyl iodide (1 eq/2 eq) was added and the reaction was allowed to warm to RT. This was left to stir overnight before being reduced *in vacuo* and taken up in water (15 mL) and extracted with EtOAc (3 x 15 mL). Organic fractions were combine, washed with brine and reduced by rotary evaporation. The pure product was obtained by MPLC (10 - 60% EtOAc in petroleum ether).

General procedure Q: Indazole-BOC Deprotection

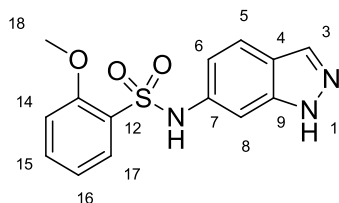
A Boc protected indazole (1 eq) was dissolved in DCM (10 mL/0.1 mmol) and TFA (1 mL/0.05 mmol) and stirred at room temperature for 2 hours before evaporating off the volatiles and redissolving in EtOAc. The organic solution was washed with a saturated NaHCO₃ solution (aq) and dried over Na₂SO₄. The product was obtained by MPLC (0-80% EtOAc in petroleum ether).

General Procedure R: PCl₃ Mediated Amide Coupling

A microwave vial was charged with the relevant carboxylic acid (1 eq.), the desired amine (2.5 eq), MeCN (2 mL/mmol) and PCl₃ (1 eq.). The resulting mixture was heated at 150 °C by microwave irradiation for 5 mins. The mixture was then quenched with a saturated NaHCO₃ Solution and diluted with H₂O. The the solution was extracted with EtOAc (3 x 30 mL) and combined organic layers were washed with brine (50 mL), dried over Na₂SO₄, and concentrated *in vacuo*. The pure product was obtained by MPLC (10- 80% EtOAc in petroleum ether).

5.6 Synthetic Procedures

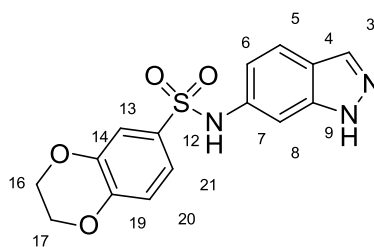
N-(1*H*-Indazol-6-yl)-2-methoxybenzenesulfonamide (31)



2-methoxybenzenethiol (0.24 ml, 2 mmol) was dissolved in acetonitrile (3 mL) and Hydrogen peroxide (30% in water, 6 mmol, 0.68ml) was added, the vessel was cooled in ice whilst thionyl chloride (2 mmol, 0.15 ml) was added dropwise. The mixture was stirred until conversion to the sulfonyl chloride was complete by TLC. 6-Amino-indazole (266 mg, 2 mmol) dissolved in pyridine (3 ml) was added to the solution and stirred for a further 16 h. The resulting solution was acidified with hydrochloric acid solution (2 M, 10 mL) and extracted with EtOAc (3 x 10ml). The combined organic fractions were washed with brine and evaporated under low pressure. The resulting residue was purified by medium pressure liquid chromatography (0-70% EtOAc in petroleum spirit over 30 column volumes) to give a white solid (43.4 mg, 7%).

R_f 0.35 (EtOAc /Petrol, 1:1); m.p. 221°C; UV λ_{\max} (EtOH/nm) 286.0, 213.5; IR $\nu_{\max}/\text{cm}^{-1}$: 3353 (SO_2NH), 1590, 1479; $^1\text{H-NMR}$ (500 MHz, $\text{DMSO-}d_6$) δ ppm 3.89 (3H, s, H-18), 6.91 (1H, d, J = 8.6 Hz, H-6), 7.01 (1H, dd, J = 7.4, 7.4 Hz, H-16), 7.15 (1H, d, J = 8.2 Hz, H-14), 7.22 (1H, s, H-8), 7.51-7.56 (2H, m, H-15, H-5), 7.77 (1H, d, J = 7.4 Hz, H-17), 7.89 (1H, s, H-3), 10.13 (1H, s-br, SOONH), 12.80 (1H, s-br, N-1); $^{13}\text{C-NMR}$ (125 MHz, $\text{DMSO-}d_6$) δ ppm 56.1 (C-18), 99.1 (C-8), 112.8 (C-14), 114.4 (C-6), 119.5 (C-4), 120.0 (C-16), 120.9 (C-5), 126.2 (C-12), 130.3 (C-17), 133.3 (C-3), 135.0 (C-15), 136.2 (C-7), 140.1 (C-9), 156.3 (C-13); MS (ES^+) m/z 304.2 $[\text{M}+\text{H}]^+$; HRMS calcd for $\text{C}_{14}\text{H}_{14}\text{N}_3\text{O}_3\text{S}$ 304.0750 $[\text{M}+\text{H}]^+$ found 304.0750.

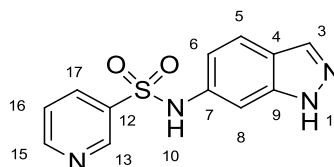
***N*-(1*H*-Indazol-6-yl)-2,3-dihydrobenzo[*b*][1,4]dioxine-6-sulfonamide (34)**



Prepared according to general procedure A with following reagents and quantities: 6-amino-indazole (100 mg, 0.75 mmol), pyridine (1.5 mL), THF (2 mL) and 1,4-benzodioxan-6-sulfonyl chloride (194 mg, 0.75 mmol) to give a white solid (37.1 mg, 15%).

R_f 0.39 (EtOAc /Petrol, 1:1). m.p. 196°C. UV λ_{\max} (EtOH/nm) 288, 207. IR $\nu_{\max}/\text{cm}^{-1}$ 3384 (SO₂NH) 2111, 1633, 1495, 1142. ¹H-NMR (500 MHz, DMSO-*d*₆) δ ppm 4.24-4.27 (4H, m, H-16₂, H-17₂), 6.89 (1H, d, J = 8.7, 1.6 Hz, H-6), 6.97 (1H, d, J = 8.9 Hz, H-20), 7.23-7.26 (1H, m, H-21, H-8, H-13), 7.61 (1H, d, J = 8.7 Hz, H-5), 7.94 (1H, s, H-3), 10.33 (1H, br, SO₂NH), 12.87 (1H, s-br, N-1). ¹³C-NMR (125 MHz, DMSO-*d*₆) δ ppm 63.9 (C-17), 64.3 (C-16), 99.4 (C-8), 114.5 (C-6), 115.6 (C-13), 117.6 (C-20), 119.6 (C-4), 120.3 (C-21), 121.2 (C-5), 131.8 (C-12), 133.4 (C-3), 136.1 (7CH), 140.1 (C-9), 143.2 (C-19), 147.2 (C-14); MS (ES⁺) m/z 332.2 [M+H]⁺. HRMS calcd for C₁₅H₁₄N₃O₄S [M+H]⁺ 332.700 found 332.0703

***N*-(1*H*-Indazol-6-yl)pyridine-3-sulfonamide (37)**

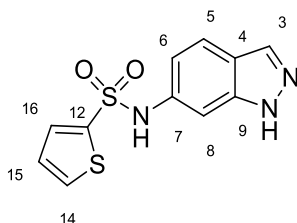


Pyridine-3-sulfonic acid (1g, 6.28 mmol) was dissolved in phosphorousoxychloride (7 ml) with phosphorouspentachloride (1.96 g, 9.42 mmol) and was heated at 135 °C for c.a. 18 h. After this time the solution was reduced to a residue under low pressure and taken in ice cold water (c.a. 20 ml). This was then baseified with saturated sodium hydrogencarbonate solution (20 ml) and extracted with diethylether. This was reduced under low pressure and used in the next reaction without purification. 6-aminoindazole (837 mg, 6.28 mmol) in anhydrous pyridine (5 ml) was added to the

sulphonyl chloride, previously taken in 5ml THF. The solution was stirred at RT under nitrogen for c.a. 3 h before being reduced to a residue and taken in sodium hydrogencarbonate (20 ml) and extracted with EtOAc (3 x 15ml). Combined organic fractions were washed with brine, reduced under low pressure and purified by medium pressure liquid chromatography (0-70% EtOAc in petroleum ether) giving the title compound as an off white solid (284.3 mg, 16%).

R_f 0.28 (EtOAc /Petrol, 1:1); m.p. 216°C; UV λ_{\max} (EtOH/nm) 267, 209, 199.5; IR $\nu_{\max}/\text{cm}^{-1}$ 2745 (NNH), 1636, 1467, 1416; $^1\text{H-NMR}$ (500 MHz, DMSO- d_6) δ ppm 6.88 (1H, dd, J = 8.6, 1.7 Hz, H-6), 7.27 (1H, s, H-8) 7.59 (1H, dd, J = 8.1, 4.7 Hz H-16), 7.63 (1H, d, J = 8.6 Hz, H-5), 7.97 (1H, s, H-3), 8.11 (1H, dt, J = 8.1, 1.6 Hz, H-17), 8.76 (1H, dd, J = 4.7, 1.6 Hz, H-15) 8.89 (1H, d, J = 1.9 Hz, H-13) 10.62 (1H, s-br, SOONH), 12.26 (1H, s-br, N-1); $^{13}\text{C-NMR}$ (125 MHz, DMSO- d_6) δ ppm 100.7 (C-8), 115.1 (C-6), 120.1 (C-4), 120.4 (C-5), 124.4 (C-16), 133.5 (C-3), 134.6 (C-17), 135.3 (C-7), 135.6 (C-12), 140.0 (C-9), 147.0 (C-13), 153.5 (C-15); MS (ES^+) m/z 275.2 [$\text{M}+\text{H}$] $^+$; HRMS calcd for $\text{C}_{12}\text{H}_{11}\text{N}_4\text{O}_2\text{S}$ [$\text{M}+\text{H}$] $^+$ 275.0602 found 275.0602.

***N*-(1*H*-Indazol-6-yl)thiophene-2-sulfonamide (38)**

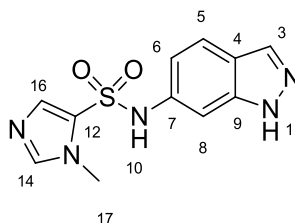


Prepared according to general procedure A with following reagents and quantities: 6-amino-indazole (100 mg, 0.75 mmol), pyridine (1.5 mL), THF (2 mL) and 2-thiophenesulfonyl chloride (137 mg, 0.75 mmol) to give a light pink solid (32.8 mg, 16%).

R_f 0.39 (EtOAc /Petrol, 1:1). m.p. 169-170°C. UV λ_{\max} (EtOH/nm) 298, 258, 213. IR $\nu_{\max}/\text{cm}^{-1}$ 3341 (SO_2NH) 3139 (NNH), 1628, 1497, 1332, 1146, 853. $^1\text{H-NMR}$ (500MHz, DMSO- d_6) δ ppm 6.91 (1H, d, J = 8.6 Hz, H-6), 7.09 (1H, dd, J = 3.7 & 4.7 Hz, H-15), 7.32 (1H, s, H-8), 7.53 (1H, d, J = 3.7 Hz, H-16), 7.64 (1H, d, J = 8.7 Hz, H-5), 7.86 (1H, d, J = 4.7 Hz, H-14), 7.90 (1H, s, H-3), 10.54 (1H, s-br, SOONH), 12.91 (1H, s-br, N-1). $^{13}\text{C-NMR}$ (125 MHz, DMSO- d_6) δ ppm 100.4 (C-8), 115.0 (C-6), 120.0 (C-4), 121.2 (C-5), 127.6 (C-

15), 132.3 (C-16), 133.3 (C-14), 133.4 (C-3), 135.7 (C-7), 139.8 (C-12), 140.1 (C-9); MS (ES⁺) m/z 280.2 [M+H]⁺; HRMS calcd for C₁₁H₁₀N₃O₂S₂ 280.01 [M+H]⁺ 280.0205 found 280.0205.

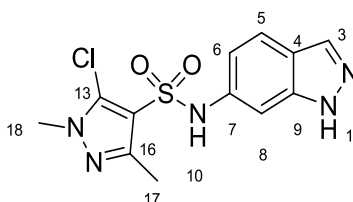
***N*-(1*H*-Indazol-6-yl)-1-methyl-1*H*-imidazole-5-sulfonamide (40)**



Prepared according to general procedure A with following reagents and quantities: 6-amino-indazole (100 mg, 0.75 mmol), pyridine (1.5 mL), THF (2 mL) and 1-methyl-1*H*-imidazole-5-sulfonyl chloride (181 mg, 0.75 mmol) to give an off white solid (50.9 mg, 25%).

R_f 0.34 (EtOAc /Petrol, 1:1). m.p. 262°C; UV λ_{max} (EtOH/nm) 297.5, 285.5, 208.5; IR ν_{max}/cm^{-1} 3427 (SO₂NH), 1631, 1531, 1326, 1146, 991, 945, 798. ¹H-NMR (500 MHz, DMSO-*d*₆) δ ppm 3.63 (3H, s, H-17), 6.93 (1H, d, J = 8.6 Hz, H-6), 7.33 (1H, s, H-8), 7.57 (1H, d, J = 8.6 Hz, H-5), 7.73 (1H, s, H-14), 7.98 (1H, s, H-16), 7.93 (1H, s, H-3), 10.31 (1H, s-br, SOONH), 12.84 (1H, s-br, N-1). ¹³C-NMR (125 MHz, DMSO-*d*₆) δ ppm 33.4 (C-17), 98.9 (C-8), 114.4 (C-6), 119.3 (C-4), 120.8 (C-5), 125.2 (C-16), 133.3 (C-3), 136.5 (C-7), 138.4 (C-12), 139.7 (C-14), 140.2 (C-9); MS (ES⁺) m/z 378.2 [M+H]⁺; HRMS calcd for C₁₁H₁₂N₅O₂S 278.0706 [M+H]⁺ found 278.0706.

5-Chloro-*N*-(1*H*-indazol-6-yl)-1,3-dimethyl-1*H*-pyrazole-4-sulfonamide (41)

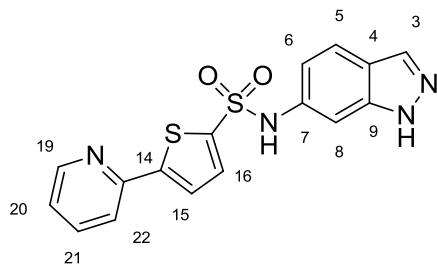


Prepared according to general procedure A with following reagents and quantities: 6-amino-indazole (100 mg, 0.75 mmol), pyridine (1.5 mL), THF (2 mL) and 5-chloro-1,3-dimethyl-1*H*-pyrazole-4-sulfonyl chloride (172 mg, 0.75 mmol) followed by semi-

preparative HPLC (50% MeCN in H₂O with 1% formic acid) to give a white solid (121.7 mg, 50%).

*R*_f 0.41 (EtOAc /Petrol, 1:1); m.p. 221°C; UV λ_{max} (EtOH/nm) 298, 286.5, 212; IR ν_{max}/cm⁻¹ 3374 (SO₂NH), 1635, 1501, 1333, 1126, 941, 910, 855, 686. ¹H-NMR (500 MHz, DMSO-*d*₆) δ ppm 2.27 (3H, s, H-17), 3.69 (3H, s, H-18), 6.89 (1H, dd, *J* = 8.7, 1.8 Hz, H-6), 7.33 (1H, d, *J* = 1.8 Hz, H-8), 7.63 (1H, d, *J* = 8.7 Hz, H-5), 7.96 (1H, s, H-3), 10.56 (1H, s-br, SOONH), 12.91 (1H, s-br, N-1). ¹³C-NMR (125 MHz, DMSO-*d*₆) δ ppm 13.3 (C-17), 36.4 (C-18), 99.1 (C-8), 114.3 (C-6), 114.3 (C-16), 119.6 (C-4), 121.3 (C-5), 128.9 (C-9), 133.4 (C-3), 135.7 (C-12), 140.1 (C-7), 147.6 (C-13); MS (ES⁺) *m/z* 326.2 [M+H]⁺; HRMS calcd for C₁₂H₁₃³⁵ClN₅O₂S 326.0473 [M+H]⁺ 326.0479.

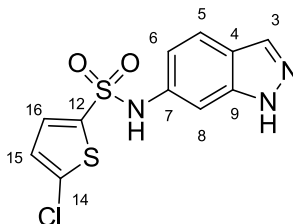
***N*-(1*H*-Indazol-6-yl)-5-(pyridin-2-yl)thiophene-2-sulfonamide (42)**



Prepared according to general procedure A with following reagents and quantities: 6-amino-indazole (100 mg, 0.75 mmol), pyridine (1.5 mL), THF (2 mL) and 5-(pyridin-2-yl)thiophene-2-sulfonyl chloride (195 mg, 0.75 mmol) followed by semi-preparative HPLC (60% MeCN in H₂O) to give a white solid (47.5 mg, 18%).

*R*_f 0.44 (EtOAc /Petrol, 1:1); m.p. 220°C; UV λ_{max} (EtOH/nm) 363.5, 311, 211.5; IR ν_{max}/cm⁻¹ 3253 (SO₂NH), 1634, 1427, 1350, 1149, 943, 773, 661; ¹H-NMR (500 MHz, DMSO-*d*₆) δ ppm 6.95 (1H, dd, *J* = 8.7, 1.7 Hz, H-6), 7.35-7.37 (1H, m, H-8), 7.35-7.37 (1H, m, H-20), 7.54 (1H, d, *J* = 4.0 Hz, H-16), 7.65 (1H, d, *J* = 8.7 Hz, H-5), 7.76 (1H, d, *J* = 4.0 Hz, H-15), 7.87 (1H, dd, *J* = 7.8, 1.6 Hz, H-21), 7.96-7.98 (1H, m, H-3), 7.96-7.98 (1H, m, H-22), 8.53 (1H, d, *J* = 4.3 Hz, H-19), 10.65 (1H, s-br, SOONH), 12.93 (1H, s-br, N-1). ¹³C-NMR (125 MHz, DMSO-*d*₆) δ ppm 100.4 (C-8), 115.0 (C-6), 119.4 (C-22), 120.0 (C-4), 121.3 (C-5), 123.8 (C-20), 124.7 (C-15), 133.3 (C-16), 133.5 (C-3), 135.6 (C-9), 137.5 (C-21), 140.1 (C-7), 140.6 (C-12), 149.6 (C-19), 150.1 (C-17), 150.6 (C-14); MS (ES⁺) *m/z* 357.2 [M+H]⁺; HRMS calcd for C₁₆H₁₃N₄O₂S₂ 357.0474 [M+H]⁺ found 357.0479.

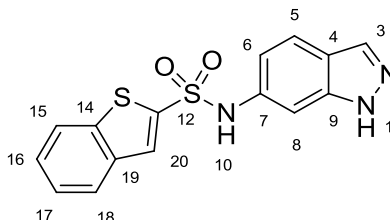
5-Chloro-*N*-(1*H*-indazol-6-yl)thiophene-2-sulfonamide (43)



Prepared according to general procedure A with following reagents and quantities: 6-amino-indazole (100 mg, 0.75 mmol), pyridine (1.5 mL), THF (2 mL) and 4-chlorothiophene-2-sulfonyl chloride (163 mg, 0.75 mmol) to give an orange solid (28.8 mg, 12%).

R_f 0.32 (EtOAc /Petrol, 1:1). m.p. 180°C. UV λ_{\max} (EtOH/nm) 271, 210.5. IR $\nu_{\max}/\text{cm}^{-1}$ 3401 (SO₂NH) 2723 (NNH), 1632, 1488, 1406, 1078, 992, 947. ¹H-NMR (500 MHz, DMSO-*d*₆) δ ppm 6.90 (1H, d, J = 8.2 Hz, H-6), 7.16 (1H, d, J = 4.9 Hz, H-15) 7.31 (1H, s, H-8), 7.39 (1H, d, J = 4.9 Hz, H-16), 7.66 (1H, d, J = 8.2 Hz, H-5), 7.98 (1H, s, H-3), 10.67 (1H, s-br, SOONH), 12.94 (1H, s-br, N-1). ¹³C-NMR (125 MHz, DMSO-*d*₆) δ ppm 100.8 (C-8), 115.2 (C-6), 120.2 (C-4), 121.4 (C-5), 127.96 (C-15), 132.3 (C-16), 133.5 (C-3), 135.1 (C-12), 135.2 (C-7), 138.0 (C-14), 140.0 (C-9). MS (ES⁺) m/z 314.2 [M+H]⁺; HRMS calcd for C₁₁H₉³⁵ClN₃O₂S 313.9819 [M+H]⁺ found 313.9820.

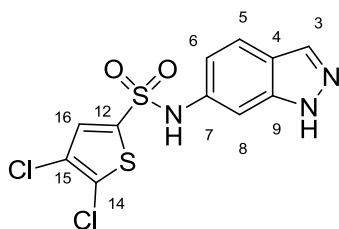
***N*-(1*H*-indazol-6-yl)benzo[*b*]thiophene-2-sulfonamide (44)**



Prepared according to general procedure A with following reagents and quantities: 6-amino-indazole (100 mg, 0.75 mmol), pyridine (1.5 mL), THF (2 mL) and benzo[*b*]thiophene-2-sulfonyl chloride (175 mg, 0.75 mmol) to give a white solid (94.5 mg, 38%).

R_f 0.37 (EtOAc /Petrol, 1:1). m.p. 193 °C. UV λ_{\max} (EtOH/nm) 270.5, 212.5. IR $\nu_{\max}/\text{cm}^{-1}$ 3403 (SO₂NH), 1634, 1501, 1325, 1241, 1142, 1070, 946, 746. ¹H-NMR (500 MHz, DMSO-*d*₆) δ ppm 6.97 (1H, d, J =8.6 Hz, H-6), 7.37 (1H, s, H-8), 7.44 (1H, dd, J = 7.0 Hz, H-17), 7.49 (1H, dd, J = 7.0 Hz, H-16), 7.65 (1H, d, J =8.6 Hz, H-5), 7.97 (1H, s, H-3), 7.97 (1H, s, H-20), 7.98 (1H, d, J =7.9 Hz H-18), 7.98 (1H, d, J =8.1 Hz H-15), 10.79 (1H, s-br, SOONH), 12.93 (1H, s-br, N-1). ¹³C-NMR (125 MHz, DMSO-*d*₆) δ ppm 100.6 (C-8), 115.1 (C-6), 120.1 (C-4), 121.3 (C-5), 123.0 (C-15), 125.5 (C-17), 125.8 (C-18), 127.4 (C-16), 129.5 (C-20), 133.4 (C-3), 135.4 (C-7), 137.1 (C-19), 140.0 (C-9), 140.3 (C-12), 140.8 (C-14); MS (ES⁺) m/z 330.2 [M+H]⁺; HRMS calcd for C₁₅H₁₂N₃O₂S₂ 330.0365 [M+H]⁺ found 330.0370.

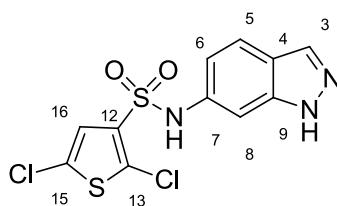
4,5-Dichloro-*N*-(1*H*-indazol-6-yl)thiophene-2-sulfonamide (45)



Prepared according to general procedure A with following reagents and quantities: 6-amino-indazole (100 mg, 0.75 mmol), pyridine (1.5 mL), THF (2 mL) and 4,5-dichlorothiophene-2-sulfonyl chloride (187 mg, 0.75 mmol) to give a off white solid (24 mg, 9%).

R_f 0.35 (EtOAc /Petrol, 1:1). m.p. 234 °C. UV λ_{\max} (EtOH/nm) 269, 212. IR $\nu_{\max}/\text{cm}^{-1}$ 3423 (SO₂NH) 3062 (NNH), 1633, 1320, 1162, 1022, 974, 853. ¹H-NMR (500 MHz, DMSO-*d*₆) δ ppm 6.94 (1H, d, J = 7.9 Hz, H-6), 7.34 (1H, s, H-8), 7.64 (1H, s, H-16), 7.71 (1H, d, J = 7.9 Hz, H-5), 8.02 (1H, s, H-3), 10.84 (1H, s-br, SOONH), 12.98 (1H, s-br, N-1). ¹³C-NMR (125 MHz, DMSO-*d*₆) δ ppm 101.4 (C-8), 115.3 (C-6), 120.4 (C-4), 121.6 (C-5), 123.9 (C-15), 130.1 (C-14), 131.0 (C-16), 133.5 (C-12), 134.7 (C-3), 137.1 (C-9), 140.0 (C-7); MS (ES⁺) m/z 348.1 [M+H]⁺; HRMS calcd for C₁₁H₈³⁵Cl₂N₃O₂S₂ 347.9435 [M+H]⁺ found 347.9435.

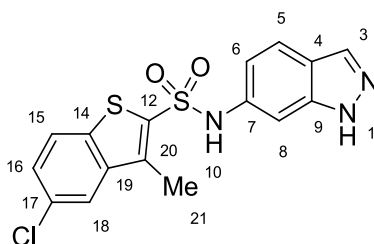
2,5-Dichloro-*N*-(1*H*-indazol-6-yl)thiophene-3-sulfonamide (46)



Prepared according to general procedure A with following reagents and quantities: 6-amino-indazole (100 mg, 0.75 mmol), pyridine (1.5 mL), THF (2 mL) and 2,5-dichlorothiophene-3-sulfonyl chloride (187 mg, 0.75 mmol) to give a light pink solid (96 mg, 37%).

R_f 0.34 (EtOAc /Petrol, 1:1); m.p. 197-198°C; UV λ_{\max} (EtOH/nm) 264.5; IR $\nu_{\max}/\text{cm}^{-1}$ 3408 (SO₂NH) 3104 (NNH), 3354, 1632, 1354, 1154, 1130, 1041, 851. ¹H-NMR (500 MHz, DMSO-*d*₆) δ ppm 6.92 (1H, d, J = 7.7 Hz, H-6), 7.27 (1H, s, H-8), 7.31 (1H, s, H-16), 7.67 (1H, d, J = 7.7 Hz, H-5), 7.98 (1H, s, H-3), 10.82 (1H, s-br, SOONH), 12.92 (1H, s-br, N-1); ¹³C-NMR (125 MHz, DMSO-*d*₆) δ ppm 100.4 (C-8), 114.8 (C-6), 120.1 (C-4), 121.4 (C-5), 126.5 (C-15), 126.7 (C-16), 129.7 (13CCl), 133.4 (C-3), 134.9 (12CH), 135.5 (C-7), 140.1 (C-9); MS (ES⁺) m/z 348.1 [M+H]⁺; HRMS calcd for C₁₁H₈³⁵Cl₂N₃O₂S₂ 348. [M+H]⁺ 347.9427 found 347.9427.

5-Chloro-*N*-(1*H*-indazol-6-yl)-3-methylbenzo[*b*]thiophene-2-sulfonamide (47)

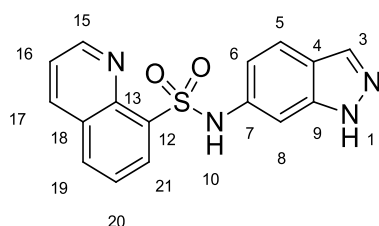


Prepared according to general procedure A with following reagents and quantities: 6-amino-indazole (100 mg, 0.75 mmol), pyridine (1.5 mL), THF (2 mL) and 5-chloro-3-methylbenzo[*b*]thiophene-2-sulfonyl chloride (211 mg, 0.75 mmol) to give a grey solid (122.4 mg, 43%).

R_f 0.37 (EtOAc /Petrol, 1:1); m.p. 232 °C; UV λ_{\max} (EtOH/nm) 285.0, 240.5, 209.5; IR $\nu_{\max}/\text{cm}^{-1}$ 3359 (SO₂NH), 1631, 1329, 1150, 1077, 944, 859; ¹H-NMR (500 MHz, DMSO-

d_6) δ ppm 2.51 (3H, s, H-21), 6.94 (1H, d, $J=8.1$ Hz, H-6), 7.34 (1H, s, H-8), 7.51 (1H, d, $J=7.8$ Hz, H-16), 7.63 (1H, d, $J=8.1$ Hz H-5), 7.97 (1H, s, H-3), 7.97 (1H, s, H-18), 8.02 (1H, d, $J=7.8$ Hz, H-15), 10.89 (1H, s-br, SOONH), 12.93 (1H, s-br, H-1); ^{13}C -NMR (125 MHz, DMSO- d_6) δ ppm 11.9 (C-21) 100.8 (C-8), 115.7 (C-6), 120.1 (C-4), 121.3 (C-5), 123.4 (C-18), 124.6 (C-15), 127.6 (C-16), 130.5 (C-17), 133.4 (C-3), 135.0 (C-7), 136.3 (C-20), 136.4 (C-12), 137.1 (C-14), 140.0 (C-9), 140.3 (C-19); MS (ES^+) m/z 378.2 $[\text{M}+\text{H}]^+$; HRMS calcd for $\text{C}_{16}\text{H}_{13}^{35}\text{ClN}_3\text{O}_2\text{S}_2$ 378.0132 $[\text{M}+\text{H}]^+$ found 378.0136.

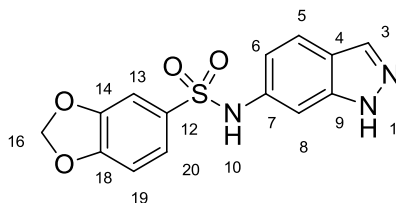
***N*-(1*H*-Indazol-6-yl)quinoline-8-sulfonamide (48)**



Prepared according to general procedure A with following reagents and quantities: 6-amino-indazole (100 mg, 0.75 mmol), pyridine (1.5 mL), THF (2 mL) and 8-quinolinesulfonyl chloride (171 mg, 0.75 mmol) to give a grey solid (110.7 mg, 45%).

R_f 0.34 (EtOAc /Petrol, 1:1) m.p. 237°C. UV λ_{max} (EtOH/nm) 274.5, 214. IR $\nu_{\text{max}}/\text{cm}^{-1}$ 1633, 1492, 1135, 939, 900, 785, 685. ^1H -NMR (500 MHz, DMSO- d_6) δ ppm 6.88 (1H, dd, $J = 8.6, 1.7$ Hz, H-6), 7.20 (1H, s, H-8) 7.47 (1H, d, $J = 8.6$ Hz, H-5), 7.70 (1H, dd, $J = 7.8, 7.8$ Hz, H-20), 7.73 (1H, dd, $J = 8.4, 4.2$, Hz, H-16) 7.84 (1H, s, H-3), 8.25 (1H, dd, $J = 7.8, 1.1$ Hz, H-19), 8.25 (1H, dd, $J = 7.8, 1.1$ Hz, H-21), 8.50 (1H, dd, $J = 8.4, 1.6$, Hz, H-17), 9.17 (1H, dd, $J = 4.2, 1.6$ Hz, H-15), 10.22 (1H, s-br, SOONH), 12.75 (1H, s-br, N-1). ^{13}C -NMR (125 MHz, DMSO- d_6) δ ppm 99.5 (C-8), 114.7 (C-6), 119.5 (C-4), 120.8 (C-5), 122.6 (C-16), 125.6 (C-20), 128.4 (18C), 132.1 (C-21), 133.2 (C-3), 134.3 (C-19). 135.1 (C-12), 136.0 (C-7), 137.0 (C-17), 139.9 (C-9), 142.7 (13C), 151.45 (C-15); MS (ES^+) m/z 325.3 $[\text{M}+\text{H}]^+$; HRMS calcd for $\text{C}_{11}\text{H}_8\text{ClN}_3\text{O}_2\text{S}_2$ $[\text{M}+\text{H}]^+$ 325.0753 found 325.0753.

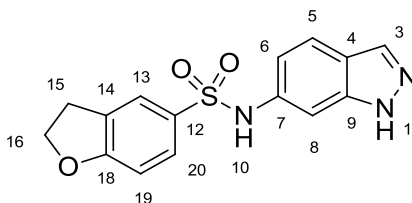
***N*-(1*H*-Indazol-6-yl)benzo[*d*][1,3]dioxole-5-sulfonamide (50)**



Prepared according to general procedure A with following reagents and quantities: 6-amino-indazole (100 mg, 0.75 mmol), pyridine (1.5 mL), THF (2 mL) and 1,3-benzodioxole-5-sulfonylchloride (166 mg, 0.75 mmol) to give a off white solid (106.2 mg, 45%).

R_f 0.37 (EtOAc /Petrol, 1:1). m.p. 196°C. UV λ_{\max} (EtOH/nm) 289.5, 207.5, 197.5. IR $\nu_{\max}/\text{cm}^{-1}$ 3358 (SO₂NH), 2899 (NNH), 1630, 1482, 1249, 1140, 1037, 914, 805, 702. ¹H-NMR (500 MHz, DMSO-*d*₆) δ ppm 6.11 (2H, s, H-16₂), 6.90 (1H, d, J = 7.7 Hz, H-6), 7.00 (1H, d, J = 6.7 Hz, H-19), 7.23 (1H, s, H-13), 7.26 (1H, s, H-8), 7.31 (1H, d, J = 6.7 Hz, H-20), 7.61 (1H, d, J = 7.7 Hz, H-5), 7.95 (1H, s, H-3), 10.23 (1H, s-br, SOONH), 12.87 (1H, s-br, N-1). ¹³C-NMR (125 MHz, DMSO-*d*₆) δ ppm 99.8 (C-8), 102.5 (C-16), 106.3 (C-13), 108.2 (C-19), 114.7 (C-6), 119.7 (C-4), 121.2 (C-5), 122.5 (C-20), 132.6 (C-12), 133.4 (C-3), 136.0 (C-7), 140.1 (C-9), 147.8 (C-14), 151.0 (18C); MS (ES⁺) m/z 318.3 [M+H]⁺; HRMS calcd for C₁₄H₁₂N₃O₄S 318.0543 [M+H]⁺ found 318.0548.

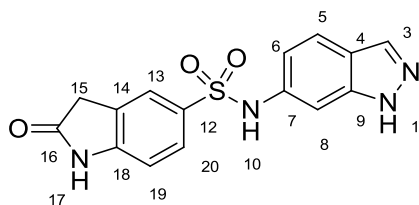
***N*-(1*H*-Indazol-6-yl)-2,3-dihydrobenzofuran-5-sulfonamide (51)**



Prepared according to general procedure A with following reagents and quantities: 6-amino-indazole (100 mg, 0.75 mmol), pyridine (1.5 mL), THF (2 mL) and 2,3-dihydrobenzo[*b*]furan-5-sulfonylchloride (164 mg, 0.75 mmol) to give an off white solid (121.8 mg, 51%).

R_f 0.35 (EtOAc /Petrol, 1:1). m.p. 194°C. UV λ_{\max} (EtOH/nm) 298, 287.5, 250, 200. IR $\nu_{\max}/\text{cm}^{-1}$ 3314 (SO₂NH), 1633, 1445, 1354, 1244, 1144, 1113, 1065, 921, 687. ¹H-NMR (500 MHz, DMSO-*d*₆) δ ppm 3.18 (2H, t, J =9.0 Hz, H-15), 4.58 (2H, t, J =9.0 Hz, H-16₂), 6.85 (1H, d, J =8.5 Hz, H-19), 6.89 (1H, d, J = 8.9 Hz, H-6), 7.26 (1H, s, H-8), 7.54 (1H, d, J = 8.5 Hz, H-20), 7.60 (1H, d, J = 9.0 Hz, H-5), 7.63 (1H, s, H-13), 7.94 (1H, s, H-3), 10.23 (1H, s-br, SOONH), 12.85 (1H, s-br, N-1). ¹³C-NMR (125 MHz, DMSO-*d*₆) δ ppm 28.3 (C-15), 72.2 (C-16), 99.4 (C-8), 109.0 (C-19), 114.6 (C-6), 119.6 (C-4), 121.2 (C-5), 124.0 (C-13), 128.1 (C-20), 128.1 (C-12), 131.0 (C-7), 133.4 (C-3), 136.3 (C-14), 140.1 (C-9), 163.2 (18C); MS (ES⁺) m/z 316.3 [M+H]⁺; HRMS calcd for C₁₅H₁₄N₃O₃S 316.0750 [M+H]⁺ found 316.0755.

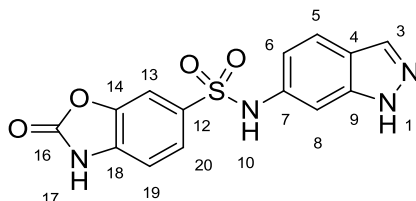
***N*-(1*H*-Indazol-6-yl)-2-oxoindoline-5-sulfonamide (52)**



Prepared according to general procedure A with following reagents and quantities: 6-amino-indazole (100 mg, 0.75 mmol), pyridine (1.5 mL), THF (2 mL) and 2-oxindole-5-sulfonylchloride (174 mg, 0.75 mmol) to give a pure product as a white solid (172.6 mg, 70%).

R_f 0.38 (EtOAc /Petrol, 1:1). m.p. 268°C; UV λ_{\max} (EtOH/nm) 265.5, 207; IR $\nu_{\max}/\text{cm}^{-1}$ 3377 (SO₂NH), 2891 (NNH), 1707 (C=O), 1611, 1617, 1480. ¹H-NMR (500MHz, DMSO-*d*₆) δ ppm 3.53 (2H, s, CH₂), 6.88 (1H, d, J = 8.2 Hz, H-6), 6.89 (1H, dd, J = 8.7 & 1.7 Hz H19), 7.25 (1H, s, H-8), 7.59 (1H, d, J = 8.6 Hz, H-5), 7.56 (1H, s, H-13), 7.62 (1H, d, J = 8.7 Hz, H-20), 7.93 (1H, s, H-3), 10.30 (1H, s-br, SO₂NH), 10.75 (1H, s-br, CONH) 12.84 (1H, br s, H-1). ¹³C-NMR (125MHz, DMSO-*d*₆) δ ppm 35.5 (C-15), 99.4 (C-8), 108.9 (C-19) 114.5 (C-6), 119.6 (C-4), 121.2 (C-5), 122.7 (C-13), 126.7 (C-14), 127.5 (C-20), 131.8 (C-12), 133.4 (C-3), 136.2 (C-7), 140.1 (C-9), 147.8 (C-18), 176.3 (C-16); MS (ES⁺) m/z 329.3 [M+H]⁺; HRMS calcd for C₁₅H₁₃N₄O₃S 329.0708 [M+H]⁺ found 329.0703.

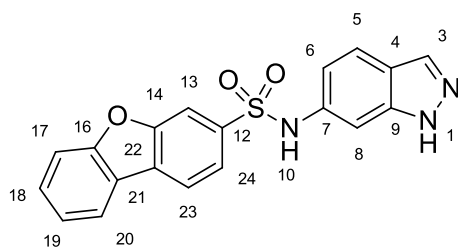
***N*-(1*H*-Indazol-6-yl)-2-oxo-2,3-dihydrobenzo[*d*]oxazole-6-sulfonamide (53)**



Prepared according to general procedure A with following reagents and quantities: 6-amino-indazole (100 mg, 0.75 mmol), pyridine (1.5 mL), THF (2 mL) and 2-oxo-2,3-dihydro-1,3-benzoxazole-6-sulfonyl chloride (176 mg, 0.75 mmol) to give a white solid (84.4 mg, 34%).

R_f 0.41 (EtOAc /Petrol, 1:1). m.p. 308°C. UV λ_{\max} (EtOH/nm) 280.5, 248 IR $\nu_{\max}/\text{cm}^{-1}$ 3372 (SO₂NH), 2898 (NNH), 1765 (C=O), 1488, 1347, 1151, 942, 700. ¹H-NMR (500 MHz, DMSO-*d*₆) δ ppm 6.89 (1H, dd, J = 8.6, 1.8 Hz, H-6), 7.18 (1H, d, J = 8.2 Hz H-19), 7.26 (1H, s, H-8) 7.56 (1H, dd, J = 8.2, 1.8 Hz H-20), 7.60 (1H, d, J = 8.6 Hz, H-5), 7.63 (1H, d, J = 1.8 Hz, H-13), 7.94 (1H, s, H-3), 10.38 (1H, s-br, SOONH), 12.11 (1H, s-br, NHCOO) 12.86 (1H, s-br, N-1). ¹³C-NMR (125 MHz, DMSO-*d*₆) δ ppm 99.9 (C-8), 107.8 (C-13), 109.8 (C-19), 114.8 (C-6), 119.8 (C-4), 121.3 (C-5), 123.4 (C-20), 132.7 (C-12), 133.4 (C-3), 134.5 (18C). 135.9 (C-7), 140.1 (C-9), 142.8 (C-14), 154.0 (C-16); MS (ES⁺) m/z 331.2 [M+H]⁺; HRMS calcd for C₁₄H₁₁N₄O₄S 331.0500 [M+H]⁺ found 331.0496.

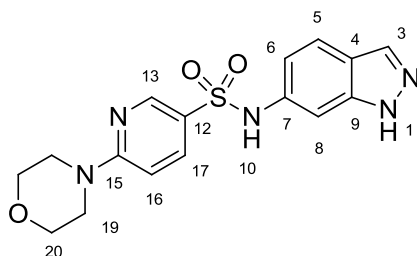
***N*-(1*H*-indazol-6-yl)dibenzo[*b,d*]furan-3-sulfonamide (54)**



Prepared according to general procedure A with following reagents and quantities: 6-amino-indazole (100 mg, 0.75 mmol), pyridine (1.5 mL), THF (2 mL) and dibenzo[*b,d*]furan-3-sulfonyl chloride (200 mg, 0.75 mmol) to give a white solid (40.7 mg, 15%).

R_f 0.42 (EtOAc /Petrol, 1:1). m.p. 310 °C; UV λ_{\max} (EtOH/nm) 287.5, 209.0; IR $\nu_{\max}/\text{cm}^{-1}$ 3314 (SO₂NH), 1632, 1500; ¹H-NMR (500 MHz, DMSO-*d*₆) δ ppm 6.93 (1H, d, J =8.6 Hz, H-6), 7.28 (1H, s, H-8), 7.46 (1H, t, J = 7.5 Hz, H-18), 7.60 (1H, d, J = 8.60 Hz, H-5), 7.60 (1H, m, H-19), 7.75 (1H, d, J = 78.2 Hz, H-20), 7.90 (1H, m, H-23), 7.90 (1H, m, H-24H), 7.90 (1H, s, H-3), 8.27 (1H, d, J = 7.5 Hz, H-17), 8.65 (1H, s, H-13) 10.46 (1H, s-br, SOONH), 12.83 (1H, s-br, N-1). ¹³C-NMR (125 MHz, DMSO-*d*₆) δ ppm 100.3 (C-8), 112.0 (C-20), 112.6 (C-23), 115.0 (C-6), 119.8 (C-4), 120.8 (C-13), 121.3 (C-5), 121.9 (C-17), 122.4 (21C), 123.9 (C-18), 123.9 (22C), 126.0 (C-24), 128.9 (C-19), 133.4 (C-3), 134.5 (C-12), 136.0 (C-7), 140.0 (C-9), 156.2 (C-16), 157.2 (C-14); MS (ES⁺) m/z 364.2 [M+H]⁺; HRMS calcd for C₁₉H₁₄N₃O₃S 364.0750 [M+H]⁺ found 364.0754.

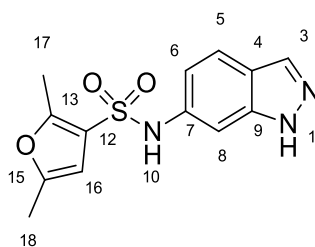
***N*-(1*H*-Indazol-6-yl)-6-morpholinopyridine-3-sulfonamide (67)**



Prepared according to general procedure A with following reagents and quantities: 6-amino-indazole (100 mg, 0.75 mmol), pyridine (1.5 mL), THF (2 mL) and 6-(morpholin-4-yl)pyridine-3-sulfonyl chloride (198 mg, 0.75 mmol) to give a grey solid (165.6 mg, 61%).

R_f 0.39 (EtOAc /Petrol, 1:1); m.p. 218-219°C. UV λ_{\max} (EtOH/nm) 274.5, 210.5 IR $\nu_{\max}/\text{cm}^{-1}$ 3237 (SO₂NH) 2856 (NNH), 1633, 1586, 1491, 1141, 1103, 941. ¹H-NMR (500 MHz, DMSO-*d*₆) δ ppm 3.53 (4H, t, J = 4.8 Hz, H-19), 3.62 (4H, t, J = 4.8 Hz, H-20), 6.85 (1H, d, J = 9.2 Hz, H-16), 6.91 (1H, dd, J = 8.7, 1.8 Hz, H-6), 7.29 (1H, s, H-8) 7.61 (1H, d, J = 8.7 Hz, H-5), 7.70 (1H, dd, J = 9.2, 2.5 Hz, H-17), 7.94 (1H, s, H-3), 8.39 (1H, d, J = 2.5 Hz, H-13), 10.27 (1H, s-br, SOONH), 12.87 (1H, s-br, N-1). ¹³C-NMR (125 MHz, DMSO-*d*₆) δ ppm 44.3 (C-19), 65.7 (C-20), 99.4 (C-8), 106.0 (C-16), 114.6 (C-6), 119.7 (C-4), 121.3 (C-5), 122.9 (C-12), 133.4 (C-3), 135.7 (C-17), 136.2 (C-7), 140.2 (C-9), 147.3 (C-13), 159.8 (C-15); MS (ES⁺) m/z 360.3 [M+H]⁺; HRMS calcd for C₁₆H₁₈N₅O₃S 360.1125 [M+H]⁺ found 360.1116.

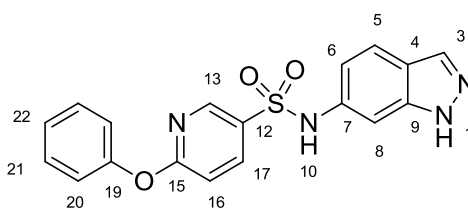
***N*-(1*H*-Indazol-6-yl)-2,5-dimethylfuran-3-sulfonamide (372)**



Prepared according to general procedure A with following reagents and quantities: 6-amino-indazole (100 mg, 0.75 mmol), pyridine (1.5 mL), THF (2 mL) and 2,5-dimethylfuran-3-sulfonyl chloride (146 mg, 0.75 mmol) to give a white solid (83 mg, 38%).

R_f 0.36 (EtOAc /Petrol, 1:1). m.p. 163 °C; UV λ_{\max} (EtOH/nm) 298.0, 286.0, 214.5; IR $\nu_{\max}/\text{cm}^{-1}$ 3330 (SO₂NH), 1633, 1500; ¹H-NMR (500 MHz, DMSO-*d*₆) δ ppm 2.16 (3H, s, H-18), 2.33 (3H, s, H-17), 6.18 (1H, s, H-16), 6.91 (1H, d, J =8.6 Hz, H-6), 7.27 (1H, s, H-8), 7.64 (1H, d, J =8.6 Hz, H-5), 7.97 (1H, s, H-3), 10.29 (1H, s-br, SOONH), 12.90 (1H, s-br, N-1); ¹³C-NMR (125 MHz, DMSO-*d*₆) δ ppm 12.3 (C-17), 12.8 (C-18), 99.6 (C-8), 105.1 (C-16), 114.7 (C-6), 119.7 (C-4), 120.7 (C-12), 121.2 (C-5), 133.4 (C-3), 136.1 (C-7), 140.1 (C-9), 150.7 (C-15), 153.8 (13C); MS (ES⁺) m/z 292.2 [M+H]⁺; HRMS calcd for C₁₃H₁₄N₃O₃S 292.0750 [M+H]⁺ found 292.0755.

***N*-(1*H*-Indazol-6-yl)-6-phenoxy pyridine-3-sulfonamide (373)**

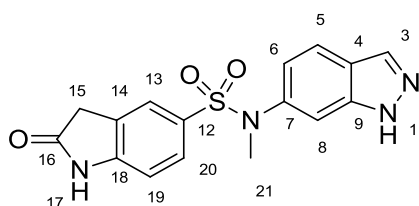


Prepared according to general procedure A with following reagents and quantities: 6-amino-indazole (100 mg, 0.75 mmol), pyridine (1.5 mL), THF (2 mL) and 6-phenoxy pyridine-3-sulfonyl chloride (203 mg, 0.75 mmol) to give a white solid (114.3 mg, 42%).

R_f 0.24 (EtOAc /Petrol, 1:1); m.p. 178°C; UV λ_{\max} (EtOH/nm) 210.5, 198; IR $\nu_{\max}/\text{cm}^{-1}$ 3082 (SO₂NH), 1635, 1581, 1463; ¹H-NMR (500 MHz, DMSO-*d*₆) δ ppm 6.91 (1H, dd, J =

8.6, 1.8 Hz, H-6), 7.15 (2H, d, $J = 7.8$ Hz H-20), 7.15 (1H, d, $J = 7.8$ Hz H-16) 7.26 (1H, t, $J = 7.5$ Hz H-22) 7.29 (1H, s, H-8) 7.42 (2H, t, $J = 7.8$ Hz, H-21), 7.64 (1H, d, $J = 8.6$ Hz, H-5), 7.97 (1H, s, H-3), 8.12 (1H, dd, $J = 8.8, 2.5$ Hz, H-17), 8.47 (1H, d, $J = 2.5$ Hz, H-13), 10.54 (1H, s-br, SOONH), 12.90 (1H, s-br, N-1); ^{13}C -NMR (125 MHz, DMSO- d_6) δ ppm 100.3 (C-8), 111.9 (C-16) 114.9 (C-6), 120 (C-4), 121.5 (C-5), 121.6 (C-20), 125.5 (C-22), 129.8 (C-21), 130.5 (C-12), 133.4 (C-3), 135.4 (C-7). 138.6 (C-17), 140.1 (C-9), 146.6 (C-13), 152.6 (C-19), 165.4 (C-15); MS (ES^+) m/z 367.2 $[\text{M}+\text{H}]^+$; HRMS calcd for $\text{C}_{18}\text{H}_{15}\text{N}_4\text{O}_3\text{S}$ 367.0863 $[\text{M}+\text{H}]^+$ found 367.0859.

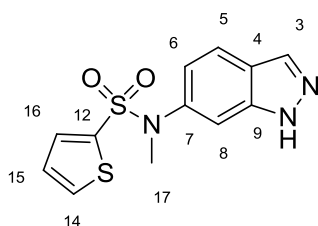
***N*-(1*H*-Indazol-6-yl)-*N*-methyl-2-oxoindoline-5-sulfonamide (83)**



Prepared according to general procedure A with following reagents and quantities: *N*-methyl-1*H*-indazol-6-amine (32 mg, 0.22 mmol), pyridine (1.5 mL), THF (2 mL) and 2-oxindole-5-sulfonylchloride (50 mg, 0.22 mmol) to give a light pink solid (32 mg, 43%).

R_f 0.34 (EtOAc /Petrol, 1:1); m.p. 229-231 $^{\circ}\text{C}$; UV λ_{max} (EtOH/nm) 262.0, 207.5; IR $\nu_{\text{max}}/\text{cm}^{-1}$ 3398 (SO_2N), 2873, 1699 (C=O), 1618, 1478, 1326, 1240, 1152; ^1H -NMR (500 MHz, DMSO- d_6) δ ppm 3.53 (2H, s, H-15), 6.88 (1H, d, $J = 8.4$ Hz, H-6), 6.89 (1H, dd, $J = 8.7, 1.7$ Hz H-19), 7.25 (1H, s, H-8), 7.59 (1H, d, $J = 8.4$ Hz, H-5), 7.56 (1H, s, H-13), 7.62 (1H, d, $J = 8.7$ Hz, H-20), 7.93 (1H, s, H-3), 10.30 (1H, s-br, SOONH), 10.75 (1H, s-br, H-17) 12.84 (1H, br, H-1); ^{13}C -NMR (125 MHz, DMSO- d_6) δ ppm 35.5 (C-15), 99.4 (C-8), 108.9 (C-19) 114.5 (C-6), 119.6 (C-4), 121.2 (C-5), 122.7 (C-13), 126.7 (C-14), 127.5 (C-20), 131.8 (C-12), 133.4 (C-3), 136.2 (C-7), 140.1 (C-9), 147.8 (C-18), 176.3 (C-16); MS (ES^+) m/z 329.3 $[\text{M}+\text{H}]^+$; HRMS calcd for $\text{C}_{16}\text{H}_{15}\text{N}_4\text{O}_3\text{S}$ 343.0859 $[\text{M}+\text{H}]^+$ found 343.0858.

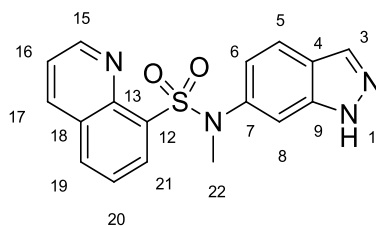
***N*-(1*H*-Indazol-6-yl)-*N*-methylthiophene-2-sulfonamide (84)**



Prepared according to general procedure A with following reagents and quantities: *N*-methyl-1*H*-indazol-6-amine (41 mg, 0.27 mmol), pyridine (1.5 mL), THF (2 mL) and 2-thiophenesulfonyl chloride (50 mg, 0.27 mmol) to give a white solid (30 mg, 38%).

R_f 0.37 (EtOAc /Petrol, 1:1); m.p. 172-173 °C; UV λ_{\max} (EtOH/nm) 255.5, 210.0; IR $\nu_{\max}/\text{cm}^{-1}$ 3360 (SO₂N) 3106, 1627, 1343, 1162; ¹H-NMR (500 MHz, DMSO-*d*₆) δ ppm 6.87 (1H, d, J = 8.6 Hz, H-6), 7.24 (1H, dd, J = 3.7, 4.9Hz, H-15), 7.26 (1H, s, H-8), 7.49 (1H, d, J = 3.7Hz, H-16), 7.73 (1H, d, J = 8.6 Hz, H-5), 8.01 (1H, d, J = 4.9Hz, H-14), 8.08 (1H, s, H-3), 13.13 (1H, s-br, H-1) ; ¹³C-NMR (125 MHz, DMSO-*d*₆) δ ppm 38.4 (C-17), 108.0 (C-8), 119.2 (C-6), 120.8 (C-5), 121.8 (C-4), 128.0 (C-15), 133.2 (C-16), 133.5 (C-3), 134.0 (C-14), 138.9 (C-7), 139.5 (C-9), 153.2 (C-12); MS (ES⁺) m/z 294.2 [M+H]⁺; HRMS calcd for C₁₂H₁₂N₃O₂S₂ 294.0365 [M+H]⁺ found 294.0364.

***N*-(1*H*-Indazol-6-yl)-*N*-methylquinoline-8-sulfonamide (85)**

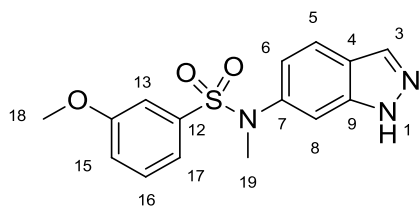


Prepared according to general procedure B with following reagents and quantities: methyl iodide (13 μ L, 0.22 mmol), K₂CO₃ (20 mg, 0.15 mmol) and *N*-(1*H*-indazol-6-yl)-quinoline-8-sulfonamide (47 mg, 0.15 mmol) in DMF (4 mL) this gave the title compound as a grey solid (13.6 mg, 28%).

R_f 0.35 (EtOAc /Petrol, 1:1); m.p. 158°C; UV λ_{\max} (EtOH/nm) 288.0, 213.0; IR $\nu_{\max}/\text{cm}^{-1}$ 3318 (SO₂NH), 1626, 1474; ¹H-NMR (500 MHz, DMSO-*d*₆) δ ppm 3.69 (3H, s, H-22), 6.78 (1H, dd, J = 8.6, 1.7 Hz, H-6), 7.22 (1H, s, H-8) 7.53 (1H, d, J = 8.6 Hz, H-5), 7.63 (1H, dd,

$J = 7.8, 7.8$ Hz, H-20), 7.75 (1H, dd, $J = 8.4, 4.2$, Hz, H-16), 7.95 (1H, s, H-3), 8.21 (1H, dd, $J = 7.8, 1.1$ Hz, H-19), 8.26 (1H, dd, $J = 7.8, 1.1$ Hz, H-21), 8.55 (1H, dd, $J = 8.4, 1.6$, Hz, H-17), 9.15 (1H, dd, $J = 4.2, 1.6$ Hz, H-15), 12.92 (1H, s-br, N-1); ^{13}C -NMR (125 MHz, DMSO- d_6) δ ppm 40.2 (C-22), 107.2 (C-8), 118.7 (C-6), 120.7 (C-5), 121.1 (C-4), 122.6 (C-16), 125.6 (C-20), 128.6 (18C), 132.9 (C-19), 133.3 (C-3), 134.2 (C-21), 136.6 (C-12), 136.9 (C-17), 139.2 (C-7), 139.6 (C-9), 143.3 (13C), 151.5 (C-15); MS (ES^+) m/z 339.2 $[\text{M}+\text{H}]^+$; HRMS calcd for $\text{C}_{17}\text{H}_{15}\text{N}_4\text{O}_2\text{S}$ 339.0910 $[\text{M}+\text{H}]^+$ found 339.0916.

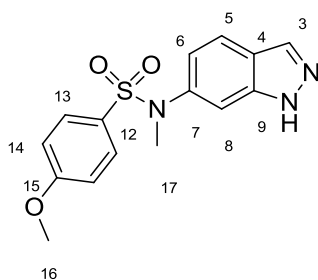
***N*-(1*H*-Indazol-6-yl)-3-methoxy-*N*-methylbenzenesulfonamide (86)**



Prepared according to general procedure B with following reagents and quantities: Methyl iodide (12 μL , 0.20 mmol), K_2CO_3 (18 mg, 0.13 mmol) and *N*-(1*H*-indazol-6-yl)-3-methoxybenzenesulfonamide (40 mg, 0.13 mmol) in DMF (3 mL) this gave the title compound as a grey solid (17 mg, 41%).

R_f 0.38 (EtOAc /Petrol, 1:1); m.p. 84-86 $^\circ\text{C}$; UV λ_{max} (EtOH/nm) 289.5; IR $\nu_{\text{max}}/\text{cm}^{-1}$: 3356 (SO_2NH), 1627, 1479; ^1H -NMR (500 MHz, DMSO- d_6) δ ppm 3.21 (3H, s, H-19), 3.70 (3H, s, H-18), 6.85 (1H, dd, $J = 8.6, 1.7$ Hz, H-6), 6.93 (1H, s, H-13), 7.10 (1H, d, $J = 7.7$ Hz, H-15), 7.23 (1H, s, H-8), 7.28 (1H, dd, $J = 8.2, 2.3$ Hz, H-17), 7.53 (1H, dd, $J = 8.0$ Hz, H-16), 7.72 (1H, d, $J = 8.6$ Hz, H-5), 8.08 (1H, s, H-3), 13.10 (1H, s-br, N-1); ^{13}C -NMR (125 MHz, DMSO- d_6) δ ppm 38.42 (C-19) 55.46 (C-18), 107.9 (C-8), 112.1 (C-13), 119.2 (C-6), 119.3 (C-17), 119.6 (C-15), 120.7 (C-5), 121.7 (C-4), 130.4 (C-16), 133.5 (C-3), 137.1 (C-12), 139.1 (C-7), 139.5 (C-9), 159.2 (C-14); MS (ES^+) m/z 318.2 $[\text{M}+\text{H}]^+$; HRMS calcd for $\text{C}_{15}\text{H}_{16}\text{N}_3\text{O}_3\text{S}$ 318.0907 $[\text{M}+\text{H}]^+$ found 318.0911.

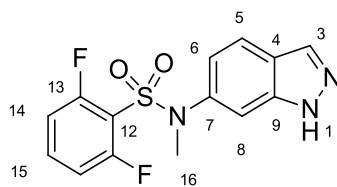
***N*-(1*H*-indazol-6-yl)-4-methoxy-*N*-methylbenzenesulfonamide (87)**



Prepared according to general procedure A with following reagents and quantities: *N*-methyl-1*H*-indazol-6-amine (36 mg, 0.24 mmol), pyridine (1.5 mL), THF (2 mL) and 2-thiophenesulfonyl chloride (50 mg, 0.24 mmol) to give a white solid (31 mg, 42%).

R_f 0.36 (EtOAc /Petrol, 1:1); m.p. 162-164 °C; UV λ_{\max} (EtOH/nm) 244.0; IR $\nu_{\max}/\text{cm}^{-1}$ 3350 (SO₂N), 3042, 1626, 1593, 1500, 1307; ¹H-NMR (500 MHz, DMSO-*d*₆) δ ppm 3.18 (3H, s, H-17), 3.83 (3H, s, H-16), 6.91 (1H, d, J = 8.6 Hz, H-6), 7.15 (2H, d, J = 8.2 Hz, H-14), 7.22 (1H, s, H-8), 7.15 (2H, d, J = 8.2 Hz, H-13), 7.70 (1H, d, J = 8.6 Hz, H-5), 7.89 (1H, s, H-3), 12.80 (1H, br, H-1); ¹³C-NMR (125 MHz, DMSO-*d*₆) δ ppm 38.3 (C-17) 56.1 (C-16), 99.1 (C-8), 112.8 (C-14), 114.4 (C-6), 119.5 (C-4), 120.9 (C-5), 126.2 (C-12), 133.3 (C-3), 135.0 (C-13), 136.2 (C-7), 140.1 (C-9) 162.7 (C-15); MS (ES⁺) m/z 317.3 [M+H]⁺; HRMS calcd for C₁₅H₁₆N₃O₃S 318.0907 [M+H]⁺ found 318.0906.

2,6-Difluoro-*N*-(1*H*-indazol-6-yl)-*N*-methylbenzenesulfonamide (88)

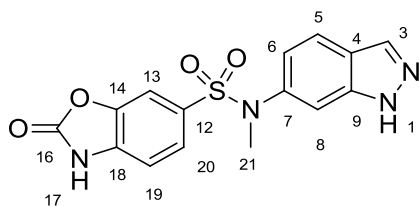


Prepared according to general procedure B with following reagents and quantities: Methyl iodide (12 μ L, 0.22 mmol), K₂CO₃ (18 mg, 0.13 mmol) and 2,6-difluoro-*N*-(1*H*-indazol-6-yl)-benzenesulfonamide (40 mg, 0.13 mmol) in DMF (4 mL) this gave the title compound as a grey solid (10.2 mg, 24%).

R_f 0.36 (EtOAc /Petrol, 1:1); m.p. 170 °C; UV λ_{\max} (EtOH/nm) 271.0, 211.0; IR $\nu_{\max}/\text{cm}^{-1}$: 3328 (SO₂NH), 1611, 1464; ¹H-NMR (500 MHz, DMSO-*d*₆) δ ppm 3.38 (3H, s, H-16₃),

6.96 (1H, dd, $J = 8.6, 1.7$ Hz, H-6), 7.29 (2H, t, $J = 8.8$ Hz, 2xH-14), 7.38 (1H, s, H-8), 7.75 (1H, d, $J = 8.6$ Hz, H-5), 7.76 (1H, dddd, $J = 6.1, 6.1, 8.5, 8.5$, H-15), 8.08 (1H, s, H-3), 13.14 (1H, br, H-1); ^{13}C -NMR (125 MHz, DMSO- d_6) δ ppm 38.5 (C-16), 108.0 (C-8), 113.5 (d, $J_{\text{FC}} = 27$ Hz, C-14), 114.7 (C-12), 118.8 (C-6), 121.1 (C-15), 121.8 (C-4), 133.5 (C-3), 136 (t, $J_{\text{FC}} = 11.1$ Hz, C-15), 138.1 (C-7), 139.6 (C-9), 158.87 (d, $J_{\text{FC}} = 257$ Hz, C-13), 158.91 (d, $J_{\text{FC}} = 257$ Hz, C-13); ^{19}F NMR (470 MHz, DMSO- d_6) δ -105.9; MS (ES^+) m/z 324.2 $[\text{M}+\text{H}]^+$; HRMS calcd for $\text{C}_{14}\text{H}_{12}\text{F}_2\text{N}_3\text{O}_2\text{S}$ 324.0613 $[\text{M}+\text{H}]^+$ found 324.0611.

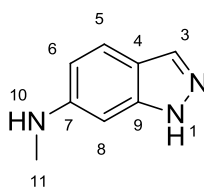
***N*-(1*H*-Indazol-6-yl)-*N*-methyl-2-oxo-2,3-dihydrobenzo[d]oxazole-6-sulfonamide (89)**



Prepared according to general procedure A with following reagents and quantities: *N*-methyl-1*H*-indazol-6-amine (50 mg, 0.34 mmol), pyridine (1.5 mL), THF (2 mL) and 2-thiophenesulfonyl chloride (80 mg, 0.34 mmol) to give a white solid (50 mg, 43%).

R_f 0.41 (EtOAc /Petrol, 1:1); m.p. 271-273 °C; UV λ_{max} (EtOH/nm) 287.5, 251.5; IR $\nu_{\text{max}}/\text{cm}^{-1}$ 3237 (SO_2N), 1762 (C=O), 1620, 1482, 1346; ^1H -NMR (500 MHz, DMSO- d_6) δ ppm 3.21 (3H, s, H-21₃), 6.83 (1H, dd, $J = 8.5$ Hz, H-6), 7.22 (1H, d, $J = 8.3$ Hz, H-19), 7.23 (1H, s, H-8) 7.27 (1H, dd, $J = 8.3, 1.7$ Hz H-20), 7.46 (1H, d, $J = 1.7$ Hz, H-13), 7.70 (1H, d, $J = 8.5$ Hz, H-5), 8.08 (1H, s, H-3), 12.21 (1H, br, H-17) 13.08 (1H, br, H-1); ^{13}C -NMR (125 MHz, DMSO- d_6) δ ppm 39.1(C-21), 108.1(C-8), 108.7 (C-13), 109.7 (C-19), 119.4 (C-6), 120.7 (C-5), 121.7(C-4), 124.4 (C-20), 129.2 (C-12), 133.5 (C-3), 134.8 (C-18), 139.1 (C-7), 139.6 (C-9), 142.9 (C-14), 154.1 (C-16); MS (ES^+) m/z 345.2 $[\text{M}+\text{H}]^+$; HRMS calcd for $\text{C}_{15}\text{H}_{13}\text{N}_4\text{O}_4\text{S}$ 345.0652 $[\text{M}+\text{H}]^+$ found 345.0650.

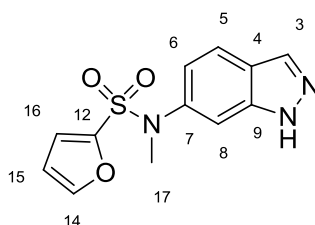
***N*-Methyl-1*H*-indazol-6-amine (90)**



6-Aminoindazole (1.0 g, 7.5 mmol) was taken in freshly prepared sodium methoxide solution (900 mg of sodium in 20 mL MeOH) followed by paraformaldehyde (340mg, 10.5 mmol) and stirred at room temperature for 5 hours. After this time sodium borohydride (280 mg, 7.5 mmol) was added and the mixture refluxed at 80 °C for 2 hours. The solution was hydrolysed in sodium hydroxide (1 M, 10 mL) and extracted with ethyl acetate (3 x 10 mL). Combined organic fractions were washed with brine (10 mL) and dried over Na₂SO₄. The compound was purified MPLC (0-60% EtOAc in petroleum spirit over 20 column volumes). The pure product was isolated as a light brown solid (423 mg, 38%).

*R*_f 0.25 (EtOAc /Petrol, 1:1); m.p. 137-138°C; UV λ_{max} (EtOH/nm) 306.4, 267.0, 236.4, 218.8, 217.0; IR ν_{max}/cm⁻¹ 3409, 3188, 1613, 1357, 948, 802; ¹H-NMR (500 MHz, DMSO-*d*₆) δ ppm; 2.71 (3H, d, *J* = 4.7 Hz, H-11), 5.87 (1H, d, *J* = 4.7 Hz, H-10), 6.29 (1H, s, H-8), 6.49 (1H, d, *J* = 8.7 Hz H-6), 7.38 (1H, d, *J* = 8.7 Hz, H-5), 7.74 (1H, s, H-3), 12.35 (1H, br, H-1); ¹³C-NMR (125 MHz, DMSO-*d*₆) δ ppm; 29.8 (C-11), 86.3 (C-8), 111.9 (C-6), 115.0 (C-4), 120.3 (C-5), 133.1 (C-3), 142.2 (C-9), 149.0 (C-7); MS (ES⁺) *m/z* 148.2 [M+H]⁺; HRMS calcd for C₈H₁₀N₃ 148.0869 [M+H]⁺ found 148.0866.

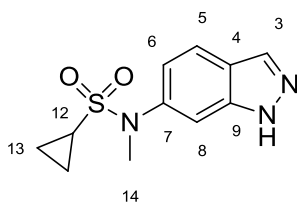
***N*-(1*H*-Indazol-6-yl)-*N*-methylfuran-2-sulfonamide (91)**



Prepared according to general procedure **A** with the following reagents and quantities: *N*-methyl-1*H*-indazol-6-amine (34 mg, 0.24 mmol), pyridine (1.5 mL) and 2-furansulfonyl chloride (48 μL, 0.29 mmol) to give a light brown solid (41 mg, 62%).

R_f 0.37 (Et₂O); m.p. 152-154 °C; UV λ_{\max} (EtOH/nm) 288.8, 216.0; IR $\nu_{\max}/\text{cm}^{-1}$ 3337, 3126, 1356, 1151; ¹H-NMR (500 MHz, CDCl₃) δ ppm 3.39 (1H, s, H-17), 6.49 (1H, s, H-16), 6.90-6.91 (2H, m, H-6, H-15), 7.44 (1H, s, H-8), 7.59 (1H, s, H-14), 7.67 (1H, d, J = 8.2 Hz, H-5), 8.04 (1H, s, H-3); ¹³C-NMR (125 MHz, CDCl₃) δ ppm 39.2 (C-17), 109.3 (C-8), 111.3 (C-16), 113.0 (C-4), 117.6 (C-15), 119.8 (C-6), 121.5 (C-5), 134.7 (C-3), 139.7 (C-7), 146.4 (C-14), 147.2 (C-12); MS (ES⁺) m/z 278.2 [M+H]⁺; HRMS calcd for C₁₂H₁₂N₃O₃S 278.0594 [M+H]⁺ found 278.0594

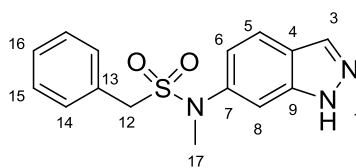
***N*-(1*H*-indazol-6-yl)-*N*-methylcyclopropanesulfonamide (92)**



Prepared according to general procedure B with following reagents and quantities: methyl iodide (9.6 μ L, 0.22 mmol), K₂CO₃ (38 mg, 0.27 mmol) and *N*-(1*H*-indazol-6-yl)cyclopropanesulfonamide (43 mg, 0.18 mmol) in DMF (8 mL) this gave the title compound as a clear yellow oil (26 mg, 57%).

R_f 0.37 (Et₂O); UV λ_{\max} (EtOH/nm) 287.8, 265.8, 210.0; IR $\nu_{\max}/\text{cm}^{-1}$ 3333, 3183, 1330, 1137; ¹H-NMR (500 MHz, CDCl₃) δ ppm 0.92-0.96 (2H, m, H-13), 1.08-1.12 (2H, m, H-13), 2.41-2.45 (1H, m, H-12), 3.41 (1H, s, H-17), 6.85 (1H, dd, J = 8.7, 1.7 Hz, H-6), 7.60 (1H, s, H-8), 7.73 (1H, d, J = 8.7 Hz, H-5), 8.07 (1H, s, H-3); ¹³C-NMR (125 MHz, CDCl₃) δ ppm 4.8 (C-13), 27.0 (C-12), 39.0 (C-14), 109.0 (C-8), 119.8 (C-6), 121.4 (C-5), 122.2 (C-4), 134.7 (C-3), 140.2 (C-7), 140.5 (C-9); MS (ES⁺) m/z 252.3 [M+H]⁺; HRMS calcd for C₁₁H₁₄N₃O₂S 252.0801 [M+H]⁺ found 252.0801.

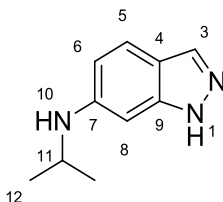
***N*-(1*H*-indazol-6-yl)-*N*-methyl-1-phenylmethanesulfonamide (93)**



Prepared according to general procedure **A** using *N*-methyl-1*H*-indazol-6-amine (60 mg, 0.41 mmol) and phenylmethanesulfonyl chloride (93 mg, 0.49 mmol) in pyridine (2.5 mL). The product was isolated as a white solid (97 mg, 79%).

R_f 0.44 (Et₂O); m.p. 134-136 °C; UV λ_{\max} (EtOH/nm) 310.2, 244.2, 215.6; IR $\nu_{\max}/\text{cm}^{-1}$ 3345, 3109, 3037, 2921, 2863, 2811, 1614; ¹H-NMR (500 MHz, CDCl₃) δ ppm; 2.76 (3H, s, H-17), 4.57 (2H, s, H-12), 6.51 (1H, dd, J = 8.7, 2.0 Hz, H-6), 6.06 (1H, d, J = 2.0 Hz, H-8), 7.03 (2H, d, J = 7.4 Hz, H-14), 7.11 (2H, dd, J = 7.4, Hz, 7.5 H-15), 7.21 (1H, t, J = 7.5 Hz, H-16), 7.36 (1H, d, J = 8.7 Hz, H-5), 8.04 (1H, s, H-3); ¹³C-NMR (125 MHz, CDCl₃) δ ppm; 30.4 (C-17), 59.6 (C-12), 91.6 (C-8), 113.6 (C-6), 118.6 (C-4), 121.3 (C-5), 126.8 (C-13), 128.5 (C-15), 129.1 (C-16), 130.8 (C-14), 141.2 (C-3), 144.2 (C-9), 150.8 (C-7); MS (ES⁺) m/z 302.2 [M+H]⁺.

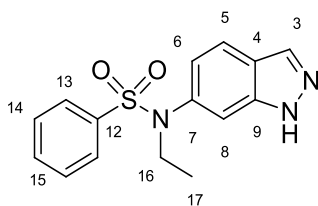
***N*-Isopropyl-1*H*-indazol-6-amine (95)**



6-Aminoindazole (100 mg, 0.75 mmol) was dissolved in acetonitrile (3 mL) and potassium iodide (12 mg, 0.08 mmol) added whilst under N₂. 2-Bromopropane (24 μ L, 0.25 mmol) was added and the reaction was subjected to microwave radiation to a temperature of 150 °C for 10 minutes and then a further 10 minutes to 170 °C. The resulting mixture was diluted with water (10 mL) and extracted with EtOAc (3 x 10 mL), combined organic fractions were washed with brine (10 mL) and dried over Na₂SO₄. The resulting solution was reduced to a residue under vacuum and purified by MPLC (0-60% EtOAc in petroleum ether). The pure product was isolated as a brown solid (17 mg, 39%).

R_f 0.61 (Et₂O); m.p. 83-84 °C; UV λ_{\max} (EtOH/nm) 309.2, 268.2, 236.8, 220.4; IR $\nu_{\max}/\text{cm}^{-1}$ 3303, 3191, 1633, 1358, 1128, 846; ¹H-NMR (500 MHz, DMSO-*d*₆) δ ppm 1.17 (6H, d, J = 6.2 Hz, H-12), 3.35 (1H, m, J = 6.2 Hz, H-11), 5.59 (1H, d, J = 7.2, H-10), 6.34 (1H, s, H-8), 6.51 (1H, d, J = 8.3 Hz, H-6), 7.37 (1H, d, J = 8.3 Hz, H-5), 7.71 (1H, s, H-3), 12.28 (1H, br, H-1); ¹³C-NMR (125 MHz, DMSO-*d*₆) δ ppm 22.2 (C-12), 43.2 (C-11), 87.3 (C-8), 112.3 (C-6), 114.9 (C-4), 120.4 (C-5), 133.2 (C-3), 142.3 (C-7), 147.1 (C-9); MS (ES⁺) m/z 176.2 [M+H]⁺

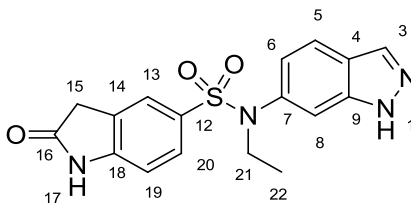
***N*-Ethyl-*N*-(1*H*-indazol-6-yl)benzenesulfonamide (97)**



Prepared according to general procedure A using 1*H*-indazol-6-amine (100 mg, 0.75 mmol) and benzenesulfonyl chloride (96 μ L, 0.75 mmol) in pyridine (2 mL). The material generated (*N*-(1*H*-indazol-6-yl)benzenesulfonamide) was used directly without purification according to general procedure B with the following reagents and quantities: ethyl iodide (60 μ L, 0.75 mmol) and K₂CO₃ (104 mg, 0.75 mmol) in DMF (4 mL) this gave the title compound as a grey solid (74 mg, 35%).

R_f 0.38 (EtOAc /Petrol, 1:1); m.p. 149-151 °C; UV λ_{\max} (EtOH/nm) 208.0; IR $\nu_{\max}/\text{cm}^{-1}$ 3298, 1625, 1334, 1156, 1057, 937, 726; ¹H-NMR (500 MHz, DMSO-*d*₆) δ ppm 1.00 (3H, t, J = 7.1 Hz, H-17), 3.67 (2H, q, J = 7.1 Hz, H-16), 6.72 (1H, dd, J = 8.6, 1.7 Hz, H-6), 7.20 (1H, s, H-8), 7.59-7.60 (4H, m, H-14, H-13), 7.70-7.72 (2H, m, H-5, H-15), 8.09 (1H, s, H-3), 13.12 (1H, s-br(1H, s-br, H-1); ¹³C-NMR (125 MHz, DMSO-*d*₆) δ ppm 13.9 (C-17), 45.5 (C-16), 110.5 (C-8), 120.7 (C-6), 120.8 (C-5), 122.1 (C-4), 127.2 (C-13), 129.2 (C-14), 133.1 (C-15), 133.5 (C-3), 136.2 (C-7), 137.9 (C-12), 139.7 (C-9); MS (ES⁺) m/z 302.3 [M+H]⁺; HRMS calcd for C₁₅H₁₆N₃O₂S 302.0958 [M+H]⁺ found 302.0956.

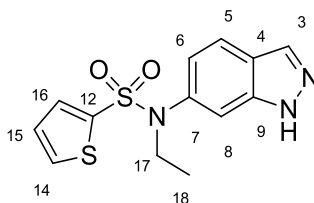
***N*-Ethyl-*N*-(1*H*-indazol-6-yl)-2-oxoindoline-5-sulfonamide (98)**



Prepared according to general procedure B with following reagents and quantities: ethyliodide (10 μ L, 0.12 mmol), K_2CO_3 (17 mg, 0.12 mmol) and *N*-(1*H*-indazol-6-yl)-2-oxoindoline-5-sulfonamide (40 mg, 0.12 mmol) in DMF (2 mL) this gave the title compound as a grey solid (19.2 mg, 44%).

R_f 0.36 (EtOAc /Petrol, 1:1); m.p. 128-130 $^{\circ}C$; UV λ_{max} (EtOH/nm) 266.4, 208.2; IR ν_{max}/cm^{-1} 3218, 2928, 1703, 1617, 1480, 1332, 1141, 1061; 1H -NMR (500 MHz, DMSO- d_6) δ ppm 0.98, (3H, t, J = 7.0 Hz, H-22), 3.57 (2H, s, H-15), 3.62 (2H, q, J = 7.0 Hz, H-21), 6.75 (1H, dd, J = 8.5, 1.6 Hz, H-6), 6.92 (1H, d, J = 8.2 Hz, H-19), 7.18 (1H, s, H-8), 7.37 (1H, d, J = 8.2 Hz, H-20), 7.45 (1H, s, H-13), 7.71 (1H, d, J = 8.5 Hz, H-5), 8.09 (1H, s, H-3), 10.85 (1H, br, H-17) 13.11 (1H, br, H-1); ^{13}C -NMR (125 MHz, DMSO- d_6) δ ppm 13.8 (C-22), 35.6 (C-15), 45.4 (C-21), 108.9 (C-19), 110.5 (C-8), 120.7 (C-5), 121.0 (C-6), 122.0 (C-4), 123.5 (C-13), 126.7 (C-14), 128.2 (C-20), 133.5 (C-3), 136.6 (C-7), 139.7 (C-9), 147.9 (C-18), 153.2 (C-12), 176.4 (C-16); MS (ES^+) m/z 357.4 $[M+H]^+$; HRMS calcd for $C_{17}H_{17}N_4O_3S$ 357.1016 $[M+H]^+$ found 357.1016.

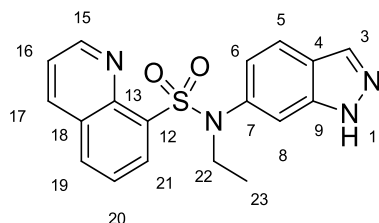
***N*-Ethyl-*N*-(1*H*-indazol-6-yl)thiophene-2-sulfonamide (99)**



Prepared according to general procedure A using 1*H*-indazol-6-amine (100 mg, 0.75 mmol) and thiophene-2-sulfonyl chloride (137 mg, 0.75 mmol) in pyridine (2 mL). The material generated (*N*-(1*H*-indazol-6-yl)thiophene-2-sulfonamide) was used directly without purification according to general procedure B with the following reagents and quantities: ethyliodide (60 μ L, 0.75 mmol) and K_2CO_3 (104 mg, 0.75 mmol) in DMF (4 mL) this gave the title compound as a grey solid (44.8 mg, 20% (over two steps)).

R_f 0.33 (EtOAc /Petrol, 1:1); m.p. 174-176 °C; UV λ_{\max} (EtOH/nm) 253.4, 210.4; IR $\nu_{\max}/\text{cm}^{-1}$ 3317, 1333, 1157, 938; $^1\text{H-NMR}$ (500MHz, DMSO- d_6) δ ppm 1.03 (3H, t, J = 7.1 Hz, H-18), 3.69 (2H, q, J = 7.1 Hz, H-17), 6.89 (1H, dd, J = 8.6, 1.7 Hz, H-6), 7.23-7.25 (2H, m, H-15, H-8), 7.52 (1H, dd, J = 1.3, 3.7 Hz, H-16), 7.74 (1H, d, J = 8.6 Hz, H-5), 8.02 (1H, dd, J = 5.0, 1.3 Hz, H-14), 8.10 (1H, s, H-3), 13.16 (1H, s-br, H-1). $^{13}\text{C-NMR}$ (125 MHz, DMSO- d_6) δ ppm 13.9 (C-18), 45.6 (C-17), 110.4 (C-8), 120.7 (C-6), 120.9 (C-5), 122.2 (C-4), 128.0 (C-15), 132.8 (C-16), 133.5 (C-3), 133.7 (C-14), 136.0 (C-7), 137.8 (C-12), 139.6 (C-9); MS (ES^+) m/z 308.3 $[\text{M}+\text{H}]^+$; HRMS calcd for $\text{C}_{13}\text{H}_{14}\text{N}_3\text{O}_2\text{S}_2$ 308.0522 $[\text{M}+\text{H}]^+$ found 308.0520.

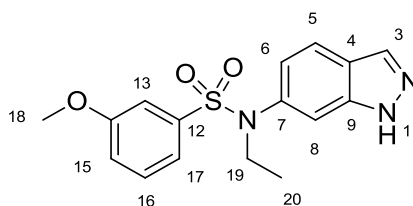
***N*-Ethyl-*N*-(1*H*-indazol-6-yl)quinoline-8-sulfonamide (100)**



Prepared according to general procedure B with following reagents and quantities: ethyliodide (10 μL , 0.12 mmol), K_2CO_3 (17 mg, 0.12 mmol) and *N*-(1*H*-indazol-6-yl)-quinoline-8-sulfonamide (40 mg, 0.12 mmol) in DMF (3 mL) this gave the title compound as a grey solid (22.3 mg, 51%).

R_f 0.37 (EtOAc /Petrol, 1:1); m.p. 168-169 °C; UV λ_{\max} (EtOH/nm) 289.2, 212.2; IR $\nu_{\max}/\text{cm}^{-1}$ 3307, 2931, 1493, 1324, 1128, 941, 704; $^1\text{H-NMR}$ (500 MHz, DMSO- d_6) δ ppm 1.09 (3H, t, J = 7.2 Hz, H-23), 4.24 (2H, q, J = 7.2 Hz, H-22), 6.61 (1H, dd, J = 8.7, 1.6 Hz, H-6), 7.14 (1H, s, H-8), 7.54 (1H, d, J = 8.7 Hz, H-5), 7.59 (1H, dd, J = 7.7, 7.7 Hz, H-20), 7.78 (1H, dd, J = 8.4, 4.2, Hz, H-16), 7.98 (1H, s, H-3), 8.09 (1H, dd, J = 7.7, 1.2 Hz, H-19), 8.27 (1H, dd, J = 7.7, 1.1 Hz, H-21), 8.58 (1H, dd, J = 8.4, 1.7, Hz, H-17), 9.18 (1H, dd, J = 4.2, 1.6 Hz, H-15), 12.98 (1H, br, H-1); $^{13}\text{C-NMR}$ (125 MHz, DMSO- d_6) δ ppm 15.0 (C-23), 47.9 (C-22), 110.7 (C-8), 120.8 (C-5), 121.0 (C-6), 121.8 (C-4), 122.6 (C-16), 125.6 (C-20), 128.6 (C-18), 132.7 (C-19), 133.4 (C-3), 134.0 (C-21), 136.4 (C-7), 136.7 (C-12), 137.0 (C-17), 139.6 (C-9), 143.2 (13C), 151.5 (C-15); MS (ES^+) m/z 353.4 $[\text{M}+\text{H}]^+$; HRMS calcd for $\text{C}_{18}\text{H}_{17}\text{N}_4\text{O}_2\text{S}$ 353.1067 $[\text{M}+\text{H}]^+$ found 353.1064.

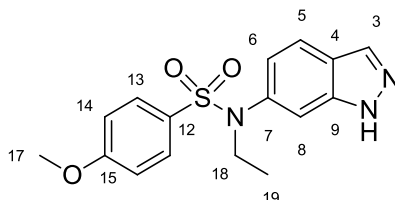
***N*-Ethyl-*N*-(1*H*-indazol-6-yl)-3-methoxybenzenesulfonamide (101)**



Prepared according to general procedure B with following reagents and quantities: ethyliodide (11 μ L, 0.13 mmol), K_2CO_3 (18 mg, 0.13 mmol) and *N*-(1*H*-indazol-6-yl)-3-methoxybenzenesulfonamide (40 mg, 0.13 mmol) in DMF (3 mL) this gave the title compound as a grey solid (24.5 mg, 56%).

R_f 0.37 (EtOAc /Petrol, 1:1); m.p. 63-64 $^{\circ}C$; UV λ_{max} (EtOH/nm) 285.0, 203.6; IR ν_{max}/cm^{-1} : 3352, 2935, 1595, 1477, 1319, 1239, 1159, 941; 1H -NMR (500 MHz, $DMSO-d_6$) δ ppm 0.99 (3H, t, J = 7.0 Hz, H-20), 3.66 (2H, q, J = 7.0 Hz, H-19), 3.74 (3H, s, H-18), 6.74 (1H, dd, J = 8.7, 1.8 Hz, H-6), 6.93 (1H, dd, J = 2.3, 2.3 Hz, H-13), 7.16 (1H, ddd, J = 8.0, 1.9, 2.3 Hz, H-15), 7.22 (1H, s, H-8), 7.28 (1H, ddd, J = 8.0, 2.3, 1.9 Hz, H-17), 7.51 (1H, dd, J = 8.0, 8.0 Hz, H-16), 7.72 (1H, d, J = 8.7 Hz, H-5), 8.09 (1H, s, H-3), 13.15 (1H, br, H-1); ^{13}C -NMR (125 MHz, $DMSO-d_6$) δ ppm 13.9 (C-20), 45.4 (C-19), 55.5 (C-18), 110.5 (C-8), 111.9 (C-13), 119.1 (C-17), 119.4 (C-15), 120.8 (C-5), 121.4 (C-4), 122.1 (C-6), 130.5 (C-16), 133.6 (C-3), 136.2 (C-7), 138.0 (C-12), 139.0 (C-9), 159.3 (C-14); MS (ES^+) m/z 332.4 $[M+H]^+$; HRMS calcd for $C_{16}H_{18}N_3O_3S$ 332.1063 $[M+H]^+$ found 332.1062.

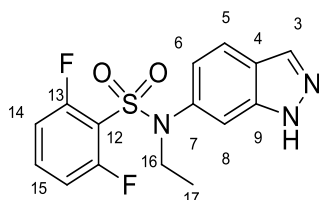
***N*-Ethyl-*N*-(1*H*-indazol-6-yl)-4-methoxybenzenesulfonamide (102)**



Prepared according to general procedure B using *N*-ethyl-1*H*-indazol-6-amine (40 mg, 0.24 mmol) and 4-methoxybenzene-1-sulfonyl chloride (51 mg, 0.24 mmol) in pyridine (2 mL). The title compound was obtained as a light green solid (21 mg, 25%).

R_f 0.38 (EtOAc /Petrol, 1:1); m.p. 146-148 °C; UV λ_{\max} (EtOH/nm) 245.6, 202.0; IR $\nu_{\max}/\text{cm}^{-1}$ 3400, 2937, 1593, 1326, 1260, 1154, 939; $^1\text{H-NMR}$ (500 MHz, DMSO- d_6) δ ppm 0.98 (3H, t, J = 7.1 Hz, H-19), 3.63 (2H, q, J = 7.1 Hz, H-18), 3.85, (3H, s, H-17), 6.73 (1H, dd, J = 8.5, 1.7 Hz, H-6), 7.10 (2H, d, J = 8.9 Hz H-14), 7.12 (1H, s, H-8), 7.51 (2H, d, J = 8.9 Hz, H-13), 7.71 (1H, d, J = 8.5 Hz, H-5), 8.08 (1H, s, H-3), 13.11 (1H, br, H-1); $^{13}\text{C-NMR}$ (125 MHz, DMSO- d_6) δ ppm 13.9 (C-19), 45.1 (C-18), 55.7 (C-17), 110.8 (C-8), 114.3 (C-14), 120.8 (C-6), 120.9 (C-5), 125.1 (C-4), 129.4 (C-12), 129.5 (C-13), 133.6 (C-3), 136.5 (C-7), 139.7 (C-9), 162.6 (C-18); MS (ES^+) m/z 332.3 $[\text{M}+\text{H}]^+$; HRMS calcd for $\text{C}_{16}\text{H}_{18}\text{N}_3\text{O}_3\text{S}$ 332.1063 $[\text{M}+\text{H}]^+$ found 332.1060.

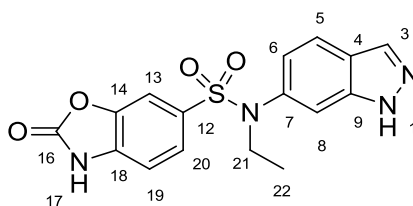
***N*-Ethyl-2,6-difluoro-*N*-(1*H*-indazol-6-yl)benzenesulfonamide (103)**



Prepared according to general procedure A using 1*H*-indazol-6-amine (100 mg, 0.75 mmol) and 2,6-difluorobenzene-1-sulfonyl chloride (102 μL , 0.75 mmol) in pyridine (2 mL). The material generated (*N*-(1*H*-indazol-6-yl)benzenesulfonamide) was used directly without purification according to general procedure B with the following reagents and quantities: ethyl iodide (60 μL , 0.75 mmol) and K_2CO_3 (104 mg, 0.75 mmol) in DMF (4 mL) this gave the title compound as a grey solid (12 mg, 10%).

R_f 0.39 (EtOAc /Petrol, 1:1); m.p. 83-85 °C; UV λ_{\max} (EtOH/nm) 289.2, 264.0, 209.0; IR $\nu_{\max}/\text{cm}^{-1}$ 3362, 2882, 1610, 1464, 1362, 1171, 1002, 939; $^1\text{H-NMR}$ (500 MHz, DMSO- d_6) δ ppm 1.05 (3H, t, J = 7.0 Hz, H-17), 3.85 (2H, q, J = 7.0 Hz, H-16), 6.86 (1H, d, J = 8.4 Hz, H-6), 7.28 (2H, dd, J = 9.15 Hz, H-14), 7.36 (1H, s, H-8), 7.73-7.79 (2H, m, H-15, H-5), 8.10 (1H, s, H-3), 13.17 (1H, s-br, H-1); $^{13}\text{C-NMR}$ (125 MHz, DMSO- d_6) δ ppm 14.1 (C-17), 46.0 (C-16), 110.7 (C-8), 113.5 (d, J_{FC} = 23.5 Hz, C-14), 113.5 (d, J_{FC} = 23.5 Hz, C-14'), 120.4 (C-6), 121.2 (C-5), 122.2 (C-4), 133.6 (C-3), 133.6 (C-12), 135.1 (C-7), 136.1 (t, J_{FC} = 11.4 Hz, C-15), 139.7 (C-9), 158.8 (d, J_{FC} = 257.3 Hz, C-13), 158.8 (d, J_{FC} = 257.3 Hz, C-13'); $^{19}\text{F-NMR}$ (470 MHz, DMSO- d_6) δ -106.2; MS (ES^+) m/z 338.3 $[\text{M}+\text{H}]^+$; HRMS calcd for $\text{C}_{15}\text{H}_{14}\text{F}_2\text{N}_3\text{O}_2\text{S}$ 338.0769 $[\text{M}+\text{H}]^+$ found 338.0764.

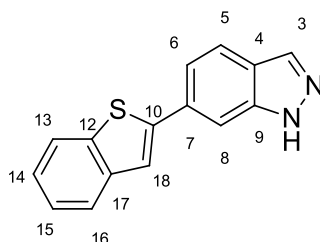
***N*-Ethyl-*N*-(1*H*-indazol-6-yl)-2-oxo-2,3-dihydrobenzo[*d*]oxazole-6-sulfonamide (104)**



Prepared according to general procedure B with following reagents and quantities: ethyliodide (10 μ L, 0.12mmol), K_2CO_3 (17 mg, 0.12 mmol) and *N*-(1*H*-indazol-6-yl)-2-oxo-2,3-dihydrobenzo[*d*]oxazole-6-sulfonamide (40 mg, 0.12 mmol) in DMF (2 mL) this gave the title compound as a grey solid (16.8 mg, 43%).

R_f 0.37 (EtOAc /Petrol, 1:1); m.p. 239-241 $^{\circ}$ C; UV λ_{max} (EtOH/nm) 252.2, 203.8; IR ν_{max}/cm^{-1} 3370, 3072, 1775, 1631, 1487, 1329, 1147, 940; 1H -NMR (500 MHz, DMSO- d_6) δ ppm 1.21 (3H, t, J = 7.2 Hz, H-22), 3.81 (2H, q, J = 7.2 Hz, H-21), 6.91 (1H, dd, J = 8.7, 1.7 Hz, H-6), 7.28 (1H, s, H-8), 7.44 (1H, d, J = 8.3 Hz, H-19), 7.60 (1H, d, J = 8.7 Hz, H-5), 7.65 (1H, dd, J = 8.3, 1.7 Hz, H-20), 7.70 (1H, d, J = 1.7 Hz, H-13), 7.93 (1H, s, H-3), 10.44 (1H, br, H-17), 12.86 (1H, br, H-1); ^{13}C -NMR (125 MHz, DMSO- d_6) δ ppm 12.6 (C-22), 37.1 (C-21), 99.7 (C-8), 107.9 (C-13), 109.1 (C-19), 114.6 (C-6), 119.8 (C-4), 121.3 (C-5), 123.4 (C-20), 132.9 (C-12), 133.4 (C-3), 134.8 (C-18), 135.9 (C-7), 140.1 (C-9), 141.5 (C-14), 153.2 (C-18); MS (ES^+) m/z 359.4 [$M+H$] $^+$; HRMS calcd for $C_{16}H_{15}N_4O_4S$ 359.0809 [$M+H$] $^+$ found 359.0809.

6-(Benzo[*b*]thiophen-2-yl)-1*H*-indazole (111)

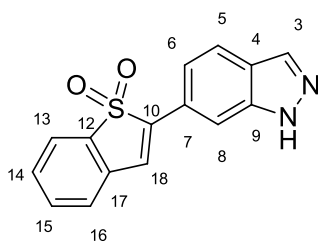


6-Bromoindazole (100 mg, 0.51 mmol), benzo[*b*]thiophen-2-ylboronic acid (90 mg, 0.51 mmol) and Na_2CO_3 (64 mg, 0.61 mmol) in water (0.3 mL) were added to dioxane (2.7 mL) and the solution was degassed with nitrogen for *ca.* 15 minutes. Palladium tetrakis (6 mg, 0.05 mmol) was added and the solution degassed again for a further 15 minutes. After this time the reaction was subjected to microwave radiation to a

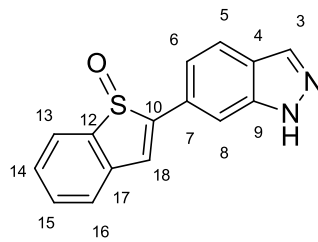
temperature of 110 °C for 30 minutes. After this time further equivalence of benzo[*b*]thiophen-2-ylboronic acid (90 mg, 0.51 mmol), Na₂CO₃ (64 mg, 0.61 mmol) and Palladium tetrakis (6 mg, 0.05 mmol) with repeated 15 minute degassing. This was again heated in a microwave initiator at 110°C for 30 minutes before being filtered through Celite® (washing with EtOAc (15 mL)) and being diluted in water (15 mL). The aqueous was extracted with EtOAc (3 x 10 mL) and the combined organic extraction was washed with brine, dried over Na₂SO₄ and purified by MPLC (0-50% EtOAc in petroleum ether over 20 CV). 97.7 mg (77%) of pure orange solid was isolated.

*R*_f 0.30 (EtOAc /Petrol, 1:1); m.p. 254-255°C; UV λ_{max} (EtOH/nm) 319.8, 257.4, 234.0, 214.8; IR ν_{max}/cm⁻¹ 3296, 1620, 1073, 943, 836, 751; ¹H-NMR (500 MHz, DMSO-*d*₆) δ ppm 7.36 (1H, dd, *J* = 8.9, 8.9 Hz, H-15), 7.42 (1H, dd, *J* = 8.9, 8.9 Hz, H-14), 7.60 (1H, d, *J* = 8.7, H-6), 7.87-7.89 (3H, m, H-8, H-13, H16), 7.97 (1H, s, H-18), 8.00 (1H, d, *J* = 8.7, H-5), 8.12 (1H, s, H-3), 13.21 (1H, br, H-1); ¹³C-NMR (125 MHz, DMSO-*d*₆) δ ppm 107.9 (C-8), 118.5 (C-6), 121.4 (C-13), 122.0 (C-5), 123.3 (C-4), 124.4 (C-17), 125.4 (C-18), 125.9 (C-16), 130.5 (C-15), 130.8 (C-10), 133.9 (C-3), 134.5 (C-14), 136.3 (C-12), 139.6 (C-9), 141.4(C-7); MS (ES⁺) *m/z* 251.2 [M+H]⁺.

2-(1*H*-Indazol-6-yl)benzo[*b*]thiophene 1,1-dioxide (112) and 2-(1*H*-indazol-6-yl)benzo[*b*]thiophene 1-oxide (113)



67



68

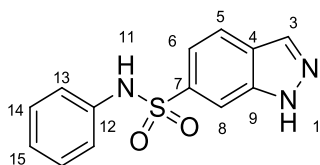
6-(Benzo[*b*]thiophen-2-yl)-1*H*-indazole (66 mg, 0.26 mmol) was dissolved in anhydrous DCM (2 mL) and *m*-CPBA (84 mg, 0.36 mmol, 0.74%) was added at 0 °C in portions over 5 minutes whilst under N₂. This was left at RT overnight before being filtered through Celite® (washing with DCM), the filtrate was washed with Na₂SO₃ solution, NaHCO₃ solution and dried over Na₂SO₄. This solution was reduced to a residue under vacuum

and purified by MPLC (0-70% EtOAc in petroleum ether) to give **112** as a dull orange solid (41 mg, 55%) and **113** as a grey solid (11 mg, 15%).

112 - R_f 0.38 (EtOAc /Petrol, 1:1); m.p. 224-225 °C; UV λ_{\max} (EtOH/nm) 339.2, 313.6, 240.2, 202.8; IR $\nu_{\max}/\text{cm}^{-1}$ 3169, 3128, 2867, 1284, 1145, 834, 755; ^1H -NMR (500 MHz, DMSO- d_6) δ ppm 7.60 (1H, d, J = 8.7, H-6), 7.65 (1H, dd, J = 8.9, 8.9 Hz, H-15), 7.68 (1H, d, J = 8.9, H-16), 7.77 (1H, dd, J = 8.9, 8.9 Hz, H-14), 7.96 (1H, d, J = 8.7 Hz, H-5), 7.98 (1H, J = 8.9 Hz, H-13), 8.07 (1H, s, H-8), 8.11 (1H, s, H-18), 8.19 (1H, s, H-3), 13.38 (1H, br, H-1); ^{13}C -NMR (125 MHz, DMSO- d_6) δ ppm 107.9 (C-8), 118.5 (C-6), 121.4 (C-13), 122.0 (C-5), 123.3 (C-4), 124.4 (C-17), 125.4 (C-18), 125.9 (C-16), 130.5 (C-15), 130.8 (C-10), 133.9 (C-3), 134.5 (C-14), 136.3 (C-12), 139.6 (C-9), 141.4 (C-7); MS (ES^+) m/z 283.3 $[\text{M}+\text{H}]^+$; HRMS calcd for $\text{C}_{15}\text{H}_{11}\text{N}_2\text{O}_2\text{S}$ 285.0536 $[\text{M}+\text{H}]^+$ found 285.0536.

113 - R_f 0.33 (EtOAc /Petrol, 1:1); m.p. 206-208 °C; UV λ_{\max} (EtOH/nm) 352.6, 241.4, 201.2; IR $\nu_{\max}/\text{cm}^{-1}$ 3252, 2921, 1061, 998, 845, 752; ^1H -NMR (500 MHz, DMSO- d_6) δ ppm 7.55 (1H, dd, J = 8.9, 8.9 Hz, H-15), 7.60 (1H, d, J = 8.7, H-6), 7.66 (1H, dd, J = 8.9, 8.9 Hz, H-14), 7.71 (1H, d, J = 8.9, H-16), 7.91 (1H, s, H-18), 7.92 (1H, d, J = 8.7 Hz, H-5), 8.04 (1H, s, H-8), 8.06 (1H, J = 8.9 Hz, H-13), 8.16 (1H, s, H-3), 13.32 (1H, br, H-1); MS (ES^+) m/z 267.3 $[\text{M}+\text{H}]^+$; HRMS calcd for $\text{C}_{15}\text{H}_{11}\text{N}_2\text{OS}$ 267.0587 $[\text{M}+\text{H}]^+$ found 267.0587.

***N*-phenyl-1*H*-indazole-6-sulfonamide (114)**

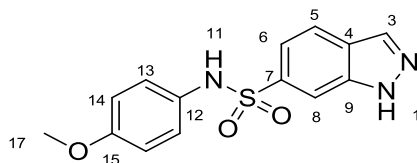


Prepared according to general procedure M using the following varied reagents and quantities: aniline (70 mg, 0.75 mmol); giving a dark grey solid (12 mg, 6%).

R_f 0.33 (EtOAc /Petrol, 1:1); m.p. 152-154 °C; UV λ_{\max} (EtOH/nm) 299.0, 263.2, 216.6; IR $\nu_{\max}/\text{cm}^{-1}$ 3248, 1315, 1150, 938, 715; ^1H -NMR (500 MHz, DMSO- d_6) δ ppm 7.09 (1H, t, J = 7.3 Hz, H-15), 7.18 (2H, d, J = 7.9 Hz, H-13), 7.29 (2H, dd, J = 7.9, 7.3 Hz, H-14), 7.55 (1H, d, J = 8.5 Hz, H-6), 8.01-8.04 (2H, m, H-5, H-8), 8.30 (1H, s, H-3), 10.44 (1H, s-br, H-11), 13.61 (1H, s-br, H-1); ^{13}C -NMR (125 MHz, DMSO- d_6) δ ppm 110.0 (C-8), 117.5 (C-6), 120.1 (C-13), 121.9 (C-5), 124.1 (C-15), 124.6 (C-4), 129.1 (C-14), 134.0 (C-3), 136.9 (C-

7), 137.6 (C-12), 138.3 (C-9); MS (ES⁺) m/z 274.3 [M+H]⁺; HRMS calcd for C₁₃H₁₂N₃O₂S 274.0645 [M+H]⁺ found 274.0646.

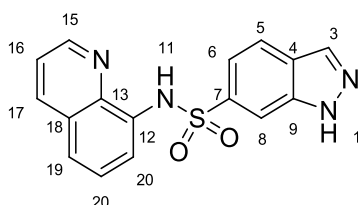
***N*-(4-methoxyphenyl)-1*H*-indazole-6-sulfonamide (115)**



Prepared according to general procedure M using the following varied reagents and quantities: 4-methoxyaniline (80 mg, 0.64 mmol); giving a grey solid (25 mg, 11%).

R_f 0.28 (EtOAc /Petrol, 1:1); m.p. 157-159 °C; UV λ_{\max} (EtOH/nm) 217.5; IR $\nu_{\max}/\text{cm}^{-1}$ 3259, 1615, 1508, 1318, 1148, 943, 717; ¹H-NMR (500 MHz, DMSO-*d*₆) δ ppm 3.64 (3H, s, H-17), 6.77 (2H, d, J = 8.7 Hz, H-14), 6.97 (2H, d, J = 8.7 Hz, H-13), 7.42 (1H, d, J = 8.5 Hz, H-6), 7.85 (1H, s, H-8), 7.93 (1H, d, J = 8.5 Hz, H-5), 8.21 (1H, s, H-3), 9.95 (1H, s-br, H-11), 13.47 (1H, s-br, H-1); ¹³C-NMR (125 MHz, DMSO-*d*₆) δ ppm 55.1 (C-17), 109.9 (C-8), 114.2 (C-14), 117.7 (C-6), 121.7 (C-5), 123.5 (C-13), 124.6 (C-4), 130.0 (C-12), 134.0 (C-3), 136.9 (C-7), 138.4 (C-9) 156.5 (C-15); MS (ES⁺) m/z 304.3 [M+H]⁺; HRMS calcd for C₁₄H₁₄N₃O₃S 304.0750 [M+H]⁺ found 304.0753.

***N*-(quinolin-8-yl)-1*H*-indazole-6-sulfonamide (116)**

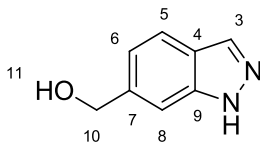


Prepared according to general procedure M using the following varied reagents and quantities: quinolin-8-amine (108 mg, 0.75 mmol); giving a grey solid (11.3 mg, 5%).

R_f 0.46 (EtOAc /Petrol, 1:1); m.p. 201-203 °C; UV λ_{\max} (EtOH/nm) 304.0, 228.6, 200.0; IR $\nu_{\max}/\text{cm}^{-1}$ 3355, 3268, 2924, 1504, 1253, 1054, 713; ¹H-NMR (500 MHz, DMSO-*d*₆) δ ppm 7.52 (1H, dd, J = 7.9, 7.9 Hz, H-20), 7.57 (1H, dd, J = 8.3, 4.2, Hz, H-16), 7.60 (1H, d, J = 8.6 Hz, H-6), 7.65 (1H, dd, J = 7.9, 1.0 Hz, H-19), 7.72 (1H, dd, J = 7.9, 1.0 Hz, H-21), 7.86 (1H, d, J = 8.6 Hz, H-5), 8.14 (1H, s, H-8), 8.16 (1H, s, H-3), 8.33 (1H, dd, J = 8.3, 1.7, Hz, H-17), 8.84 (1H, dd, J = 4.2, 1.7 Hz, H-15), 13.51 (1H, s-br, H-1); ¹³C-NMR (125 MHz,

DMSO-*d*₆) δ ppm 110.2 (C-8), 116.8 (C-12), 117.7 (C-6), 121.8 (C5), 122.3 (C-16), 123.1 (C-21), 124.7 (C-4), 126.6 (C-20), 128.1 (C-18), 133.6 (C-19), 133.9 (C-3), 136.5 (C-17), 137.0 (C-7), 138.2(C-9), 138.8 (C-13), 149.4 (C-15); MS (ES⁺) m/z 325.3 [M+H]⁺; HRMS calcd for C₁₆H₁₃N₄O₂S 325.0754 [M+H]⁺ found 325.0753.

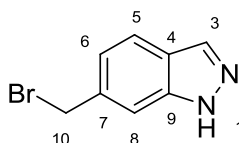
(1*H*-Indazol-6-yl)methanol (125)



1*H*-indazole-6-carbaldehyde (100 mg, 0.68 mmol) was dissolved in ethanol (4 mL) and sodium borohydride (32 mg, 0.85mmol) was added and the solution was stirred at RT for c.a. 3 h. NaOH solutuion (2 M in H₂O, 10ml) was added and the solution extracted with EtOAc (3 x 10ml). Combined organic fractions were washed with brine and dried over NaSO₄. This solution was reduced to a residue under reduced pressure and purified by MPLC (0-70% EtOAc in petroleum spirit over 30 column volumes) to give the title product as a white solid (87 mg, 89%).

R_f 0.32 (Et₂O); m.p. 156-158 °C; IR $\nu_{\max}/\text{cm}^{-1}$ 3121, 2861, 1354, 1028, 1007, 946, 848; ¹H-NMR (500 MHz, DMSO-*d*₆) δ ppm 4.62 (2H, d, J = 5.4 Hz, H-10), 5.26 (1H, t, J = 5.4 Hz, H-11), 7.04 (1H, d, J = 8.4 Hz, H-6), 7.46 (1H, s, H-8), 7.67 (1H, d, J = 8.4 Hz H-5), 8.00 (1H, s, H-3), 12.95 (1H, s-br, H-1); ¹³C-NMR (125 MHz, DMSO-*d*₆) δ ppm 63.1 (C-10), 106.9 (C-8), 119.5 (C-6), 120.0 (C-5), 121.8 (C-4), 133.2 (C-3), 140.1 (C-9), 140.8 (C-7); MS (ES⁺) m/z 149.3 [M+H]⁺.

6-(bromomethyl)-1*H*-indazole (126)

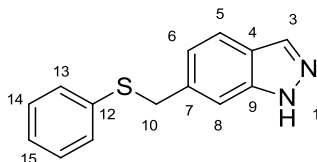


(1*H*-Indazol-6-yl)methanol (200 mg, 1.3 mmol) was dissolved in anhydrous DCM in dry glassware, under an inert atmosphere. Thionylbromide (0.21ml, 2.7mmol) was added

via syringe followed by DMF (0.01 mL, 0.13 mmol). The reaction was stirred at 0°C and warmed to RT over 4 h. The reaction mix was evaporated to a residue and purified by MPLC (0-10% methanol in DCM) to give the title product as an orange solid (244 mg, 86%).

R_f 0.44 (Et₂O); m.p. >300 °C; UV λ_{\max} (EtOH/nm) 262.8, 217.8; IR $\nu_{\max}/\text{cm}^{-1}$ 2766, 2615, 1635, 1353, 1146, 828, 661; ¹H-NMR (500 MHz, DMSO-*d*₆) δ ppm 4.88 (2H, s, H-10), 7.18 (1H, d, J = 8.4 Hz, H-6), 7.65 (1H, s, H-8), 7.75 (1H, d, J = 8.4 Hz H-5), 8.07 (1H, s, H-3), 13.40 (1H, s-br, H-1); ¹³C-NMR (125 MHz, DMSO-*d*₆) δ ppm; 63.5 (C-10), 107.6 (C-8), 120.3 (C-6), 120.6 (C-5), 122.1 (C-4), 133.4 (C-3), 140.6 (C-9), 140.8 (C-7); MS (ES⁺) m/z 211.2 [M+H]⁺.

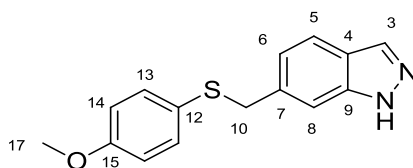
6-((Phenylthio)methyl)-1H-indazole (127)



Thiophenol sodium salt (1M in THF, 0.38 mL, 0.42 mmol) was dissolved in EtOH (2 mL) and 6-(bromomethyl)-1H-indazole (80 mg, 0.38 mmol) was added, this was stirred at RT for 4 h. The reaction was diluted with water (10 mL) and extracted with EtOAc (3 x 10 mL), combined organic fractions were washed with brine and dried over Na₂SO₄. The material was purified by MPLC (0-80% EtOAc in petroleum ether) giving the title compound as an off white solid (40 mg, 40%).

R_f 0.49 (EtOAc /Petrol, 1:1); m.p. 147-149°C; UV λ_{\max} (EtOH/nm) 254.0, 210.5; IR $\nu_{\max}/\text{cm}^{-1}$ 3269, 1578, 1483, 1068, 943; ¹H-NMR (500 MHz, DMSO-*d*₆) δ ppm 4.39 (2H, s, H-10), 7.13 (1H, d, J = 8.4 Hz, H-6), 7.18 (1H, t, J = 7.4 Hz, H-15), 7.28 (2H, t, J = 8.0 Hz, H-14), 7.35 (2H, d, J = 8.0 Hz, H-13), 7.48 (1H, s, H-8), 7.68 (1H, d, J = 8.4 Hz, H-5), 8.05 (1H, s, H-3), 12.98 (1H, s-br, H-1); ¹³C-NMR (125 MHz, DMSO-*d*₆) δ ppm 37.0 (C-10), 109.7 (C-8), 120.4 (C-5), 121.7 (C-6), 121.9 (C-5), 125.8 (C-15), 128.3 (C-13), 128.9 (C-14), 133.3 (C-3), 135.5 (C-7), 136.0 (C-12) 139.9 (C-9); MS (ES⁺) m/z 241.2 [M+H]⁺; HRMS calcd for C₁₄H₁₃N₂S 241.0794 [M+H]⁺ found 241.0797.

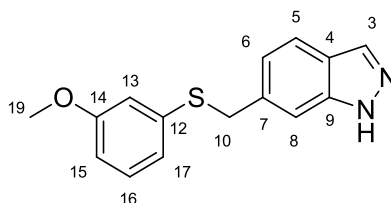
6-(((4-Methoxyphenyl)thio)methyl)-1*H*-indazole (128)



Sodium hydroxide (22 mg, 0.56 mmol) was dissolved in EtOH (2.5 mL), 4-methoxybenzenethiol (0.046 mL, 0.38 mmol) was added followed by 6-(bromomethyl)-1*H*-indazole (80 mg, 0.38 mmol) this was stirred at RT for 4 h. The reaction was diluted with water (10 mL) and extracted with EtOAc (3 x 10 mL), combined organic fractions were washed with brine and dried over Na₂SO₄. The material was purified by MPLC (0-80% EtOAc in petroleum ether) giving the title compound as light brown solid (40 mg, 40%).

*R*_f 0.36 (EtOAc /Petrol, 1:1); m.p. 117-119°C; UV λ_{max} (EtOH/nm) 211.5, 348.0; IR ν_{max}/cm⁻¹ 3182, 1588, 1491, 1241, 1027, 944; ¹H-NMR (500 MHz, DMSO-*d*₆) δ ppm 3.72 (3H, s, H-17), 4.24 (2H, s, H-10), 6.86 (2H, d, *J* = 8.9 Hz, H-14), 7.06 (1H, d, *J* = 8.2 Hz, H-6), 7.28 (2H, d, *J* = 8.9 Hz, H-13), 7.34 (1H, s, H-8), 7.66 (1H, d, *J* = 8.2 Hz, H-5), 8.00 (1H, s, H-3), 12.95 (1H, s-br, H-1); ¹³C-NMR (125 MHz, DMSO-*d*₆) δ ppm 39.7 (C-10) 55.1 (C-17), 109.6 (C-8), 114.6 (C-14), 120.3 (C-5), 121.7 (C-4, C-6), 125.6 (C-12), 132.4 (C-13), 133.3 (C-3), 136.0 (C-7), 139.9 (C-9) 158.4 (C-15); MS (ES⁺) *m/z* 271.2 [M+H]⁺; HRMS calcd for C₁₅H₁₅N₂OS 271.0900 [M+H]⁺ found 271.0904.

6-(((3-Methoxyphenyl)thio)methyl)-1*H*-indazole (129)

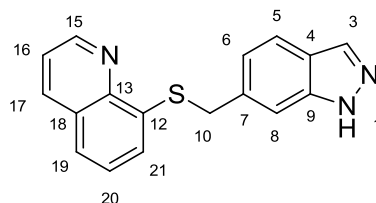


Sodium hydroxide (21 mg, 0.47 mmol) was dissolved in water (1 mL) and added to a solution of 3-methoxybenzenethiol (0.059 mL, 0.47 mmol) and 6-(bromomethyl)-1*H*-indazole (100 mg, 0.47 mmol) in toluene (3 mL). Tetra-*n*-butylammonium bromide (15 mg, 0.05 mmol) was added to the mixture which was then stirred vigorously for

18 h at RT. The reaction was diluted with water (10 mL) and extracted with EtOAc (3 x 10 mL), combined organic fractions were washed with brine (10 mL) and dried over Na₂SO₄. The material was purified by MPLC (0-80% EtOAc in petroleum ether) giving the title compound as a yellow solid (25 mg, 20%).

*R*_f 0.38 (EtOAc /Petrol, 1:1); m.p. 96-98°C; UV λ_{max} (EtOH/nm) 287.0, 254.5, 214.0; IR ν_{max}/cm⁻¹ 3128, 2935, 1573, 1245, 1035, 850; ¹H-NMR (500 MHz, DMSO-*d*₆) δ ppm 3.71 (3H, s, H-19), 4.40 (2H, s, H-10), 6.73 (1H, d, *J* = 8.2 Hz, H-15), 6.89 (1H, s, H-13), 6.91 (1H, d, *J* = 8.2 Hz, H-17), 7.14 (1H, d, *J* = 8.4 Hz, H-6), 7.46 (1H, dd, *J* = 8.0, 8.0 Hz, H-16), 7.51 (1H, s, H-8), 7.69 (1H, d, *J* = 8.4 Hz, H-5), 8.01 (1H, s, H-3), 13.00 (1H, s-br, H-1); ¹³C-NMR (125 MHz, DMSO-*d*₆) δ ppm 36.6 (C-10), 55.0 (C-19), 109.8 (C-8), 111.6 (C-15), 113.2 (C-13), 120.1 (C-17), 120.4 (C-5), 121.7 (C-6), 121.9 (C-4), 129.8 (C-16), 133.3 (C-3), 135.5 (C-7), 137.5 (C-12), 139.9 (C-9), 159.5 (C-14); MS (ES⁺) *m/z* 271.4 [M+H]⁺; HRMS calcd for C₁₅H₁₅N₂OS 271.0900 [M+H]⁺ found 271.0896.

8-(((1*H*-Indazol-6-yl)methyl)thio)quinoline (130)

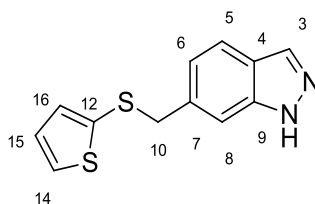


Sodium hydroxide (42 mg, 1.03 mmol) was dissolved in water (2 mL) and added to a solution of 3-quinoline-8-thiol HCl salt (94 mg, 0.47 mmol) and 6-(bromomethyl)-1*H*-indazole (100 mg, 0.47 mmol) in toluene (3 mL). Tetra-*n*-butylammonium bromide (15 mg, 0.05 mmol) was added to the mixture which was then stirred vigorously for 18 h at RT. The reaction was diluted with water (10 mL) and extracted with EtOAc (3 x 10 mL), combined organic fractions were washed with brine (10 mL) and dried over Na₂SO₄. The material was purified by MPLC (0-80% EtOAc in petroleum ether) giving the title compound as an off white solid (49 mg, 36%).

*R*_f 0.50 (EtOAc /Petrol, 1:1); m.p. 187-190°C; UV λ_{max} (EtOH/nm) 340.5, 290.0, 251.5; IR ν_{max}/cm⁻¹ 3293, 3055, 1490, 1350, 936, 832; ¹H-NMR (500 MHz, DMSO-*d*₆) δ ppm 4.50 (2H, s, H-10), 7.25 (1H, d, *J* = 8.3 Hz, H-6), 7.52 (1H, dd, *J* = 7.8, 7.8 Hz, H-20), 7.82 (1H, dd, *J* = 8.4, 4.3, Hz, H-16), 7.64-7.67 (2H, m, H-8, H-19), 7.72 (1H, dd, *J* = 8.1, 1.0 Hz, H-

21), 7.72 (1H, d, $J = 8.3$ Hz, H-5), 8.03 (1H, s, H-3), 8.36 (1H, dd, $J = 8.3, 1.7$, Hz, H-17), 8.90 (1H, dd, $J = 4.2, 1.7$ Hz, H-15), 13.00 (1H, s-br, H-1); ^{13}C -NMR (125 MHz, $\text{DMSO-}d_6$) δ ppm 34.5 (C-10), 109.8 (C-8), 120.2 (C-5), 121.9 (C-5), 122.0 (C-4), 122.1 (C-16), 123.9 (C-21), 124.1 (C-19), 126.7 (C-20), 127.8 (C-18), 133.3 (C-3), 135.1 (C-7), 136.5 (C-17), 138.1 (C-12), 140.1 (C-9), 144.4 (C-13), 149.3 (C-15); MS (ES^+) m/z 292.3 $[\text{M}+\text{H}]^+$; HRMS calcd for $\text{C}_{17}\text{H}_{14}\text{N}_3\text{S}$ 292.0903 $[\text{M}+\text{H}]^+$ found 292.0901.

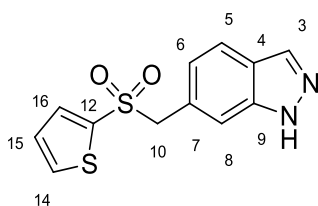
6-((Thiophen-2-ylthio)methyl)-1*H*-indazole (131)



Cs_2CO_3 (109 mg, 0.57 mmol) was dissolved in THF (2 mL), thiophene-2-thiol (0.036 mL, 0.38 mmol) was added followed by 6-(bromomethyl)-1*H*-indazole (80 mg, 0.38 mmol) this was stirred at RT for 4 h. The reaction was diluted with water (10 mL) and extracted with EtOAc (3 x 10 mL), combined organic fractions were washed with brine and dried over Na_2SO_4 . The material was purified by MPLC (0-80% EtOAc in petroleum ether) giving the title compound as a light pink solid (33 mg, 35%).

R_f 0.39 (EtOAc /Petrol, 1:1). m.p. 104-107°C. UV λ_{max} (EtOH/nm) 212.5; IR $\nu_{\text{max}}/\text{cm}^{-1}$ 3266, 1625, 1346, 1346, 944, 855, 696. ^1H -NMR (500MHz, $\text{DMSO-}d_6$) δ ppm 4.19 (2H, s, H-10), 6.98 (1H, dd, $J = 5.2, 3.5$ Hz, H-15), 7.01-7.04 (2H, m, H-6, H-14), 7.27 (1H, s, H-8), 7.56 (1H, dd, $J = 1.3, 5.2$ Hz, H-16), 7.67 (1H, d, $J = 8.3$ Hz, H-5), 8.02 (1H, s, H-3), 12.98 (1H, s-br, H-1); ^{13}C -NMR (125 MHz, $\text{DMSO-}d_6$) δ ppm 42.9 (C-10), 110.0 (C-8), 120.4 (C-5), 121.8 (C-6), 127.8 (C-15), 130.2 (C-16), 133.7 (C-3), 135.6 (C-14); MS (ES^+) m/z 247.2 $[\text{M}+\text{H}]^+$; HRMS calcd for $\text{C}_{12}\text{H}_{11}\text{N}_2\text{S}_2$ 247.0358 $[\text{M}+\text{H}]^+$ found 247.0361.

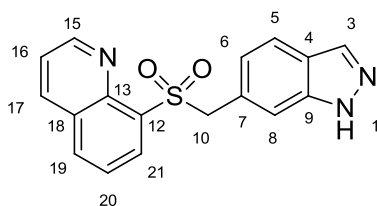
6-((Thiophen-2-ylsulfonyl)methyl)-1*H*-indazole (120)



6-((Thiophen-2-ylthio)methyl)-1*H*-indazole (12.5 mg, 0.05 mmol) was dissolved in MeOH (1 mL) and Oxone[®] solution (0.07 mL, 0.15 mmol, 1.5 M in H₂O:MeOH(1:1)) was added. This was stirred for c.a. 18 h before dilution with water (10 mL) and extraction with EtOAc (3 x 10 mL), combined organic fractions were washed with brine and dried over Na₂SO₄. The material was purified by MPLC (0-80% EtOAc in petroleum ether) giving the title compound as a pink solid (9 mg, 63%).

*R*_f 0.31 (EtOAc /Petrol, 1:1). m.p. 201-203°C. UV λ_{max} (EtOH/nm) 291.5, 255.5, 213.0; IR ν_{max}/cm⁻¹ 3359, 1398, 1295, 1140, 942, 673; ¹H-NMR (500MHz, DMSO-*d*₆) δ ppm 4.90 (2H, s, H-10), 6.89 (1H, d, *J* = 8.3 Hz, H-6), 7.21 (1H, dd, *J* = 3.8, 4.9 Hz, H-15), 7.38 (1H, s, H-8), 7.57 (1H, dd, *J* = 1.3, 3.8 Hz, H-16), 7.67 (1H, d, *J* = 8.3 Hz, H-5), 8.03 (1H, dd, *J* = 4.9, 1.3 Hz, H-14), 8.05 (1H, s, H-3), 13.12 (1H, s-br, H-1); MS (ES⁺) *m/z* 279.2 [M+H]⁺; HRMS calcd for C₁₂H₁₁N₂O₂S₂ 279.0256 [M+H]⁺ found 279.0261.

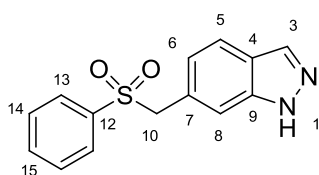
8-(((1*H*-Indazol-6-yl)methyl)sulfonyl)quinoline (121)



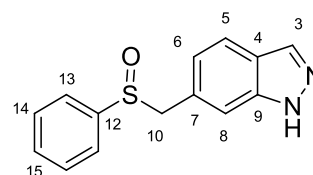
8-(((1*H*-Indazol-6-yl)methylthio)quinoline (15 mg, 0.05 mmol) was dissolved in MeOH (2 mL) and Oxone[®] solution (0.1 mL, 0.15 mmol, 1.5 M in H₂O:MeOH(1:1)) was added and the mixture stirred for 18 h. After this time the reaction was diluted with water (10 mL) and extracted with EtOAc (3 x 10 mL), combined organic fractions were washed with brine (10 mL) and dried over Na₂SO₄. The material was purified by MPLC (0-80% EtOAc in petroleum ether) giving the title compound as a yellow solid (8 mg, 47%).

R_f 0.44 (EtOAc /Petrol, 1:1); m.p. 178-180°C; UV λ_{\max} (EtOH/nm) 282.0, 214.5; IR $\nu_{\max}/\text{cm}^{-1}$ 3309, 2929, 1493, 1296, 1113, 832; $^1\text{H-NMR}$ (500 MHz, DMSO- d_6) δ ppm 5.37 (2H, s, H-10), 6.74 (1H, d, $J = 8.3$ Hz, H-6), 7.25 (1H, s, H-8) 7.54 (1H, d, $J = 8.3$ Hz, H-5), 7.67 (1H, dd, $J = 8.0, 8.0$ Hz, H-20), 7.82 (1H, dd, $J = 8.4, 4.3$, Hz, H-16), 7.97 (1H, s, H-3), 8.14 (1H, dd, $J = 7.4, 1.5$ Hz, H-19), 8.35 (1H, dd, $J = 8.0, 1.5$ Hz, H-21), 8.63 (1H, dd, $J = 8.5, 1.8$, Hz, H-17), 9.27 (1H, dd, $J = 4.3, 1.8$ Hz, H-15), 12.98 (1H, s-br, H-1); $^{13}\text{C-NMR}$ (125 MHz, DMSO- d_6) δ ppm 40.2 (C-10), 107.2 (C-8), 118.7 (C-6), 120.7 (C-5), 121.1 (C-4), 122.6 (C-16), 125.6 (C-20), 128.6 (18C), 132.9 (C-19), 133.3 (C-3), 134.2 (C-21), 136.6 (C-12), 136.9 (C-17), 139.2 (C-7), 139.6 (C-9), 143.3 (13C), 151.5 (C-15); MS (ES^+) m/z 273.3 $[\text{M}+\text{H}]^+$; HRMS calcd for $\text{C}_{17}\text{H}_{14}\text{N}_3\text{O}_2\text{S}$ 324.0801 $[\text{M}+\text{H}]^+$ found 324.0806.

6-((Phenylsulfonyl)methyl)-1H-indazole (122) and 6-((phenylsulfinyl)methyl)-1H-indazole (132)



122



132

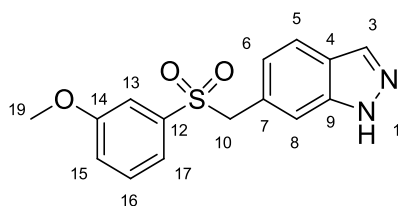
6-((Phenylthio)methyl)-1H-indazole (50 mg, 0.21 mmol) was dissolved in MeOH (1 mL) and Oxone® solution (0.41 mL, 0.63 mmol, 1.5 M in $\text{H}_2\text{O}:\text{MeOH}(1:1)$) was added. This was stirred for c.a. 18 h before dilution with water (10 mL) and extraction with EtOAc (3 x 10 mL), combined organic fractions were washed with brine and dried over Na_2SO_4 . The material was purified by MPLC (0-80% EtOAc in petroleum ether) giving the **15** as a white solid (11 mg, 19%) and **20** as a white solid (24 mg, 45%).

122 - R_f 0.38 (EtOAc /Petrol, 1:1); m.p. 195-197°C; UV λ_{\max} (EtOH/nm) 291.5, 258.5, 212.0; IR $\nu_{\max}/\text{cm}^{-1}$ 3397, 1281, 1149, 1083, 937; $^1\text{H-NMR}$ (500 MHz, DMSO- d_6) δ ppm 4.83 (2H, s, H-10), 6.87 (1H, d, $J = 8.3$ Hz, H-6), 7.35 (1H, s, H-8), 7.58 (2H, dd, $J = 7.4, 8.2$ Hz, H-14), 7.65 (1H, d, $J = 8.3$ Hz, H-5), 7.69-7.72 (3H, m, H-15, H-13), 8.05 (1H, s, H-

3), 13.09 (1H, s-br, H-1); ^{13}C -NMR (125 MHz, DMSO- d_6) δ ppm 60.9 (C-10), 112.6 (C-8), 120.1 (C-5), 122.5 (C-4), 123.1 (C-6), 126.4 (C-7), 128.0 (C-13), 129.1 (C-14), 133.4 (C-3), 133.7 (C-15), 138.4 (C-12) 139.6 (C-9); MS (ES $^+$) m/z 273.3 [M+H] $^+$; HRMS calcd for C₁₄H₁₂N₂O₂S 273.0692 [M+H] $^+$ found 273.0697.

132 - R_f 0.42 (EtOAc /Petrol, 1:1); m.p. 184-186°C; UV λ_{max} (EtOH/nm) 379.5, 259.0, 212.0; IR ν_{max} /cm $^{-1}$ 3169, 1626, 1357, 1012, 938; ^1H -NMR (500 MHz, DMSO- d_6) δ ppm 4.21 (1H, d, J = 13.1 Hz, H-10A), 4.40 (1H, d, J = 13.1 Hz, H-10B) 6.82 (1H, d, J = 8.2 Hz, H-6), 7.31 (1H, s, H-8), 7.52 (5H, m, H-15, H-14, H-13), 7.63 (1H, d, J = 8.2 Hz, H-5), 8.04 (1H, s, H-3), 13.07 (1H, s-br, H-1); ^{13}C -NMR (125 MHz, DMSO- d_6) δ ppm 62.0 (C-10), 111.9 (C-8), 120.0 (C-5), 122.3 (C-4), 122.8 (C-6), 124.4 (C-13), 128.2 (C-7), 128.9 (C-14), 130.8 (C-15), 133.3 (C-3), 139.0 (C-12) 143.4 (C-9); MS (ES $^+$) m/z 257.3 [M+H] $^+$; HRMS calcd for C₁₄H₁₂N₂OS 257.0743 [M+H] $^+$ found 257.0747.

6-(((3-Methoxyphenyl)sulfonyl)methyl)-1H-indazole (123)

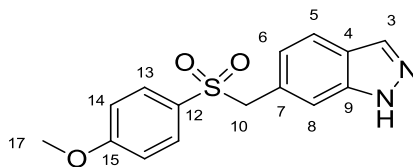


6-(((3Methoxyphenyl)thio)methyl)-1H-indazole (13.5 mg, 0.05mmol) was dissolved in MeOH (2 mL) and Oxone $^{\circ}$ solution (0.1 mL, 0.15 mmol, 1.5M in H₂O:MeOH(1:1)) was added and the mixture stirred for 18 h. After this time the reaction was diluted with water (10 mL) and extracted with EtOAc (3 x 10 mL), combined organic fractions were washed with brine (10 mL) and dried over Na₂SO₄. The material was purified by MPLC (0-80% EtOAc in petroleum ether) giving the title compound as an off white solid (6 mg, 42%).

R_f 0.30 (EtOAc /Petrol, 1:1); m.p. 160-162°C; UV λ_{max} (EtOH/nm) 290.5, 258.0; IR ν_{max} /cm $^{-1}$ 3350, 2929, 1596, 1481, 1300, 1143, 854; ^1H -NMR (500 MHz, DMSO- d_6) δ ppm 3.74 (3H, s, H-19), 4.83 (2H, s, H-10), 6.91 (1H, d, J = 8.3 Hz, H-6), 7.21 (1H, dd, J = 2.3, 1.8 Hz, H-13), 7.24-7.28 (2H, m, H-15, H-17), 7.37 (1H, s, H-8), 7.48 (1H, dd, J = 7.9, 7.9 Hz, H-16), 7.66 (1H, d, J = 8.3 Hz, H-5), 8.05 (1H, s, H-3), 13.10 (1H, s-br, H-1); ^{13}C -NMR (125 MHz, DMSO- d_6) δ ppm 55.5 (C-19), 60.8 (C-10), 112.5 (C-13), 112.7 (C-8),

120.0 (C-17), 120.1 (C-15), 120.1 (C-5), 122.5 (C-4), 123.2 (C-6), 126.4 (C-7), 130.3 (C-16), 133.4 (C-3), 139.6 (C-12), 139.6 (C-9) 159.2 (C-15); MS (ES⁺) *m/z* 303.3 [M+H]⁺; HRMS calcd for C₁₅H₁₅N₂O₃S 303.0798 [M+H]⁺ found 303.0803.

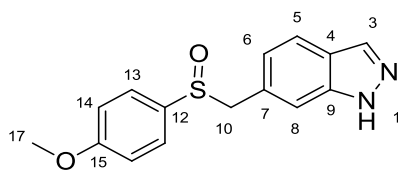
6-(((4-Methoxyphenyl)sulfonyl)methyl)-1*H*-indazole (124)



6-(((4-Methoxyphenyl)thio)methyl)-1*H*-indazole (27.5 mg, 0.1mmol) was dissolved in MeOH (2 mL) and Oxone[®] solution (0.2 mL, 0.3 mmol, 1.5M in H₂O:MeOH(1:1)) was added. This was stirred for c.a. 18 h before a further addition of Oxone[®] solution was made (0.2 mL, 0.3 mmol, 1.5 M). The reaction was stirred for 1.5 h more before dilution with water (10 mL) and extraction with EtOAc (3 x 10 mL), combined organic fractions were washed with brine and dried over Na₂SO₄. The material was purified by MPLC (0-80% EtOAc in petroleum ether) giving the title compound as a white solid (22 mg, 72%).

R_f 0.32 (EtOAc /Petrol, 1:1); m.p. 156-158^oC; UV λ_{max} (EtOH/nm) 291.0, 242.0; IR ν_{max}/cm⁻¹ 3396, 2590, 1595, 1260, 1143, 827; ¹H-NMR (500 MHz, DMSO-*d*₆) δ ppm 3.83 (3H, s, H-17), 4.75 (2H, s, H-10), 6.87 (1H, d, *J* = 8.3 Hz, H-6), 7.08 (2H, d, *J* = 8.9 Hz, H-14), 7.33 (1H, s, H-8), 7.61 (2H, d, *J* = 8.9 Hz, H-13), 7.65 (1H, d, *J* = 8.3 Hz, H-5), 8.05 (1H, s, H-3), 13.08 (1H, s-br, H-1); ¹³C-NMR (125 MHz, DMSO-*d*₆) δ ppm 55.7 (C-17), 61.2 (C-10), 112.5 (C-8), 114.2 (C-14), 120.1 (C-5), 122.4 (C-4), 123.1 (C-6), 126.7 (C-7), 130.0 (C-12), 130.3 (C-13), 133.4 (C-3), 139.6 (C-9) 163.1 (C-15); MS (ES⁺) *m/z* 303.3 [M+H]⁺; HRMS calcd for C₁₅H₁₅N₂O₃S 303.0798 [M+H]⁺ found 303.0800.

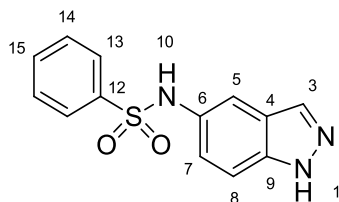
6-(((4-Methoxyphenyl)sulfinyl)methyl)-1*H*-indazole (133)



6-(((4-methoxyphenyl)thio)methyl)-1*H*-indazole (84 mg, 0.31 mmol) was dissolved in MeOH (1.5 mL) and cooled to 0°C with stirring, sodium periodate (74 mg, 0.34 mmol) was added in portions over 3 minutes and the reaction mixture was allowed to warm to RT overnight. Water (10 mL) was added and the mixture extracted with EtOAc (3 x 10 mL), combined organic fractions were washed with brine and dried over Na₂SO₄. The material was purified by MPLC (0-80% EtOAc in petroleum ether) giving the title compound as a white solid (71 mg, 80%).

*R*_f 0.38 (EtOAc /Petrol, 1:1); m.p. 167-168°C; UV λ_{max} (EtOH/nm) 251.4, 203.6; IR ν_{max}/cm⁻¹ 3171, 2957, 1593, 1494, 1248, 1019, 832; ¹H-NMR (500 MHz, DMSO-*d*₆) δ ppm 3.81 (3H, s, H-17), 4.21 (1H, d, *J* = 12.4 Hz, H-10), 4.32 (1H, d, *J* = 12.4 Hz, H-10) 6.83 (1H, d, *J* = 8.3 Hz, H-6), 7.07 (2H, d, *J* = 8.9 Hz, H-14), 7.28 (1H, s, H-8), 7.47 (2H, d, *J* = 8.9 Hz, H-13), 7.64 (1H, d, *J* = 8.3 Hz, H-5), 8.04 (1H, s, H-3), 13.06 (1H, s-br, H-1); ¹³C-NMR (125 MHz, DMSO-*d*₆) δ ppm 55.5 (C-17), 62.3 (C-10), 111.8 (C-8), 114.4 (C-14), 120.0 (C-5), 122.2 (C-4), 122.8 (C-6), 126.2 (C-13), 128.4 (C-7), 133.3 (C-3), 134.3 (C-12), 139.8 (C-9), 161.3 (C-15); MS (ES⁺) *m/z* 287.3 [M+H]⁺; HRMS calcd for C₁₅H₁₅N₂O₂S 287.0849 [M+H]⁺ found 287.0848.

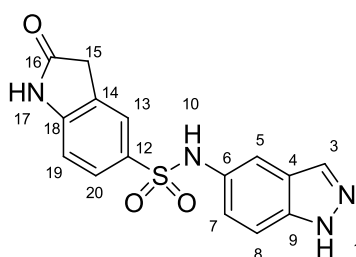
N-(1*H*-Indazol-5-yl)benzenesulfonamide (134)



Prepared according to general procedure A using 1*H*-indazol-5-amine (100 mg, 0.75 mmol) and benzenesulfonyl chloride (96 μL, 0.75 mmol). The title compound was obtained as a grey solid (48 mg, 30%).

R_f 0.36 (EtOAc /Petrol, 1:1); m.p. 176-178 °C; UV λ_{\max} (EtOH/nm) 299.0, 207.6; IR $\nu_{\max}/\text{cm}^{-1}$ 3437, 3361, 1734, 1449, 1151, 945, 687; $^1\text{H-NMR}$ (500 MHz, DMSO- d_6) δ ppm 7.07 (1H, dd, J = 9.0, 1.8 Hz, H-7), 7.40-7.42 (2H, m, H-5, H-8), 7.50 (2H, dd, J = 7.7, 7.7 Hz, H-14), 7.56 (1H, tt, J = 7.7, 1.4 Hz, H-15), 7.69 (2H, dd, J = 7.7, 1.4 Hz H-13), 7.98 (1H, s, H-3), 10.07 (1H, s-br, H-10), 13.02 (1H, s-br, H-1); $^{13}\text{C-NMR}$ (125 MHz, DMSO- d_6) δ ppm 110.6 (C-8), 112.8 (C-5), 122.2 (C-7), 122.8 (C-4), 126.6 (C-13), 129.1 (C-14), 130.2 (C-6), 132.7 (C-15), 133.4 (C-3), 137.6 (C-12), 139.4 (C-9); MS (ES^+) m/z 274.3 [$\text{M}+\text{H}$] $^+$; HRMS calcd for $\text{C}_{13}\text{H}_{12}\text{N}_3\text{O}_2\text{S}$ 274.0645 [$\text{M}+\text{H}$] $^+$ found 274.0643.

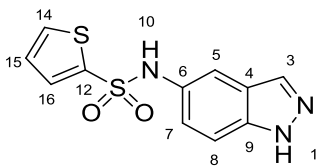
***N*-(1*H*-Indazol-5-yl)-2-oxoindoline-5-sulfonamide (135)**



Prepared according to general procedure A using 1*H*-indazol-5-amine (100 mg, 0.75 mmol) and 2-oxoindoline-5-sulfonyl chloride (173 mg, 0.75 mmol). The title compound was obtained as a green solid (12 mg, 5%).

R_f 0.25 (EtOAc /Petrol, 1:1); m.p. 230-232 °C; UV λ_{\max} (EtOH/nm) 263.6, 204.4; IR $\nu_{\max}/\text{cm}^{-1}$ 3286, 2844, 1703, 1617, 1481, 1138, 1067; $^1\text{H-NMR}$ (500 MHz, DMSO- d_6) δ ppm 3.52 (2H, s, H-15), 6.85 (1H, d, J = 8.2 Hz, H-19), 7.09 (1H, dd, J = 8.9, 1.9 Hz, H-7), 7.40-7.42 (2H, m, H-5, H-8), 7.51-7.54 (2H, m, H-13, H-20), 7.98 (1H, s, H-3), 9.95 (1H, s-br, H-17), 10.71 (1H, s-br, H-10), 13.01 (1H, s-br, H-1); $^{13}\text{C-NMR}$ (125 MHz, DMSO- d_6) δ ppm 35.5 (C-15), 108.8 (C-19), 110.6 (C-8), 112.3 (C-5), 122.0 (C-7), 122.8 (C-13), 122.8 (C-4), 126.5 (C-14), 127.5 (C-20), 130.4 (C-6), 131.9 (C-12), 133.4 (C-3), 137.5 (C-9), 147.6 (C-18), 176.4 (C-16); MS (ES^+) m/z 329.3 [$\text{M}+\text{H}$] $^+$; HRMS calcd for $\text{C}_{15}\text{H}_{13}\text{N}_4\text{O}_3\text{S}$ 329.0703 [$\text{M}+\text{H}$] $^+$ found 329.0754.

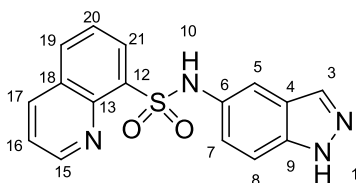
***N*-(1*H*-Indazol-5-yl)thiophene-2-sulfonamide (136)**



Prepared according to general procedure A using 1*H*-indazol-5-amine (100 mg, 0.75 mmol) and thiophene-2-sulfonyl chloride (136 mg, 0.75 mmol). The title compound was obtained as a light orange solid (166 mg, 79%).

R_f 0.36 (EtOAc /Petrol, 1:1); m.p. 170-172 °C; UV λ_{\max} (EtOH/nm) 283.4, 235.8, 200.0; IR $\nu_{\max}/\text{cm}^{-1}$ 3443, 3384, 2730, 1738, 1495, 1139, 728; $^1\text{H-NMR}$ (500 MHz, DMSO- d_6) δ ppm 7.08 (1H, dd, J = 3.8, 5.0 Hz, H-15), 7.12 (1H, dd, J = 2.6, 8.9 Hz, H-7), 7.43-7.47 (3H, m, H-5, H-8, H-16), 7.85 (1H, dd, J = 1.4, 5.0 Hz, H-14), 8.03 (1H, s, H-3), 10.19 (1H, s-br, H-10), 13.06 (1H, s-br, H-1); $^{13}\text{C-NMR}$ (125 MHz, DMSO- d_6) δ ppm 110.6 (C-8), 113.2 (C-5), 122.4 (C-7), 122.8 (C-4), 127.5 (C-15), 129.9 (C-6), 132.1 (C-16), 133.06 (C-14), 133.5 (C-3), 137.8 (C-9), 139.8 (C-12); MS (ES^+) m/z 280.3 [$\text{M}+\text{H}$] $^+$; HRMS calcd for $\text{C}_{11}\text{H}_{10}\text{N}_3\text{O}_2\text{S}_2$ 280.0209 [$\text{M}+\text{H}$] $^+$ found 280.0209.

***N*-(1*H*-Indazol-5-yl)quinoline-8-sulfonamide (137)**

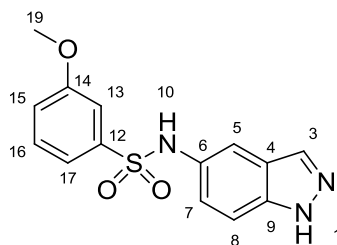


Prepared according to general procedure A using 1*H*-indazol-5-amine (100 mg, 0.75 mmol) and quinoline-8-sulfonyl chloride (171 mg, 0.75 mmol). The title compound was obtained as a grey solid (15 mg, 6%).

R_f 0.46 (EtOAc /Petrol, 1:1); m.p. 258-260 °C; UV λ_{\max} (EtOH/nm) 278.8, 215.4; IR $\nu_{\max}/\text{cm}^{-1}$ 3259, 2927, 1493, 1318, 1163, 1140, 830; $^1\text{H-NMR}$ (500 MHz, DMSO- d_6) δ ppm 7.01 (1H, dd, J = 8.9, 1.6 Hz, H-7), 7.25 (1H, d, J = 8.9 Hz, H-8), 7.32 (1H, d, J = 1.6 Hz, H-5), 7.64 (1H, dd, J = 7.6, 7.6 Hz, H-20), 7.76 (1H, dd, J = 8.3, 4.2 Hz, H-16), 7.87 (1H, s, H-3), 8.23 (1H, dd, J = 7.6, 1.4 Hz, H-19), 8.26 (1H, dd, J = 7.6, 1.4 Hz, H-21), 8.53 (1H, dd, J = 8.3, 1.8 Hz, H-17), 9.20 (1H, dd, J = 4.2, 1.8 Hz, H-15), 9.84 (1H, s-br, H-10), 12.90 (1H, s-br, H-1); $^{13}\text{C-NMR}$ (125 MHz, DMSO- d_6) δ ppm 110.3 (C-8), 112.1 (C-5),

121.9 (C-7), 122.5 (C-4), 122.6 (C-16), 128.3 (C-19), 130.3 (C-6), 131.9 (C-21), 133.2 (C-3), 134.0 (C-18), 135.1 (C-13), 137.0 (C-17), 137.4 (C-9), 142.7 (C-12), 151.5 (C-15); MS (ES^+) m/z 325.4 $[\text{M}+\text{H}]^+$; HRMS calcd for $\text{C}_{16}\text{H}_{13}\text{N}_4\text{O}_2\text{S}$ 325.0754 $[\text{M}+\text{H}]^+$ found 325.0752.

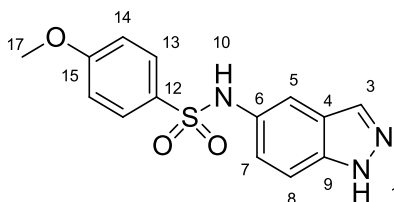
***N*-(1*H*-Indazol-5-yl)-3-methoxybenzenesulfonamide (138)**



Prepared according to general procedure A using 1*H*-indazol-5-amine (100 mg, 0.75 mmol) and 3-methoxybenzene-1-sulfonyl chloride (106 μL , 0.75 mmol). The title compound was obtained as a white solid (139 mg, 63%).

R_f 0.34 (EtOAc /Petrol, 1:1); m.p. 170-172 $^{\circ}\text{C}$; UV λ_{max} (EtOH/nm) 284.4, 202.0; IR $\nu_{\text{max}}/\text{cm}^{-1}$ 3368, 3243, 1484, 1311, 1157, 809; ^1H -NMR (500 MHz, $\text{DMSO}-d_6$) δ ppm 3.73 (3H, s, H-19), 7.09 (1H, dd, $J=9.0, 1.8$ Hz, H-7), 7.13 (1H, ddd, $J=0.8, 2.5, 8.3$ Hz, H-15), 7.50 (1H, dd, $J=1.7, 2.5$ Hz, H-13), 7.24 (1H, ddd, $J=7.7, 1.7, 0.8$ Hz, H-17), 7.39-7.43 (3H, m, H-5, H-8, H-16), 8.00 (1H, s, H-3), 10.06 (1H, s-br, H-10), 13.03 (1H, s-br, H-1); ^{13}C -NMR (125 MHz, $\text{DMSO}-d_6$) δ ppm 55.5 (C-19), 110.6 (C-8), 111.7 (C-13), 112.9 (C-5), 118.5 (C-15), 118.8 (C-17), 122.2 (C-7), 122.8 (C-4), 130.1 (C-6), 130.3 (C-16), 133.4 (C-3), 137.6 (C-9), 140.6 (C-12), 159.2 (C-14); MS (ES^+) m/z 304.4 $[\text{M}+\text{H}]^+$; HRMS calcd for $\text{C}_{14}\text{H}_{14}\text{N}_3\text{O}_3\text{S}$ 304.0750 $[\text{M}+\text{H}]^+$ found 304.0751.

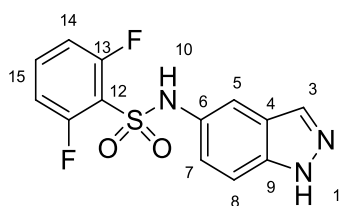
***N*-(1*H*-Indazol-5-yl)-4-methoxybenzenesulfonamide (139)**



Prepared according to general procedure A using 1*H*-indazol-5-amine (100 mg, 0.75 mmol) and 4-methoxybenzene-1-sulfonyl chloride (155 mg, 0.75 mmol). The title compound was obtained as a white solid (143 mg, 63%).

R_f 0.35 (EtOAc /Petrol, 1:1); m.p. 187-189 °C; UV λ_{\max} (EtOH/nm) 299.6, 241.6, 202.2; IR $\nu_{\max}/\text{cm}^{-1}$ 3357, 3238, 1592, 1498, 1259, 1151, 811; ^1H -NMR (500 MHz, DMSO- d_6) δ ppm 3.77 (3H, s, H-17), 7.01 (2H, d, J = 8.9 Hz, H-14), 7.07 (1H, dd, J = 9.0, 1.8 Hz, H-7), 7.40-7.41 (2H, m, H-5, H-8), 7.61 (2H, d, J = 8.9 Hz, H-13), 7.99 (1H, s, H-3), 9.91 (1H, s-br, H-10), 13.00 (1H, s-br, H-1); ^{13}C -NMR (125 MHz, DMSO- d_6) δ ppm 55.5 (C-17), 110.6 (C-8), 112.5 (C-5), 114.2 (C-14), 122.1 (C-7), 122.8 (C-4), 128.8 (C-13), 130.4 (C-6), 131.0 (C-12), 133.4 (C-3), 137.6 (C-9), 162.2 (C-15); MS (ES^+) m/z 304.3 $[\text{M}+\text{H}]^+$; HRMS calcd for $\text{C}_{14}\text{H}_{14}\text{N}_3\text{O}_3\text{S}$ 304.0750 $[\text{M}+\text{H}]^+$ found 304.0749.

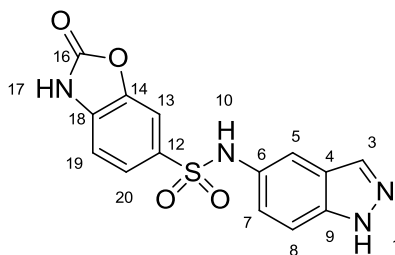
2,6-Difluoro-*N*-(1*H*-indazol-5-yl)benzenesulfonamide (140)



Prepared according to general procedure A using 1*H*-indazol-5-amine (100 mg, 0.75 mmol) and 2,6-difluorobenzene-1-sulfonyl chloride (101 μL , 0.75 mmol). The title compound was obtained as a yellow solid (58 mg, 25%).

R_f 0.37 (EtOAc /Petrol, 1:1); m.p. 243-245 °C; UV λ_{\max} (EtOH/nm) 299.2, 255.6, 210.2; IR $\nu_{\max}/\text{cm}^{-1}$ 3386, 2981, 1613, 1467, 1353, 1169, 1002, 772; ^1H -NMR (500 MHz, DMSO- d_6) δ ppm 7.16 (1H, dd, J = 8.6, 1.6 Hz, H-7), 7.22 (2H, dd, J = 9.0, 9.0 Hz, H-14), 7.46 (1H, d, J = 8.6 Hz, H-8), 7.49 (1H, d, J = 1.6 Hz, H-5), 7.76 (1H, dddd, J = 6.1, 6.1, 8.5, 8.5, H-15), 8.02 (1H, s, H-3), 10.66 (1H, s-br, H-10), 13.08 (1H, s-br, H-1); ^{13}C -NMR (125 MHz, DMSO- d_6) δ ppm 110.9 (C-8), 112.4 (C-5), 113.3 (d, J_{FC} = 23.4 Hz, C-14), 113.3 (d, J_{FC} = 23.4 Hz, C-14'), 116.4 (C-12), 121.7 (C-7), 122.7 (C-4), 129.2 (C-6), 133.5 (C-3), 135.8 (t, J_{FC} = 11.1 Hz, C-15), 137.7 (C-9), 158.9 (d, J_{FC} = 256.8 Hz, C-13), 158.9 (d, J_{FC} = 256.8 Hz, C-13); ^{19}F NMR (470 MHz, DMSO- d_6) δ -107.5; MS (ES^+) m/z 310.3 $[\text{M}+\text{H}]^+$; HRMS calcd for $\text{C}_{13}\text{H}_{10}\text{F}_2\text{N}_3\text{O}_2\text{S}$ 310.0456 $[\text{M}+\text{H}]^+$ found 310.0457.

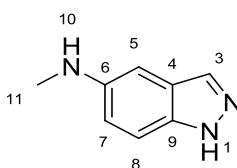
***N*-(1*H*-Indazol-5-yl)-2-oxo-2,3-dihydrobenzo[*d*]oxazole-6-sulfonamide (141)**



Prepared according to general procedure A using 1*H*-indazol-5-amine (100 mg, 0.75 mmol) and 2-oxo-2,3-dihydrobenzo[*d*]oxazole-6-sulfonyl chloride (175 mg, 0.75 mmol). The title compound was obtained as a grey solid (24 mg, 10%).

R_f 0.24 (EtOAc /Petrol, 1:1); m.p. >300 °C; UV λ_{\max} (EtOH/nm) 286.8, 247.8, 202.8; IR $\nu_{\max}/\text{cm}^{-1}$ 3382, 3242, 1770, 1484, 1347, 1168, 947; $^1\text{H-NMR}$ (500 MHz, DMSO- d_6) δ ppm 7.08 (1H, dd, J = 8.9, 2.0 Hz, H-7), 7.15 (1H, d, J = 8.2 Hz, H-19), 7.40-7.42 (2H, m, H-5, H-8), 7.46 (1H, dd, J = 8.2, 1.6 Hz, H-20), 7.56 (1H, d, J = 1.6 Hz, H-13), 8.00 (1H, s, H-3), 10.04 (1H, s-br, H-10), 12.10 (1H, s-br, H-17), 13.03 (1H, s-br, H-1); $^{13}\text{C-NMR}$ (125 MHz, DMSO- d_6) δ ppm 107.8 (C-13), 109.7 (C-19), 110.7 (C-8), 112.8 (C-5), 122.2 (C-7), 122.8 (C-4), 123.5 (C-20), 130.1 (C-6), 132.6 (C-18), 133.4 (C-3), 137.6 (C-9), 140.4 (C-12), 142.8 (C-14), 154.1 (C-16); MS (ES^+) m/z 331.4 [$\text{M}+\text{H}$] $^+$; HRMS calcd for $\text{C}_{14}\text{H}_{11}\text{N}_4\text{O}_4\text{S}$ 331.0496 [$\text{M}+\text{H}$] $^+$ found 331.0497.

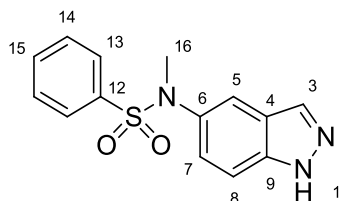
***N*-Methyl-1*H*-indazol-5-amine (150)**



5-Aminoindazole (1.0 g, 7.5 mmol) was taken in freshly prepared sodium methoxide solution (sodium (900 mg) in MeOH (20 mL)) followed by paraformaldehyde (340 mg, 10.5 mmol) and stirred at RT for 5 h. After this time sodium borohydride (280 mg, 7.5 mmol) was added and the mixture refluxed at 80°C for 2 h. The solution was hydrolysed in sodium hydroxide (1 M, 10 mL) and extracted with EtOAc (3 x 10 mL). Combined organic fractions were washed with brine (10 mL) and dried over Na_2SO_4 . The compound was purified by MPLC (0-60% EtOAc in petroleum ether). The pure product was isolated as a brown solid (622 mg, 62%).

R_f 0.23 (EtOAc /Petrol, 1:1); m.p. 144-145 °C (lit: 144-146 °C)¹⁹⁹; UV λ_{\max} (EtOH/nm) 334.0, 216.2; IR $\nu_{\max}/\text{cm}^{-1}$ 3432, 3137, 1500, 954, 853, 797; $^1\text{H-NMR}$ (500 MHz, DMSO- d_6) δ ppm 2.68 (3H, d, J = 5.2 Hz, H-11), 5.39 (1H, d, J = 5.2 Hz, H-10), 6.57 (1H, s, H-5), 6.79 (1H, d, J = 8.9 Hz H-7), 7.27 (1H, d, J = 8.9 Hz, H-8), 7.77 (1H, s, H-3), 12.59 (1H, br, H-1); $^{13}\text{C-NMR}$ (125 MHz, DMSO- d_6) δ ppm 30.5 (C-11), 96.0 (C-5), 110.4 (C-7), 117.8 (C-8), 123.9 (C-4), 131.7 (C-3), 134.3 (C-6), 144.4 (C-9); MS (ES^+) m/z 148.02 $[\text{M}+\text{H}]^+$;

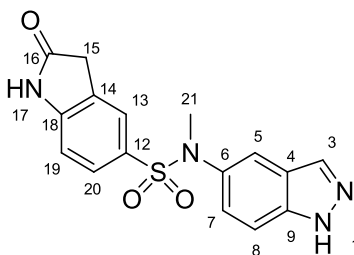
***N*-(1*H*-Indazol-5-yl)-*N*-methylbenzenesulfonamide (142)**



Prepared according to general procedure A using *N*-methyl-1*H*-indazol-5-amine (80 mg, 0.54 mmol) and benzenesulfonyl chloride (70 μL , 0.54 mmol). The title compound was obtained as an off white solid (68 mg, 44%).

R_f 0.38 (EtOAc /Petrol, 1:1); m.p. 154.5-155.3 °C; UV λ_{\max} (EtOH/nm) 292.4, 209.0; IR $\nu_{\max}/\text{cm}^{-1}$ 3145, 2948, 1504, 1446, 1345, 1158, 954, 726; $^1\text{H-NMR}$ (500 MHz, DMSO- d_6) δ ppm 3.19 (3H, s, H-16), 7.05 (1H, dd, J = 9.0, 2.0 Hz, H-7), 7.42 (1H, d, J = 2.0 Hz, H-5), 7.48 (1H, d, J = 9.0 Hz, H-8), 7.51 (2H, dd, J = 8.3, 1.6 Hz, H-13), 7.57 (2H, dd, J = 8.3, 8.3 Hz, H-14), 7.69 (1H, tt, J = 8.3, 1.6 Hz H-15), 8.05 (1H, s, H-3), 13.19 (1H, s-br, H-1); $^{13}\text{C-NMR}$ (125 MHz, DMSO- d_6) δ ppm 38.6 (C-16), 110.3 (C-8), 118.5 (C-5), 122.6 (C-4), 125.4 (C-7), 127.5 (C-13), 129.2 (C-14), 133.2 (C-15), 133.8 (C-3), 133.9 (C-6), 135.9 (C-12), 138.6 (C-9); MS (ES^+) m/z 288.3 $[\text{M}+\text{H}]^+$; HRMS calcd for $\text{C}_{14}\text{H}_{14}\text{N}_3\text{O}_2\text{S}$ 288.0801 $[\text{M}+\text{H}]^+$ found 288.0801.

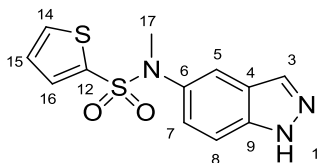
***N*-(1*H*-Indazol-5-yl)-*N*-methyl-2-oxoindoline-5-sulfonamide (143)**



Prepared according to general procedure A using *N*-methyl-1*H*-indazol-5-amine (80 mg, 0.54 mmol) and 2-oxoindoline-5-sulfonyl chloride (126 mg, 0.54 mmol). The title compound was obtained as a dull white solid (9 mg, 4%).

R_f 0.26 (EtOAc /Petrol, 1:1); m.p. 249-251 °C; UV λ_{\max} (EtOH/nm) 263.0, 210.4; IR $\nu_{\max}/\text{cm}^{-1}$ 3186, 2861, 1711, 1618, 1480, 1340, 1237, 1147; ^1H -NMR (500 MHz, DMSO- d_6) δ ppm 3.15 (3H, s, H-21), 3.55 (2H, s, H-15), 6.91 (1H, d, J = 8.3 Hz, H-19), 7.06 (1H, dd, J = 8.7, 2.0 Hz, H-7), 7.78 (1H, dd, J = 8.3, 1.7 Hz, H-20), 7.38 (1H, s, H-13), 7.45 (1H, d, J = 2.0 Hz, H-5), 7.48 (1H, d, J = 8.7 Hz, H-8), 8.06 (1H, s, H-3), 10.84 (1H, s-br, H-17), 13.17 (1H, s-br, H-1); ^{13}C -NMR (125 MHz, DMSO- d_6) δ ppm 35.6 (C-15), 38.6 (C-21), 108.9 (C-19), 110.2 (C-8), 118.5 (C-5), 122.6 (C-4), 123.7 (C-13), 125.6 (C-7), 126.6 (C-14), 128.2 (C-12), 128.4 (C-20), 133.9 (C-3), 134.1 (C-6), 138.6 (C-9), 148.0 (C-18), 176.4 (C-16); MS (ES^+) m/z 343.4 $[\text{M}+\text{H}]^+$; HRMS calcd for $\text{C}_{16}\text{H}_{15}\text{N}_4\text{O}_3\text{S}$ 343.0859 $[\text{M}+\text{H}]^+$ found 343.0858.

***N*-(1*H*-Indazol-5-yl)-*N*-methylthiophene-2-sulfonamide (144)**

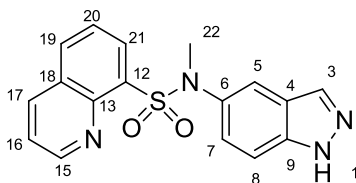


Prepared according to general procedure A using *N*-methyl-1*H*-indazol-5-amine (80 mg, 0.54 mmol) and thiophene-2-sulfonyl chloride (99 mg, 0.54 mmol). The title compound was obtained as a pink solid (74 mg, 74%).

R_f 0.37 (EtOAc /Petrol, 1:1); m.p. 164-165 °C; UV λ_{\max} (EtOH/nm) 212.0; IR $\nu_{\max}/\text{cm}^{-1}$ 3260, 3150, 1506, 1341, 1160, 942, 708; ^1H -NMR (500 MHz, DMSO- d_6) δ ppm 3.23 (3H, s, H-17), 7.09 (1H, dd, J = 2.0, 8.8 Hz, H-7), 7.24 (1H, dd, J = 3.8, 5.0 Hz, H-15), 7.46 (1H, dd, J = 3.8, 1.3 Hz, H-16), 7.48 (1H, d, J = 2.0 Hz, H-5), 7.51 (1H, d, J = 8.8 Hz, H-8), 8.01

(1H, dd, $J = 1.3, 5.0$ Hz, H-14), 8.07 (1H, s, H-3), 13.20 (1H, s-br, H-1); ^{13}C -NMR (125 MHz, DMSO- d_6) δ ppm 38.6 (C-17), 110.3 (C-8), 118.5 (C-5), 122.6 (C-4), 125.4 (C-7), 128.0 (C-15), 133.1 (C-16), 133.6 (C-3), 133.9 (C-6, C-14), 135.6 (C-12), 138.7 (C-9); MS (ES^+) m/z 294.3 $[\text{M}+\text{H}]^+$; HRMS calcd for $\text{C}_{12}\text{H}_{12}\text{N}_3\text{O}_2\text{S}_2$ 294.0365 $[\text{M}+\text{H}]^+$ found 294.0365.

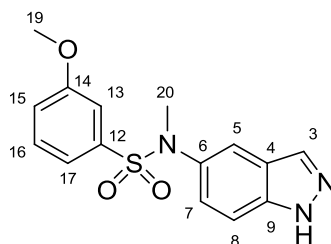
***N*-(1*H*-Indazol-5-yl)-*N*-methylquinoline-8-sulfonamide (145)**



Prepared according to general procedure A using *N*-methyl-1*H*-indazol-5-amine (80 mg, 0.54 mmol) and quinoline-8-sulfonyl chloride (124 mg, 0.54 mmol). The title compound was obtained as a white solid (105 mg, 56%).

R_f 0.49 (EtOAc / Petrol, 1:1); m.p. 164-166 °C; UV λ_{max} (EtOH/nm) 286.6, 214.6; IR $\nu_{\text{max}}/\text{cm}^{-1}$ 3304, 2943, 1495, 1325, 1158, 1127, 938, 786; ^1H -NMR (500 MHz, DMSO- d_6) δ ppm 3.66 (3H, s, H-22), 6.97 (1H, dd, $J = 8.9, 1.6$ Hz, H-7), 7.33 (1H, d, $J = 8.9$ Hz, H-8), 7.42 (1H, d, $J = 1.6$ Hz, H-5), 7.60 (1H, dd, $J = 7.7, 7.7$ Hz, H-20), 7.75 (1H, dd, $J = 8.4, 4.2$ Hz, H-16), 7.95 (1H, s, H-3), 8.13 (1H, dd, $J = 7.7, 1.4$ Hz, H-19), 8.25 (1H, dd, $J = 7.7, 1.4$ Hz, H-21), 8.56 (1H, dd, $J = 8.4, 1.8$ Hz, H-17), 9.16 (1H, dd, $J = 4.2, 1.8$ Hz, H-15), 13.08 (1H, s-br, H-1); ^{13}C -NMR (125 MHz, DMSO- d_6) δ ppm 40.9 (C-22), 110.4 (C-8), 118.9 (C-5), 122.5 (C-16), 122.7 (C-4), 125.4 (C-7), 125.6 (C-20), 128.6 (C-13), 132.8 (C-19), 133.7 (C-3, C-18), 134.0 (C-21), 136.7 (C-6), 136.9 (C-17), 138.3 (C-9), 143.4 (C-12), 151.5 (C-15); MS (ES^+) m/z 339.3 $[\text{M}+\text{H}]^+$; HRMS calcd for $\text{C}_{17}\text{H}_{15}\text{N}_4\text{O}_2\text{S}$ 339.0910 $[\text{M}+\text{H}]^+$ found 339.0909.

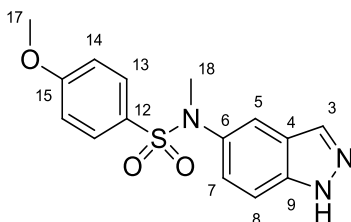
***N*-(1*H*-Indazol-5-yl)-3-methoxy-*N*-methylbenzenesulfonamide (146)**



Prepared according to general procedure A using *N*-methyl-1*H*-indazol-5-amine (80 mg, 0.54 mmol) and 3-methoxybenzene-1-sulfonyl chloride (77 μ L, 0.54 mmol). The title compound was obtained as a white solid (67 mg, 38%).

R_f 0.36 (EtOAc /Petrol, 1:1); m.p. 158-160 $^{\circ}$ C; UV λ_{\max} (EtOH/nm) 285.4, 203.4; IR $\nu_{\max}/\text{cm}^{-1}$ 3150, 2953, 1428, 1344, 1243, 1053, 956, 848, 712; ^1H -NMR (500 MHz, DMSO- d_6) δ ppm 3.19 (3H, s, H-20), 3.71 (3H, s, H-19), 7.09 (1H, dd, J = 9.0, 1.8 Hz, H-7), 6.92 (1H, dd, J = 1.8, 2.3 Hz, H-13), 7.06-7.08 (2H, m, H-7, H-17), 7.13 (1H, ddd, J = 0.7, 2.3, 8.3 Hz, H-15), 7.46 (1H, d, J = 2.0 Hz, H-5), 7.48-7.51 (2H, m, H-8, H-16), 8.07 (1H, s, H-3), 13.19 (1H, s-br, H-1); ^{13}C -NMR (125 MHz, DMSO- d_6) δ ppm 38.6 (C-20), 55.4 (C-18), 110.2 (C-8), 112.2 (C-13), 118.5 (C-5), 119.2 (C-15), 119.7 (C-17), 122.6 (C-4), 125.4 (C-7), 130.4 (C-16), 133.8 (C-3), 133.9 (C-6), 137.1 (C-12), 138.6 (C-9), 159.2 (C-14); MS (ES^+) m/z 318.3 $[\text{M}+\text{H}]^+$; HRMS calcd for $\text{C}_{15}\text{H}_{16}\text{N}_3\text{O}_3\text{S}$ 318.0907 $[\text{M}+\text{H}]^+$ found 318.0905.

***N*-(1*H*-Indazol-5-yl)-4-methoxy-*N*-methylbenzenesulfonamide (147)**

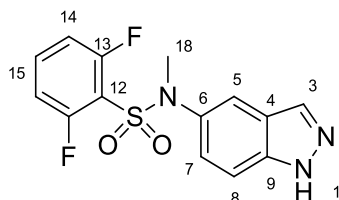


Prepared according to general procedure A using *N*-methyl-1*H*-indazol-5-amine (80 mg, 0.54 mmol) and 4-methoxybenzene-1-sulfonyl chloride (112 mg, 0.54 mmol). The title compound was obtained as a light green solid (19 mg, 11%).

R_f 0.34 (EtOAc /Petrol, 1:1); m.p. 66-68 $^{\circ}$ C; UV λ_{\max} (EtOH/nm) 247.8, 201.6; IR $\nu_{\max}/\text{cm}^{-1}$ 3349, 2945, 1594, 1496, 1336, 1256, 1155, 939, 832; ^1H -NMR (500 MHz, DMSO- d_6) δ ppm 3.15 (3H, s, H-18), 3.84 (3H, s, H-17), 7.05-7.09 (3H, m, H-7, H-14), 7.42-7.43 (3H, m, H-5, H-13), 7.49 (1H, d, J = 8.8 Hz, H-8), 8.06 (1H, s, H-3), 13.18 (1H, s-br, H-1); ^{13}C -

NMR (125 MHz, DMSO- d_6) δ ppm 38.5 (C-18), 55.6 (C-17), 110.2 (C-8), 114.3 (C-14), 118.4 (C-5), 122.6 (C-4), 125.5 (C-7), 127.5 (C-6), 129.7 (C-13), 133.9 (C-3), 134.0 (C-12), 138.6 (C-9), 162.7 (C-15); MS (ES⁺) m/z 318.4 [M+H]⁺; HRMS calcd for C₁₅H₁₆N₃O₃S 318.0907 [M+H]⁺ found 318.0908.

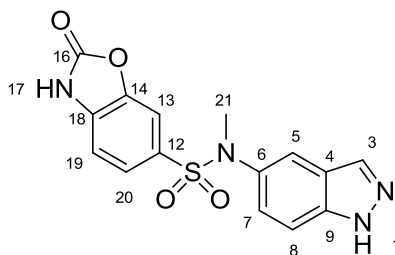
2,6-Difluoro-*N*-(1*H*-indazol-5-yl)-*N*-methylbenzenesulfonamide (148)



Prepared according to general procedure A using *N*-methyl-1*H*-indazol-5-amine (80 mg, 0.54 mmol) and 2,6-difluorobenzene-1-sulfonyl chloride (74 μ L, 0.54 mmol). The title compound was obtained as a grey solid (89 mg, 48%).

R_f 0.40 (EtOAc /Petrol, 1:1); m.p. 216.8-217.1 °C; UV λ_{\max} (EtOH/nm) 209.0; IR $\nu_{\max}/\text{cm}^{-1}$ 3327, 1609, 1462, 1361, 1170, 941, 799; ¹H-NMR (500 MHz, DMSO- d_6) δ ppm 3.35 (3H, s, H-16), 7.18 (1H, dd, J = 8.8, 1.9 Hz, H-7), 7.28 (2H, dd, J = 8.9, 8.9 Hz, H-14), 7.51 (1H, d, J = 8.8 Hz, H-8), 7.60 (1H, d, J = 1.9 Hz, H-5), 7.76 (1H, dddd, J = 6.1, 6.1, 8.5, 8.5, H-15), 8.07 (1H, s, H-3), 13.21 (1H, s-br, H-1); ¹³C-NMR (125 MHz, DMSO- d_6) δ ppm 38.8 (C-16), 110.6 (C-8), 113.6 (d, J_{FC} = 23.5 Hz, C-14), 113.6 (d, J_{FC} = 23.2 Hz, C-14'), 114.6 (C-12), 118.8 (C-5), 122.7 (C-4), 125.3 (C-7), 132.7 (C-6), 134.0 (C-3) 136.2 (t, J_{FC} = 11.2 Hz, C-15), 138.7 (C-9), 158.9 (d, J_{FC} = 257.6 Hz, C-13), 158.9 (d, J_{FC} = 257.3 Hz, C-13); ¹⁹F NMR (470 MHz, DMSO- d_6) δ -105.7 MS (ES⁺) m/z 324.3 [M+H]⁺; HRMS calcd for C₁₄H₁₂F₂N₃O₂S 324.0613 [M+H]⁺ found 324.0611.

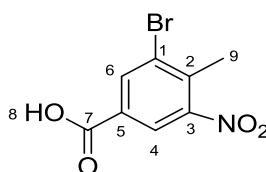
***N*-(1*H*-Indazol-5-yl)-*N*-methyl-2-oxo-2,3-dihydrobenzo[*d*]oxazole-6-sulfonamide (149)**



Prepared according to general procedure A using *N*-methyl-1*H*-indazol-5-amine (80 mg, 0.54 mmol) and 2-oxo-2,3-dihydrobenzo[*d*]oxazole-6-sulfonyl chloride (127 mg, 0.54 mmol). The title compound was obtained as a grey solid (32 mg, 26%).

R_f 0.25 (EtOAc /Petrol, 1:1); m.p. 256-257°C; UV λ_{\max} (EtOH/nm) 281.6, 253.0, 205.6; IR $\nu_{\max}/\text{cm}^{-1}$ 3633, 2991, 2725, 1772, 1485, 1348, 1168, 706; $^1\text{H-NMR}$ (500 MHz, DMSO- d_6) δ ppm 3.18 (3H, s, H-21), 7.05 (1H, dd, J = 8.9, 2.0 Hz, H-7), 7.21 (1H, d, J = 8.1 Hz, H-19), 7.24 (1H, dd, J = 8.1, 1.6 Hz, H-20), 7.43 (1H, d, J = 1.6 Hz, H-13), 7.45 (1H, d, J = 2.0 Hz, H-5), 7.48 (1H, d, J = 8.8 Hz, H-8), 8.05 (1H, s, H-3), 12.21 (1H, s-br, H-17), 13.18 (1H, s-br, H-1); $^{13}\text{C-NMR}$ (125 MHz, DMSO- d_6) δ ppm 38.7 (C-21), 108.7 (C-5), 109.7 (C-19), 110.3 (C-8), 118.7 (C-13), 122.6 (C-4), 124.4 (C-20), 125.5 (C-7), 129.1 (C-12), 133.8 (C-3), 133.9 (C-6), 134.8 (C-14), 138.6 (C-9), 142.9 (C-18), 154.2 (C-16); MS (ES^+) m/z 345.3 $[\text{M}+\text{H}]^+$; HRMS calcd for $\text{C}_{15}\text{H}_{13}\text{N}_4\text{O}_4\text{S}$ 345.0652 $[\text{M}+\text{H}]^+$ found 345.0653.

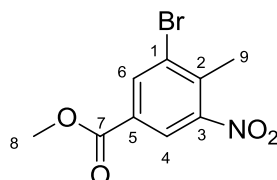
3-Bromo-4-methyl-5-nitrobenzoic acid (161)



Dibromisocyanuric acid (870 mg, 3.0 mmol) was dissolved in sulphuric acid (20 mL) and added in portions to a solution of 4-methyl-3-nitrobenzoic acid (1.00 g, 5.5 mmol) in concentrated sulphuric acid (15 mL) over *ca.* 5 minutes. This solution was stirred overnight before addition of ice (100 g) and extraction with ethyl acetate (3 x 50 mL). Combined organic fractions were washed with brine (50 mL) and dried over Na_2SO_4 . The pure product was isolated by MPLC (0-80% EtOAc in petroleum ether) giving the title compound as a pale yellow solid (1.34 g, 92%).

R_f 0.13 (Et₂O); m.p. 188-189 °C (Lit 184.5-185.5 °C)²⁰⁰; UV λ_{\max} (EtOH/nm) 229.2, 209.4; IR $\nu_{\max}/\text{cm}^{-1}$ 3086, 2815, 2539, 1696; ¹H-NMR (500 MHz, DMSO-*d*₆) δ ppm; 2.54 (3H, s, H-9), 8.32 (1H, d, J = 1.6 Hz, H-4), 8.35 (1H, d, J = 1.6 Hz, H-6), 13.84 (1H, s-br, H-8); ¹³C-NMR (125 MHz, DMSO-*d*₆) δ ppm; 19.3 (C-9), 123.8 (C-4), 126.5 (C-2), 131.0 (C-1), 136.0 (C-5), 136.3 (C-6), 150.8 (C-3), 164.4 (C-7); MS (ES⁺) m/z 260.3 [M(⁷⁹Br)+H]⁺.

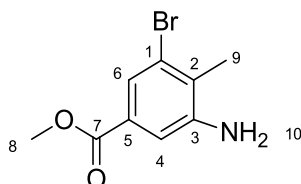
Methyl 3-bromo-4-methyl-5-nitrobenzoate (160)



3-bromo-4-methyl-5-nitrobenzoic acid (200 mg, 0.38 mmol) was dissolved in methanol (3 mL) and concentrated sulphuric acid (0.5 mL) was added. This mixture was heated at 60 °C for 18 hours then reduced under low pressure giving a residue which was redissolved in EtOAc (15 mL) and washed with water (10 mL), saturated NaHCO₃ solution (aq, 10 mL), brine (10 mL) then dried over Na₂SO₄ and the solvent removed *in vacuo* giving the desired material as an orange solid (193 mg, 92 %).

R_f 0.20 (Et₂O); m.p. 56-58 °C; UV λ_{\max} (EtOH/nm) 296.8, 230.6, 208.2; IR $\nu_{\max}/\text{cm}^{-1}$ 3423, 3079, 1717, 1607; ¹H-NMR (500 MHz, CDCl₃) δ ppm; 2.61 (3H, s, H-9), 3.95 (3H, s, H-8), 8.34 (1H, d, J = 1.4 Hz, H-4), 8.42 (1H, d, J = 1.4 Hz, H-6), ¹³C-NMR (125 MHz, CDCl₃) δ ppm; 19.7 (C-9), 52.94 (C-8), 124.0 (C-4), 127.3 (C-1), 129.9 (C-5), 136.9 (C-6), 137.1 (C-2), 151.2 (C-3), 163.9 (C-7); MS (ES⁺) m/z 274.3 [M(⁷⁹Br)+H]⁺.

Methyl 3-amino-5-bromo-4-methylbenzoate (162)

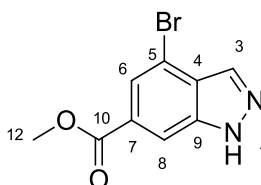


3-bromo-4-methyl-5-nitrobenzoic acid (500 mg, 1.8 mmol) was dissolved in a methanol-acetic acid solution (4:1, 10:2.5 mL) under nitrogen and zinc powder (1.25 g, 18.3 mmol) was added. This mixture was heated to 60 °C for 1 hour then filtered through Celite® and washed with MeOH (15 mL). The filtrate was reduced *in vacuo* and

purified by MPLC (0-80% EtOAc in petroleum ether) giving the desired material as an orange solid (424 mg, 95 %).

R_f 0.21 (Et₂O); m.p. 117-118 °C; UV λ_{\max} (EtOH/nm) 325.4, 231.2; IR $\nu_{\max}/\text{cm}^{-1}$ 3468, 3365, 3232, 1703, 1631; ¹H-NMR (500 MHz, DMSO-*d*₆) δ ppm; 2.20 (3H, s, H-9), 3.80 (3H, s, H-8), 5.56 (2H, s, H-10), 7.25 (1H, d, J = 1.6 Hz, H-4), 7.29 (1H, d, J = 1.6 Hz, H-6); ¹³C-NMR (125 MHz, DMSO-*d*₆) δ ppm; 17.2 (C-9), 52.1 (C-8), 113.5 (C-4), 119.6 (C-6), 124.7 (C-5), 125.0 (C-2), 128.8 (C-1), 148.4 (C-3), 165.5 (C-7); MS (ES⁺) m/z 244.3 [M(⁷⁹Br)+H]⁺.

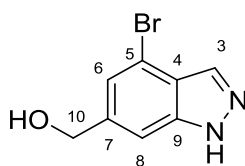
Methyl 4-bromo-1*H*-indazole-6-carboxylate (163)



Methyl 3-amino-5-bromo-4-methylbenzoate (30 mg, 0.12 mmol) was dissolved in acetic acid (2 mL) and NaNO₂ (9.4 mg, 0.14 mmol) in H₂O (0.5 mL) was added. The reaction was stirred for *ca.* 15 minutes then diluted with H₂O (10 mL) and extracted with EtOAc (3 x 10 mL), combined organic fractions were washed with brine (10 mL) and dried over Na₂SO₄ before purification by MPLC (0-95% EtOAc in petroleum ether) giving the desired product as a pale orange solid (29.5 mg, 94%).

R_f 0.59 (Et₂O); m.p. 166-168 °C; UV λ_{\max} (EtOH/nm) 312.2, 266.6, 226.2; IR $\nu_{\max}/\text{cm}^{-1}$ 3116, 3062, 2952, 2844, 1728, 1227; ¹H-NMR (500 MHz, CDCl₃) δ ppm; 3.97 (3H, s, H-12), 8.00 (1H, s, H-8), 8.16 (1H, s, H-3), 8.22 (1H, s, H-6); ¹³C-NMR (125 MHz, CDCl₃) δ ppm; 52.7 (C-12), 111.5 (C-8), 114.5 (C-5), 124.4 (C-4), 126.9 (C-6), 129.8 (C-7), 135.2 (C-3), 139.9 (C-9), 166.1 (C-10); MS (ES⁺) m/z 253.3 [M(⁷⁹Br)+H]⁺.

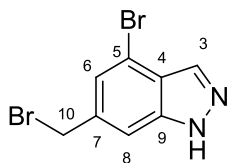
(4-Bromo-1*H*-indazol-6-yl)methanol (164)



Prepared according to general procedure **G** using Methyl 4-bromo-1*H*-indazole-6-carboxylate (1.565 g, 5.03 mmol) and LiAlH₄ (2M in THF, 6.29 mL, 12.60 mmol). The product was isolated as a white solid (1.14 g, 82%).

m.p. 210-212°C; UV λ_{max} (EtOH/nm) 288.2, 267.8, 212.8; IR ν_{max} /cm⁻¹ 3122, 3078, 2881; ¹H-NMR (500 MHz, MeOD) δ ppm; 4.73 (2H, s, H-10), 7.35 (1H, s, H-6), 7.53 (1H, s, H-8), 7.99 (1H, s, H-3); ¹³C-NMR (125 MHz, MeOD) δ ppm; 63.2 (C-10), 106.7 (C-8), 110.9 (C-4), 113.4 (C-5), 122.7 (C-6), 133.2 (C-3), 135.2 (C-3), 142.3 (C-7), 143.4 (C-9); MS (ES⁺) m/z 227.3 [M(⁷⁹Br)+H]⁺.

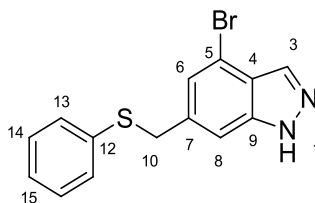
4-Bromo-6-(bromomethyl)-1*H*-indazole (159)



Prepared according to general procedure **H** using (4-bromo-1*H*-indazol-6-yl)methanol (1.14 g, 5.02 mmol), SOBr₂ (0.78 mL, 10.03 mmol) and DMF (0.04 mL, 0.5 mmol). The product was isolated as an orange solid (838 mg, 58%).

M.p. No clear m.p., decomposition range 222-225 °C; UV λ_{max} (EtOH/nm) 296.2, 266.2, 221.2; IR ν_{max} /cm⁻¹ 3149, 3110, 2967, 663; ¹H-NMR (500 MHz, DMSO-*d*₆) δ ppm; 4.87 (2H, s, H-10), 7.43 (1H, s, H-6), 7.69 (1H, s, H-8), 8.04 (1H, s, H-3), 13.55 (1H, s-br, H-1); ¹³C-NMR (125 MHz, DMSO-*d*₆) δ ppm; 34.0 (C-10), 113.0(C-8), 113.9 (C-5), 123.2 (C-4), 124.5 (C-6), 133.1 (C-3), 137.6 (C-7), 140.3 (C-9); MS (ES⁺) m/z 291.3 [M(⁷⁹Br)+H]⁺.

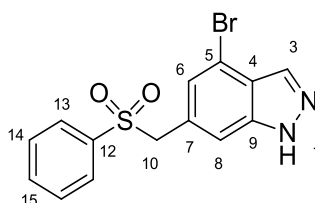
4-Bromo-6-((phenylthio)methyl)-1*H*-indazole (166)



4-Bromo-6-(bromomethyl)-1*H*-indazole (200 mg, 0.69 mmol) was taken in anhydrous THF (15 mL) under N₂ and lithium thiophenolate (0.76 mL, 0.76 mmol, 1.1 eq) was added. The solution was stirred for 4 hours at room temperature before dilution with NaOH solution (2 M, aq, 10 mL) and extraction with EtOAc (3 x 10 mL). Combined organic fractions were washed with brine (10 mL) and dried over Na₂SO₄. This material was reduced by rotary evaporator and purified by MPLC (0-80% EtOAc in petroleum ether) giving the desired product as an off white solid (201 mg, 91%).

m.p. Not clear; decomposition range 280-282 °C; UV λ_{max} (EtOH/nm) 298.2, 258.2; IR ν_{max} /cm⁻¹ 3150, 3108, 2964; ¹H-NMR (500 MHz, DMSO-*d*₆) δ ppm; 4.87 (2H, s, H-10), 7.11 (1H, s, H-6), 7.38 (1H, s, H-8), 7.60 (2H, dd, *J* = 7.8, 8.0 Hz, H-14), 7.73-7.75 (3H, m, H-15, H-13), 8.03 (1H, s, H-3), 13.49 (1H, s-br, H-1); ¹³C-NMR (125 MHz, DMSO-*d*₆) δ ppm; 60.0 (C-10), 112.4 (C-8), 112.4 (C-5), 123.3 (C-4), 125.7 (C-6), 128.1 (C-13), 128.1 (C-7), 129.2 (C-14), 133.0 (C-3), 133.9 (C-15), 138.1 (C-12) 140.1 (C-9); MS (ES⁺) *m/z* 319.2 [M(⁷⁹Br)+H]⁺.

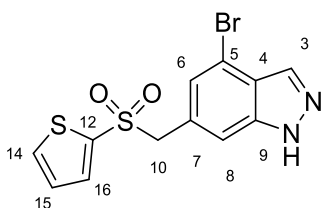
4-Bromo-6-((phenylsulfonyl)methyl)-1*H*-indazole (169)



Prepared according to general procedure **K** using 4-bromo-6-((phenylthio)methyl)-1*H*-indazole (200 mg, 0.63 mmol) and Oxone[®] (1.15 g, 1.89 mmol). The product was isolated as an off white solid (142.3 mg, 65%).

R_f 0.41 (Et₂O); m.p. 187-188 °C; UV λ_{\max} (EtOH/nm) 293.8, 271.2, 264.0, 216.0; IR $\nu_{\max}/\text{cm}^{-1}$ 3119, 2921, 1303, 1144, 950, 727; ¹H-NMR (500 MHz, DMSO-*d*₆) δ ppm; 4.87 (2H, s, H-10), 7.11 (1H, s, H-6), 7.37 (1H, s, H-8), 7.60 (2H, dd, J = 7.5, 8.0 Hz, H-14), 7.73-7.75 (3H, m, H-15, H-13), 8.02 (1H, s, H-3), 13.49 (1H, s-br, H-1); ¹³C-NMR (125 MHz, DMSO-*d*₆) δ ppm; 60.1 (C-10), 112.4 (C-8), 112.4 (C-5), 123.3 (C-4), 125.7 (C-6), 128.1 (C-13), 128.1 (C-7), 129.2 (C-14), 133.0 (C-3), 133.9 (C-15), 138.2 (C-12) 140.1 (C-9); MS (ES⁺) m/z 353.2 [M+H]⁺; HRMS calcd for C₁₄H₁₂BrN₂O₂S 350.9797 & 352.9776 [M+H]⁺ found 350.9803 & 352.9777.

4-Bromo-6-((thiophen-2-ylsulfonyl)methyl)-1*H*-indazole (170)

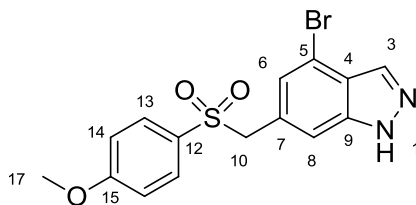


4-Bromo-6-(bromomethyl)-1*H*-indazole (100 mg, 0.34 mmol) was taken in anhydrous THF (2 mL) under N₂ and was added dropwise to a solution of thiophene-2-thiol (0.065 mL, 0.69 mmol, 2 eq) in pyridine (4 mL). The solution was stirred for 4 hours at room temperature before removal of solvent by V10. The resulting residue was suspended in NaOH solution (2 M, aq, 10 mL) and extracted into EtOAc (3 x10 mL). Combined organic fractions were washed with brine (10 mL) and dried over Na₂SO₄. This material was reduced by rotary evaporator and purified by MPLC (0-80% EtOAc in petroleum ether) giving 4-bromo-6-((thiophen-2-ylthio)methyl)-1*H*-indazole as an off white solid (89 mg, 73%). Isolated material was used directly in the next step with out characterisation according to general procedure **K** using: 4-bromo-6-((thiophen-2-ylthio)methyl)-1*H*-indazole (139 mg, 0.43 mmol) and Oxone[®] (782 mg, 1.29 mmol). The product was isolated as an off white solid (152 mg, 77%).

R_f 0.35 (Et₂O). m.p. 182-183 °C. UV λ_{\max} (EtOH/nm) 294.4, 216.0; IR $\nu_{\max}/\text{cm}^{-1}$ 3118, 2925, 1307, 1146, 951, 686; ¹H-NMR (500MHz, DMSO-*d*₆) δ ppm; 4.95 (2H, s, H-10), 7.14 (1H, s, H-6), 7.24 (1H, dd, J = 3.9, 4.9 Hz, H-15), 7.41 (1H, s, H-8), 7.61 (1H, dd, J = 1.3, 3.9 Hz, H-16), 8.03 (1H, s, H-3), 8.06 (1H, dd, J = 4.9, 1.3 Hz, H-14), 13.51 (1H, s-br, H-1). ¹³C-NMR (125 MHz, DMSO-*d*₆) δ ppm; 61.7 (C-10), 112.3 (C-8), 112.5 (C-5), 123.4

(C-4), 125.5 (C-6), 128.2 (C-15), 128.4 (C-12), 133.1 (C-3), 134.8 (C-16), 135.7 (C-14), 138.6 (C-7), 140.1 (C-9); MS (ES⁺) m/z 359.1 [M(⁷⁹Br)+H]⁺.

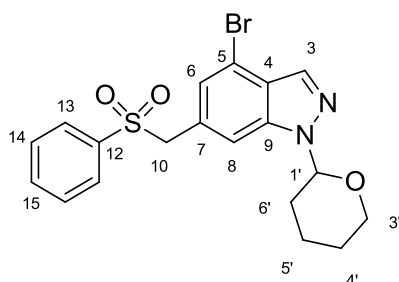
4-Bromo-6-(((4-methoxyphenyl)sulfonyl)methyl)-1H-indazole (171)



4-Bromo-6-(bromomethyl)-1H-indazole (200 mg, 0.69 mmol) was taken in anhydrous THF (2 mL) under N₂ and was added dropwise to a solution of *p*-methoxythiophenol (0.17 mL, 1.38 mmol, 2 eq) in pyridine (4 mL). The solution was stirred for 4 hours at room temperature before removal of solvent by V10. The resulting residue was suspended in NaOH solution (2 M, aq, 10 mL) and extracted into EtOAc (3 x10 mL). Combined organic fractions were washed with brine (10 mL) and dried over Na₂SO₄. This material was reduced by rotary evaporator and purified by MPLC (0-80% EtOAc in petroleum ether) giving 4-bromo-6-(((4-methoxyphenyl)thio)methyl)-1H-indazole as an off white solid (61 mg, 25%). Isolated material was used directly in the next step without characterisation according to general procedure **K** using: 4-bromo-6-(((4-methoxyphenyl)thio)methyl)-1H-indazole (61 mg, 0.17 mmol) and Oxone[®] (320 mg, 0.52 mmol). The product was isolated as an off white solid (63 mg, 95%)

R_f 0.36 (Et₂O); m.p. 181-182°C; UV λ_{max} (EtOH/nm) 294.0, 242.0, 216.8, 202.4; IR ν_{max}/cm^{-1} 3319, 2930, 1593, 1295, 1261, 1142, 1058, 833; ¹H-NMR (500 MHz, DMSO-*d*₆) δ ppm; 3.85 (3H, s, H-17), 4.79 (2H, s, H-10), 7.35 (3H, m, H-6, H-14), 7.35 (1H, s, H-8), 7.63 (2H, d, J = 8.8 Hz, H-13), 8.03 (1H, s, H-3), 13.48 (1H, s-br, H-1); ¹³C-NMR (125 MHz, DMSO-*d*₆) δ ppm; 55.8 (C-17), 60.4 (C-10), 112.3 (C-8), 112.4 (C-5), 114.3 (C-14), 123.2 (C-4), 125.7 (C-6), 128.5 (C-7), 129.7 (C-12), 130.4 (C-13), 133.0 (C-3), 140.1 (C-9) 163.3 (C-15); MS (ES⁺) m/z 383.2 [M(⁷⁹Br)+H]⁺.

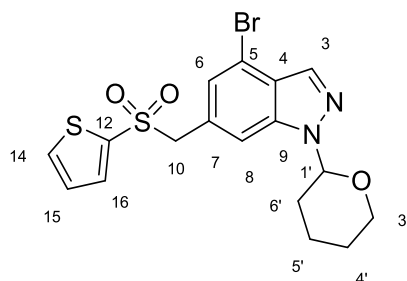
4-Bromo-6-((phenylsulfonyl)methyl)-1-(tetrahydro-2H-pyran-2-yl)-1H-indazole (173)



Prepared according to general procedure **C** 4-bromo-6-((phenylsulfonyl)methyl)-1H-indazole (60 mg, 0.17 mmol), *p*-TSA (3 mg, 0.02 mmol) and DHP (47 μ L, 0.51 mmol). The product was isolated as an off white solid (103 mg, 71%).

m.p. 151-153 $^{\circ}$ C; UV λ_{max} (EtOH/nm) 296.5, 264.0, 219.5; IR ν_{max} /cm $^{-1}$ 3066, 2937, 2844, 1304, 1156, 1080; ^1H -NMR (500 MHz, CDCl $_3$) δ ppm; 1.64-1.75 (3H, m, H-4', H-5', H-5'), 2.00-2.03 (1H, m, H-6'), 2.10-2.13 (1H, m, H-4'), 2.40-2.43 (1H, m, H-6'), 3.66-3.69 (1H, m, H-3'), 3.92-3.95 (1H, m, H-3'), 4.39 (2H, d, J = 5.1 Hz, H-10), 5.72 (1H, dd, J = 2.9, 9.1 Hz, H-1'), 6.97 (1H, d, J = 1.1 Hz, H-6), 7.29 (1H, s, H-8), 7.48 (2H, dd, J = 7.5, 8.1 Hz, H-14), 7.63 (1H, tt, J = 1.2, 7.5 Hz, H-15), 7.67 (2H, dd, J = 8.1, 1.2 Hz, H-13), 7.99 (1H, s, H-3); ^{13}C -NMR (125 MHz, CDCl $_3$) δ ppm; 22.3 (C-4') 25.0 (C-5'), 29.3 (C-6'), 62.7 (C-10), 67.4 (C-3'), 85.8 (C-1'), 112.0 (C-8), 114.5 (C-4), 126.5 (C-6), 127.7 (C-), 128.7 (C-13), 129.1 (C-14), 133.8 (C-3), 133.9 (C-15); MS (ES $^{+}$) m/z 435.2 [M+H] $^{+}$; HRMS calcd for C $_{19}$ H $_{20}$ BrN $_2$ O $_3$ S 435.0373 & 437.0351 [M+H] $^{+}$ found 435.0371 & 437.0348.

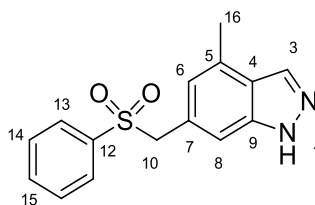
4-Bromo-1-(tetrahydro-2H-pyran-2-yl)-6-((thiophen-2-ylsulfonyl)methyl)-1H-indazole (174)



Prepared according to general procedure **C** using 4-bromo-6-((thiophen-2-ylsulfonyl)methyl)-1H-indazole (117 mg, 0.33 mmol), *p*-TSA (6 mg, 0.03 mmol) and DHP (84 μ L, 0.99 mmol). The product was isolated as an off white solid (103 mg, 71%)

m.p. 64-66°C; UV λ_{max} (EtOH/nm) 293.1, 260.2, 220.1; IR ν_{max} /cm⁻¹ 3374, 2928, 1355, 1147; ¹H-NMR (500 MHz, DMSO-*d*₆) δ ppm; 1.55-1.59 (2H, m, H-5', H-4'), 1.73-1.76 (1H, m, H-4'), 1.93-1.96 (1H, m, H-5'), 1.99-2.03 (1H, m, H-6'), 2.27-2.30 (1H, m, H-6'), 3.66-3.71 (1H, m, H-3'), 3.86-3.89 (1H, m, H-3'), 4.94 (2H, s, H-10), 5.72 (1H, dd, *J* = 2.0, 9.2 Hz, H-1'), 7.25 (1H, s, H-6), 7.27 (1H, dd, *J* = 4.8, 3.6 Hz, H-15), 7.51 (1H, s, H-8), 7.34 (1H, dd, *J* = 1.0, 3.6 Hz, H-16), 8.08-8.09 (2H, m, H-5, H-14); ¹³C-NMR (125 MHz, DMSO-*d*₆) δ ppm; 22.2 (C-4') 25.1 (C-5'), 28.9 (C-6'), 62.6 (C-10), 67.4 (C-3'), 85.4 (C-1'), 62.3 (C-10), 113.3 (C-8), 112.5 (C-5), 123.2 (C-4), 125.5 (C-6), 127.9 (C-15), 129.0 (C-12), 133.3 (C-3), 134.7 (C-16), 136.0 (C-14), 139.1 (C-7), 140.2 (C-9); MS (ES⁺) *m/z* 442.4 [M(⁷⁹Br)+H]⁺.

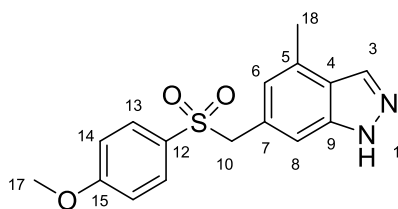
4-Methyl-6-((phenylsulfonyl)methyl)-1*H*-indazole (172)



Prepared according to general procedure **L** using 4-bromo-6-((phenylsulfonyl)methyl)-1-(tetrahydro-2*H*-pyran-2-yl)-1*H*-indazole (45 mg, 0.10 mmol), Pd(dppf)Cl₂.DCM (7 mg, 0.01 mmol), Cs₂CO₃ (51 mg, 0.15 mmol) and methylboronic acid (19 mg, 0.31 mmol). The product was isolated as an off white solid (12.4 mg, 41%).

*R*_f 0.40 (Et₂O); m.p. 120-122 °C; UV λ_{max} (EtOH/nm) 293.8, 258.2, 216.0; IR ν_{max} /cm⁻¹ 3337, 2357, 1625, 1446, 1305, 1148, 1083, 686; ¹H-NMR (500 MHz, DMSO-*d*₆) δ ppm; 2.46 (3H, s, H-16), 4.76 (2H, s, H-10), 6.65 (1H, s, H-6), 7.14 (1H, s, H-8), 7.59 (2H, dd, *J* = 7.5, 8.0 Hz, H-14), 7.71-7.74 (3H, m, H-15, H-13), 8.09 (1H, s, H-3), 13.04 (1H, s-br, H-1); ¹³C-NMR (125 MHz, DMSO-*d*₆) δ ppm; 18.3 (C-16), 61.0 (C-10), 110.2 (C-8), 122.9 (C-6), 123.0 (C-4), 126.4 (C-5), 128.0 (C-13), 129.1 (C-14), 129.9 (C-7), 132.4 (C-3), 133.7 (C-15), 138.5 (C-12), 139.6 (C-9); MS (ES⁺) *m/z* 287.3 [M+H]⁺; HRMS calcd for C₁₅H₁₅N₂O₂S 287.0849 [M+H]⁺ found 287.0852.

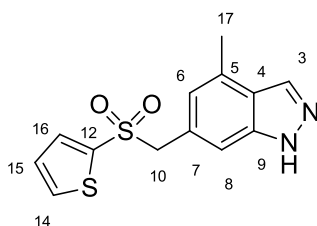
6-(((4-Methoxyphenyl)sulfonyl)methyl)-4-methyl-1*H*-indazole (180)



Prepared according to general procedure **C** using 4-bromo-6-(((4-methoxyphenyl)sulfonyl)methyl)-1*H*-indazole (63 mg, 0.17 mmol), *p*-TSA (3 mg, 0.02 mmol) and DHP (42 μ L, 0.50 mmol). 4-Bromo-6-(((4-methoxyphenyl)sulfonyl)methyl)-1-(tetrahydro-2*H*-pyran-2-yl)-1*H*-indazole was isolated as an off white solid (44 mg, 58%) and used in the next step without characterisation according to general procedure **L** using 4-bromo-6-(((4-methoxyphenyl)sulfonyl)methyl)-1-(tetrahydro-2*H*-pyran-2-yl)-1*H*-indazole (44 mg, 0.09 mmol), Pd(dppf)Cl₂·DCM (6 mg, 0.01 mmol), Cs₂CO₃ (46 mg, 0.14 mmol) and methyboronic acid (19 mg, 0.31 mmol). The product was isolated as an off white solid (15.8 mg, 52%).

*R*_f 0.37 (Et₂O); m.p. 189-191 °C; UV λ_{max} (EtOH/nm) 293.0, 242.0, 216.0; IR ν_{max} /cm⁻¹ 3329, 2929, 1602, 1401, 1304, 1145, 1014, 854, 722; ¹H-NMR (500 MHz, CDCl₃) δ ppm; 2.52 (3H, s, H-18), 3.85 (3H, s, H-17), 4.36 (2H, s, H-10), 6.67 (1H, s, H-6), 6.89 (2H, d, *J* = 8.9 Hz, H-14), 7.09 (1H, s, H-8), 7.56 (2H, d, *J* = 8.9 Hz, H-13), 8.09 (1H, s, H-3); ¹³C-NMR (125 MHz, CDCl₃) δ ppm; 18.6 (C-18), 55.7 (C-17), 63.5 (C-10), 109.8 (C-8), 114.1 (C-14), 120.1 (C-4), 123.9 (C-6), 127.3 (C-5), 129 (C-12), 130.3 (C-13), 133.4 (C-3), 139.6 (C-9), 163.1 (C-15); MS (ES⁺) *m/z* 317.3 [M+H]⁺.

4-Methyl-6-((thiophen-2-ylsulfonyl)methyl)-1*H*-indazole (179)

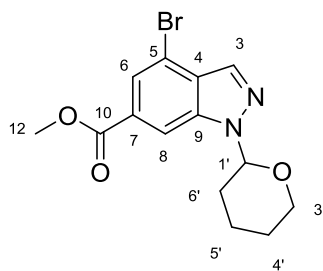


Prepared according to general procedure **L** using 4-bromo-1-(tetrahydro-2*H*-pyran-2-yl)-6-((thiophen-2-ylsulfonyl)methyl)-1*H*-indazole (50 mg, 0.11 mmol),

Pd(dppf)Cl₂.DCM (6 mg, 0.01 mmol), Cs₂CO₃ (55 mg, 0.17 mmol) and methyboronic acid (21 mg, 0.34 mmol). The product was isolated as an off white solid (18 mg, 54%).

R_f 0.34 (EtOAc /Petrol, 1:1). m.p. 115-117 °C. UV λ_{max} (EtOH/nm) 257.4, 215.8; IR ν_{max} /cm⁻¹ 3181, 1400, 1308, 1149, 849, 738; ¹H-NMR (500MHz, CDCl₃) δ ppm; 2.54 (3H, s, H-17), 4.50 (2H, s, H-10), 6.70 (1H, s, H-6), 7.05 (1H, dd, *J* = 3.8, 4.9 Hz, H-15), 7.19 (1H, s, H-8), 7.39 (1H, dd, *J* = 1.8, 3.8 Hz, H-16), 7.65 (1H, dd, *J* = 4.9, 1.8 Hz, H-14), 8.11 (1H, s, H-3); ¹³C-NMR (125 MHz, CDCl₃) δ ppm; 18.6 (C-17), 64.4 (C-10), 109.7 (C-8), 123.6 (C-6), 127.0 (C-4), 127.7 (C-15), 134.4 (C-14), 134.9 (C-16), 138.7 (C-3) *N.B. not all are carbons visible*; MS (ES⁺) *m/z* 293.3 [M+H]⁺; HRMS calcd for C₁₃H₁₃N₂O₂S₂ 293.0413 [M+H]⁺ found 293.0415.

Methyl 4-bromo-1-(tetrahydro-2H-pyran-2-yl)-1H-indazole-6-carboxylate (181)

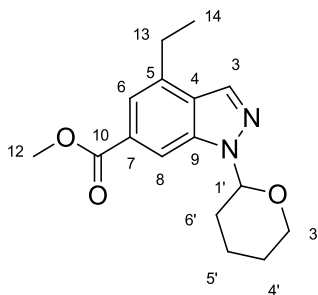


Crude methyl 4-bromo-1H-indazole-6-carboxylate (302 mg, 1.18 mmol) was dissolved in anhydrous DCM (20 mL) under N₂ and *p*-TSA (0.1 eq, 23 mg, 0.12 mmol) was added followed by DHP (3 eq, 322 μ L, 3.53 mmol). The solution was stirred at room temperature for *ca.* 18 hours then saturated NaHCO₃ solution (aq, 15 mL) was added and the solution extracted with DCM (3 x 10 mL). Combined organic fractions were dried using a phase separator and reduced to a residue by rotary evaporator. This material was purified by MPLC (0-80% EtOAc in petroleum ether) giving the desired product as a pale orange solid (330 g, 82%).

m.p. 110-112 °C; UV λ_{max} (EtOH/nm) 314.6, 267.0, 227.4; IR ν_{max} /cm⁻¹ 3107, 2948, 2855, 1715; ¹H-NMR (500 MHz, DMSO-*d*₆) δ ppm; 1.45-1.50 (1H, m, H-4'), 1.59-1.62 (1H, m, H-4'), 1.76-1.79 (1H, m, H-5') 2.00-2.06 (2H, m, H-5', H-6'), 2.37-2.40 (1H, m, H-6'B), 3.81-3.86 (2H, m, H-3') 3.93 (3H, s, H-12), 6.08 (1H, dd, *J* = 2.0, 9.0 Hz, H-1'), 7.88 (1H, d, *J* = 1.0 Hz, H-6), 8.24 (1H, s, H-3), 8.41 (1H, s, H-8); ¹³C-NMR (125 MHz, DMSO-*d*₆) δ

ppm; 21.8 (C-4') 24.7 (C-5'), 28.8 (C-6'), 52.7 (C-12), 66.4 (C-3'), 84.1 (C-1'), 112.0 (C-8), 113.5 (C-4), 123.6 (C-6), 127.1 (C-5), 128.9 (C-7), 133.3 (C-3), 139.2 (C-9), 165.3 (C-10); MS (ES⁺) m/z 339.2 [M+H]⁺; HRMS calcd for C₁₄H₁₆BrN₂O₃ 339.0339 & 341.0318 [M+H]⁺ found 339.0341 & 341.0315.

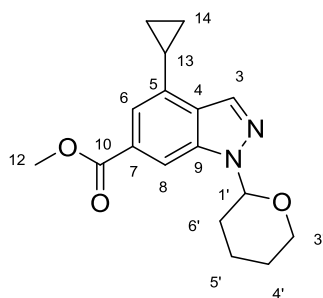
Methyl 4-ethyl-1-(tetrahydro-2H-pyran-2-yl)-1H-indazole-6-carboxylate (182)



Prepared according to general procedure **F** using Methyl 4-bromo-1-(tetrahydro-2H-pyran-2-yl)-1H-indazole-6-carboxylate (250 mg, 0.74 mmol), ethylboronic acid (165 mg, 2.21 mmol), Cs₂CO₃ (360 mg, 1.11 mmol) and Pd(dppf)Cl₂.DCM (6 mg, 0.07 mmol) in 1,4-dioxane (5 mL). The product was isolated as a white solid (184 mg, 87%).

m.p. 88-90 °C; UV λ_{max} (EtOH/nm) 314.8, 272.2, 263.8, 227.8; IR ν_{max} /cm⁻¹ 2943, 2850, 1714, 1266; ¹H-NMR (500 MHz, CDCl₃) δ ppm; 1.37 (3H, t, J = 7.6 Hz, H-14), 1.64-1.69 (1H, m, H-5'), 1.74-1.80 (2H, m, H-4', H-5'), 2.05-2.10 (1H, m, H-6'), 2.14-2.18 (1H, m, H-4'), 2.55-2.62 (1H, m, H-6'), 2.99 (2H, t, J = 7.6 Hz, H-13), 3.76-3.81 (1H, m, H-3'), 3.96 (3H, s, H-12), 4.03-4.06 (1H, m, H-3'), 5.77 (1H, dd, J = 3.0, 9.8 Hz, H-1'), 7.64 (1H, s, H-6), 8.10 (1H, s, H-8), 8.16 (1H, s, H-3); ¹³C-NMR (125 MHz, CDCl₃) δ ppm; 14.8 (C-14), 22.7 (C-4') 25.1 (C-5'), 26.2 (C-13), 29.5 (C-6'), 52.3 (C-12), 67.7 (C-3'), 85.4 (C-1'), 110.1 (C-8), 120.0 (C-6), 127.0 (C-4), 128.5 (C-5), 132.7 (C-3), 137.9 (C-9), 139.2 (C-7), 167.6 (C-10); MS (ES⁺) m/z 289.2 [M+H]⁺; HRMS calcd for C₁₆H₂₁N₂O₃ 289.1547 [M+H]⁺ found 289.1549.

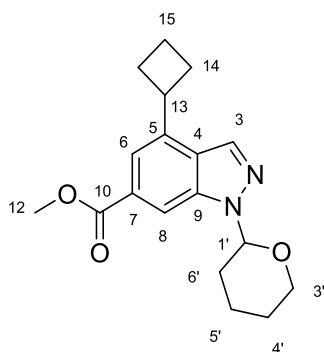
Methyl 4-cyclopropyl-1-(tetrahydro-2H-pyran-2-yl)-1H-indazole-6-carboxylate (183)



Prepared according to general procedure **F** using Methyl 4-bromo-1-(tetrahydro-2H-pyran-2-yl)-1H-indazole-6-carboxylate (250 mg, 0.74 mmol), cyclopropylboronic acid (185 mg, 2.21 mmol), Cs₂CO₃ (360 mg, 1.11 mmol) and Pd(dppf)Cl₂.DCM (6 mg, 0.07 mmol) in 1,4-dioxane (5 mL). The product was isolated as a white solid (157 mg, 71%).

UV λ_{max} (EtOH/nm) 320.6, 273.2, 265.2, 229.2; IR ν_{max} /cm⁻¹ 3083, 2945, 2851, 1714; ¹H-NMR (500 MHz, CDCl₃) δ ppm; 0.91-0.94 (2H, m, H-14), 1.07-1.11 (2H, m, H-14), 1.65-1.69 (1H, m, H-5'), 1.73-1.79 (2H, m, H-4', H-5'), 2.05-2.08 (1H, m, H-6'), 2.15-2.18 (1H, m, H-4'), 2.23-2.28 (1H, m, H-13), 2.54-2.65 (1H, m, H-6'), 3.75-3.80 (1H, m, H-3'), 3.94 (3H, s, H-12), 4.02-4.05 (1H, m, H-3'), 5.76 (1H, dd, J = 2.7, 9.6 Hz, H-1'), 7.41 (1H, s, H-6), 8.11 (1H, s, H-8), 8.19 (1H, s, H-3); ¹³C-NMR (125 MHz, CDCl₃) δ ppm; 8.6 (C-14), 13.4 (C-13), 22.8 (C-4') 25.2 (C-5'), 29.6 (C-6'), 52.4 (C-12), 67.8 (C-3'), 85.5 (C-1'), 109.8 (C-8), 117.0 (C-6), 127.7 (C-4), 128.6 (C-5), 132.9 (C-3), 138.1 (C-9), 139.6 (C-7), 167.7 (C-10); MS (ES⁺) m/z 301.3 [M+H]⁺; HRMS calcd for C₁₇H₂₁N₂O₃ 301.1547 [M+H]⁺ found 301.1546.

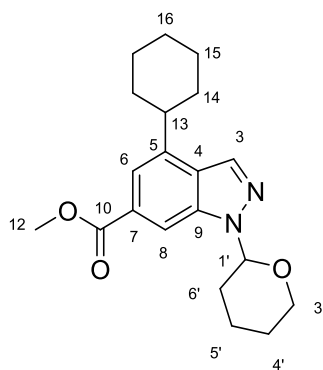
Methyl 4-cyclobutyl-1-(tetrahydro-2H-pyran-2-yl)-1H-indazole-6-carboxylate (374)



Prepared according to general procedure **F** using Methyl 4-bromo-1-(tetrahydro-2H-pyran-2-yl)-1H-indazole-6-carboxylate (250 mg, 0.74 mmol), cyclobutylboronic acid (219 mg, 2.21 mmol), Cs₂CO₃ (360 mg, 1.11 mmol) and Pd(dppf)Cl₂.DCM (60 mg, 0.07 mmol) in 1,4-dioxane (5 mL). The product was isolated as a white solid (74 mg, 32%).

m.p. 100-102 °C; UV λ_{max} (EtOH/nm) 316.4, 272.6, 228.0; IR ν_{max} /cm⁻¹ 2943, 2856, 1717; ¹H-NMR (500 MHz, CDCl₃) δ ppm; 1.65-1.69 (1H, m, H-5'), 1.73-1.80 (2H, m, H-4', H-5'), 1.91-1.97 (1H, m, H-15), 2.06-2.10 (1H, m, H-6'), 2.14-2.19 (2H, m, H-15, H-4'), 2.31-2.39 (2H, m, H-14), 2.48-2.53 (2H, m, H-14), 2.57-2.60 (1H, m, H-6'), 3.76-3.81 (1H, m, H-3'), 3.93-3.99 (4H, m, H-12, H-13), 4.02-4.05 (1H, m, H-3'), 5.78 (1H, dd, *J* = 2.7, 9.6 Hz, H-1'), 7.65 (1H, s, H-6), 8.06 (1H, s, H-3), 8.15 (1H, s, H-8); ¹³C-NMR (125 MHz, CDCl₃) δ ppm; 18.7 (C-15), 22.7 (C-4'), 25.1 (C-5'), 29.1 (C-14), 29.5 (C-6'), 38.2 (C-13), 52.3 (C-12), 67.7 (C-3'), 85.3 (C-1'), 110.0 (C-8), 118.0 (C-6), 126.0 (C-4), 128.4 (C-5), 133.0 (C-3); MS (ES⁺) *m/z* 315.3 [M+H]⁺; HRMS calcd for C₁₈H₂₃N₂O₃ 315.1703 [M+H]⁺ found 315.1703

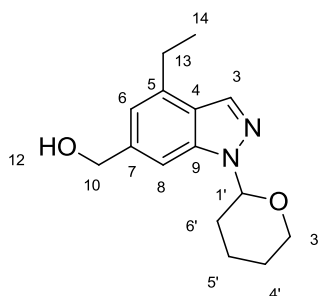
Methyl 4-cyclohexyl-1-(tetrahydro-2H-pyran-2-yl)-1H-indazole-6-carboxylate (375)



Prepared according to general procedure **F** using Methyl 4-bromo-1-(tetrahydro-2H-pyran-2-yl)-1H-indazole-6-carboxylate (250 mg, 0.74 mmol), cyclohexylboronic acid (283 mg, 2.21 mmol), Cs₂CO₃ (360 mg, 1.11 mmol) and Pd(dppf)Cl₂.DCM (60 mg, 0.07 mmol) in 1,4-dioxane (5 mL). The product was isolated as a white solid (83 mg, 33%).

m.p. 96-98 °C; UV λ_{max} (EtOH/nm) 316.2, 271.4, 264.0, 228.0; IR ν_{max}/cm⁻¹ 2936, 2852, 1714; ¹H-NMR (500 MHz, CDCl₃) δ ppm; 1.31-1.38 (1H, m, H-16), 1.44-1.54 (2H, m, H-15), 1.58-1.67 (3H, m, H-14, H-5'), 1.76-1.82 (3H, m, H-4', H-5', H-16), 1.89-1.92 (2H, m, H-15), 1.97-2.01 (2H, m, H-14), 2.06-2.09 (1H, m, H-6'), 2.15-2.17 (1H, m, H-4'), 2.57-2.61 (1H, m, H-6'), 2.95-3.01 (1H, m, H-13), 3.76-3.81 (1H, m, H-3'), 3.96 (3H, s, H-12), 4.03-4.06 (1H, m, H-3'), 5.77 (1H, dd, *J* = 2.7, 9.7 Hz, H-1'), 7.66 (1H, s, H-6), 8.13 (1H, s, H-8), 8.14 (1H, s, H-3); ¹³C-NMR (125 MHz, CDCl₃) δ ppm; 22.7 (C-4') 25.1 (C-5'), 26.2 (C-16), 26.9 (C-15), 29.5 (C-6'), 33.7 (C-14), 42.1 (C-13), 52.3 (C-12), 67.8 (C-3'), 85.3 (C-1'), 110.0 (C-8), 118.1 (C-6), 126.6 (C-4), 128.5 (C-5), 132.7 (C-3), 139.2 (C-9), 141.8 (C-7), 167.7 (C-10); MS (ES⁺) *m/z* 343.2 [M+H]⁺; HRMS calcd for C₂₀H₂₇N₂O₃ 343.2016 [M+H]⁺ found 343.2015

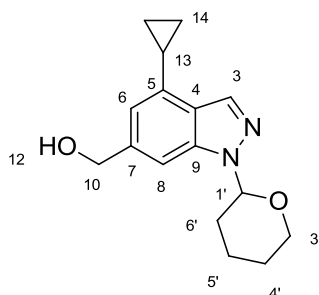
(4-Ethyl-1-(tetrahydro-2H-pyran-2-yl)-1H-indazol-6-yl)methanol (184)



Prepared according to general procedure **G** using Methyl 4-ethyl-1-(tetrahydro-2H-pyran-2-yl)-1H-indazole-6-carboxylate (368 mg, 1.28 mmol), LiAlH₄ (1M in THF, 2.6 mL, 2.21 mmol) in THF (30 mL). The product was isolated as a white solid (284 mg, 86%).

UV λ_{max} (EtOH/nm) 290.8, 256.4, 218.8; IR ν_{max} /cm⁻¹ 3368, 2932, 2855; ¹H-NMR (500 MHz, CDCl₃) δ ppm; 1.38 (3H, t, J = 7.6 Hz, H-14), 1.62-1.66 (1H, m, H-5'), 1.70-1.80 (2H, m, H-4', H-5'), 2.03-2.06 (1H, m, H-6'), 2.12-2.17 (1H, m, H-4'), 2.54-2.61 (1H, m, H-6'), 2.94 (2H, q, J = 7.6 Hz, H-13), 3.71-3.76 (1H, m, H-3'), 4.02-4.05 (1H, m, H-3'), 4.80 (2H, s, H-10), 5.69 (1H, dd, J = 2.4, 9.7 Hz, H-1'), 6.94 (1H, s, H-6), 7.42 (1H, s, H-8), 8.03 (1H, s, H-3); ¹³C-NMR (125 MHz, CDCl₃) δ ppm; 14.9 (C-14), 22.8 (C-4'), 25.1 (C-5'), 26.3 (C-13), 29.5 (C-6'), 65.7 (C-10), 67.7 (C-3'), 85.3 (C-1'), 105.5 (C-8), 118.9 (C-6), 123.9 (C-4), 132.6 (C-3), 138.1 (C-5), 139.9 (C-9), 140.2 (C-7); MS (ES⁺) m/z 261.2 [M+H]⁺; HRMS calcd for C₁₅H₂₁N₂O₂ 261.1598 [M+H]⁺ found 261.1596.

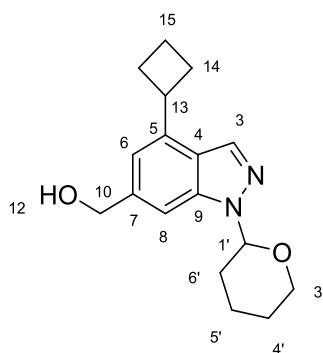
(4-Cyclopropyl-1-(tetrahydro-2H-pyran-2-yl)-1H-indazol-6-yl)methanol (185)



Prepared according to general procedure **G** using methyl 4-cyclopropyl-1-(tetrahydro-2H-pyran-2-yl)-1H-indazole-6-carboxylate (900 mg, 3.00 mmol), LiAlH₄ (1M in THF, 6 mL, 5.99 mmol) in THF (40 mL). The product was isolated as a white solid (760 mg, 93%).

UV λ_{\max} (EtOH/nm) 294.0, 259.8, 221.6; IR $\nu_{\max}/\text{cm}^{-1}$ 3353, 2935, 2853; $^1\text{H-NMR}$ (500 MHz, CDCl_3) δ ppm; 0.87-0.91 (2H, m, H-14), 1.05-1.09 (2H, m, H-14), 1.64-1.69 (1H, m, H-5'), 1.72-1.81 (2H, m, H-4', H-5'), 2.06-2.07 (1H, m, H-6'), 2.15-2.17 (1H, m, H-4'), 2.21-2.27 (1H, m, H-13), 2.54-2.61 (1H, m, H-6'), 3.73-3.78 (1H, m, H-3'), 3.94 (3H, s, H-12), 4.02-4.05 (1H, m, H-3'), 5.18 (2H, d, $J = 5.6$ Hz, H-10), 5.70 (1H, dd, $J = 2.5, 9.4$ Hz, H-1'), 7.76 (1H, s, H-6), 7.37 (1H, s, H-8), 8.12 (1H, s, H-3); $^{13}\text{C-NMR}$ (125 MHz, CDCl_3) δ ppm; 8.4 (C-14), 13.4 (C-13), 22.7 (C-4') 25.1 (C-5'), 29.4 (C-6'), 66.8 (C-10), 67.6 (C-3'), 85.2 (C-1'), 107.2 (C-8), 117.2 (C-6), 124.7 (C-4), 126.8 (C-5), 132.7 (C-3), 138.2 (C-9), 139.6 (C-7); MS (ES^+) m/z 273.4 $[\text{M}+\text{H}]^+$; HRMS calcd for $\text{C}_{16}\text{H}_{21}\text{N}_2\text{O}_2$ 273.1598 $[\text{M}+\text{H}]^+$ found 273.1598.

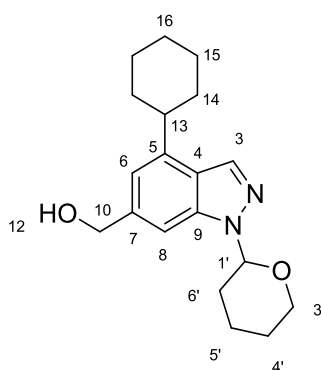
(4-Cyclobutyl-1-(tetrahydro-2H-pyran-2-yl)-1H-indazol-6-yl)methanol (376)



Prepared according to general procedure **G** using Methyl 4-cyclobutyl-1-(tetrahydro-2H-pyran-2-yl)-1H-indazole-6-carboxylate (101 mg, 0.32 mmol) and LiAlH_4 (1M in THF, 0.64 mL, 0.64 mmol). The product was isolated as an off white solid (58 mg, 64%).

UV λ_{\max} (EtOH/nm) 297.0, 257.6; IR $\nu_{\max}/\text{cm}^{-1}$ 3349, 2940, 2877; $^1\text{H-NMR}$ (500 MHz, CDCl_3) δ ppm; 1.62-1.67 (1H, m, H-5'), 1.73-1.78 (2H, m, H-4', H-5'), 1.88-1.95 (1H, m, H-15), 2.03-2.07 (1H, m, H-6'), 2.10-2.18 (2H, m, H-15, H-4'), 2.27-2.36 (2H, m, H-14), 2.44-2.51 (2H, m, H-14), 2.55-2.61 (1H, m, H-6'), 3.71-3.76 (1H, m, H-3'), 3.92 (1H, tt, $J = 8.6, 8.6$ Hz, H-13), 4.02-4.05 (1H, m, H-3'), 4.82 (2H, s, H-10), 5.69 (1H, dd, $J = 2.8, 9.6$ Hz, H-1'), 6.96 (1H, s, H-6), 7.42 (1H, s, H-8), 7.98 (1H, s, H-3); $^{13}\text{C-NMR}$ (125 MHz, CDCl_3) δ ppm; 18.7 (C-15), 22.8 (C-4'), 25.1 (C-5'), 29.1 (C-14), 29.4 (C-6'), 38.3 (C-13), 65.8 (C-10), 67.7 (C-3'), 85.3 (C-1'), 105.5 (C-8), 117.0 (C-6), 122.9 (C-4), 133.0 (C-3), 139.9 (C-5), 140.0 (C-7), 140.2 (C-9); MS (ES^+) m/z 287.3 $[\text{M}+\text{H}]^+$; HRMS calcd for $\text{C}_{17}\text{H}_{23}\text{N}_2\text{O}_2$ 287.1754 $[\text{M}+\text{H}]^+$ found 287.1756

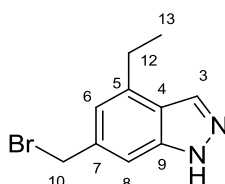
(4-Cyclohexyl-1-(tetrahydro-2H-pyran-2-yl)-1H-indazol-6-yl)methanol (377)



Prepared according to general procedure **G** using Methyl 4-hexyl-1-(tetrahydro-2H-pyran-2-yl)-1H-indazole-6-carboxylate (125.7 mg, 0.37 mmol) and LiAlH_4 (1M in THF, 0.74 mL, 0.74 mmol). The product was isolated as an off white solid (95 mg, 82%).

UV λ_{max} (EtOH/nm) 298.4, 261.0, 222.3; IR ν_{max} /cm⁻¹ 3354, 2932, 2833; ¹H-NMR (500 MHz, CDCl_3) δ ppm; 1.29-1.35 (1H, m, H-16), 1.44-1.52 (2H, m, H-15), 1.55-1.64 (3H, m, H-14, H-5'), 1.74-1.82 (3H, m, H-4', H-5', H-16), 1.88-1.90 (2H, m, H-15), 1.96-1.99 (2H, m, H-14), 2.04-2.07 (1H, m, H-6'), 2.14-2.16 (1H, m, H-4'), 2.57-2.60 (1H, m, H-6'), 2.92-2.97 (1H, m, H-13), 3.72-3.77 (1H, m, H-3'), 4.04-4.06 (1H, m, H-3'), 4.81 (2H, s, H-10), 5.70 (1H, dd, $J = 2.5, 9.5$ Hz, H-1'), 7.00 (1H, s, H-6), 7.42 (1H, s, H-8), 8.06 (1H, s, H-3); ¹³C-NMR (125 MHz, CDCl_3) δ ppm; 22.8 (C-4'), 25.2 (C-5'), 26.3 (C-16), 26.9 (C-15), 29.4 (C-6'), 33.8 (C-14), 42.6 (C-13), 65.9 (C-10), 67.7 (C-3'), 85.3 (C-1'), 105.5 (C-8), 117.1 (C-6), 123.5 (C-4), 128.5 (C-5), 132.7 (C-3), 140.0 (C-9), 140.1 (C-7), 142.1 (C-5); MS (ES^+) m/z 315.3 [$\text{M}+\text{H}$]⁺; HRMS calcd for $\text{C}_{19}\text{H}_{27}\text{N}_2\text{O}_2$ 315.2067 [$\text{M}+\text{H}$]⁺ found 315.2069.

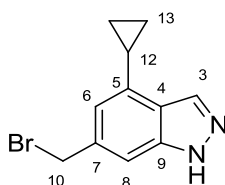
6-(Bromomethyl)-4-ethyl-1H-indazole (186)



Prepared according to general procedure **H** using (4-ethyl-1-(tetrahydro-2H-pyran-2-yl)-1H-indazol-6-yl)methanol (258 mg, 0.99 mmol), SOBr_2 (179 μL , 2.30 mmol), DMF (9 μL , 0.12 mmol) in DCM (30 mL) followed by MeOH.HCl (1.25 M, 5 mL). The product was isolated as an off white solid (153 mg, 64%).

m.p. 104-106 °C; UV λ_{max} (EtOH/nm) 263.6, 219.8, 292.2; IR ν_{max} /cm⁻¹ 3084, 2968, 2875; ¹H-NMR (500 MHz, DMSO-*d*₆) δ ppm; 1.29 (3H, t, *J* = 7.6 Hz, H-13), 2.92 (2H, q, *J* = 7.6 Hz, H-12), 4.88 (2H, s, H-10), 6.97 (1H, s, H-6), 7.44 (1H, s, H-8), 8.14 (1H, s, H-3); ¹³C-NMR (125 MHz, DMSO-*d*₆) δ ppm; 15.3 (C-13), 26.6 (C-12), 63.6 (C-10), 105.2 (C-8), 118.1 (C-6), 121.9 (C-4), 132.3 (C-3), 136.7 (C-5), 140.8 (C-9), 141.7 (C-7); MS (ES⁺) *m/z* 238.2 [M+H]⁺.

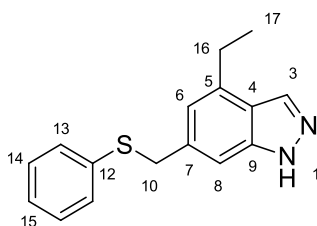
6-(Bromomethyl)-4-cyclopropyl-1*H*-indazole (187)



Prepared according to general procedure **H** using (4-cyclopropyl-1-(tetrahydro-2*H*-pyran-2-yl)-1*H*-indazol-6-yl)methanol (720 mg, 2.65 mmol), SOBr₂ (410 μ L, 5.29 mmol), DMF (20 μ L, 0.27 mmol) in DCM (65 mL) followed by MeOH.HCl (1.25 M, 10 mL). The product was isolated a white solid (573 mg, 91%).

*R*_f 0.51 (Et₂O); UV λ_{max} (EtOH/nm) 296.4, 266.8, 220.2; IR ν_{max} /cm⁻¹ 3172, 3111, 2996, 2855; ¹H-NMR (500 MHz, CDCl₃) δ ppm 0.91-0.95 (2H, m, H-13), 1.08-1.12 (2H, m, H-13), 2.24-2.28 (1H, m, H-12), 4.58 (2H, s, H-10), 6.80 (1H, s, H-6), 7.32 (1H, s, H-8), 8.18 (1H, s, H-3); ¹³C-NMR (125 MHz, CDCl₃) δ ppm; 8.5 (C-13), 13.5 (C-12), 34.2 (C-10), 107.2 (C-8), 117.8 (C-6), 123.5 (C-4), 133.7 (C-3), 136.9 (C-7), 138.5 (C-5), 140.1 (C-9); MS (ES⁺) *m/z* 253.2 [M+H]⁺; HRMS calcd for C₁₁H₁₂BrN₂ 251.0178 & 253.0158 [M+H]⁺ found 251.1018 & 253.0159.

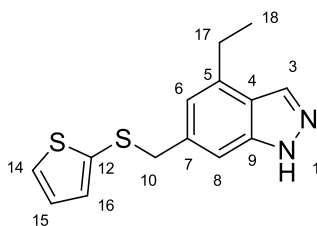
4-Ethyl-6-((phenylthio)methyl)-1*H*-indazole (188)



Prepared according to general procedure I using 6-(bromomethyl)-4-ethyl-1*H*-indazole (45 mg, 0.19 mmol) and lithium thiophenolate (1 M in THF, 0.28 mL, 0.28 mmol) in DMF (3 mL). The product was isolated a white solid (45 mg, 89%).

UV λ_{max} (EtOH/nm) 205.0, 264.2, 302.4; IR ν_{max} /cm⁻¹ 33186, 2965, 2931, 2870; ¹H-NMR (500 MHz, CDCl₃) δ ppm; 1.23 (3H, t, *J* = 7.7 Hz, H-17), 2.84 (2H, q, *J* = 7.7 Hz, H-16), 4.15 (2H, s, H-10), 6.45 (1H, s, H-6), 7.16 (1H, s, H-8), 7.22 (1H, tt, *J* = 1.1, 8.1 Hz, H-15), 7.28-7.1 (2H, m, H-14), 7.85 (1H, s, H-3), 7.46-7.50 (1H, m, H-13); ¹³C-NMR (125 MHz, CDCl₃) δ ppm; 14.6 (C-17), 26.2 (C-16), 63.9 (C-10), 109.7 (C-8), 121.7 (C-6), 126.02 (C-4), 127.2 (C-5), 127.5 (C-13), 129.0 (C-14), 130.9 (C-3), 131.3 (C-15), 135.4 (C-7), 137.0 (C-12), 138.8 (C-9); MS (ES⁺) *m/z* 269.2 [M+H]⁺; HRMS calcd for C₁₆H₁₆N₂S 269.1112 [M+H]⁺ found 269.1109.

4-Ethyl-6-((thiophen-2-ylthio)methyl)-1*H*-indazole (189)

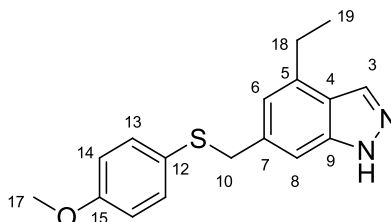


Prepared according to general procedure I using 6-(bromomethyl)-4-ethyl-1*H*-indazole (45 mg, 0.19 mmol), Cs₂CO₃ (67 mg, 0.21 mmol) and 2-thiolthiophene (27 μ L, 0.28 mmol) in DMF (6 mL). The product was isolated a grey solid (33 mg, 63%).

UV λ_{max} (EtOH/nm) 219.1, 215.8; IR ν_{max} /cm⁻¹ 3172, 3101, 2962, 2972; ¹H-NMR (500 MHz, CDCl₃) δ ppm; 1.34 (3H, t, *J* = 7.6 Hz, H-18) 2.94 (2H, q, *J* = 7.6 Hz, H-17), 4.05 (2H, s, H-10), 6.86 (1H, s, H-6), 6.88-6.92 (2H, m, H-15, H-16), 7.05 (1H, s, H-8), 7.31 (1H, dd,

$J = 1.2, 5.2$ Hz, H-14), 8.10 (1H, s, H-3); ^{13}C -NMR (125 MHz, CDCl_3) δ ppm; 14.7 (C-18), 26.3 (C-17), 44.4 (C-10), 107.4 (C-8), 120.0 (C-6), 127.5 (C-15), 129.9 (C-14), 133.4 (C-3), 134.5 (C-16), 137.3 (C-3), 137.8 (C-7), 140.4 (C-9); MS (ES^+) m/z 275.1 $[\text{M}+\text{H}]^+$; HRMS calcd for $\text{C}_{14}\text{H}_{15}\text{N}_2\text{S}$ 275.0675 $[\text{M}+\text{H}]^+$ found 275.0671.

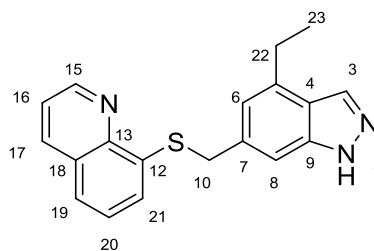
4-Ethyl-6-(((4-methoxyphenyl)thio)methyl)-1H-indazole (190)



Prepared according to general procedure I using 6-(bromomethyl)-4-ethyl-1H-indazole (45 mg, 0.19 mmol), Cs_2CO_3 (67 mg, 0.21 mmol) and 4-methoxythiophenol (35 μL , 0.28 mmol) in DMF (4 mL). The product was isolated as a white solid (34 mg, 61%).

UV λ_{max} (EtOH/nm) 263.6, 219.8, 292.2; IR $\nu_{\text{max}}/\text{cm}^{-1}$ 3177, 3103, 2930, 1491, 1241; ^1H -NMR (500 MHz, CDCl_3) δ ppm; 1.34 (3H, t, $J = 7.6$ Hz, H-19), 2.93 (2H, q, $J = 7.6$ Hz, H-18), 3.77 (3H, s, H-17), 4.08 (2H, s, H-10), 6.77 (2H, d, $J = 8.9$ Hz, H-14), 6.87 (1H, s, H-6), 7.08 (1H, s, H-8), 7.24 (2H, d, $J = 8.9$ Hz, H-13), 8.08 (1H, s, H-3); ^{13}C -NMR (125 MHz, CDCl_3) δ ppm; 14.7 (C-19), 26.3 (C-18), 41.8 (C-10), 55.5 (C-17), 107.2 (C-8), 114.5 (C-14), 121.0 (C-6), 122.0 (C-4), 125.8 (C-5), 126.3 (C-12), 133.1 (C-3), 134.3 (C-13), 137.9 (C-7), 140.3 (C-9) 159.3 (C-15); MS (ES^+) m/z 299.3 $[\text{M}+\text{H}]^+$; HRMS calcd for $\text{C}_{17}\text{H}_{19}\text{N}_2\text{OS}$ 299.1213 $[\text{M}+\text{H}]^+$ found 299.1213.

8-(((4-Ethyl-1H-indazol-6-yl)methyl)thio)quinoline (191)

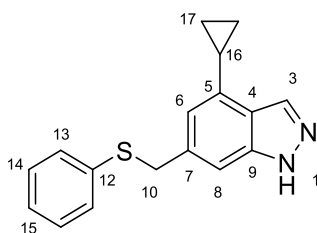


Prepared according to general procedure I using 6-(bromomethyl)-4-ethyl-1H-indazole (50 mg, 0.21 mmol), Cs_2CO_3 (143 mg, 0.44 mmol) and 8-quinolinethiol hydrochloride

(62 mg, 0.31 mmol) in DMF (2 mL). The product was isolated as a white solid (54 mg, 81%).

R_f 0.45 (EtOAc /Petrol, 1:1); UV λ_{\max} (EtOH/nm) 335.8, 292.0, 252.6, 205.8; $^1\text{H-NMR}$ (500 MHz, CDCl_3) δ ppm; 1.33 (3H, t, $J = 7.7$ Hz, H-23), 2.92 (2H, q, $J = 7.2$ Hz, H-22), 4.42 (2H, s, H-10), 7.02 (1H, s, H-6), 7.44-7.47 (2H, m, H-8, H-20), 7.51 (1H, dd, $J = 8.6$, 4.5 Hz, H-16), 8.05 (1H, dd, $J = 7.0$ Hz, H-19), 7.65 (1H, dd, $J = 7.8$ Hz, H-21), 8.22 (1H, dd, $J = 8.6$ Hz, H-17), 9.05 (1H, s, H-3); MS (ES^+) m/z 320.3 $[\text{M}+\text{H}]^+$.

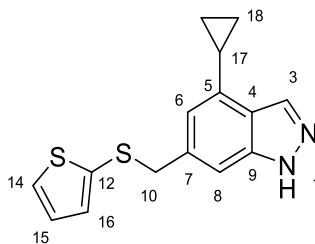
4-Cyclopropyl-6-((phenylthio)methyl)-1H-indazole (192)



Prepared according to general procedure I using 6-(bromomethyl)-4-cyclopropyl-1H-indazole (100 mg, 0.40 mmol) and lithium thiophenolate (1M in THF, 1.2 mL, 1.20 mmol) in DMF (6 mL). The product was isolated a white solid (108 mg, 97%).

R_f 0.69 (Et_2O); m.p. 87-89 $^\circ\text{C}$; UV λ_{\max} (EtOH/nm) 292.4, 257.0, 218.8; IR $\nu_{\max}/\text{cm}^{-1}$ 3108, 3049, 2996, 2851; $^1\text{H-NMR}$ (500 MHz, CDCl_3) δ ppm; 0.86 (2H, m, H-17), 1.06 (2H, m, H-17), 2.22 (1H, m, H-16), 4.18 (2H, s, H-10), 6.71 (1H, s, H-6), 7.18-7.20 (2H, m, H-8, H-15), 7.24-7.26 (2H, m, H-14), 7.29-7.31 (2H, m, H-13), 8.16 (1H, s, H-3); $^{13}\text{C-NMR}$ (125 MHz, CDCl_3) δ ppm; 8.4 (C-17), 13.4 (C-16), 39.7 (C-10), 106.8 (C-8), 117.9 (C-6), 122.5 (C-4), 126.6 (C-15), 128.9 (C-13), 130.1 (C-14), 133.1 (C-3), 136.1 (C-5), 137.3 (C-7), 137.9 (C-12), 140.2 (C-9); MS (ES^+) m/z 281.4 $[\text{M}+\text{H}]^+$; HRMS calcd for $\text{C}_{17}\text{H}_{16}\text{N}_2\text{S}$ 281.1107 $[\text{M}+\text{H}]^+$ found 281.1107.

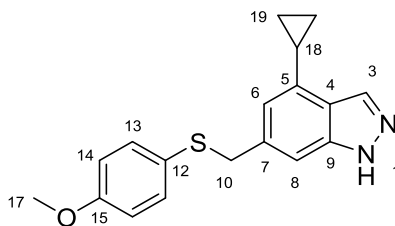
4-Cyclopropyl-6-((thiophen-2-ylthio)methyl)-1*H*-indazole (193)



Prepared according to general procedure I using 6-(bromomethyl)-4-cyclopropyl-1*H*-indazole (100 mg, 0.40 mmol), Cs₂CO₃ (143 mg, 0.44 mmol) and 2-thiolthiophene (56 μ L, 0.60 mmol) in DMF (6 mL). The product was isolated a grey solid (111 mg, 98%).

R_f 0.63 (Et₂O); m.p. 79-81 °C; UV λ_{\max} (EtOH/nm) 217.6; IR ν_{\max} /cm⁻¹ 3177, 3112, 3055, 2997, 2925, 2883, 1620; ¹H-NMR (500 MHz, CDCl₃) δ ppm; 0.84-0.87 (2H, m, H-18), 1.04-1.07 (2H, m, H-18), 2.20-2.26 (1H, m, H-17), 4.02 (2H, s, H-10), 6.59 (1H, s, H-6), 6.82-6.91 (2H, m, H-15, H-16), 7.02 (1H, s, H-8), 7.30 (1H, dd, J = 1.3, 5.1 Hz, H-14), 8.17 (1H, s, H-3), 10.49 (1H, s-br, H-1); ¹³C-NMR (125 MHz, CDCl₃) δ ppm; 8.5 (C-18), 13.4 (C-17), 44.4 (C-10), 107.0 (C-8), 117.7 (C-6), 122.7 (C-4), 127.5 (C-15), 129.9 (C-14), 133.4 (C-3), 134.5 (C-16), 136.9 (C-7), 137.7 (C-5), 140.3 (C-9); MS (ES⁺) m/z 287.2 [M+H]⁺; HRMS calcd for C₁₅H₁₄N₂S₂ 287.0671 [M+H]⁺ found 287.0671.

4-Cyclopropyl-6-(((4-methoxyphenyl)thio)methyl)-1*H*-indazole (194)

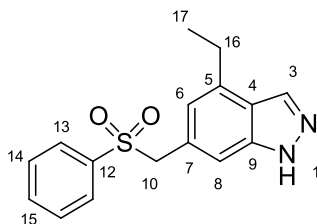


Prepared according to general procedure I using 6-(bromomethyl)-4-cyclopropyl-1*H*-indazole (100 mg, 0.40 mmol), Cs₂CO₃ (143 mg, 0.44 mmol) and 4-methoxythiophenol (74 μ L, 0.60 mmol) in DMF (6 mL). The product was isolated a white solid (105 mg, 85%).

R_f 0.64 (Et₂O); IR ν_{\max} /cm⁻¹ 3177, 3000, 1588, 1498, 1241; ¹H-NMR (500 MHz, CDCl₃) δ ppm; 0.84 (2H, m, H-19), 1.04 (2H, m, H-19), 2.21 (1H, m, H-18), 3.76 (3H, s, H-17), 4.04

(2H, s, H-10), 6.61 (1H, s, H-6), 6.79 (2H, d, $J = 8.7$ Hz, H-14), 7.04 (1H, s, H-8), 7.23 (2H, d, $J = 8.9$ Hz, H-13), 8.16 (1H, s, H-3); ^{13}C -NMR (125 MHz, CDCl_3) δ ppm; 8.4 (C-19), 13.2 (C-18), 41.8 (C-10), 55.4 (C-17), 106.8 (C-8), 114.5 (C-14), 117.8 (C-6), 122.5 (C-4), 125.9 (C-5), 132.7 (C-12), 133.3 (C-3), 134.3 (C-13), 137.6 (C-7), 140.3 (C-9) 159.3 (C-15); MS (ES^+) m/z 311.4 $[\text{M}+\text{H}]^+$; HRMS calcd for $\text{C}_{18}\text{H}_{18}\text{N}_2\text{OS}$ 311.1213 $[\text{M}+\text{H}]^+$ found 311.1212.

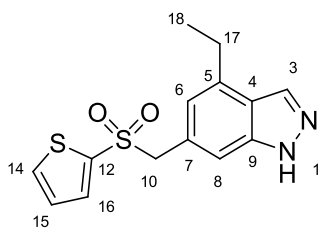
4-Ethyl-6-((phenylsulfonyl)methyl)-1*H*-indazole (196)



Prepared according to general procedure **K** using 4-ethyl-6-((phenylthio)methyl)-1*H*-indazole (35 mg, 0.13 mmol) and Oxone[®] (240 mg, 0.78 mmol) in MeOH (3 mL) and H_2O (3 mL). The product was isolated as an off white solid (31 mg, 79%).

R_f 0.42 (Et_2O); m.p. 76-78 $^\circ\text{C}$; UV λ_{max} (EtOH/nm) 294.2, 215.6; IR $\nu_{\text{max}}/\text{cm}^{-1}$ 3341, 2966, 1622, 1305, 1147, 1083, 686; ^1H -NMR (500 MHz, $\text{DMSO}-d_6$) δ ppm; 1.15 (3H, t, $J = 7.5$ Hz, H-17), 2.79 (2H, q, $J = 7.5$ Hz, H-16), 4.77 (2H, s, H-10), 6.54 (1H, s, H-6), 7.21 (1H, s, H-8), 7.57 (2H, dd, $J = 7.4, 8.4$ Hz, H-14), 7.70-7.73 (3H, m, H-15, H-13), 8.11 (1H, s, H-3), 13.05 (1H, s-br, H-1); ^{13}C -NMR (125 MHz, $\text{DMSO}-d_6$) δ ppm; 14.5 (C-17), 25.5 (C-16), 61.1 (C-10), 110.3 (C-8), 121.1 (C-6), 122.2 (C-4), 126.5 (C-5), 128.1 (C-13), 129.0 (C-14), 132.1 (C-3), 133.7 (C-15), 136.1 (C-7), 138.4 (C-12), 139.8 (C-9); MS (ES^+) m/z 301.3 $[\text{M}+\text{H}]^+$; HRMS calcd for $\text{C}_{16}\text{H}_{17}\text{N}_2\text{O}_2\text{S}$ 301.1005 $[\text{M}+\text{H}]^+$ found 301.1008.

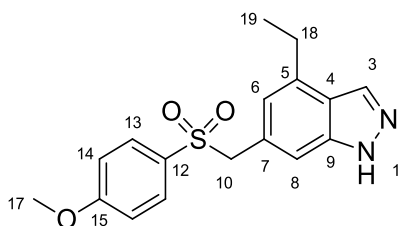
4-Ethyl-6-((thiophen-2-ylsulfonyl)methyl)-1*H*-indazole (198)



Prepared according to general procedure **K** using 4-ethyl-6-((thiophen-2-ylthio)methyl)-1*H*-indazole (20 mg, 0.07 mmol) and Oxone® (134 mg, 0.44 mmol) in MeOH (2.5 mL) and H₂O (2.5 mL). The product was isolated as a grey solid (17 mg, 75%).

R_f 0.37 (Et₂O); m.p. 90-92 °C; UV λ_{\max} (EtOH/nm) 294.2, 257.2, 215.8; IR ν_{\max} /cm⁻¹ 3166, 3103, 1593, 1496, 1252, 1136, 1084, 829, 696; ¹H-NMR (500 MHz, CDCl₃) δ ppm; 1.26 (3H, t, J = 7.5 Hz, H-18) 2.88 (2H, q, J = 7.5 Hz, H-17), 4.51 (2H, s, H-10), 6.63 (1H, s, H-6), 7.03 (1H, dd, J = 3.9, 4.8 Hz, H-15), 7.23 (1H, s, H-8), 7.36 (1H, dd, J = 1.8, 3.9 Hz, H-16), 7.64 (1H, dd, J = 4.8, 1.8 Hz, H-14), 8.16 (1H, s, H-3); ¹³C-NMR (125 MHz, CDCl₃) δ ppm; 14.7 (C-18), 26.2 (C-17), 64.5 (C-10), 109.0 (C-8), 122.0 (C-6), 127.2 (C-4), 127.7 (C-15), 134.4 (C-14), 134.9 (C-16), 138.6 (C-3), 140.4 (C-9) not all carbons visible; MS (ES⁺) m/z 307.3 [M+H]⁺.

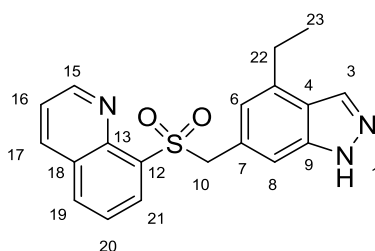
4-Ethyl-6-(((4-methoxyphenyl)sulfonyl)methyl)-1*H*-indazole (200)



Prepared according to general procedure **K** using 4-ethyl-6-(((4-methoxyphenyl)thio)methyl)-1*H*-indazole (20 mg, 0.07 mmol) and Oxone® (124 mg, 0.40 mmol) in MeOH (2.5 mL) and H₂O (2.5 mL). The product was isolated as a white solid (21 mg, 95%).

R_f 0.39 (Et₂O); m.p. 169-171 °C; UV λ_{\max} (EtOH/nm) 293.8, 241.8, 216.6; IR $\nu_{\max}/\text{cm}^{-1}$ 3337, 2965, 1592; ¹H-NMR (500 MHz, CDCl₃) δ ppm; 1.23 (3H, t, J = 7.6 Hz, H-19), 2.85 (2H, q, J = 7.6 Hz, H-18), 3.83 (3H, s, H-17), 4.39 (2H, s, H-10), 6.54 (1H, s, H-6), 6.87 (2H, d, J = 8.9 Hz, H-14), 7.21 (1H, s, H-8), 7.54 (2H, d, J = 8.9 Hz, H-13), 8.08 (1H, s, H-3); ¹³C-NMR (125 MHz, CDCl₃) δ ppm; 14.7 (C-19), 26.1 (C-18), 55.7 (C-17), 63.5 (C-10), 109.9 (C-8), 114.1 (C-14), 122.1 (C-6), 122.9 (C-4), 127.5 (C-5), 129.5 (C-12), 130.9 (C-13), 133.4 (C-3), 137.8 (C-7), 140.1 (C-9) 163.8 (C-15); MS (ES⁺) m/z 331.4 [M+H]⁺.

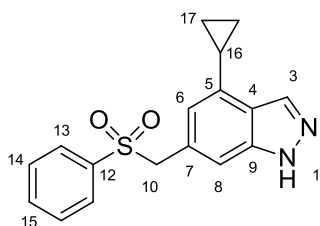
8-(((4-Ethyl-1H-indazol-6-yl)methyl)sulfonyl)quinoline (202)



Prepared according to general procedure **K** using 8-(((4-ethyl-1H-indazol-6-yl)methyl)thio)quinoline (44 mg, 0.14 mmol) and Oxone® (125 mg, 0.83 mmol) in MeOH (2.5 mL) and H₂O (2.5 mL). The product was isolated as a white solid (39 mg, 86%).

m.p. 226-229 °C; UV λ_{\max} (EtOH/nm) 254.8, 215.8; IR $\nu_{\max}/\text{cm}^{-1}$ 3313, 2930, 1295, 1118; ¹H-NMR (500 MHz, CDCl₃) δ ppm; 1.06 (3H, t, J = 7.6 Hz, H-23), 2.74 (2H, q, J = 7.6 Hz, H-22), 5.26 (2H, s, H-10), 6.56 (1H, s, H-6), 7.20 (1H, s, H-8), 7.53 (1H, dd, J = 7.6, 8.1 Hz, H-20), 7.64 (1H, dd, J = 8.3, 4.3 Hz, H-16), 7.99 (1H, s, H-3), 8.05 (1H, dd, J = 1.4, 8.3 Hz, H-19), 8.25 (1H, dd, J = 7.6, 1.4 Hz, H-21), 8.31 (1H, dd, J = 8.3, 1.7 Hz, H-17), 9.26 (1H, dd, J = 4.3, 1.7 Hz, H-15); ¹³C-NMR (125 MHz, CDCl₃) δ ppm 14.4 (C-23), 25.9 (C-22), 62.0 (C-10), 109.7 (C-8), 121.8 (C-6), 122.3 (C-4), 122.9 (C-16), 125.7 (C-20), 127.5 (C-12), 128.8 (C-18), 132.8 (C-21), 134.3 (C-19), 135.4 (C-3), 136.8 (C-17), 137.6 (C-5), 144.4 (C-13), 151.6 (C-15); MS (ES⁺) m/z 352.3 [M+H]⁺.

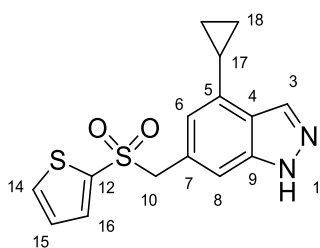
4-Cyclopropyl-6-((phenylsulfonyl)methyl)-1H-indazole (197)



Prepared according to general procedure **K** using 4-cyclopropyl-6-((phenylthio)methyl)-1H-indazole (92 mg, 0.33 mmol) and Oxone® (607 mg, 1.98 mmol) in MeOH (6 mL) and H₂O (4 mL). The product was isolated as an off white solid (103 mg, 99%).

R_f 0.35 (Et₂O); m.p. 155-157 °C; UV λ_{max} (EtOH/nm) 297.4, 261.4, 225.2, 221.4; IR ν_{max}/cm^{-1} 3348, 3178, 2924, 1620; ¹H-NMR (500 MHz, CDCl₃) δ ppm; 0.63 (2H, m, H-17), 1.00 (2H, m, H-17), 2.14 (1H, m, H-16), 4.38 (2H, s, H-10), 6.24 (1H, s, H-6), 7.17 (1H, s, H-8), 7.43 (2H, dd, J = 7.6, 7.9 Hz, H-14), 7.59-7.63 (3H, m, H-15, H-13), 8.17 (1H, s, H-3); ¹³C-NMR (125 MHz, CDCl₃) δ ppm; 8.5 (C-17), 13.1 (C-16), 63.3 (C-10), 109.5 (C-8), 118.7 (C-6), 123.6 (C-4), 127.0 (C-5), 128.7 (C-13), 128.9 (C-14), 133.7 (C-3), 133.8 (C-15), 137.9 (C-7), 139.0 (C-12), 139.9 (C-9); MS (ES⁺) m/z 313.4 [M+H]⁺; HRMS calcd for C₁₇H₁₆N₂O₂S 313.1005 [M+H]⁺ found 313.1004.

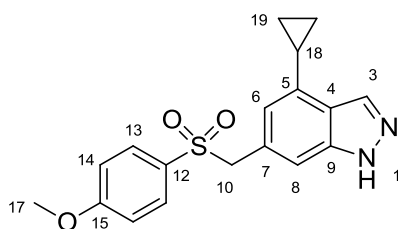
4-Cyclopropyl-6-((thiophen-2-ylsulfonyl)methyl)-1H-indazole (199)



Prepared according to general procedure **K** using 4-cyclopropyl-6-((thiophen-2-ylthio)methyl)-1H-indazole (110 mg, 0.38 mmol) and Oxone® (710 mg, 2.30 mmol) in MeOH (5 mL) and H₂O (5 mL). The product was isolated as a pink solid (111 mg, 91%).

R_f 0.49 (Et₂O); m.p. 114-116 °C; UV λ_{\max} (EtOH/nm) 297.4, 258.8, 217.2; IR $\nu_{\max}/\text{cm}^{-1}$ 3338, 3099, 2921, 2852, 1620; ¹H-NMR (500 MHz, CDCl₃) δ ppm; 0.70 (2H, m, H-18), 1.02 (2H, m, H-18), 2.16 (1H, m, H-17), 4.47 (2H, s, H-10), 6.33 (1H, s, H-6), 7.03 (1H, dd, J = 3.8, 4.8 Hz, H-15), 7.22 (1H, s, H-8), 7.35 (1H, dd, J = 1.2, 3.8 Hz, H-16), 7.64 (1H, dd, J = 4.8, 1.2 Hz, H-14), 8.18 (1H, s, H-3); ¹³C-NMR (125 MHz, CDCl₃) δ ppm; 8.6 (C-18), 13.2 (C-17), 64.5 (C-10), 109.6 (C-8), 118.5 (C-6), 123.6 (C-4), 127.0 (C-5), 127.7 (C-15), 133.5 (C-3), 133.9 (C-14), 134.9 (C-16), 138.2 (C-7), 138.5 (C-12); MS (ES⁺) m/z 319.3 [M+H]⁺; HRMS calcd for C₁₅H₁₄N₂O₂S₂ 319.0569 [M+H]⁺ found 319.0570.

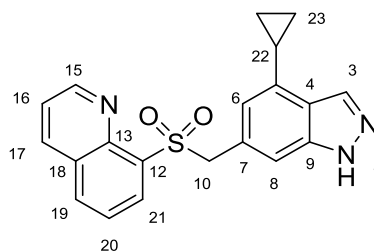
4-Cyclopropyl-6-(((4-methoxyphenyl)sulfonyl)methyl)-1H-indazole (201)



Prepared according to general procedure **K** using 4-cyclopropyl-6-(((4-methoxyphenyl)thio)methyl)-1H-indazole (84 mg, 0.27 mmol) and Oxone[®] (497 mg, 1.62 mmol) in MeOH (6 mL) and H₂O (4 mL). The product was isolated as a white solid (32 mg, 34%).

R_f 0.34 (Et₂O); m.p. 192-194 °C; UV λ_{\max} (EtOH/nm) 296.4, 241.2, 217.2, 202.6; IR $\nu_{\max}/\text{cm}^{-1}$ 3345, 2922, 1591; ¹H-NMR (500 MHz, CDCl₃) δ ppm; 0.66 (2H, m, H-19), 1.01 (2H, m, H-19), 2.16 (1H, m, H-18), 3.85 (3H, s, H-17), 4.35 (2H, s, H-10), 6.26 (1H, s, H-6), 6.88 (2H, d, J = 8.9 Hz, H-14), 7.15 (1H, s, H-8), 7.51 (2H, d, J = 8.9 Hz, H-13), 8.17 (1H, s, H-3); ¹³C-NMR (125 MHz, CDCl₃) δ ppm; 8.5 (C-19), 13.1 (C-18), 55.7 (C-17), 63.5 (C-10), 109.4 (C-8), 114.1 (C-14), 118.9 (C-6), 123.2 (C-4), 127.5 (C-5), 129.4 (C-12), 130.9 (C-13), 133.6 (C-3), 137.9 (C-7), 139.8 (C-9), 163.8 (C-15); MS (ES⁺) m/z 343.4 [M+H]⁺; HRMS calcd for C₁₈H₁₈N₂O₃S 343.1111 [M+H]⁺ found 343.1110.

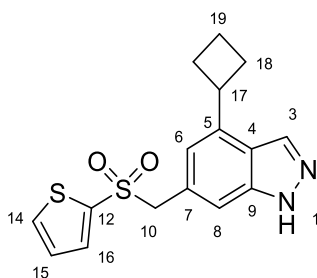
8-(((4-cyclopropyl-1H-indazol-6-yl)methyl)sulfonyl)quinolone (203)



Prepared according to general procedure I using 6-(bromomethyl)-4-cyclopropyl-1H-indazole (100 mg, 0.40 mmol), Cs₂CO₃ (274 mg, 0.84 mmol) and 8-quinolinethiol hydrochloride (119 mg, 0.60 mmol) in DMF (4 mL). 8-(((4-cyclopropyl-1H-indazol-6-yl)methyl)thio)quinoline was isolated as a white solid (94 mg, 70%). Isolated material was used in the next step without characterisation according to general procedure K using 8-(((4-cyclopropyl-1H-indazol-6-yl)methyl)thio)quinoline (84 mg, 0.28 mmol) and Oxone[®] (258 mg, 1.69 mmol) in MeOH (4 mL) and H₂O (4 mL). The title product was isolated as a white solid (85 mg, 97%).

m.p. 225-227 °C; UV λ_{max} (EtOH/nm) 295.4, 252.4, 205.2; IR ν_{max}/cm⁻¹ 3174, 2995, 1354, ; ¹H-NMR (500 MHz, CDCl₃) δ ppm; 0.37-0.38 (2H, m, H-23), 0.85-0.88 (2H, m, H-23), 2.01-2.04 (1H, m, H-22), 5.21 (2H, s, H-10), 6.23 (1H, s, H-6), 7.17 (1H, s, H-8), 7.52 (1H, dd, *J* = 7.6, 7.6 Hz, H-20), 7.64 (1H, dd, *J* = 8.3, 4.2 Hz, H-16), 8.05-8.06 (1H, m, H-19, H-3), 8.22 (1H, dd, *J* = 7.6, 1.4 Hz, H-21), 8.31 (1H, dd, *J* = 8.3, 1.7 Hz, H-17), 9.25 (1H, dd, *J* = 4.2, 1.7 Hz, H-15); ¹³C-NMR (125 MHz, CDCl₃) δ ppm 8.32 (C-23), 21.9 (C-22), 62.0 (C-10), 109.4 (C-8), 118.5 (C-6), 122.3 (C-4, C-16), 125.7 (C-20), 127.5 (C-12), 128.8 (C-18), 132.8 (C-21), 134.3 (C-19), 135.3 (C-3), 136.9 (C-17), 137.6 (C-5), 144.4 (C-13), 151.6 (C-15); MS (ES⁺) *m/z* 332.3 [M+H]⁺.

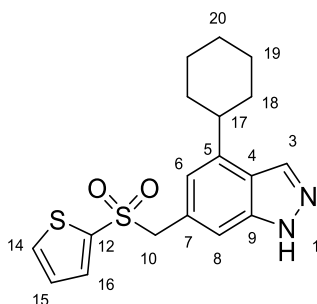
4-Cyclobutyl-6-((thiophen-2-ylsulfonyl)methyl)-1*H*-indazole (204)



Prepared according to general procedure **H** using: (4-Cyclobutyl-1-(tetrahydro-2*H*-pyran-2-yl)-1*H*-indazol-6-yl)methanol (49 mg, 0.17 mmol), SOBr₂ (27 μ L, 0.34 mmol) and DMF (2 μ L, 0.02 mmol) in DCM (10 mL). Crude material was engaged in general procedure **I** using: Cs₂CO₃ (45 mg, 0.14 mmol) and 2-thiolthiophene (10 μ L, 0.11 mmol) in DMF (4 mL). Crude material was engaged in general procedure **K** using: Oxone[®] (30 mg, 0.05 mmol) in MeOH (2 mL) and H₂O (2 mL). The product was isolated as a light grey solid (6 mg, 11% over three steps).

UV λ_{max} (EtOH/nm) 295.0, 257.0, 216.2; IR ν_{max} /cm⁻¹ 2952, 1035; ¹H-NMR (500 MHz, CDCl₃) δ ppm; 1.22-1.27 (1H, m, H-19), 1.90-1.93 (1H, m, H-19), 2.14-2.22 (3H, m, H-18, H-17), 2.44-2.49 (2H, m, H-18), 4.55 (2H, s, H-10), 6.94 (1H, s, H-6), 7.09 (1H, dd, *J* = 3.9, 4.8 Hz, H-15), 7.37 (1H, s, H-8), 7.45 (1H, d, *J* = 3.9 Hz, H-16), 7.70 (1H, dd, *J* = 4.8 Hz, H-14); ¹³C-NMR (125 MHz, CDCl₃) δ ppm; 18.6 (C-19), 29.0 (C-18), 37.8 (C-17), 64.5 (C-10), 127.9 (C-15), 134.8 (C-16), 135.0 (C-14); MS (ES⁺) *m/z* 333.3 [M+H]⁺.

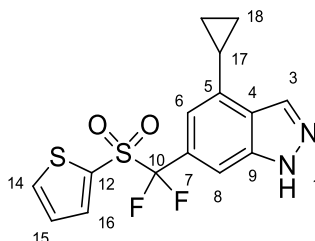
4-Cyclohexyl-6-((thiophen-2-ylsulfonyl)methyl)-1*H*-indazole (206)



Prepared according to general procedure **H** using: (4-Cyclobutyl-1-(tetrahydro-2H-pyran-2-yl)-1H-indazol-6-yl)methanol (89 mg, 0.28 mmol), SOBr₂ (44 μ L, 0.34 mmol) and DMF (3 μ L, 0.04 mmol) in DCM (10 mL). Crude material was engaged in general procedure **I** using: Cs₂CO₃ (45 mg, 0.14 mmol) and 2-thiolthiophene (10 μ L, 0.11 mmol) in DMF (4 mL). Crude material was engaged in general procedure **K** using: Oxone® (30 mg, 0.05 mmol) in MeOH (2 mL) and H₂O (2 mL). The product was isolated as a grey solid (9 mg, 9% over three steps).

UV λ_{max} (EtOH/nm) 304.5, 294.5, 256.5, 216.0; IR ν_{max} /cm⁻¹ 3363, 2924, 2851, 1147, 1009; ¹H-NMR (500 MHz, CDCl₃) δ ppm; 1.28-1.32 (1H, m, H-20), 1.44-1.47 (4H, m, H-18, H19), 1.79-1.82 (1H, m, H-20), 1.87-1.91 (4H, m, H-18, H-19), 2.87-2.91 (1H, m, H-17), 4.53 (2H, s, H-10), 6.86 (1H, s, H-6), 7.06 (1H, dd, J = 3.8, 4.8 Hz, H-15), 7.38-7.40 (2H, ms, H-8, H-16), 7.66 (1H, d, J = 4.8 Hz, H-14; ¹³C-NMR (125 MHz, CDCl₃) δ ppm; 26.1 (C-20), 26.7 (C-19), 33.7 (C-18), 42.1 (C-17), 64.5 (C-10), 111.5 (C-8), 121.8 (C-6), 127.8 (C-15), 130.6 (C-5), 134.7 (C-14), 135.0 (C-16), 138.5 (C-12); MS (ES⁺) m/z 361.2 [M+H]⁺.

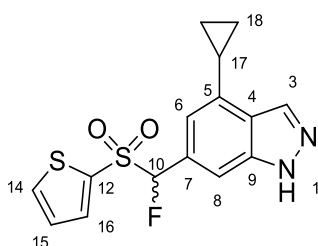
4-Cyclopropyl-6-(difluoro(thiophen-2-ylsulfonyl)methyl)-1H-indazole (211)



4-Cyclopropyl-6-((thiophen-2-ylsulfonyl)methyl)-1H-indazole (85 mg, 0.27 mmol) was dissolved in anhydrous THF (3 mL) at -78 °C and *N*-fluorobenzenesulfonimide (NFSI) (185 mg, 0.59 mmol) was added followed by *n*-BuLi (2.5 M in hexanes, 342 μ L, 0.86 mmol) dropwise over ca. 10 minutes. The solution was stirred at -78 °C for 2 h then allowed to warm to room temperature and stirred for a further 16 h after which the reaction was quenched with NH₄Cl solution (saturated aqueous, 5 mL) and extracted with EtOAc (3 x 10 mL). Combined organic fractions were washed with brine (10 mL), dried over Na₂SO₄ and reduced *in vacuo*. Reverse phase flash chromatography (0-80 % MeCN (0.1% HCOOH) in H₂O (0.1% HCOOH)) was performed to give the title compound as a white solid (47 mg, 49%).

R_f 0.53 (Et₂O); m.p. 170-172 °C; UV λ_{\max} (EtOH/nm) 305.6, 262.8, 217.6; IR ν_{\max} /cm⁻¹ 3273, 3114, 1337, 1165; ¹H-NMR (500 MHz, CDCl₃) δ ppm; 0.93 (2H, m, H-18), 1.13 (2H, m, H-18), 2.30 (1H, m, H-17), 6.98 (1H, s, H-6), 7.27 (1H, dd, J = 3.9, 5.0 Hz, H-15), 7.69 (1H, s, H-8), 7.85 (1H, dd, J = 1.3, 3.9 Hz, H-16), 7.92 (1H, dd, J = 5.0, 1.3 Hz, H-14), 8.28 (1H, s, H-3); ¹³C-NMR (125 MHz, CDCl₃) δ ppm; 8.8 (C-18), 13.6 (C-17), 107.7 (C-8), 114.9 (C-6), 122.0 (C-4), 125.0 (C-7) 128.4 (C-15), 132.4 (C-12), 133.9 (C-3), 137.6 (C-14), 138.3 (C-16), 138.8 (C-5); ¹⁹F NMR (470 MHz, CDCl₃) δ -100.4; MS (ES⁺) m/z 355.3 [M+H]⁺.

4-Cyclopropyl-6-(difluoro(thiophen-2-ylsulfonyl)methyl)-1H-indazole (212)

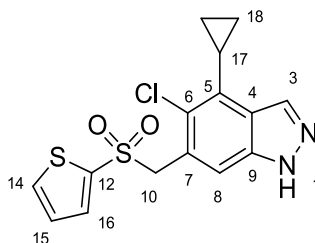


4-Cyclopropyl-6-((thiophen-2-ylsulfonyl)methyl)-1H-indazole (200 mg, 0.63 mmol) was dissolved in anhydrous THF (7 mL) at -78 °C and *N*-fluorobenzenesulfonimide (NFSI) (435 mg, 1.38 mmol) was added followed by *n*-BuLi (2.5 M in hexanes, 880 μ L, 0.22 mmol) dropwise over ca. 10 minutes. The solution was stirred at -78 °C for 2 h then allowed to warm to room temperature and stirred for a further 16 h after which the reaction was cooled back down to -78 °C and *N*-fluorobenzenesulfonimide (NFSI) (197 mg, 0.63 mmol) was added followed by *n*-BuLi (2.5 M in hexanes, 251 μ L, 0.63 mmol) and stirred for a further 3 h. The reaction was quenched with NH₄Cl solution (saturated aqueous, 5 mL) and extracted with EtOAc (3 x 10 mL). Combined organic fractions were washed with brine (10 mL), dried over Na₂SO₄ and reduced *in vacuo*. Reverse phase flash chromatography (0-80 % MeCN (0.1% HCOOH) in H₂O (0.1% HCOOH) was performed to give the title compound as a white solid (70 mg, 33%).

m.p. 168-170 °C; UV λ_{\max} (EtOH/nm) 306.0, 262.8, 218.0; IR ν_{\max} /cm⁻¹ 3268, 3110, 1335, 1163; ¹H-NMR (500 MHz, CDCl₃) δ ppm; 0.78-0.86 (2H, m, H-18), 1.07-1.09 (2H, m, H-18), 2.23-2.24 (1H, m, H-17), 6.15 (1H, s, H-10A), 6.24 (1H, s, H-10B), 6.71 (1H, s, H-6), 7.16 (1H, dd, J = 3.9, 5.0 Hz, H-15), 7.26 (1H, s, H-8), 7.61 (1H, d, J = 3.0 Hz, H-16), 7.79 (1H, d, J = 4.9 Hz, H-14), 8.33 (1H, s, H-3); ¹³C-NMR (125 MHz, CDCl₃) δ ppm; 8.8 (C-18),

13.6 (C-17), 122.0 (C-4), 125.0 (C-7) 128.4 (C-15), 132.4 (C-12), 133.9 (C-3), 137.6 (C-14), 138.3 (C-16), 138.8 (C-5); ^{19}F NMR (470 MHz, CDCl_3) δ -172.4; MS (ES^+) m/z 337.3 $[\text{M}+\text{H}]^+$; HRMS calcd for $\text{C}_{15}\text{H}_{14}\text{N}_2\text{O}_2\text{FS}_2$ 337.0475 $[\text{M}+\text{H}]^+$ found 337.0477.

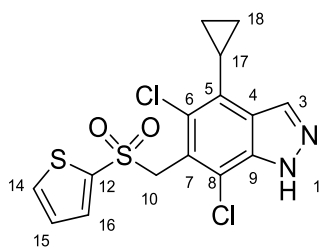
5-Chloro-4-cyclopropyl-6-((thiophen-2-ylsulfonyl)methyl)-1*H*-indazole (222)



4-Cyclopropyl-6-((thiophen-2-ylsulfonyl)methyl)-1*H*-indazole (100 mg, 0.32 mmol) was dissolved in MeOH (3 mL) and a solution of brine (1 mL) Oxone® (193 mg, 0.63 mmol) and H_2O (2 mL) was added. The resulting mixture was stirred overnight before dilution with H_2O (10 mL) and extraction with EtOAc (3 x 10 mL). Combined organic fractions were dried over Na_2SO_4 and purified by MPLC (0-60 % EtOAc in petroleum ether) to yield the title compound as a white solid (40 mg, 36%) and three further compounds shown below.

m.p. 192-194 °C; UV λ_{max} (EtOH/nm) 317.0, 306.4, 256.4, 221.8; IR $\nu_{\text{max}}/\text{cm}^{-1}$ 3421, 3088, 1302, 1150; ^1H -NMR (500 MHz, $\text{DMSO}-d_6$) δ ppm; 0.86-0.89 (2H, m, H-18), 1.09-1.13 (2H, m, H-18), 2.15-2.18 (1H, m, H-17), 5.02 (2H, s, H-10), 7.21 (1H, dd, J = 3.8, 5.1 Hz, H-15), 7.47 (1H, s, H-8), 7.51 (1H, dd, J = 1.3, 3.8 Hz, H-16), 8.08 (1H, dd, J = 5.1, 1.3 Hz, H-14), 8.16 (1H, s, H-3) 13.33 (1H, s, H-1); ^{13}C -NMR (125 MHz, $\text{DMSO}-d_6$) δ ppm; 8.1 (C-18), 14.0 (C-17), 61.1 (C-10), 113.2 (C-8), 123.5 (C-6), 124.9 (C-4), 126.8 (C-7) 127.8 (C-5), 128.7 (C-15), 132.6 (C-3), 133.6 (C-3), 135.5 (C-16), 136.5 (C-14), 138.4 (C-12); MS (ES^+) m/z 353.2 $[\text{M}+\text{H}]^+$; HRMS calcd for $\text{C}_{15}\text{H}_{14}\text{N}_2\text{O}_2^{35}\text{ClS}_2$ 353.0180 $[\text{M}+\text{H}]^+$ found 353.0183.

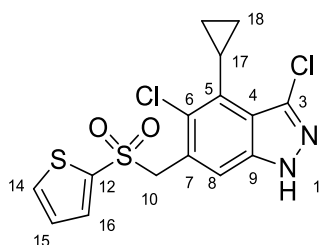
5,7-Dichloro-4-cyclopropyl-6-((thiophen-2-ylsulfonyl)methyl)-1*H*-indazole (223)



Isolated from procedure above (**222**) as a white solid (25 mg, 21%).

m.p. 210-212 °C; UV λ_{max} (EtOH/nm) 312.8, 257.4, 222.0; IR ν_{max} /cm⁻¹ 3214, 3115, 1311, 1154; ¹H-NMR (500 MHz, DMSO-*d*₆) δ ppm; 0.90-0.93 (2H, m, H-18), 1.14-1.17 (2H, m, H-18), 2.16-2.22 (1H, m, H-17), 5.13 (2H, s, H-10), 7.25 (1H, dd, *J* = 3.8, 4.9 Hz, H-15), 7.62 (1H, dd, *J* = 1.3, 3.8 Hz, H-16), 8.15 (1H, dd, *J* = 4.9, 1.3 Hz, H-14), 8.30 (1H, s, H-3) 13.83 (1H, s, H-1); ¹³C-NMR (125 MHz, DMSO-*d*₆) δ ppm; 8.2 (C-18), 14.1 (C-17), 59.7 (C-10), 116.9 (C-8), 122.9 (C-6), 124.0 (C-4), 128.7 (C-7) 129.0 (C-15), 133.2 (C-5), 134.0 (C-3), 135.9 (C-16), 137.0 (C-14), 137.2 (C-9), 140.1 (C-12); MS (ES⁺) *m/z* 387.1 [M+H]⁺; HRMS calcd for C₁₅H₁₃N₂O₂³⁵Cl₂S₂ 386.9790 [M+H]⁺ found 386.9791.

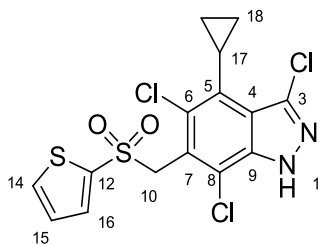
3,5-Dichloro-4-cyclopropyl-6-((thiophen-2-ylsulfonyl)methyl)-1*H*-indazole (224)



Isolated from procedure above (**222**) as a white solid (30 mg, 24%).

m.p. 200-202 °C; UV λ_{max} (EtOH/nm) 322.6, 311.2, 226.4; IR ν_{max} /cm⁻¹ 3243, 3083, 1314, 1127; ¹H-NMR (500 MHz, DMSO-*d*₆) δ ppm; 0.63-0.64 (2H, m, H-18), 1.15-1.17 (2H, m, H-18), 1.98-2.02 (1H, m, H-17), 5.02 (2H, s, H-10), 7.21 (1H, dd, *J* = 3.8, 5.1 Hz, H-15), 7.48 (1H, dd, *J* = 1.3, 3.8 Hz, H-16), 7.56 (1H, s, H-8), 8.09 (1H, dd, *J* = 5.1, 1.3 Hz, H-14), 13.58 (1H, s, H-1); ¹³C-NMR (125 MHz, DMSO-*d*₆) δ ppm; 10.5 (C-18), 11.9 (C-17), 60.8 (C-10), 114.7 (C-8), 120.6 (C-4), 126.8 (C-7), 128.7 (C-15) 129.9 (C-6), 132.4 (C-3), 133.3 (C-5), 135.7 (C-16), 136.7 (C-14), 138.9 (C-12) 139.9 (C-9); MS (ES⁺) *m/z* 387.1 [M+H]⁺; HRMS calcd for C₁₅H₁₃N₂O₂³⁵Cl₂S₂ 386.9790 [M+H]⁺ found 386.9793.

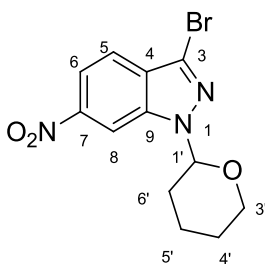
3,5,7-Trichloro-4-cyclopropyl-6-((thiophen-2-ylsulfonyl)methyl)-1*H*-indazole (225)



Isolated from procedure above (**222**) as a white solid (28 mg, 21%).

m.p. 247-249 °C; UV λ_{max} (EtOH/nm) 329.4, 317.0, 226.6; IR ν_{max} /cm⁻¹ 3373, 3096, 1320, 1132; ¹H-NMR (500 MHz, DMSO-*d*₆) δ ppm; 0.69-0.70 (2H, m, H-18), 1.20-1.22 (2H, m, H-18), 2.01-2.04 (1H, m, H-17), 5.13 (2H, s, H-10), 7.25 (1H, dd, *J* = 3.8, 4.9 Hz, H-15), 7.61 (1H, dd, *J* = 1.3, 3.8 Hz, H-16), 8.15 (1H, dd, *J* = 5.1, 1.3 Hz, H-14), 14.09 (1H, s, H-1); ¹³C-NMR (125 MHz, DMSO-*d*₆) δ ppm; 10.6 (C-18), 11.9 (C-17), 59.5 (C-10), 118.2 (C-8), 121.3 (C-6), 124.7 (C-4), 129.1 (C-15) 130.7 (C-7), 132.9 (C-5), 133.6 (C-3), 136.1 (C-16), 137.2 (C-14), 138.4 (C-9) 139.8 (C-12); MS (ES⁺) *m/z* 423.1 [M+H]⁺; HRMS calcd for C₁₅H₁₂N₂O₂³⁵Cl₃S₂ 420.9400 [M+H]⁺ found 420.9400.

3-Bromo-6-nitro-1-(tetrahydro-2*H*-pyran-2-yl)-1*H*-indazole (233)

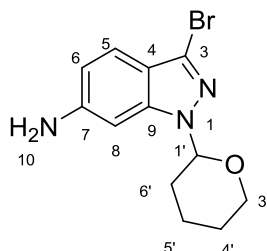


Prepared according to general procedure **C** using 3-bromo-6-nitro-1*H*-indazole (4.5 g, 18.7 mmol), DHP (4.75 mL, 56.0 mmol) and *p*-TSA (355 mg, 1.87 mmol) in DCM (80 mL). The product was isolated as a pure white solid (5.24 g, 86%).

*R*_f 0.41 (Et₂O); M.p. 124-126 °C; UV λ_{max} (EtOH/nm) 339.4, 255.4, 207.8; IR ν_{max} /cm⁻¹ 3073, 2941, 2865, 1523; ¹H-NMR (500 MHz, CDCl₃) δ ppm; 1.67-1.81 (3H, m, H-5'A, H-5', H-4'), 2.11-2.17 (2H, m, H-4', H-6'), 2.48-2.54 (1H, m, H-6') 3.76-3.81 (1H, m, H-3'), 4.00-4.04 (1H, m, H-3'), 5.77 (1H, dd, *J* = 2.3, 8.7 Hz, H-1'), 8.09 (1H, d, *J* = 8.9 Hz, H-6),

7.73 (1H, d, J = 8.9 Hz, H-5), 8.55 (1H, s, H-8); ^{13}C -NMR (125 MHz, CDCl_3) δ ppm; 22.0 (C-4'), 24.9 (C-5'), 29.3 (C-6'), 67.5 (C-3'), 86.3 (C-1'), 107.6 (C-8), 116.7 (C-6), 121.5 (C-5), 122.1 (C-3), 127.6 (C-4), 139.3 (C-9), 147.5 (C-7); MS (ES^+) m/z 326.4 [$\text{M}-\text{H}$] $^-$; HRMS calcd for $\text{C}_{12}\text{H}_{13}\text{BrN}_3\text{O}_3$ 326.0135 & 328.0114 [$\text{M}+\text{H}$] $^+$ found 326.0139 & 328.0118.

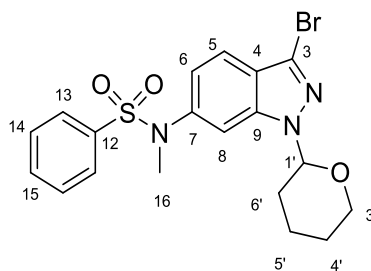
3-Bromo-1-(tetrahydro-2H-pyran-2-yl)-1H-indazol-6-amine (234)



Prepared according to general procedure E using 3-bromo-6-nitro-1-(tetrahydro-2H-pyran-2-yl)-1H-indazole (428 mg, 1.32 mmol) in EtOAc (50 mL, 0.05M). The product was isolated as a brown solid, (380 mg, 98%).

R_f 0.34 (Et_2O); m.p. $<60^\circ\text{C}$; UV λ_{max} (EtOH/nm) 303.0, 285.4, 239.8, 220.2; IR $\nu_{\text{max}}/\text{cm}^{-1}$ 3449, 3351, 3226, 2936, 2936, 2851, 1623; ^1H -NMR (500 MHz, CDCl_3) δ ppm; 1.61-1.63 (1H, m, H-5'), 1.70 (2H, m, H-5', H-4'), 2.00-2.04 (1H, m, H-6'), 2.12-2.14 (1H, m, H-4'), 2.49-2.52 (1H, m, H-6'), 3.67-3.72 (1H, m, H-3'), 4.00-4.03 (1H, m, H-3'), 5.51 (1H, dd, J = 2.7, 9.2 Hz, H-1'), 6.61 (1H, dd, J = 1.5, 8.5 Hz, H-6), 6.69 (1H, d, J = 1.5 Hz, H-8), 7.33 (1H, d, J = 8.5 Hz, H-5); ^{13}C -NMR (125 MHz, CDCl_3) δ ppm; 22.5 (C-5'), 25.1 (C-4'), 29.2 (C-6'), 67.4 (C-3'), 85.3 (C-1'), 92.9 (C-8), 113.6 (C-6), 118.2 (C-4), 121.2 (C-5), 122.2 (C-3), 142.4 (C-9), 147.0 (C-7); MS (ES^+) m/z 296.2 [$\text{M}+\text{H}$] $^+$; HRMS calcd for $\text{C}_{12}\text{H}_{15}\text{BrN}_3\text{O}$ 296.0393 & 298.0373 [$\text{M}+\text{H}$] $^+$ found 296.0398 & 298.0375.

***N*-(3-Bromo-1-(tetrahydro-2*H*-pyran-2-yl)-1*H*-indazol-6-yl)-*N*-methylbenzenesulfonamide (238)**

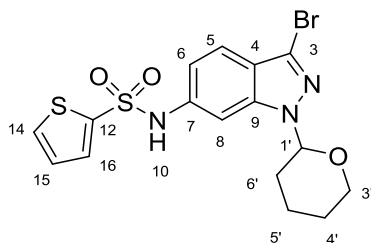


Formic acid (184 μ L, 4.88 mmol) was added drop wise to acetic anhydride (238 μ L, 2.44 mmol) at 0°C and stirred for *ca.* five minutes before heating to 60°C and stirred for a further hour. The solution was allowed to cool and 3-bromo-1-(tetrahydro-2*H*-pyran-2-yl)-1*H*-indazol-6-amine (360 mg, 1.22 mmol) in THF (20 mL) was added in one portion and stirred for 1 hour. After this time the solution was reduced to a white solid under vacuum. The crude *N*-(3-bromo-1*H*-indazol-6-yl)formamide was suspended in THF (20 mL) and borane (3.05 mL, 1M in THF, 3.05 mmol) was added. The solution was stirred under reflux for 16 hours then allowed to cool, volatiles were removed by rotary evaporator. The residue was suspended in methanolic HCl (1.25M, 6 mL) and heated to reflux for 3 hours. The solution was reduced to a residue and purified using MPLC (0-80% EtOAc in petroleum ether) giving 3-bromo-*N*-methyl-1-(tetrahydro-2*H*-pyran-2-yl)-1*H*-indazol-6-amine as a white solid 195 mg, 51%. Isolated material was used in the next step with out characterisation according to general procedure **A** using 3-bromo-*N*-methyl-1-(tetrahydro-2*H*-pyran-2-yl)-1*H*-indazol-6-amine (285 mg, 0.92 mmol) in pyridine (10 mL) and benzenesulphonyl chloride (176 μ L, 1.38 mmol) to give the product as an off white solid (373 mg, 90%).

m.p. 59-61 °C; UV λ_{max} (EtOH/nm) 295.6, 272.8, 216.0; IR ν_{max} /cm⁻¹ 2937, 2854; ¹H-NMR (500 MHz, CDCl₃) δ ppm; 1.61-1.75 (3H, m, H-4', H-5', H-5'), 2.01-2.05 (1H, m, H-6'), 2.10-2.12 (1H, m, H-4'), 2.45-2.48 (1H, m, H-6'), 3.23 (3H, s, H-16), 3.65-3.70 (1H, m, H-3'), 3.96-3.99 (1H, m, H-3'), 5.59 (1H, dd, *J* = 2.8, 9.5 Hz, H-1'), 6.81 (1H, dd, *J* = 8.6, 1.8 Hz, H-6), 7.11 (1H, d, *J* = 1.8 Hz, H-8), 7.45-7.47 (3H, m, H-14, H-5), 7.56 (2H, dd, *J* = 1.5, 8.8 Hz, H-13), 7.89 (1H, tt, *J* = 1.5, 8.6, H-15); ¹³C-NMR (125 MHz, CDCl₃) δ ppm; 22.3 (C-4') 24.9 (C-5'), 29.3 (C-6'), 38.6 (C-16), 67.4 (C-3'), 85.6 (C-1'), 109.7 (C-8), 120.5

(C-6), 120.7 (C-5), 121.9 (C-5), 123.4 (C-3), 127.9 (C-13), 128.9 (C-14), 132.9 (C-15), 136.4 (C-12), 140.4 (C-7), 141.2 (C-9); MS (ES⁺) m/z 449.2 [M(⁷⁹Br)+H]⁺.

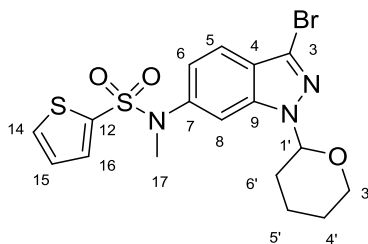
***N*-(3-Bromo-1-(tetrahydro-2*H*-pyran-2-yl)-1*H*-indazol-6-yl)thiophene-2-sulfonamide
(235)**



Prepared according to general procedure **A** using 3-bromo-1-(tetrahydro-2*H*-pyran-2-yl)-1*H*-indazol-6-amine (1 g, 3.38 mmol) and 2-thiophenesulphonyl chloride (920 mg, 5.06 mmol) in pyridine (10 mL) and (THF 10 mL) to give the product as an off white solid (1.46 g, 98%).

m.p. 74-76 °C; UV λ_{max} (EtOH/nm) 292.6, 218.8, 257.4; IR ν_{max} /cm⁻¹ 3342, 3099, 2937, 2859, 1332, 1155; ¹H-NMR (500 MHz, DMSO-*d*₆) δ ppm; 1.53-1.60 (2H, m, H-4'), 1.75-1.77 (1H, m, H-5'), 1.95-2.00 (2H, m, H-5', H-6'), 2.23-2.29 (1H, m, H-6'), 3.68-3.73 (1H, m, H-3'), 3.84-3.87 (1H, m, H-3'), 5.71 (1H, dd, J = 2.0, 9.0 Hz, H-1'), 7.06 (1H, dd, J = 8.9, 1.5 Hz, H-6), 7.11 (1H, dd, J = 4.9, 3.8 Hz, H-15), 7.47-7.49 (2H, m, H-8, H-5), 7.61 (1H, dd, J = 1.3, 3.8 Hz, H-16), 7.89 (1H, dd, J = 1.3, 4.9, H-14), 10.77 (1H, s-br, H-10); ¹³C-NMR (125 MHz, DMSO-*d*₆) δ ppm; 21.7 (C-4') 24.7 (C-5'), 28.6 (C-6'), 66.4 (C-3'), 84.5 (C-1'), 100.1 (C-8), 116.7 (C-6), 120.1 (C-4), 120.5 (C-5), 120.6 (C-3), 127.5 (C-15), 132.6 (C-14), 133.3 (C-16), 138.5 (C-12), 140.1 (C-9), 140.7 (C-7); MS (ES⁺) m/z 442.8 [M(⁷⁹Br)+H]⁺.

***N*-(3-Bromo-1-(tetrahydro-2*H*-pyran-2-yl)-1*H*-indazol-6-yl)-*N*-methylthiophene-2-sulfonamide (237)**



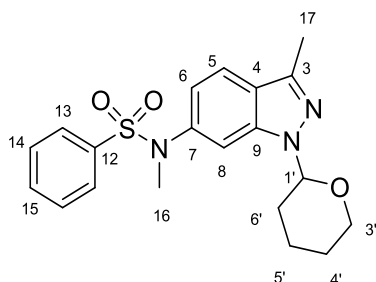
Formic acid (184 μ L, 4.88 mmol) was added drop wise to acetic anhydride (238 μ L, 2.44 mmol) at 0°C and stirred for *ca.* five minutes before heating to 60°C and stirred for a further hour. The solution was allowed to cool and 3-bromo-1-(tetrahydro-2*H*-pyran-2-yl)-1*H*-indazol-6-amine (360 mg, 1.22 mmol) in THF (20 mL) was added in one portion and stirred for 1 hour. After this time the solution was reduced to a white solid under vacuum. The crude *N*-(3-bromo-1*H*-indazol-6-yl)formamide was suspended in THF (20 mL) and borane (3.05 mL, 1M in THF, 3.05 mmol) was added. The solution was stirred under reflux for 16 hours then allowed to cool, volatiles were removed by rotary evaporator. The residue was suspended in methanolic HCl (1.25M, 6 mL) and heated to reflux for 3 hours. The solution was reduced to a residue and purified using MPLC (0-80% EtOAc in petroleum ether) giving 3-bromo-*N*-methyl-1-(tetrahydro-2*H*-pyran-2-yl)-1*H*-indazol-6-amine as a white solid 195 mg, 51%. Isolated material was used in the next step with out characterisation according to general procedure **A** using 3-bromo-*N*-methyl-1-(tetrahydro-2*H*-pyran-2-yl)-1*H*-indazol-6-amine (173 mg, 0.56 mmol) in pyridine (6 mL) and 2-thiophenesulphonyl chloride (122 mg, 0.67 mmol) to give the product as white solid (137 mg, 54%).

Or

Prepared according to general procedure **B** with following reagents and quantities: methyl iodide (56 μ L, 0.90 mmol), K₂CO₃ (75 mg, 0.54 mmol) and *N*-(3-Bromo-1-(tetrahydro-2*H*-pyran-2-yl)-1*H*-indazol-6-yl)thiophene-2-sulfonamide (200 mg, 0.45 mmol) in DMF (3 mL) this gave the title compound as a white solid (201 mg, 98%).

m.p. 95-97 °C; UV λ_{max} (EtOH/nm) 296.6, 263.8, 218.2; IR ν_{max} /cm⁻¹ 3070, 2935, 2866, 1349, 1148; ¹H-NMR (500 MHz, CDCl₃) δ ppm; 1.62-1.76 (3H, m, H-4', H5'), 2.04-2.07 (1H, m, H-6'), 2.11-2.14 (1H, m, H-5'), 3.31 (3H, s, H-17), 3.68-3.73 (1H, m, H-3'), 3.97-4.00 (1H, m, H-3'), 5.61 (1H, dd, J = 2.7, 9.0 Hz, H-1'), 6.87 (1H, dd, J = 8.6, 1.7 Hz, H-6), 7.08 (1H, dd, J = 4.9, 3.8 Hz, H-15), 7.34 (1H, dd, J = 1.3, 3.8 Hz, H-16), 7.47 (1H, d, J = 1.7 Hz, H-8), 7.50 (1H, d, J = 8.6 Hz, H-5), 7.60 (1H, dd, J = 1.3, 4.9, H-14); ¹³C-NMR (125 MHz, CDCl₃) δ ppm; 22.3 (C-4') 25.0 (C-5'), 29.2 (C-6'), 38.7 (C-17), 67.4 (C-3'), 85.6 (C-1'), 110.0 (C-8), 120.3 (C-6), 120.8 (C-5), 122.0 (C-4), 123.6 (C-3), 127.4 (C-15), 132.3 (C-14), 133.0 (C-16), 136.6 (C-12), 140.4 (C-9), 140.9 (C-7); MS (ES⁺) m/z 455.2 [M(⁷⁹Br)+H]⁺.

***N*-methyl-*N*-(3-methyl-1-(tetrahydro-2*H*-pyran-2-yl)-1*H*-indazol-6-yl)benzenesulfonamide (243)**

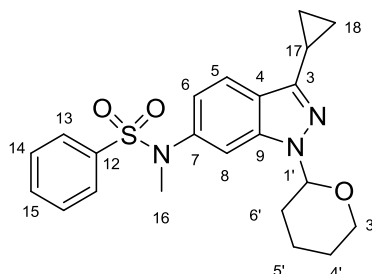


Prepared according to general procedure **F** using *N*-(3-bromo-1-(tetrahydro-2*H*-pyran-2-yl)-1*H*-indazol-6-yl)-*N*-methylbenzenesulfonamide (50 mg, 0.11 mmol), trimethyl boroxine (16 μ L, 0.11 mmol), Cs₂CO₃ (54 mg, 0.16 mmol) and Pd(dppf)Cl₂.DCM (9 mg, 0.01 mmol) in 1,4-dioxane (2 mL). The product was isolated as a white solid (42 mg, 99%).

m.p. 62-64 °C; UV λ_{max} (EtOH/nm) 295.0, 265.6, 219.8; IR ν_{max} /cm⁻¹ 2927, 2854, 1345, 1169; ¹H-NMR (500 MHz, CDCl₃) δ ppm; 1.60-1.62 (1H, m, H5'), 1.71-1.73 (2H, m, H-4', H5'), 1.99-2.01 (1H, m, H-6'), 2.10-2.24 (1H, m, H-4'), 2.48-2.50 (1H, m, H-6'), 2.54 (3H, s, H-17), 3.24 (3H, s, H-16), 3.67-3.71 (1H, m, H-3'), 4.03-4.05 (1H, m, H-3'), 5.61 (1H, dd, J = 2.4, 10.0 Hz, H-1'), 6.72 (1H, dd, J = 8.5, 1.6 Hz, H-6), 7.31 (1H, d, J = 1.6 Hz, H-8), 7.46 (2H, dd, J = 8.2, 8.2 Hz, H-14), 7.49 (1H, d, J = 8.5 Hz, H-5), 7.57-7.60 (3H, m, H-15, H-13); ¹³C-NMR (125 MHz, CDCl₃) δ ppm; 12.0 (C-17), 22.9 (C-4') 25.1 (C-5'), 29.7 (C-6'), 38.8 (C-16), 67.9 (C-3'), 85.1 (C-1'), 109.3 (C-8), 119.1 (C-6), 120.6 (C-5), 123.3 (C-

4), 128.0 (C-13), 128.8 (C-14), 132.7 (C-15), 136.7 (C-12), 140.0 (C-9), 140.3 (C-7), 142.7 (C-3); MS (ES⁺) *m/z* 386.1 [M+H]⁺.

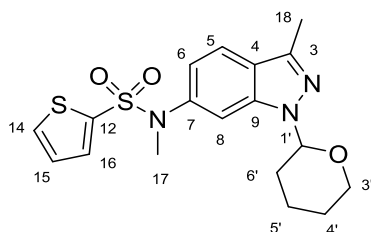
***N*-(3-Cyclopropyl-1-(tetrahydro-2*H*-pyran-2-yl)-1*H*-indazol-6-yl)-*N*-methylbenzenesulfonamide (244)**



Prepared according to general procedure **F** using *N*-(3-bromo-1-(tetrahydro-2*H*-pyran-2-yl)-1*H*-indazol-6-yl)-*N*-methylbenzenesulfonamide (50 mg, 0.11 mmol), cyclopropyl boronic acid (29 mg, 0.33 mmol), Cs₂CO₃ (54 mg, 0.16 mmol) and Pd(dppf)Cl₂.DCM (9 mg, 0.01 mmol) in 1,4-dioxane (3 mL). The product was isolated as a white solid (33 mg, 80%).

m.p. 67-69 °C; UV λ_{max} (EtOH/nm) 300.4, 217.6; IR ν_{max}/cm⁻¹ 2936, 2856, 1345, 1169; ¹H-NMR (500 MHz, CDCl₃) δ ppm; 0.99-1.05 (4H, m, H-18), 1.59-1.61 (1H, m, H-5'), 1.66-1.73 (2H, m, H-5', H-4'), 1.95-1.98 (1H, m, H-6'), 2.08-2.11 (1H, m, H-4'), 2.15-2.18 (1H, m, H-17), 2.43-2.46 (1H, m, H-6'), 3.24 (3H, s, H-16), 3.63-3.69 (1H, m, H-3'), 3.99-4.01 (1H, m, H-3'), 5.51 (1H, dd, *J* = 2.7, 9.8 Hz, H-1'), 6.72 (1H, dd, *J* = 8.6, 1.7 Hz, H-6), 7.28 (1H, *J* = 1.7 Hz, H-8), 7.46 (2H, dd, *J* = 7.6, 7.6 Hz, H-14), 7.56-7.60 (4H, m, H-13, H-15, H-5); ¹³C-NMR (125 MHz, CDCl₃) δ ppm; 7.1 (C-18), 8.3 (C-17), 22.7 (C-4') 25.1 (C-5'), 29.4 (C-6'), 38.8 (C-17), 67.7 (C-3'), 85.4 (C-1'), 109.5 (C-8), 119.2 (C-6), 120.5 (C-5), 122.8 (C-4), 128.0 (C-13), 128.7 (C-14), 132.7 (C-15), 136.7 (C-12), 139.9 (C-9), 140.4 (C-7), 147.5 (C-3); MS (ES⁺) *m/z* 412.3 [M+H]⁺.

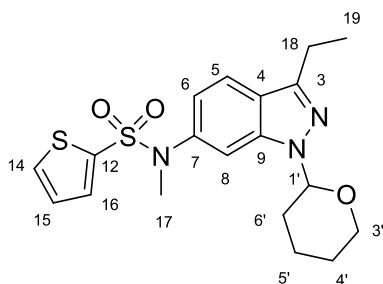
***N*-Methyl-*N*-(3-methyl-1-(tetrahydro-2*H*-pyran-2-yl)-1*H*-indazol-6-yl)thiophene-2-sulfonamide (239)**



Prepared according to general procedure **F** using *N*-(3-Bromo-1-(tetrahydro-2*H*-pyran-2-yl)-1*H*-indazol-6-yl)-*N*-methylthiophene-2-sulfonamide (80 mg, 0.18 mmol), trimethyl boroxine (25 μ L, 0.18 mmol), Cs_2CO_3 (86 mg, 0.26 mmol) and $\text{Pd}(\text{dppf})\text{Cl}_2\cdot\text{DCM}$ (14 mg, 0.02 mmol) in 1,4-dioxane (3 mL). The product was isolated as a white solid (50 mg, 71%).

m.p. 59-61 $^\circ\text{C}$; UV λ_{max} (EtOH/nm) 295.1, 242.6, 218.6; IR $\nu_{\text{max}}/\text{cm}^{-1}$ 33092, 2928, 2853, 1349, 1148; ^1H -NMR (500 MHz, CDCl_3) δ ppm; 1.59-1.62 (1H, m, H-5'), 1.72-1.76 (2H, m, H-4', H-5'), 2.00-2.03 (1H, m, H-6'), 2.11-2.13 (1H, m, H-4'), 2.47-2.53 (1H, m, H-6'), 2.54 (3H, s, H-18), 3.31 (3H, s, H-17), 3.68-3.73 (1H, m, H-3'), 4.03-4.05 (1H, m, H-3'), 5.55 (1H, dd, $J = 2.4, 10.0$ Hz, H-1'), 6.78 (1H, dd, $J = 8.6, 1.4$ Hz, H-6), 7.08 (1H, dd, $J = 4.8, 3.8$ Hz, H-15), 7.34 (1H, dd, $J = 1.0, 3.8$ Hz, H-16), 7.36 (1H, d, $J = 1.4$ Hz, H-8), 7.52 (1H, d, $J = 8.6$ Hz, H-5), 7.59 (1H, dd, $J = 1.0, 4.8$, H-14); ^{13}C -NMR (125 MHz, CDCl_3) δ ppm; 12.0 (C-18), 22.5 (C-4'), 25.1 (C-5'), 29.6 (C-6'), 38.9 (C-17), 67.9 (C-3'), 85.1 (C-1'), 109.4 (C-8), 118.9 (C-6), 120.7 (C-5), 123.5 (C-4), 127.3 (C-15), 132.1 (C-14), 132.9 (C-16), 136.9 (C-12), 139.7 (C-9), 140.3 (C-7), 142.7 (C-3); MS (ES^+) m/z 392.3 $[\text{M}+\text{H}]^+$.

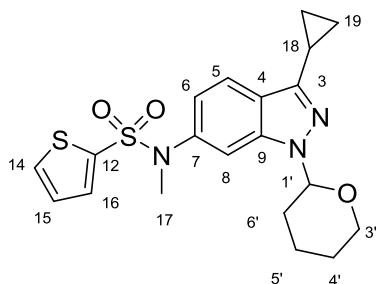
***N*-(3-Ethyl-1-(tetrahydro-2*H*-pyran-2-yl)-1*H*-indazol-6-yl)-*N*-methylthiophene-2-sulfonamide (240)**



Prepared according to general procedure **F** using *N*-(3-Bromo-1-(tetrahydro-2*H*-pyran-2-yl)-1*H*-indazol-6-yl)-*N*-methylthiophene-2-sulfonamide (80 mg, 0.18 mmol), ethyl boronic acid (39 mg, 0.53 mmol), Cs₂CO₃ (86 mg, 0.26 mmol) and Pd(dppf)Cl₂.DCM (14 mg, 0.02 mmol) in 1,4-dioxane (3 mL). The product was isolated as a white solid (50 mg, 71%).

m.p. 63-65 °C; UV λ_{max} (EtOH/nm) 294.8, 256.3, 218.2; IR ν_{max} /cm⁻¹ 3089, 2935, 2856, 1349, 1050; ¹H-NMR (500 MHz, CDCl₃) δ ppm; 1.37 (3H, t, *J* = 7.3 Hz, H-19), 1.61-1.63 (1H, m, H-5'), 1.72-1.75 (2H, m, H-4', H-5'), 1.99-2.02 (1H, m, H-6'), 2.11-2.13 (1H, m, H-4'), 2.48-2.51 (1H, m, H-6'), 2.96 (2H, q, *J* = 7.3 Hz, H-18), 3.31 (3H, s, H-17), 3.68-3.72 (1H, m, H-3'), 4.01-4.05 (1H, m, H-3'), 5.55 (1H, dd, *J* = 2.4, 9.9 Hz, H-1'), 6.79 (1H, dd, *J* = 8.7, 1.7 Hz, H-6), 7.09 (1H, dd, *J* = 4.8, 3.8 Hz, H-15), 7.34-7.36 (2H, m, H-8, H-16), 7.56-7.60 (2H, m, H-14, H-5); ¹³C-NMR (125 MHz, CDCl₃) δ ppm; 13.5 (C-19), 20.5 (C-18), 22.8 (C-4'), 25.1 (C-5'), 29.6 (C-6'), 38.9 (C-17), 67.9 (C-3'), 85.4 (C-1'), 109.5 (C-8), 118.9 (C-6), 120.8 (C-5), 122.7 (C-4), 127.3 (C-15), 132.0 (C-14), 132.9 (C-16), 137.0 (C-12), 139.6 (C-9), 140.4 (C-7), 147.8 (C-3); MS (ES⁺) *m/z* 406.2 [M+H]⁺.

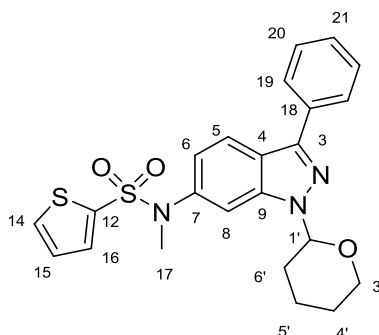
***N*-(3-Cyclopropyl-1-(tetrahydro-2*H*-pyran-2-yl)-1*H*-indazol-6-yl)-*N*-methylthiophene-2-sulfonamide (241)**



Prepared according to general procedure **F** using *N*-(3-Bromo-1-(tetrahydro-2*H*-pyran-2-yl)-1*H*-indazol-6-yl)-*N*-methylthiophene-2-sulfonamide (75 mg, 0.16 mmol), cyclopropyl boronic acid (42 mg, 0.49 mmol), Cs₂CO₃ (80 mg, 0.25 mmol) and Pd(dppf)Cl₂.DCM (13 mg, 0.02 mmol) in 1,4-dioxane (3 mL). The product was isolated as a white solid (66 mg, 96%).

m.p. 63-65 °C; UV λ_{max} (EtOH/nm) 298.8, 219.0; IR ν_{max}/cm⁻¹ 3068, 2927, 2854, 1347, 1168; ¹H-NMR (500 MHz, CDCl₃) δ ppm; 0.99-1.05 (4H, m, H-18), 1.59-1.62 (1H, m, H-5'), 1.69-1.73 (2H, m, H-5', H-4'), 1.96-1.99 (1H, m, H-6'), 2.10-2.12 (1H, m, H-4'), 2.14-2.18 (1H, m, H-17), 2.45-2.47 (1H, m, H-6'), 3.31 (3H, s, H-16), 3.66-3.70 (1H, m, H-3'), 3.99-4.02 (1H, m, H-3'), 5.53 (1H, dd, *J* = 2.6, 9.8 Hz, H-1'), 6.78 (1H, dd, *J* = 8.6, 1.6 Hz, H-6), 7.08 (1H, dd, *J* = 4.9, 3.8 Hz, H-15), 7.35 (2H, m, H-8, H-16), 7.58-7.60 (2H, m, H-14, H-5); ¹³C-NMR (125 MHz, CDCl₃) δ ppm; 7.1 (C-18), 8.3 (C-17), 22.7 (C-4') 25.1 (C-5'), 29.4 (C-6'), 38.9 (C-17), 67.7 (C-3'), 85.4 (C-1'), 109.6 (C-8), 119.0 (C-6), 120.7 (C-5), 122.9 (C-4), 127.3 (C-15), 132.0 (C-14), 132.9 (C-16), 137.0 (C-12), 139.6 (C-9), 140.4 (C-7), 147.5 (C-3); MS (ES⁺) *m/z* 418.2 [M+H]⁺.

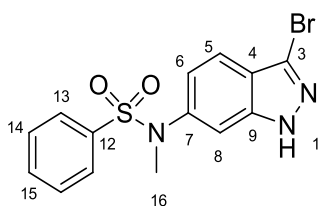
***N*-methyl-*N*-(3-phenyl-1-(tetrahydro-2*H*-pyran-2-yl)-1*H*-indazol-6-yl)thiophene-2-sulfonamide (242)**



Prepared according to general procedure **F** using *N*-(3-Bromo-1-(tetrahydro-2*H*-pyran-2-yl)-1*H*-indazol-6-yl)-*N*-methylthiophene-2-sulfonamide (80 mg, 0.18 mmol), phenyl boronic acid (64 mg, 0.53 mmol), Cs₂CO₃ (86 mg, 0.26 mmol) and Pd(dppf)Cl₂.DCM (14 mg, 0.02 mmol) in 1,4-dioxane (3 mL). The product was isolated as a white solid (79 mg, 99%).

m.p. 156-158 °C; UV λ_{max} (EtOH/nm) 308.2, 246.4, 218.8; IR ν_{max}/cm⁻¹ 3087, 2926, 2852, 1349, 1039; ¹H-NMR (500 MHz, CDCl₃) δ ppm; 1.65-1.68 (1H, m, H-5'), 1.72-1.79 (2H, m, H-4', H-5'), 2.09-2.12 (1H, m, H-6'), 2.16-2.19 (1H, m, H-4'), 2.57-2.63 (1H, m, H-6'), 3.34 (3H, s, H-17), 3.73-3.77 (1H, m, H-3'), 4.02-4.04 (1H, m, H-3'), 5.72 (1H, dd, *J* = 2.6, 9.3 Hz, H-1'), 6.88 (1H, dd, *J* = 8.6, 1.4 Hz, H-6), 7.09 (1H, dd, *J* = 5.0, 3.8 Hz, H-15), 7.37 (1H, d, *J* = 1.4 Hz, H-8), 7.40 (1H, t, *J* = 7.3 Hz, H-21), 7.47-7.50 (3H, m, H-16, H-20), 7.60 (1H, dd, *J* = 1.2, 5.0 Hz, H-14), 7.89 (1H, d, *J* = 8.6 Hz, H-5), 7.93 (2H, d, *J* = 7.3, H-19); ¹³C-NMR (125 MHz, CDCl₃) δ ppm; 22.5 (C-4') 25.1 (C-5'), 29.4 (C-6'), 38.9 (C-17), 67.5 (C-3'), 85.7 (C-1'), 109.9 (C-8), 120.0 (C-6), 121.7 (C-5), 121.8 (C-4), 127.4 (C-15), 127.6 (C-19), 128.2 (C-21), 128.8 (C-20), 132.1 (C-14), 132.9 (C-16), 133.1 (C-18), 136.9 (C-12), 139.6 (C-9), 140.9 (C-7), 144.6 (C-3); MS (ES⁺) *m/z* 454.3 [M+H]⁺.

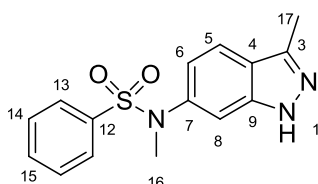
***N*-(3-Bromo-1*H*-indazol-6-yl)-*N*-methylbenzenesulfonamide (250)**



Prepared according to general procedure **A** using 3-bromo-*N*-methyl-1*H*-indazol-6-amine (45 mg, 0.19 mmol) in pyridine (1.5 mL) and benzenesulphonyl chloride (28 μ L, 0.22 mmol) to give the product as an off white solid (35 mg, 48%).

R_f 0.51 (Et₂O); m.p. 158-159 °C; UV λ_{\max} (EtOH/nm) 294.2, 212.8; IR $\nu_{\max}/\text{cm}^{-1}$ 3325, 3065, 2929, 1622; ¹H-NMR (500 MHz, CDCl₃) δ ppm; 3.25 (1H, s, H-16) 6.85 (1H, d, J = 8.7 Hz, H-6), 7.42 (1H, s, H-8), 7.46 (2H, dd, J = 7.7, 7.7 Hz, H-14), 7.51 (1H, d, J = 8.7 Hz, H-5), 7.56 (2H, d, J = 7.7 Hz, H-13), 7.59 (1H, t, J = 7.7 Hz, H-15) 10.83 (1H, s-br, H-1); ¹³C-NMR (125 MHz, CDCl₃) δ ppm; 38.5 (C-16), 109.2 (C-8), 120.2 (C-6), 120.6 (C-5), 122.0 (C-4), 122.9 (C-9), 127.8 (C-13), 129.0 (C-14), 133.1 (C-15), 136.3 (C-12), 141.0 (C-3), 141.5 (C-7); MS (ES⁺) m/z 368.2 [M+H]⁺; HRMS calcd for C₁₄H₁₂BrN₃O₂S 365.9906/367.9885 [M+H]⁺ found 365.9901/367.9875.

***N*-Methyl-*N*-(3-methyl-1*H*-indazol-6-yl)benzenesulfonamide (251)**

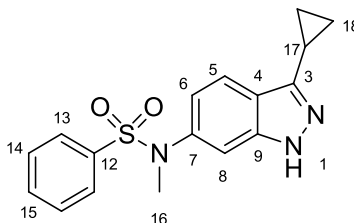


Prepared according to general procedure **D** using *N*-methyl-*N*-(3-methyl-1-(tetrahydro-2*H*-pyran-2-yl)-1*H*-indazol-6-yl)benzenesulfonamide (38 mg, 0.10 mmol) in MeOH.HCl (1.25 M, 3 mL) giving the title compound via semi-preparatory HPLC (H₂O (0.1% HCOOH) : MeCN (13:7)) as a white solid (7 mg, 24 %).

R_f 0.56 (Et₂O); m.p. <60 °C; UV λ_{\max} (EtOH/nm) 293.8, 213.6; IR $\nu_{\max}/\text{cm}^{-1}$ 3357, 3175, 3062, 2924, 1623; ¹H-NMR (500 MHz, CDCl₃) δ ppm; 2.57 (3H, s, H-17), 3.25 (3H, s, H-16), 6.79 (1H, dd, J = 1.7, 8.6 Hz, H-6), 7.26 (1H, s, H-8), 7.45 (2H, dd, J = 7.5, 8.1 Hz, H-14), 7.54-7.59 (4H, m, H-15, H-13, H-5); ¹³C-NMR (125 MHz, CDCl₃) δ ppm; 12.0 (17),

38.6 (C-16), 108.6 (C-8), 119.0 (C-6), 120.5 (C-5), 121.9 (C-4), 127.9 (C-13), 128.8 (C-14), 132.9 (C-15), 136.5 (C-12), 140.4 (C-7) 143.5 (C-3); MS (ES⁺) m/z 302.2 [M+H]⁺; HRMS calcd for C₁₅H₁₆N₃O₂S 302.0958 [M+H]⁺ found 302.0955.

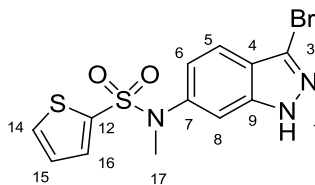
***N*-(3-Cyclopropyl-1*H*-indazol-6-yl)-*N*-methylbenzenesulfonamide (252)**



Prepared according to general procedure **D** using *N*-(3-cyclopropyl-1-(tetrahydro-2*H*-pyran-2-yl)-1*H*-indazol-6-yl)-*N*-methylbenzenesulfonamide (25 mg, 0.06 mmol) in MeOH.HCl (1.25 M, 6 mL) giving the title compound as a white solid (13 mg, 67%)

R_f 0.59 (Et₂O); m.p. 63-65 °C; UV λ_{max} (EtOH/nm) 298.2, 265.6, 215.2; IR ν_{max}/cm^{-1} 3352, 3172, 2925, 1622; ¹H-NMR (500 MHz, CDCl₃) δ ppm; 1.04-1.07 (4H, m, H-18), 2.19 (1H, m, H-17), 3.24 (3H, s, H-16), 6.79 (1H, d, J = 8.6 Hz, H-6), 7.23 (1H, s, H-8), 7.45 (2H, dd, J = 7.6, 7.8 Hz, H-14), 7.56-7.60 (3H, m, H-15, H-13), 7.63 (1H, d, J = 8.6 Hz, H-5); ¹³C-NMR (125 MHz, CDCl₃) δ ppm; 7.3 (18), 8.1 (C-17), 38.6 (C-16), 108.6 (C-8), 119.0 (C-6), 120.5 (C-5), 127.9 (C-13), 128.8 (C-14), 132.9 (C-15), 136.5 (C-12), 140.4 (C-7); MS (ES⁺) m/z 328.3 [M+H]⁺.

***N*-(3-Bromo-1*H*-indazol-6-yl)-*N*-methylthiophene-2-sulfonamide (245)**

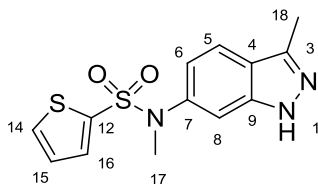


Prepared according to general procedure **D** using *N*-(3-bromo-1-(tetrahydro-2*H*-pyran-2-yl)-1*H*-indazol-6-yl)-*N*-methylthiophene-2-sulfonamide (25 mg, 0.06 mmol) in MeOH.HCl (1.25 M, 4 mL) giving the title compound as a pale orange solid (19 mg, 92%)

R_f 0.48 (Et₂O); m.p. 158-160 °C; UV λ_{max} (EtOH/nm) 294.0, 214.6; IR ν_{max}/cm^{-1} 3286, 3099, 2923, 1622; ¹H-NMR (500 MHz, CDCl₃) δ ppm; 3.32 (3H, s, H-17), 6.91 (1H, d, J = 8.7 Hz, H-6), 7.09 (1H, dd, J = 4.5, 3.8 Hz, H-15), 7.34 (1H, d, J = 3.8 Hz, H-16), 7.43 (1H,

d, $J = 1.6$ Hz, H-8), 7.54 (1H, d, $J = 8.7$ Hz, H-5), 7.87 (1H, d, $J = 4.9$ Hz, H-14), 10.49 (1H, s-br, H-1); ^{13}C -NMR (125 MHz, CDCl_3) δ ppm; 38.6 (C-17), 109.2 (C-8), 120.2 (C-6), 120.7 (C-5), 123.1 (C-4), 127.5 (C-15), 132.4 (C-14), 133.0 (C-16), 136.5 (C-12), 140.1 (C-9), 141.3 (C-7); MS (ES^+) m/z 372.1 $[\text{M}(^{79}\text{Br})+\text{H}]^+$.

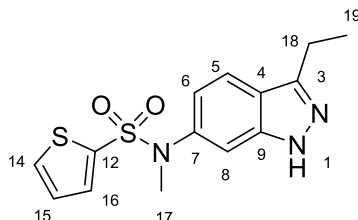
***N*-(3-Ethyl-1*H*-indazol-6-yl)-*N*-methylthiophene-2-sulfonamide (246)**



Prepared according to general procedure **D** using *N*-methyl-*N*-(3-methyl-1-(tetrahydro-2*H*-pyran-2-yl)-1*H*-indazol-6-yl)thiophene-2-sulfonamide (55 mg, 0.14 mmol) in MeOH.HCl (1.25 M, 5 mL) giving the title compound as a white solid (13 mg, 31 %)

R_f 0.58 (Et_2O); m.p. 172-174°C; UV λ_{max} (EtOH/nm) 214.8; IR $\nu_{\text{max}}/\text{cm}^{-1}$ 3270, 3104, 2935, 1351, 1159; ^1H -NMR (500 MHz, CDCl_3) δ ppm; 2.57 (3H, s, H-18), 3.31 (3H, s, H-17), 6.84 (1H, dd, $J = 8.6, 1.4$ Hz, H-6), 7.07 (1H, dd, $J = 4.8, 3.9$ Hz, H-15), 7.29 (1H, s, H-8), 7.33 (1H, dd, $J = 1.0, 3.9$ Hz, H-16), 7.57-7.59 (2H, m, H-14, H-5); ^{13}C -NMR (125 MHz, CDCl_3) δ ppm; 12.0 (C-18), 38.7 (C-17), 108.7 (C-8), 118.9 (C-6), 120.6 (C-5), 121.2 (C-4), 127.4 (C-15), 132.2 (C-14), 132.8 (C-16), 136.7 (C-12), 140.0 (C-9), 141.1 (C-7), 148.7 (C-3); MS (ES^+) m/z 308.2 $[\text{M}+\text{H}]^+$; HRMS calcd for $\text{C}_{13}\text{H}_{14}\text{N}_3\text{O}_2\text{S}_2$ 308.0522 $[\text{M}+\text{H}]^+$ found 308.0521.

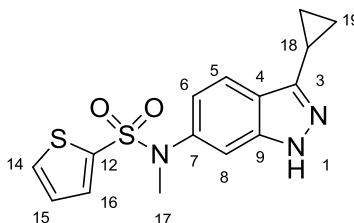
***N*-(3-Ethyl-1*H*-indazol-6-yl)-*N*-methylthiophene-2-sulfonamide (247)**



Prepared according to general procedure **D** using *N*-methyl-*N*-(3-ethyl-1-(tetrahydro-2*H*-pyran-2-yl)-1*H*-indazol-6-yl)thiophene-2-sulfonamide (65 mg, 0.16 mmol) in MeOH.HCl (1.25 M, 5 mL) giving the title compound as a light pink solid (32 mg, 63%)

R_f 0.62 (Et₂O); m.p. 54-56 °C; UV λ_{\max} (EtOH/nm) 217.0; IR $\nu_{\max}/\text{cm}^{-1}$ 3367, 3172, 3107, 2969, 2933, 1623; ¹H-NMR (500 MHz, CDCl₃) δ ppm; 1.41 (3H, t, J = 7.6 Hz, H-19), 2.99 (2H, q, J = 7.6 Hz, H-18), 3.31 (3H, s, H-17), 6.85 (1H, dd, J = 8.6, 1.7 Hz, H-6), 7.07 (1H, dd, J = 4.9, 3.8 Hz, H-15), 7.29 (1H, d, J = 1.7 Hz, H-8), 7.34 (1H, dd, J = 1.2, 3.8 Hz, H-16), 7.58 (1H, dd, J = 1.2, 4.9 Hz, H-14), 7.66 (1H, d, J = 8.6 Hz, H-5); ¹³C-NMR (125 MHz, CDCl₃) δ ppm; 13.3 (C-19), 20.4 (C-18), 38.8 (C-17), 108.7 (C-8), 118.9 (C-6), 120.6 (C-5), 121.2 (C-4), 127.4 (C-15), 132.2 (C-14), 132.9 (C-16), 136.7 (C-12), 140.0 (C-9), 141.1 (C-7), 148.7 (C-3); MS (ES⁺) m/z 322.2 [M+H]⁺; HRMS calcd for C₁₄H₁₆N₃O₂S₂ 322.0678 [M+H]⁺ found 322.0673.

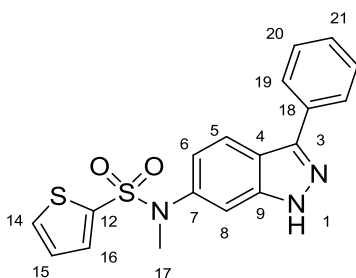
***N*-(3-Cyclopropyl-1*H*-indazol-6-yl)-*N*-methylthiophene-2-sulfonamide (248)**



Prepared according to general procedure **D** using *N*-(3-cyclopropyl-1-(tetrahydro-2*H*-pyran-2-yl)-1*H*-indazol-6-yl)-*N*-methylthiophene-2-sulfonamide (66 mg, 0.16 mmol) in MeOH.HCl (1.25 M, 8 mL) giving the title compound as a pale orange solid (13 mg, 24%).

R_f 0.55 (Et₂O); m.p. <60 °C; UV λ_{\max} (EtOH/nm) 298.2, 217.4; IR $\nu_{\max}/\text{cm}^{-1}$ 3365, 3172, 3092, 3004, 2929, 1622; ¹H-NMR (500 MHz, CDCl₃) δ ppm; 1.03-1.07 (4H, m, H-19), 2.18-2.22 (1H, m, H-18), 3.31 (3H, s, H-17), 6.85 (1H, dd, J = 8.6, 1.7 Hz, H-6), 7.07 (1H, dd, J = 4.9, 3.8 Hz, H-15), 7.27 (1H, d, J = 1.7 Hz, H-8), 7.34 (1H, dd, J = 1.2, 3.8 Hz, H-16), 7.58 (1H, dd, J = 1.2, 4.9 Hz, H-14), 7.66 (1H, d, J = 8.6 Hz, H-5); ¹³C-NMR (125 MHz, CDCl₃) δ ppm; 7.3 (C-19), 8.1 (C-18), 38.7 (C-17), 108.7 (C-8), 118.9 (C-6), 120.6 (C-5), 121.6 (C-4), 127.4 (C-15), 132.2 (C-14), 132.9 (C-16), 136.7 (C-12), 140.0 (C-9), 141.2 (C-7), 148.8 (C-3); MS (ES⁺) m/z 334.2 [M+H]⁺.

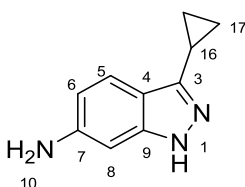
***N*-Methyl-*N*-(3-phenyl-1*H*-indazol-6-yl)thiophene-2-sulfonamide (249)**



Prepared according to general procedure **D** using *N*-methyl-*N*-(3-phenyl-1-(tetrahydro-2*H*-pyran-2-yl)-1*H*-indazol-6-yl)thiophene-2-sulfonamide (68 mg, 0.15 mmol) in MeOH.HCl (1.25 M, 5 mL) giving the title compound as a pale orange solid (50 mg, 90%)

R_f 0.71 (Et₂O); m.p. 67-69 °C; UV λ_{\max} (EtOH/nm) 305.2, 244.8, 216.0; IR ν_{\max} /cm⁻¹ 3354, 3167, 3108, 2931, 1623; ¹H-NMR (500 MHz, CDCl₃) δ ppm; 3.32 (3H, s, H-17), 6.94 (1H, dd, J = 8.7, 1.7 Hz, H-6), 7.07 (1H, dd, J = 5.0, 3.7 Hz, H-15), 7.34 (1H, d, J = 1.7 Hz, H-8), 7.36 (1H, dd, J = 1.2, 3.7 Hz, H-16), 7.43 (1H, tt, J = 7.4, 1.1 Hz, H-21), 7.51, (2H, dd, J = 7.4, 5.8 Hz, H-20), 7.58 (1H, dd, J = 1.2, 5.0 Hz, H-14), 7.92-7.94 (3H, m, H-5, H-19); ¹³C-NMR (125 MHz, CDCl₃) δ ppm; 38.7 (C-17), 108.9 (C-8), 120.2 (C-6), 120.2 (C-4), 121.6 (C-5), 127.4 (C-15), 127.5 (C-19), 128.4 (C-21), 129.0 (C-20), 132.3 (C-14), 132.9 (C-16), 133.0 (C-18), 136.7 (C-12), 140.0 (C-9), 141.2 (C-7), 145.8 (C-3); MS (ES⁺) m/z 370.3 [M+H]⁺; HRMS calcd for C₁₈H₁₆N₃O₂S₂ 370.0678 [M+H]⁺ found 370.0671.

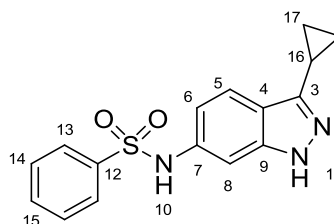
3-Cyclopropyl-1*H*-indazol-6-amine (254)



Prepared according to general procedure **F** using 3-bromo-6-nitro-1-(tetrahydro-2*H*-pyran-2-yl)-1*H*-indazole (250 mg, 0.75 mmol), cyclopropyl boronic acid (200 mg, 2.25 mmol), Pd(dppf)Cl₂.DCM (12 mg, 0.02 mmol) and Cs₂CO₃ (375 mg, 1.15 mmol) in 1,4-dioxane (9 mL) to give the crude intermediate 3-cyclopropyl-6-nitro-1*H*-indazole (91 mg, 58%). Isolated material was immediately progressed into general procedure **E** using 3-cyclopropyl-6-nitro-1*H*-indazole (90 mg, 0.44 mmol) in EtOAc (20 mL, 0.015M). The product was isolated as a white solid, (71.3 mg, 93%).

R_f 0.44 (Et₂O); m.p. 175-176 °C; UV λ_{\max} (EtOH/nm) 294.4, 224.6; IR $\nu_{\max}/\text{cm}^{-1}$ 3374, 3181, 3080, 2941, 2894, 1625; ¹H-NMR (500 MHz, DMSO-*d*₆) δ ppm; 0.87-0.93 (4H, m, H-17), 2.08-2.12 (1H, m, H-16), 5.52 (2H, s-br, H-10), 6.42-6.44 (1H, m, H-8, H-6), 7.35 (1H, d, J = 9.2 Hz, H-5) 11.76 (1H, s-br, H-1); ¹³C-NMR (125 MHz, DMSO-*d*₆) δ ppm; 7.1 (C-17), 8.0 (C-16), 90.6 (C-8), 111.3 (C-6), 114.3 (C-4), 119.8 (C-5), 143.2 (C-9), 145.9 (C-7), 147.4 (C-3); MS (ES⁺) m/z 174.2 [M+H]⁺; HRMS calcd for C₁₀H₁₂N₃ 174.1026 [M+H]⁺ found 174.1023.

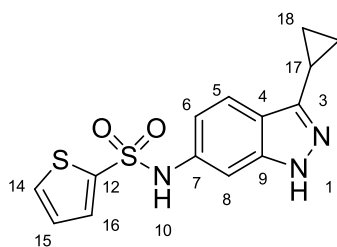
***N*-(3-Cyclopropyl-1*H*-indazol-6-yl)benzenesulfonamide (255)**



Prepared according to general procedure **A** using 3-cyclopropyl-1*H*-indazol-6-amine (22 mg, 0.13 mmol) in pyridine (1 mL) and benzenesulphonyl chloride (18 μ L, 0.14 mmol) to give the product as an off white solid (16.5 mg, 41%).

R_f 0.53 (Et₂O); m.p. 73-75 °C; UV λ_{\max} (EtOH/nm) 294.0, 216.4; IR $\nu_{\max}/\text{cm}^{-1}$ 3248, 3067, 2923, 1629; ¹H-NMR (500 MHz, CDCl₃) δ ppm; 1.00-1.02 (4H, m, H-17), 2.14 (1H, m, H-16), 6.76 (1H, d, J = 8.6 Hz, H-6), 7.28 (1H, s, H-8), 7.37 (1H, s-br, H-10), 7.41 (2H, dd, J = 7.4, 7.4 Hz, H-14), 7.51 (1H, t, J = 7.4 Hz, H-15), 7.57 (1H, d, J = 8.6 Hz, H-5), 7.67 (2H, d, J = 7.5 Hz, H-13); ¹³C-NMR (125 MHz, CDCl₃) δ ppm; 7.3 (17), 8.1 (C-16), 102.1 (C-8), 115.6 (C-6), 121.2 (C-5), 127.2 (C-13), 129.1 (C-14), 133.1 (C-15), 135.5 (C-9), 139.0 (C-12), 141.6 (C-7), 148.6 (C-3); MS (ES⁺) m/z 314.3 [M+H]⁺; HRMS calcd for C₁₆H₁₅N₃O₂S 314.0958 [M+H]⁺ found 314.0953.

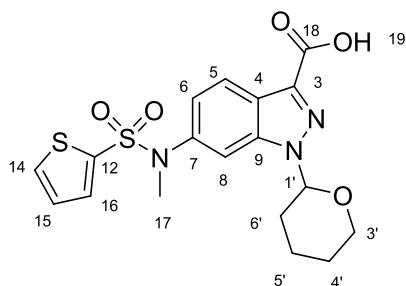
***N*-(3-Cyclopropyl-1*H*-indazol-6-yl)thiophene-2-sulfonamide (256)**



Prepared according to general procedure **A** using 3-cyclopropyl-1*H*-indazol-6-amine (22 mg, 0.13 mmol) in pyridine (1 mL) and 2-thiophenesulphonyl chloride (25 mg, 0.14 mmol) to give the product as an off white solid (18.5 mg, 46%).

R_f 0.48 (Et₂O); m.p. 178-180 °C; UV λ_{\max} (EtOH/nm) 293.8, 221.6; IR $\nu_{\max}/\text{cm}^{-1}$ 3384, 3103, 2922, 2860, 1626; ¹H-NMR (500 MHz, DMSO-*d*₆) δ ppm; 0.90, (2H, m, H-18A), 0.95 (2H, m, H-18B), 2.19 (1H, m, H-17), 6.87 (1H, dd, J = 8.6, 1.6 Hz, H-6), 7.10 (1H, dd, J = 4.9, 3.8 Hz, H-15), 7.22 (1H, d, J = 1.6 Hz, H-8), 7.51 (1H, dd, J = 1.2, 3.8 Hz, H-16), 7.64 (1H, d, J = 8.6 Hz, H-5), 7.87 (1H, dd, J = 1.2, 4.8 Hz, H-14), 10.49 (1H, s-br, H-10), 12.42 (1H, s-br, H-1); ¹³C-NMR (125 MHz, DMSO-*d*₆) δ ppm; 7.4 (C-18), 7.8 (C-17), 100.5 (C-8), 114.1 (C-6), 118.8 (C-4), 120.5 (C-5), 127.6 (C-15), 132.3 (C-16), 133.3 (C-14), 135.7 (C-7), 139.8 (C-12), 141.2 (C-9), 146.4 (C-3); MS (ES⁺) m/z 320.2 [M+H]⁺; HRMS calcd for C₁₄H₁₃N₃O₂S₂ 320.0522 [M+H]⁺ found 320.0518.

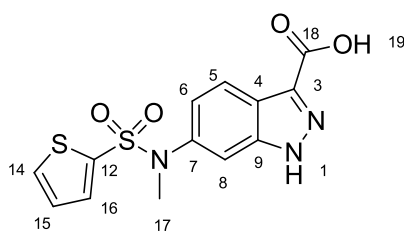
6-(*N*-Methylthiophene-2-sulfonamido)-1-(tetrahydro-2*H*-pyran-2-yl)-1*H*-indazole-3-carboxylic acid (261)



Prepared according to general procedure **N** using: *N*-(3-bromo-1-(tetrahydro-2*H*-pyran-2-yl)-1*H*-indazol-6-yl)-*N*-methylthiophene-2-sulfonamide (100 mg, 0.22 mmol), Pd(OAc)₂ (5 mg, 0.02 mmol), XantPhos (4,5-Bis(diphenylphosphino)-9,9-dimethylxanthene, 25 mg, 0.04 mmol) lithium formate monohydrate (61 mg, 0.88 mmol), Et₃N (122 μ L, 0.88 mmol) and Ac₂O (83 μ L, 0.88 mmol) in DMF (2 mL) to give the product as a white solid (88 mg, 95%).

¹H-NMR (500 MHz, DMSO-*d*₆) δ ppm; 1.56-1.51 (2H, m, H-5', H-5'), 1.71-1.79 (1H, m, H-4'), 1.96-2.00 (2H, m, H-6', H-4'), 2.28-2.34 (1H, m, H-6'), 3.28 (3H, s, H-17), 3.71-3.76 (1H, m, H-3'), 4.86-4.88 (1H, m, H-3'), 5.93 (1H, dd, *J* = 2.5, 9.4 Hz, H-1'), 7.10 (1H, dd, *J* = 8.6, 1.6 Hz, H-6), 7.26 (1H, dd, *J* = 4.8, 3.7 Hz, H-15), 7.52 (1H, dd, *J* = 3.7, 1.4 Hz, H-16), 7.60 (1H, d, *J* = 1.6 Hz, H-8), 8.03-8.05 (2H, m, H-14, H-5); ¹³C-NMR (125 MHz, DMSO-*d*₆) δ ppm; 22.2 (C-4') 25.1 (C-5'), 29.2 (C-6'), 39.0 (C-17), 67.1 (C-3'), 85.1 (C-1'), 109.9 (C-8), 122.3 (C-5), 122.9 (C-6), 126.8 (C-4), 128.5 (C-15), 133.9 (C-16), 134.7 (C-14), 135.1 (C-12), 140.3 (C-7), 168.2 (C-18); MS (ES⁺) *m/z* 422.4 [M+H]⁺.

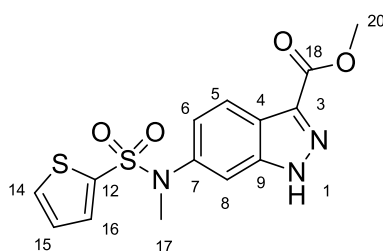
Methyl 6-(*N*-methylthiophene-2-sulfonamido)-1*H*-indazole-3-carboxylate (257)



6-(*N*-Methylthiophene-2-sulfonamido)-1-(tetrahydro-2*H*-pyran-2-yl)-1*H*-indazole-3-carboxylic acid (45 mg, 0.11 mmol) was dissolved in MeCN (3 mL) and concentrated HCL (0.5 mL) was added and the solution was stirred for 3 hours then reduced to a residue under vacuum. The title compound was obtained after MPCL (20-95% EtOAc in petrol) as an off white solid (25 mg, 69 %).

R_f 0.27 (10% MeOH in DCM); m.p. 231-233 °C; UV λ_{\max} (EtOH/nm) 294.2, 208.8; IR $\nu_{\max}/\text{cm}^{-1}$ 3246, 1712, 1338, 1142; $^1\text{H-NMR}$ (500 MHz, DMSO- d_6) δ ppm; 3.27 (3H, s, H-17), 7.05 (1H, dd, J = 8.8, 1.9 Hz, H-6), 7.24 (1H, dd, J = 4.8, 3.7 Hz, H-15), 7.37 (1H, d, J = 1.9 Hz, H-8), 7.49 (1H, dd, J = 1.4, 3.7 Hz, H-16), 8.00-8.02 (2H, m, H-5, H-14), 13.07 (1H, s-br, H-19), 13.83 (1H, s-br, H-1); $^{13}\text{C-NMR}$ (125 MHz, DMSO- d_6) δ ppm; 38.8 (C-17), 109.2 (C-8), 122.0 (C-5), 128.5 (C-15), 133.8 (C-16), 134.7 (C-14), 135.9 (C-12), 139.8 (C-7); MS (ES^+) m/z 338.3 [$\text{M}+\text{H}$] $^+$.

Methyl 6-(*N*-methylthiophene-2-sulfonamido)-1*H*-indazole-3-carboxylate (258)

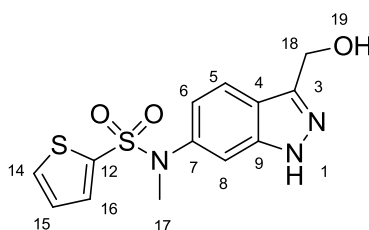


Prepared according to general procedure **D** using 6-(*N*-Methylthiophene-2-sulfonamido)-1-(tetrahydro-2*H*-pyran-2-yl)-1*H*-indazole-3-carboxylic acid (60 mg, 0.14 mmol) in MeOH.HCl (1.25 M, 5 mL) and MeOH (5 mL) giving the title compound as a white solid (48 mg, 97 %).

R_f 0.36 (10% MeOH in DCM); m.p. 139-141 °C; UV λ_{\max} (EtOH/nm) 294.8, 234.0, 208.4; IR $\nu_{\max}/\text{cm}^{-1}$ 3257, 3093, 2951, 1720, 1349, 1130; $^1\text{H-NMR}$ (500 MHz, DMSO- d_6) δ ppm;

3.17 (3H, s, H-17), 3.93 (3H, s, H-20), 6.62 (1H, dd, $J = 8.7, 1.7$ Hz, H-6), 7.24 (1H, dd, $J = 5.0, 3.8$ Hz, H-15), 7.40 (1H, d, $J = 1.7$ Hz, H-8), 7.50 (1H, dd, $J = 1.3, 3.8$ Hz, H-16), 8.00-8.02 (2H, m, H-5, H-14), 14.00 (1H, s-br, H-1); ^{13}C -NMR (125 MHz, DMSO- d_6) δ ppm; 38.8 (C-17), 52.2 (C-20), 109.4 (C-8), 121.5 (C-4), 121.7 (C-5), 122.2 (C-6), 128.5 (C-15), 133.8 (C-16), 134.7 (C-14), 135.9 (C-12), 140.0 (C-7), 141.1 (C-9), 151.0 (C-3) 162.9 (C-18); MS (ES^+) m/z 352.3 $[\text{M}+\text{H}]^+$.

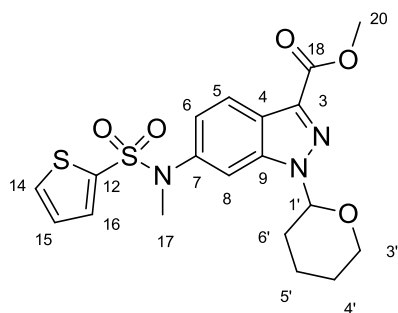
***N*-(3-(Hydroxymethyl)-1*H*-indazol-6-yl)-*N*-methylthiophene-2-sulfonamide (259)**



Prepared according to general procedure **G** using Methyl 6-(*N*-methylthiophene-2-sulfonamido)-1*H*-indazole-3-carboxylate (34 mg, 0.1 mmol) and LiAlH_4 (1M in THF, 0.2 mL, 0.20 mmol). The product was isolated as a grey solid (15 mg, 47%).

R_f 0.33 (10% MeOH in DCM); m.p. 166-168 $^{\circ}\text{C}$; UV λ_{max} (EtOH/nm) 291.8, 214.0; IR $\nu_{\text{max}}/\text{cm}^{-1}$ 3234, 2926, 1350, 1161, 1014; ^1H -NMR (500 MHz, CD_3OD) δ ppm; 3.30 (3H, s, H-17), 4.58 (1H, s, H-19), 4.94 (2H, s, H-18), 6.90 (1H, dd, $J = 8.7, 1.7$ Hz, H-6), 7.15 (1H, dd, $J = 4.9, 3.9$ Hz, H-15), 7.27 (1H, d, $J = 1.7$ Hz, H-8), 7.37 (1H, dd, $J = 1.1, 3.9$ Hz, H-16), 7.79-7.81 (2H, m, H-5, H-14); ^{13}C -NMR (125 MHz, CD_3OD) δ ppm; 37.8 (C-17), 65.7 (C-18), 108.3 (C-8), 119.3 (C-6), 120.6 (C-5), 127.2 (C-15), 132.7 (C-16), 132.8 (C-14), MS (ES^+) m/z 324.2 $[\text{M}+\text{H}]^+$; HRMS calcd for $\text{C}_{13}\text{H}_{14}\text{N}_3\text{O}_3\text{S}_2$ 324.0471 $[\text{M}+\text{H}]^+$ found 324.0473.

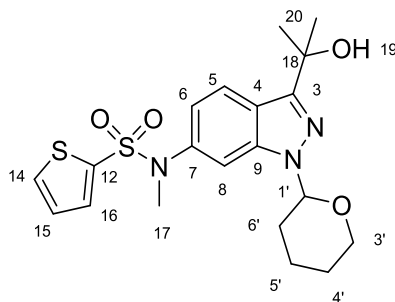
Methyl 6-(*N*-methylthiophene-2-sulfonamido)-1-(tetrahydro-2*H*-pyran-2-yl)-1*H*-indazole-3-carboxylate (262)



Prepared according to general procedure **N** using: *N*-(3-bromo-1-(tetrahydro-2*H*-pyran-2-yl)-1*H*-indazol-6-yl)-*N*-methylthiophene-2-sulfonamide (50 mg, 0.11 mmol), Pd(OAc)₂ (3 mg, 0.01 mmol), XantPhos (4,5-Bis(diphenylphosphino)-9,9-dimethylxanthene, 13 mg, 0.02 mmol), methyl formate (27 μ L, 0.44 mmol), Et₃N (61 μ L, 0.44 mmol) and Ac₂O (42 μ L, 0.44 mmol) in DMF (2 mL) to give the product as a white solid (31 mg, 65%).

m.p. 65-67 °C; UV λ_{max} (EtOH/nm) 298.6, 245.6, 211.6; IR ν_{max} /cm⁻¹ 3090, 2926, 2854, 1674, 1348, 1167; ¹H-NMR (500 MHz, CDCl₃) δ ppm; 1.68-1.81 (3H, m, H-4', H-4', H-5'), 2.07-2.18 (2H, m, H-6', H-5'), 2.54-2.58 (1H, m, H-6'), 2.78 (3H, s, H-20), 3.31 (3H, s, H-17), 3.74-3.78 (1H, m, H-3'), 3.98-4.02 (1H, m, H-3'), 5.76 (1H, dd, J = 2.8, 9.0 Hz, H-1'), 6.88 (1H, dd, J = 8.7, 1.8 Hz, H-6), 7.07 (1H, dd, J = 5.0, 3.8 Hz, H-15), 7.32 (1H, dd, J = 1.3, 3.8 Hz, H-16), 7.59 (1H, dd, J = 1.3, 5.0 Hz, H-14), 7.60 (1H, d, J = 1.8 Hz, H-8), 8.23 (1H, d, J = 8.7 Hz, H-5); ¹³C-NMR (125 MHz, CDCl₃) δ ppm; 22.1 (C-4'), 24.9 (C-5'), 26.7 (C-20), 29.1 (C-6'), 38.7 (C-17), 67.4 (C-3'), 86.1 (C-1'), 110.5 (C-8), 121.7 (C-6), 122.2 (C-4), 123.3 (C-5), 127.4 (C-15), 132.3 (C-14), 132.9 (C-16), 136.7 (C-12), 140.1 (C-7), 140.7 (C-9), 142.6 (C-3), 195.0 (C-18); MS (ES⁺) m/z 437.2 [M+H]⁺; HRMS calcd for C₁₉H₂₂N₃O₅S₂ 436.0995 [M+H]⁺ found 436.0991.

***N*-(3-(2-hydroxypropan-2-yl)-1-(tetrahydro-2*H*-pyran-2-yl)-1*H*-indazol-6-yl)-*N*-methylthiophene-2-sulfonamide (378)**

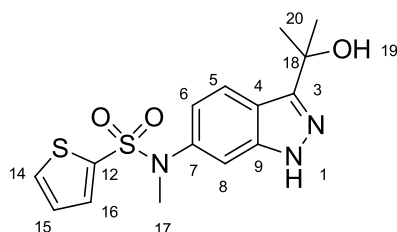


Methyl 6-(*N*-methylthiophene-2-sulfonamido)-1-(tetrahydro-2*H*-pyran-2-yl)-1*H*-indazole-3-carboxylate (127 mg, 0.29 mmol) was taken in THF (1.5 mL) under N₂ at 0 °C. Methylmagnesium bromide (3M in Et₂O, 341 µL, 1.02 mmol) was added dropwise and the solution was stirred for 3 hours. The solution was filtered through celite and reduced to a residue under vacuum. The title compound was purified by MPLC (0-80% EtOAc in petrol) to give a white solid (110 mg, 87%).

N-(3-(2-hydroxypropan-2-yl)-1-(tetrahydro-2*H*-pyran-2-yl)-1*H*-indazol-6-yl)-*N*-methylthiophene-2-sulfonamide (37 mg, 0.09 mmol) was dissolved in THF (1 mL) and H₂SO₄ (aq) (0.4 M, 1 mL) was added. The solution was stirred for 48 h at RT before a further addition of H₂SO₄ (conc., 22 µL). After another 48 h the solution was diluted with H₂O (5 mL) and extracted into EtOAc (2 x 10 mL), combined organic fractions were dried over Na₂SO₄ and reduced *in vacuo* and purified by reversephase flash chromatography (0-80 % MeCN (0.1% HCOOH) in H₂O (0.1% HCOOH) to give the the title compound as a white solid (12 mg, 39%).

*R*_f 0.46 (Et₂O); m.p. 76-78 °C; UV λ_{max} (EtOH/nm) 292.8, 214.4; IR ν_{max}/cm⁻¹ 3345, 2975, 1340, 1162; ¹H-NMR (500 MHz, CDCl₃) δ ppm; 1.74 (6H, s, H-20), 3.30 (3H, s, H-17), 6.85 (1H, dd, *J* = 8.7, 1.6 Hz, H-6), 7.08 (1H, dd, *J* = 5.0, 3.8 Hz, H-15), 7.34 (1H, d, *J* = 1.6 Hz, H-8), 7.37 (1H, dd, *J* = 1.3, 3.8 Hz, H-16), 7.59 (1H, dd, *J* = 5.0, 1.3 Hz, H-14), 7.85 (1H, d, *J* = 8.7 Hz, H-5); ¹³C-NMR (125 MHz, CDCl₃) δ ppm; 30.5 (C-20), 38.7 (C-17), 71.3 (C-18), 108.9 (C-8), 119.1 (C-6), 122.4 (C-5), 127.4 (C-15), 132.3 (C-14), 132.9 (C-16), 136.8 (C-12), 140.0 (C-7), 141.7 (C-9), 152.8 (C-3); MS (ES⁺) *m/z* 350.2 [M-H]⁻; HRMS calcd for C₁₅H₁₈N₃O₃S₂ 352.0784 [M+H]⁺ found 352.0786.

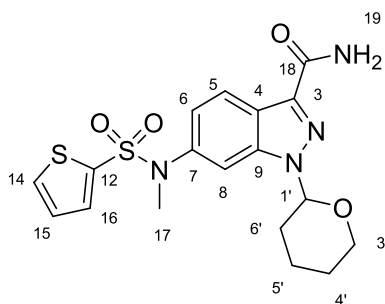
***N*-(3-(2-hydroxypropan-2-yl)-1*H*-indazol-6-yl)-*N*-methylthiophene-2-sulfonamide
(260)**



N-(3-(2-hydroxypropan-2-yl)-1-(tetrahydro-2*H*-pyran-2-yl)-1*H*-indazol-6-yl)-*N*-methylthiophene-2-sulfonamide (37 mg, 0.09 mmol) was dissolved in THF (1 mL) and H₂SO₄ (aq) (0.4 M, 1 mL) was added. The solution was stirred for 48 h at RT before a further addition of H₂SO₄ (conc., 22 μ L). After another 48 h the solution was diluted with H₂O (5 mL) and extracted into EtOAc (2 x 10 mL), combined organic fractions were dried over Na₂SO₄ and reduced *in vacuo* and purified by reversephase flash chromatography (0-80 % MeCN (0.1% HCOOH) in H₂O (0.1% HCOOH) to give the the title compound as a white solid (12 mg, 39%).

*R*_f 0.46 (Et₂O); m.p. 76-78 °C; UV λ_{max} (EtOH/nm) 292.8, 214.4; IR ν_{max} /cm⁻¹ 3345, 2975, 1340, 1162; ¹H-NMR (500 MHz, CDCl₃) δ ppm; 1.74 (6H, s, H-20), 3.30 (3H, s, H-17), 6.85 (1H, dd, *J* = 8.7, 1.6 Hz, H-6), 7.08 (1H, dd, *J* = 5.0, 3.8 Hz, H-15), 7.34 (1H, d, *J* = 1.6 Hz, H-8), 7.37 (1H, dd, *J* = 1.3, 3.8 Hz, H-16), 7.59 (1H, dd, *J* = 5.0, 1.3 Hz, H-14), 7.85 (1H, d, *J* = 8.7 Hz, H-5); ¹³C-NMR (125 MHz, CDCl₃) δ ppm; 30.5 (C-20), 38.7 (C-17), 71.3 (C-18), 108.9 (C-8), 119.1 (C-6), 122.4 (C-5), 127.4 (C-15), 132.3 (C-14), 132.9 (C-16), 136.8 (C-12), 140.0 (C-7), 141.7 (C-9), 152.8 (C-3); MS (ES⁺) *m/z* 350.2 [M-H]⁻; HRMS calcd for C₁₅H₁₈N₃O₃S₂ 352.0784 [M+H]⁺ found 352.0786.

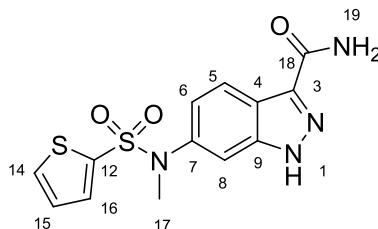
6-(*N*-Methylthiophene-2-sulfonamido)-1-(tetrahydro-2*H*-pyran-2-yl)-1*H*-indazole-3-carboxamide (266)



Prepared according to general procedure **O** using: 6-(*N*-Methylthiophene-2-sulfonamido)-1-(tetrahydro-2*H*-pyran-2-yl)-1*H*-indazole-3-carboxylic acid (65 mg, 0.15 mmol), CDI (50 mg, 0.31 mmol) and ammonia (1M in 1,4-dioxane, 772 μ L, 0.39 mmol) in THF (3 mL) giving the title compound as a white solid (18 mg, 27%).

UV λ_{max} (EtOH/nm) 297.0, 259.5, 237.1, 210.8; IR ν_{max} /cm⁻¹ 3469, 3335, 3177, 2930, 2855; ¹H-NMR (500 MHz, CDCl₃) δ ppm;) 1.61-1.79 (3H, m, H-5', H-5', H-4'), 2.06-2.09 (1H, m, H-6'), 2.13-2.16 (1H, m, H-4'), 2.49-2.55 (1H, m, H-6'), 3.32 (3H, s, H-17), 3.74-3.78 (1H, m, H-3'), 4.01-4.04 (1H, m, H-3'), 5.58 (1H, s-br, H-19), 5.55 (1H, dd, J = 2.8, 9.4 Hz, H-1'), 6.82 (1H, dd, J = 8.7, 1.7 Hz, H-6), 6.92 (1H, s-br, H-19), 7.07 (1H, dd, J = 5.0, 3.8 Hz, H-15), 7.32 (1H, dd, J = 3.8, 1.4, H-16), 7.59 (1H, dd, J = 5.0, 1.4 Hz, H-14), 7.61 (1H, d, J = 1.7 Hz, H-8), 8.23 (1H, d, J = 8.7 Hz, H-5); ¹³C-NMR (125 MHz, CDCl₃) δ ppm; 22.3 (C-4') 24.9 (C-5'), 29.2 (C-6'), 38.7 (C-17), 67.6 (C-3'), 85.7 (C-1'), 110.8 (C-8), 120.8 (C-6), 122.5 (C-4), 123.3 (C-5), 127.4 (C-15), 132.3 (C-14), 132.9 (C-16), 135.0 (C-12), 140.1 (C-7), 140.8 (C-9), 164.1 (C-18); MS (ES⁺) m/z 321.4 [M+H]⁺;

6-(*N*-Methylthiophene-2-sulfonamido)-1*H*-indazole-3-carboxamide (263)

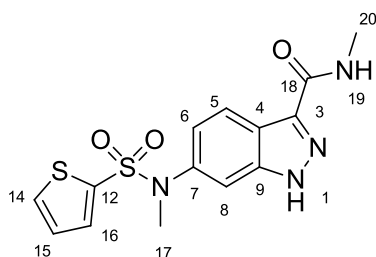


Prepared according to general procedure **D** using 6-(*N*-methylthiophene-2-sulfonamido)-1-(tetrahydro-2*H*-pyran-2-yl)-1*H*-indazole-3-carboxamide (18 mg, 0.04

mmol) in MeOH.HCl (1.25 M, 3 mL) giving the title compound as a white solid (6 mg, 42%).

UV λ_{max} (EtOH/nm) 295.0, 232.0, 209.0; IR ν_{max} /cm⁻¹ 3391, 2922, 2852, 1735, 1581, 1158; ¹H-NMR (500 MHz, CD₃OD) δ ppm; 3.32 (3H, s, H-17), 6.99 (1H, dd, J = 8.7, 1.7 Hz, H-6), 7.16 (1H, dd, J = 4.9, 3.8 Hz, H-15), 7.38-7.39 (2H, m, H-8, H-16), 7.81 (1H, dd, J = 4.9, 1.2 Hz, H-14), 8.12 (1H, d, J = 8.7 Hz, H-5); ¹³C-NMR (125 MHz, CD₃OD) δ ppm; 37.7 (C-17), 108.8 (C-8), 121.0 (C-6), 112.8 (C-5), 127.2 (C-15), 132.7 (C-14), 132.9 (C-16), 136.1 (C-12), 140.1 (C-7), 140.8 (C-9), 156.8 (C-18); MS (ES⁺) m/z 337.4 [M+H]⁺.

***N*-methyl-6-(*N*-methylthiophene-2-sulfonamido)-1*H*-indazole-3-carboxamide (264)**

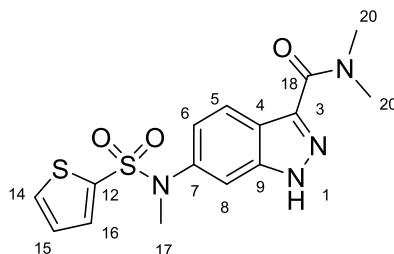


Prepared according to general procedure **O** using: 6-(*N*-Methylthiophene-2-sulfonamido)-1-(tetrahydro-2*H*-pyran-2-yl)-1*H*-indazole-3-carboxylic acid (50 mg, 0.12 mmol), CDI (39 mg, 0.24 mmol) and methylamine (2M in THF, 148 μ L, 0.30 mmol) in THF (2 mL) giving *N*-Methyl-6-(*N*-methylthiophene-2-sulfonamido)-1-(tetrahydro-2*H*-pyran-2-yl)-1*H*-indazole-3-carboxamide as a white solid (48 mg, 93 %). Isolated material was used immediately in the next step without full characterisation according to general procedure **D** using: *N*-methyl-6-(*N*-methylthiophene-2-sulfonamido)-1-(tetrahydro-2*H*-pyran-2-yl)-1*H*-indazole-3-carboxamide (18 mg, 0.04 mmol) in MeOH.HCl (1.25 M, 5 mL) giving the title compound as a white solid (20 mg, 47%).

m.p. 266-268 °C; UV λ_{max} (EtOH/nm) 295.6, 232.6, 209.6; IR ν_{max} /cm⁻¹ 3426, 3107, 2939, 1646, 1554, 1338, 1143; ¹H-NMR (500 MHz, DMSO-*d*₆) δ ppm; 2.82 (3H, d, J = 4.7 Hz, H-20), 3.27 (3H, s, H-17), 6.99 (1H, dd, J = 8.7, 1.7 Hz, H-6), 7.23 (1H, dd, J = 5.0, 3.7 Hz, H-15), 7.34 (1H, d, J = 1.7 Hz, H-8), 7.49 (1H, dd, J = 1.1, 3.7 Hz, H-16), 8.01 (1H, dd, J = 5.0, 1.1 Hz, H-14), 8.09 (1H, d, J = 8.7 Hz, H-5) 8.38 (1H, q, J = 4.7 Hz, H-19), 13.59 (1H, s-br, H-1); ¹³C-NMR (125 MHz, DMSO-*d*₆) δ ppm; 26.0 (C-20), 38.8 (C-17), 109.0 (C-8), 120.9 (C-4), 121.2 (C-6), 122.3 (C-5), 128.5 (C-15), 133.7 (C-16), 134.6 (C-14), 136.0 (C-12),

139.0 (C-3), 139.8 (C-7), 141.2 (C-9), 162.9 (C-18); MS (ES^+) m/z 351.3 $[\text{M}-\text{H}]^-$; HRMS calcd for $\text{C}_{14}\text{H}_{15}\text{N}_4\text{O}_3\text{S}_2$ 351.0580 $[\text{M}+\text{H}]^+$ found 351.0581.

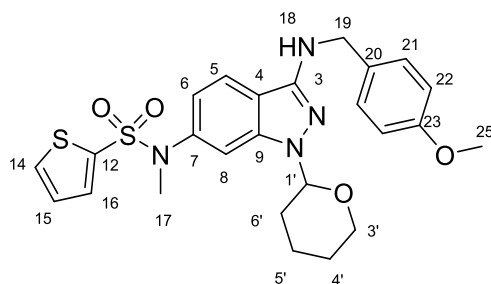
***N,N*-dimethyl-6-(*N*-methylthiophene-2-sulfonamido)-1*H*-indazole-3-carboxamide (265)**



Prepared according to general procedure **O** using: 6-(*N*-Methylthiophene-2-sulfonamido)-1-(tetrahydro-2*H*-pyran-2-yl)-1*H*-indazole-3-carboxylic acid (50 mg, 0.12 mmol), CDI (39 mg, 0.24 mmol) and dimethylamine (2M in THF, 148 μL , 0.30 mmol) in THF (2 mL) giving *N,N*-Dimethyl-6-(*N*-methylthiophene-2-sulfonamido)-1-(tetrahydro-2*H*-pyran-2-yl)-1*H*-indazole-3-carboxamide as a white solid (36 mg, 67%). Isolated material was used immediately in the next step without full characterisation according to general procedure **D** using: *N,N*-dimethyl-6-(*N*-methylthiophene-2-sulfonamido)-1-(tetrahydro-2*H*-pyran-2-yl)-1*H*-indazole-3-carboxamide (18 mg, 0.04 mmol) in MeOH.HCl (1.25 M, 5 mL) giving the title compound as a white solid (15 mg, 34%).

m.p. 230-232 $^{\circ}\text{C}$; UV λ_{max} (EtOH/nm) 294.4, 210.4; IR $\nu_{\text{max}}/\text{cm}^{-1}$ 3092, 2925, 2855, 1598, 1346, 1143; ^1H -NMR (500 MHz, $\text{DMSO}-d_6$) δ ppm; 3.07 (3H, s, H-17), 3.26 (3H, s, H-20A), 3.36 (3H, s, H-20B), 6.94 (1H, dd, $J = 8.7, 1.8$ Hz, H-6), 7.24 (1H, dd, $J = 5.0, 3.9$ Hz, H-15), 7.32 (1H, d, $J = 1.8$ Hz, H-8), 7.49 (1H, dd, $J = 1.3, 3.9$ Hz, H-16), 7.90 (1H, d, $J = 8.7$ Hz, H-5), 8.01 (1H, dd, $J = 5.0, 1.3$ Hz, H-14), 13.61 (1H, s-br, H-1); ^{13}C -NMR (125 MHz, $\text{DMSO}-d_6$) δ ppm; 36.0 (C-17), 38.8 (C-20A), 38.9 (C-20B), 108.8 (C-8), 117.7 (C-4), 121.0 (C-6), 122.3 (C-5), 128.5 (C-15), 133.8 (C-16), 134.6 (C-14), 136.0 (C-12), 139.6 (C-3), 139.8 (C-7), 140.5 (C-9), 163.4 (C-18); MS (ES^+) m/z 365.2 $[\text{M}-\text{H}]^-$; HRMS calcd for $\text{C}_{15}\text{H}_{17}\text{N}_4\text{O}_3\text{S}_2$ 365.0737 $[\text{M}+\text{H}]^+$ found 365.0733

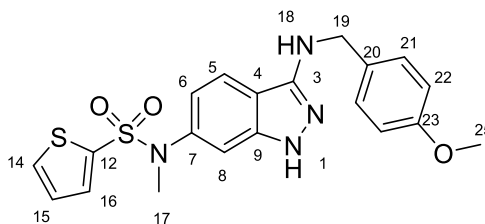
***N*-(3-((4-methoxybenzyl)amino)-1-(tetrahydro-2*H*-pyran-2-yl)-1*H*-indazol-6-yl)-*N*-methylthiophene-2-sulfonamide (274)**



Cs_2CO_3 (392 mg, 1.21 mmol), $\text{Pd}_2(\text{dba})_3$ (39 mg, 0.04 mmol) and BrettPhos (2-(dicyclohexylphosphino)3,6-dimethoxy-2',4',6'-triisopropyl-1,1'-biphenyl, 58 mg, 0.11 mmol) were deposited in a 20 mL dry microwave vial under N_2 and dissolved in 1,4-dioxane (6 mL). 4-Methoxyphenyl)methanamine (112 μL , 0.86 mmol) was added and the solution was degassed with N_2 for *ca.* 10 minutes before heating at 100 $^\circ\text{C}$ for another 10 minutes. The solution was allowed to cool and *N*-(3-Bromo-1-(tetrahydro-2*H*-pyran-2-yl)-1*H*-indazol-6-yl)thiophene-2-sulfonamide (197 mg, 0.43 mmol) was added. The solution was heated to 100 $^\circ\text{C}$ for 18 h, allowed to cool then filtered through Celite[®]. The filtrate was reduced to a residue under vacuum and purified by MPLC (0-80% EtOAc in petrol) to give an off white solid (103 mg, 47%)

R_f 0.47 (Et₂O); m.p. 48-50 $^\circ\text{C}$; UV λ_{max} (EtOH/nm) 332.2, 236.2, 216.4; IR $\nu_{\text{max}}/\text{cm}^{-1}$ 3373, 3094, 2926, 2853; $^1\text{H-NMR}$ (500 MHz, CDCl_3) δ ppm; 1.56-1.61 (1H, m, H-5'), 1.69-1.74 (2H, m, H-4', H-5'), 1.97-1.99 (1H, m, H-6'), 2.11-2.12 (1H, m, H-4'), 2.49-2.51 (1H, m, H-6'), 3.29 (3H, s, H-17), 3.65-3.70 (1H, m, H-3'), 3.81 (3H, s, H-25), 4.02-4.05 (1H, m, H-3'), 4.53 (2H, s, H-19), 5.43 (1H, dd, $J = 2.2, 9.7$ Hz, H-1'), 6.66 (1H, dd, $J = 8.7, 1.7$ Hz, H-6), 6.89 (2H, d, $J = 8.5$ Hz, H-22), 7.07 (1H, dd, $J = 4.9, 3.8$ Hz, H-15), 7.23 (1H, d, $J = 1.7$ Hz, H-8), 7.32 (1H, dd, $J = 1.2, 3.8$ Hz, H-16), 7.34-7.37 (3H, m, H-5, H-21), 7.58 (1H, dd, $J = 1.2, 4.9$ Hz, H-14); $^{13}\text{C-NMR}$ (125 MHz, CDCl_3) δ ppm; 22.9 (C-4'), 25.2 (C-5'), 29.4 (C-6'), 38.8 (C-17), 47.8 (C-19), 55.3 (C-25), 67.7 (C-3'), 85.0 (C-1'), 109.1 (C-8), 114.0 (C-22), 115.0 (C-4), 117.6 (C-6), 119.6 (C-5), 127.3 (C-15), 129.5 (C-21), 131.8 (C-20), 132.0 (C-14), 132.9 (C-16), 136.7 (C-12), 140.3 (C-7), 141.3 (C-9), 149.4 (C-3), 159.0 (C-23); MS (ES^+) m/z 513.3 $[\text{M}+\text{H}]^+$.

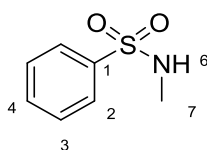
***N*-(3-((4-Methoxybenzyl)amino)-1*H*-indazol-6-yl)-*N*-methylthiophene-2-sulfonamide (275)**



N-(3-((4-methoxybenzyl)amino)-1-(tetrahydro-2*H*-pyran-2-yl)-1*H*-indazol-6-yl)-*N*-methylthiophene-2-sulfonamide (50 mg, 0.11 mmol) was dissolved in MeOH (8 mL) and concentrated AcOH (2 mL) and heated at reflux for 2 hrs. the solution was reduced to a residue *in vacuo* and partitioned between H₂O (10 mL) and EtOAc (3 x 8 mL). Combined organic fractions were washed with saturated NaHCO₃ (aq, 10 mL) and brine (10 mL) then dried over Na₂SO₄. This solution was purified by MPLC (0-80% EtOAc in petroleum ether) giving the title compound as a white solid (42 mg, 43%)

*R*_f 0.60 (Et₂O); m.p. 61-63 °C; UV λ_{max} (EtOH/nm) 327.6, 242.2; IR ν_{max}/cm⁻¹ 3385, 3094, 2926, 1613; ¹H-NMR (500 MHz, CDCl₃) δ ppm; 3.29 (3H, s, H-17), 3.81 (3H, s, H-25), 4.53 (2H, s, H-19), 6.75 (1H, dd, *J* = 8.6, 1.7 Hz, H-6), 6.89 (2H, d, *J* = 8.4 Hz, H-22), 7.06 (1H, dd, *J* = 4.9, 3.8 Hz, H-15), 7.13 (1H, d, *J* = 1.7 Hz, H-8), 7.32 (1H, dd, *J* = 1.2, 3.8 Hz, H-16), 7.36 (2H, d, *J* = 8.4 Hz, H-21), 7.41 (1H, d, *J* = 8.6 Hz, H-5), 7.57 (1H, dd, *J* = 1.2, 4.9 Hz, H-14); ¹³C-NMR (125 MHz, CDCl₃) δ ppm; 38.7 (C-17), 47.7 (C-19), 55.3 (C-25), 108.4 (C-8), 113.5 (C-4), 114.1 (C-22), 117.7 (C-6), 119.5 (C-5), 127.4 (C-15), 129.2 (C-21), 131.5 (C-20), 132.2 (C-14), 132.8 (C-16), 136.7 (C-12), 140.7 (C-7), 142.3 (C-9), 150.5 (C-3), 159.0 (C-23); MS (ES⁺) *m/z* 429.3 [M+H]⁺; HRMS calcd for C₂₀H₂₁N₄O₃S₂ 429.1050 [M+H]⁺ found 429.1046.

***N*-Methylbenzenesulfonamide (276)**

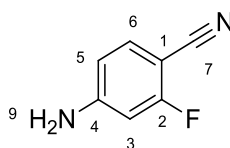


Prepared according to general procedure **J** with following reagents and quantities:

Benzene sulphonyl chloride (255 μ L, 2.00 mmol) and methylamine (2 M in THF, 2.1 mL, 4.20 mmol) in DCM (6 mL) to give a clear liquid (322 mg, 94%).

R_f 0.56 (Et_2O); UV λ_{max} (EtOH/nm) 264.4, 226.0; IR $\nu_{\text{max}}/\text{cm}^{-1}$ 3287; ^1H -NMR (500 MHz, CDCl_3) δ ppm; 2.60 (3H, d, $J = 5.5$ Hz, H-7), 5.09 (1H, d, $J = 5.5$ Hz, H-6), 7.49 (2H, dd, $J = 7.4, 7.4$ Hz, H-3), 7.56 (1H, t, $J = 7.4$ Hz, H-4), 7.85 (2H, d, $J = 7.4$ Hz, H-2); ^{13}C -NMR (125 MHz, CDCl_3) δ ppm; 29.3 (C-7), 127.2 (C-2), 129.2 (C-3), 132.7 (C-4), 138.7 (C-1); MS (ES^+) m/z 172.2 $[\text{M}+\text{H}]^+$; Aligns with literature data.²⁰¹

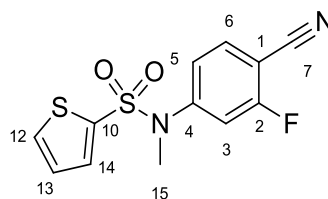
4-Amino-2-fluorobenzonitrile (277)



2-Fluoro-4-nitrobenzonitrile (5.0 g, 30 mmol) was dissolved in a methanol-acetic acid solution (4:1, 75 mL) under N_2 and zinc powder (9.8 g, 151 mmol) was added over 10 minutes. This mixture was heated to 50 $^\circ\text{C}$ for 4 h then filtered through Celite® and washed with MeOH (30 mL). The filtrate was reduced under low pressure and purified by MPLC (0-80% EtOAc in petroleum ether) giving the desired material as a brown solid (2.46 g, 61 %).

R_f 0.44 (Et_2O); m.p. 108-110 $^\circ\text{C}$ (lit: 103-105 $^\circ\text{C}$); UV λ_{max} (EtOH/nm) 272.4, 217.0; IR $\nu_{\text{max}}/\text{cm}^{-1}$ 3446, 3347, 2216; ^1H -NMR (500 MHz, $\text{DMSO}-d_6$) δ ppm; 6.42-6.46 (2H, m, H-3, H-5), 6.54 (2H, s-br, H-9), 7.41 (1H, dd, $J_H = 6.1, J_F = 8.4$ Hz, H-6); ^{13}C -NMR (125 MHz, $\text{DMSO}-d_6$) δ ppm; 99.5 (d, $J_{\text{FC}} = 22.5$ Hz, C-3), 110.7 (C-5), 116.4 (C-1), 134.5 (d, $J_{\text{FC}} = 2.8$ Hz, C-7), 143.3 (C-6), 156.1 (d, $J_{\text{FC}} = 12.3$ Hz, C-4), 163.8-165.7 (d, $J_{\text{FC}} = 250.5$ Hz, C-2); ^{19}F NMR (470 MHz, $\text{DMSO}-d_6$) δ -109.3; MS (ES^+) m/z 137.1 $[\text{M}+\text{H}]^+$; Aligns with literature data.²⁰³

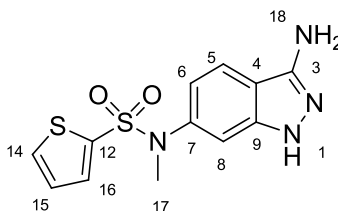
***N*-(4-Cyano-3-fluorophenyl)-*N*-methylthiophene-2-sulfonamide (279)**



Prepared according to general procedure **A** with following reagents and quantities: 2-Fluoro-4-nitrobenzonitrile (1.53 g, 11.2 mmol), pyridine (20 mL), THF (40 mL) and 2-thiophenesulfonyl chloride (2.24 g, 12.3 mmol) to give *N*-(4-cyano-3-fluorophenyl)thiophene-2-sulfonamide as off white solid (1.7g, 54%) and used directly in the next step according to general procedure **B** with following reagents and quantities: *N*-(4-cyano-3-fluorophenyl)thiophene-2-sulfonamide (1.08 g, 3.86 mmol), DMF (35 mL), methyl iodide (200 μ L, 8.48 mmol) and K_2CO_3 (586 mg, 4.24 mmol) to give an off white solid (1.1 g, 99%).

m.p. 98-100 $^{\circ}C$; UV λ_{max} (EtOH/nm) 253.4; IR ν_{max}/cm^{-1} 3117, 3056, 2901, 2237, 1354, 1151; 1H -NMR (500 MHz, $CDCl_3$) δ ppm; 7.10-7.14 (3H, m, H-3, H-5, H-13), 7.41 (1H, dd, $J = 1.3, 3.8$ Hz, H-14), 7.56-7.59 (1H, dd, $J_H = 7.8, J_F = 1.0$ Hz, H-6), 7.63 (1H, dd, $J = 1.3, 4.9$ Hz, H-12); ^{13}C -NMR (125 MHz, $DMSO-d_6$) δ ppm; 37.5 (C-15), 99.5 (d, $J_{FC} = 15.7$ Hz, C-1), 113.3 (d, $J_{FC} = 15.7$ Hz, C-3), 113.4 (C-7), 121.3 (d, $J_{FC} = 3.5$ Hz, C-5), 127.7 (C-13), 133.2 (C-12), 133.3 (C-14), 133.5 (C-6), 143.3 (C-10), 147.2 (d, $J_{FC} = 9.9$ Hz, C-4), 162.0-164.1 (d, $J_{FC} = 260.1$ Hz, C-2); ^{19}F NMR (470 MHz, $DMSO-d_6$) δ -104.0; MS (ES^+) m/z 297.2 $[M+H]^+$.

***N*-(3-Amino-1*H*-indazol-6-yl)-*N*-methylthiophene-2-sulfonamide (269)**

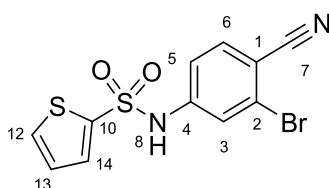


N-(4-Cyano-3-fluorophenyl)-*N*-methylthiophene-2-sulfonamide (100 mg, 0.34 mmol) was taken in THF (2 mL) under N_2 at room temperature and hydrazine (33 μ M, 0.68 mmol) was added and the solution stirred overnight. After this time H_2O (5 mL) was

added and the solution extracted with EtOAc (3 x 5 mL). Organic fractions were combined and washed with brine (10mL) and dried over Na₂SO₄ before subsection to purification by MPLC (0-10% MeOH in DCM) giving the title compound as a white solid (62 mg, 59 %).

*R*_f 0.31 (10% MeOH in DCM); m.p. 222-224 °C; UV λ_{max} (EtOH/nm) 316.8, 236.0; IR ν_{max}/cm⁻¹ 3378, 3309, 3052, 1340, 1160; ¹H-NMR (500 MHz, DMSO-*d*₆) δ ppm; 3.22 (3H, s, H-17), 5.38 (2H, s, H-18), 6.62 (1H, dd, *J* = 8.5, 1.8 Hz, H-6), 6.95 (1H, d, *J* = 1.8 Hz, H-8), 7.23 (1H, dd, *J* = 5.0, 3.8 Hz, H-15), 7.47 (1H, dd, *J* = 1.3, 3.8 Hz, H-16), 7.61 (1H, d, *J* = 8.5 Hz, H-5), 7.57 (1H, dd, *J* = 1.3, 5.0 Hz, H-14), 11.43 (1H, s-br, H-1); ¹³C-NMR (125 MHz, DMSO-*d*₆) δ ppm; 38.9 (C-17), 107.9 (C-8), 113.5 (C-4), 116.6 (C-6), 121.0 (C-5), 128.4 (C-15), 133.5 (C-16), 134.4 (C-14), 136.3 (C-12), 139.6 (C-7), 141.6 (C-3), 149.6 (C-9); MS (ES⁺) *m/z* 309.2 [M+H]⁺.

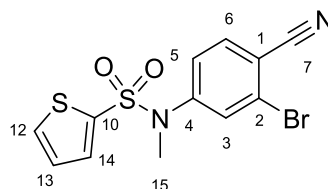
***N*-(3-Bromo-4-cyanophenyl)thiophene-2-sulfonamide (280)**



Prepared according to general procedure A with following reagents and quantities: 4-amino-2-bromobenzonitrile (1 g, 5.08 mmol), pyridine (10 mL) and 2-thiophenesulfonyl chloride (968 mg, 5.33 mmol) to give an off white solid (1.5 g, 88%).

m.p. 182-184 °C; UV λ_{max} (EtOH/nm) 271.8, 210.2; IR ν_{max}/cm⁻¹ 3477, 3309, 3210, 2222, 1589, 1162; ¹H-NMR (500 MHz, DMSO-*d*₆) δ ppm; 7.18 (1H, dd, *J* = 3.8, 4.9 Hz, H-13), 7.32 (1H, dd, *J* = 8.6, 2.0 Hz, H-5), 7.51 (1H, d, *J* = 2.0 Hz, H-3), 7.74 (1H, dd, *J* = 3.8, 1.4 Hz, H-12), 7.85 (1H, d, *J* = 8.6 Hz, H-6), 8.00 (1H, dd, *J* = 4.9, 1.4 Hz, H-14), 11.43 (1H, s-br, H-8); ¹³C-NMR (125 MHz, DMSO-*d*₆) δ ppm; 109.1 (C-1), 117.9 (C-5), 122.0 (C-3), 125.8 (C-2), 128.5 (C-13), 134.0 (C-12), 135.1 (C-14), 136.4 (C-6), 139.5 (C-10), 143.6 (C-4), 144.9 (C-7); MS (ES⁺) *m/z* 343.2 [M(⁷⁹Br)+H]⁺;

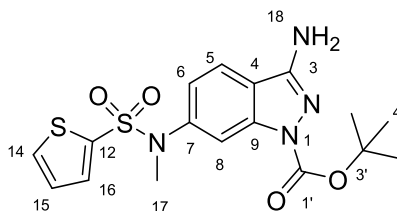
***N*-(3-Bromo-4-cyanophenyl)-*N*-methylthiophene-2-sulfonamide (281)**



Prepared according to general procedure B with the following reagents and quantities: *N*-(4-cyano-3-bromophenyl)thiophene-2-sulfonamide (1.5 g, 4.4 mmol), DMF (30 mL), methyliodide (234 μ L, 5.28 mmol) and K_2CO_3 (911 mg, 6.60 mmol) to give an off white solid (1.25 g, 80%).

m.p. 82-84 $^{\circ}C$; UV λ_{max} (EtOH/nm) 270.6, 256.4, 206.8; IR ν_{max}/cm^{-1} 3105, 2227, 1594, 1358; 1H -NMR (500 MHz, $DMSO-d_6$) δ ppm; 3.25 (3H, s, H-15), 7.12 (1H, dd, J = 3.8, 5.0 Hz, H-13), 7.30 (1H, dd, J = 8.5, 2.0 Hz, H-5), 7.41 (1H, dd, J = 3.8, 1.3 Hz, H-12), 7.51 (1H, d, J = 2.0 Hz, H-3), 7.61 (1H, d, J = 8.6 Hz, H-6), 7.64 (1H, dd, J = 1.3, 5.0 Hz, H-14); ^{13}C -NMR (125 MHz, $CDCl_3$) δ ppm; 37.5 (C-15), 113.9 (C-1), 116.7 (C-7), 124.6 (C-5), 125.5 (C-4), 127.7 (C-13), 129.7 (C-3), 133.1 (C-10), 133.4 (C-14), 134.4 (C-12), 135.9 (C-5), 145.9 (C-2); MS (ES^+) m/z 355.4 [$M(^{79}Br)+H$] $^+$.

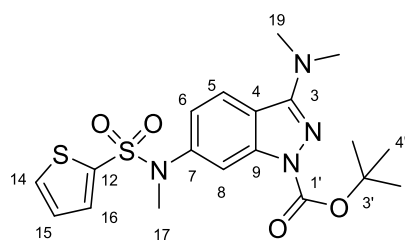
***tert*-Butyl 3-amino-6-(*N*-methylthiophene-2-sulfonamido)-1*H*-indazole-1-carboxylate (282)**



N-(4-Cyano-3-bromoophenyl)-*N*-methylthiophene-2-sulfonamide (50 mg, 0.14 mmol), and *t*-butylcarbazate (23 mg, 0.17 mmol), copper(I) bromide (4 mg, 0.03) and potassium carbonate (39 mg, 0.28 mmol) were taken in DMSO (2 mL) under N_2 at room temperature was added and the solution stirred overnight at 80 $^{\circ}C$. After this time aqueous NH_4Cl (saturated, 5 mL) was added and the solution extracted with EtOAc (3 x 5 mL). Organic fractions were combined and washed with brine (10mL) and dried over Na_2SO_4 before subjection to purification by MPLC (0-80% EtOAc in petroleum ether) giving the title compound as a white solid (19 mg, 34%).

$^1\text{H-NMR}$ (500 MHz, $\text{DMSO-}d_6$) δ ppm; 1.54 (9H, s, H-4'), 3.24 (3H, s, H-17), 6.38 (2H, s, H-18), 7.06 (1H, dd, $J = 8.4, 1.7$ Hz, H-6), 7.24 (1H, dd, $J = 5.0, 3.8$ Hz, H-15), 7.49 (1H, dd, $J = 1.4, 3.8$ Hz, H-16), 7.64 (1H, s, H-8), 7.80 (1H, d, $J = 8.4$ Hz, H-5), 8.02 (1H, dd, $J = 1.3, 5.0$ Hz, H-14); $^{13}\text{C-NMR}$ (125 MHz, $\text{DMSO-}d_6$) δ ppm; 28.3 (C-4'), 38.7 (C-17), 83.2 (C-3'), 112.6 (C-8), 118.6 (C-4), 121.4 (C-5), 121.8 (C-6), 128.5 (C-15), 134.0 (C-16), 134.7 (C-14), 135.6 (C-12), 140.3 (C-9), 142.1 (C-7), 152.6 (C-3); MS (ES^+) m/z 409.2 $[\text{M}+\text{H}]^+$; HRMS calcd for $\text{C}_{17}\text{H}_{21}\text{N}_4\text{O}_4\text{S}_2$ 409.0999 $[\text{M}+\text{H}]^+$ found 409.0996.

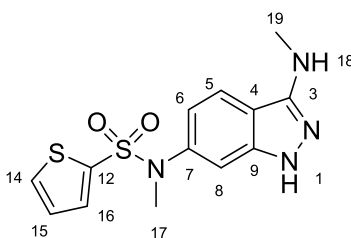
***tert*-Butyl 3-(dimethylamino)-6-(*N*-methylthiophene-2-sulfonamido)-1*H*-indazole-1-carboxylate (284)**



Prepared according to general procedure **P** with the following reagents and quantities: *tert*-butyl 3-amino-6-(*N*-methylthiophene-2-sulfonamido)-1*H*-indazole-1-carboxylate (30 mg, 0.07 mmol), NaH (5 mg, 0.19), MeI (9 μL , 0.15 mmol), in DMF (4 mL) giving the title compound as an off white solid (12 mg, 37 %).

$^1\text{H-NMR}$ (500 MHz, CDCl_3) δ ppm; 1.42 (9H, s, H-4'), 3.31 (3H, s, H-17), 3.38 (3H, s, H-19), 3.96 (3H, s, H-19), 6.70 (1H, dd, $J = 8.7, 1.8$ Hz, H-6), 7.07 (1H, dd, $J = 4.9, 3.8$ Hz, H-15), 7.26 (1H, m, H-8), 7.33 (1H, dd, $J = 3.8, 1.2$ Hz, H-16), 7.52 (1H, d, $J = 8.7$ Hz, H-5), 7.58 (1H, dd, $J = 1.2, 4.9$ Hz, H-14); $^{13}\text{C-NMR}$ (125 MHz, CDCl_3) δ ppm; 28.2 (C-4'), 35.5 (C-19), 36.9 (C-19), 38.7 (C-17), 81.0 (C-3'), 108.6 (C-8), 117.2 (C-4), 117.9 (C-6), 122.8 (C-5), 127.4 (C-15), 132.1 (C-16), 132.8 (C-14), 136.8 (C-12), 139.6 (C-9), 140.7 (C-7), 143.9 (C-3), 154.3 (C-1'); MS (ES^+) m/z 437.5 $[\text{M}+\text{H}]^+$;

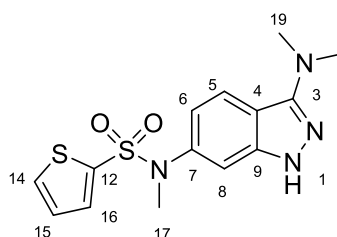
***N*-Methyl-*N*-(3-(methylamino)-1*H*-indazol-6-yl)thiophene-2-sulfonamide (270)**



Prepared according to general procedure **P** with the following reagents and quantities: *tert*-butyl 3-amino-6-(*N*-methylthiophene-2-sulfonamido)-1*H*-indazole-1-carboxylate (65 mg, 0.16 mmol), NaH (5 mg, 0.19), MeI (7 μ L, 0.16 mmol), in DMF (4 mL) giving *tert*-butyl 3-(methylamino)-6-(*N*-methylthiophene-2-sulfonamido)-1*H*-indazole-1-carboxylate as an off white solid (16 mg, 23 %). Isolated material was used immediately in the next step without full characterisation according to general procedure **Q** with the following reagents and quantities: *tert*-butyl 3-(methylamino)-6-(*N*-methylthiophene-2-sulfonamido)-1*H*-indazole-1-carboxylate (16 mg, 0.04 mmol), in DCM (5 mL) and TFA (1 mL) giving the title compound as a yellow solid (7 mg, 57 %).

m.p. 179-181 $^{\circ}$ C; UV λ_{max} (EtOH/nm) 332.8, 241.0; IR ν_{max} /cm $^{-1}$ 3318, 3207, 2925, 1342, 1148; ^1H -NMR (500 MHz, CDCl $_3$) δ ppm; 3.30 (3H, s, H-17), 3.78 (3H, s, H-19), 4.02 (1H, s-br, H-18), 6.64 (1H, dd, J = 8.6, 1.7 Hz, H-6), 7.07-7.09 (2H, m, H-15, H-8), 7.34 (1H, dd, J = 1.3, 3.8 Hz, H-16), 7.41 (1H, d, J = 8.6 Hz, H-5), 7.59 (1H, dd, J = 1.3, 5.0 Hz, H-14); ^{13}C -NMR (125 MHz, CDCl $_3$) δ ppm; 34.9 (C-19), 38.7 (C-17), 108.0 (C-8), 113.6 (C-4), 116.7 (C-6), 119.9 (C-5), 127.3 (C-15), 132.1 (C-14), 132.9 (C-16), 136.8 (C-12), 140.1 (C-7), 141.3 (C-3), 146.8 (C-9); MS (ES $^{+}$) m/z 323.2 [M+H] $^{+}$.

***N*-(3-(Dimethylamino)-1*H*-indazol-6-yl)-*N*-methylthiophene-2-sulfonamide (271)**

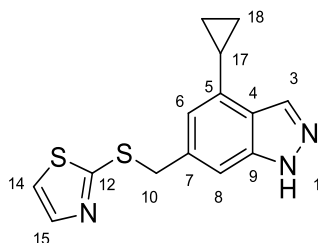


Prepared according to general procedure **Q** with the following reagents and quantities: *tert*-butyl 3-(methylamino)-6-(*N*-methylthiophene-2-sulfonamido)-1*H*-indazole-1-

carboxylate (16 mg, 0.04 mmol), in DCM (5 mL) and TFA (1 mL) giving the title compound as an orange solid (8 mg, 86 %).

m.p. 155-157 °C; UV λ_{max} (EtOH/nm) 340.2, 245.8; IR ν_{max} /cm⁻¹ 3396, 2921, 2852, 1342, 1145; ¹H-NMR (500 MHz, CDCl₃) δ ppm; 3.07 (3H, s, H-19), 3.30 (3H, s, H-17), 3.80 (3H, s, H-19), 6.61 (1H, d, *J* = 8.6 Hz, H-6), 7.03 (1H, s, H-8), 7.07 (1H, dd, *J* = 5.0, 3.8 Hz, H-15), 7.33 (1H, dd, *J* = 1.3, 3.8 Hz, H-16), 7.38 (1H, d, *J* = 8.6 Hz, H-5), 7.58 (1H, dd, *J* = 1.3, 5.0 Hz, H-14); ¹³C-NMR (125 MHz, CDCl₃) δ ppm; 38.8 (C-17), 107.8 (C-8), 113.3 (C-4), 116.2 (C-6), 119.7 (C-5), 127.3 (C-15), 132.1 (C-14), 132.8 (C-16), 136.8 (C-12), 140.5 (C-7), 150.1 (C-9); MS (ES⁺) *m/z* 337.2 [M+H]⁺.

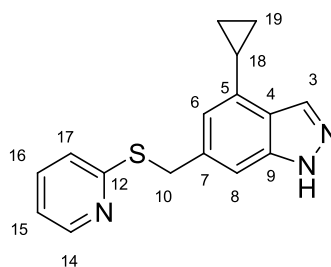
2-(((4-Cyclopropyl-1H-indazol-6-yl)methyl)thio)thiazole (289)



Prepared according to general procedure I using 6-(bromomethyl)-4-cyclopropyl-1H-indazole (50 mg, 0.20 mmol), Cs₂CO₃ (71 mg, 0.22 mmol) and 2-mercaptothiazole (35 mg, 0.30 mmol) in DMF (3 mL). The product was isolated a pale yellow solid (55 mg, 97%).

*R*_f 0.44 (10% MeOH in DCM); m.p. 75-77 °C; UV λ_{max} (EtOH/nm) 297.2, 260.2, 217.8; IR ν_{max} /cm⁻¹ 3353, 3175, 3109, 3000, 2918; ¹H-NMR (500 MHz, DMSO-*d*₆) δ ppm; 0.64 (2H, m, H-18), 1.01 (2H, m, H-18), 2.23 (1H, m, H-17), 5.00 (2H, s, H-10), 6.29 (1H, s, H-6), 7.22 (1H, s, H-8), 8.18 (1H, s, H-3), 8.23-8.25 (2H, m, H-14, H-15), 13.09 (1H, s-br, H-1); ¹³C-NMR (125 MHz, DMSO-*d*₆) δ ppm; 9.5 (C-18), 13.2 (C-17), 61.0 (C-10), 110.4 (C-8), 117.5 (C-6), 123.3 (C-4), 126.0 (C-7), 129.4 (C-15), 132.6 (C-3), 137.4 (C-5), 140.1 (C-9), 145.6 (C-15), 164.6 (C-12); MS (ES⁺) *m/z* 320.2 [M+H]⁺; HRMS calcd for C₁₄H₁₄N₃S₂ 288.0624 [M+H]⁺ found 288.0624.

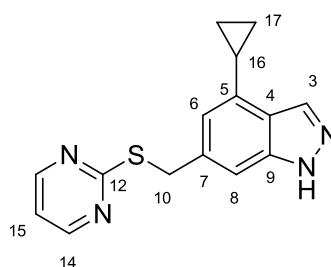
4-Cyclopropyl-6-((pyridin-2-ylthio)methyl)-1*H*-indazole (290)



Prepared according to general procedure I using 6-(bromomethyl)-4-cyclopropyl-1*H*-indazole (50 mg, 0.20 mmol), Cs₂CO₃ (71 mg, 0.22 mmol) and pyridine-2-thiol (33 mg, 0.30 mmol) in DMF (3 mL). The product was isolated a white solid (50 mg, 89%).

*R*_f 0.55 (10% MeOH in DCM); m.p. 49-51 °C; UV λ_{max} (EtOH/nm) 294.0, 251.8, 215.4; IR ν_{max}/cm⁻¹ 3166, 3103, 2997, 2928, 1121; ¹H-NMR (500 MHz, CDCl₃) δ ppm; 0.88 (2H, m, H-19), 1.06 (2H, m, H-19), 2.22 (1H, m, H-17), 4.54 (2H, s, H-10), 6.82 (1H, s, H-6), 7.03 (1H, dd, *J* = 4.3, 6.5 Hz, H-15) 7.18 (1H, d, *J* = 8.1 Hz, H-17), 7.39 (1H, s, H-8), 7.50 (1H, dt, *J* = 8.1, 1.8 Hz, H-16), 8.15 (1H, s, H-3), 8.49 (1H, d, *J* = 4.3 Hz, H-14); ¹³C-NMR (125 MHz, CDCl₃) δ ppm; 8.4 (C-19), 13.5 (C-18), 35.1 (C-10), 107.1 (C-8), 118.0 (C-6), 119.9 (C-15) 122.5 (C-4, C-17), 133.2 (C-3), 136.6 (C-16), 137.4 (C-7), 137.9 (C-5), 140.3 (C-9), 149.0 (C-14), 158.4 (C-12); MS (ES⁺) *m/z* 282.2 [M+H]⁺; HRMS calcd for C₁₆H₁₆N₃S 282.1059 [M+H]⁺ found 282.1055.

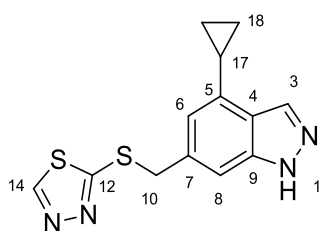
4-Cyclopropyl-6-((pyrimidin-2-ylthio)methyl)-1*H*-indazole (291)



Prepared according to general procedure I using 6-(bromomethyl)-4-cyclopropyl-1*H*-indazole (50 mg, 0.20 mmol), Cs₂CO₃ (71 mg, 0.22 mmol) and 2-mercaptopyrimidine (33 mg, 0.30 mmol) in DMF (3 mL). The product was isolated a white solid (56 mg, 99%).

R_f 0.52 (10% MeOH in DCM); m.p. 137-139 °C; UV λ_{\max} (EtOH/nm) 291.0, 254.2, 216.4; IR $\nu_{\max}/\text{cm}^{-1}$ 3178, 3104, 2926, 1374; $^1\text{H-NMR}$ (500 MHz, CDCl_3) δ ppm; 0.83 (2H, m, H-17), 1.00 (2H, m, H-17), 2.16 (1H, m, H-16), 4.43 (2H, s, H-10), 6.78 (1H, s, H-6), 6.91 (1H, t, $J = 4.9$ Hz, H-15), 7.32 (1H, s, H-8), 8.08 (1H, s, H-3), 8.47 (2H, d, $J = 4.9$ Hz, H-14); $^{13}\text{C-NMR}$ (125 MHz, CDCl_3) δ ppm; 8.4 (C-17), 13.5 (C-16), 35.7 (C-10), 107.0 (C-8), 116.7 (C-15), 118.0 (C-6), 122.7 (C-4), 133.6 (C-3), 136.8 (C-9), 137.8 (C-7), 140.3 (C-5), 157.3 (C-14), 172.1 (C-12); MS (ES^+) m/z 283.2 $[\text{M}+\text{H}]^+$; HRMS calcd for $\text{C}_{15}\text{H}_{15}\text{N}_4\text{S}$ 283.1012 $[\text{M}+\text{H}]^+$ found 283.1010.

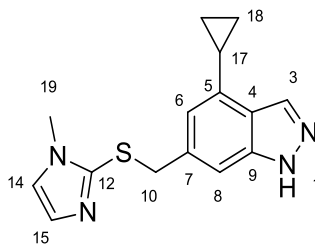
2-(((4-Cyclopropyl-1H-indazol-6-yl)methyl)thio)-1,3,4-thiadiazole (292)



Prepared according to general procedure I using 6-(bromomethyl)-4-cyclopropyl-1H-indazole (50 mg, 0.20 mmol), Cs_2CO_3 (71 mg, 0.22 mmol) and 2-mercapto-1,3,4-thiadiazole (35 mg, 0.30 mmol) in DMF (3 mL). The product was isolated as an off white solid (57 mg, 99%).

R_f 0.36 (10% MeOH in DCM); m.p. 157-159 °C; UV λ_{\max} (EtOH/nm) 264.4, 218.0; IR $\nu_{\max}/\text{cm}^{-1}$ 3185, 3084, 1368, 1064; $^1\text{H-NMR}$ (500 MHz, $\text{DMSO-}d_6$) δ ppm; 0.83 (2H, m, H-18), 1.05 (2H, m, H-18), 2.29 (1H, m, H-17), 4.66 (2H, s, H-10), 6.77 (1H, s, H-6), 7.39 (1H, s, H-8), 8.16 (1H, s, H-3), 9.51 (1H, s, H-14), 13.04 (1H, s-br, H-1); $^{13}\text{C-NMR}$ (125 MHz, $\text{DMSO-}d_6$) δ ppm; 9.4 (C-18), 13.6 (C-17), 38.7 (C-10), 107.9 (C-8), 116.6 (C-6), 122.7 (C-4), 132.6 (C-3), 134.9 (C-7), 137.7 (C-5), 140.1 (C-9), 154.7 (C-14), 165.5 (C-12); MS (ES^+) m/z 289.2 $[\text{M}+\text{H}]^+$; HRMS calcd for $\text{C}_{13}\text{H}_{13}\text{N}_4\text{S}_2$ 289.0576 $[\text{M}+\text{H}]^+$ found 289.0574.

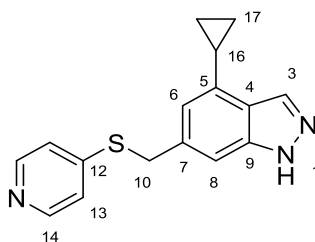
4-Cyclopropyl-6-(((1-methyl-1*H*-imidazol-2-yl)thio)methyl)-1*H*-indazole (293)



Prepared according to general procedure I using 6-(bromomethyl)-4-cyclopropyl-1*H*-indazole (50 mg, 0.20 mmol), Cs₂CO₃ (71 mg, 0.22 mmol) and 2-mercapto-1-methylimidazole (34 mg, 0.30 mmol) in DMF (3 mL). The product was isolated a white solid (55 mg, 97%).

*R*_f 0.50 (10% MeOH in DCM); m.p. 53-55 °C; UV λ_{max} (EtOH/nm) 294.6, 259.6, 218.2; IR ν_{max}/cm⁻¹ 3102, 3010, 2930, 2871, 1279; ¹H-NMR (500 MHz, CDCl₃) δ ppm; 0.83 (2H, m, H-18), 1.05 (2H, m, H-18), 2.20 (1H, m, H-17), 3.21 (3H, s, H-19), 4.22 (2H, s, H-10), 6.54 (1H, s, H-6), 6.84 (1H, s, H-14), 7.04 (1H, s, H-8), 7.14 (1H, s, H-15), 8.13 (1H, s, H-3), 10.53 (1H, s-br, H-1); ¹³C-NMR (125 MHz, CDCl₃) δ ppm; 8.5 (C-18), 13.4 (C-17), 33.2 (C-19), 40.5 (C-10), 106.8 (C-8), 117.3 (C-6), 122.5 (C-14), 122.7 (C-4), 129.7 (C-15), 133.5 (C-3), 136.9 (C-7), 137.9 (C-5), 140.2 (C-9), 140.5 (C-12); MS (ES⁺) *m/z* 285.2 [M+H]⁺; HRMS calcd for C₁₅H₁₇N₄S 285.1168 [M+H]⁺ found 285.1165.

4-Cyclopropyl-6-((pyridin-4-ylthio)methyl)-1*H*-indazole (294)

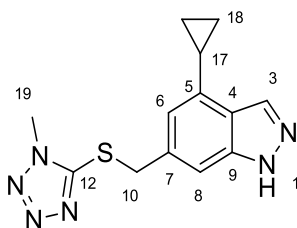


Prepared according to general procedure I using 6-(bromomethyl)-4-cyclopropyl-1*H*-indazole (50 mg, 0.20 mmol), Cs₂CO₃ (71 mg, 0.22 mmol) and 4-mercapto-1-methylimidazole (33 mg, 0.30 mmol) in DMF (3 mL). The product was isolated a white solid (46 mg, 83%).

*R*_f 0.53 (10% MeOH in DCM); m.p. 148-150 °C; UV λ_{max} (EtOH/nm) 265.4, 216.0; IR ν_{max}/cm⁻¹ 3000, 2852, 2810, 1572, 936; ¹H-NMR (500 MHz, CDCl₃) δ ppm; 0.91 (2H, m,

H-17), 1.09 (2H, m, H-17), 2.25 (1H, m, H-16), 4.29 (2H, s, H-10), 6.79 (1H, s, H-6), 7.13 (1H, d, $J = 6.3$ Hz, H-13), 7.32 (1H, s, H-8), 8.16 (1H, s, H-3), 8.38 (2H, d, $J = 6.3$ Hz, H-14), 10.30 (1H, s, H-1); ^{13}C -NMR (125 MHz, CDCl_3) δ ppm; 8.6 (C-17), 13.6 (C-16), 36.2 (C-10), 106.7 (C-8), 117.3 (C-6), 120.9 (C-14), 123.0 (C-4), 133.7 (C-3), 134.7 (C-7), 138.4 (C-5), 140.3 (C-9), 149.2 (C-13); MS (ES^+) m/z 314.3 $[\text{M}+\text{H}]^+$; HRMS calcd for $\text{C}_{16}\text{H}_{16}\text{N}_3\text{S}$ 282.1059 $[\text{M}+\text{H}]^+$ found 282.1055.

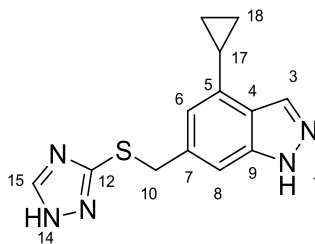
4-Cyclopropyl-6-(((1-methyl-1H-tetrazol-5-yl)thio)methyl)-1H-indazole (295)



Prepared according to general procedure I using 6-(bromomethyl)-4-cyclopropyl-1H-indazole (50 mg, 0.20 mmol), Cs_2CO_3 (71 mg, 0.22 mmol) and 2-methyl-1H-tetrazole-5-thiol (34 mg, 0.30 mmol) in DMF (3 mL). The product was isolated a white solid (57 mg, 99%).

R_f 0.38 (10% MeOH in DCM); m.p. 51-53 $^\circ\text{C}$; UV λ_{max} (EtOH/nm) 296.8, 261.8, 229.2; IR $\nu_{\text{max}}/\text{cm}^{-1}$ 3183, 2999, 1170, 937; ^1H -NMR (500 MHz, CDCl_3) δ ppm; 0.89 (2H, m, H-18), 1.09 (2H, m, H-18), 2.23 (1H, m, H-17), 3.80 (3H, s, H-19), 4.61 (2H, s, H-10), 6.76 (1H, s, H-6), 7.35 (1H, s, H-8), 8.18 (1H, s, H-3); ^{13}C -NMR (125 MHz, CDCl_3) δ ppm; 8.7 (C-18), 13.6 (C-17), 33.5 (C-19), 38.4 (C-10), 107.8 (C-8), 117.5 (C-6), 134.9 (C-3), 138.7 (C-5), 153.7 (C-12); MS (ES^+) m/z 287.2 $[\text{M}+\text{H}]^+$; HRMS calcd for $\text{C}_{13}\text{H}_{15}\text{N}_6\text{S}$ 287.1073 $[\text{M}+\text{H}]^+$ found 287.1071.

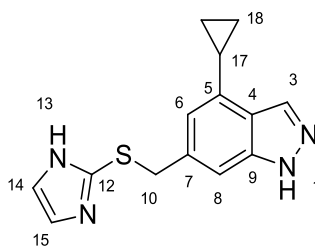
6-(((1*H*-1,2,4-Triazol-3-yl)thio)methyl)-4-cyclopropyl-1*H*-indazole (296)



Prepared according to general procedure I using 6-(bromomethyl)-4-cyclopropyl-1*H*-indazole (50 mg, 0.20 mmol), Cs₂CO₃ (71 mg, 0.22 mmol) and 3-mercapto-1,2,4-triazole (31 mg, 0.30 mmol) in DMF (3 mL). The product was isolated a white solid (50 mg, 93%).

*R*_f 0.46 (10% MeOH in DCM); m.p. 79-81 °C; UV λ_{max} (EtOH/nm) 295.0, 261.4, 219.0; IR ν_{max}/cm⁻¹ 3099, 2913, 2853, 938; ¹H-NMR (500 MHz, DMSO-*d*₆) δ ppm; 0.81 (2H, m, H-18), 1.03 (2H, m, H-18), 2.25 (1H, m, H-17), 4.42 (2H, s, H-10), 6.67 (1H, s, H-6), 7.27 (1H, s, H-8), 8.13 (1H, s, H-3), 8.49 (1H, s, H-15), 12.96 (1H, s, H-1), 14.07 (1H, s-br, H-14); ¹³C-NMR (125 MHz, DMSO-*d*₆) δ ppm; 9.3 (C-18), 13.6 (C-17), 36.6 (C-10), 107.3 (C-8), 116.5 (C-6), 122.4 (C-4), 124.7 (C-7), 132.4 (C-3), 137.3 (C-5), 140.3 (C-9), 145.7 (C-15), 163.2 (C-12); MS (ES⁺) *m/z* 272.2 [M+H]⁺; HRMS calcd for C₁₃H₁₄N₅S 272.0964 [M+H]⁺ found 272.0963.

6-(((1*H*-Imidazol-2-yl)thio)methyl)-4-cyclopropyl-1*H*-indazole (297)

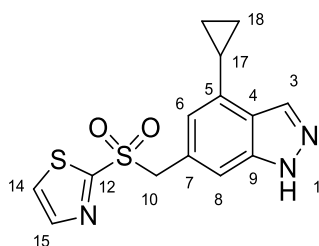


Prepared according to general procedure I using 6-(bromomethyl)-4-cyclopropyl-1*H*-indazole (50 mg, 0.20 mmol), Cs₂CO₃ (71 mg, 0.22 mmol) and 2-sulphonyl-1*H*-imidazole (30 mg, 0.30 mmol) in DMF (3 mL). The product was isolated a white solid (54 mg, 99%).

*R*_f 0.38 (10% MeOH in DCM); m.p. 102-104 °C; UV λ_{max} (EtOH/nm) 294.8, 259.4, 218.8; IR ν_{max}/cm⁻¹ 3091, 3007, 2911; ¹H-NMR (500 MHz, DMSO-*d*₆) δ ppm; 0.77 (2H, m, H-18),

1.02 (2H, m, H-18), 2.24 (1H, m, H-17), 4.29 (2H, s, H-10), 6.49 (1H, s, H-6), 7.07 (1H, s, H-8), 7.15 (2H, s, H-14), 8.12 (1H, s, H-3), 12.27 (1H, s-br, H-13), 12.09 (1H, s-br, H-1); ^{13}C -NMR (125 MHz, DMSO- d_6) δ ppm; 9.3 (C-18), 13.5 (C-17), 61.3 (C-10), 107.2 (C-8), 116.3 (C-6), 122.5 (C-4), 126.2 (C-5), 132.4 (C-3), 136.9 (C-7), 140.3 (C-9), 143.3 (C-12); MS (ES^+) m/z 271.2 $[\text{M}+\text{H}]^+$; HRMS calcd for $\text{C}_{14}\text{H}_{15}\text{N}_4\text{S}$ 271.1012 $[\text{M}+\text{H}]^+$ found 271.1009.

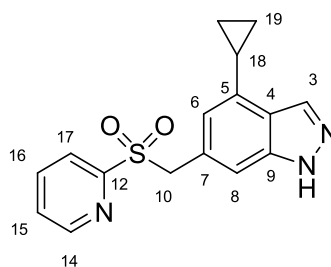
2-(((4-Cyclopropyl-1H-indazol-6-yl)methyl)sulfonyl)thiazole (298)



Prepared according to general procedure **K** using 2-(((4-cyclopropyl-1H-indazol-6-yl)methyl)thio)thiazole (53 mg, 0.18 mmol) and Oxone® (340 mg, 1.20 mmol) in MeOH (10 mL) and H₂O (5 mL). The product was isolated as an off white solid (38 mg, 65%).

R_f 0.38 (10% MeOH in DCM); m.p. 75-77 °C; UV λ_{max} (EtOH/nm) 297.2, 260.2, 217.8; IR $\nu_{\text{max}}/\text{cm}^{-1}$ 3353, 3175, 3109, 3000, 2918; ^1H -NMR (500 MHz, DMSO- d_6) δ ppm; 0.64 (2H, m, H-18), 1.01 (2H, m, H-18), 2.23 (1H, m, H-17), 5.00 (2H, s, H-10), 6.29 (1H, s, H-6), 7.22 (1H, s, H-8), 8.18 (1H, s, H-3), 8.23-8.25 (2H, m, H-14, H-15), 13.09 (1H, s-br, H-1); ^{13}C -NMR (125 MHz, DMSO- d_6) δ ppm; 9.5 (C-18), 13.2 (C-17), 61.0 (C-10), 110.4 (C-8), 117.5 (C-6), 123.3 (C-4), 126.0 (C-7), 129.4 (C-15), 132.6 (C-3), 137.4 (C-5), 140.1 (C-9), 145.6 (C-15), 164.6 (C-12); MS (ES^+) m/z 320.2 $[\text{M}+\text{H}]^+$; HRMS calcd for $\text{C}_{14}\text{H}_{14}\text{N}_3\text{O}_2\text{S}_2$ 320.0522 $[\text{M}+\text{H}]^+$ found 320.0522.

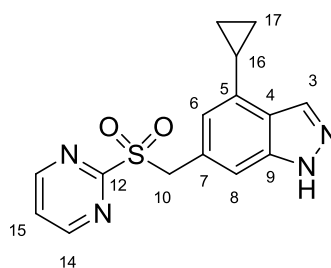
4-Cyclopropyl-6-((pyridin-2-ylsulfonyl)methyl)-1*H*-indazole (299)



Prepared according to general procedure **K** using 4-cyclopropyl-6-((pyridin-2-ylthio)methyl)-1*H*-indazole (40 mg, 0.14 mmol) and Oxone® (262 mg, 0.85 mmol) in MeOH (5 mL) and H₂O (5 mL). The product was isolated as an off white solid (19 mg, 42%).

R_f 0.50 (10% MeOH in DCM); m.p. 88-90 °C; UV λ_{max} (EtOH/nm) 297.6, 260.4, 216.6; IR ν_{max} /cm⁻¹ 3329, 3181, 3092, 3002, 1307, 1164, 1106; ¹H-NMR (500 MHz, DMSO-*d*₆) δ ppm; 0.59 (2H, m, H-19), 0.99 (2H, m, H-19), 2.21 (1H, m, H-17), 4.88 (2H, s, H-10), 6.27 (1H, s, H-6), 7.19 (1H, s, H-8), 7.77-7.80 (2H, m, H-15, H-17), 8.05 (1H, ddd, *J* = 7.6, 7.6, 1.3 Hz, H-16), 8.16 (1H, s, H-3), 8.89 (1H, d, *J* = 4.0 Hz, H-14), 13.04 (1H, s, H-1); ¹³C-NMR (125 MHz, DMSO-*d*₆) δ ppm; 9.4 (C-19), 13.2 (C-18), 58.1 (C-10), 110.3 (C-8), 117.7 (C-6), 123.2 (C-4, C-15), 126.5 (C-7), 128.5 (C-17), 132.6 (C-3), 137.1 (C-5), 139.3 (C-16), 140.1 (C-9), 150.8 (C-14), 156.5 (C-12); MS (ES⁺) *m/z* 314.3 [M+H]⁺; HRMS calcd for C₁₆H₁₆N₃O₂S 314.0958 [M+H]⁺ found 314.0959.

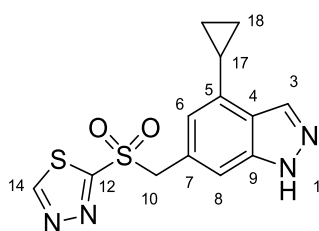
4-Cyclopropyl-6-((pyrimidin-2-ylsulfonyl)methyl)-1*H*-indazole (300)



Prepared according to general procedure **K** using 4-cyclopropyl-6-((pyrimidin-2-ylthio)methyl)-1*H*-indazole (50 mg, 0.18 mmol) and Oxone® (327 mg, 1.06 mmol) in MeOH (10 mL) and H₂O (5 mL). The product was isolated as an off white solid (32 mg, 58%).

R_f 0.48 (10% MeOH in DCM); m.p. 179-181 °C; UV λ_{\max} (EtOH/nm) 297.0, 261.8, 217.6; IR $\nu_{\max}/\text{cm}^{-1}$ 3240, 3079, 1318, 1121; ^1H -NMR (500 MHz, DMSO- d_6) δ ppm; 0.69 (2H, m, H-17), 1.03 (2H, m, H-17), 2.25 (1H, m, H-16), 5.04 (2H, s, H-10), 6.51 (1H, s, H-6), 7.30 (1H, s, H-8), 7.88 (1H, t, J = 4.9 Hz, H-15), 8.18 (1H, s, H-3), 9.12 (2H, d, J = 4.9 Hz, H-14), 13.07 (1H, s, H-1); ^{13}C -NMR (125 MHz, DMSO- d_6) δ ppm; 9.4 (C-17), 13.4 (C-16), 57.4 (C-10), 110.6 (C-8), 118.2 (C-6), 123.1 (C-4), 125.2 (C-15), 125.8 (C-7), 132.6 (C-3), 137.3 (C-5), 140.1 (C-9), 159.6 (C-15), 165.3 (C-12); MS (ES $^+$) m/z 315.3 [M+H] $^+$; HRMS calcd for C₁₅H₁₅N₄O₂S 315.0910 [M+H] $^+$ found 315.0909.

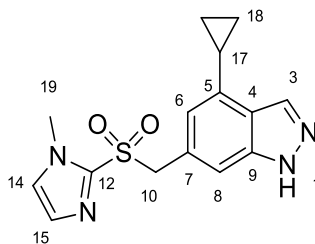
2-(((4-Cyclopropyl-1H-indazol-6-yl)methyl)sulfonyl)-1,3,4-thiadiazole (301)



Prepared according to general procedure **K** using 2-(((4-cyclopropyl-1H-indazol-6-yl)methyl)thio)-1,3,4-thiadiazole (50 mg, 0.17 mmol) and Oxone® (320 mg, 1.04 mmol) in MeOH (10 mL) and H₂O (5 mL). The product was isolated as an off white solid (31 mg, 56%).

R_f 0.36 (10% MeOH in DCM); m.p. 173-175 °C; UV λ_{\max} (EtOH/nm) 298.4, 261.0, 218.0; IR $\nu_{\max}/\text{cm}^{-1}$ 3242, 3086, 2914, 1618; ^1H -NMR (500 MHz, DMSO- d_6) δ ppm; 0.66 (2H, m, H-18), 1.03 (2H, m, H-18), 2.25 (1H, m, H-17), 5.21 (2H, s, H-10), 6.41 (1H, s, H-6), 7.27 (1H, s, H-8), 8.21 (1H, s, H-3), 9.93 (1H, s, H-14), 13.13 (1H, s-br, H-1); ^{13}C -NMR (125 MHz, DMSO- d_6) δ ppm; 9.5 (C-18), 13.2 (C-17), 61.7 (C-10), 110.7 (C-8), 117.8 (C-6), 123.4 (C-4), 125.3 (C-5), 132.7 (C-3), 137.7 (C-7), 140.1 (C-9), 160.6 (C-14), 168.3 (C-12); MS (ES $^+$) m/z 321.2 [M+H] $^+$; HRMS calcd for C₁₃H₁₃N₄O₂S₂ 321.0474 [M+H] $^+$ found 321.0475.

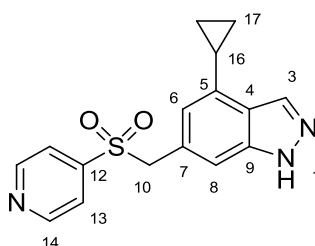
4-Cyclopropyl-6-(((1-methyl-1*H*-imidazol-2-yl)sulfonyl)methyl)-1*H*-indazole (302)



Prepared according to general procedure **K** using 4-cyclopropyl-6-(((1-methyl-1*H*-imidazol-2-yl)thio)methyl)-1*H*-indazole (59 mg, 0.20 mmol) and Oxone® (340 mg, 1.20 mmol) in MeOH (5 mL) and H₂O (5 mL). The product was isolated as an off white solid (50 mg, 77%).

R_f 0.44 (10% MeOH in DCM); m.p. 86-88°C; UV λ_{\max} (EtOH/nm) 306.6, 297.6, 241.4, 216.8; IR $\nu_{\max}/\text{cm}^{-1}$ 3337, 3114, 3003, 2920; ¹H-NMR (500 MHz, DMSO-*d*₆) δ ppm; 0.66 (2H, m, H-18), 1.02 (2H, m, H-18), 2.26 (1H, m, H-17), 3.29 (3H, s, H-19), 4.82 (2H, s, H-10), 6.18 (1H, s, H-6), 7.18 (1H, s, H-8), 7.20 (1H, s, H-15), 7.42 (1H, s, H-14), 8.22 (1H, s, H-3), 13.11 (1H, s-br, H-1); ¹³C-NMR (125 MHz, DMSO-*d*₆) δ ppm; 9.5 (C-18), 13.2 (C-17), 34.7 (C-19), 61.9 (C-10), 110.4 (C-8), 117.4 (C-6), 123.3 (C-4), 126.2 (C-7), 127.5 (C-14), 129.3 (C-15), 132.6 (C-3), 137.4 (C-5), 140.0 (C-9), 140.7 (C-12); MS (ES⁺) m/z 317.3 [M+H]⁺; HRMS calcd for C₁₅H₁₇N₄O₂S 317.1067 [M+H]⁺ found 317.1064.

4-Cyclopropyl-6-((pyridin-4-ylsulfonyl)methyl)-1*H*-indazole (303)

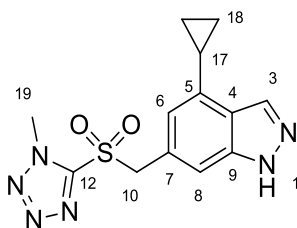


Prepared according to general procedure **K** using 4-cyclopropyl-6-((pyridin-4-ylthio)methyl)-1*H*-indazole (52 mg, 0.19 mmol) and Oxone® (114 mg, 0.38 mmol) in MeOH (10 mL) and H₂O (5 mL). The product was isolated as an off white solid (30 mg, 52%).

R_f 0.47 (10% MeOH in DCM); m.p. 159-161 °C; UV λ_{\max} (EtOH/nm) 296.6, 261.8, 217.6; IR $\nu_{\max}/\text{cm}^{-1}$ 3569, 3088, 3023, 2974, 1311, 1163; ¹H-NMR (500 MHz, DMSO-*d*₆) δ ppm;

0.58 (2H, m, H-17), 1.00 (2H, m, H-17), 2.23 (1H, m, H-16), 4.90 (2H, s, H-10), 6.31 (1H, s, H-6), 7.19 (1H, s, H-8), 7.66 (2H, d, $J = 4.5$ Hz, H-13), 8.18 (1H, s, H-3), 8.85 (2H, d, $J = 4.5$ Hz, H-14), 13.07 (1H, s, H-1); ^{13}C -NMR (125 MHz, $\text{DMSO}-d_6$) δ ppm; 9.3 (C-17), 13.2, (C-16), 60.8 (C-10), 110.3 (C-8), 117.8 (C-6), 121.9 (C-13), 123.2 (C-4), 126.3 (C-7), 132.6 (C-3), 137.2 (C-5), 140.0 (C-9), 146.6 (C-12), 151.4 (C-14); MS (ES^+) m/z 314.3 $[\text{M}+\text{H}]^+$; HRMS calcd for $\text{C}_{16}\text{H}_{16}\text{N}_3\text{O}_2\text{S}$ 314.0958 $[\text{M}+\text{H}]^+$ found 314.0958.

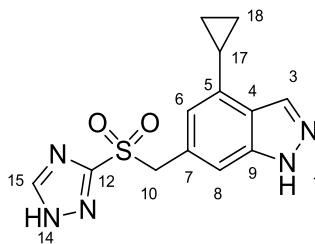
4-Cyclopropyl-6-(((1-methyl-1H-tetrazol-5-yl)sulfonyl)methyl)-1H-indazole (304)



Prepared according to general procedure **K** using 4-cyclopropyl-6-(((1-methyl-1H-tetrazol-5-yl)sulfonyl)methyl)-1H-indazole (50 mg, 0.18 mmol) and Oxone[®] (321 mg, 1.04 mmol) in MeOH (10 mL) and H_2O (5 mL). The product was isolated as an off white solid (31 mg, 56%).

R_f 0.33 (10% MeOH in DCM); m.p. 86-88 $^{\circ}\text{C}$; UV λ_{max} (EtOH/nm) 298.6, 260.4, 217.8; IR $\nu_{\text{max}}/\text{cm}^{-1}$ 3386, 3181, 2919, 1618; ^1H -NMR (500 MHz, CDCl_3) δ ppm; 0.81 (2H, m, H-18), 1.11 (2H, m, H-18), 2.22 (1H, m, H-17), 3.79 (3H, s, H-19), 4.88 (2H, s, H-10), 6.50 (1H, s, H-6), 7.23 (1H, s, H-8), 8.22 (1H, s, H-3); ^{13}C -NMR (125 MHz, CDCl_3) δ ppm; 9.1 (C-18), 13.3 (C-17), 35.8 (C-19), 62.9 (C-10), 110.1 (C-8), 118.5 (C-6), 123.7 (C-4), 139.5 (C-5), 152.3 (C-12); MS (ES^+) m/z 319.3 $[\text{M}+\text{H}]^+$; HRMS calcd for $\text{C}_{13}\text{H}_{15}\text{N}_6\text{O}_2\text{S}$ 319.0972 $[\text{M}+\text{H}]^+$ found 319.0971.

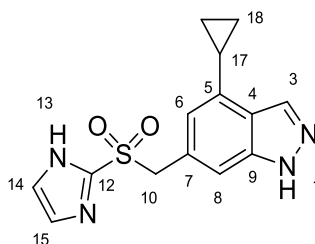
6-(((1*H*-1,2,4-Triazol-3-yl)sulfonyl)methyl)-4-cyclopropyl-1*H*-indazole (305)



Prepared according to general procedure **K** using 6-(((1*H*-1,2,4-triazol-3-yl)thio)methyl)-4-cyclopropyl-1*H*-indazole (58 mg, 0.21 mmol) and Oxone® (340 mg, 1.20 mmol) in MeOH (10 mL) and H₂O (5 mL). The product was isolated as a white solid (23 mg, 36%).

R_f 0.40 (10% MeOH in DCM); m.p. 250-252 °C; UV λ_{\max} (EtOH/nm) 297.0, 260.6, 219.2; IR $\nu_{\max}/\text{cm}^{-1}$ 3250, 3136, 3001, 1310; ¹H-NMR (500 MHz, DMSO-*d*₆) δ ppm; 0.68 (2H, m, H-18), 1.03 (2H, m, H-18), 2.25 (1H, m, H-17), 4.86 (2H, s, H-10), 6.38 (1H, s, H-6), 7.22 (1H, s, H-8), 8.18 (1H, s, H-3), 8.92 (1H, s, H-15), 13.08 (1H, s, H-1), 15.03 (1H, s-br, H-14); ¹³C-NMR (125 MHz, DMSO-*d*₆) δ ppm; 9.4 (C-18), 13.3 (C-17), 60.5 (C-10), 110.4 (C-8), 117.9 (C-6), 123.2 (C-4), 126.0 (C-7), 132.5 (C-3), 137.1 (C-5), 140.1 (C-9); MS (ES⁺) m/z 304.2 [M+H]⁺; HRMS calcd for C₁₃H₁₄N₅O₂S 304.0863 [M+H]⁺ found 304.0862.

6-(((1*H*-Imidazol-2-yl)sulfonyl)methyl)-4-cyclopropyl-1*H*-indazole (306)

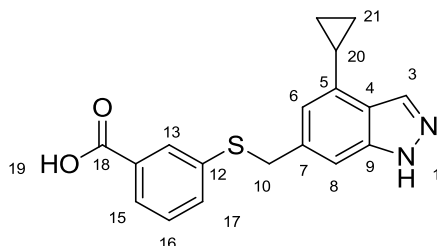


Prepared according to general procedure **K** using 6-(((1*H*-imidazol-2-yl)thio)methyl)-4-cyclopropyl-1*H*-indazole (50 mg, 0.19 mmol) and Oxone® (340 mg, 1.20 mmol) in MeOH (5 mL) and H₂O (5 mL). The product was isolated as an off white solid (45 mg, 80%).

R_f 0.41 (10% MeOH in DCM); m.p. 216-218 °C; UV λ_{\max} (EtOH/nm) 297.2, 216.0; IR $\nu_{\max}/\text{cm}^{-1}$ 3371, 3080, 2983, 2884, 2768, 1587; ¹H-NMR (500 MHz, DMSO-*d*₆) δ ppm; 0.64 (2H, m, H-18), 0.99 (2H, m, H-18), 2.22 (1H, m, H-17), 4.80 (2H, s, H-10), 6.16 (1H,

s, H-6), 7.14 (1H, s, H-8), 7.32 (2H, s, H-14), 8.18 (1H, s, H-3), 13.08 (1H, s-br, H-1); ^{13}C -NMR (125 MHz, DMSO- d_6) δ ppm; 9.5 (C-18), 13.2 (C-17), 61.3 (C-10), 110.2 (C-8), 117.3 (C-6), 123.2 (C-4), 126.5 (C-5), 132.5 (C-3), 137.3 (C-7), 140.1 (C-9), 142.1 (C-12); MS (ES^+) m/z 303.3 $[\text{M}+\text{H}]^+$; HRMS calcd for $\text{C}_{14}\text{H}_{15}\text{N}_4\text{O}_2\text{S}$ 303.0910 $[\text{M}+\text{H}]^+$ found 303.0908.

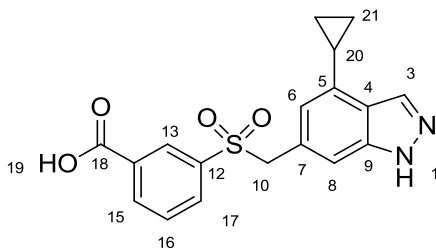
3-(((4-Cyclopropyl-1H-indazol-6-yl)methyl)thio)benzoic acid (312)



Prepared according to general procedure I using 6-(bromomethyl)-4-cyclopropyl-1H-indazole (100 mg, 0.40 mmol), Cs_2CO_3 (324 mg, 1.00 mmol) and 3-mercaptobenzoic acid (74 mg, 0.48 mmol) in DMF (4 mL). The product was isolated a white solid (118 mg, 92%).

^1H -NMR (500 MHz, DMSO- d_6) δ ppm; 0.79-0.83 (2H, m, H-21), 0.99-1.02 (2H, m, H-21), 2.17-2.25 (1H, m, H-20), 4.62 (2H, s, H-10), 6.54 (1H, d, $J = 9.9$ Hz, H-15), 6.67 (1H, s, H-6), 7.25 (1H, s, H-8), 7.71 (1H, dd, $J = 7.8, 7.8$ Hz, H-16), 7.88 (1H, d, $J = 7.8$ Hz, H-17), 8.14 (1H, s, H-13), 8.17 (1H, s, H-3), 13.06 (1H, s-br, H-1), 13.50 (1H, s-br, H-19); ^{13}C -NMR (125 MHz, DMSO- d_6) δ ppm; 7.5 (C-21), 12.6 (C-20), 64.1 (C-10), 104.7 (C-8), 114.8 (C-6), 122.4 (C-4), 127.1 (C-5), 128.5 (C-13), 130.5 (C-16), 132.0 (C-3), 134.9 (C-17), 135.2 (C-15), 137.0 (C-7), 137.8 (C-12), 171.4 C-18; MS (ES^+) m/z 325.3 $[\text{M}+\text{H}]^+$; HRMS calcd for $\text{C}_{18}\text{H}_{17}\text{N}_2\text{O}_2\text{S}$ 325.1005 $[\text{M}+\text{H}]^+$ found 325.1009.

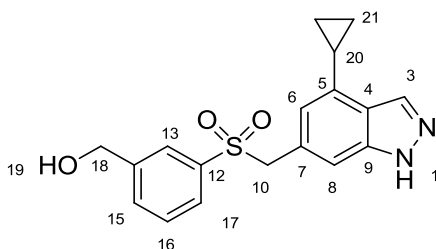
3-(((4-Cyclopropyl-1*H*-indazol-6-yl)methyl)sulfonyl)benzoic acid (310)



Prepared according to general procedure **K** 3-(((4-cyclopropyl-1*H*-indazol-6-yl)methyl)thio)benzoic acid (100 mg, 0.31 mmol) and Oxone® (568 mg, 1.85 mmol) in MeOH (20 mL) and H₂O (10 mL). The product was isolated as a white solid (33 mg, 30%).

R_f 0.12 (10% MeOH in DCM); m.p. 246-248 °C; UV λ_{\max} (EtOH/nm) 297.4, 261.2, 217.6; IR $\nu_{\max}/\text{cm}^{-1}$ 3318, 2922, 1684, 1297, 1152; ¹H-NMR (500 MHz, DMSO-*d*₆) δ ppm; 0.55 (2H, m, H-21), 0.96 (2H, m, H-21), 2.21 (1H, m, H-20), 4.81 (2H, s, H-10), 6.25 (1H, s, H-6), 7.19 (1H, s, H-8), 7.71 (1H, dd, $J = 7.8, 7.8$ Hz, H-16), 7.88 (1H, d, $J = 7.8$ Hz, H-17), 8.14 (1H, s, H-13), 8.17 (1H, s, H-3), 13.06 (1H, s-br, H-1), 13.50 (1H, s-br, H-19); ¹³C-NMR (125 MHz, DMSO-*d*₆) δ ppm; 9.1 (C-21), 13.1 (C-20), 61.5 (C-10), 110.3 (C-8), 117.9 (C-6), 123.1 (C-4), 126.9 (C-7), 129.4 (C-13), 130.1 (C-16), 132.4 (C-3), 132.6 (C-17), 134.6 (C-15), 137.0 (C-5), 139.3 (C-12), 166.3 (C-18); MS (ES⁺) m/z 357.2 [M+H]⁺; HRMS calcd for C₁₈H₁₇N₂O₄S 357.0904 [M+H]⁺ found 357.0904.

(3-(((4-cyclopropyl-1*H*-indazol-6-yl)methyl)sulfonyl)phenyl)methanol (311)

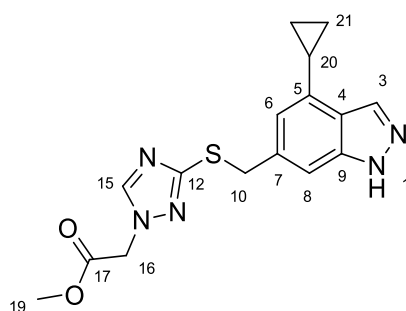


3-(((4-Cyclopropyl-1*H*-indazol-6-yl)methyl)sulfonyl)benzoic acid (207 mg, 0.58 mmol) was taken in THF (15 mL) at 0 °C under N₂ and borane.THF complex (1M, 1.45 mL, 1.45 mmol) was added by syringe over 5 minutes. The reaction mix was stirred for 18 h after which time the solution was quenched with H₂O (5 mL) and extracted with EtOAc

(3 x 10 mL). The title compound was isolated after MPLC (0-70% EtOAc in petroleum ether) as a white solid (65 mg, 33%).

R_f 0.22 (10% MeOH in DCM); m.p. 146-148 °C; UV λ_{\max} (EtOH/nm) 297.2, 261.6, 216.4; IR $\nu_{\max}/\text{cm}^{-1}$ 3299, 3000, 1293, 1139; $^1\text{H-NMR}$ (500 MHz, DMSO- d_6) δ ppm; 0.59 (2H, m, H-21), 0.98 (2H, m, H-21), 2.22 (1H, m, H-20), 4.55 (2H, s, H-18), 4.72 (2H, s, H-10), 5.44 (1H, s-br, H-10), 6.28 (1H, s, H-6), 7.20 (1H, s, H-8), 7.51-7.55 (2H, m, H-16, H-17), 7.64 (1H, d, J = 6.7 Hz, H-15), 7.70 (1H, s, H-13), 8.17 (1H, s, H-3), 13.06 (1H, s, H-1); $^{13}\text{C-NMR}$ (125 MHz, DMSO- d_6) δ ppm; 9.1 (C-21), 13.1 (C-20), 61.5 (C-10), 110.3 (C-8), 117.9 (C-6), 123.1 (C-4), 126.9 (C-7), 129.4 (C-13), 130.1 (C-16), 132.4 (C-3), 132.6 (C-17), 134.6 (C-15), 137.0 (C-5), 139.3 (C-12), 166.3 (C-18); MS (ES^+) m/z 343.3 [$\text{M}+\text{H}$] $^+$; HRMS calcd for $\text{C}_{18}\text{H}_{19}\text{N}_2\text{O}_3\text{S}$ 343.1111 [$\text{M}+\text{H}$] $^+$ found 343.1114.

Methyl 2-(3-(((4-cyclopropyl-1H-indazol-6-yl)methyl)thio)-1H-1,2,4-triazol-1-yl)acetate (314)

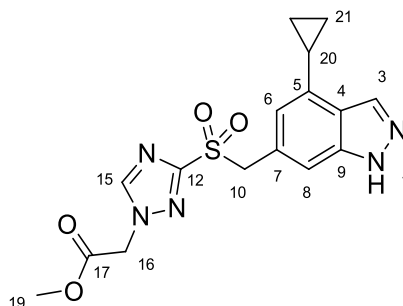


6-(((1H-1,2,4-Triazol-3-yl)thio)methyl)-4-cyclopropyl-1H-indazole (200 mg, 0.74 mmol) and Cs_2CO_3 (289 mg, 0.89 mmol) was dissolved in anhydrous DMF (10 mL) and methyl bromoacetate (81 μL , 0.89 mmol) was added. The reaction was stirred for 48 hrs at rt under N_2 before removal of DMF *in vacuo*. The residue was resuspended in EtOAc and water, organic fractions were extracted and combined before purification by MPLC (0-80% EtOAc in petroleum ether) giving the title compound as an off white solid (23 mg, 10%)

R_f 0.49 (10% MeOH in DCM); m.p. 105-107 °C; UV λ_{\max} (EtOH/nm) 297.0, 261.0, 218.2; IR $\nu_{\max}/\text{cm}^{-1}$ 3181, 2999, 2950, 1746, 1219, 1174; $^1\text{H-NMR}$ (500 MHz, CDCl_3) δ ppm; 0.87 (2H, m, H-21), 1.08 (2H, m, H-21), 2.21 (1H, m, H-20), 3.70 (3H, s, H-19), 4.46 (2H, s, H-10), 4.74 (2H, s, H-16), 6.68 (1H, s, H-6), 7.20 (1H, s, H-8), 7.96 (1H, s, H-15), 8.15

(1H, s, H-3); ^{13}C -NMR (125 MHz, CDCl_3) δ ppm; 8.6 (C-21), 13.5 (C-20), 39.2 (C-10), 49.4 (C-16), 52.9 (C-19), 107.1 (C-8), 117.3 (C-6), 123.0 (C-4), 133.5 (C-7), 135.5 (C-3), 138.4 (C-5), 140.1 (C-9), 151.9 (C-15), 152.5 (C-12), 166.7 (C-17); MS (ES^+) m/z 344.3 $[\text{M}+\text{H}]^+$; HRMS calcd for $\text{C}_{16}\text{H}_{18}\text{N}_5\text{O}_2\text{S}$ 344.1176 $[\text{M}+\text{H}]^+$ found 344.1177.

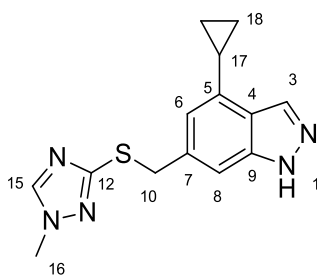
Methyl 2-(3-(((4-cyclopropyl-1H-indazol-6-yl)methyl)sulfonyl)-1H-1,2,4-triazol-1-yl)acetate (308)



Prepared according to general procedure **K** using methyl 2-(3-(((4-cyclopropyl-1H-indazol-6-yl)methyl)thio)-1H-1,2,4-triazol-1-yl)acetate (23 mg, 0.07 mmol) and Oxone[®] (124 mg, 0.20 mmol) in MeOH (2 mL) and H_2O (0.5 mL). The product was isolated as a white solid (8 mg, 30%).

R_f 0.43 (10% MeOH in DCM); m.p. 181-183 $^{\circ}\text{C}$; UV λ_{max} (EtOH/nm) 298.6, 261.0, 215.8; IR $\nu_{\text{max}}/\text{cm}^{-1}$ 3222, 1745, 1326, 1143; ^1H -NMR (500 MHz, CDCl_3) δ ppm; 0.81 (2H, m, H-21), 1.08 (2H, m, H-21), 2.22 (1H, m, H-20), 3.72 (3H, s, H-19), 4.76 (2H, s, H-10), 5.00 (2H, s, H-16), 6.55 (1H, s, H-6), 7.25 (1H, s, H-8), 8.08 (1H, s, H-15), 8.20 (1H, s, H-3); ^{13}C -NMR (125 MHz, CDCl_3) δ ppm; 8.8 (C-21), 13.3 (C-20), 51.7 (C-16), 53.1 (C-19), 62.0 (C-10), 110.0 (C-8), 118.9 (C-6), 124.3 (C-4), 138.8 (C-5), 140.1 (C-9), 150.4 (C-12), 151.0 (C-15), 166.6 (C-17); MS (ES^+) m/z 376.2 $[\text{M}+\text{H}]^+$; HRMS calcd for $\text{C}_{16}\text{H}_{18}\text{N}_5\text{O}_4\text{S}$ 376.1074 $[\text{M}+\text{H}]^+$ found 376.1075.

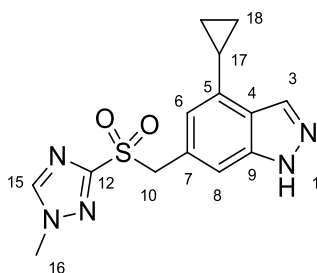
4-Cyclopropyl-6-(((1-methyl-1H-1,2,4-triazol-3-yl)thio)methyl)-1H-indazole (313)



6-(((1H-1,2,4-Triazol-3-yl)thio)methyl)-4-cyclopropyl-1H-indazole (70 mg, 0.26 mmol) and Cs_2CO_3 (92 mg, 0.28 mmol) was dissolved in anhydrous DMF (3 mL) and methyl iodide (13 μL , 0.28 mmol) was added. The reaction was stirred for 48 hrs at rt under N_2 before removal of DMF *in vacuo*. The residue was resuspended in EtOAc and water, organic fractions were extracted and combined before purification by MPLC (0-80% EtOAc in petroleum ether) giving the title compound as an off white solid (13 mg, 18%)

R_f 0.52 (10% MeOH in DCM); m.p. 158-160 $^\circ\text{C}$; UV λ_{max} (EtOH/nm) 295.0, 261.8, 218.6; IR $\nu_{\text{max}}/\text{cm}^{-1}$ 3251, 3101, 2999, 2950, 1356, 1283; $^1\text{H-NMR}$ (500 MHz, CDCl_3) δ ppm; 0.88 (2H, m, H-18), 1.06 (2H, m, H-18), 2.22 (1H, m, H-17), 3.86 (3H, s, H-16), 4.41 (2H, s, H-10), 6.80 (1H, s, H-6), 7.33 (1H, s, H-8), 7.98 (1H, s, H-15), 8.14 (1H, s, H-3); $^{13}\text{C-NMR}$ (125 MHz, CDCl_3) δ ppm; 8.4 (C-18), 13.5 (C-17), 36.3 (C-16), 37.0 (C-10), 107.0 (C-8), 117.9 (C-6), 122.7 (C-4), 133.6 (C-3), 136.8 (C-7), 137.8 (C-5), 140.3 (C-9), 144.5 (C-15), 160.6 (C-12); MS (ES^+) m/z 286.3 $[\text{M}+\text{H}]^+$; HRMS calcd for $\text{C}_{14}\text{H}_{16}\text{N}_5\text{S}$ 286.1121 $[\text{M}+\text{H}]^+$ found 286.1124.

4-Cyclopropyl-6-(((1-methyl-1H-1,2,4-triazol-3-yl)sulfonyl)methyl)-1H-indazole (307)

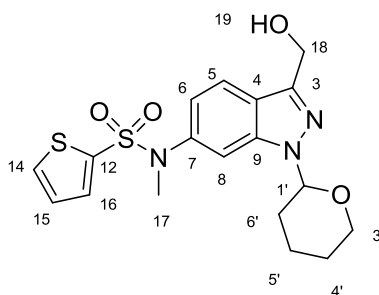


Prepared according to general procedure **K** using 4-cyclopropyl-6-(((1-methyl-1H-1,2,4-triazol-3-yl)thio)methyl)-1H-indazole (10 mg, 0.03 mmol) and Oxone[®] (64 mg, 0.11

mmol) in MeOH (4 mL) and H₂O (1 mL). The product was isolated as a white solid (11 mg, 63%).

R_f 0.48 (10% MeOH in DCM); m.p. 158-160 °C; UV λ_{max} (EtOH/nm) 297.4, 261.0, 218.8; IR ν_{max} /cm⁻¹ 3375, 3113, 1325, 1137; ¹H-NMR (500 MHz, DMSO-*d*₆) δ ppm; 0.71 (2H, m, H-18), 1.05 (2H, m, H-18), 2.27 (1H, m, H-17), 3.97 (3H, s, H-16), 4.85 (2H, s, H-10), 6.43 (1H, s, H-6), 7.25 (1H, s, H-8), 8.19 (1H, s, H-3), 8.84 (1H, s, H-15) 13.08 (1H, s-br, H-1); ¹³C-NMR (125 MHz, DMSO-*d*₆) δ ppm; 9.3 (C-18), 13.5 (C-17), 37.3 (C-16), 60.5 (C-10), 110.5 (C-8), 118.0 (C-6), 123.2 (C-4), 125.8 (C-7), 132.5 (C-3), 137.2 (C-5), 140.2 (C-9), 147.4 (C-15), 160.6 (C-12); MS (ES⁺) *m/z* 318.3 [M+H]⁺; HRMS calcd for C₁₄H₁₆N₅O₂S 318.1019 [M+H]⁺ found 318.1023.

***N*-(3-(Hydroxymethyl)-1-(tetrahydro-2*H*-pyran-2-yl)-1*H*-indazol-6-yl)-*N*-methylthiophene-2-sulfonamide (324)**

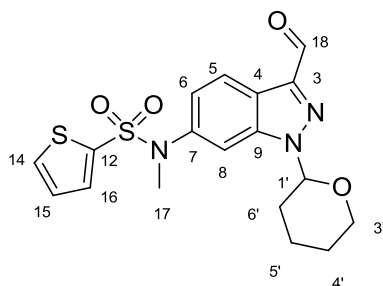


Prepared according to general procedure **G** with the following reagents and quantities: methyl 6-(*N*-methylthiophene-2-sulfonamido)-1-(tetrahydro-2*H*-pyran-2-yl)-1*H*-indazole-3-carboxylate (87 mg, 0.23 mmol) and LiAlH₄ (1M in THF, 0.51 mL, 0.51 mmol) in THF (3 mL). The product was isolated as a grey solid (73 mg, 90%).

m.p. 65-67 °C; UV λ_{max} (EtOH/nm) 2293.2, 216.8; IR ν_{max} /cm⁻¹ 3371, 3092, 2931, 2855, 1347, 1146; ¹H-NMR (500 MHz, CDCl₃) δ ppm; 1.63-1.66 (1H, m, H-5'), 1.71-1.75 (2H, m, H-4', H-5'), 2.02-2.04 (1H, m, H-6'), 2.12-2.14 (1H, m, H-4'), 2.49-2.52 (1H, m, H-6'), 3.32 (3H, s, H-17), 3.69-3.75 (1H, m, H-3'), 4.02-4.05 (1H, m, H-3'), 5.02 (2H, s, H-18), 5.61 (1H, dd, *J* = 2.5, 9.8 Hz, H-1'), 6.81 (1H, dd, *J* = 8.6, 1.7 Hz, H-6), 7.08 (1H, dd, *J* = 4.9, 3.9 Hz, H-15), 7.35 (1H, dd, *J* = 1.3, 3.8 Hz, H-16), 7.45 (1H, d, *J* = 1.7 Hz, H-8), 7.59 (1H, dd, *J* = 1.3, 4.8 Hz, H-14), 7.70 (1H, d, *J* = 8.6 Hz, H-5); ¹³C-NMR (125 MHz, CDCl₃) δ ppm; 22.7 (C-4') 25.0 (C-5'), 29.5 (C-6'), 38.8 (C-17), 58.5 (C-18), 67.8 (C-3'), 85.3 (C-1'),

109.8 (C-8), 119.5 (C-6), 121.0 (C-5), 121.9 (C-4), 127.4 (C-15), 132.1 (C-14), 132.9 (C-16), 136.9 (C-12), 140.0 (C-9), 145.1 (C-3); MS (ES⁺) *m/z* 408.5 [M+H]⁺.

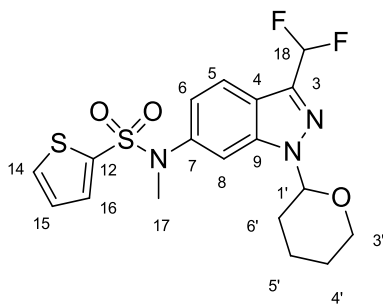
***N*-(3-Formyl-1-(tetrahydro-2*H*-pyran-2-yl)-1*H*-indazol-6-yl)-*N*-methylthiophene-2-sulfonamide (323)**



N-(3-(Hydroxymethyl)-1-(tetrahydro-2*H*-pyran-2-yl)-1*H*-indazol-6-yl)-*N*-methylthiophene-2-sulfonamide (73 mg, 0.18 mmol) was dissolved in DCM (12 mL) under N₂. Dess–Martin periodinane (0.3 M in DCM, 661 μL, 0.20 mmol) was added dropwise over five minutes at RT and stirred for 3h. Sodium thiosulfate (sat. aq, 15 mL) was added and the organic fraction separated and purified by MPLC (0-70% EtOAc in petroleum ether) to give the title compound as an off white solid (70 mg, 96%).

¹H-NMR (500 MHz, CDCl₃) δ ppm; 1.69-1.82 (3H, m, THP), 2.11-2.19 (2H, m, THP), 2.51-2.57 (1H, m, THP), 3.32 (3H, s, H-17), 3.75-3.80 (1H, m, THP), 3.98-4.02 (1H, m, THP), 5.68 (1H, dd, *J* = 2.6, 8.8 Hz, H-1'), 6.93 (1H, dd, *J* = 8.7, 1.8 Hz, H-6), 7.09 (1H, dd, *J* = 5.0, 3.8 Hz, H-15), 7.34 (1H, dd, *J* = 1.3, 3.8 Hz, H-16), 7.60 (1H, dd, *J* = 1.3, 5.0 Hz, H-14), 7.64 (1H, d, *J* = 1.7 Hz, H-8), 8.18 (1H, d, *J* = 8.7 Hz, H-5), 10.23 (1H, s, H-18); ¹³C-NMR (125 MHz, CDCl₃) δ ppm; 22.0 (C-THP), 24.9 (C-THP), 29.1 (C-THP), 38.7 (C-17), 67.4 (C-THP), 86.2 (C-THP), 110.7 (C-8), 121.4 (C-4), 122.1 (C-6), 122.5 (C-5), 127.4 (C-15), 132.3 (C-14), 133.0 (C-16), 136.6 (C-12), 140.5 (C-7), 140.8 (C-9), 143.2 (C-3), 187.1 (C-18); MS (ES⁺) *m/z* 322.2 [M+H]⁺.

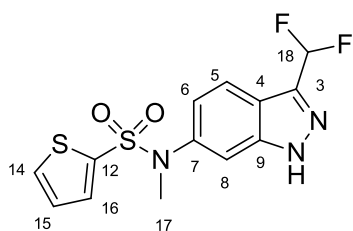
***N*-(3-(difluoromethyl)-1-(tetrahydro-2*H*-pyran-2-yl)-1*H*-indazol-6-yl)-*N*-methylthiophene-2-sulfonamide (325)**



N-(3-Formyl-1-(tetrahydro-2*H*-pyran-2-yl)-1*H*-indazol-6-yl)-*N*-methylthiophene-2-sulfonamide (70 mg, 0.17 mmol) was dissolved in toluene (1 mL) under N₂ at rt dexoxfluor (2.7 M in toluene, 642 μ L, 1.73 mmol) was added and the solution heated to 60 °C and stirred for 18h. The solution was quenched with NaHCO₃ (sat. aq, 5 mL) and extracted with DCM (3 x 5 mL), organic fractions were combined and purified by MPLC (0-60 % EtOAc in petroleum ether) to give the title compound as a white solid (28 mg, 37%).

R_f 0.42 (Et₂O); m.p. 65-67 °C; UV λ_{max} (EtOH/nm) 211.6, 256.0; IR ν_{max} /cm⁻¹ 3097, 2939, 2856, 1352, 1013; ¹H-NMR (500 MHz, CDCl₃) δ ppm; 1.67-1.78 (3H, m, THP), 2.04-2.07 (1H, m, THP), 2.12-2.15 (1H, m, THP), 2.44-2.51 (1H, m, THP), 3.32 (3H, s, H-17), 3.70-3.75 (1H, m, THP), 3.98-4.01 (1H, m, THP), 5.68 (1H, dd, *J* = 2.6, 9.2 Hz, H-1'), 6.88 (1H, dd, *J* = 8.7, 1.7 Hz, H-6), 6.94 (1H, t, *J_{HF}* = 54.4 Hz, H-18), 7.09 (1H, dd, *J* = 5.0, 3.8 Hz, H-15), 7.35 (1H, dd, *J* = 1.3, 3.8 Hz, H-16), 7.54 (1H, d, *J* = 1.7 Hz, H-8), 7.60 (1H, dd, *J* = 1.3, 5.0 Hz, H-14), 7.81 (1H, d, *J* = 8.7 Hz, H-5); ¹³C-NMR (125 MHz, CDCl₃) δ ppm; 22.2 (C-THP), 24.9 (C-THP), 29.2 (C-THP), 38.7 (C-17), 67.5 (C-THP), 85.6 (C-THP), 110.3 (C-8), 112.3 (t, *J_{CF}* = 232.8, C-18), 120.0 (C-4), 120.7 (C-6), 121.2 (C-5), 127.4 (C-15), 132.3 (C-16), 133.0 (C-14), 136.7 (C-12), 139.0 (t, *J_{CF}* = 30.9, C-3), 140.4 (C-7), 140.5 (C-9); MS (ES⁺) *m/z* 344.3 [M+H]⁺; HRMS calcd for C₁₈H₂₀N₃O₃F₂S₂ 428.0909 [M+H]⁺ found 428.0905.

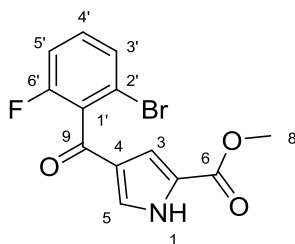
***N*-(3-(Difluoromethyl)-1*H*-indazol-6-yl)-*N*-methylthiophene-2-sulfonamide (322)**



Prepared according to general procedure **D** using *N*-(3-(difluoromethyl)-1-(tetrahydro-2*H*-pyran-2-yl)-1*H*-indazol-6-yl)-*N*-methylthiophene-2-sulfonamide (27 mg, 0.01 mmol) in MeOH.HCl (1.25 M, 5 mL) giving the title compound as a white solid (21 mg, 95%).

R_f 0.34 (Et₂O); m.p. 194-196°C; UV λ_{\max} (EtOH/nm) 254.8, 211.8; IR ν_{\max} /cm⁻¹ 3341, 1343, 1160; ¹H-NMR (500 MHz, CD₃OD) δ ppm; 3.32 (3H, s, H-17), 7.02 (1H, dd, J = 8.7, 1.8 Hz, H-6), 7.04 (1H, t, J_{HF} = 54.3 Hz, H-18), 7.17 (1H, dd, J = 5.0, 3.8 Hz, H-15), 7.38 (1H, d, J = 1.8 Hz, H-8), 7.40 (1H, dd, J = 1.3, 3.8 Hz, H-16), 7.79 (1H, d, J = 8.7 Hz, H-5), 7.81 (1H, dd, J = 1.3, 5.0 Hz, H-14); ¹³C-NMR (125 MHz, CD₃OD) δ ppm; 37.7 (C-17), 108.7 (C-8), 112.6 (t, J_{CF} = 234.4, C-18), 118.2 (C-4), 120.0 (C-5), 120.7 (C-6), 127.3 (C-15), 132.8 (C-16), 132.9 (C-14), 136.1 (C-12), 139.3 (t, J_{CF} = 30.8, C-3), 140.5 (C-7), 141.2 (C-9); ¹⁹F NMR (470 MHz, CDCl₃) δ -113.1; MS (ES⁺) m/z 344.3 [M+H]⁺; HRMS calcd for C₁₃H₁₂N₃O₂F₂S₂ 344.0334 [M+H]⁺ found 344.0333.

Methyl 4-(2-bromo-6-fluorobenzoyl)-1*H*-pyrrole-2-carboxylate (328)

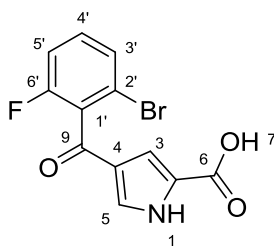


2-bromo, 6-fluorobenzoic acid (5 g, 23 mmol) was taken in THF (30 mL) and SOCl₂ (4.95 mL, 69 mmol) was added followed by and DMF (0.2 mL, 2.3 mmol). The solution was stirred at room temperature for 3 hours before volatiles were removed by rotary evaporator the resulting crude material was used directly in the next step. AlCl₃ (3.8 g, 29 mmol) was suspended in DCM (30 mL) and Methyl 1*H*-pyrrole-2-carboxylate (3.83 g,

11.5 mmol) and crude 2-bromo,6-fluorobenzoyl chloride (5.46 g, 23 mmol) were added. The solution was stirred at room temperature for 18 hours before addition of HCl (1M in H₂O, 20 mL) and stirring for a further 2 hours. The product was extracted with DCM (3 x 30 mL) and combined organic fractions were washed with NaCO₃ (saturated aqueous solution, 50 mL) and brine (40 mL). The organic solution was dried over Na₂SO₄ and concentrated *in vacuo* for purification by MPLC (10-70% EtOAc in petrol) giving the title compound as a brown solid (2.4 g, 65%).

R_f 0.21 (8:2 Petrol/EtOAc); m.p. 142-144 °C; $C_{\lambda_{max}}$ (EtOH/nm) 286.5, 231.5; IR ν_{max}/cm^{-1} 3230, 3002, 2953, 1730, 1637, 1599, 1564, 1508; 1H NMR (500 MHz, DMSO-*d*₆) δ ppm; 3.80 (3H, s, H-8), 6.99 (1H, s-br, H-3), 7.40 (1H, dd, J = 8.3, 8.9 Hz, H-4'), 7.48-7.53 (2H, m, H-3', H-5), 7.59 (1H, d, J = 8.3 Hz, H-5'), 12.88 (1H, s, H-1); ^{13}C NMR (125 MHz, DMSO-*d*₆) δ ppm 51.7 (C-8), 114.7 (C-3), 115.3 (d, J_{CF} = 22.1 Hz, C-5'), 118.9 (d, J_{CF} = 5.2 Hz, C-2'), 124.5 (C-2/4), 125.0 (C-2/4), 128.8 (d, J_{CF} = 2.9 Hz, C-3'), 129.7 (d, J_{CF} = 22.8 Hz, C-1'), 130.1 (C-5), 132.3 (d, J_{CF} = 9.0 Hz, C-4'), 158.5 (d, J_{CF} = 245.9 Hz, C-6'), 160.2 (C-6), 184.6 (C-9); ^{19}F NMR (471 MHz, DMSO-*d*₆) δ -113.8 (ArF); MS (ES⁺) m/z 326.3 [M(^{79}Br)+H]⁺, 328.3 [M(^{81}Br)+H]⁺; HRMS (ESI) calcd for C₁₃H₁₀BrFNO₃ [M(^{79}Br)+H]⁺ 325.9823, found 325.9823.

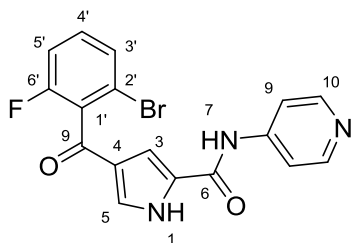
4-(2-Bromo-6-fluorobenzoyl)-1H-pyrrole-2-carboxylic acid (329)



Methyl 4-(2-bromo-6-fluorobenzoyl)-1H-pyrrole-2-carboxylate (1.4 g, 4.3 mmol), was dissolved in THF (20 mL) and LiOH.H₂O (3.6 g, 80 mmol) in H₂O (40 mL) was added. The solution was stirred at 65 °C for 18 hours then acidified to pH 3/4 using HCl (1M in H₂O). The product was extracted using EtOAc (3 x 30 mL) and washed with brine (40 mL). Organic solution was dried over Na₂SO₄ and reduced *in vacuo* to give the title compound as a white solid (1.2 g, 90%).

R_f 0.15 (9:1 DCM/MeOH); m.p. 210-211 °C; λ_{\max} (EtOH/nm) 281.0; IR $\nu_{\max}/\text{cm}^{-1}$ 3342, 1690, 1648, 1561; ^1H NMR (500 MHz, DMSO- d_6) δ ppm 6.94 (1H, s-br, H-3), 7.39- 7.43 (2H, m, H-5, H-5'), 7.50 (1H, ddd, J = 6.3, 8.3, 8.4 Hz, H-4'), 7.59 (1H, d, J = 8.3 Hz, H-3'), 12.68 (1H, s, H-1), 12.90 (1H, s, H-7); ^{13}C NMR (125 MHz, DMSO- d_6) δ ppm 114.2 (C-3), 115.3 (d, J_{CF} = 21.7 Hz, C-5'), 118.9 (d, J_{CF} = 5.2 Hz, C-2), 124.9 (C-2/4), 125.8 (C-2/4), 128.8 (d, J_{CF} = 3.1 Hz, C-3'), 129.7 (C-5), 129.9 (d, J_{CF} = 22.7 Hz, C-1'), 132.2 (d, J_{CF} = 8.7 Hz, C-4'), 158.4 (d, J_{CF} = 249.9 Hz, C-6'), 161.3 (C-6), 184.6 (C-8); ^{19}F NMR (471 MHz, DMSO- d_6) δ -113.84; MS (ES^-) m/z 310.1 [$\text{M}(^{79}\text{Br})\text{-H}^-$], 312.1 [$\text{M}(^{81}\text{Br})\text{-H}^-$]; HRMS (ESI) calcd for $\text{C}_{12}\text{H}_6\text{BrFNO}_3$ 309.9521 $\text{M}(^{79}\text{Br})\text{-H}^-$ found 309.9518.

4-(2-Bromo-6-fluorobenzoyl)-*N*-(pyridin-4-yl)-1*H*-pyrrole-2-carboxamide (327)

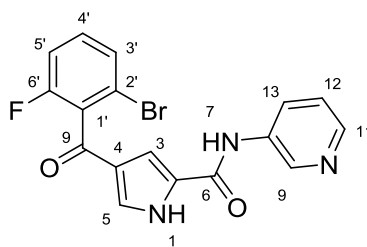


Prepared according to general procedure **R** with the following reagents and quantities:

4-(2-bromo-6-fluorobenzoyl)-1*H*-pyrrole-2-carboxylic acid (540 mg, 1.73 mmol), PCl_3 (151 μL , 1.73 mmol) and 4-aminopyridine (407 mg, 4.33 mmol) in MeCN (11 mL) to give the title compound as a white solid (497 mg, 74%).

R_f 0.32 (19:1 DCM/MeOH); m.p. 312-314 °C; λ_{\max} (EtOH/nm) 291.5, 270.5; IR $\nu_{\max}/\text{cm}^{-1}$ 3344, 3112, 2958, 1627, 1591, 1557, 1506; ^1H NMR (500 MHz, DMSO- d_6) δ ppm 7.42-7.46 (1H, m, H-5'), 7.49-7.54 (3H, m, H-3, H-4', H-5), 7.61-7.62 (1H, m, H-3'), 7.73 (2H, d, J = 6.4 Hz, H-9), 8.46 (2H, d, J = 6.4 Hz, C-10), 10.35 (1H, s, H-6), 12.74 (1H, s, H-1); ^{13}C NMR (125 MHz, DMSO- d_6) δ ppm 112.1 (C-3), 113.7 (C-9), 115.4 (d, J_{CF} = 21.6 Hz, C-5'), 119.0 (d, J_{CF} = 5.1 Hz, C-2'), 125.0 (C-2/4), 128.0 (C-2/4), 128.9 (d, J_{CF} = 2.9 Hz, C-3'), 129.8 (C-1'), 132.2 (d, J_{CF} = 8.9 Hz, C-4'), 145.6 (C-10), 150.3 (C-8), 158.5 (d, J_{CF} = 247.8 Hz, C-1'), 159.0 (C-6), 184.9 (C-9); HRMS calcd for $\text{C}_{17}\text{H}_{11}\text{BrFN}_3\text{O}_2$ 388.0091 [$\text{M}(^{79}\text{Br})\text{+H}^+$] found 388.0088.

4-(2-Bromo-6-fluorobenzoyl)-*N*-(pyridin-3-yl)-1*H*-pyrrole-2-carboxamide (17)



Prepared according to general procedure **R** with the following reagents and quantities: 4-(2-bromo-6-fluorobenzoyl)-1*H*-pyrrole-2-carboxylic acid (500 mg, 1.60 mmol), PCl₃ (140 μL, 1.60 mmol) and 3-aminopyridine (377 mg, 4.00 mmol) in MeCN (10 mL) to give the title compound as a white solid (547 mg, 88%).

*R*_f 0.31 (19:1 DCM/MeOH); m.p. 138-140 °C; λ_{max} (EtOH/nm) 288.0; IR ν_{max}/cm⁻¹ 3127, 2960, 1635, 1599, 1534; ¹H NMR (500 MHz, DMSO-*d*₆) δ ppm 7.39 (1H, dd, *J* = 4.7, 8.4 Hz, H-12), 7.42-7.48 (3H, m, H-3, H-5', H-5), 7.52 (1H, ddd, *J* = 6.2, 8.3, 8.4 Hz, H-4'), 7.61-7.63 (1H, m, H-3'), 8.14 (1H, ddd, *J* = 1.5, 2.5, 8.4 Hz, H-13), 8.30 (1H, dd, *J* = 1.5, 4.7 Hz, H-11), 8.89 (1H, d, *J* = 2.5 Hz, H-9), 10.24 (1H, s, H-7), 12.70 (1H, s, H-1); ¹³C NMR (125 MHz, DMSO-*d*₆) δ ppm 111.7 (C-3), 115.4 (d, *J*_{CF} = 21.7 Hz, C-5'), 119.0 (d, *J*_{CF} = 5.2 Hz, C-2'), 123.6 (C-12), 124.9 (C-2/4), 127.0 (C-2/4), 128.8 (d, *J*_{CF} = 2.5 Hz, C-3'), 129.4 (C-1'), 130.0 (C-9), 132.1 (d, *J*_{CF} = 8.7 Hz, C-4'), 135.5 (C-13), 141.6 (C-12), 144.4 (C-8), 158.5 (d, *J*_{CF} = 245.6 Hz, C-6'), 158.7 (C-6), 184.9 (C-9); HRMS calcd for C₁₇H₁₁BrFN₃O₂ 388.0091 [M(⁷⁹Br)+H]⁺ found 388.0090.

Abbreviations

ABC	ATP binding cassette transporters
ADMET	Adsorption, distribution, metabolism, excretion and toxicity
ADP	Adenosine diphosphate
ALK	Anaplastic lymphoma tyrosine kinase receptor
aq	aqueous
ATP	Adenosine triphosphate
AUC	Area under curve
BAD	Bcl-2-associated death promoter
bFGF	fibroblast growth factor
Boc	<i>tert</i> -butyloxycarbonyl
CDI	1,1'-Carbonyldiimidazole
CDK	cyclin dependant kinase
CRT-DL	Cancer Research Technology Discovery Labs
DAST	diethylaminosulfur trifluoride
DCM	Dichloromethane
DFG	aspartate, phenylalanine, glycine
DHP	dihydropyran
DMB	dimethoxy benzyl
DNA	Deoxyribonucleic acid
EDG	Electron donating group
EGF	epidermal growth factor
EGTA	ethylene glycol tetraacetic acid

ERK5	Extracellular signal regulated kinase 5
Et ₂ O	diethyl ether
EtOAc	Ethyl acetate
EWG	Electron withdrawing group
FDA	Food and Drugs Administration
GAB1	Grb2-associated binder
GE	Group efficiency
GPCR	G-protein coupled receptor
HBA	Hydrogen bond acceptor
HBD	Hydrogen bond donor
hERG	Human ether-a-go-go related gene product
HPLC	High performance liquid chromatography
HRMS	High resolution mass spectrometry
HTS	High throughput screen
ID	Identification
IMAP	immobilised metal affinity polarisation
IP	intraperitoneal
IR	infrared
IV	intravenous
LAD	Lck-associated adaptor
LCMS	liquid chromatography-mass spectrometry
LE	Ligand efficiency
LEI	Ligand efficiency index
LIF	Leukaemia inhibitory factor

LipE	lipophilic ligand efficiency
LLE	lipophilic ligand efficiency
MAPK	Mitogen activated protein kinase
MAPKK	MAPK kinase
MAPKKK	MAPK kinase kinase
MDR	multidrug resistance
MDR1	multidrug resistance 1
MLM	Mouse liver microsome
MPLC	Medium pressure liquid chromatography
MW	Molecular weight
NBD	nucleotide binding domain
NFG	nerve growth factor
NFSI	<i>N</i> -Fluorobenzenesulfonimide
NLK	Nemo-like kinase
NMP	<i>N</i> -methyl-2-pyrrolidone
NMR	Nuclear magnetic resonance spectroscopy
PDB	Protein database
PDGF	platelet derived growth factor
PEG	polyethylene glycol
P-gp	P-glycoprotein
PLP	piecewise linear potential
PMB	Para-methoxy benzyl
PML	promyelocytic leukaemia protein
PO	oral administration

PPB	Plasma protein binding
<i>p</i> -TSA	<i>para</i> -toluenesulfonic
QED	quantitative estimate of drug likeness
Rb	retinoblastoma protein
RTV	Relative tumour volumes
SAR	structure activity relationship
SDS	sodium dodecyl sulphate
SEM	Trimethylsilyl ethoxymethyl
TAD	transactivation domain
TFE	Trifluoroethanol
THP	Tetrahydropyran
TLC	Thin layer chromatography
TMD	transmembrane domain
TNBC	Triple negative breast cancer
tPSA	topological polar surface area
Tris	tris(hydroxymethyl)aminomethane
Ts	Tosyl
UK	United Kingdom
UV	Ultraviolet
V _{dss}	volume of distribution at steady state
VEGF	vascular endothelial growth factor

References

1. Drews, J. Drug discovery: a historical perspective. *Science* **2000**, 287, 1960-1964.
2. Williams, K. J. The introduction of 'chemotherapy' using arsphenamine – the first magic bullet. *J. R. Soc. Med.* **2009**, 102, 343-348.
3. Newman, D. J.; Cragg, G. M.; Snader, K. M. The influence of natural products upon drug discovery. *Nat. Prod. Rep.* **2000**, 17, 215-234.
4. Gordon, E. M.; Gallop, M. A.; Patel, D. V. Strategy and Tactics in Combinatorial Organic Synthesis. Applications to Drug Discovery. *Acc. Chem. Res.* **1996**, 29, 144-154.
5. Lander, E. S. Initial impact of the sequencing of the human genome. *Nature* **2011**, 470, 187-197.
6. Bhatt, A. Evolution of Clinical Research: A History Before and Beyond James Lind. *Perspectives in Clinical Research* **2010**, 1, 6-10.
7. Anonymous <http://www.fda.gov/AboutFDA/WhatWeDo/History/> (accessed 07/15, 2015).
8. Nicolaou, K. C.; Hale, C. R. H.; Nilewski, C.; Ioannidou, H. A. Constructing molecular complexity and diversity: total synthesis of natural products of biological and medicinal importance. *Chem. Soc. Rev.* **2012**, 41, 5185-5238.
9. Guerra-Bubb, J.; Croteau, R.; Williams, R. M. The Early Stages of Taxol Biosynthesis: An Interim Report on the Synthesis and Identification of Early Pathway Metabolites. *Nat. Prod. Rep.* **2012**, 29, 683-696.
10. Patrick, G. L. *An Introduction to Medicinal Chemistry, Fourth Edition*; Oxford University Press: New York, 2009; , pp 752.

11. Kappe, C. O.; Dallinger, D. The impact of microwave synthesis on drug discovery. *Nat Rev Drug Discov* **2006**, *5*, 51-63.
12. Anonymous What is the European Lead Factory?
<https://www.europeanleadfactory.eu/about/unique-high-quality-compounds-and-advanced-screening/> (accessed 07/17, 2015).
13. Harris, C. J.; Hill, R. D.; Sheppard, D. W.; Slater, M. J.; Stouten, P. F. The design and application of target-focused compound libraries. *Comb. Chem. High Throughput Screen.* **2011**, *14*, 521-531.
14. Welsch, M. E.; Snyder, S. A.; Stockwell, B. R. Privileged scaffolds for library design and drug discovery. *Curr. Opin. Chem. Biol.* **2010**, *14*, 347-361.
15. Virshup, A. M.; Contreras-Garcia, J.; Wipf, P.; Yang, W.; Beratan, D. N. Stochastic Voyages into Uncharted Chemical Space Produce a Representative Library of All Possible Drug-Like Compounds. *J. Am. Chem. Soc.* **2013**, *135*, 7296-7303.
16. Leeson, P. D.; Springthorpe, B. The influence of drug-like concepts on decision-making in medicinal chemistry. *Nat Rev Drug Discov* **2007**, *6*, 881-890.
17. Lipinski, C. A.; Lombardo, F.; Dominy, B. W.; Feeney, P. J. Experimental and computational approaches to estimate solubility and permeability in drug discovery and development settings¹. *Adv. Drug Deliv. Rev.* **2001**, *46*, 3-26.
18. Bickerton, G. R.; Paolini, G. V.; Besnard, J.; Muresan, S.; Hopkins, A. L. Quantifying the chemical beauty of drugs. *Nat Chem* **2012**, *4*, 90-98.
19. Leeson, P. Chemically beauty contest. *Nature* **2012**, *481*, 455-456.

20. Kola, I.; Landis, J. Can the pharmaceutical industry reduce attrition rates? *Nat Rev Drug Discov* **2004**, *3*, 711-716.
21. Hopkins, A. L.; Keseru, G. M.; Leeson, P. D.; Rees, D. C.; Reynolds, C. H. The role of ligand efficiency metrics in drug discovery. *Nat. Rev. Drug Discov.* **2014**, *13*, 105-121.
22. Cancer Research UK Worldwide Cancer statistics: Cancer Research UK.
<http://info.cancerresearchuk.org/cancerstats/world/> (accessed 20/03, 2012).
23. Loeb, L. A. Human cancers express mutator phenotypes: origin, consequences and targeting. *Nature reviews.Cancer* **2011**, *11*, 450-457.
24. Stratton, M. R.; Campbell, P. J.; Futreal, P. A. The cancer genome. *Nature* **2009**, *458*, 719-724.
25. Hanahan, D.; Weinberg, R. A. Hallmarks of Cancer: The Next Generation. *Cell* **2011**, *144*, 646-674.
26. Hanahan, D.; Weinberg, R. A. The hallmarks of cancer. *Cell* **2000**, *100*, 57-70.
27. Thurston, D. E. *Chemistry and Pharmacology of Anticancer Drugs*; CRC Press: Boca Raton, 2007; .
28. Nygren, P. What is cancer chemotherapy? *Acta Oncologica* **2001**, *40*, 166-174.
29. Gunnars, B.; Nygren, P.; Glimelius, B. Assessment of Quality of Life During Chemotherapy. *Acta Oncologica* **2001**, *40*, 175-184.
30. Druker, B. J.; Talpaz, M.; Resta, D. J.; Peng, B.; Buchdunger, E.; Ford, J. M.; Lydon, N. B.; Kantarjian, H.; Capdeville, R.; Ohno-Jones, S.; Sawyers, C. L. Efficacy and safety of a specific

inhibitor of the BCR-ABL tyrosine kinase in chronic myeloid leukemia. *N. Engl. J. Med.* **2001**, *344*, 1031-1037.

31. Nagar, B.; Bornmann, W. G.; Pellicena, P.; Schindler, T.; Veach, D. R.; Miller, W. T.; Clarkson, B.; Kuriyan, J. Crystal structures of the kinase domain of c-Abl in complex with the small molecule inhibitors PD173955 and imatinib (STI-571). *Cancer Res.* **2002**, *62*, 4236-4243.

32. Cohen, P. Protein kinases--the major drug targets of the twenty-first century? *Nat. Rev. Drug Discov.* **2002**, *1*, 309-315.

33. Shah, N. P.; Nicoll, J. M.; Nagar, B.; Gorre, M. E.; Paquette, R. L.; Kuriyan, J.; Sawyers, C. L. Multiple BCR-ABL kinase domain mutations confer polyclonal resistance to the tyrosine kinase inhibitor imatinib (STI571) in chronic phase and blast crisis chronic myeloid leukemia. *Cancer. Cell.* **2002**, *2*, 117-125.

34. Cohen, P. Protein kinases [mdash] the major drug targets of the twenty-first century? *Nat Rev Drug Discov* **2002**, *1*, 309-315.

35. Knight, Z. A.; Shokat, K. M. Features of Selective Kinase Inhibitors. *Chem. Biol.* **2005**, *12*, 621-637.

36. Zuccotto, F.; Ardini, E.; Casale, E.; Angiolini, M. Through the 'Gatekeeper Door': Exploiting the Active Kinase Conformation. *J. Med. Chem.* **2010**, *53*, 2681-2694.

37. Morphy, R. Selectively Nonselective Kinase Inhibition: Striking the Right Balance. *J. Med. Chem.* **2010**, *53*, 1413-1437.

38. Zhang, J.; Yang, P. L.; Gray, N. S. Targeting cancer with small molecule kinase inhibitors. *Nat. Rev. Cancer.* **2009**, *9*, 28-39.

39. Cronan, M. R.; Nakamura, K.; Johnson, N. L.; Granger, D. A.; Cuevas, B. D.; Wang, J. G.; Mackman, N.; Scott, J. E.; Dohlman, H. G.; Johnson, G. L. Defining MAP3 kinases required for MDA-MB-231 cell tumor growth and metastasis. *Oncogene* **2011**, .
40. Pearson, G.; Robinson, F.; Beers Gibson, T.; Xu, B.; Karandikar, M.; Berman, K.; Cobb, M. H. Mitogen-Activated Protein (MAP) Kinase Pathways: Regulation and Physiological Functions. *Endocrine Reviews* **2001**, 22, 153-183.
41. Garai, A.; Zeke, A.; Gogl, G.; Toro, I.; Fordos, F.; Blankenburg, H.; Barkai, T.; Varga, J.; Alexa, A.; Emig, D.; Albrecht, M.; Remenyi, A. Specificity of linear motifs that bind to a common mitogen-activated protein kinase docking groove. *Sci. Signal.* **2012**, 5, ra74.
42. Cargnello, M.; Roux, P. P. Activation and Function of the MAPKs and Their Substrates, the MAPK-Activated Protein Kinases. *Microbiology and Molecular Biology Reviews* **March 2011**, 75, 50-83.
43. Goldsmith, Z. G.; Dhanasekaran, D. N. G protein regulation of MAPK networks. *Oncogene* **2007**, 26, 3122-3142.
44. Kolch, W. Meaningful relationships: the regulation of the Ras/Raf/MEK/ERK pathway by protein interactions. *Biochem. J.* **2000**, 351, 289-305.
45. Dhanasekaran, D. N.; Kashef, K.; Lee, C. M.; Xu, H.; Reddy, E. P. Scaffold proteins of MAP-kinase modules. *Oncogene* **2007**, 26, 3185-3202.
46. Tanoue, T.; Adachi, M.; Moriguchi, T.; Nishida, E. A conserved docking motif in MAP kinases common to substrates, activators and regulators. *Nat. Cell Biol.* **2000**, 2, 110-116.
47. Drew, B. A.; Burow, M. E.; Beckman, B. S. MEK5/ERK5 pathway: The first fifteen years. *Biochimica et Biophysica Acta (BBA) - Reviews on Cancer* **2012**, 1825, 37-48.

48. Lee, J. D.; Ulevitch, R. J.; Han, J. Primary structure of BMK1: a new mammalian map kinase. *Biochem. Biophys. Res. Commun.* **1995**, *213*, 715-724.
49. Lochhead, P. A.; Gilley, R.; Cook, S. J. ERK5 and its role in tumour development. *Biochem. Soc. Trans.* **2012**, *40*, 251-256.
50. Sun, W.; Kesavan, K.; Schaefer, B.; Garrington, T.; Ware, M.; Johnson, N.; Gelfand, E.; Johnson, G. MEKK2 associates with the adapter protein Lad/RIBP and regulates the MEK5-BMK1/ERK5 pathway. *J. Biol. Chem.* **2001**, *276*, 5093-5100.
51. Kamakura, S.; Moriguchi, T.; Nishida, E. Activation of the protein kinase ERK5/BMK1 by receptor tyrosine kinases - Identification and characterization of a signaling pathway to the nucleus. *J. Biol. Chem.* **1999**, *274*, 26563-26571.
52. Nakaoka, Y.; Nishida, K.; Fujio, Y.; Izumi, M.; Terai, K.; Oshima, Y.; Sugiyama, S.; Matsuda, S.; Koyasu, S.; Yamauchi-Takahara, K.; Hirano, T.; Kawase, I.; Hirota, H. Activation of gp130 transduces hypertrophic signal through interaction of scaffolding/docking protein Gab1 with tyrosine phosphatase SHP2 in cardiomyocytes. *Circ. Res.* **2003**, *93*, 221-229.
53. Qiagen ERK5 Signaling.
<https://www.qiagen.com/qb/products/genes%20and%20pathways/pathway%20details/?pwid=163&action=Accept> (accessed 07/23, 2015).
54. Wang, X.; Tournier, C. Regulation of cellular functions by the ERK5 signalling pathway. *Cell. Signal.* **2006**, *18*, 753-760.
55. Sun, W.; Wei, X.; Kesavan, K.; Garrington, T. P.; Fan, R.; Mei, J.; Anderson, S. M.; Gelfand, E. W.; Johnson, G. L. MEK kinase 2 and the adaptor protein Lad regulate extracellular signal-regulated kinase 5 activation by epidermal growth factor via Src. *Mol. Cell. Biol.* **2003**, *23*, 2298-2308.

56. Nakamura, K.; Johnson, G. PB1 domains of MEKK2 and MEKK3 interact with the MEK5 PB1 domain for activation of the ERK5 pathway. *J. Biol. Chem.* **2003**, *278*, 36989-36992.
57. Zhou, G.; Bao, Z.; Dixon J. Components of a New Human Protein-Kinase Signal-Transduction Pathway. *J. Biol. Chem.* **1995**, *270*, 12665-12669.
58. English, J.; Vanderblit, C.; Xu, S.; Marcus, S.; Cobb, M. Isolation of Mek5 and Differential Expression of Alternatively Spliced Forms. *J. Biol. Chem.* **1995**, *270*, 28897-28902.
59. Seyfried, J.; Wang, X.; Kharebava, G.; Tournier, C. A novel mitogen-activated protein kinase docking site in the N terminus of MEK5 alpha organizes the components of the extracellular signal-regulated kinase 5 signaling pathway. *Mol. Cell. Biol.* **2005**, *25*, 9820-9828.
60. Buschbeck, M.; Ullrich, A. The unique C-terminal tail of the mitogen-activated protein kinase ERK5 regulates its activation and nuclear shuttling. *J. Biol. Chem.* **2005**, *280*, 2659-2667.
61. Yang, Q.; Lee, J. Targeting the BMK1 MAP Kinase Pathway in Cancer Therapy. *Clinical Cancer Research* **2011**, *17*, 3527-3532.
62. Kondoh, K.; Terasawa, K.; Morimoto, H.; Nishida, E. Regulation of nuclear translocation of extracellular signal-regulated kinase 5 by active nuclear import and export mechanisms. *Mol. Cell. Biol.* **2006**, *26*, 1679-1690.
63. Kato, Y.; Tapping, R. I.; Huang, S.; Watson, M. H.; Ulevitch, R. J.; Lee, J. Bmk1/Erk5 is required for cell proliferation induced by epidermal growth factor. *Nature* **1998**, *395*, 713-716.
64. Wisdom, R.; Johnson, R. S.; Moore, C. c-Jun regulates cell cycle progression and apoptosis by distinct mechanisms. *EMBO J.* **1999**, *18*, 188-197.
65. Mulloy, R.; Salinas, S.; Philips, A.; Hipkind, R. A. Activation of cyclin D1 expression by the ERK5 cascade. *Oncogene* **2003**, *22*, 5387-5398.

66. Schreiber, M.; Kolbus, A.; Piu, F.; Szabowski, A.; Mohle-Steinlein, U.; Tian, J.; Karin, M.; Angel, P.; Wagner, E. F. Control of cell cycle progression by c-Jun is p53 dependent. *Genes Dev.* **1999**, *13*, 607-619.
67. iBiology, D. Morgan (accessed 10/01/2016)
- <http://www.ibiology.org/ibioseminars/cell-biology/david-morgan-part-2.html>
68. Perez-Madrigal, D.; Finegan, K. G.; Paramo, B.; Tournier, C. The extracellular-regulated protein kinase 5 (ERK5) promotes cell proliferation through the down-regulation of inhibitors of cyclin dependent protein kinases (CDKs). *Cell. Signal.* **2012**, *24*, 2360-2368.
69. Yang, Q.; Deng, X.; Lu, B.; Cameron, M.; Fearn, C.; Patricelli, M. P.; Yates III, J. R.; Gray, N. S.; Lee, J. Pharmacological Inhibition of BMK1 Suppresses Tumor Growth through Promyelocytic Leukemia Protein. *Cancer Cell* **2010**, *18*, 258-267.
70. Potthoff, M. J.; Olson, E. N. MEF2: a central regulator of diverse developmental programs. *Development* **2007**, *134*, 4131-4140.
71. Lu, J.; McKinsey, T. A.; Nicol, R. L.; Olson, E. N. Signal-dependent activation of the MEF2 transcription factor by dissociation from histone deacetylases. *Proc. Natl. Acad. Sci. U. S. A.* **2000**, *97*, 4070-4075.
72. Nishimoto, S.; Kusakabe, M.; Nishida, E. Requirement of the MEK5-ERK5 pathway for neural differentiation in *Xenopus* embryonic development. *EMBO Rep.* **2005**, *6*, 1064-1069.
73. Hayashi, M.; Lee, J. Role of the BMK1/ERK5 signaling pathway: lessons from knockout mice. *Journal of Molecular Medicine-Jmm* **2004**, *82*, 800-808.
74. Hayashi, M.; Lee, J. Role of the BMK1/ERK5 signaling pathway: lessons from knockout mice. *Journal of Molecular Medicine* **2004**, *82*, 800-808.

75. Hayashi, M.; Tapping, R. I.; Chao, T.; Lo, J.; King, C. C.; Yang, Y.; Lee, J. BMK1 Mediates Growth Factor-induced Cell Proliferation through Direct Cellular Activation of Serum and Glucocorticoid-inducible Kinase. *Journal of Biological Chemistry* **2001**, *276*, 8631-8634.
76. Hayashi, M.; Kim, S.; Imanaka-Yoshida, K.; Yoshida, T.; Abel, E.; Eliceiri, B.; Yang, Y.; Ulevitch, R.; Lee, J. Targeted deletion of BMK1/ERK5 in adult mice perturbs vascular integrity and leads to endothelial failure. *J. Clin. Invest.* **2004**, *113*, 1138-1148.
77. Ramsay, A. K.; McCracken, S. R. C.; Soofi, M.; Fleming, J.; Yu, A. X.; Ahmad, I.; Morland, R.; Machesky, L.; Nixon, C.; Edwards, D. R.; Nuttall, R. K.; Seywright, M.; Marquez, R.; Keller, E.; Leung, H. Y. ERK5 signalling in prostate cancer promotes an invasive phenotype. *Br. J. Cancer* **2011**, *104*, 664-672.
78. Gialeli, C.; Theocharis, A. D.; Karamanos, N. K. Roles of matrix metalloproteinases in cancer progression and their pharmacological targeting. *FEBS J.* **2011**, *278*, 16-27.
79. Beroukhi, R.; Mermel, C. H.; Porter, D.; Wei, G.; Raychaudhuri, S.; Donovan, J.; Barretina, J.; Boehm, J. S.; Dobson, J.; Urashima, M.; Mc Henry, K. T.; Pinchback, R. M.; Ligon, A. H.; Cho, Y. J.; Haery, L.; Greulich, H.; Reich, M.; Winckler, W.; Lawrence, M. S.; Weir, B. A.; Tanaka, K. E.; Chiang, D. Y.; Bass, A. J.; Loo, A.; Hoffman, C.; Prensner, J.; Liefeld, T.; Gao, Q.; Yecies, D.; Signoretti, S.; Maher, E.; Kaye, F. J.; Sasaki, H.; Tepper, J. E.; Fletcher, J. A.; Tabernero, J.; Baselga, J.; Tsao, M. S.; Demichelis, F.; Rubin, M. A.; Janne, P. A.; Daly, M. J.; Nucera, C.; Levine, R. L.; Ebert, B. L.; Gabriel, S.; Rustgi, A. K.; Antonescu, C. R.; Ladanyi, M.; Letai, A.; Garraway, L. A.; Loda, M.; Beer, D. G.; True, L. D.; Okamoto, A.; Pomeroy, S. L.; Singer, S.; Golub, T. R.; Lander, E. S.; Getz, G.; Sellers, W. R.; Meyerson, M. The landscape of somatic copy-number alteration across human cancers. *Nature* **2010**, *463*, 899-905.
80. Dang, C. MYC on the Path to Cancer. *Cell* **2012**, *149*, 22-35.

81. Anonymous ERK5 Is a Potential Therapeutic Target in ALK-Positive Neuroblastoma. *Cancer Discovery* **2014**, *4*, 1363-1363.
82. CRUK Prostate cancer statistics. <http://www.cancerresearchuk.org/health-professional/cancer-statistics/statistics-by-cancer-type/prostate-cancer#heading-Three> (accessed 07/26, 2015).
83. Ortiz-Ruiz, M.; Álvarez-Fernández, S.; Parrott, T.; Zaknoen, S.; Burrows, F. J.; Ocaata, A.; Pandiella, A.; Esparas-Ogando, A. Therapeutic potential of ERK5 targeting in triple negative breast cancer. *Oncotarget* **2014**, *5*, 11308-11318.
84. Mehta, P. B.; Jenkins, B. L.; McCarthy, L.; Thilak, L.; Robson, C. N.; Neal, D. E.; Leung, H. Y. MEK5 overexpression is associated with metastatic prostate cancer, and stimulates proliferation, MMP-9 expression and invasion. *Oncogene* **2003**, *22*, 1381-1389.
85. McCracken, S. R. C.; Ramsay, A.; Heer, R.; Mathers, M. E.; Jenkins, B. L.; Edwards, J.; Robson, C. N.; Marquez, R.; Cohen, P.; Leung, H. Y. Aberrant expression of extracellular signal-regulated kinase 5 in human prostate cancer. *Oncogene* **2007**, *27*, 2978-2988.
86. Nagel, S.; Burek, C.; Venturini, L.; Scherr, M.; Quentmeier, H.; Meyer, C.; Rosenwald, A.; Drexler, H. G.; MacLeod, R. A. F. Comprehensive analysis of homeobox genes in Hodgkin lymphoma cell lines identifies dysregulated expression of HOXB9 mediated via ERK5 signaling and BMI1. *Blood* **2007**, *109*, 3015-3023.
87. Sticht, C.; Freier, K.; Knoepfle, K.; Flechtenmacher, C.; Pungs, S.; Hofele, C. M.; Hahn, M.; Joos, S.; Lichter, P. Activation of MAP kinase signaling through ERK5 but not ERK1 expression is associated with lymph node metastases in oral squamous cell carcinoma (OSCC). *Neoplasia* **2008**, *10*, 462-U26.

88. Garaude, J.; Cherni, S.; Kaminski, S.; Delepine, E.; Chable-Bessia, C.; Benkirane, M.; Borges, J.; Pandiella, A.; Iniguez, M. A.; Fresno, M.; Mpskind, R. A.; Villalba, M. ERK5 activates NF-kappa B in leukemic T cells and is essential for their growth in vivo. *Journal of Immunology* **2006**, *177*, 7607-7617.
89. Nagel, S.; Burek, C.; Venturini, L.; Scherr, M.; Quentmeier, H.; Meyer, C.; Rosenwald, A.; Drexler, H. G.; MacLeod, R. A. F. Comprehensive analysis of homeobox genes in Hodgkin lymphoma cell lines identifies dysregulated expression of HOXB9 mediated via ERK5 signaling and BMI1. *Blood* **2007**, *109*, 3015-3023.
90. Ramos-Nino, M. E.; Blumen, S. R.; Sabo-Attwood, T.; Pass, H.; Carbone, M.; Testa, J. R.; Altomare, B. A.; Mossman, B. T. HGF mediates cell proliferation of human mesothelioma cells through a PI3K/MEK5/Fra-1 pathway. *American Journal of Respiratory Cell and Molecular Biology* **2008**, *38*, 209-217.
91. Finegan, K. G.; Perez-Madrigal, D.; Hitchin, J. R.; Davies, C. C.; Jordan, A. M.; Tournier, C. ERK5 Is a Critical Mediator of Inflammation-Driven Cancer. *Cancer Res.* **2015**, *75*, 742-753.
92. Down, K.; Bamborough, P.; Alder, C.; Campbell, A.; Christopher, J. A.; Gerelle, M.; Ludbrook, S.; Mallett, D.; Mellor, G.; Miller, D. D.; Pearson, R.; Ray, K.; Solanke, Y.; Somers, D. The discovery and initial optimisation of pyrrole-2-carboxamides as inhibitors of p38 alpha MAP kinase. *Bioorg. Med. Chem. Lett.* **2010**, *20*, 3936-3940.
93. Herberich, B.; Jackson, C.; Wurz, R. P.; Pettus, L. H.; Sherman, L.; Liu, Q.; Henkle, B.; Saris, C. J. M.; Wong, L. M.; Chmait, S.; Lee, M. R.; Mohr, C.; Hsieh, F.; Tasker, A. S. Identification of triazolopyridazinones as potent p38 alpha inhibitors. *Bioorg. Med. Chem. Lett.* **2012**, *22*, 1226-1229.

94. Deng, X.; Yang, Q.; Kwiatkowski, N.; Sim, T.; McDermott, U.; Settleman, J. E.; Lee, J.; Gray, N. S. Discovery of a benzo[e]pyrimido-[5,4-b][1,4]diazepin-6(11H)-one as a Potent and Selective Inhibitor of Big MAP Kinase 1. *ACS Med. Chem. Lett.* **2011**, *2*, 195-200.
95. Deng, X.; Elkins, J. M.; Zhang, J.; Yang, Q.; Erazo, T.; Gomez, N.; Choi, H. G.; Wang, J.; Dzamko, N.; Lee, J.; Sim, T.; Kim, N.; Alessi, D. R.; Lizcano, J. M.; Knapp, S.; Gray, N. S. Structural determinants for ERK5 (MAPK7) and leucine rich repeat kinase 2 activities of benzo[e]pyrimido-[5,4-b]diazepine-6(11H)-ones. *Eur. J. Med. Chem.* **2013**, *70*, 758-767.
96. Elkins, J. M.; Wang, J.; Deng, X.; Pattison, M. J.; Arthur, J. S.; Erazo, T.; Gomez, N.; Lizcano, J. M.; Gray, N. S.; Knapp, S. X-ray Crystal Structure of ERK5 (MAPK7) in Complex with a Specific Inhibitor. *J. Med. Chem.* **2013**, *56*, 4413-4421.
97. Deng, X.; Yang, Q.; Kwiatkowski, N.; Sim, T.; McDermott, U.; Settleman, J. E.; Lee, J.; Gray, N. S. Discovery of a benzo[e]pyrimido-[5,4-b][1,4]diazepin-6(11H)-one as a Potent and Selective Inhibitor of Big MAP Kinase 1. *Acs Medicinal Chemistry Letters* **2011**, *2*, 195-200.
98. Tatake, R. J.; O'Neill, M. M.; Kennedy, C. A.; Wayne, A. L.; Jakes, S.; Wu, D.; Kugler Jr., S. Z.; Kashem, M. A.; Kaplita, P.; Snow, R. J. Identification of pharmacological inhibitors of the MEK5/ERK5 pathway. *Biochem. Biophys. Res. Commun.* **2008**, *377*, 120-125.
99. Goh, K. C.; Novotny-Diermayr, V.; Hart, S.; Ong, L. C.; Loh, Y. K.; Cheong, A.; Tan, Y. C.; Hu, C.; Jayaraman, R.; William, A. D.; Sun, E. T.; Dymock, B. W.; Ong, K. H.; Ethirajulu, K.; Burrows, F.; Wood, J. M. TG02, a novel oral multi-kinase inhibitor of CDKs, JAK2 and FLT3 with potent anti-leukemic properties. *Leukemia* **2012**, *26*, 236-243.
100. Molecular devices IMAF Assays - Screening Kinase Assays, Phosphatase, Phosphodiesterase Assays. <http://www.moleculardevices.com/Products/Assay-Kits/Enzymes/IMAF-Assays.html> (accessed 30/03, 2012).

101. Patson, B.; B Cohen, ,Roger; Olszanski, A. J. Pharmacokinetic evaluation of axitinib. *Expert Opin. Drug Metab. Toxicol.* **2012**, *8*, 259-270.
102. Swahn, B.; Huerta, F.; Kallin, E.; Malmström, J.; Weigelt, T.; Viklund, J.; Womack, P.; Xue, Y.; Öhberg, L. Design and synthesis of 6-anilinoindazoles as selective inhibitors of c-Jun N-terminal kinase-3. *Bioorg. Med. Chem. Lett.* **2005**, *15*, 5095-5099.
103. Bamborough, P.; Angell, R. M.; Bhamra, I.; Brown, D.; Bull, J.; Christopher, J. A.; Cooper, A. W. J.; Fazal, L. H.; Giordano, I.; Hind, L.; Patel, V. K.; Ranshaw, L. E.; Sims, M. J.; Skone, P. A.; Smith, K. J.; Vickerstaff, E.; Washington, M. N-4-Pyrimidinyl-1H-indazol-4-amine inhibitors of Lck: Indazoles as phenol isosteres with improved pharmacokinetics RID C-5543-2009. *Bioorg. Med. Chem. Lett.* **2007**, *17*, 4363-4368.
104. Bardelle, C.; Barlaam, B.; Brooks, N.; Coleman, T.; Cross, D.; Ducray, R.; Green, I.; Lambert-van der Brempt, C.; Olivier, A.; Read, J. Inhibitors of the tyrosine kinase EphB4. Part 3: Identification of non-benzodioxole-based kinase inhibitors. *Bioorg. Med. Chem. Lett.* **2010**, *20*, 6242-6245.
105. Bauer, D.; Whittington, D. A.; Coxon, A.; Bready, J.; Harriman, S. P.; Patel, V. F.; Polverino, A.; Harmange, J. Evaluation of indazole-based compounds as a new class of potent KDR/VEGFR-2 inhibitors. *Bioorg. Med. Chem. Lett.* **2008**, *18*, 4844-4848.
106. Blanchard, S.; William, A. D.; Lee, A. C. -; Poulsen, A.; Teo, E. L.; Deng, W.; Tu, N.; Tan, E.; Goh, K. L.; Ong, W. C.; Ng, C. P.; Goh, K. C.; Bonday, Z.; Sun, E. T. Synthesis and evaluation of alkenyl indazoles as selective Aurora kinase inhibitors. *Bioorg. Med. Chem. Lett.* **2010**, *20*, 2443-2447.
107. Di Grandi, M. J.; Berger, D. M.; Hopper, D. W.; Zhang, C.; Dutia, M.; Dunnick, A. L.; Torres, N.; Levin, J. I.; Diamantidis, G.; Zapf, C. W.; Bloom, J. D.; Hu, Y.; Powell, D.; Wojciechowicz, D.;

Collins, K.; Frommer, E. Novel pyrazolopyrimidines as highly potent B-Raf inhibitors. *Bioorg. Med. Chem. Lett.* **2009**, *19*, 6957-6961.

108. Feng, Y.; Cameron, M. D.; Frackowiak, B.; Griffin, E.; Lin, L.; Ruiz, C.; Schroter, T.; LoGrasso, P. Structure-activity relationships, and drug metabolism and pharmacokinetic properties for indazole piperazine and indazole piperidine inhibitors of ROCK-II. *Bioorg. Med. Chem. Lett.* **2007**, *17*, 2355-2360.

109. Foloppe, N.; Fisher, L.; Francis, G.; Howes, R.; Kierstan, P.; Potter, A. Identification of a buried pocket for potent and selective inhibition of Chk1: Prediction and verification. *Bioorg. Med. Chem.* **2006**, *14*, 1792-1804.

110. Goodman, K. B.; Cui, H.; Dowdell, S. E.; Gaitanopoulos, D. E.; Ivy, R. L.; Sehon, C. A.; Stavenger, R. A.; Wang, G. Z.; Viet, A. Q.; Xu, W.; Ye, G.; Semus, S. F.; Evans, C.; Fries, H. E.; Jolivet, L. J.; Kirkpatrick, R. B.; Dul, E.; Khandekar, S. S.; Yi, T.; Jung, D. K.; Wright, L. L.; Smith, G. K.; Behm, D. J.; Bentley, R.; Doe, C. P.; Hu, E.; Lee, D. Development of dihydropyridone indazole amides as selective Rho-kinase inhibitors. *J. Med. Chem.* **2007**, *50*, 6-9.

111. Hu, Y.; Cole, D.; Denny, R. A.; Anderson, D. R.; Ipek, M.; Ni, Y.; Wang, X.; Thaisrivongs, S.; Chamberlain, T.; Hall, J. P.; Liu, J.; Luong, M.; Lin, L.; Telliez, J.; Gopalsamy, A. Discovery of indazoles as inhibitors of Tpl2 kinase. *Bioorg. Med. Chem. Lett.* **2011**, *21*, 4758-4761.

112. Ko, J. H.; Yeon, S. W.; Ryu, J. S.; Kim, T.; Song, E.; You, H.; Park, R.; Ryu, C. Synthesis and biological evaluation of 5-arylamino-6-chloro-1H-indazole-4,7-diones as inhibitors of protein kinase B/Akt. *Bioorg. Med. Chem. Lett.* **2006**, *16*, 6001-6005.

113. Lee, J.; Choi, H.; Kim, K.; Jeong, S.; Park, J.; Baek, C.; Lee, S. Synthesis and biological evaluation of 3,5-diaminoindazoles as cyclin-dependent kinase inhibitors. *Bioorg. Med. Chem. Lett.* **2008**, *18*, 2292-2295.

114. McBride, C.; Renhowe, P.; Gesner, T.; Jansen, J.; Lin, J.; Ma, S.; Zhou, Y.; Shafer, C. 3-benzimidazol-2-yl-1H-indazoles as potent c-ABL inhibitors. *Bioorg. Med. Chem. Lett.* **2006**, *16*, 3789-3792.
115. Shafer, C. M.; Lindvall, M.; Bellamacina, C.; Gesner, T. G.; Yabannavar, A.; Jia, W.; Lin, S.; Walter, A. 4-(1H-Indazol-5-yl)-6-phenylpyrimidin-2(1H)-one analogs as potent CDC7 inhibitors. *Bioorg. Med. Chem. Lett.* **2008**, *18*, 4482-4485.
116. Sutherlin, D. P.; Bao, L.; Berry, M.; Castanedo, G.; Chuckowree, I.; Dotson, J.; Folks, A.; Friedman, L.; Goldsmith, R.; Gunzner, J.; Heffron, T.; Lesnick, J.; Lewis, C.; Mathieu, S.; Murray, J.; Nonomiya, J.; Pang, J.; Pegg, N.; Prior, W. W.; Rouge, L.; Salphati, L.; Sampath, D.; Tian, Q.; Tsui, V.; Wan, N. C.; Wang, S.; Wei, B.; Wiesmann, C.; Wu, P.; Zhu, B.; Olivero, A. Discovery of a Potent, Selective, and Orally Available Class I Phosphatidylinositol 3-Kinase (PI3K)/Mammalian Target of Rapamycin (mTOR) Kinase Inhibitor (GDC-0980) for the Treatment of Cancer. *J. Med. Chem.* **2011**, *54*, 7579-7587.
117. Takahashi, H.; Shinoyama, M.; Komine, T.; Nagao, M.; Suzuki, M.; Tsuchida, H.; Katsuyama, K. Novel dihydrothieno[2,3-e]indazole derivatives as I kappa B kinase inhibitors. *Bioorg. Med. Chem. Lett.* **2011**, *21*, 1758-1762.
118. Trujillo, J. I.; Kiefer, J. R.; Huang, W.; Thorarensen, A.; Xing, L.; Caspers, N. L.; Day, J. E.; Mathis, K. J.; Kretzmer, K. K.; Reitz, B. A.; Weinberg, R. A.; Stegeman, R. A.; Wrightstone, A.; Christine, L.; Compton, R.; Li, X. 2-(6-Phenyl-1H-indazol-3-yl)-1H-benzo[d]imidazoles: Design and synthesis of a potent and isoform selective PKC-zeta inhibitor. *Bioorg. Med. Chem. Lett.* **2009**, *19*, 908-911.
119. Barnwell, N.; Cornwall, P.; Horner, D.; Knott, J.; Liddon, J. Development of an Extremely Efficient Oxidative Chlorination Reaction: The Value of Routine Data Collection. *Org. Process Res. Dev.* **2010**, *14*, 278-288.

120. Shear, N. H.; Spielberg, S. P.; Grant, D. M.; Tang, B. K.; Kalow, W. Differences in Metabolism of Sulfonamides Predisposing to Idiosyncratic Toxicity. *Ann. Intern. Med.* **1986**, *105*, 179-184.
121. Li, X.; Chu, S.; Feher, V. A.; Khalili, M.; Nie, Z.; Margosiak, S.; Nikulin, V.; Levin, J.; Sprankle, K. G.; Tedder, M. E.; Almassy, R.; Appelt, K.; Yager, K. M. Structure-Based Design, Synthesis, and Antimicrobial Activity of Indazole-Derived SAH/MTA Nucleosidase Inhibitors. *J. Med. Chem.* **2003**, *46*, 5663-5673.
122. Wyatt, P. G.; Woodhead, A. J.; Berdini, V.; Boulstridge, J. A.; Carr, M. G.; Cross, D. M.; Davis, D. J.; Devine, L. A.; Early, T. R.; Feltell, R. E.; Lewis, E. J.; McMenamin, R. L.; Navarro, E. F.; O'Brien, M. A.; O'Reilly, M.; Reule, M.; Saxty, G.; Seavers, L. C. A.; Smith, D.; Squires, M. S.; Trewartha, G.; Walker, M. T.; Woolford, A. J. -. Identification of N-(4-piperidinyl)-4-(2,6-dichlorobenzoylamino)-1H-pyrazole-3-carboxamide (AT7519), a novel cyclin dependent kinase inhibitor using fragment-based X-ray crystallography and structure based drug design. *J. Med. Chem.* **2008**, *51*, 4986-4999.
123. Morris, E. J.; Jha, S.; Restaino, C. R.; Dayananth, P.; Zhu, H.; Cooper, A.; Carr, D.; Deng, Y.; Jin, W.; Black, S.; Long, B.; Liu, J.; Dinunzio, E.; Windsor, W.; Zhang, R.; Zhao, S.; Angagaw, M. H.; Pinheiro, E. M.; Desai, J.; Xiao, L.; Shipps, G.; Hruza, A.; Wang, J.; Kelly, J.; Paliwal, S.; Gao, X.; Babu, B. S.; Zhu, L.; Daublain, P.; Zhang, L.; Lutterbach, B. A.; Pelletier, M. R.; Philippar, U.; Siliphaivanh, P.; Witter, D.; Kirschmeier, P.; Bishop, W. R.; Hicklin, D.; Gilliland, D. G.; Jayaraman, L.; Zawel, L.; Fawell, S.; Samatar, A. A. Discovery of a novel ERK inhibitor with activity in models of acquired resistance to BRAF and MEK inhibitors. *Cancer. Discov.* **2013**, *3*, 742-750.

124. Dalvie, D. K.; Kalgutkar, A. S.; Khojasteh-Bakht, S.; Obach, R. S.; O'Donnell, J. P. Biotransformation Reactions of Five-Membered Aromatic Heterocyclic Rings. *Chem. Res. Toxicol.* **2002**, *15*, 269-299.
125. Eicher, T.; Hauptmann, S.; Speicher, A. *The chemistry of heterocycles: Structure, reactions, syntheses and applications, second edition*. Wiley: Weinheim, 2003; .
126. Schmidt, A.; Beutler, A.; Snovydovych, B. Recent Advances in the Chemistry of Indazoles. *European Journal of Organic Chemistry* **2008**, *2008*, 4073-4095.
127. Lohou, E.; Sopkova-de, O. S.; Schumann-Bard, P.; Boulouard, M.; Stiebing, S.; Rault, S.; Collot, V. New hypotheses for the binding mode of 4- and 7-substituted indazoles in the active site of neuronal nitric oxide synthase. *Bioorg. Med. Chem.* **2012**, *20*, 5296-5304.
128. Lundgren, R. J.; Stradiotto, M. Palladium-Catalyzed Cross-Coupling of Aryl Chlorides and Tosylates with Hydrazine. *Angewandte Chemie International Edition* **2010**, *49*, 8686-8690.
129. Coşkun, N.; Çetin, M. A new regioselective synthesis and ambient light photochemistry of quinazolin-1-oxides. *Tetrahedron* **2007**, *63*, 2966-2972.
130. Jin, T.; Yamamoto, Y. An Efficient, Facile, and General Synthesis of 1H-Indazoles by 1,3-Dipolar Cycloaddition of Arynes with Diazomethane Derivatives. *Angewandte Chemie International Edition* **2007**, *46*, 3323-3325.
131. Lukin, K.; Hsu, M. C.; Fernando, D.; Leanna, M. R. New Practical Synthesis of Indazoles via Condensation of o-Fluorobenzaldehydes and Their O-Methyloximes with Hydrazine. *J. Org. Chem.* **2006**, *71*, 8166-8172.

132. Lukin, K.; Hsu, M. C.; Fernando, D.; Leanna, M. R. New Practical Synthesis of Indazoles via Condensation of o-Fluorobenzaldehydes and Their O-Methyloximes with Hydrazine. *J. Org. Chem.* **2006**, *71*, 8166-8172.
133. Xu, L.; Peng, Y.; Pan, Q.; Jiang, Y.; Ma, D. Assembly of Substituted 3-Aminoindazoles from 2-Bromobenzonitrile via a CuBr-Catalyzed Coupling/Condensation Cascade Process. *J. Org. Chem.* **2013**, *78*, 3400-3404.
134. Duan, J.; Cai, X.; Meng, F.; Lan, L.; Hart, C.; Matteucci, M. Potent Antitubulin Tumor Cell Cytotoxins Based on 3-Aroyl Indazoles. *J. Med. Chem.* **2007**, *50*, 1001-1006.
135. Jin, T.; Yamamoto, Y. An Efficient, Facile, and General Synthesis of 1H-Indazoles by 1,3-Dipolar Cycloaddition of Arynes with Diazomethane Derivatives. *Angewandte Chemie International Edition* **2007**, *46*, 3323-3325.
136. Liu, Z.; Wang, L.; Tan, H.; Zhou, S.; Fu, T.; Xia, Y.; Zhang, Y.; Wang, J. Synthesis of 1H-indazoles from N-tosylhydrazones and nitroaromatic compounds. *Chem. Commun.* **2014**, *50*, 5061-5063.
137. Pelc, M.; Huang, W.; Trujillo, J.; Baldus, J.; Turner, S.; Kleine, P.; Yang, S.; Thorarensen, A. An Efficient and Regioselective Difluoromethylation of 3-Iodoindazole with Chlorodifluoromethane. *Synlett* **2010**, *2010*, 219-222.
138. Ben-Yahia, A.; Naas, M.; El Kazzouli, S.; Essassi, E. M.; Guillaumet, G. Direct C-3-arylations of 1H-indazoles. *European Journal of Organic Chemistry* **2012**, 7075.
139. Hattori, K.; Yamaguchi, K.; Yamaguchi, J.; Itami, K. Pd- and Cu-catalyzed C-H arylation of indazoles. *Tetrahedron* **2012**, *68*, 7605.

140. Nagaradja, E.; Chevallier, F.; Roisnel, T.; Dorcet, V.; Halauko, Y. S.; Ivashkevich, O. A.; Matulis, V. E.; Mongin, F. Deproto-metallation using a mixed lithium-zinc base and computed CH acidity of 1-aryl 1H-benzotriazoles and 1-aryl 1H-indazoles. *Organic and Biomolecular Chemistry* **2014**, *12*, 1475.
141. Ye, M.; Edmunds, A. J. F.; Morris, J. A.; Sale, D.; Zhang, Y.; Yu, J. A robust protocol for Pd(ii)-catalyzed C-3 arylation of (1H) indazoles and pyrazoles: Total synthesis of nigellidine hydrobromide. *Chemical Science* **2013**, *4*, 2374.
142. Fernandez, P.; Bellamy, T.; Kling, M.; Madge, D.; Selwood, D. A convenient route to the soluble guanylate cyclase activator YC-1 and its N2 regioisomer. *Heterocycles* **2001**, *55*, 1813-+.
143. Unsinn, A.; Knochel, P. Regioselective zincation of indazoles using TMP2Zn and Negishi cross-coupling with aryl and heteroaryl iodides. *Chem. Commun.* **2012**, *48*, 2680-2682.
144. Slade, D. J.; Pelz, N. F.; Bodnar, W.; Lampe, J. W.; Watson, P. S. Indazoles: Regioselective Protection and Subsequent Amine Coupling Reactions. *J. Org. Chem.* **2009**, *74*, 6331-6334.
145. Bahrami, K.; Khodaei, M. M.; Soheilzad, M. Direct Conversion of Thiols to Sulfonyl Chlorides and Sulfonamides. *J. Org. Chem.* **2009**, *74*, 9287-9291.
146. Karaman, R.; Blasko, A.; Almarsson, O.; Arasasingham, R.; Bruice, T. C. Symmetrical and unsymmetrical quadruply aza-bridged, closely interspaced, cofacial bis(5,10,15,20-tetraphenylporphyrin)s. 2. Synthesis, characterization, and conformational effects of solvents. *J. Am. Chem. Soc.* **1992**, *114*, 4889-4898.
147. Blotny, G. A new, mild preparation of sulfonyl chlorides. *Tetrahedron Lett.* **2003**, *44*, 1499-1501.

148. Tajbakhsh, M.; Hosseinzadeh, R.; Alinezhad, H.; Ghahari, S.; Heydari, A.; Khaksar, S. Catalyst-Free One-Pot Reductive Alkylation of Primary and Secondary Amines and N,N-Dimethylation of Amino Acids Using Sodium Borohydride in 2,2,2-Trifluoroethanol. *Synthesis-Stuttgart* **2011**, 490-496.
149. Salvatore, R. N.; Nagle, A. S.; Jung, K. W. Cesium Effect: High Chemoselectivity in Direct N-Alkylation of Amines. *J. Org. Chem.* **2002**, 67, 674-683.
150. Romera, J. L.; Cid, J. M.; Trabanco, A. A. Potassium iodide catalysed monoalkylation of anilines under microwave irradiation. *Tetrahedron Lett.* **2004**, 45, 8797-8800.
151. Knight, Z. A.; Shokat, K. M. Features of selective kinase inhibitors. *Chem. Biol.* **2005**, 12, 621-637.
152. Yang, L.; Xue, X.; Zhang, Y. Simple and Efficient Synthesis of Belinostat. *Synthetic Communications* **2010**, 40, 2520-2524.
153. Choong, I. C.; Lew, W.; Lee, D.; Pham, P.; Burdett, M. T.; Lam, J. W.; Wiesmann, C.; Luong, T. N.; Fahr, B.; DeLano, W. L.; McDowell, R. S.; Allen, D. A.; Erlanson, D. A.; Gordon, E. M.; O'Brien, T. Identification of Potent and Selective Small-Molecule Inhibitors of Caspase-3 through the Use of Extended Tethering and Structure-Based Drug Design. *J. Med. Chem.* **2002**, 45, 5005-5022.
154. Leahy, J. W.; Buhr, C. A.; Johnson, H. W. B.; Kim, B. G.; Baik, T.; Cannoy, J.; Forsyth, T. P.; Jeong, J. W.; Lee, M. S.; Ma, S.; Noson, K.; Wang, L.; Williams, M.; Nuss, J. M.; Brooks, E.; Foster, P.; Goon, L.; Heald, N.; Holst, C.; Jaeger, C.; Lam, S.; Loughheed, J.; Nguyen, L.; Plonowski, A.; Song, J.; Stout, T.; Wu, X.; Yakes, M. F.; Yu, P.; Zhang, W.; Lamb, P.; Raeber, O. Discovery of a Novel Series of Potent and Orally Bioavailable Phosphoinositide 3-Kinase \hat{I}^3 Inhibitors. *J. Med. Chem.* **2012**, 55, 5467-5482.

155. DORSETT, M.; GRISAR, J.; HICKEY, K.; POHL, R.; HUDAK, W.; LEWIS, R.
Aminoalkenylbenzenesulfonamides with Hypotensive and Histamine-Releasing Properties. *J. Med. Chem.* **1970**, *13*, 895-&.
156. Kochi, J. K. The Mechanism of the Sandmeyer and Meerwein Reactions. *J. Am. Chem. Soc.* **1957**, *79*, 2942-2948.
157. Nagle, A.; Salvatore, R.; Chong, B.; Jung, K. Efficient synthesis of beta-amino bromides. *Tetrahedron Lett.* **2000**, *41*, 3011-3014.
158. Harada, K.; Makino, K.; Shima, N.; Okuyama, H.; Esumi, T.; Kubo, M.; Hioki, H.; Asakawa, Y.; Fukuyama, Y. Total synthesis of riccardin C and (\pm)-cavicularin via Pd-catalyzed Ar–Ar cross couplings. *Tetrahedron* **2013**, *69*, 6959-6968.
159. Wang, L.; Zhang, Y. Indium-mediated Coupling Reaction of Sulfonyl Chlorides with Alkyl Bromides in Water. A Facile Synthesis of Sulfones. *J. Chem. Res. (S)* **1998**, *0*, 588-589.
160. Sun, X.; Wang, L.; Zhang, Y. A convenient synthesis of sulfones using zinc mediated coupling reaction of sulfonyl chlorides with alkyl halides in aqueous media. *Synthetic Communications* **1998**, *28*, 1785-1791.
161. Rao Volla, C. M.; Vogel, P. Iron-catalyzed desuffinylative C-C cross-coupling reactions of sulfonyl chlorides with grignard reagents. *Angewandte Chemie-International Edition* **2008**, *47*, 1305-1307.
162. Ragni, R.; Orselli, E.; Kottas, G. S.; Omar, O. H.; Badudri, F.; Pedone, A.; Naso, F.; Farinola, G. M.; De Cola, L. Iridium(III) Complexes with Sulfonyl and Fluorine Substituents: Synthesis, Stereochemistry and Effect of Functionalisation on their Photophysical Properties. *Chemistry-a European Journal* **2009**, *15*, 136-148.

163. Rayner, C. M. Synthesis of thiols, sulfides, sulfoxides and sulfones. *Contemp. Org. Synth.* **1995**, *2*, 409-440.
164. Glatz, G.; Gogl, G.; Alexa, A.; Remenyi, A. Structural mechanism for the specific assembly and activation of the extracellular signal regulated kinase 5 (ERK5) module. *J. Biol. Chem.* **2013**, *288*, 8596-8609.
165. Leed, A. R.; Boettger, S. D.; Ganem, B. Studies on the synthesis of substituted phenanthrenoids. *J. Org. Chem.* **1980**, *45*, 1098-1106.
166. Carella, A.; Vives, G.; Cox, T.; Jaud, J.; Rapenne, G.; Launay, J. Synthesis of New Tripodal Tri-Functionalized Hydrotris(indazol-1-yl)borate Ligands and X-ray Structures of Their Cyclopentadieneruthenium Complexes. *European Journal of Inorganic Chemistry* **2006**, *2006*, 980-987.
167. Dijkstra, G.; Kruizinga, W. H.; Kellogg, R. M. An assessment of the causes of the "cesium effect". *J. Org. Chem.* **1987**, *52*, 4230-4234.
168. Lipinski, C. A.; Lombardo, F.; Dominy, B. W.; Feeney, P. J. Experimental and computational approaches to estimate solubility and permeability in drug discovery and development settings¹. *Adv. Drug Deliv. Rev.* **2001**, *46*, 3-26.
169. Reaction Biology Kinase Mapper.
<http://www.reactionbiology.com/webapps/site/Biochemical-Assay-Services.aspx> (accessed 03/30, 2015).
170. Lave, T.; Dupin, S.; Schmitt, C.; Chou, R. C.; Jaeck, D.; Coassolo, P. Integration of in vitro data into allometric scaling to predict hepatic metabolic clearance in man: Application to 10 extensively metabolized drugs. *J. Pharm. Sci.* **1997**, *86*, 584-590.

171. Desmoulin, F.; Gilard, V.; Malet-Martino, M.; Martino, R. Metabolism of capecitabine, an oral fluorouracil prodrug: (19)F NMR studies in animal models and human urine. *Drug Metab. Dispos.* **2002**, *30*, 1221-1229.
172. Hussain, M.; Ahmed, V.; Hill, B.; Ahmed, Z.; Taylor, S. D. A re-examination of the difluoromethylenesulfonic acid group as a phosphotyrosine mimic for PTP1B inhibition. *Bioorg. Med. Chem.* **2008**, *16*, 6764-6777.
173. Mutlib, A.; Espina, R.; Atherton, J.; Wang, J.; Talaat, R.; Scatina, J.; Chandrasekaran, A. Alternate Strategies to Obtain Mass Balance without the Use of Radiolabeled Compounds: Application of Quantitative Fluorine (19F) Nuclear Magnetic Resonance (NMR) Spectroscopy in Metabolism Studies. *Chem. Res. Toxicol.* **2012**, *25*, 572-583.
174. Xu, P.; Guo, S.; Wang, L.; Tang, P. Silver-catalyzed oxidative activation of benzylic C-H bonds for the synthesis of difluoromethylated arenes. *Angew. Chem. Int. Ed Engl.* **2014**, *53*, 5955-5958.
175. Gramec, D.; Peterlin Masic, L.; Sollner Dolenc, M. Bioactivation Potential of Thiophene-Containing Drugs. *Chem. Res. Toxicol.* **2014**, .
176. Stepan, A. F.; Walker, D. P.; Bauman, J.; Price, D. A.; Baillie, T. A.; Kalgutkar, A. S.; Aleo, M. D. Structural Alert/Reactive Metabolite Concept as Applied in Medicinal Chemistry to Mitigate the Risk of Idiosyncratic Drug Toxicity: A Perspective Based on the Critical Examination of Trends in the Top 200 Drugs Marketed in the United States. *Chem. Res. Toxicol.* **2011**, *24*, 1345-1410.
177. Evans, W. E.; Relling, M. V. Pharmacogenomics: translating functional genomics into rational therapeutics. *Science* **1999**, *286*, 487-491.

178. Lopez-Garcia, M.; Dansette, P. M.; Mansuy, D. Thiophene derivatives as new mechanism-based inhibitors of cytochromes P-450: Inactivation of yeast-expressed human liver cytochrome P-450 2C9 by tienilic acid. *Biochemistry (N. Y.)* **1994**, *33*, 166-175.
179. Rettie, A. E.; Jones, J. P. Clinical and toxicological relevance of CYP2C9: drug-drug interactions and pharmacogenetics. *Annu. Rev. Pharmacol. Toxicol.* **2005**, *45*, 477-494.
180. Narender, N.; Srinivasu, P.; Ramakrishna Prasad, M.; Kulkarni, S. J.; Raghavan, K. V. AN EFFICIENT AND REGIOSELECTIVE OXYBROMINATION OF AROMATIC COMPOUNDS USING POTASSIUM BROMIDE AND OXONE[®],*. *Synthetic Communications* **2002**, *32*, 2313-2318.
181. Barnard, C. F. J. Palladium-Catalyzed Carbonylation—A Reaction Come of Age. *Organometallics* **2008**, *27*, 5402-5422.
182. Brennfürher, A.; Neumann, H.; Beller, M. Palladium-Catalyzed Carbonylation Reactions of Aryl Halides and Related Compounds. *Angewandte Chemie International Edition* **2009**, *48*, 4114-4133.
183. Grigg, R.; Mutton, S. P. Pd-catalysed carbonylations: versatile technology for discovery and process chemists. *Tetrahedron* **2010**, *66*, 5515-5548.
184. Buchstaller, H.; Wilkinson, K.; Burek, K.; Nisar, Y. Synthesis of 3-Indazolecarboxylic Esters and Amides via Pd-Catalyzed Carbonylation of 3-Iodoindazoles. *Synthesis* **2011**, 3089-3098.
185. Cacchi, S.; Fabrizi, G.; Goggiamani, A. Palladium-Catalyzed Hydroxycarbonylation of Aryl and Vinyl Halides or Triflates by Acetic Anhydride and Formate Anions. *Org. Lett.* **2003**, *5*, 4269-4272.
186. Surry, D. S.; Buchwald, S. L. Dialkylbiaryl phosphines in Pd-catalyzed amination: a user's guide. *Chem. Sci.* **2011**, *2*, 27-50.

187. Deng, W.; Liu, L.; Zhang, C.; Liu, M.; Guo, Q. Copper-catalyzed cross-coupling of sulfonamides with aryl iodides and bromides facilitated by amino acid ligands. *Tetrahedron Lett.* **2005**, *46*, 7295-7298.

188. Pettus, L. H.; Xu, S.; Cao, G.; Chakrabarti, P. P.; Rzasa, R. M.; Sham, K.; Wurz, R. P.; Zhang, D.; Middleton, S.; Henkle, B.; Plant, M. H.; Saris, C. J. M.; Sherman, L.; Wong, L. M.; Powers, D. A.; Tudor, Y.; Yu, V.; Lee, M. R.; Syed, R.; Hsieh, F.; Tasker, A. S. 3-Amino-7-phthalazinylbenzoxisoxazoles as a Novel Class of Potent, Selective, and Orally Available Inhibitors of p38 α Mitogen-Activated Protein Kinase. *J. Med. Chem.* **2008**, *51*, 6280-6292.

189. Vigroux, A.; Bergon, M.; Bergonzi, C.; Tisnes, P. A General Acid-Catalyzed Anion Breakdown Associated with an E1cB Reaction in the Hydrolysis of Aryl N-(Substituted Phenylsulfonyl)carbamates. *J. Am. Chem. Soc.* **1994**, *116*, 11787-11796.

190. Olsen, L.; Rydberg, P.; Rod, T. H.; Ryde, U. Prediction of Activation Energies for Hydrogen Abstraction by Cytochrome P450. *J. Med. Chem.* **2006**, *49*, 6489-6499.

191. Tian, Z.; Fattahi, A.; Lis, L.; Kass, S. R. Cycloalkane and Cycloalkene C-H Bond Dissociation Energies. *J. Am. Chem. Soc.* **2006**, *128*, 17087-17092.

192. Auerbach, R.; Lewis, R.; Shinnars, B.; Kubai, L.; Akhtar, N. Angiogenesis assays: a critical overview. *Clin. Chem.* **2003**, *49*, 32-40.

193. Ambudkar, S. V.; Kim, I.; Sauna, Z. E. The power of the pump: Mechanisms of action of P-glycoprotein (ABCB1). *European Journal of Pharmaceutical Sciences* **2006**, *27*, 392-400.

194. Ludwig, J. A.; Szakács, G.; Martin, S. E.; Chu, B. F.; Cardarelli, C.; Sauna, Z. E.; Caplen, N. J.; Fales, H. M.; Ambudkar, S. V.; Weinstein, J. N.; Gottesman, M. M. Selective Toxicity of NSC73306 in MDR1-Positive Cells as a New Strategy to Circumvent Multidrug Resistance in Cancer. *Cancer Research* **2006**, *66*, 4808-4815.

195. Nobili, S.; Landini, I.; Mazzei, T.; Mini, E. Overcoming tumor multidrug resistance using drugs able to evade P-glycoprotein or to exploit its expression. *Med. Res. Rev.* **2012**, *32*, 1220-1262.
196. Pellicani, R. Z.; Stefanachi, A.; Niso, M.; Carotti, A.; Leonetti, F.; Nicolotti, O.; Perrone, R.; Berardi, F.; Cellamare, S.; Colabufo, N. A. Potent Galloyl-Based Selective Modulators Targeting Multidrug Resistance Associated Protein 1 and P-glycoprotein. *J. Med. Chem.* **2012**, *55*, 424-436.
197. Ambudkar, S.; Dey, S.; Hrycyna, C.; Ramachandra, M.; Pastan, I.; Gottesman, M. Biochemical, cellular, and pharmacological aspects of the multidrug transporter. *Annu. Rev. Pharmacol. Toxicol.* **1999**, *39*, 361-398.
198. Desai, P. V.; Raub, T. J.; Blanco, M. How hydrogen bonds impact P-glycoprotein transport and permeability. *Bioorg. Med. Chem. Lett.* **2012**, *22*, 6540-6548.
199. Soule, H. D.; Vazquez, J.; Long, A.; Albert, S.; Brennan, M. A human cell line from a pleural effusion derived from a breast carcinoma. *J. Natl. Cancer Inst.* **1973**, *51*, 1409-1416.
200. Sumitomo Pharmaceuticals Company, L. Europe Patent EP1403255 A1, 2004.
201. Leed, A. R.; Boettger, S. D.; Ganem, B. Studies on the synthesis of substituted phenanthrenoids. *J. Org. Chem.* **1980**, *45*, 1098-1106.
202. Banks, M. R.; Hudson, R. F. The reaction of N-alkylhydroxamic acids with sulphonyl chlorides. *J. Chem. Soc., Perkin Trans. 2* **1986**, 1211-1216.
203. SQUIBB BRISTOL MYERS CO USA Patent WO2013/55984 A1, 2013.